THE CITY UNIVERSITY, LONDON

THERMAL STRESSES IN STRUCTURES

A Thesis submitted to

THE CITY UNIVERSITY

for the Degree of Doctor of Philosophy
in Civil Engineering

by

Harbhajan Singh Parmar B.Sc.(Civil Eng.), M.Sc.(Struct.Eng.)
P.Eng., F.I.E.(S'pore), M.I.E.(Aust.)
C.Eng., M.I.C.E.

1978

PREFACE

The author obtained his first degree of B.Sc. (Civil Eng.) at Battersea College of Technology, University of London, in 1963 and his second degree of M.Sc. (Struct.Eng.) at the University of Surrey, in 1967.

He is a partner in the Consulting Engineering firm of M/s. Steen Sehested & Partners, which has its main centre of operation in South-East Asia and an office in London. He has designed a wide variety of buildings - educational, residential, commercial, factory buildings, warehouses, swimming pool complexes and civil engineering works - jetties, wharfs, submarine pipelines, roads, bridges etc., but has specialised in multi-storey buildings - offices, hotels and hospitals. Notable examples are (i) 45-storey Hong Leong Building (office), (ii) 40-storey Mandarin Hotel and (iii) 30-storey Tunas Building (office), all in Singapore. He is presently engaged in the design of, perhaps, the largest teaching hospital in the world and several tall buildings.

SYNOPSIS

This work is concerned with thermal stresses and deformations in structures generally. It is now well known, and is confirmed by observations of structures, that high stresses can develop due to thermal effects even at ambient temperature changes. These are usually evidenced by the appearance of extensive cracking and deflections, and sometimes by premature deterioration of concrete. In spite of considerable research into various thermal aspects, the information at present available to a practising engineer is insufficient, and these effects are therefore rarely adequately included at the design stage.

In this work, methods of predicting thermal stresses and deformations in structures, suitable for practical application in office conditions, are developed. Particular attention is paid to the basic structural forms used in practice, such as portal frames, multi-storey frames, braced frames, trusses and box girders. Other forms not discussed here may also be dealt with in a similar way, based on principles developed for these basic forms of structures. The effects of axial stresses arising from temperature changes and the effect of temperature of hydration of cement combined with early shrinkage of concrete were also investigated.

The validity of the assumptions made in the theoretical formulations was checked and confirmed by several experiments conducted on micro-concrete and perspex models.

Experiments were also conducted to investigate the thermal response and properties of concrete which are required in the analysis.

Acknowledgements

I wish to express my thanks to Dr. M. Smolira, for his help, guidance and suggestions based on his approach to thermal analysis of structures.

Appreciation is also due to [redacted], for giving a practicing consultant the opportunity to carry out this work; to [redacted], for his kindness during my stay at the University; and to the other teaching and laboratory staff, especially [redacted], for their very willing assistance.

Lastly, I would like to thank my friends, [redacted], for their encouragement and assistance.

CONTENTS

CHAPTER THREE

CHAPTER FOUR

CHAPTER FIVE

INDEX OF PLATES

NOTATIONS

A	area
B, C	constants as specified
D	flexural rigidity = $Ed^3/12(1-\mu^2)$
E, Ec etc.	modulus of elasticity, for conc. etc.
F	force
G	shear modulus of elasticity
H	horizontal reaction
I, Ix, Iy	second moment of area, x & y directions
K	bulk modulus; also constants as specified
L, l	length of member
M, m	bending moments
N	force resultant
P	load; perimeter; constants as specified
Q	quantity of heat; also constant as specified
R	radius of curvature; constants as specified; modulus of rupture
T	temperature (also Ty, T0, T1, T2)
V	vertical reactions
X, Y, Z	body forces per unit volume
a, b, c	linear dimensions
d	depth or thickness
e, e_{ij}	strain (e_{xx}, e_{yy}, e_{zz}); also eccentricity
f	flexibility coefficients (f_{11}, f_{21} etc); also dimension
h	half thickness or depth (= d/2)
k	thermal conductivity
l, m, n	direction cosines
p	pressure
q	heat flux per unit area per unit time
r, r_1	constants as specified

s, s_{12}	shrinkage; also constants as specified
t	time; also thickness
u, v, w	components of displacement vector in co-ordinate directions
x, y, z	rectangular co-ordinates; also linear dimensions
α	coefficient of linear thermal expansion; rotation; constants as specified
β	constant as specified
δ, Δ	displacements
ϵ	strain components
θ	rotation; also slope
λ, μ	Lame's elastic constants
ν	Poisson's Ratio
ρ	mass density; also lack of fit
σ, σ_{ij}	stress (σ_{xx}, σ_{yy}, σ_{zz})
Σ	summation (σ_{xx}, + σ_{yy} + σ_{zz})
τ	twist or shearing stress
ϕ	rotation
$\bar{e}$	dilatation (= e_{xx} + e_{yy} + e_{zz})
$\bar{y}$	dimension

1.00 SCOPE AND OBJECTIVES

The main objectives of this work are to develop methods of predicting thermal stresses and deformations, due to ambient temperature changes, in structures suitable for office use, and to verify the validity of the assumptions made in the mathematical formulations by experimental work. Although a considerable amount of work has been carried out by other authors to investigate the effects of ambient temperature changes, such as between day and night and annual changes etc., it appears that many problems are still not fully resolved. This work is therefore intended to further our knowledge of thermal effects on structures.

The main objectives can be categorised as follows:-

(i) To establish thermal response and properties of concrete,

(ii) To investigate the effects of ambient temperature changes on structures generally,

(iii) To check the assumptions made in the theories of thermal stresses,

(iv) To check the correlation of theoretical predictions of thermal stresses and deformations with experimental results, and

(v) To compare various methods of analysis suitable for dealing with thermal stresses.

The experimental work was carried out using 'micro-concrete' models subjected to the effect of temperature changes and on perspex models using the simulated effect of temperature. Tests were also conducted on normal and some lightweight concretes to establish thermal response and to investigate and determine material properties.

An investigation was also carried out to assess the effect of early shrinkage of concrete and the temperature of hydration of cement on stresses and deformations, as well as to predict the approximate spacing of the potential cracks.

The force-displacement method is used mostly in this work for the following reasons:-

(i) The method is not yet fully explored and therefore this work serves the dual purpose of its use in the thermal stress problems and the further exploration of the method itself.

(ii) This method gives directly the values of forces and deflections usually required by the designer (unlike the stiffness method where statical indeterminacy is expressed in relation to the number of degrees of freedom of joints).

(iii) The method is based on clear, physical interpretation of the actual response of the structure which is relatively simple to understand, and this greatly facilitates the setting out of the matrix and helps in avoiding errors.

(iv) The method is versatile and has already been used by others to resolve some complex structural problems.

(v) The matrix is usually well conditioned and no serious problems have so far been encountered in the computational processes.

1.02 INTRODUCTION

It is well known that temperature variations cause dimensional changes in structures and these result in high stresses and deformations. Modern structures are often very slender and are exposed and can therefore be subjected to the effect of seasonal and daily variations of temperature. In some parts of the world these variations could be very severe, e.g. in desert countries the daytime temperatures could rise to say 130°F, while the night temperatures could be well below freezing point. The problems created by temperature variations arise mainly because of the continuity of joints and are now prevalent virtually in all countries and these are aggravated by central heating and airconditioning. While the temperature inside the building stays relatively constant, outside members are often subjected to the effect of considerable temperature differential and tend to change their dimensions relative to the interior members. If these dimensional changes could take place completely freely, no stresses would develop. However, restraints in various forms are usually present and free dimensional changes cannot take place. This results in high thermal stresses and deformations and consequent development of cracks. Besides structural damage, thermal movements can effect architectural components such as partitions, finishes, services and floor alignments, etc.

The nature of thermal stresses and strains is complicated and still not fully understood by designers and even by researchers. This is due to the fact that it is difficult to separate the thermal effects from those due to creep, shrinkage and humidity and moisture changes. Most codes of Practices require provisions for thermal stresses in the design of structural members, but do not give sufficient guidelines to the designers on how these provisions should be made.

This results with the designer either making arbitrary provisions or no provision at all. The structure then ends up either overdesigned or underdesigned, neither of which is satisfactory. Therefore, better understanding of the magnitude of thermal stresses and movements may lead to more economical and rational design. It is intended to give the designer a scientific theory on which to base his design.

Theoretically, thermal stresses would not occur in two extreme cases, (i) if solids did not conduct heat at all, and (ii) if the heat of conduction was infinite, i.e. matter would then have constant temperature. However, since all solids have heat conduction of finite values, dimensional changes take place and, in the presence of restraints, stresses develop. The magnitude of these stresses depends on the thermal properties of materials, on the magnitude and form of the temperature gradient, and on the mass and size of members.

In a steady state of heat conduction, temperature stresses tend theoretically to zero over a long period of time because of creep, but few structures are exposed to a steady state of temperature for a period long enough to make this effect appreciable. The main sources of temperature changes are relatively short term and these are:-

(i) Ambient changes between day and night.

(ii) Heat of hydration of cement.

(iii) Various heating and airconditioning installations.

(iv) Heat generated in nuclear shields of power stations and other nuclear applications.

(v) The difference in the oil temperatures in the storage tanks of off-shore drilling platforms to that of the surrounding sea water, and

(vi) Annual seasonal changes.

It is now known that thermal response of structures depends on many parameters such as the thermal properties of the particular concrete used, on time, creep and shrinkage, temperature of hydration of cement, moisture variations, continuity of joints and even the percentage of steel used. Some of these parameters are interdependent and are often of unknown form. Because of these difficulties in practice some simplifications are introduced, which appear to be adequate for the present requirements, and for practical purposes. These simplified assumptions are as follows:-

(i) That the temperature variation in the material of the structural member can be determined independently of the magnitude of strains and stresses,

(ii) That the deformations are small and the analysis can be based on the original dimensions and configuration of a structure,

(iii) That the principle of superposition is valid and the material obeys Hooke's Law, and

(iv) That the thermal stresses can be evaluated independently of the effect of creep and shrinkage, and at the time corresponding with the steady state of stress.

This work aims to investigate the thermal effects on various structures normally encountered in the design office. Typical examples of a large number of problems are investigated so as to lay the basis of some guidelines for the designer to follow in solving the problems of thermal stresses. Experimental work aims at verification of the assumptions made. A comparison with some basic methods of analysis will be made.

This work aims also to investigate thermal properties of materials and particularly concrete for the purpose of including these parameters in the matrices.

Not considered in this work is the effects of elevated temperatures and fire in structures.

1.03 PROGRAMME OF EXPERIMENTAL WORK

(a) Experiments were carried out on micro-concrete models to determine the following:-

(i) Stresses and deformations induced in a 6-storey shear wall frame due to the effect of temperature variation in one column.

(ii) Stresses and deformations induced in a 6-storey shear wall frame due to the effect of temperature variation in the roof.

(iii) Experimental verifications of thermal response of concrete due to temperature variation by the application of heat to a large concrete block.

(iv) The variations of modulus of elasticity of various concrete mixes due to the effect of temperature variation in concrete cylinders.

(v) The modulus of elasticity and strain calibration of a reinforced micro-concrete beam from stresses induced by elastic loading.

(vi) The coefficient of linear thermal expansion and the modulus of elasticity from stresses induced by thermal effects in a reinforced micro-concrete continuous beam.

(vii) The effect on compression strength of concrete cubes of various mixes due to temperature variation.

(b) Experiments were carried out on perspex models based on simulated temperature variations to determine the following:-

(viii) Stresses and deformations induced in a 6-storey perspex shear wall frame due to the simulated effect of temperature variation in one column.

(ix) Stresses and deformations induced in a perspex truss due to the simulated effect of temperature variation in the top chord.

2.00 REVIEW OF PRESENT STATE OF KNOWLEDGE OF THERMAL EFFECTS ON STRUCTURES

2.01 SHORT REVIEW OF THE THEORY OF HEAT TRANSFER

The thermal properties of concrete and the knowledge of the laws of heat transfer are required for the analysis of thermal stresses and deformations. The basic modes of heat transfer are: conduction, convection and radiation of heat. In structural engineering, however, heat transfer by conduction is the primary mode with the other two only affecting the boundary conditions.

In a solid body heat is transferred mainly by conduction since the effects of radiation are negligible (except for transparent materials such as glass or quartz) and convection is predominant mainly in liquids and gases.

When heat is applied to a body, it is partly dissipated and partly absorbed followed by rise of temperature. For heat conduction to occur, a temperature gradient must exist and then the heat always flows in the direction of decreasing temperature. The rate of heat conduction is a property unique to the particular material but depends also on the level of the applied temperature and moisture content. The Theory of heat conduction is based on Fourier's Law, which for an isotropic body may be written as:

$$q = -k \frac{\partial T}{\partial n} \qquad 2.01.01$$

in which $\partial/\partial n$ denotes differentiation along the outward-drawn normal to the surface or more specifically in rectangular co-ordinates,

$$(qx\ ,\ qy,\ qz) = -k\ (\frac{\partial T}{\partial x}\ ,\ \frac{\partial T}{\partial y}\ ,\ \frac{\partial T}{\partial z}) \qquad 2.01.02$$

Where, the heat flux per unit area, q is in the direction of positive normal, or positive co-ordinate. The flux of heat across any surface is defined as the rate at which heat is transferred across any surface 's' at a point 'p', per unit area per unit time.

'k' is a Thermal Conductivity of a material, which depends on the chemical composition of material, its physical state and texture, and may also be a function of the level of temperature. Strictly speaking, the conductivity 'k' is therefore not constant for the same substance, but depends upon the level of temperature applied. However, when the range of temperature is limited, the change in 'k' may be neglected and in most mathematical theories it is assumed that the conductivity does not vary with the level of temperature. The units of 'k' are cal/(sec) (cm^2) ($^oc/cm$) in the C.G.S. System or Btu/(hr.)(ft^2) ($^oF/ft$) as commonly used by engineers.

When the amount of heat absorbed equals that which is dissipated, the flow of heat is said to be steady or independent of time. If the amount of heat absorbed is not equal to the amount dissipated, the flow is said to be time dependent or unsteady. The transient state is a special form of unsteady state and describes a definite change between the two limits.

In practice, the surface temperature of structures does not stay constant for sufficiently long time to develop a steady state of heat transfer, but changes periodically with the daily and annual variation of temperature.

Observations of the response of concrete members to outside temperature changes show two important phenomena which are relevant to the design of structures:

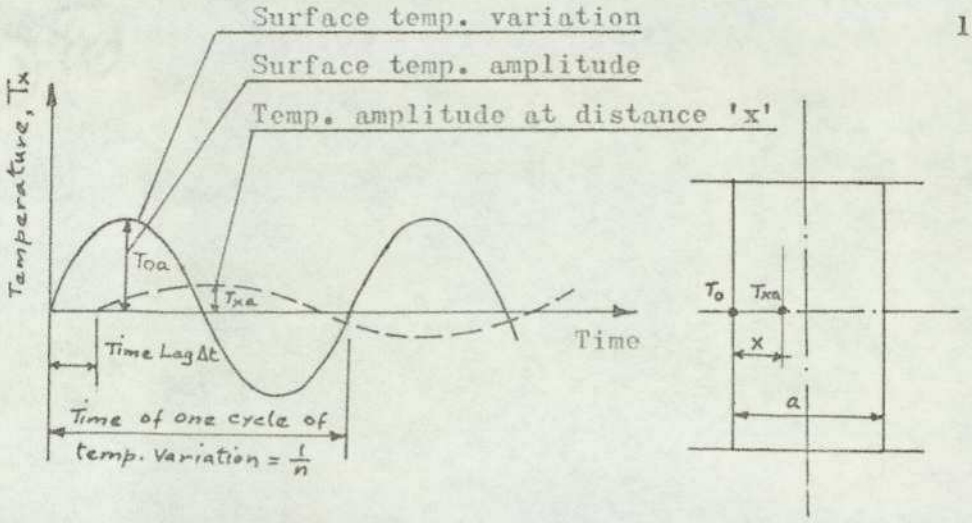

Fig. 2.011 Temperation variation inside a member for sinusoidal variation of surface temperature.

(a) a time lag, and

(b) attenuation (or damping) of intensity of temperature amplitude with the distance from the heated face of concrete.

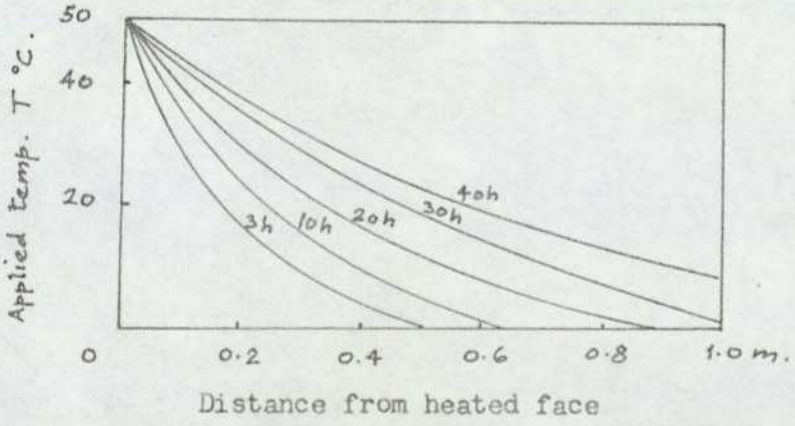

Fig. 2.012 Penetration of applied temperature at various time intervals for normal density concrete.

The time lag is due to the thermal inertia of concrete in responding to the temperature change. Fig. 2.012 shows average values of time lag in the arrival of surface temperature variation at various depths of concrete members. It can be seen from this diagram that rapid temperature changes penetrate very little into concrete, and only the amplitudes of slowly

changing temperatures penetrate deep into the mass of concrete. The lower the thermal conductivity of concrete, the greater is the time lag and the attenuation of the temperature variation.

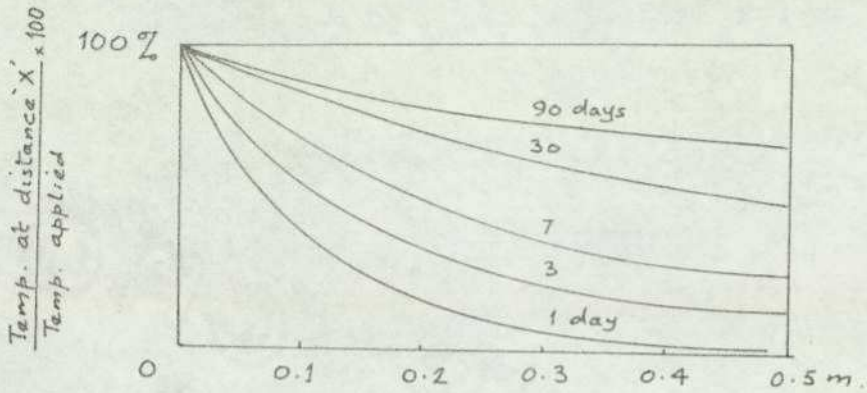

Fig. 2.013 The attenuation of surface temperature amplitudes at various depths of concrete mass.

The attenuation indicates that the temperature in concrete does not rapidly reach the value of temperature applied because of the "thermal inertia" of concrete. Fig. 2.013 shows average values of attenuation of surface temperature with depth in a normal concrete.

2.02.1 Definition of Strain Components

The strain-displacement relations are derived directly from purely geometrical considerations. The displacements are assumed to be small and are obtained, based on an initial unstressed condition at uniform temperature, To. The displacements are assumed not to effect the geometry of the element or its density (i.e. the thermal couplings are omitted).

The equations for a rectangular axis system (x,y,z) are:-

$$\left.\begin{aligned} e_{xx} &= \frac{\partial u}{\partial x} \; ; \qquad e_{yy} = \frac{\partial v}{\partial y} \; ; \qquad e_{zz} = \frac{\partial w}{\partial z} \\ e_{xy} &= \frac{\partial u}{\partial y} + \frac{\partial v}{\partial x} \; ; \; e_{yz} = \frac{\partial v}{\partial z} + \frac{\partial w}{\partial y} \; ; \; e_{zx} = \frac{\partial w}{\partial x} + \frac{\partial u}{\partial z} \end{aligned}\right\} \quad \ldots \; 2.02.101$$

Where u, v, and w are the components of the displacement vector in the x, y and z directions respectively.

From a physical point of view, the displacements in a simply connected body must be single-valved and continuous. Certain restrictions on the strains e_{ij} arise to meet this requirement and these constitute the so-called strain compatibility equations. The six strains e_{ij} are written in terms of the displacements u, v and w and by repeated differentiation and elimination of displacements the appropriate equations of compatibility are derived which are valid for both thermal and mechanical loading.

$$\left.\begin{aligned} &\text{Thus} \quad \frac{\partial^2 e_{xx}}{\partial y^2} + \frac{\partial^2 e_{yy}}{\partial x^2} = \frac{\partial^2 e_{xy}}{\partial x \partial y} \; ; \qquad \frac{\partial^2 e_{yy}}{\partial z^2} \quad \frac{\partial^2 e_{zz}}{\partial y^2} = \frac{\partial^2 e_{yz}}{\partial y \partial z} \\ &\frac{\partial^2 e_{zz}}{\partial x^2} + \frac{\partial^2 e_{xx}}{\partial z^2} = \frac{\partial^2 e_{xz}}{\partial x \partial z} \; ; \quad 2\frac{\partial^2 e_{xx}}{\partial y \partial z} = \frac{\partial}{\partial x}\left(\frac{\partial e_{zx}}{\partial y} + \frac{\partial e_{xy}}{\partial z} - \frac{\partial e_{yz}}{\partial x}\right) \\ &\frac{2\partial^2 e_{yy}}{\partial z \partial x} = \frac{\partial}{\partial y}\left(\frac{\partial e_{xy}}{\partial z} + \frac{\partial e_{yz}}{\partial x} - \frac{\partial e_{zx}}{\partial y}\right); \; \frac{2\partial^2 e_{zz}}{\partial x \partial y} = \frac{\partial}{\partial z}\left(\frac{\partial e_{yz}}{\partial x} + \frac{\partial e_{zx}}{\partial y} - \frac{\partial e_{xy}}{\partial z}\right) \end{aligned}\right\} \quad 2.02.102$$

2.02.2 Equations of State

The total strains at each point in a heated body may be considered to consist of two parts, viz. the free thermal expansion plus the strains dependent upon the stress state in the body. Since the first part is uniform in all directions at a given point in an isotropic body it can be deduced that no shear strains result - only direct strains. Therefore, the usual strain-stress relations of linear isothermal elasticity are extended for the thermoelastic case to become

$$\left.\begin{aligned} e_{xx} &= \alpha T + \left[\sigma_{xx} - U(\sigma_{yy} + \sigma_{zz})\right]/E \\ e_{yy} &= \alpha T + \left[\sigma_{yy} - U(\sigma_{xx} + \sigma_{zz})\right]/E \\ e_{zz} &= \alpha T + \left[\sigma_{zz} - U(\sigma_{xx} + \sigma_{yy})\right]/E \\ e_{xy} &= \sigma_{xy}/G \;;\; e_{yz} = \sigma_{yz}/G \;;\; e_{zx} = \sigma_{zx}/G \end{aligned}\right\} \quad \ldots\ldots 2.02.201$$

Soln. of 2.02.201 gives :-

$$\left.\begin{aligned} \sigma_{xx} &= (\lambda + 2\mu)e_{xx} + \lambda(e_{yy} + e_{zz}) - \beta T \\ \sigma_{yy} &= (\lambda + 2\mu)e_{yy} + \lambda(e_{zz} + e_{xx}) - \beta T \\ \sigma_{zz} &= (\lambda + 2\mu)e_{zz} + \lambda(e_{xx} + e_{yy}) - \beta T \\ \sigma_{xy} &= \mu e_{xy} \;;\; \sigma_{yz} = \mu e_{yz} \;;\; \sigma_{zx} = \mu e_{zx} \end{aligned}\right\} \quad 2.02.202$$

Where λ and μ, the Lamé elastic constants, are defined by

$$\left.\begin{aligned} \lambda &= UE/(1+U)(1-2U) \;;\quad \mu = E/2(1+U) = G \text{ and} \\ \beta &= E\alpha/(1-2U) \end{aligned}\right\} \quad 2.02.203$$

Equations 2.02.201 and 2.02.202 are the equations of state for the elastic regime of an isotropic solid body.

It is to be noted that E, G, U and α (and hence, λ, μ, and β) are all, in general, functions of temperature.

If the dilatation $\bar{e}$ and the sum of the normal stresses Σ are defined by

$$\bar{e} = e_{xx} + e_{yy} + e_{zz} \quad \ldots \quad 2.02.204$$

and

$$\Sigma = \sigma_{xx} + \sigma_{yy} + \sigma_{zz} \quad \ldots \quad 2.02.205$$

the following relation is obtained from (2.02.201)

$$\bar{e} = 3\alpha T + \Sigma/3K \quad \ldots \quad 2.02.206$$

where $$K = E/3(1-2\upsilon) \quad \ldots \quad 2.02.207$$

2.02.3 Equations of Equilibrium

The components of stress must satisfy the usual equations of equilibrium throughout the volume, and since these are derived from purely mechanical considerations they are the same as those for isothermal elasticity, viz:-

$$\left.\begin{aligned} \frac{\partial \sigma_{xx}}{\partial x} + \frac{\partial \sigma_{xy}}{\partial y} + \frac{\partial \sigma_{xz}}{\partial z} + X &= 0 \\ \frac{\partial \sigma_{xy}}{\partial x} + \frac{\partial \sigma_{yy}}{\partial y} + \frac{\partial \sigma_{yz}}{\partial z} + Y &= 0 \\ \frac{\partial \sigma_{xz}}{\partial x} + \frac{\partial \sigma_{yz}}{\partial y} + \frac{\partial \sigma_{zz}}{\partial z} + Z &= 0 \end{aligned}\right\} \quad \ldots \quad 2.02.301$$

with the complementary shear stress components equal, i.e.

$$\sigma_{xy} = \sigma_{yx} \;, \quad \sigma_{yz} = \sigma_{zy} \;, \quad \sigma_{zx} = \sigma_{xz} \quad \ldots \quad 2.02.302$$

If inertia effects are to be considered then, for small displacements, with ρ being the mass density

$$X = -\rho \frac{\partial^2 u}{\partial t^2} \;, \quad Y = -\rho \frac{\partial^2 v}{\partial t^2} \;, \quad Z = -\rho \frac{\partial^2 w}{\partial t^2} \quad \ldots \quad 2.02.303$$

Gravity forces may be included similarly.

2.02.4 Boundary Conditions

2.02.4.1 Traction Boundary Conditions

Not only must the components of stress satisfy the equations of equilibrium throughout the volume of the body but also at all points on the surface, i.e.

$$\begin{aligned} l\,\sigma_{xx} + m\,\sigma_{xy} + n\,\sigma_{xz} &= X_s \\ l\,\sigma_{xy} + m\,\sigma_{yy} + n\,\sigma_{yz} &= Y_s \\ l\,\sigma_{xz} + m\,\sigma_{yz} + n\,\sigma_{zz} &= Z_s \end{aligned} \qquad 2.02.4.01$$

Where l, m and n are the direction cosines of the outward drawn normal.

2.02.4.2 Displacement Boundary Conditions

The components of the displacement vector must satisfy the conditions below each point, s, on the surface,

$$U = f_1(s) \;, \quad V = f_2(s) \;, \quad W = f_3(s)$$

Where f_1, f_2 and f_3 are prescribed functions.

2.02.4.3 Mixed Boundary Conditions

In practice, neither the Traction Boundary Conditions nor the Displacement Boundary Conditions may apply independently over the entire surface of the body, and mixed boundary conditions are then involved. To generalize therefore, at each point on the surface any three of the six conditions above may be specified provided that each of the three is related to a different coordinate direction, e.g. U , V and Zs may be specified but not U , V and Ys.

It is also possible to prescribe the condition whereby a relation exists between a corresponding pair of displacement and surface force components.

2.02.5 Three Dimensional Thermoelastic Formulations

If the temperature is given at all points in a solid body the stresses and displacements at the corresponding points can be determined by the solution of equations 2.02.101, 2.02.202 and 2.02.301 subject to the appropriate boundary conditions. This is, however, a very difficult problem except in the simplest cases since the following fifteen equations must be satisfied, viz.

6 strain - displacement relations, equations 2.02.101

6 stress - strain relations, equations 2.02.202

3 equilibrium equations, equations 2.02.301

in order to determine the following fifteen unknown functions

6 stress components : $\sigma_{xx} \ldots \sigma_{xy} \ldots$

6 strain components : $e_{xx} \ldots e_{xy} \ldots$

3 displacement components : u, v, w

Various simplifications have been formulated for the solution of complex problems. However, these will not be enumerated here as these are considered outside the scope of this work.

2.02.6 Two Dimensional Formulations and Solutions

The general three-dimensional thermoelastic problem requires the determination of 15 quantities, viz. 6 stresses, 6 strains and 3 displacements, when the body forces and the boundary conditions are known. The problem becomes much simpler if some of the unknown

quantities are zero or insignificant as a result of the particular geometry or loading. Such is the case for Plane Strain and Plane Stress problems.

2.02.6.1 Plane Strain Analysis

The condition of plane strain arises when the displacement component in a given direction is zero and the other displacement components are independent of this direction. Therefore, if W in the z-direction is zero, the conditions which define plane strain are

$$U = U_{(x,Y)} \quad ; \quad V = V_{(x,Y)} \quad ; \quad W = 0 \quad \cdots \quad 2.02.601$$

It can be shown that this condition occurs in a prismatic body whose length is large compared with its cross-sectional dimensions, and for temperatures and loads which are independent of the z-coordinate; the body force component z must also be zero.

With these restrictions the general three-dimensional theory is automatically satisfied, with

$$\left.\begin{aligned} \sigma_{\bar{x}x} &= f_1(x,Y) \;, \quad \sigma_{\bar{Y}Y} = f_2(x,Y), \\ \sigma_{\bar{x}Y} &= f_3(x,Y) \;, \quad \sigma_{\bar{x}z} = \sigma_{\bar{Y}z} = 0 \end{aligned}\right\} \quad \cdots \quad 2.02.602$$

and

$$\sigma_{\bar{z}z} = f_4(x,Y) \;, \quad \text{when} \quad T = T(x,Y)$$

In fact, the third equation 2.02.201 gives

$$\sigma_{\bar{z}z} = U(\sigma_{\bar{x}x} + \sigma_{\bar{Y}Y}) - E\alpha T = f_4(x,Y) \quad \cdots \quad 2.02.603$$

The above equation defines the tractions which are necessary on the end faces of the body to maintain the state of plane strain, i.e. $e_{zz} = 0$. Since these tractions are not, in general, equal to those required, it is necessary to add to the plane solution, another solution which will

make the end tractions have their required valve. This secondary solution requires, in general, the analysis of a non-thermal, but three-dimensional problem. Thus if it is required that the surface tractions on the end faces should be zero, i.e.

$$\sigma_{zz} = \sigma_{xz} = \sigma_{yz} = 0 \quad \text{on} \quad Z = 0, L \ldots \quad 2.02.604$$

the secondary solution necessary must satisfy the conditions

$$\sigma_{xz} = \sigma_{yz} = 0 \quad \text{and} \quad \sigma_{zz} = -f_4(x,y) \quad \text{on} \quad Z = 0, L \ldots \quad 2.02.605$$

with the appropriate boundary conditions on the other faces. In specifying these conditions due note has been taken of the fact that in the plane strain solution the end shear stresses are already zero. In general, the secondary solution satisfying 2.02.605 is difficult to obtain, but by invoking Saint-Venant's principle a realistic but approximate solution is found (as shown in text later) for bodies whose length is much greater than their cross-sectional dimensions.

Saint-Venant's principle, which enables modifications to be made to the boundary conditions of a given problem, states that, "if the forces acting on a small portion of the surface of an elastic body are replaced by another statically equivalent set, only the local stress distribution is significantly altered; at more distant points in the body the resultant error is negligible".

The approximate secondary solution therefore, has the form

$$\left.\begin{aligned} \sigma_{zz} &= \frac{P}{A} + \frac{M_Y . X}{I_{YY}} + \frac{M_X . Y}{I_{XX}} \\ \sigma_{xy} &= \sigma_{xx} = \sigma_{yy} = \sigma_{xz} = \sigma_{yz} = 0 \end{aligned}\right\} \quad 2.02.606$$

2.02.6.2 Plane Stress Analysis

The condition of plane stress is defined as being a two-dimensional state of stress, e.g.

$$\sigma_{zz} = \sigma_{xz} = \sigma_{yz} = 0 \quad \cdots \quad 2.02.607$$

Substituting these values into the three-dimensional stress compatibility equations, with the body forces zero, leads to the conclusion that the temperature distribution must satisfy the equation

$$\nabla^2(\alpha T) = F(z,t) \quad \cdots \quad 2.02.608$$

if a solution to the plane stress problem is also to satisfy exactly the three-dimensional theory. Therefore, the assumptions of plane stress are less satisfactory than those for plane strain since they result in a more restrictive form of temperature distribution.

2.02.6.3 Summary of The Thermal Stress Equations in Two Dimensions

For two-dimensional problems of plane stress or plane strain the three-dimensional equations of thermo-elasticity can be reduced in the following way.

The strain-stress relations 2.02.201 and the strain-displacement relations 2.02.101 become, for the case of plane stress in thin bodies:

$$\left.\begin{aligned} e_{xx} &= \frac{1}{E}\left[\sigma_{xx} - U\sigma_{yy}\right] + \alpha T = \frac{\partial u}{\partial x} \\ e_{yy} &= \frac{1}{E}\left[\sigma_{yy} - U\sigma_{xx}\right] + \alpha T = \frac{\partial v}{\partial y} \\ e_{xy} &= \frac{1}{G}\,\sigma_{xy} = \frac{\partial u}{\partial y} + \frac{\partial v}{\partial x} \end{aligned}\right\} \quad \ldots \quad 2.02.609$$

These relations also apply to plane strain problems if the following substitutions are made, E_1, for E; U_1 for U ; α_1 for α ; where

$$\left.\begin{aligned} E_1 &= E\,(1-U^2) \\ U_1 &= U\,(1-U) \\ \alpha_1 &= \alpha\,(1+U) \end{aligned}\right\} \quad \ldots \quad 2.02.610$$

Note that $G = E/2(1+U) = E1/2(1+U_1)$ and remains the same for both formulations.

The compatibility equations in terms of strains 2.02.102 reduce to,

$$\frac{\partial^2 e_{xx}}{\partial y^2} + \frac{\partial^2 e_{yy}}{\partial x^2} = \frac{\partial^2 e_{xy}}{\partial x\,\partial y} \quad \ldots \quad 2.02.611$$

and the equilibrium equations 2.02.301 become,

$$\left.\begin{aligned} \frac{\partial \sigma_{xx}}{\partial x} + \frac{\partial \sigma_{xy}}{\partial y} + X &= 0 \\ \frac{\partial \sigma_{xy}}{\partial x} + \frac{\partial \sigma_{yy}}{\partial y} + Y &= 0 \end{aligned}\right\} \quad \ldots \quad 2.02.612$$

Using the equilibrium equations, the compatibility condition in terms of stress components becomes,

$$\left(\frac{\partial^2}{\partial x^2} + \frac{\partial^2}{\partial y^2}\right)\left(\sigma_x + \sigma_y + E\alpha T\right) = -(1+U)\left(\frac{\partial X}{\partial x} + \frac{\partial Y}{\partial y}\right) \ldots 2.02.613$$

where for plane strain the constants of equation 2.02.610 must be used.

Therefore the two-dimensional problem reduces to the determination of the stress and strain components which satisfy the compatibility equation, 2.02.613, the equilibrium equations 2.02.612 and the appropriate boundary conditions. For plain strain $e_{zz} = o$ and hence

$$\sigma_{zz} = U(\sigma_{xx} + \sigma_{yy}) - E\alpha T \quad \cdots \quad 2.02.614$$

whilst for plane stress $\sigma_{zz} = o$ and hence

$$e_{zz} = -\frac{U}{E}(\sigma_{xx} + \sigma_{yy}) + \alpha T \quad \cdots \quad 2.02.615$$

2.02.7 Analysis of Thermal Stresses in Thin Rectangular Plates and Beams

One of the causes of initial stresses in a body is non-uniform heating. With rising temperature the elements of a body expand. Such an expansion generally cannot proceed freely in a continuous body, and stresses due to the heating are set up with only a few exceptions, which are discussed later in the text.

In the following paragraph consideration is given to a special case of a one-dimensional temperature distribution i.e. if the temperature variation is the function of one co-ordinate only.

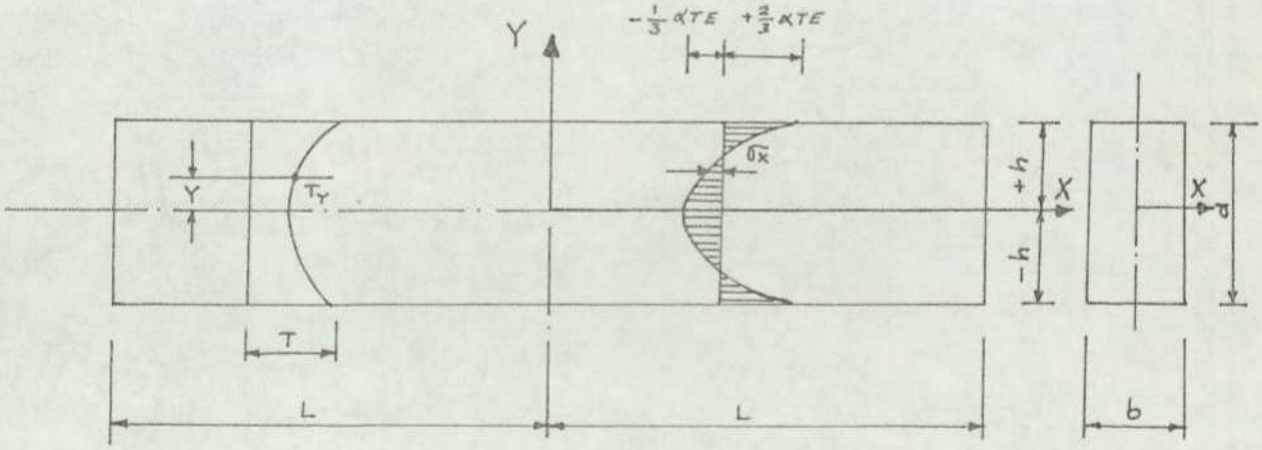

Fig. 2.0271 Thermal stresses due to symmetrical Temperature distribution

2.02.7.1 Symmetrical Temperature Distribution

The following analysis is based on the assumption of a thin rectangular plate undergoing a temperature variation which is a function only of the Y co-ordinate and is independent of the co-ordinates x and z. It is also assumed that the overall length 2L of the plate is very much greater than either the width b or the thickness 2h. The longitudinal thermal strains (αT) can be entirely suppressed by applying to each element of the plate the longitudinal compressive stress

$$\sigma_x' = -\alpha . T_Y . E \quad \cdots \quad 2.02.701$$

Since the plate is free to expand laterally the application of the stresses σ_x' will not produce any stresses in the lateral directions, and to maintain the stresses σ_x' throughout the plate, it will be necessary to distribute compressive forces of the magnitude σ_x' at the ends of the plate only. These compressive forces will completely suppress any expansion of the plate in the direction of the x-axis due to the temperature rise Ty. To obtain the thermal stresses in the plate, which is free from external forces, it is necessary to superpose on the stresses σ_x', the stresses produced in the plate by tensile forces of intensity $\alpha T E$ distributed at the ends. These forces have the resultant

$$\int_{-h}^{+h} \alpha T E \, . \, dY$$

and at a sufficient distance from the ends they will produce approximately uniformly distributed tensile stresses of the magnitude

$$\frac{1}{2h} \int_{-h}^{+h} \alpha T E \, . \, dY$$

so that the thermal stresses in the plate with free ends, at a considerable distance from the ends, will be

$$\sigma_x = \frac{1}{2h}\int_{-h}^{+h} \alpha T E \, dY - \alpha T E \quad \ldots \quad 2.02.702$$

2.02.7.2 Parabolic Temperature Distribution

Assuming, for example, that the temperature is distributed parabolically and is given by the equation

$$T_Y = T_o\left(1 - \frac{Y^2}{h^2}\right)$$

substituting into equation 2.02.702 and integrating, we obtain

$$\sigma_x = \frac{2}{3}\alpha T_o E - \alpha T_o E\left(1 - \frac{Y^2}{h^2}\right) \qquad 2.02.703$$

The stress distribution given by equation 2.02.703 is shown in Fig. 2.02721. These stresses are self-equilibrating i.e. equilibrium conditions are satisfied with regard to the forces and moments.

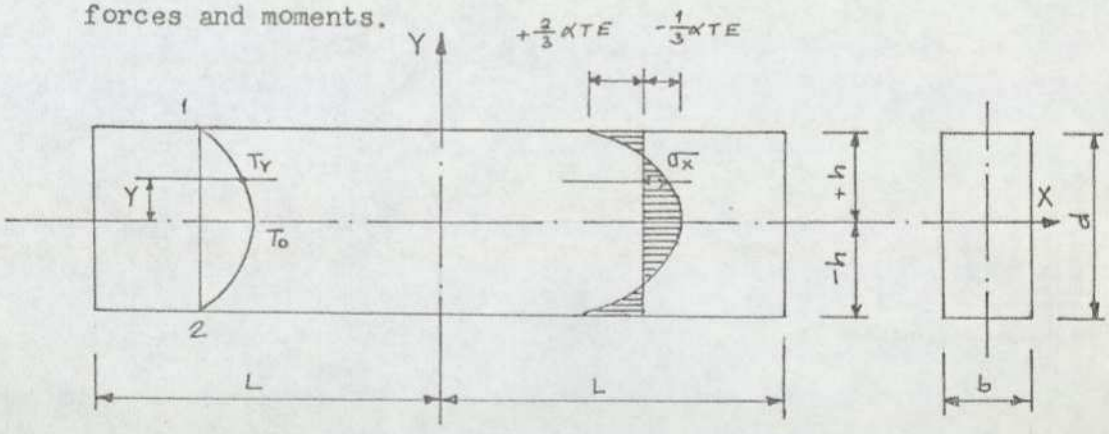

Fig. 2.02721 Thermal stresses due to Parabolic temperature distribution

2.02.7.3 Non-symmetrical Temperature Distribution

If the temperature T is not symmetrical with respect to the x-axis, the strains ϵ_x can again be suppressed by applying stresses σ_x'. In the non-symmetrical cases these stresses give rise not only to a resultant force

$$\int_{-h}^{+h} \alpha_{TE}\, dY$$

but also to a resultant couple

$$\int_{-h}^{+h} \alpha_{TE}\, Y\, dY$$

and in order to satisfy the conditions of equilibrium we must superpose on the compressive stresses σ_x' a uniform tension, determined as before, and bending stresses

$$\sigma_x'' = \sigma\, Y/h$$

determined from the condition that the moment of the forces distributed over a cross-section must be zero. Then

$$\int_{-h}^{+h} \frac{\sigma Y^2 dY}{h} - \int_{-h}^{+h} \alpha_{TEY}\, dY = 0$$

from which $\frac{\sigma}{h} = \frac{3}{2h^3}\int_{-h}^{+h} \alpha_{TEY}\, dY$, $\sigma_x'' = \frac{3Y}{2h^3}\int_{-h}^{+h} \alpha_{TEY}\, dY$

Then the total stress is

$$\sigma_x = -\alpha_{TE} + \frac{1}{2h}\int_{-h}^{+h} \alpha_{TE}\, dY + \frac{3Y}{2h^3}\int_{-h}^{+h} \alpha_{TEY}\, dY \ldots 2.02.704$$

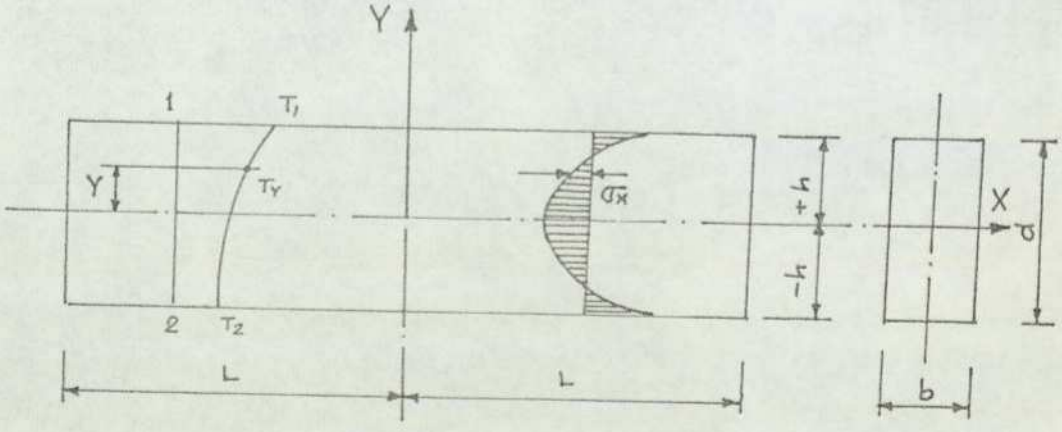

Fig. 2.0273/ Thermal stresses due to non-symmetrical temperature distribution

The above solution may be related to a plate with dimension b corresponding to its thickness, or to a beam with $2h$ corresponding to its thickness (b being its width).

Equation 2.02.704 can also be written in the form

$$\sigma_x = -E\alpha T + \frac{b}{A} N_T + bY M_T \quad \ldots \quad 2.02.705$$

in which

$$N_T = \alpha E \int_{-h}^{+h} T.dY \quad \text{and} \quad M_T = \alpha E \int_{-h}^{+h} T.Y.dY$$

Where N_T and M_T have dimensions of force and moment respectively.

The condition of zero stress at the ends cannot be satisfied because of insufficient number of constants of integration in equation 2.02.613. However, according to St. Venant's principle, any local disturbance has little effect on sections away from this point.

So far it has been assumed that the plate or beam was thin in the Z-direction.

Suppose now that the dimension in the Z-direction is large, this will be equivalent to a plate with XZ-plane as its middle plane, and a thickness $2h$. As before, letting the temperature T to be independent of x and z, and so a function of Y only.

The free thermal expansion of an element of the plate in the x- and z- directions will be completely suppressed by applying stresses $\bar{\sigma_x}$, $\bar{\sigma_z}$ obtained from equations.

$$\epsilon_x = \frac{1}{E}\left\{\bar{\sigma_x} - \upsilon\left(\bar{\sigma_x} + \bar{\sigma_z}\right)\right\}$$
$$\epsilon_y = \frac{1}{E}\left\{\bar{\sigma_y} - \upsilon\left(\bar{\sigma_x} + \bar{\sigma_z}\right)\right\}$$
$$\epsilon_z = \frac{1}{E}\left\{\bar{\sigma_z} - \upsilon\left(\bar{\sigma_x} + \bar{\sigma_y}\right)\right\}$$

by putting $\epsilon_x = \epsilon_z = -\alpha T$, $\bar{\sigma_y} = 0$, these equations then give

$$\bar{\sigma_x} = \bar{\sigma_z} = -\frac{\alpha T E}{1-\upsilon} \quad \ldots \quad 2.02.706$$

The thermal stress in the plate, free from external force, is obtained by superposing on the stresses in eqn.2.02.706, the stresses due to the application of equal and opposite distributions of force on the edges. If T is an even function of Y such that the mean value over the thickness of the plate is zero, the resultant force per unit run of edge is zero, and again, by Saint Venant's principle, it produces no stress except near the edge.

If the mean value of T is not zero, uniform tensions in the x- and z- directions corresponding to the resultant force on the edge must be superposed on the compressive stresses given by equation 2.02.706.

If in addition to this the temperature is not symmetrical with respect to the xz- plane, the bending stresses must be added. In this manner, the following

thermal stress equation can be obtained:

$$\sigma_x = \sigma_z = -\frac{\alpha T E}{1-\mu} + \frac{1}{2h(1-\mu)} \int_{-h}^{+h} \alpha T E \, dy + \frac{3y}{2h^3(1-\mu)} \int_{-h}^{+h} \alpha T E y \, dy \cdots$$

... 2.02.707

This equation is analogous to the equation 2.02.704, obtained before. By using equation 2.02.707, the thermal stresses in a plate can be calculated, if the distribution of temperature T over the Thickness of the plate is known.

2.02.7.4 Linear Temperature Distribution

If the surfaces $y = \pm h$ of a plate or beam are maintained at two different temperatures T_1 and T_2, (see fig. 2.02741) a steady state of heat flow is established after a certain time and the temperature is then given by the linear function

$$T = \frac{1}{2}(T_1 + T_2) + \frac{1}{2}(T_1 - T_2)\frac{Y}{h} \quad \cdots \quad 2.02.708$$

Substitution in equation 2.02.707 shows that the thermal stresses are zero, provided the plate or beam is not restrained. This would be the case in a simply supported beam or plate.

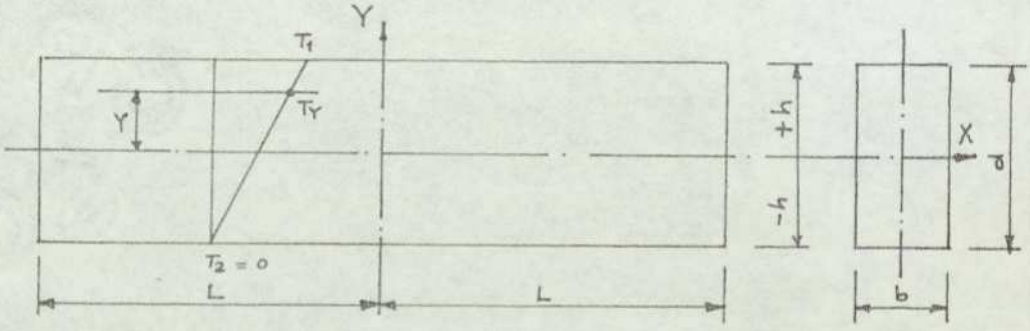

Fig 2.02741 Linear Temperature Distribution in a beam or plate

If, on the other hand, the edges are perfectly restrained against expansion and rotation, the stress induced by the heating is given by equations 2.02.706.

For instance if $T_2 = -T$, then from equation 2.02.708

$$T = T_1 \frac{Y}{h} \qquad \ldots \qquad 2.02.709$$

and equation 2.02.706 gives

$$\sigma_x = \sigma_z = -\frac{\alpha E}{1-U} \cdot T_1 \frac{Y}{h} \qquad \ldots \qquad 2.02.710$$

The Maximum stress is

$$(\sigma_x)_{max.} = (\sigma_z)_{max} = \frac{\alpha E T_1}{1-U} \qquad \ldots \qquad 2.02.711$$

If, $T_2 = o$

$$T = \frac{T_1}{2} + \frac{T_1}{2} \cdot \frac{Y}{h} \qquad \ldots \qquad 2.02.712$$

and again equation 2.02.706 gives

$$\sigma_Y = \sigma_z = -\frac{\alpha E}{1-U} \frac{T_1}{2} \left(1 + \frac{Y}{h}\right) \qquad \ldots \qquad 2.02.713$$

The maximum stress is

$$(\sigma_x)_{max.} = (\sigma_z)_{max.} = -\frac{\alpha E}{1-U} T_1 \qquad \ldots \qquad 2.02.714$$

It is seen that the stress is proportional to the coefficient of thermal expansion α, to the temperature difference T between the two faces of the plate, and to the modulus of elasticity E. The thickness h of the plate does not enter into the formula. However, in the case of a thicker plate a greater difference of temperature between the two surfaces usually exists. Therefore, it can be concluded that higher thermal stresses are to be expected in thick plates than in thin plates.

2.02.7.5 Curvilinear Temperature Distribution

If the temperature distribution is curvilinear (which is probably the most commonly occuring case in reality) then, for the purpose of the analysis, this can be 'resolved' into a linear part, and a curvilinear part with zero temperatures at the extreme fibres.

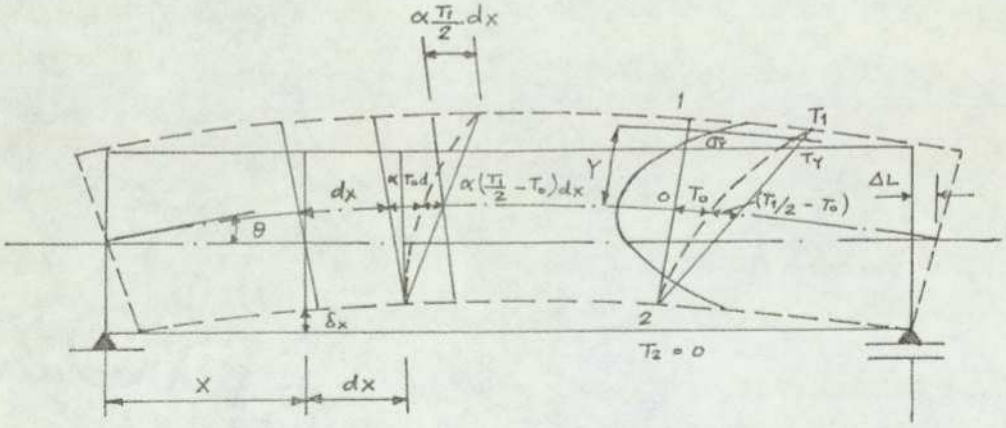

Fig 2.02751 Effect of Curvilinear Temperature Distribution on beam stresses and deformations

The first part, being a linear temperature, does not produce any stresses as can be seen by substitution of the function of the linear part of the temperature distribution into equation 2.02.704. However, linear temperature does produce deformations, which can be calculated as shown elsewhere in the text. The second part of the temperature (which may not be entirely symmetrical with respect to the neutral axis) can be assumed to result only in internal stresses, not affecting deformations by an appreciable amount. These stresses can be calculated from equation 2.02.702.

2.02.7.6 Effect of Temperature Change over a part of Cross-section of a Member

In practice, a temperature change may occur gradually over a part of the depth of the member (as specified in CP116). The partial distribution may be linear or curvilinear. However, for the purpose of analysis, a linear distribution over a part of the cross-section is assumed, as shown in Fig. 2.0276 Eqn. 2.02.704 cannot be used in this case since the temperature is not an even function of y. However, the analysis can be made as follows:-

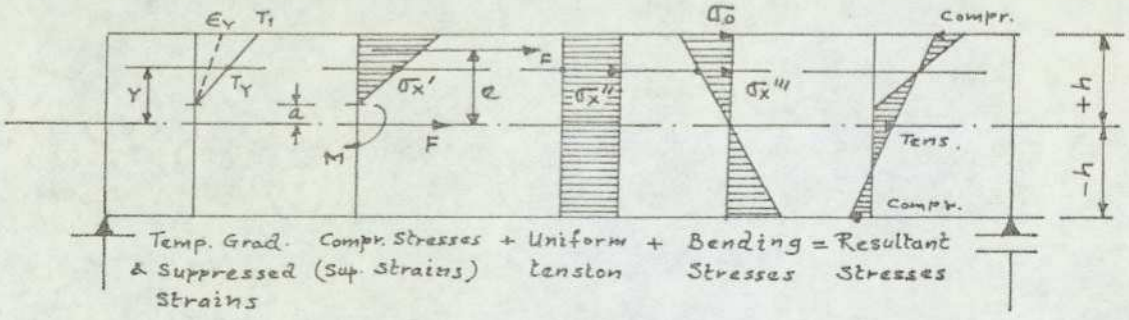

Fig 2.02761 Effect of temperature change over a part of cross-section of a member.

If a simply-supported beam is subjected to a linear temperature distribution over part of the cross-section, then, by completely suppressing strains, compressive stresses are induced of the value:

$$\sigma_x' = -\alpha E T_Y \quad \cdots \quad 2.02.715$$

and the resultant force is:

$$F = \alpha E T_1 \cdot \frac{1}{2}(h-a)b \quad \cdots \quad 2.02.716$$

This force is now applied in the opposite direction, and will, therefore, produce an average tension of the value:

$$\sigma_x'' = \frac{F}{2hb} = \frac{1}{4h} \alpha E T_1 (h-a) \quad \cdots \quad 2.02.717$$

as well as bending stress σ_o which can be calculated from the condition of equilibrium of moments as follows. The eccentricity of the force is:

$$e = a + \frac{2}{3}(h-a) = \frac{1}{3}(2h+a) \qquad \ldots \quad 2.02.718$$

and for equilibrium:

$$M = F.e = \frac{1}{2}\sigma_o\, bh \left\{\frac{2}{3}(2h)\right\} \qquad \ldots \quad 2.02.719$$

from which, by introducing the values of F and e

$$\sigma_o = \alpha E T_1 \frac{1}{4h^2}(h-a)(2h+a) \qquad \ldots \quad 2.02.720$$

and $$\sigma_x''' = \sigma_o \frac{Y}{h} \qquad \ldots \quad 2.02.721$$

The final stress is therefore:

$$\sigma_x = \sigma_x' + \sigma_x'' + \sigma_x'''$$

or $$\sigma_x = -\alpha E T_Y + \alpha E T_1 \frac{h-a}{4h}\left\{1+\left(2+\frac{a}{h}\right)\frac{Y}{h}\right\} \qquad \ldots \quad 2.02.722$$

The first term in this equation is valid only for the values of $+h > Y > a$

From eqn. 2.02.722

(a) For $a = +h$, $\sigma_x = o$ for all values of Y

(b) For $a = o$, $\sigma_x = -\alpha E T_Y + \frac{1}{2}\alpha E T_1 \left(\frac{1}{2} + \frac{Y}{h}\right)$

(c) For $a = -\frac{h}{2}$, $\sigma_x = \frac{3}{2}\alpha T_1 E\left(1+\frac{3}{2}\frac{Y}{h}\right) - \alpha E T_Y$
when $Y = o$, $T_Y = \frac{T_1}{3}$ and when $Y = -h$, $\alpha E T_Y = o$

(d) For $a = -h$, $\sigma_x = \alpha T_1 E (h+Y)/2h - \alpha E T_Y = 0$ for all values of Y
when $Y = o$, $T_Y = T_1/3$ and when $Y = -h$, $\alpha E T_Y = 0$

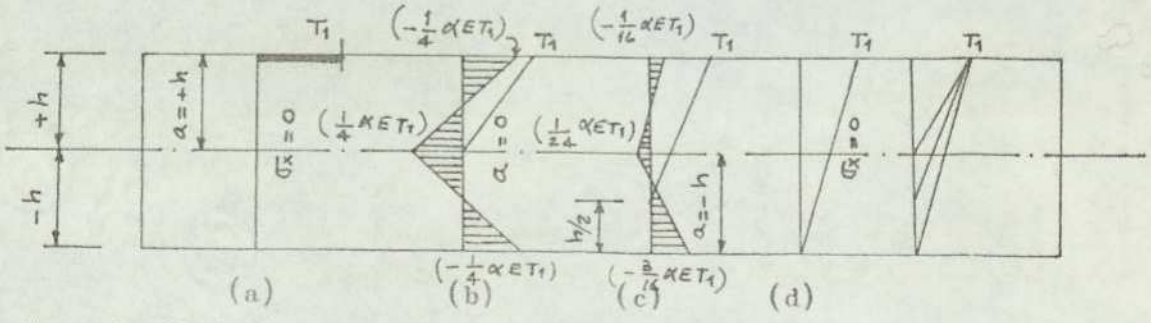

Fig. 2.02762 Variation of temperature stresses Vs depth of temperature penetration

2.03 REVIEW OF PREVIOUS WORK

A fair amount of theoretical and experimental research on (i) thermal stresses and deformations and (ii) thermal properties of materials, has been carried out by various researchers. However, it would appear that a greater concentration has been made towards the effects of elevated temperatures e.g. effects of fire. As for the effects of ambient temperature changes e.g. daily changes, many problems are still not fully resolved.

A cross-section review of some of the recent research work carried out to investigate the thermal effects which is relevant to this work is mentioned below:-

2.03.1 D. Campbell-Allen

D. Campbell-Allen (see "thermal Conductivity of Concrete" UDC 691.32.001:536.21) investigated the thermal conductivity of concrete made of three types of aggregates containing dolerite, haematite and barytes. The aim of this investigation was to relate the absorption and dissipation of heat to thermal conductivity. If this was known, then stresses and deformations could be determined analytically. However, this paper is concerned mainly with elevated temperatures as occur in nuclear power stations in hollow cylindrical shields. The parameters considered as affecting the thermal conductivity of concrete are: type of aggregate, moisture content of concrete, unit proportion, the type of cement used and the temperature of the concrete. The author has separated his experimental results into two groups, namely: the first relates the conductivity of the cement paste to that of the hydrated cement and to the percentage by volume of free water; the second relates the conductivity of concrete to the conductivity of the cement paste and the aggregate. It was shown that for atomic reactors, shielding

concrete should have a conductivity greater than 1 B.t.u./ft.h°F. It was concluded that although this can be generally achieved, the concrete must not be allowed to dry out excessively.

2.03.2 H.L. Malhotra

H.L. Malhotra (see "The Effect of Temperature on the Compressive Strength of Concrete" Department of Scientific and Industrial Research Fire Offices' Committee : Joint Fire Research Organisation) investigated the effect of temperature on the crushing strength of concrete using 2 in. diameter by 4 in. long specimens made with ordinary Portland cement, river sand and gravel aggregate, having various mix proportions and water/cement ratios. He found that (1) The effects of temperature on the crushing strength of concrete is independent of the water/cement ratio within the range normally used in its manufacture.

(2) The aggregate cement ratio has a significant effect on the strength of concrete exposed to high temperature, the proportional reduction being smaller for lean mixes than for rich mixes.

(3) Concrete under a compressive stress of the order of its design stress has a smaller proportional decrease in strength than if the stress were absent.

(4) The residual strength of heated concrete shows still further reduction in strength on cooling, being approximately 20% less than the corresponding hot strength in the temperature range 200 to 400°C for 1:4.5 and 1:6 mix concretes.

2.03.3 N.G. Zoldners

N.G. Zoldners (see "Effect of high temperatures on concretes incorporating different Aggregates" American Society for Testing and Materials, Vol.60, 1960) investigated the changes in physical properties of concrete beams and cylinders made with gravel, sandstone, limestone, and expanded slag aggregates after exposure to various temperatures ranging from 100 to 800°C.

Within the scope of the investigation, he concluded that Portland-cement concrete prepared with commercial aggregate deteriorates on exposure to dry heat at elevated temperatures. Extended deterioration of concrete is dependent to a large degree on the type of the aggregate.

Results showed evidence that flexural strength is more seriously affected by such exposure than compressive strength. The author summarised his results as follows:-

1) Concrete made with gravel, consisting predominantly of crystalline igneous and metamorphic rock, deteriorated more rapidly than limestone concrete. After 400°C exposure, the residual flexural strength of gravel concrete was only 26 per cent and the compressive strength only 85 per cent of the original strength.
2) Sandstone concrete showed a significant compressive strength gain in the lower temperature ranges. Above 500°C it deteriorated, losing strength rapidly.
3) Limestone concrete performed best of the four concretes investigated, after being exposed to temperatures up to 700°C.

4) Expanded slag concrete was strong in compression, retaining 71 per cent of its original strength after exposure at 600°C, but it retained only 16 per cent of its flexural strength after exposure to 400°C.

2.03.4 Barry P. Hughes

Barry P. Hughes (see "Temperature rises in low-heat cement concrete", Journal of the Structural Division of American Society of Civil Engineers) monitored the temperature rise due to the heat of hydration of cement in the 7'6" thick concrete of the foundation raft of an office block known as ATV Paradise Centre. The required crushing strength of concrete was 6,000 psi at 28 days. The raft was to be concreted in the summer when the ambient temperature could exceed 24°C. Furthermore, neither an interruption of the concreting programme nor the installation of cooling water pipes were considered to be practical propositions because of their cost. In order to control the temperature rise, the following steps were taken:-

(1) the use of low-heat Portland-cement,
(2) placing of additional reinforcements in the raft,
(3) flooding the surface of each bay with water as soon as possible after casting,
(4) casting the concrete in two lifts instead of a single lift, and
(5) dividing the raft into 14 bays and casting alternate bays.

The author's "most startling observation", even though low-heat Portland-cement was used, was the rapid temperature rise which occurred in the first 24 hours after placing the concrete. The

maximum temperature rise predicted for a conventional low-heat Portland-cement was about 26°C compared with an actual recorded value of 47°C, showing that the cement was not quite what it was claimed to be.

Some of the bays which were concreted in single lifts developed cracks up to 1.2mm wide and generally about 0.5mm wide. The two-lift bays also had additional reinforcement which not only reduced the average widths of the cracks still further, but also eliminated local slumping of the concrete over large diameter bars.

In spite of all the precautions taken, cracking of concrete still occurred. However, the excessive temperature rises causing the excess cracking were reduced. The author is of the opinion that a better control of temperature rise and surface cracking could have been achieved if a truly low-heat Portland-cement had been used.

2.03.5 A.K. Kar

A.K. Kar (see "Thermal Effects in Concrete Members" Ebasco Services, Inc., 21 West Street, New York, N.Y. 10006, U.S.A.) developed a method of analysis for individual concrete members having uniform capacities along their lengths, and subjected to differential (different at two faces) temperature. The method of analysis is consistant with the requirements of ultimate strength design.

The author states that unlike gravity and some other loadings for which the use of relative stiffness is adequate, dynamic and thermal loadings are directly related to the actual member stiffness. He makes recommendations for determining the average effective member stiffness, which lies between the stiffness corresponding to the cracked (i.e. at ultimate condition) and the uncracked sections.

The author claims that the method of analysis presented greatly reduces the computational efforts for determining thermal effects in concrete members.

2.03.6 K.W. Nasser and R.P. Lohtia

K.W. Nasser and R.P. Lohtia (see "Mass Concrete Properties at High Temperatures") performed tests on mass concrete cylinders for over 6 months at temperatures of 35 to 450°F. Two types of initial curing were used: some cylinders were exposed to the different temperatures at 1 day while others were heated from 14 days onwards. The strength and elastic properties of the concrete were determined at several intervals during 6 months.

Based on the test results and the available information related to the subject, Nasser and Lohtia concluded the following:-

1. Strength and elasticity beyond about 2 weeks are independent of both mass and water curing conditions in the temperature range of 35 to 205°F (1.7 to 96°C).
2. Both strength and elasticity are lower at 35°F (1.7°C) than those at 70°F (21.4°C) up to about 6 weeks, but thereafter they are the same as those at 70 and 160°F (21.4 and 71°C).
3. Beyond the minimum age of about 2 weeks, strength and elasticity are independent of temperature of curing between 70 to about 200°F (21.4 and 93°C).
4. In the temperature range of 200 to 450°F (93 to 232°C), both strength and elasticity are adversely affected by temperature and the degree of deterioration increases, both with temperature and age of curing.

5. The effect of temperature on strength and elasticity is independent of both 1 and 14 day initial curing periods at 400 and 450°F (205 and 232°C). However, at lower temperatures, the specimens initially cured for 14 days show in general better resistance to temperature than the 1 day cured specimens.
6. Although strength and elasticity show about the same temperature dependence, elasticity is more severely reduced at temperatures beyond about 200°F (93°C).
7. The deterioration in the properties of mass concrete at temperatures higher than about 200°F (93°C) is possibly due to the change of original highly cementitious tobermorite gel into weak and crystalline phases of poor cementing qualities.
8. The loss in strength and elasticity after 6 months of exposure to 450°F (232°C) is respectively about 50 and 68 per cent.

CHAPTER THREE

3.00 EXPERIMENTAL VERIFICATIONS OF THERMAL RESPONSE AND PROPERTIES OF CONCRETE

3.01 INTRODUCTION

In this section, experiments were conducted on (i) a block of normal grade concrete, (ii) micro-concrete beams and (iii) cubes and cylinders made from various mixes of concrete.

The objects of these tests were to obtain experimental data related to the thermal response and properties of concrete such as:

1. time-temperature relationship
2. temperature-distance relationship
3. time lag
4. attenuation of temperature
5. the effect of temperature on E value of concrete
6. the effect on strength of concrete at ambient temperature changes, &
7. to evaluate the coefficient of linear expansion

These data could then be used in the analysis of a structure i.e. to predict the distribution of stresses and deformations arising from temperature changes. No effort was made to check thermal conductivity and Poisson's ratio of concrete.

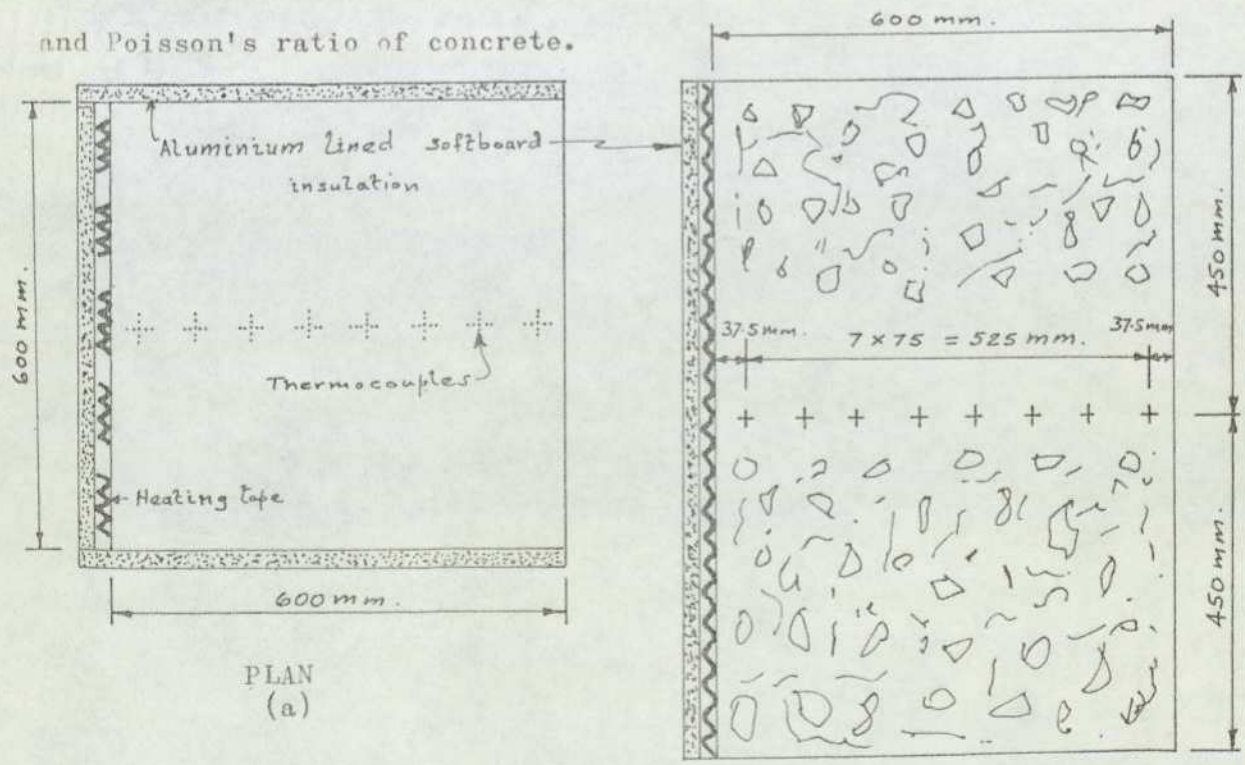

Fig. 3.011 Plan and Sectional Elevation of Model Concrete Block

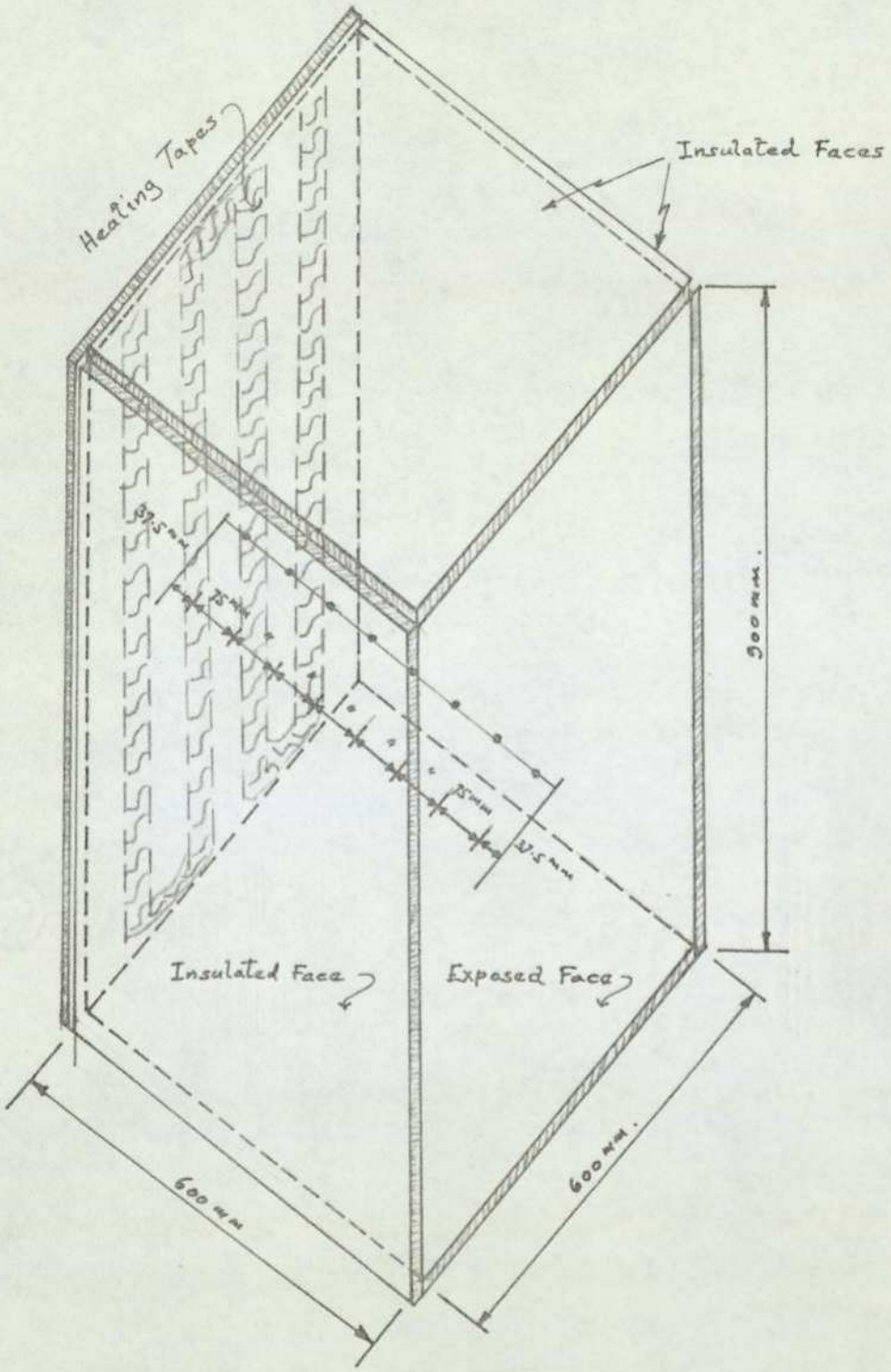

Fig. 3.012 Model Concrete Block Showing positions of Thermocouples

3.02 SECTION A: EXPERIMENT ON CONCRETE BLOCK

(Experiment 1)

3.02.1 Investigation of Thermal Response of Concrete

To investigate the above-mentioned thermal properties, a concrete block of dimensions shown in Fig. 3.012 was cast from normal grade 25 mass concrete. Before casting 8 Nos. thermocouples were positioned along the central axis of the block. The concrete block was cured by keeping it wet for 14 days. However, the actual experiment was conducted about 2½ months after casting. It was considered reasonable to assume that by this time most of the free water would have evaporated and large proportion of the shrinkage would have taken place.

3.02.1.1 Heat Input

Several methods were considered for applying heat to the block, namely

(a) Internal heating using heating coils built into the structure,

(b) A purpose-made mat, and

(c) Heating tape

Following preliminary investigations, heating tape was selected as the means of applying heat to the surface mainly for reasons of economy and ease of use for the experiment also it fulfilled the basic requirements (1) that heat output should be adjustable and (2) that there should be the capacity for the supply of enough heat to create satisfactory temperature gradient in the concrete block.

Basically, heating tape is a continuous network of wires enclosed in knitted flexible threads of fibre glass, heat output is adjustable according to the length of tape used and the supply voltage. Variations in heat output could therefore be obtained by varying the length of tape used and the supply voltage, either separately or in conjunction with each other.

Heating tape was applied on one face of the block as indicated in Fig. 3.012. Insulation softboard 12mm thick and lined with aluminium foil was applied on the outside to stop heat loss from the tape to the atmosphere. Similarly insulating softboard lined with aluminium foil was applied to the 4 adjacent faces of the block. The opposite face to the heated face was left open to the atmosphere so that a flow of heat could take place from one face to the opposite face.

The heating of the concrete block was provided through a VARIAC DURATRAK Type V6 HMT INPUT 230V 50 ~ OUTPUT 0 < 270V 3A (Range 0 to 268 volts) and an Ampere Meter (reading up to a maximum of 5 amperes.

3.02.1.2 Thermocouples

The measurement of temperature along the centre of the concrete block was carried out by means of 8 thermocouples embeded in the concrete block and connected to a direct reading temperature indicator "Resilia" instrument through a 24 station multi-switch. The "Resilia" was also fitted with a mercury thermometer. A separate alcohol thermometer was used to compare the room temperature with that shown by the "Resilia" thermometer.

Thermocouples were used because they offered the best mode for measurement of internal temperatures. This is due to the fact that one end can be made as a hot junction and the other as a cold junction. The connections could be made either by using copper-constantan wires or iron wires. Using copper-constantan wires, direct readings could be obtained whereas calibration was necessary with iron wires. In this case copper-constantan wires were available.

DATE	TIME	APPLIED VOLTAGE (VOLTS)	APPLIED AMPERAGE (AMPS)	AMBIENT ROOM TEMP. (^{o}C)	THERMOCOUPLE READINGS ^{o}C							
					T1	T2	T3	T4	T5	T6	T7	T8
21.3.77	10.48	0	0	20.00	20.00	20.00	20.00	20.00	20.00	20.00	20.00	20.00
	13.10	100	0.75	20.80	24.50	23.80	22.20	21.80	21.20	20.40	20.20	20.10
	15.15	100	0.70	21.00	26.75	24.50	23.00	22.00	21.20	20.50	20.20	20.10
	15.25	100	0.70	21.20	26.70	24.50	22.80	21.80	21.00	20.50	20.20	20.10
	17.05	100	0.70	21.20	27.50	25.50	23.50	21.80	21.50	20.60	20.40	20.20
22.3.77	10.10	100	0.70	21.00	34.20	31.50	29.20	27.00	25.20	24.10	23.50	22.20
	12.15	100	0.70	21.00	34.20	32.10	29.50	27.00	25.50	24.20	23.50	22.50
	14.00	100	0.70	21.20	34.20	32.10	29.50	27.20	25.50	24.20	23.50	22.50
	17.00	100	0.70	21.20	34.20	32.10	29.50	27.20	25.50	24.20	23.50	22.50
POWER SWITCHED OFF OVERNIGHT												
23.3.77	9.50	200	1.20	20.80	21.00	21.00	21.00	21.00	20.50	20.00	20.00	19.80
	12.25	200	1.10	21.00	34.50	28.00	23.60	21.80	20.50	20.00	19.80	19.00
	14.05	200	1.10	21.00	40.00	32.10	26.20	23.30	21.20	20.20	19.80	19.00
	16.25	200	1.10	21.10	44.00	36.00	29.50	25.00	22.00	20.50	19.90	19.00
24.3.77	10.00	200	1.10	21.20	59.50	51.50	44.00	38.00	32.20	28.50	26.00	23.80
	12.30	200	1.10	21.20	60.00	52.20	22.80	38.50	32.80	29.00	26.20	23.90
	14.30	200	1.10	21.40	60.20	52.80	45.50	38.20	33.50	29.90	26.60	24.00
	17.45	200	1.10	21.40	60.80	53.50	46.10	40.00	34.20	30.40	27.50	24.60
25.3.77	10.30	200	1.08	21.40	65.80	58.20	50.80	44.70	38.50	34.20	20.80	27.50
	12.37	200	1.08	21.60	65.80	58.20	50.80	44.50	38.50	34.20	30.80	27.50
	14.15	200	1.08	21.70	65.80	58.20	50.20	44.50	38.50	34.20	30.80	27.50
	16.30	200	1.08	22.00	65.80	58.00	50.50	44.50	38.50	34.00	30.50	27.30
POWER SWITCHED OFF OVER WEEKEND												
28.3.77	9.50	240	1.30	19.50	21.50	21.70	21.80	21.80	21.50	21.50	21.00	21.50
	11.45	240	1.21	19.25	38.00	27.70	24.20	22.70	22.20	21.80	21.50	20.50
	13.30	240	1.21	19.50	45.30	34.30	27.50	24.00	22.20	21.80	20.50	20.20
	15.30	240	1.20	19.50	51.00	40.00	32.00	26.80	23.60	22.10	21.00	20.50
	16.35	240	1.20	19.70	52.80	42.00	33.50	27.80	24.00	22.10	21.00	20.20
29.3.77	10.00	240	1.19	19.30	71.80	61.70	52.20	44.20	37.50	33.20	29.80	26.30
	11.45	240	1.19	19.30	72.50	62.40	53.40	45.50	38.30	33.80	30.20	27.20
	14.30	240	1.19	18.70	75.90	65.60	56.40	48.50	41.50	36.80	32.80	29.50
	16.40	240	1.19	19.00	75.90	65.70	56.50	48.80	41.50	36.80	32.80	29.50
30.3.77	10.00	240	1.18	19.50	80.20	70.00	61.00	53.40	45.80	40.20	36.20	31.90
	12.35	240	1.18	19.90	80.40	70.00	61.00	53.40	45.80	40.20	36.00	31.80
	16.00	240	1.18	20.20	80.50	70.00	60.80	53.20	45.80	40.20	36.00	31.60

Table: 300.01

The initial readings of all the thermocouples and the ambient room temperature were noted. The voltage was then set to 100 volts and the current switched on. From this stage onwards periodic readings, at intervals of 2 to 3 hours, were taken of all the thermocouples and the time noted. The power supply was continued overnight and the following day until the readings of the thermocouples stabilised. At this stage it was assumed that "a steady state of heat conduction", i.e. when the amount of heat absorbed is equal to the amount of heat dissipated, was reached.

The power was then switched off overnight to allow the concrete block to cool down to the ambient temperature. The experiment was continued the following day, but with the voltage increased to 200 volts. The same procedure as with applied voltage at 100 volts was repeated. However, this time it took 3 days for steady state of heat conduction to be achieved.

Once again, the power was switched off overnight to allow the concrete block to cool down. The experiment was then continued for the third time with the applied voltage increased further to 240 volts.

The results of the experiment are shown in Table: (300.01). From these results, the relationships of (i) Time against Temperature at any particular point in the concrete block and (ii) Temperature against Distance within the concrete block i.e. variation of temperature inside the block were plotted. These relationships are shown in Figs. 3.0211, 3.0212, 3.0213, 3.0214, 3.0215 and 3.0216.

THE VARIATION OF TEMPERATURE WITH TIME

AT EACH THERMOCOUPLE

(APPLIED VOLTAGE = 100 VOLTS)

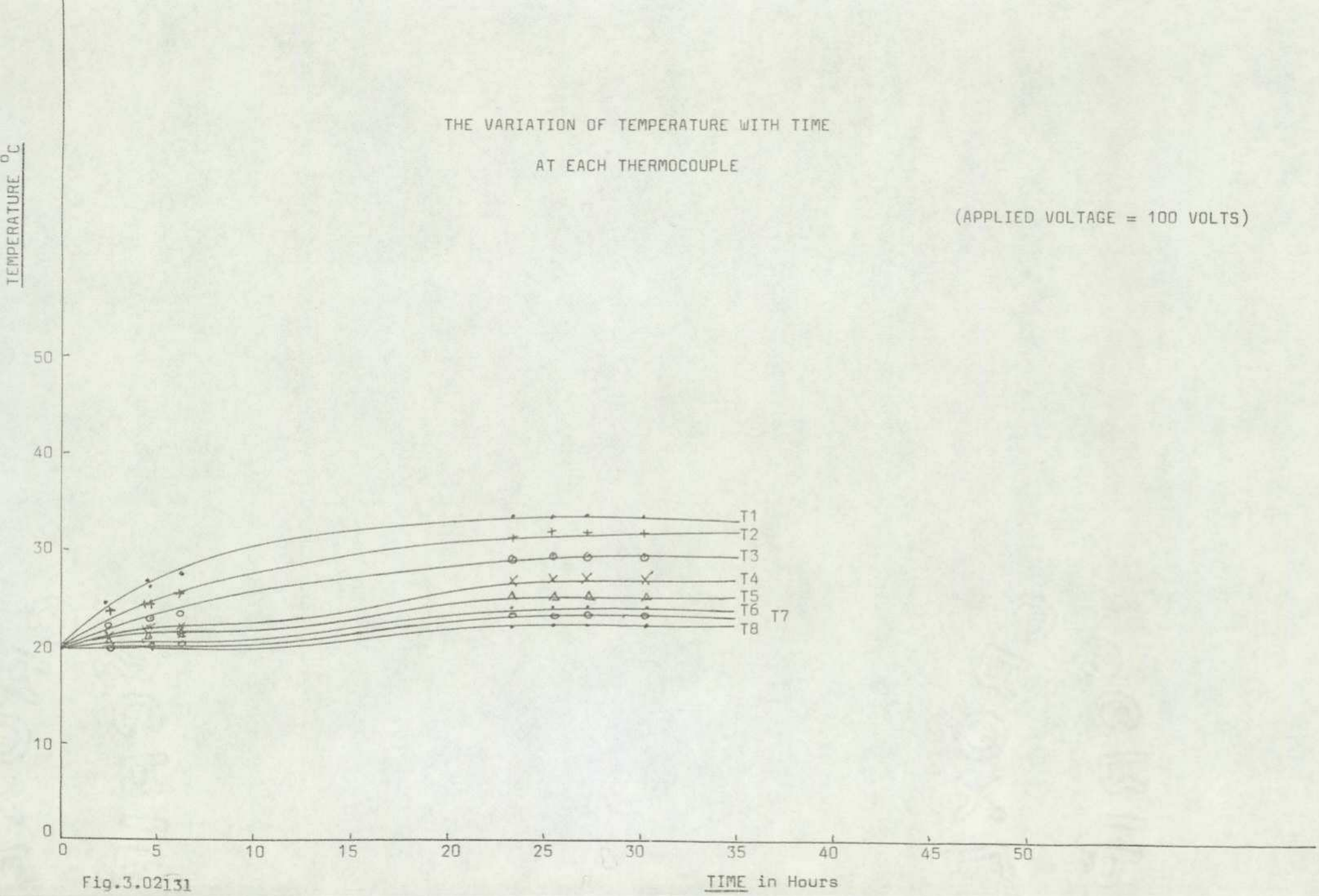

Fig.3.02131

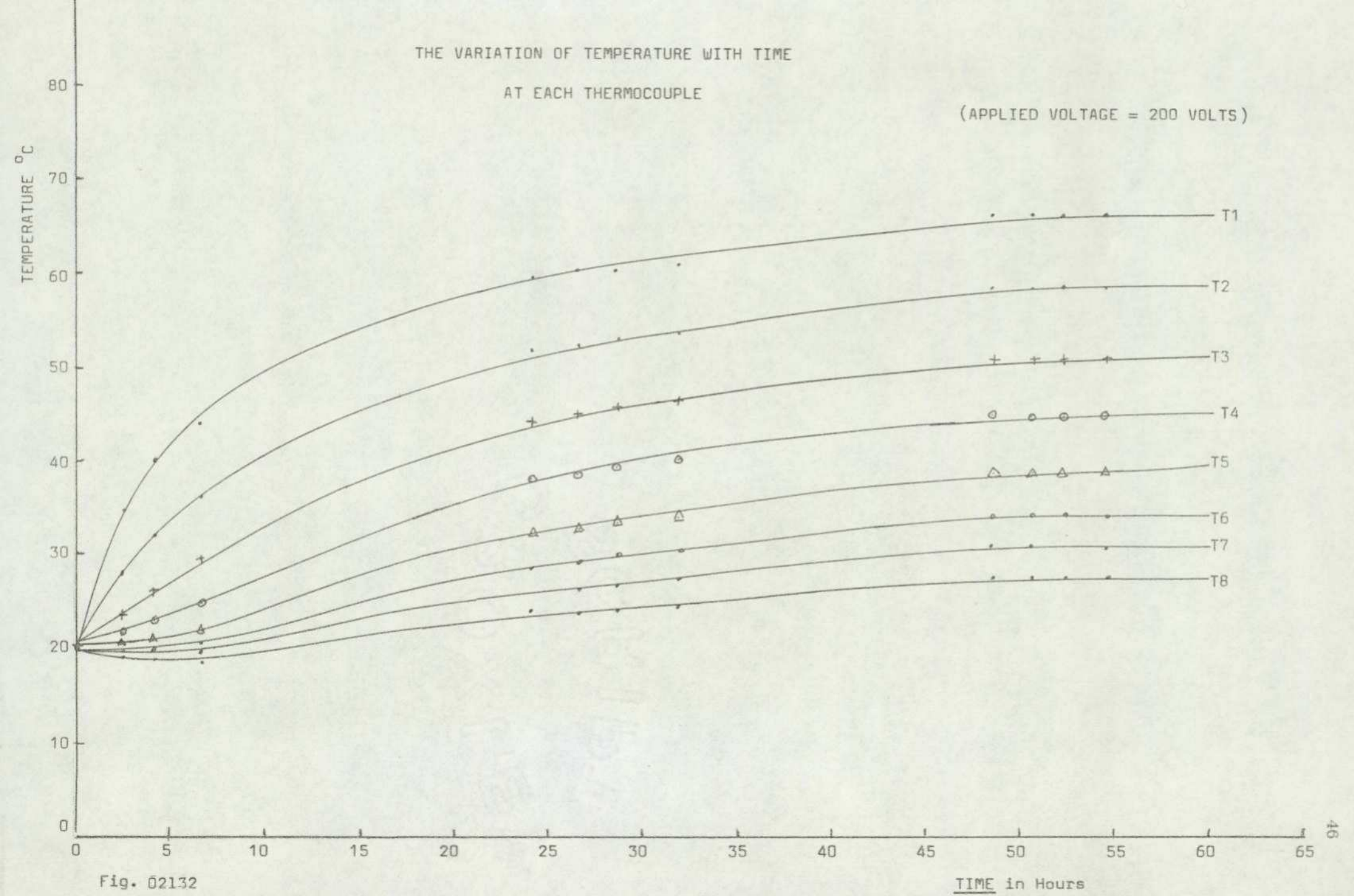
THE VARIATION OF TEMPERATURE WITH TIME
AT EACH THERMOCOUPLE
(APPLIED VOLTAGE = 200 VOLTS)
TEMPERATURE °C
0
10
20
30
40
50
60
70
80
T1
T2
T3
T4
T5
T6
T7
T8
0
5
10
15
20
25
30
35
40
45
50
55
60
65
TIME in Hours

Fig. 02132

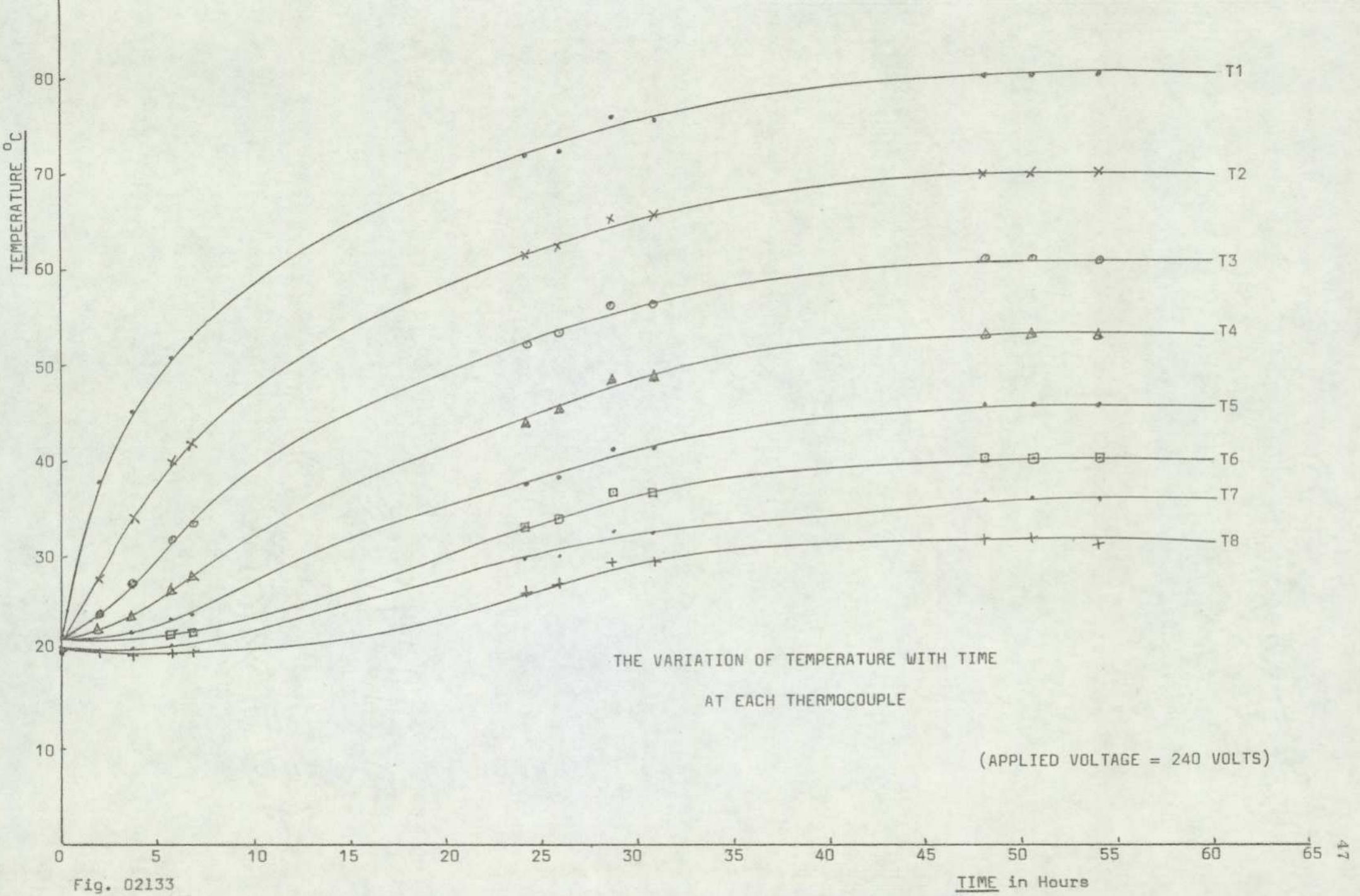
TEMPERATURE °C
80
70
60
50
40
30
20
10
T1
T2
T3
T4
T5
T6
T7
T8
THE VARIATION OF TEMPERATURE WITH TIME
AT EACH THERMOCOUPLE
(APPLIED VOLTAGE = 240 VOLTS)
0
5
10
15
20
25
30
35
40
45
50
55
60
65
TIME in Hours

Fig. 02133

PENETRATION OF APPLIED TEMPERATURE AT VARIOUS

TIME INTERVALS FOR NORMAL DENSITY CONCRETE

(APPLIED VOLTAGE = 100 VOLTS)

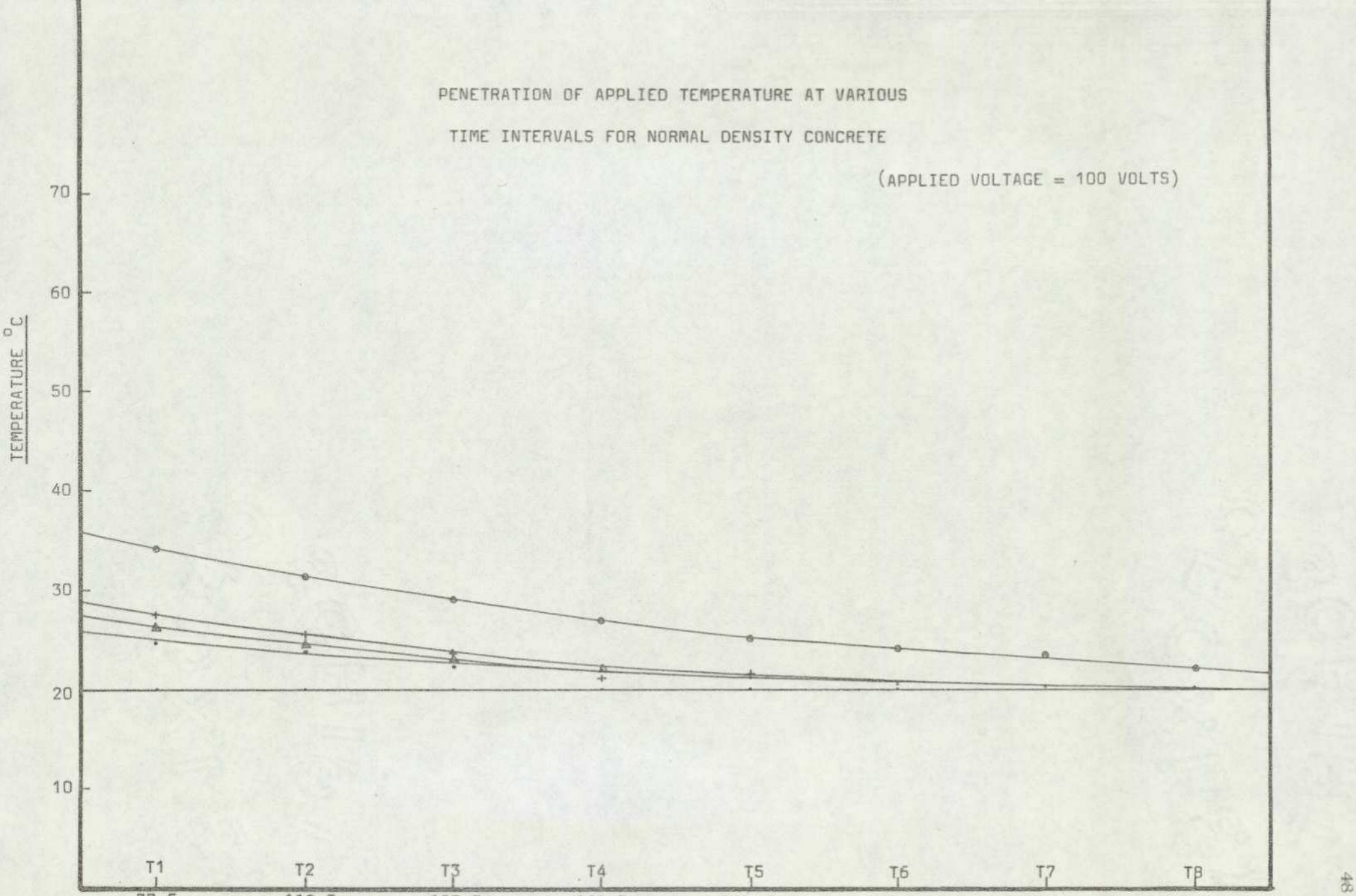

Fig. 02134

LOCATIONS OF THERMOCOUPLES - DISTANCE FROM HEATED SURFACE

PENETRATION OF APPLIED TEMPERATURE AT VARIOUS

TIME INTERVALS FOR NORMAL DENSITY CONCRETE

(APPLIED VOLTAGE = 200 VOLTS)

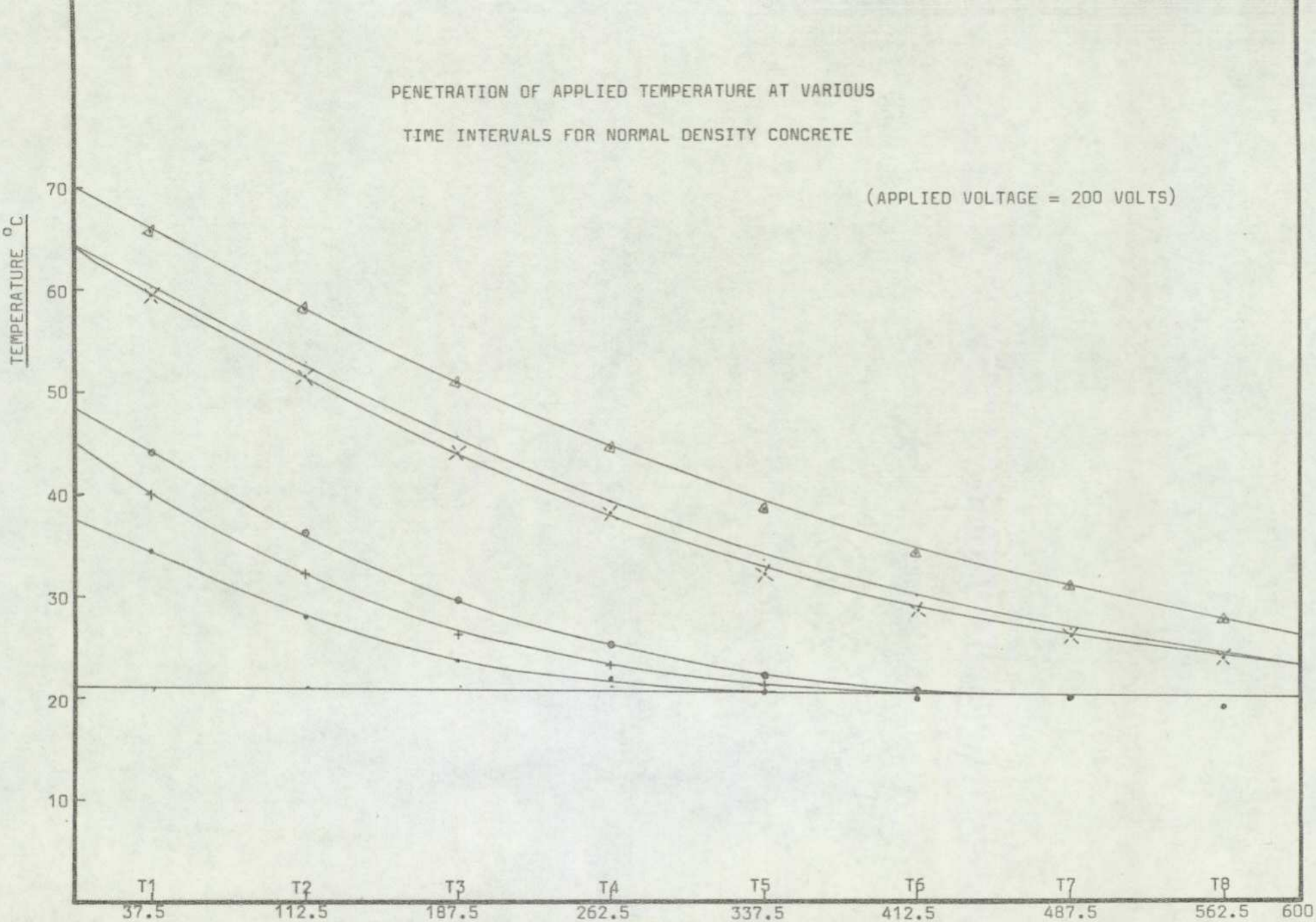

Fig. 3.02135

LOCATIONS OF THERMOCOUPLES - DISTANCE FROM HEATED SURFACE

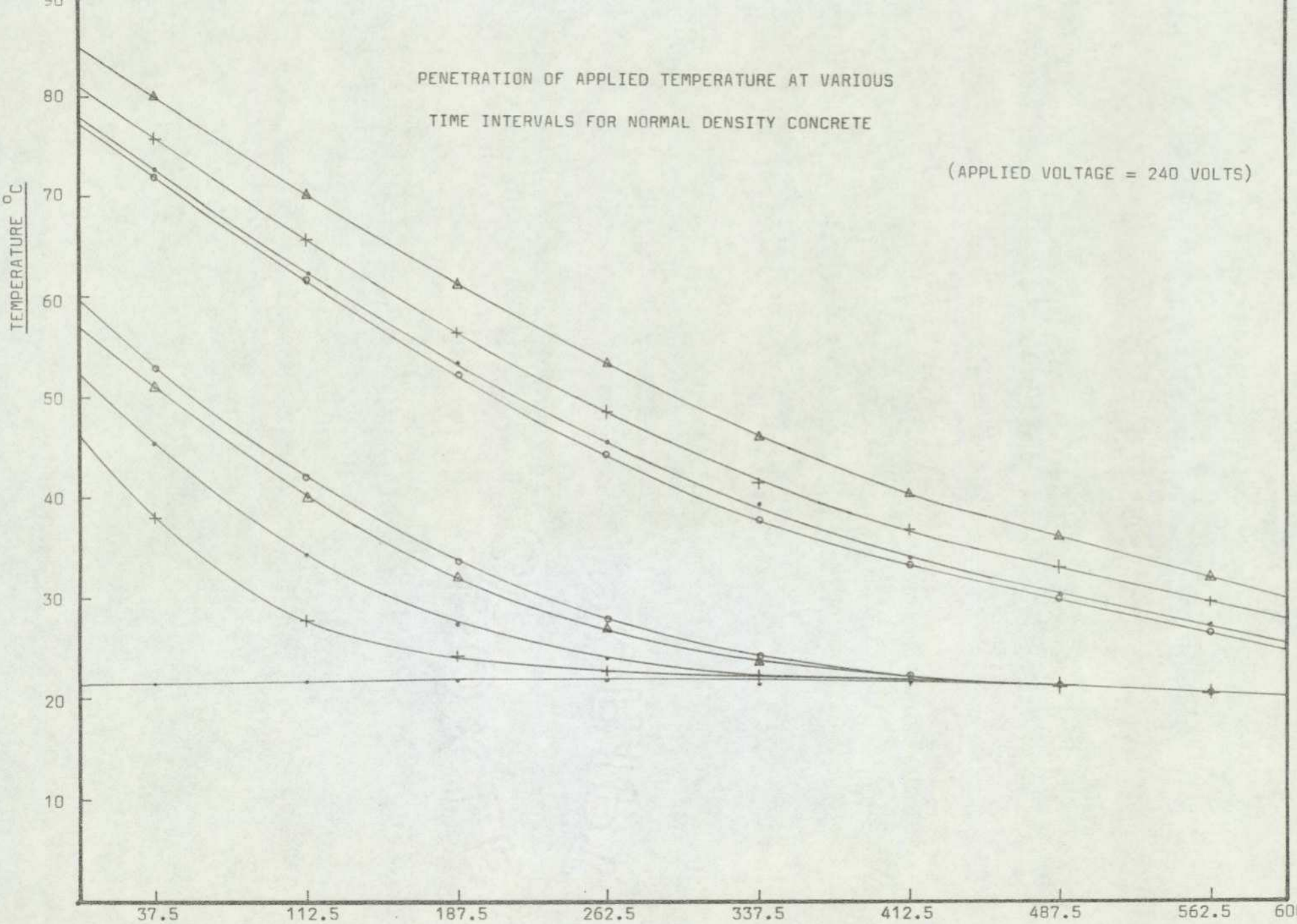
PENETRATION OF APPLIED TEMPERATURE AT VARIOUS
TIME INTERVALS FOR NORMAL DENSITY CONCRETE
(APPLIED VOLTAGE = 240 VOLTS)
TEMPERATURE °C
80
70
60
50
40
30
20
10
37.5
112.5
187.5
262.5
337.5
412.5
487.5
562.5
600
mm
LOCATIONS OF THERMOCOUPLES - DISTANCE FROM HEATED SURFACE

Fig. 3.02136

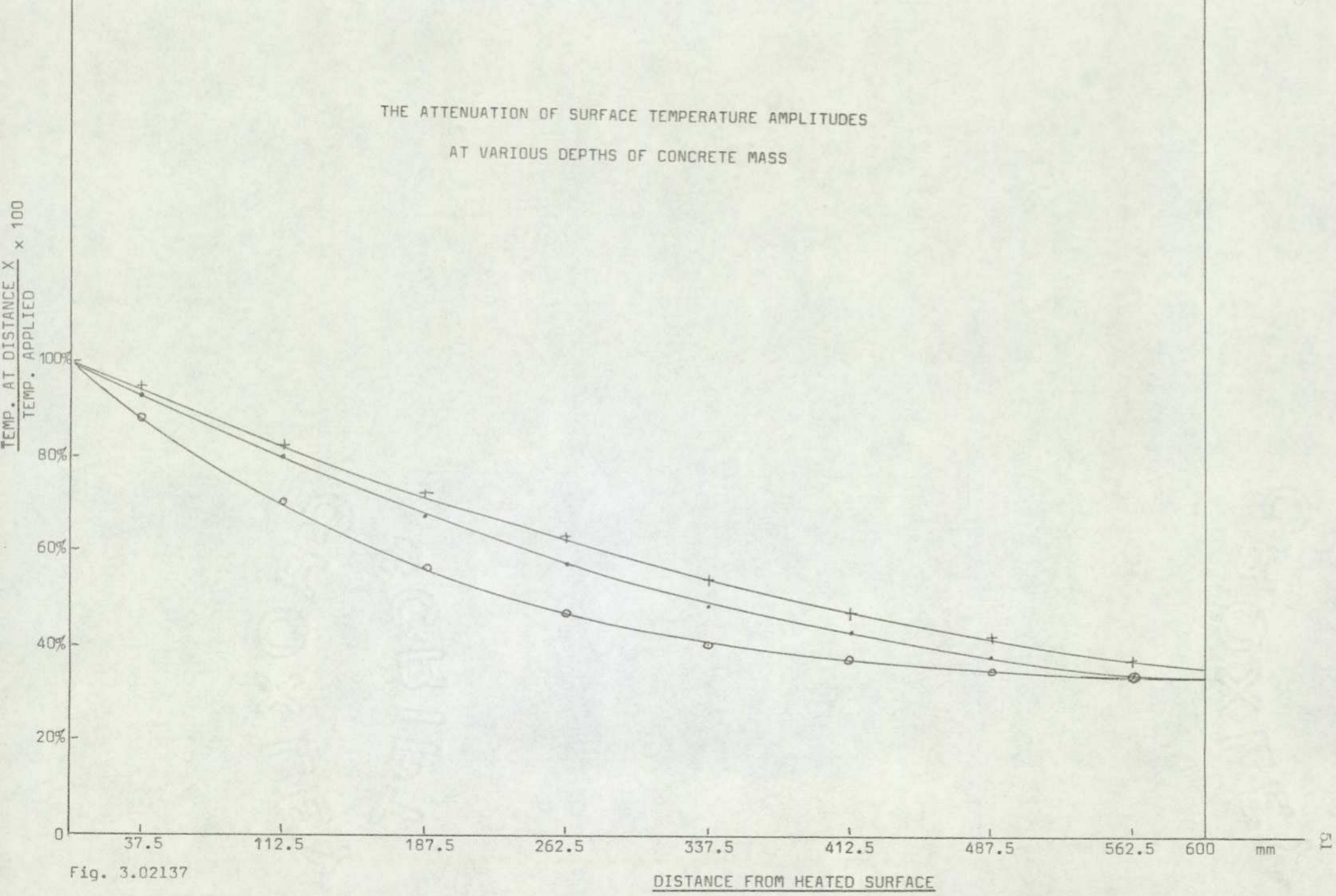
THE ATTENUATION OF SURFACE TEMPERATURE AMPLITUDES
AT VARIOUS DEPTHS OF CONCRETE MASS
TEMP. AT DISTANCE X / TEMP. APPLIED x 100
100%
80%
60%
40%
20%
0
37.5
112.5
187.5
262.5
337.5
412.5
487.5
562.5
600
mm
DISTANCE FROM HEATED SURFACE

Fig. 3.02137

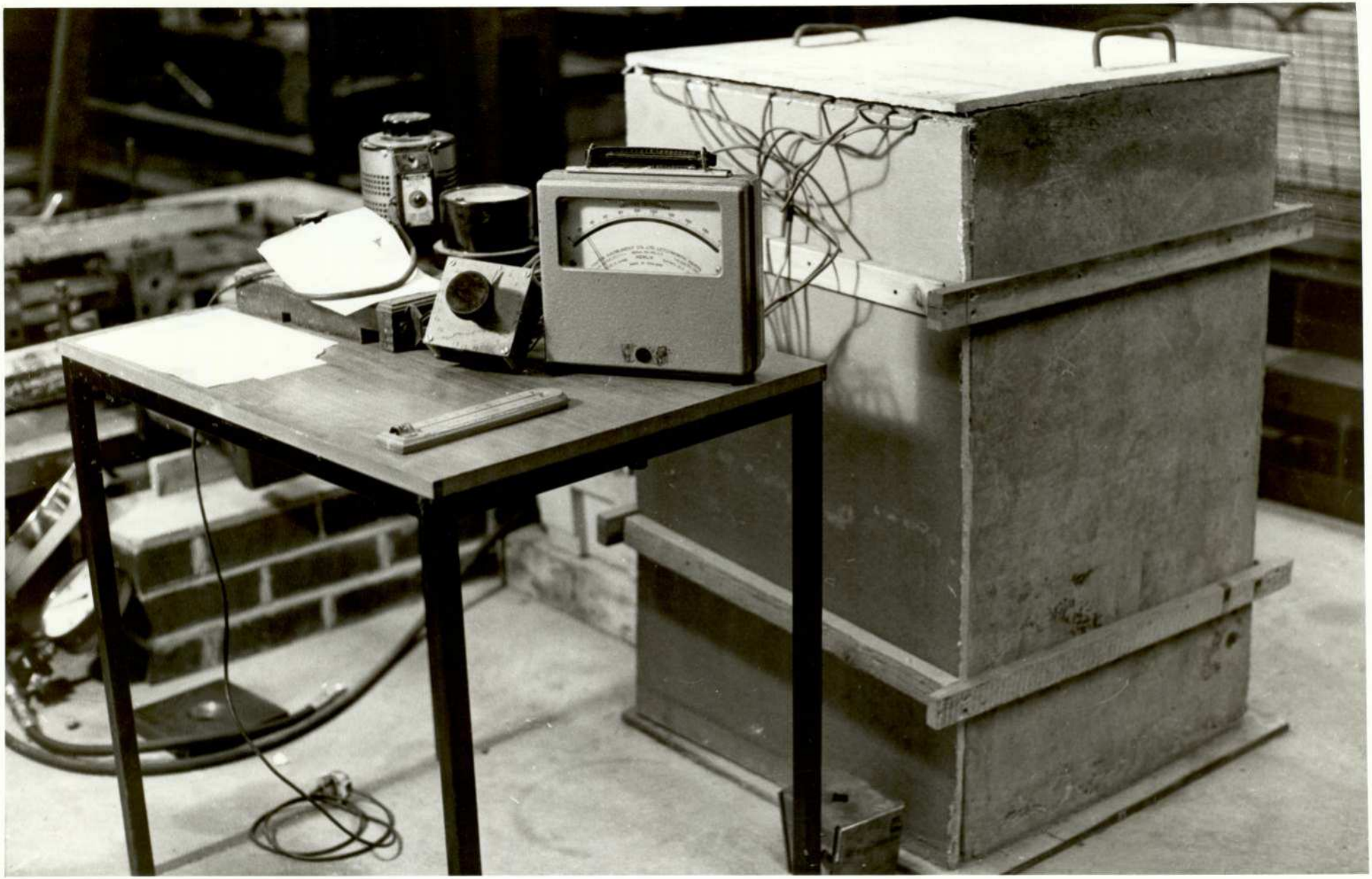

PLATE: 1 Model Concrete Block under test for thermal response of concrete.

From the results of the above experiment a further relationship of attenuation of surface temperature with depth in the concrete block was plotted and is shown in Fig. 3.0217.

3.02.1.4 Discussion of Experimental Results for Thermal Response of Concrete

The experiment was conducted for 3 different ranges of applied heat, so as to assess the thermal response of concrete.

The first experiment was conducted with a rather low applied voltage (100 volts) i.e. low applied heat. The maximum temperature reached just inside the applied face was only 22.50°C as compared to the ambient room temperature of 21.20°C. Graphs of Fig. 3.0211 show that for low range of applied heat the temperature variation in the concrete is almost linear. The graphs (Fig. 3.0214) of "Time" against "Temperature" at any point in the concrete show that "steady state of heat conduction" is reached very quickly.

The second experiment was conducted with an applied voltage of 200 volts. The maximum temperature reached just inside the applied face was 65.80°C and the minimum temperature just inside the opposite face was 27.30°C as compared to ambient room temperature of 22.00°C. The graphs of "temperature" against "distance from heated surface" (Fig. 3.0215) show that the gradients of temperature variation achieved are considerably pronounced as compared to the first experiment and the variation is curvilinear. An important observation that can be made from these graphs is that during the early part of heat application the variations are very

much more curvilinear than at a later stage and the conduction of heat is similar to a case of suddenly applied temperature. The relationship of "Time" against "Temperature" (Fig. 3.0212) shows that a "steady state of heat conduction" takes considerably longer time. These graphs also demonstrate the phenomena of time lag, i.e. the elapse of time required for the concrete to respond to the temperature change.

The third experiment was conducted with an applied voltage of 240 volts. The difference between the heat input for this case and in the case of the second experiment was relatively small. The maximum and minimum temperatures reached were 80.50°C and 31.6°C respectively as compared to an ambient room temperature of 20.20°C. As can be expected the results shown in graphs of Figs. 3.0213 and 3.0216 are similar to those of the second experiment, confirming that the results are correct.

The graphs shown in Fig. 3.0217 show "the attenuation of surface temperature amplitudes at various depths of concrete mass". The applied temperature at the surface is based on an approximate assessment deduced from the projections of curves for "temperature" against "distance from heated surface". However, in spite of the approximation the attenuation curves are similar with those obtained by other researchers.

3.03.1 Thermal Conductivity

Experiments have shown that when the steady state of temperature has been reached, the quantity of heat 'Q', which flows between two surfaces in a given time, is proportional to the difference of temperature at the surfaces and is given by the following relationship:-

$$Q = \frac{k\,(To - Tl)\,st}{d}$$

where To and Tl are the temperatures of the lower and upper surfaces of the solid in ^{o}C

s is the cross-sectional area of solid under consideration

t time in seconds for which the flow of heat is considered

d thickness in cms. of solid, and

k is the Thermal Conductivity of the substance, depending upon the material of which it is made.

Rewriting the above equation, the Thermal Conductivity is given by

$$k = \frac{Qd}{(To - Tl)\,st}$$

The units of k are cal/(sec)(cm^2)(^{o}C/cm) in the c.g.s. system or B.t.u./(hr.)(ft^2)(^{o}F/ft) in the British system. The reciprocal of the Thermal Conductivity of a substance is called its Thermal Resistivity.

In the above relationship, the solid is assumed to be homogeneous and of such a material that, when a point within it is heated, the heat flows uniformly in all directions. Such a solid is said to be isotropic, as opposed to crystalline and anisotropic solids, in which certain directions are more favourable for the conduction of heat than others.

The thermal conductivity of a material is a property of its atomic structure, and can be deduced from considerations of solid-state physics. However, these theories are not directly applicable to concrete which is heterogeneous. The conductivity of concrete is

determined by the conductivity of its constituents, and the major factors influencing the conductivity are:-

the moisture content of the concrete;

the type of aggregate;

the mix proportions;

the type of cement and

the temperature of the concrete.

The actual determination of the Thermal Conductivity of concrete is outside the scope of this work as its determination is more appropriate to Physics or Chemistry than to a civil/structural laboratory. However, the following table, taken from a paper by N.G. Zolders (ref.13), gives the values of Thermal Conductivity for concretes made from different types of aggregates.

Type of Concrete Aggregate	THERMAL CONDUCTIVITY			Room-dry concrete Density, lb per cu ft	Mean Specific Heat 25 to 400°C Btu per lb per deg. Fahr.	Heat Diffusivity, sq.ft. per hr.
	MEAN TEMPERATURE		Coefficient k, Btu in per hr. sq.ft. deg. Fahr.			
	deg.Cent.	deg.Fahr.				
Gravel	100	212	10.60			0.032
	164	327	10.60	143.9	0.229	
	402	756	8.95			0.027
Limestone	164	327	6.75	142.8	0.236	0.020
	394	740	8.04			0.024
Sandstone	95	202	15.80			0.050
	169	336	15.75	136.9	0.233	
	406	763	10.64			0.033
Expanded Slag	182	359	3.51	96.5	0.222	0.016
	398	749	3.45			

Table: 300.02

The Thermal Conductivities of some common materials taken from (ref.14) are as follows:-

Material	Thermal Conductivity B.t.u./ft.^{2}h. ^oF
Basalt	0.8
Diorite	1.3
Granite	2.0
Quartzite	1.8 to 3.1
Shale	0.5
Limestone	0.5 to 1.5
Mercury	3.6
Cast Iron	26
Mild Steel	35
Copper	221
Pure Water	0.35
Impure Water	0.3

Table: 300.03

It is seen from the tables above that the Thermal Conductivity of various materials differs considerably, and also that the Thermal Conductivity of concrete depends greatly on the type of aggregate used. It is therefore reasonable to assume that the level of thermal stresses induced in any concrete structure will depend very much on the types of material constituents used.

3.03.2 Poisson's Ratio

The ratio of the lateral strain to the longitudinal strain is defined as Poisson's ratio. If a specimen is subjected to a longitudinal stress there will be a strain in this direction equal to σ/E. There will also be a strain in all directions at right angles to the stress. It is found that for an elastic material the lateral strain is proportional to the longitudinal strain, and is of the opposite type.

The ratio

$$U = \frac{\text{lateral strain}}{\text{longitudinal strain}}$$

produced by a single stress is the Poisson's ratio. Although concrete is not truly elastic, it is usually assumed to be elastic for design purposes, and the effect of Poisson's ratio is being taken into account in some forms of structures. This property is assumed to be constant at ambient temperatures. However, it is not fully resolved whether the value of Poisson's ratio undergoes any significant change at various temperature levels, and whether thermal ratio differs from the values used for loads. The determination of Poisson's ratio itself and its change with temperature is tedious, and since its overall effect is considered to be small, a single value is normally assumed. Further work is required to investigate this property, but it was considered to be outside the scope of this work.

The value of Poisson's ratio for concrete at ambient temperatures is assumed to vary from 0.15 to 0.20. In many cases this effect is ignored, except in the case of slabs spanning in two directions.

3.03.3 Thermal Coefficient of Linear Expansion

Most substances expand when their temperature is raised and contract when cooled, and for a wide range of temperature this expansion or contraction is assumed to be proportional to the temperature change. This proportionality is expressed by the coefficient of linear thermal expansion α which is defined as the change in length which a member of unit length undergoes when its temperature is changed by $1^{o}C$.

For concrete: $\alpha_c = 0.000\ 012$ per $1^{o}C$

and for steel: $\alpha_s = 0.000\ 010$ per $1^{o}C$

If expansion or contraction of all fibres of a body is unrestrained, no stress is caused by the change in temperature. However, in most structures free expansion or contraction cannot take place, and thermal stresses take place as a result of these restraints. If these stresses exceed the materials' tensile or compressive strength, cracking or crushing of the member or damage to adjacent parts of the structure may result. However, little guidance is given in Codes of Practice as to the magnitude of these movements, and a large part of this work is therefore devoted to these aspects of the response of structures.

The thermal coefficient of linear expansion for some common rocks and hardened cement paste is shown in the table below (taken from a paper by Srdan D. Venecanin, ref.36)

Rock Type	Thermal Coefficient of linear expansion
	10^{-6} per ^{o}C
Granite	1.8 to 11.9
Diorite, andesite	4.1 to 10.3
Gabbro, basalt, diabase	3.6 to 9.7
Sandstone	4.3 to 13.9
Dolomite	6.7 to 8.6
Limestone	0.9 to 12.2
Chert	7.4 to 13.1
Marble	1.1 to 16.0
Hardened cement paste	11.0 to 20.0

Table: 300.04

The coefficient of thermal expansion of concretes made from different aggregates is shown in the table (taken from ref.21) below.

Aggregate	Thermal Expansion (10^{-6} per ^{o}C)	
	Air Storage	Wet Storage
Gravel	13.2	12.2
Granite	9.6	8.6
Quartzite	12.7	12.2
Dolerite	9.6	8.4
Sandstone	11.7	10.1
Limestone	7.3	6.1
Portland Stone	7.3	6.2
Blastfurnace Slag	10.6	9.1
Foamed Slag	12.0	9.2

Table: 300.05

3.03.4 Modulus of Elasticity of Concrete 'Ec'

The modulus of elasticity of concrete 'Ec' increases with increase of cement content, age, repetition of stress and other factors such as type of aggregate, moisture content etc. Actual values lie between 750 and 1500 times the compressive strength. However, the generally accepted arbitrary value of 'Ec' is taken as $28KN/mm^2$ and is recommended in C.P.110. This value compensates in part for errors involved in the consideration of reinforced concrete as a theoretically elastic substance and for the neglect of the tensile resistance of concrete in bending.

In problems of thermal stress analysis, the value of modulus of elasticity of concrete 'Ec', is normally assumed to remain constant. However, this is not strictly true. In an attempt to determine the effect of temperature on the modulus of elasticity of concretes made from different aggregates, an experiment was conducted on concrete cylinders made from 3 different mixes.

3.03.4.1 Experiment on Concrete Cylinders

(Experiment II)

Concrete Cylinders 150mm. dia. 300mm. high were made from 3 different mixes. The cylinders were cured by immersion in water for at least two to three weeks. Gauge lengths of 200mm. were marked on each cylinder by fixing studs with epoxy adhesives. Two cylinders from each mix were tested in compression at ambient room temperatures. One cylinder from each mix was heated to $60^{\circ}C$ and one to $100^{\circ}C$ and similarly tested in compression. The cylinders were heated in an electric oven for 24 hours in the case of $60^{\circ}C$, and over 100 hours in the case of $100^{\circ}C$. It should be noted that all heated specimens were tested in the hot state, by applying the test load immediately after removal from the oven.

RESULTS OF CYLINDER TESTS

(150mm. dia. x 300mm. high)

DEMEC GAUGE (200mm. Gauge Length and 0.096 x 10^{-4} Strain per div.)

Type of Conc. Mix	Cylinder No.	Date of Casting	Date of Testing	Age at Test Days	Temp. of Cylinder at Test °C	Test Load in KN.	DEMEC Gauge Reading	Calc. Value of Modulus 'Ec' N/mm²
Micro-Conc. Mix	1	21.4.77	27.5.77	35days	Ambient 22°C	0 100 200 300	740.0 711.5 686.0 664.5	23.43×10^3
	2	21.4.77	27.5.77	35days	Ambient 22°C	0 100 200 300	739.0 701.0 670.0 646.0	19.02×10^3
	3	21.4.77	27.5.77	35days	Heated for 24 hours 60°C	0 100 200 300	780.0 757.0 739.0 712.0	25.64×10^3
	4	10.5.77	27.5.77	17days	Heated for 24 hours 60°C	0 100 200 300	762.0 713.0 678.0 635.0	13.93×10^3
	5	10.5.77	31.5.77	21days	Heated for 117 hours 100°C	0 100 200 300	796.0 755.0 724.5 693.0	16.93×10^3
	6	21.4.77	31.5.77	39days	Heated for 117 hours 100°C	0 100 200 300	748.0 704.5 672.5 638.5	15.92×10^3
Aglite Mix	7	20.6.77	18.7.77	28days	Ambient 21°C	0 45 90 135 180	732.0 685.0 650.0 622.0 593.0	7.64×10^3

Table: 300.06(a)

Type of Conc. Mix	Cylinder No.	Date of Casting	Date at Testing	Age at Test Days	Temp. of Cylinder at Test °C	Test Load in KN.	DEMEC Gauge Reading	Calc. Value of Modulus 'Ec' N/mm^2
Aglite Mix	8	20.6.77	18.7.77	28days	Ambient 21°C	0	743.0	10.51x10^3
						45	717.0	
						90	693.0	
						135	670.0	
						180	642.0	
	9	20.6.77	20.7.77	30days	60°C	0	734.0	11.93x10^3
						45	705.0	
						90	681.0	
						135	661.0	
						180	645.0	
	10	20.6.77	27.7.77	37days	100°C	0	752.0	8.23x10^3
						45	696.0	
						90	670.0	
						135	645.0	
						180	623.0	
Lytag Mix	11	20.6.77	18.7.77	28days	Ambient 21°C	0	940.0	11.67x10^3
						35	908.0	
						70	885.0	
						105	868.0	
						140	849.0	
	12	20.6.77	18.7.77	28days	Ambient 21°C	0	685.0	5.23x10^3
						35	593.0	
						70	547.0	
						105	517.0	
						140	482.0	
	13	20.6.77	20.7.77	30days	60°C	0	735.0	11.29x10^3
						35	701.0	
						70	677.0	
						105	658.0	
						140	641.0	
	14	20.6.77	27.7.77	37days	100°C	0	788.0	7.98x10^3
						35	738.0	
						70	703.0	
						105	679.0	
						140	655.0	

Table: 300.06(b)

3.03.4.2 Compression Test Procedure

Each cylinder was placed in a hydraulically controlled compression machine. Load was applied slowly in a dummy run to a limit well within the elastic range and then unloaded. No readings of the change in gauge length was taken. The rate of increase of applied load was adjusted so that each increment was applied for the same duration. The cylinder was then loaded for the second time, also in a dummy run. The purpose of the dummy runs was to ensure that the load was applied evenly and to stabilize the behaviour of the concrete.

After twice dummy loading, the cylinder was finally loaded for the test proper. The load was applied in increments of 45 KN or 100 KN to a maximum of 140 KN for Lytag, 180 KN for Aglite and 300 KN for Micro-concrete. For each increment readings of strain were taken by means of a Demec Gauge. The above experiment was repeated on a total of 14 cylinders made from the 3 different mixes. The results of the experiments on cylinders are shown on the following sheets.

3.03.4.3 Sample Calculation for the Modulus of Elasticity 'Ec' from Cylinder Test Results

Demec Gauge Reading at zero load = 740.0

Demec Gauge Reading at 300 KN load = 664.5

Difference = 75.5

Strain per div. = 0.096×10^{-4}

" for 75.5 div. = $0.096 \times 10^{-4} \times 75.5$

Modulus of Elasticity 'Ec' = $\frac{\text{Stress}}{\text{Strain}}$

$$= \frac{300 \times 10^{3} \times 4}{\pi 150^{2} \times 0.096 \times 10^{-4} \times 75.5}$$

$$= 23.43 \times 10^{3} \text{ N/mm}^2$$

3.03.4.4 Discussion of Results of Tests on Cylinders

The main aim of tests on cylinders was to determine and to compare the value of Modulus of Elasticity, Ec, of different types of concretes, and the change in the value of Ec due to the thermal effect. A total of 14 cylinders, 6 of Micro-concrete and 4 each of Aglite and Lytag concrete, were tested. Because of various practical difficulties, it was not possible to test all the cylinders at the same age.

Micro-concrete Mix

The results of tests on cylinders of Micro-concrete show a slightly higher value of Ec at 60°C in comparison to 22°C at the same age of 35 days, whereas the value of Ec falls considerably at 100°C and a slightly longer age of 39 days. The following conclusions are drawn from the results:-

(i) At low or intermediate temperatures there is no significant change in Ec (the slight increase being due to normal variations in cylinder strength).

(ii) At 100°C the value of Ec begins to drop rather rapidly, (fig. 3.0351)

The above results compare favourably with those obtained by K.W. Nasser and R.P. Lohtia in their extensive testing of "Mass Concrete Properties at High Temperatures", as shown in Table: 300.08.

Aglite Mix

The results of tests on cylinders of Aglite concrete show similar behaviour to that shown by Micro-concrete, the only difference being that generally the values of Ec for this mix are low in comparison. A point to note is that both Micro-concrete and Aglite concrete show slightly higher Ec values at 60°C. It would appear that heating at low temperatures and for short durations may be accelerating the curing process and thus increasing the compressive strength and the Ec value.

Lytag Mix

The results of tests on cylinders of Lytag concrete also exhibit similar behaviour to that of Micro-concrete and Aglite concrete, with the exception of one cylinder tested at ambient temperature which gives a very low value of Ec. This is probably due to some imperfections or faults in the making of the cylinder, resulting in internal voids and consequently much greater strains.

In view of the limited range of specimens tested, the results cannot be considered to be completely conclusive. However, there is sufficient correlation with results of research by others that it is reasonable to accept that elasticity of concrete is adversely affected by temperature, and that the degree of deterioration increases both with temperature and age of curing.

3.03.5 Cube Strength of Concrete

3.03.5.1 Experiment on Concrete Cubes

(Experiment III)

As part of the investigation on the effect of temperature on various properties of concrete, tests were also carried out on 100mm cubes to assess the effect on the crushing strength of concrete made from different mixes.

The procedure of testing was similar to the test on cylinders except that no dummy loads were applied. The cubes were tested directly to failure loads.

3.03.5.2 Discussion of Results of Tests on Cubes

The results of compressive tests on 100mm cubes show that, within the test temperature range, the compressive strength increases with age and with increase in temperature. This is shown quite clearly by the Aglite and Lytag concretes, fig.3.0351, whereas the Micro-concrete results for the effect of temperature are somewhat inconsistent. For comparison, the results obtained by K.W. Nasser and R.P. Lohtia are shown in Table: 300.07. Although strength and elasticity show about the same temperature dependence, elasticity is more severely reduced at temperatures of 100°C or beyond.

PLATE: 11 Micro-Concrete Cylinder under compression test.

RATIO OF COMPRESSIVE STRENGTH AT VARIOUS TEMPERATURES AND AGES TO THE ONE AT 70°F (21.4°C) FOR BOTH CONCRETES A AND B

Age days	Compressive strength, psi (kgf/cm²) at 70 °F (21.4 °C)	Ratio of compressive strength at indicated temperature to that at 70 °F (21.4 °C)						
		35 °F (1.7 °C)	160 °F (71 °C)	250 °F (121 °C)	300 °F (149 °C)	350 °F (177 °C)	400 °F (205 °C)	450 °F (232 °C)
4	4200 (290)	0.68	1.17	1.09	1.15	1.20	1.10	1.07
14	5300 (372)	0.83	0.97	1.01	0.93	0.95	0.79	0.75
21	5810 (408)	1.06	0.97	0.85	0.77	0.69	0.62	0.58
180	6080 (427)	1.12	0.97	0.78	0.68	0.59	0.56	0.50
4	5400 (380)	-	0.95	0.95	1.07	0.95	0.88	0.80
14	5500 (386)	-	1.01	1.05	1.02	0.97	0.79	0.75
21	5850 (412)	-	1.05	1.07	0.87	0.73	0.63	0.59
180	6100 (428)	-	1.05	1.05	0.80	0.64	0.56	0.53

Table: 300.07 (ref. 16)

RATIO OF MODULUS OF ELASTICITY AT VARIOUS TEMPERATURES AND AGES TO THE ONE AT 70°F (21.4°C) FOR BOTH CONCRETES A AND B

Type of concrete	Age days	Modulus of elasticity E_c 10^6 psi (10^5 kfg/cm²) at 70 °F (21.4°C)	Ratio of E_c at indicated temperatures to that at 70 °F (21.4 °C)						
			35 °F (1.7°C)	160 °F (71°C)	250 °F (121°C)	300 °F (149°C)	350 °F (177°C)	400 °F (205°C)	450 °F (232°C)
A (heated after 1 day of casting)	14	5.05 (3.55)	0.81	0.84	0.80	0.77	0.58	0.51	0.44
	28	5.12 (3.59)	0.86	0.89	0.75	0.72	0.51	0.48	0.40
	91	5.20 (3.66)	0.96	0.94	0.68	0.64	0.51	0.42	0.35
	180	5.30 (3.72)	1.04	0.98	0.64	0.60	0.49	0.39	0.29
B (heated after 14 days of casting	14	5.20 (3.66)	-	0.86	0.86	0.80	0.62	0.51	0.44
	28	5.25 (3.69)	-	0.90	0.86	0.76	0.58	0.46	0.39
	91	5.40 (3.79)	-	0.97	0.88	0.71	0.53	0.41	0.33
	180	5.50 (3.86)	-	1.02	0.88	0.67	0.50	0.37	0.28

Table: 300.08 (ref. 16)

Test Cubes

(100mm. Cubes)

Type of Concrete Mix.	Cube No.	Date of casting	Date of testing	Age at Test days	Temperature of Cube at Test	Failure Load in KN	Compressive Strength in N/mm^2
Micro-Concrete Mix	1	10.5.77	27.5.77	17	Ambient 22 °C	436.0	43.60
	2	10.5.77	27.5.77	17	Ambient 22 °C	447.0	44.70
	3	21.4.77	27.5.77	35	Ambient 22 °C	539.0	53.90
	4	21.4.77	27.5.77	35	Ambient 22 °C	595.0	59.50
	5	21.4.77	27.5.77	35	60 °C (heated for 24 hours)	571.0	57.10
	6	10.5.77	27.5.77	17	60 °C (heated for 24 hours)	445.0	44.50
	7	21.4.77	31.5.77	39	100 °C (heated for 117 hours)	516.0	51.60
	8	10.5.77	31.5.77	39	100 °C (heated for 117 hours	427.0	42.70
Aglite Mix	9	20.6.77	18.7.77	28	Ambient 21 °C	270.0	27.00
	10	20.6.77	18.7.77	28	Ambient 21 °C	294.0	29.40
	11	20.6.77	20.7.77	30	60 °C	314.0	31.40
	12	20.6.77	22.7.77	32	100 °C	348.0	34.80
Lytag Mix	13	20.6.77	18.7.77	28	Ambient 21 °C	195.0	19.50
	14	20.6.77	18.7.77	28	Ambient 21 °C	200.0	20.00
	15	20.6.77	20.7.77	30	60 °C	245.0	24.50
	16	20.6.77	22.7.77	32	100 °C	281.0	28.10

Table: 300.09

TECHNICAL DATA PERTAINING TO VARIOUS CONCRETES USED IN EXPERIMENTAL WORK

1. Micro Concrete: Mainly consists of Ordinary Portland Cement and fine river aggregate (Zone 2 Thames Valley) normally used for ordinary concrete. Suitable and mainly used for small experimental members.

   Mix Design: 1.0 cement
   2.8 fine aggregate
   0.4 w/c

2. Lytag Concrete: A lightweight aggregate concrete made from Ordinary Portland Cement and sintered pulverized fuel ash collected from Electric Power Stations burning pulverized fuel. It has a density of 100 to 110 lb/ft^3 and a thermal insulation 50% better than normal dense concrete.

   Mix Design: 1.0 cement
   4.0 aggregate (in the ratio of 5 fine to 7 coarse)
   water/cement ratio to give medium workability, also, depending on absorption, property of aggregate.

3. Aglite Concrete: A lightweight aggregate concrete made from Ordinary Portland Cement and foamed slag from pig-iron blast furnaces. It has slightly better thermal insulation value than normal dense concrete.

   Mix Design: 1.0 cement
   4.0 aggregate (in ratio of 5 fine to 7 coarse)
   water/cement ratio to give medium workability.

Table: 300.10

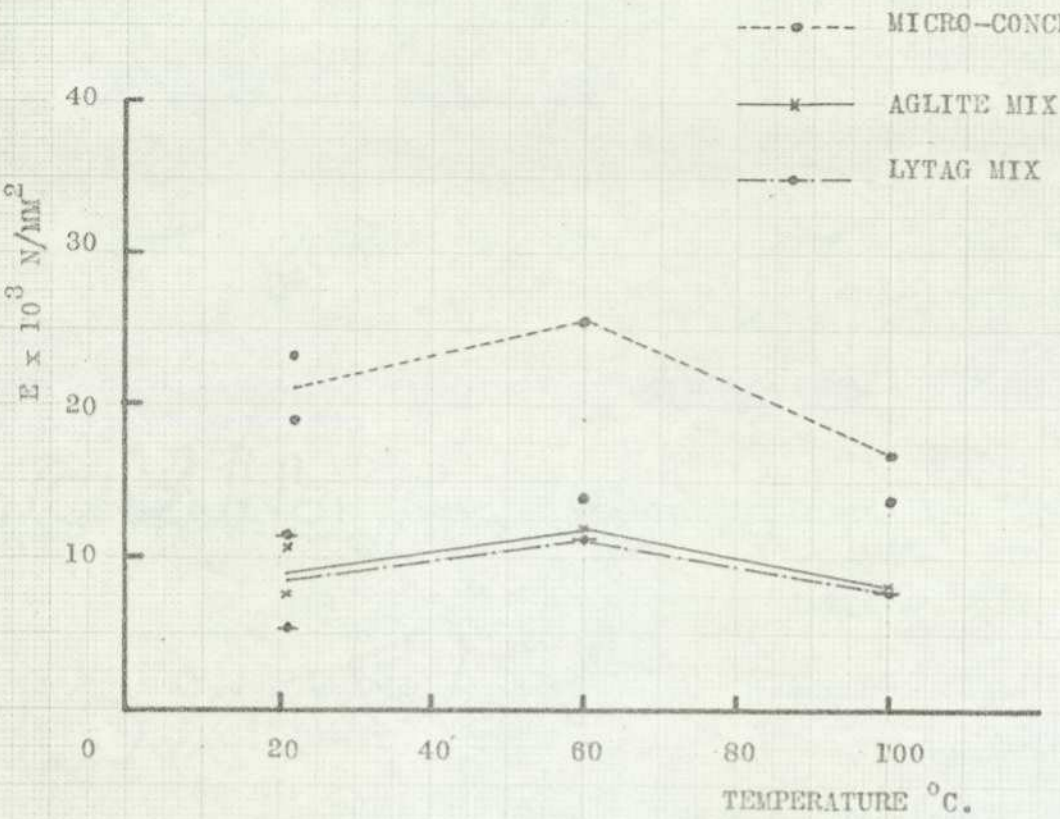
MICRO-CONCRETE
AGLITE MIX
LYTAG MIX
E x 10^3 N/mm^2
40
30
20
10
0
20
40
60
80
100
TEMPERATURE °C.

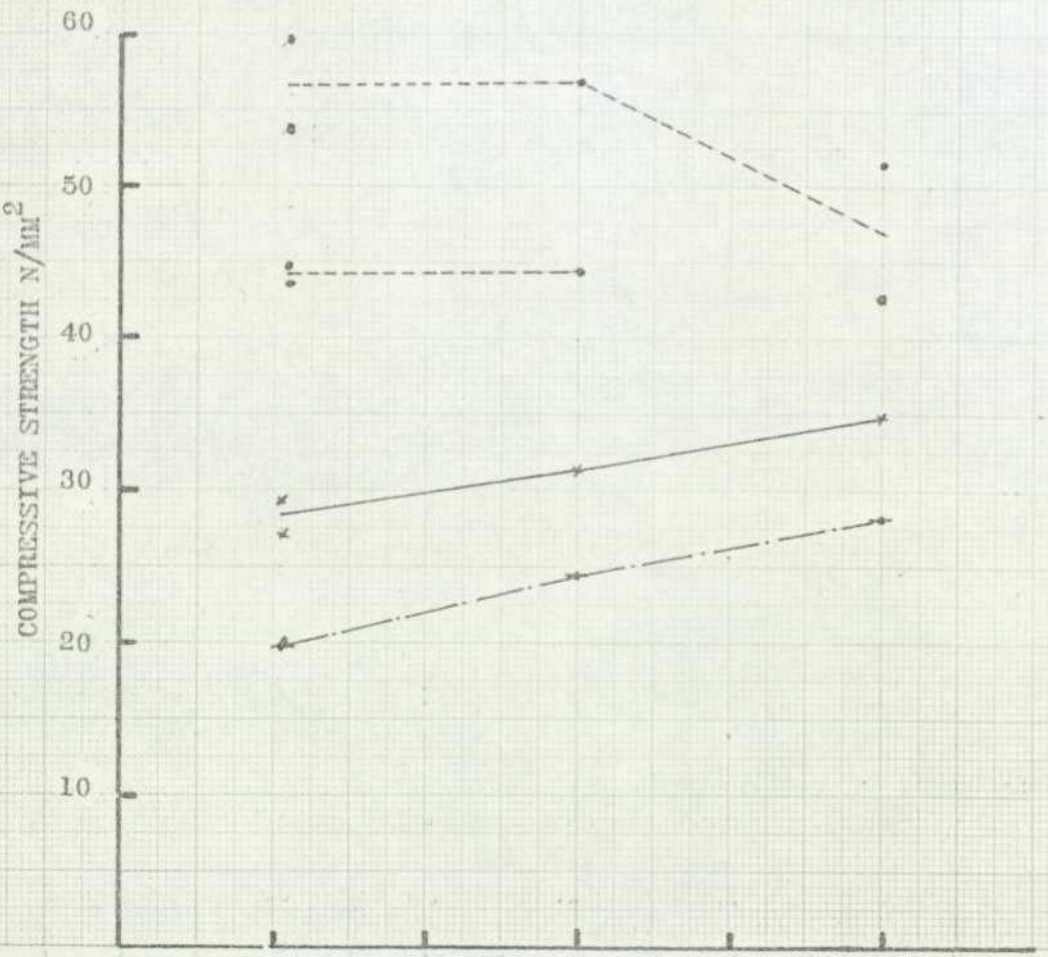
COMPRESSIVE STRENGTH N/mm^2
60
50
40
30
20
10
0
20
40
60
80
100
TEMPERATURE °C.

Fig. 3.0351

3.03.6 Experiment to Determine the Elastic Modulus and Strain Calibration of a Continuous Beam

(Experiment IV)

(Stresses induced by Elastic Loading of a Continuous Beam)

Two reinforced Micro-concrete beams of identical properties as shown in Fig. 3.071 & 2 were cast.

To establish the value of Young's Modulus 'E' and to obtain the relationship between gauge reading and strains, (and therefore stresses and bending moments) one Micro-concrete beam was tested in flexure as shown in Fig. 3.0361.

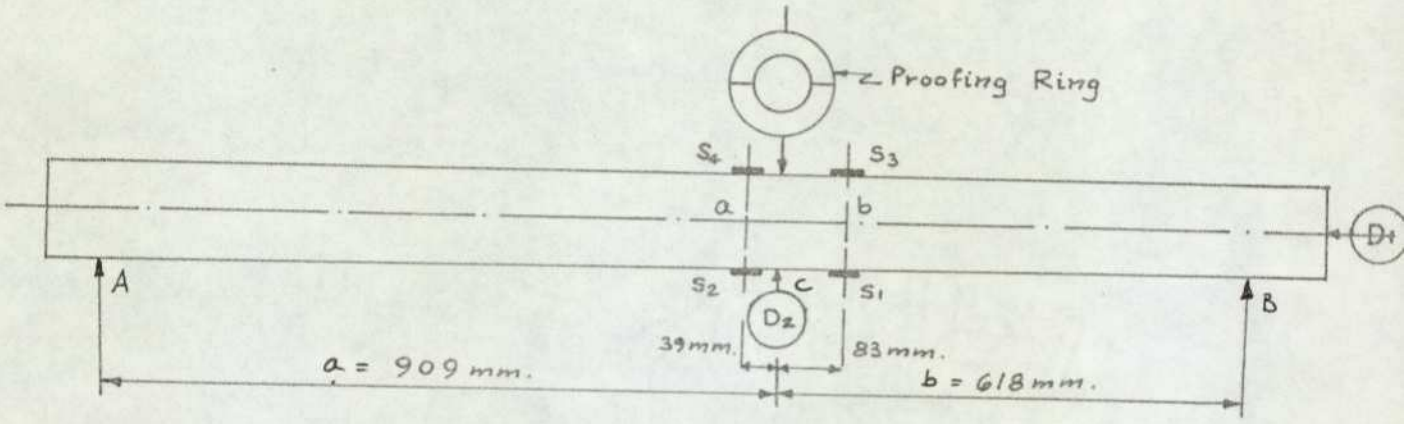

Fig. 3.0361 Reinforced Micro-concrete beam, showing dimensions and instrumentation

For a simply-supported beam, the deflection at any point, distance 'x' from support A, is given by the expression

$$EI\ \Delta y = -\frac{Pbx^3}{6L} + \frac{P}{6}(x-a)^3 + \frac{PbLx}{6} \quad \frac{Pb^3x}{6L}$$

when $x = a$

$$\Delta y = \frac{Pa^2b^2}{3EIL}$$

where Δy = deflection of beam in direction y

P = point load applied at point C

L = total length of beam between supports = a + b

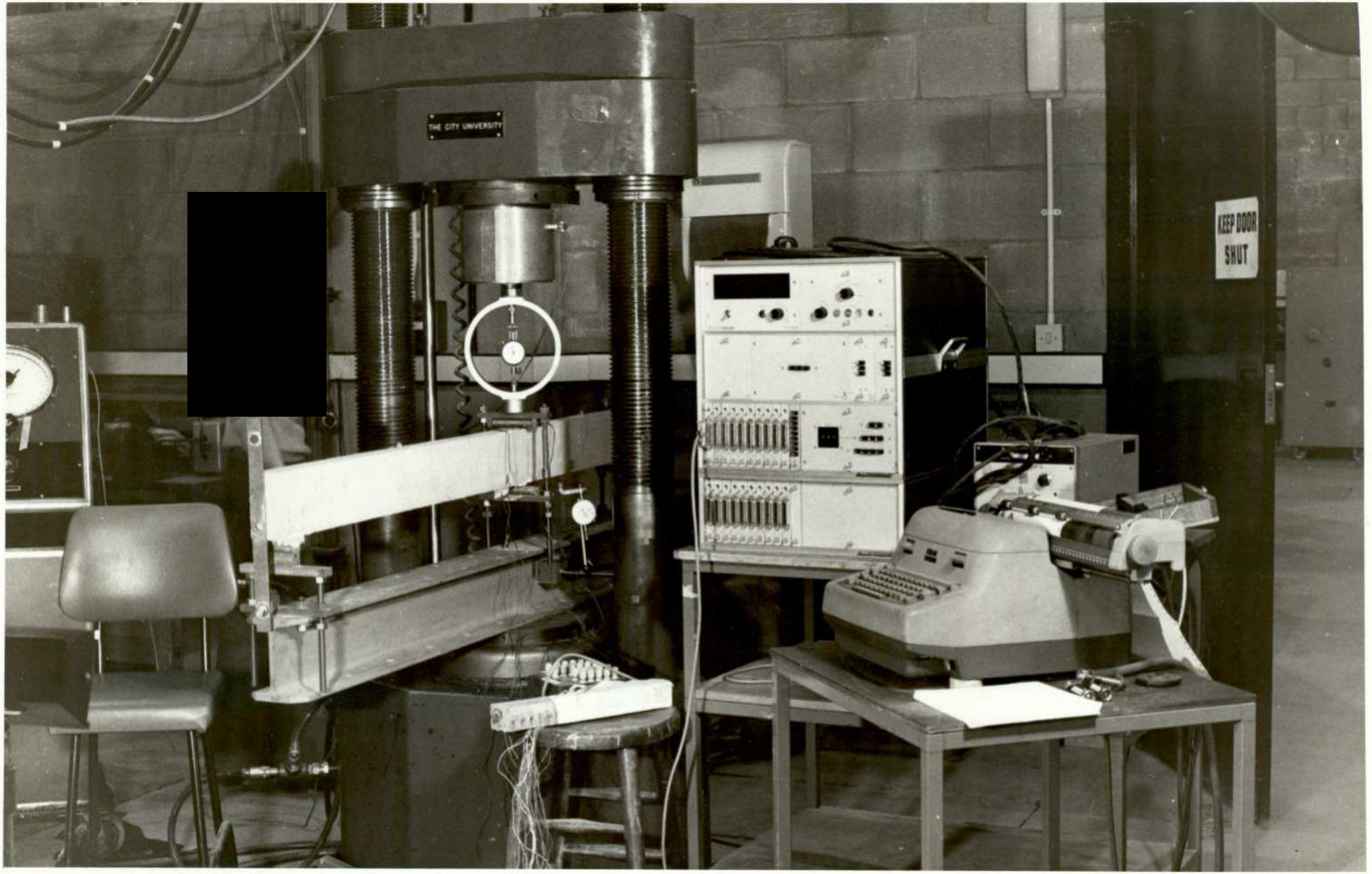

PLATE: 111 Reinforced micro-concrete beam under test for the determination of elastic modulus and strain calibration (stresses induced by elastic loading of beam).

Transposing gives

$$E = \frac{Pa^2b^2}{3IL\Delta y} = \frac{a^2b^2}{3IL} \quad \frac{P}{\Delta y}$$

now $$I = \frac{bd^3}{12} = \frac{50 \times 120^3}{12} = 7{,}200{,}000 \text{ mm}^4$$

$$a = 909 \text{ mm}$$

$$b = 618 \text{ mm}$$

$$E = \frac{P}{\Delta y} \quad \frac{909^2 \times 618^2}{3 \times 7{,}200{,}000 \times 1527} = \frac{P}{\Delta y} \ (9.5678)$$

where the value of $\frac{P}{\Delta y}$ (from graph) = 3557.1688

$$E = 3557.1688 \times 9.5678 = 34034.28 \text{ N/mm}^2 \approx 34{,}000 \text{ N/mm}^2$$

Relationship between gauge reading and stress is derived from

$$\sigma = \frac{My}{I} = \frac{Pbay}{LI}$$

$$\text{Max. } \sigma \text{ at (a)} = \frac{2769 \times 618 \times (909 - 39) \times 120}{1527 \times 7{,}200{,}000 \times 2} = 8.1248 \text{ N/mm}^2$$

$$\text{and Max. } \sigma \text{ at (b)} = \frac{2769 \times 909 \times (618 - 83) \times 120}{1527 \times 7{,}200{,}000 \times 2} = 7.3489 \text{ N/mm}^2$$

Corresponding strain gauge readings for the above stresses

at location (a) $G_2 = 83.75 - 10.5 = 73.25$

$G_4 = 36.25 - 0 = 36.25$

Average = $(73.25 + 36.25)\frac{1}{2}$

= 54.75

at location (b) $G_1 = 149.50 - 10.75 = 138.75$

$G_3 = 25.00 - 0 = 25.00$

Average = $(138.75 + 25.00)\frac{1}{2}$

= 81.88

Therefore, stress per division at (a) $\sigma = \frac{8.1248}{54.75} = 0.1484 \text{ N/mm}^2$

(b) $\sigma = \frac{7.3489}{81.88} = 0.0898 \text{ N/mm}^2$

Average stress reading per div. = $(0.1484 + 0.0898)\frac{1}{2}$

= 0.1191

Relationship between gauge reading and Bending Moment

Max. B.M. at load point = $\frac{Pba}{L}$

Max. B.M. at point (a) = $\frac{2769 \times 618\ (909 - 39)}{1527}$ = 974,970.88 N-mm

Max. B.M. at point (b) = $\frac{2769 \times 909\ (618 - 83)}{1527}$ = 881,863.94 N-mm

Corresponding strain gauge readings for the above Bending Moments

at location (a) Average of G_2 and G_4 = 54.75

at location (b) Average of G_1 and G_3 = 81.88

Therefore, B.M. per division at (a) B.M. = $\frac{974,970.88}{54.75}$ = 17,807.69 N-mm

(b) B.M. = $\frac{881863.94}{81.88}$ = 10,770.20 N-mm

Average B.M. per division at (a) & (b) = $(17,807.69 + 10,770.20)\frac{1}{2}$

= 14,288.95 N-mm

Note: the large difference in the strain gauge readings at the two locations on the beam.

The readings of gauges (2) and (4) are considered faulty. The correct calibration for the strain gauges then becomes 10,770.20 N-mm bending moment per division.

FLEXURAL TEST ON A BEAM

DIAL GAUGE READING D_1	DIAL GAUGE READING D_2	PROOF READING	LOAD IN	
			lb.	N
128.80	1,287.00	0	0	0
128.70	1,283.20	10.0	83.009	369.0
128.25	1,279.20	15.0	124.514	554.0
127.80	1,274.00	20.0	166.018	738.0
127.30	1,267.90	25.0	207.523	923.0
125.70	1,256.70	35.0	290.532	1,292.0
125.30	1,246.50	45.0	373.541	1,662.0
124.50	1,235.90	55.0	456.550	2,031.0
124.00	1,225.60	65.0	539.559	2,400.0
123.20	1,208.90	75.0	622.568	2,769.0
UNLOADING				
122.20	1,206.90	65.0	539.559	2,400.0
120.90	1,219.10	55.0	456.550	2,031.0
119.20	1,229.00	45.0	373.541	1,662.0
120.10	1,239.70	35.0	290.532	1,292.0
120.30	1,250.00	25.0	207.523	923.0
121.00	1,257.00	20.0	166.018	738.0
121.70	1,263.10	15.0	124.514	554.0
123.40	1,269.10	10.0	83.009	369.0
125.60	1,281.90	0	0	0

Table: 300.11

31.5.77

STRAIN GAUGE READINGS LOADING				APPLIED LOAD IN N.
G1	G2	G3	G4	
-0272	-0148	-0119	-0480	0
-0273	-0147	-0118	-0478	
-0272	-0146	-0118	-0479	
-0282	-0153	-0115	-0473	369.0
-0283	-0152	-0115	-0473	
-0282	-0153	-0114	-0473	
-0289	-0156	-0113	-0473	554.0
-0288	-0156	-0114	-0471	
-0289	-0157	-0114	-0472	
-0297	-0159	-0114	-0472	738.0
-0298	-0161	-0113	-0471	
-0297	-0160	-0114	-0471	
-0306	-0163	-0112	-0468	923.0
-0306	-0163	-0114	-0468	
-0306	-0164	-0113	-0468	
-0321	-0170	-0109	-0463	1,292.0
-0320	-0171	-0108	-0464	
-0320	-0171	-0108	-0464	
-0337	-0176	-0106	-0458	1,662.0
-0335	-0177	-0106	-0457	
-0335	-0178	-0104	-0459	
-0355	-0185	-0100	-0453	2,031.0
-0355	-0184	-0098	-0454	
-0357	-0185	-0100	-0453	
-0381	-0193	-0097	-0448	2,400.0
-0384	-0192	-0096	-0449	
-0383	-0193	-0097	-0447	
-0423	-0233	-0093	-0443	2,769.0
-0423	-0235	-0091	-0442	
-0426	-0240	-0092	-0442	

Table: 300.12(a)

STRAIN GAUGE READINGS UNLOADING				APPLIED LOAD IN N.
G1	G2	G3	G4	
-0415	-0236	-0095	-0447	
-0416	-0235	-0095	-0447	2,400.0
-0417	-0233	-0097	-0446	
-0404	-0228	-0100	-0451	
-0403	-0227	-0100	-0452	2,031.0
-0404	-0228	-0099	-0450	
-0388	-0220	-0102	-0455	
-0387	-0219	-0103	-0455	1,662.0
-0388	-0219	-0103	-0457	
-0372	-0213	-0107	-0460	
-0372	-0212	-0107	-0460	1,292.0
-0371	-0210	-0106	-0461	
-0353	-0202	-0109	-0466	
-0355	-0203	-0110	-0465	923.0
-0354	-0202	-0110	-0465	
-0344	-0198	-0112	-0467	
-0343	-0196	-0112	-0467	738.0
-0343	-0198	-0113	-0468	
-0333	-0193	-0116	-0472	
-0334	-0193	-0114	-0470	554.0
-0333	-0192	-0115	-0473	
-0325	-0189	-0116	-0474	
-0325	-0189	-0117	-0473	369.0
-0325	-0188	-0117	-0475	
-0304	-0178	-0120	-0479	
-0302	-0179	-0119	-0480	0
-0304	-0177	-0121	-0479	

Table: 300.12(b)

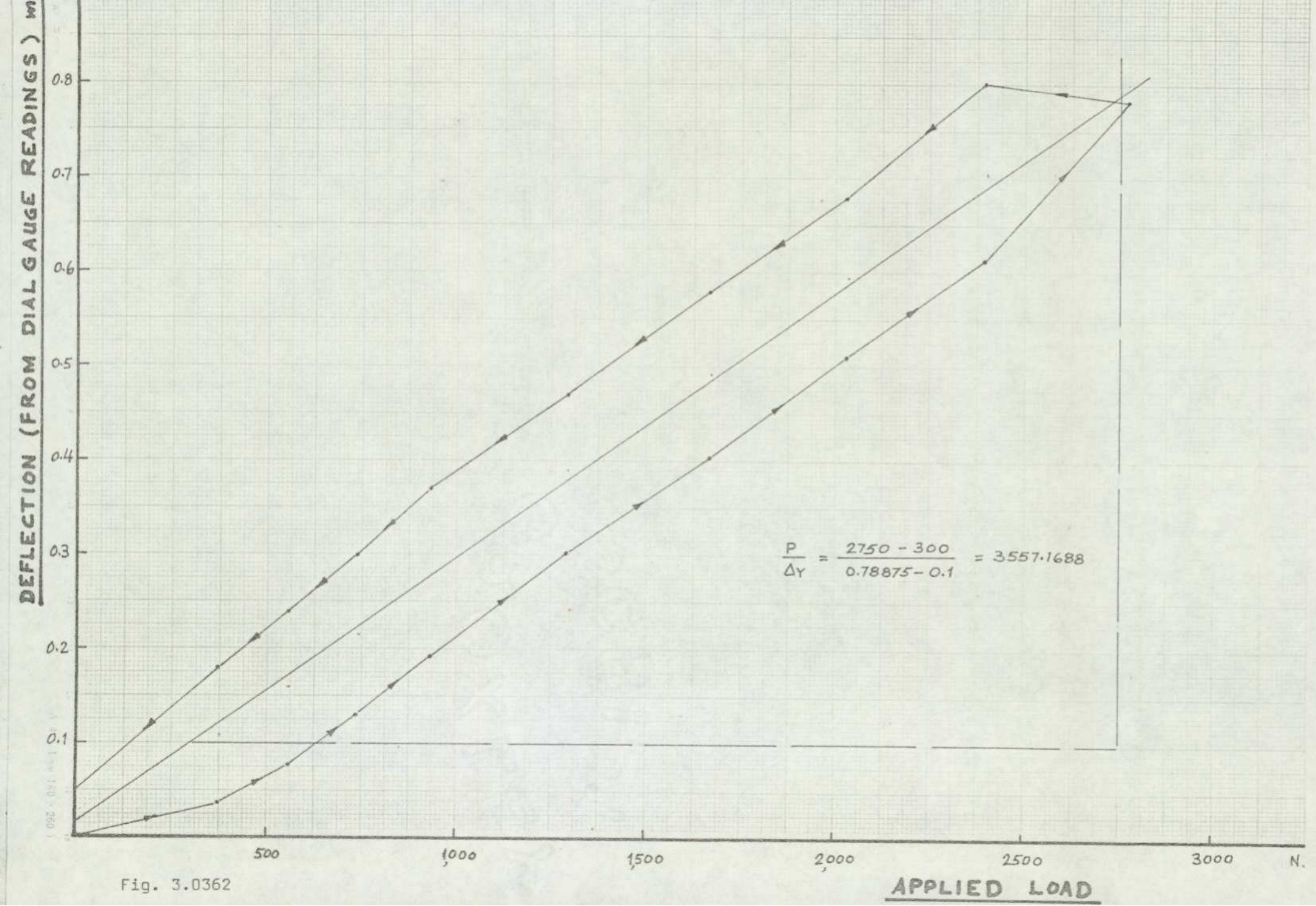
DEFLECTION (FROM DIAL GAUGE READINGS) m
0.8
0.7
0.6
0.5
0.4
0.3
0.2
0.1
500
1,000
1,500
2,000
2500
3000
N.
APPLIED LOAD
$\frac{P}{\Delta_Y} = \frac{2750 - 300}{0.78875 - 0.1} = 3557.1688$

Fig. 3.0362

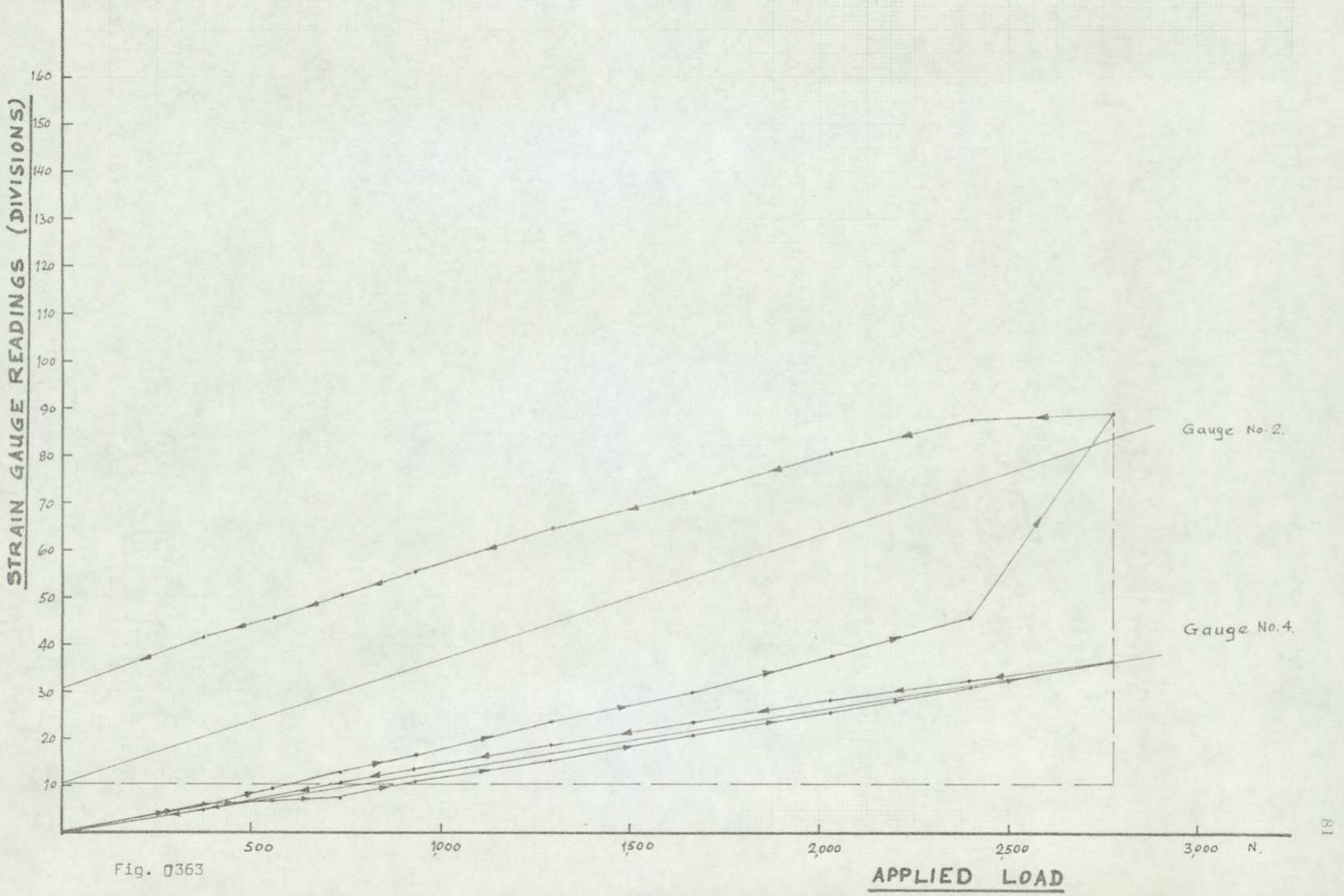
STRAIN GAUGE READINGS (DIVISIONS)
160
150
140
130
120
110
100
90
80
70
60
50
40
30
20
10
500
1,000
1,500
2,000
2,500
3,000
N.
APPLIED LOAD
Gauge No. 2.
Gauge No. 4.

Fig. 0363

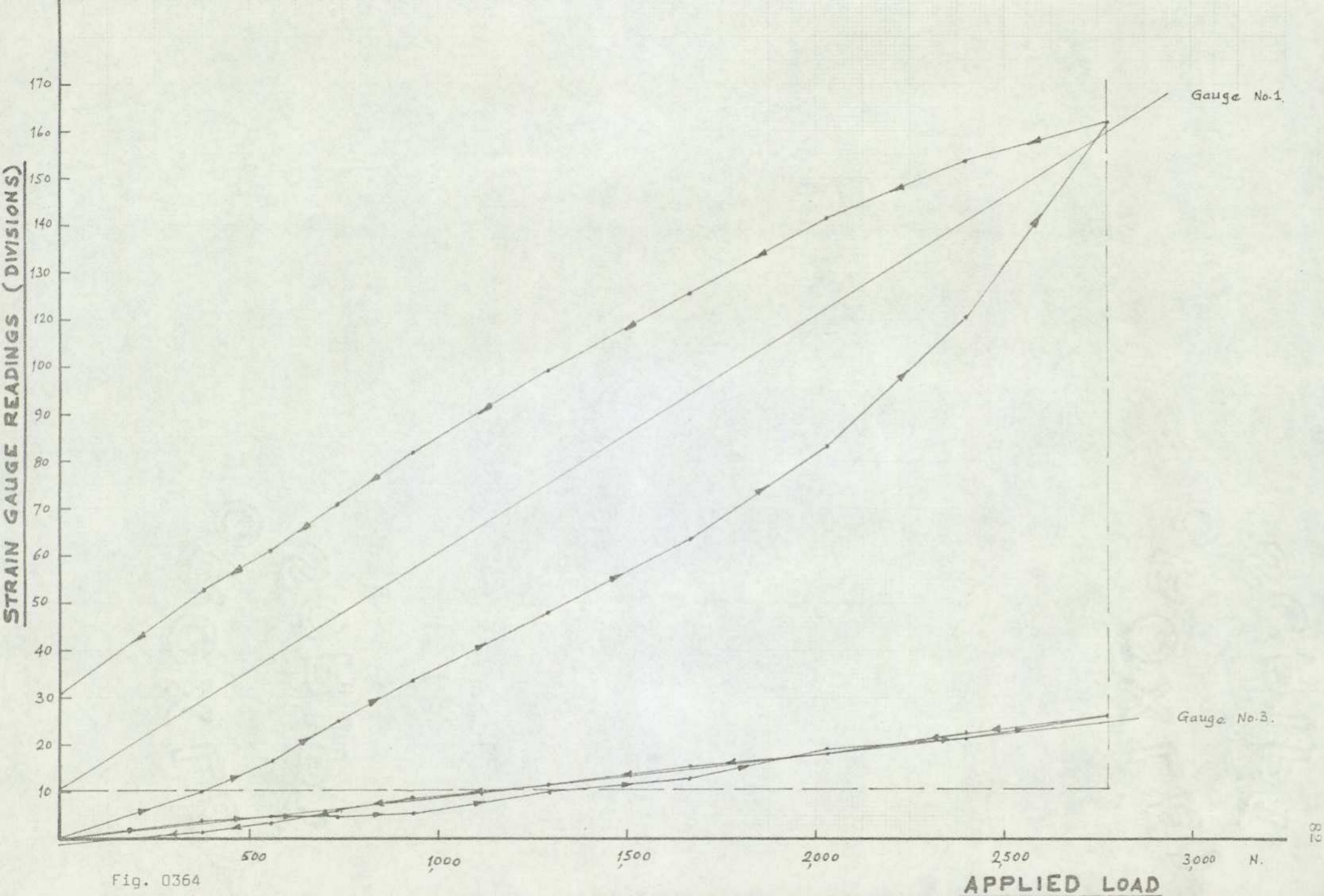
STRAIN GAUGE READINGS (DIVISIONS)
170
160
150
140
130
120
100
90
80
70
60
50
40
30
20
10
Gauge No.1.
Gauge No.3.
500
1,000
1,500
2,000
2,500
3,000
N.
APPLIED LOAD

Fig. 0364

3.03.6.1 Discussion of Results of Experiment to Determine The Elastic Modulus and Strain Calibration of a Continuous Beam

Experiment (IV)

Stresses induced by elastic loading of a continuous beam.

The value of E = 34,000 N/mm^2, obtained for the reinforced concrete continuous beam, appears, at first sight, to be on the high side. However, an inspection of the dimensional and reinforcement details shows that the percentage of longitudinal steel (2.62%) provided is fairly high. Therefore, taking into consideration the contribution of steel to the strength of the composite section, the value of E obtained can be taken to be reasonable. This result compares favourably with that obtained in experiment (V) where the value of E (= 31,600 N/mm^2) is calculated from stresses induced by thermal effects in a continuous beam.

3.03.7 Experiment to Determine the Coefficient of Linear Thermal Expansion and the Modulus of Elasticity

(Experiment V)

(Stresses induced by Thermal Effects in a Continuous Beam)

To establish the value of the coefficient of linear thermal expansion, α, and the modulus of elasticity, E, of reinforced Micro-concrete, an experiment was conducted on a beam shown in Fig. 3.0371 & 2.

For the purpose of measurement of temperature, 6 thermocouples, 3 per span per section, were cast into the beam at locations indicated in the diagram. The thermocouples were connected to a temperature indicator "Resilia" multi-switch instrument.

For the measurement of strains 4 strain gauges were fixed, 2 at the top and 2 at the bottom of the beam, at two locations indicated in the diagram. The strain gauges were connected to a direct reading data logger.

For the measurement of extension of the beam, a dial gauge was located at one end while the other end of the beam was placed against a rigid non-yielding bracket, so that beam extension could only take place in the direction of the gauge. A roller support was provided at the dial gauge end to permit free, frictionless movement. A rigid collar was provided at the middle support to prevent the beam from lifting off.

Heating tape was applied to the top surface of the beam. Then the beam was insulated on three sides by means of aluminium lined soft board. The bottom surface of the beam was left open so that heat could flow from the top surface to the bottom.

Heat was supplied at a fixed voltage until a steady state of temperature flow was achieved. Readings of thermocouples, strain gauges and dial gauge were recorded every couple of hours. The results are shown in Tables: 300.13 and 300.14.

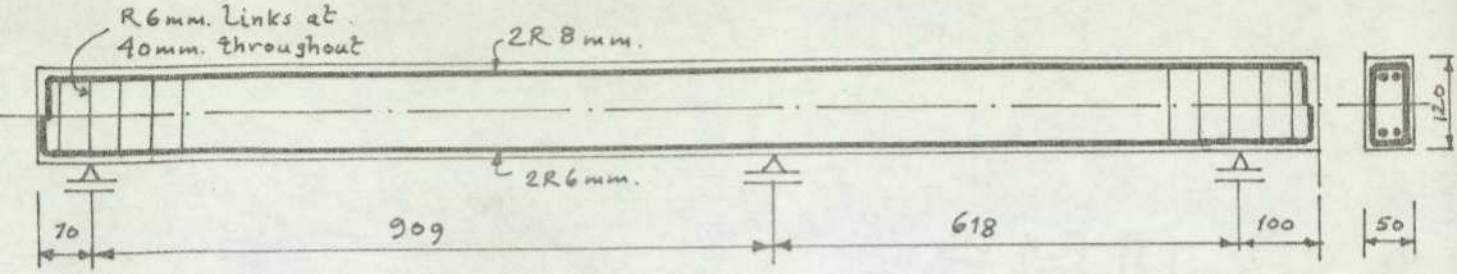

DIMENSIONAL AND REINFORCEMENT DETAILS OF MODEL BEAM

(All dimensions are in mm.)

Fig. 3.0371

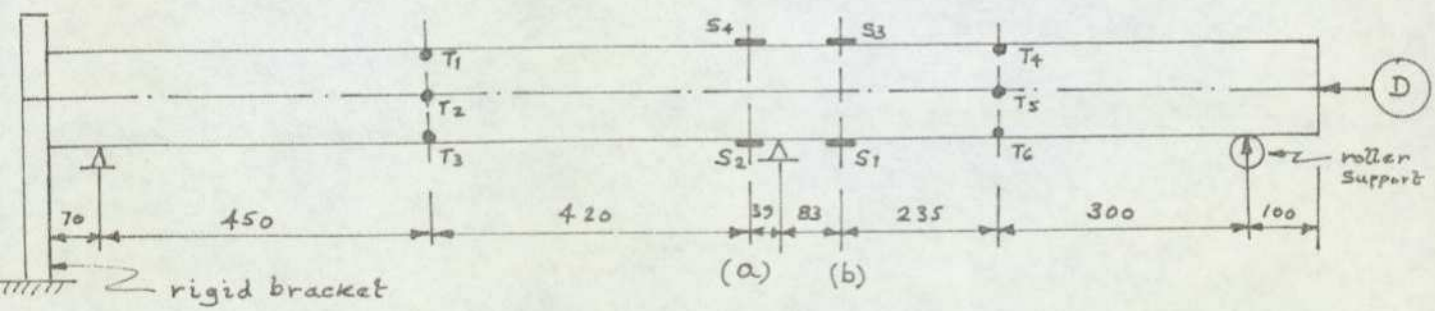

Fig. 3.0372

INSTRUMENTATION

T_1 to T_6 --- Thermocouples

S_1 to S_4 --- Strain Gauges

D --- Dial Gauge

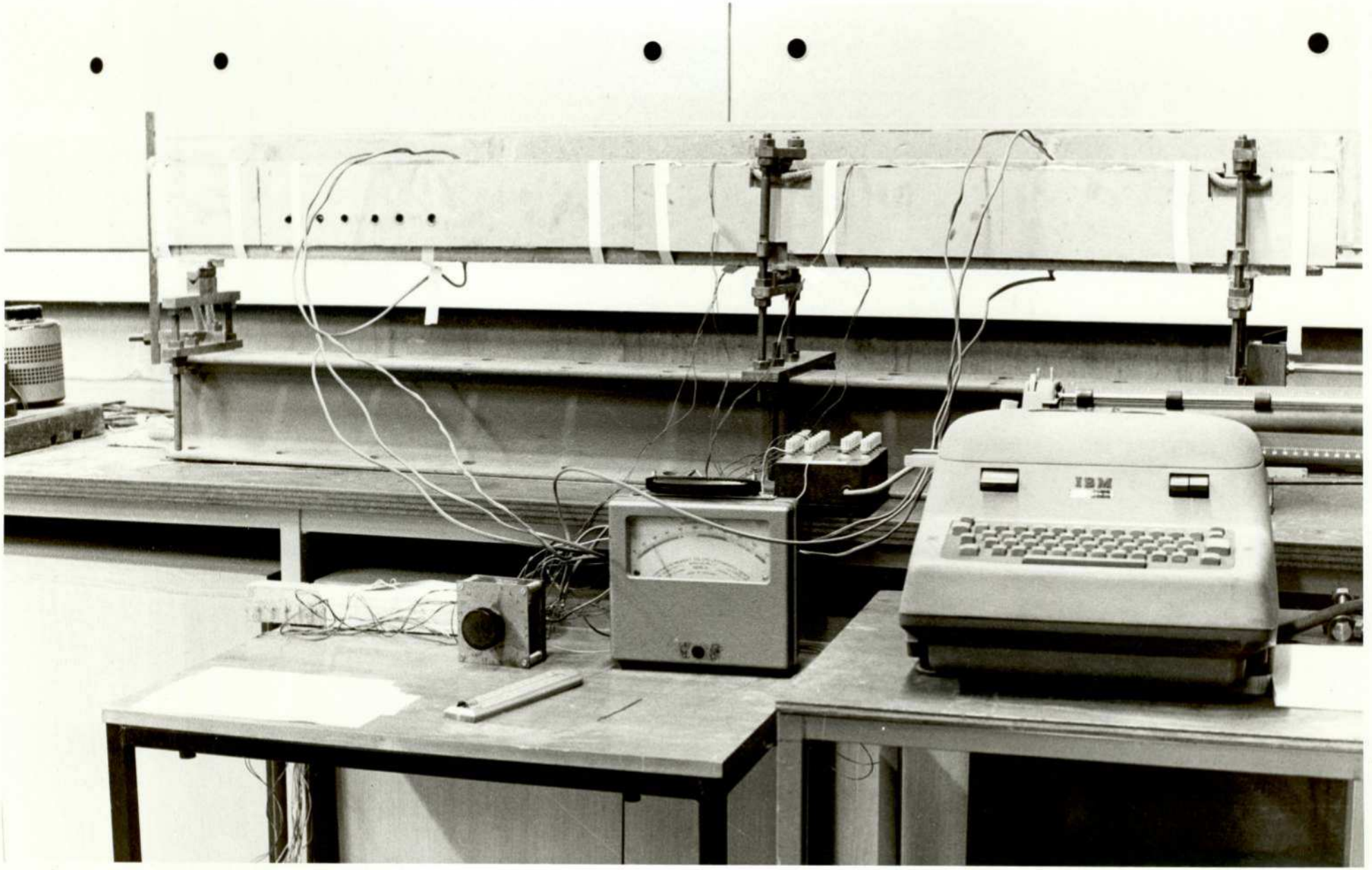

PLATE: 1V Reinforced micro-concrete beam under test for the determination of the coefficient of linear thermal expansion and the modulus of elasticity (stresses induced by thermal effect). VIEW ONE

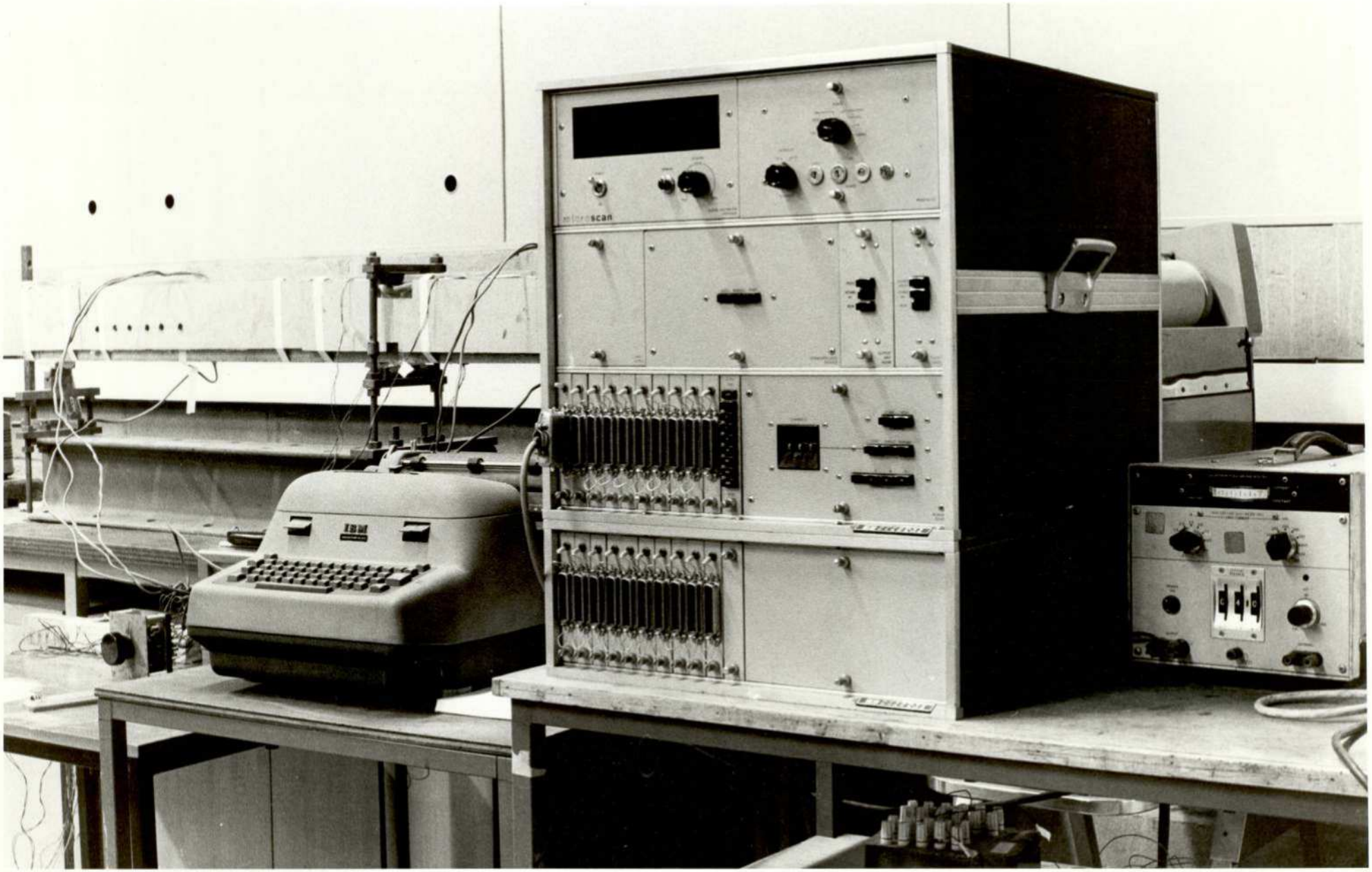

PLATE: V Reinforced micro-concrete beam under test for the determination of the coefficient of linear thermal expansion and the modulus of elasticity (stresses induced by thermal effect). VIEW TWO

EXPERIMENT ON TWO-SPAN BEAM FOR THE EFFECT OF LINEAR TEMPERATURE DISTRIBUTION

Thursday, 26th. May, 1977.

DATE	TIME	STRAIN GAUGE READINGS			
26.5.77	10.00	-0181	-0135	-0150	-0527
		-0182	-0136	-0151	-0528
		-0180	-0136	-0150	-0528
	12.45	-0129	-0099	-0076	-0370
		-0128	-0098	-0075	-0370
		-0129	-0099	-0076	-0371
		-0127	-0099	-0074	-0371
	14.30	-0169	-0129	-0088	-0478
		-0168	-0128	-0087	-0477
		-0170	-0130	-0088	-0479
	15.40	-0167	-0127	-0085	-0473
		-0169	-0129	-0085	-0474
		-0167	-0128	-0085	-0474
	16.40	-0168	-0129	-0085	-0470
		-0167	-0129	-0084	-0471
		-0168	-0129	-0085	-0472
27.5.77	9.30	-0153	-0117	-0059	-0444
		-0153	-0118	-0060	-0443
		-0153	-0118	-0059	-0442

Table: 300.13

DATE	TIME	AMBIENT ROOM TEMP. °C	THERMOCOUPLE READINGS						APPLIED VOLTAGE	APPLIED AMPERAGE	DIAL GAUGE READINGS
			T_1	T_2	T_3	T_4	T_5	T_6			
26.5.77	10.00	22.00	24.20	24.20	24.20	24.20	24.20	24.20	0	0	132.7
	12.45	22.50	28.00	37.50	44.20	31.00	23.80	42.30	120	1.3	144.8
	14.30	22.70	32.10	42.20	46.50	31.80	23.60	45.20	120	1.30	150.0
	15.40	22.80	32.20	43.20	48.00	35.00	24.00	45.80	120	1.30	151.6
	16.40	22.90	31.90	43.80	48.00	32.50	23.50	46.00	120	1.30	152.7
27.5.77	9.30	22.00	33.00	47.20	51.00	34.20	23.50	48.00	120	1.30	155.5

Table: 300.14

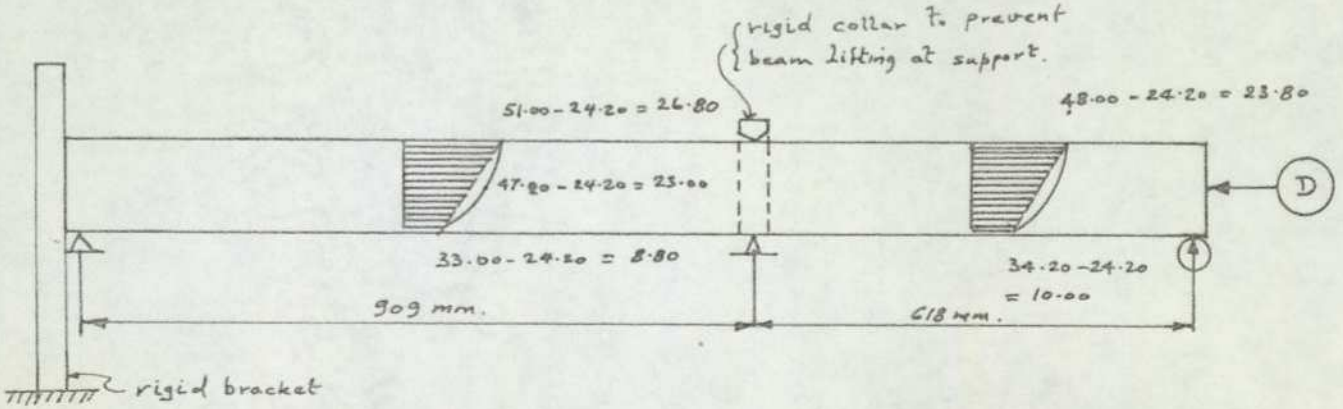

Fig. 3.0373 Temperature distribution in beam

(i) Determination of Coefficient of Linear Expansion,

From Fig. T(average) for span (1) = $(26.80+8.80)\frac{1}{2}$ = 17.8 °C

T(average) for span (2) = $(23.80+10.00)\frac{1}{2}$ = 16.9 °C

Substituting into the relationship αTL = extension, gives

$$17.8(909 + 70)\alpha + 16.9(1527 - 909 + 100)\alpha = 1.555 - 1.327$$

$$\therefore \quad \alpha = \frac{0.228}{29560.40} = 0.00000771 \text{ per 1 C}$$

(ii) Determination of Modulus of Elasticity, E

At location (a) strain gauge reading, G_2 = 18.00, G_4 = 84.70 } Average = $(88.70-18.00)\frac{1}{2}$ = 33.35

At location (b) strain gauge reading, G_1 = 28.00, G_3 = 91.00 } Average = $(91.00-28.00)\frac{1}{2}$ = 31.50

Now, from experiment for flexural test on beam

1 div. of strain reading

corresponds to an average bending moment = 10,770.20 N-mm

Bending moment due to temperature

effect at location (a) B.M. = 33.35 x 10,770.20 = 352,186.17 N-mm

(b) B.M. = 31.5 x 10,770.20 = 339,261.30 N-mm

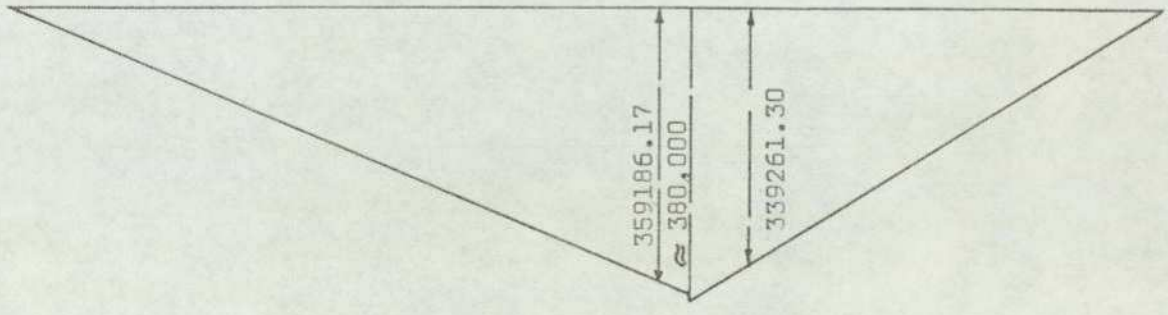

Fig. 3.0374 Bending Moment Diagram

And B.M. at point of application of load = 380,000 N-mm

Now equating this bending moment with that given by the expression

$$M = \frac{3EI\alpha T}{2d} \quad \text{gives}$$

$$\frac{3EI\alpha T}{2d} = 380,000$$

$$E = \frac{380,000 \times 2 \times 120 \times 12}{3 \times 50 \times 120 \times 0.00000771 \times 17.35} = 31,563.65 \text{ N/mm}^2$$

$$\approx 31,600 \text{ N/mm}^2$$

3.03.7.1 Discussion of Results of Experiment to determine the coefficient of Linear Thermal Expansion and the Modulus of Elasticity

Experiment (V)

Stresses induced by Thermal Effects in a continuous beam.

The results give a value of Coefficient of Linear Expansion, α = 0.00000771 per 1°C. This value of α is considered to be slightly on the low side when compared to the values of α_c = 0.000012 per 1°C for concrete and α_s = 0.000010 per 1°C for steel.

The results of determination of Modulus of Elasticity give the value of E = 31,600 N/mm^2. This value of E is considered satisfactory and compares favourably with the value of E = 34,000 N/mm^2 obtained in experiment (IV). The small discrepancy is attributed to different levels of experimental errors in the two cases. Thermal experiments, being more difficult to monitor and perform, can be assumed to have greater errors.

CHAPTER FOUR

4.00 REVIEW OF THE PRINCIPLES OF THE FORCE-DISPLACEMENT METHOD AS APPLIED TO THE EFFECT OF TEMPERATURE ON STRUCTURES

4.01 Assumptions

The analysis of thermal stresses is based on the following assumptions:-

(i) that the stresses are proportional to strains, i.e. that the Hooke's Law applies and the method is generally "linearly elastic" (although non-linear relationship between stresses and strains can be taken into account).

(ii) that the deformations are generally small, so that the equilibrium conditions can be satisfied in the original, undeformed configuration of a structure (but large deformations can also be taken into account and this leads to non-linear matrices).

(iii) that the materials are homogeneous, isotropic and uncracked.

(iv) that the principle of superposition is valid, i.e. that the various effects can be considered separately in any sequence of their action, and that these effects are additive.

(v) that the action of loads or effects is static and independent of time.

The first assumption implies that neither the temperature variations nor stresses are large when compared with the ultimate.

The second assumption implies that no distinction is needed between the coordinates of a particle before and after deformation, and that the displacement gradients are small when compared with the sizes of members.

The third assumption implies that the material properties are uniform throughout and that the material responds linearly and elastically to the applied forces.

The fourth assumption implies that if there are two or more influences acting together, their effect on stresses and deformations can be considered as additive in any sequence of their action.

The last assumption is self-explanatory. However, the method of force-displacement can be applied to non-static forces such as dynamic, wind, waves or earthquake forces, etc.

The analysis of statically indeterminate structures require that the following three conditions be satisfied simultaneously throughout the structure:-

(a) the conditions of equilibrium of forces

(b) the conditions of compatibility of deformations, and

(c) load-deflection characteristics of all members.

A system of linear homogeneous equations are set, expressing the conditions of compatibility of deformations and equilibrium of forces, from which the unknown moments and deflections are calculated simultaneously. The load-deflection characteristics of members are used in terms of angular linear or torsional flexibility coefficients.

4.02 Flexibility Coefficients

Before commencing the application of the method, it is necessary to develop the expressions for angular flexibility coefficient which will be used in setting out the conditions of compatibility of deformations for structures in which bending moments are the predominant forces.

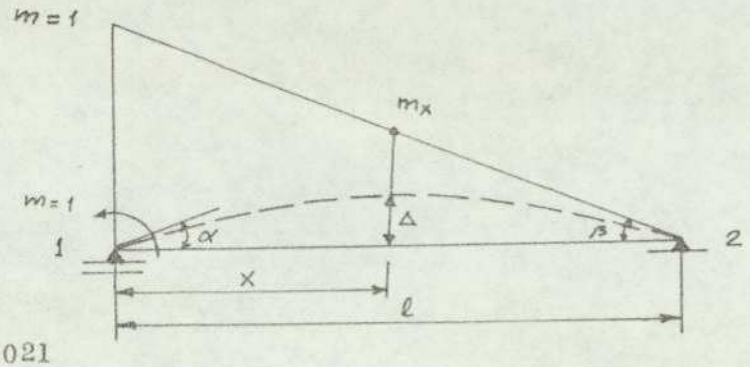

Fig. 4.021

In order to determine the angular flexibility coefficient, a simply supported beam, as shown in fig. 4.021, is subjected to a unit bending moment $m_1 = 1$. The resulting angular deformations at the ends of the beam are defined as the flexibility coefficients. These can be calculated either from the differential equation of the deflected line of a beam or from the Unit Load equation. The latter is in the general form:

$$\theta \text{ or } \Delta = \int_0^{\ell} \frac{M.m.dx}{EI}$$

in which M is the bending moment at any distance x resulting from the applied system of loading, and m_x is the moment at any distance x due to the unit force or moment applied in the direction and at the place of the required deformation.

For the case shown in fig. 4.021, M is therefore equal to m_x and

$$\alpha = \int_0^{\ell} \frac{m_x^2\, dx}{EI} = \frac{1}{EI}\int_0^{\ell} 1.\left(\frac{\ell - x}{\ell}\right)^2 dx \qquad 4.02.01$$

from which

$$\alpha = f_{11} = \frac{\ell}{3EI} \qquad 4.02.02$$

Similarly, to calculate the angle β, a unit moment is applied at 2, which gives

$$\beta = \frac{1}{EI}\int_0^{\ell} 1.\left(\frac{\ell - x}{\ell}\right).\left(\frac{x}{\ell}\right) dx \qquad 4.02.03$$

from which

$$\beta = f_{21} = \frac{\ell}{6EI} \qquad 4.02.04$$

f_{11} and f_{21} are the flexibility coefficients.

4.03 Load Functions

When loads are applied to a member, the required values in this method are the angular deformations at the ends of the beam assumed to be simply supported. Under normal loading conditions, uniformly distributed loads and point loads are the most commonly dealt with, and the load functions can be shown based on the unit load method to be as follows:-

$$\theta_a = \theta_b = \frac{w\ell^3}{24EI} \quad \text{for U.D. Load} \qquad 4.03.01$$

and

$$\left.\begin{aligned} \theta_a &= \frac{M_o}{6EI}(\ell + b) \\ \theta_b &= \frac{M_o}{6EI}(\ell + a) \end{aligned}\right\} \text{for point Load} \qquad 4.03.02$$

However, for thermal stresses, the load function that would be required would be the one that would be imposed by the effect of a linear temperature distribution or a curvilinear temperature distribution in a member, again assumed to be simply supported

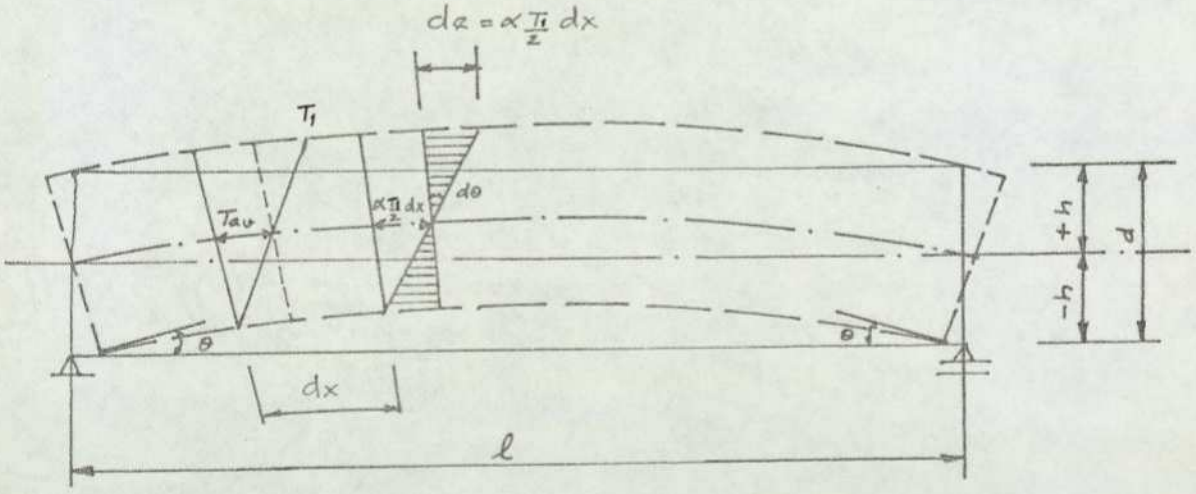

Fig 4.031 Deformations in a beam due to a linear temperature distribution

When a linear or curvilinear temperature distribution is applied to a member in the statically determinate condition as shown in fig. 4.031, it will cause the member to deflect upwards, and the axial

deformation of an element dx as well as bending deformations of the external fibres are equal to:

$$d\varepsilon = \frac{\alpha T_1}{2} dx \qquad 4.03.03$$

and the angular change in an element is:

$$d\theta = \frac{d\varepsilon}{h} = \alpha\left(\frac{T_1}{2}\right)\frac{dx}{h} \qquad 4.03.04$$

from which

$$\theta = \int_0^{\ell/2} d\theta = \frac{\alpha T_1 \ell}{2d} \qquad 4.03.05$$

since the curvature of the beam is

$$\frac{1}{R} = \frac{d\theta}{dx} = \frac{M}{EI} = \frac{\alpha T_1}{d} \qquad 4.03.06$$

from which

$$R = \frac{d}{\alpha T_1} \qquad 4.03.07$$

and

$$M = \frac{\alpha T_1 EI}{d} = \frac{2EI\theta}{\ell} \qquad 4.03.08$$

Equation 4.03.08 can alternatively be obtained by the force-displacement method from:

$$M\left(\frac{\ell}{3EI} + \frac{\ell}{6EI}\right) = \theta = \frac{\alpha T_1 \ell}{2d}.$$

The deflection Δ at any point on the beam can be calculated by the Unit load method, which gives

$$\Delta = \frac{\alpha T_1 ab}{2d} \qquad 4.03.09$$

where a and b are the distances from left and right to the point at which deflection is required.

If $a = b = \frac{\ell}{2}$

$$\Delta \text{ max.} = \frac{\alpha T_1 \ell^2}{8d} \qquad 4.03.10$$

It is interesting to note that where the effect of temperature is concerned, neither θ nor Δ depend on the actual stiffness of the member, but the equivalent bending moment (constant throughout the length of the beam) which would produce a similar curvature in a beam, is:

$$M = \frac{\alpha T_1 EI}{d} = M^F$$

i.e. it depends on the actual stiffness of the beam, but does not depend on the length of the beam.

4.04 Application of the Force-Displacement Method to the analysis of structures

4.04.1 Combined linear and constant temperature distribution in a column of a single-storey frame

The basic approach to the force-displacement method is to let the frame deflect to its equilibrium position defined by the unknown deflection Δ_o as shown in fig. 4.041

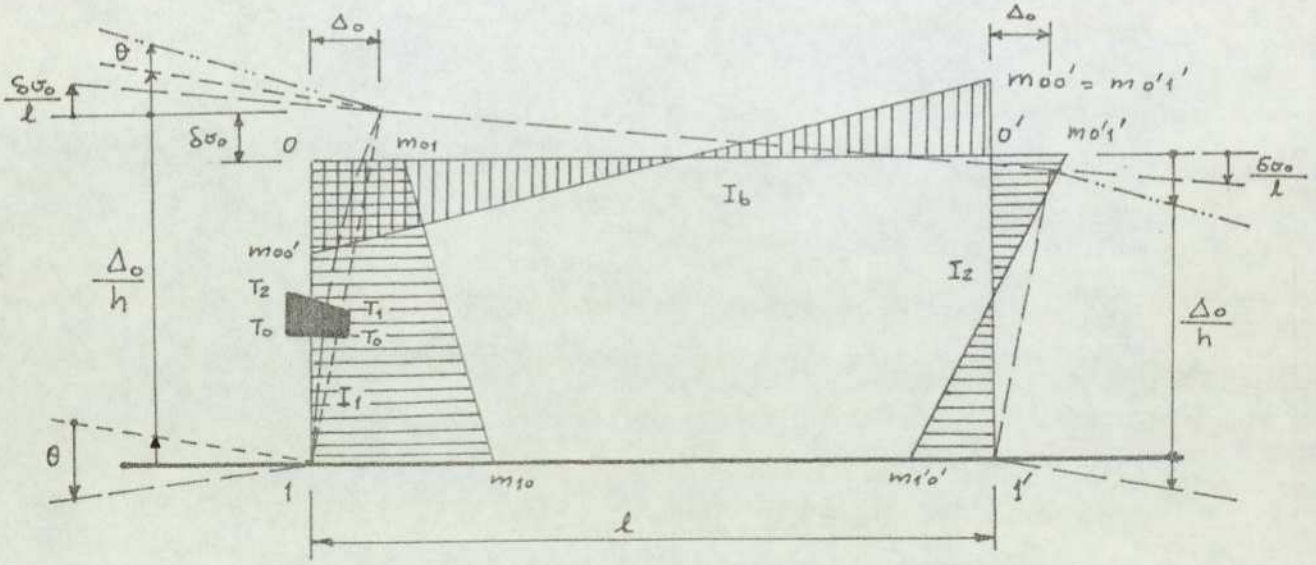

Fig. 4.0411 Assumed bending moments and deformations diagrams for combined linear and constant temperature distribution in a column.

The distribution of bending moments are assumed arbitrarily of any form, but the rest of the procedure must closely correspond to this assumption. A negative sign of bending moments or deflections obtained from the solution will indicate that the original assumption was incorrect

4.04.1.1 Sign Convention

The sign convention in this method is not related to the clockwise direction or to the hogging or sagging moments. The sign convention follows from the use of the principle of Virtual Work, so that the displacement set should correspond to the force set, i.e. the same sign must be used for both: if a moment is assumed positive, then the corresponding deformation is also positive. In other words: moments are positive if their action closes the assumed discontinuity, and negative if it increases.

The next step is to release all the members from their continuity at the joints so that each member becomes statically determinate and stresses are zero. In this released configuration, all the discontinuities between the respective members meeting at each joint are noted.

Next, statically indeterminate bending moments of such magnitude as are necessary are re-applied so as to restore the structure to full compatibility of deformations at all joints simultaneously. This procedure assures that strains or deflections in the adjoining elements will become compatible.

The setting out of the conditions of compatibility of deformations requires a knowledge of the stress-strain or the load-deflection characteristics of each element (see following page). The number of independent conditions of compatibility of deformations depend on the number of members meeting at a joint, e.g. with two members, only one such condition is required and with three members, two independent conditions are required and so on.

Referring to Fig.4.04/1, the compatibility conditions at all joints are as follows:-

F100' $$m_{10}\frac{h}{6EI_1} + m_{01}\left(\frac{h}{3EI_1} + \frac{l}{3EI_b}\right) - m_{01}'\frac{l}{6EI_b} = \frac{\Delta_0}{h} + \theta - \frac{\delta v_0}{l}$$

F10 $$m_{10}\frac{h}{3EI_1} + m_{01}\frac{h}{6EI_1} = -\frac{\Delta_0}{h} + \theta$$

F1'0'0 $$-m_{10}'\frac{h}{6EI_2} + m_{01}'\left(\frac{h}{3EI_2} + \frac{l}{3EI_b}\right) - m_{01}\frac{l}{6EI_b} = \frac{\Delta_0}{h} - \frac{\delta v_0}{l}$$

F1'0' $$m_{10}'\frac{h}{3EI_2} - m_{01}'\frac{h}{6EI_2} = \frac{\Delta_0}{h}$$

In the above equations, $$\frac{\delta v_0}{l} = \left\{T_1 + (T_2 - T_1)\frac{1}{2}\right\}\alpha\frac{h}{l}$$

$$\theta = \alpha(T_2 - T_1)\frac{h}{2d}$$

The second set of conditions which a structure must satisfy are the conditions of equilibrium of forces. This means that all members (and the whole structure) must be in equilibrium with the external forces. In this case only one such condition is required which can be written as follows:

E11' $$\frac{m_{10} - m_{01}}{h} - \frac{m_{10}' + m_{01}'}{h} = 0$$

The above five equations can now be arranged in a matrix form and solved for the unknown bending moments and deflections.

CHAPTER FIVE

5.00 ANALYSIS OF THERMAL STRESSES AND DEFORMATIONS OF VARIOUS STRUCTURES

5.01 THERMAL STRESSES IN CONTINUOUS BEAMS

5.01.1 Constant temperature distribution in continuous beams

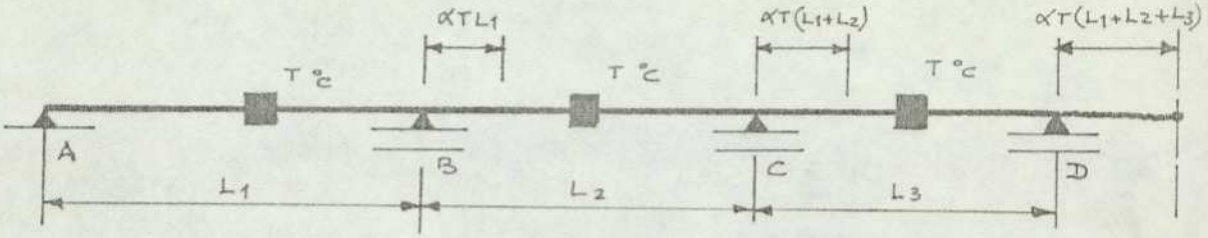

(a)

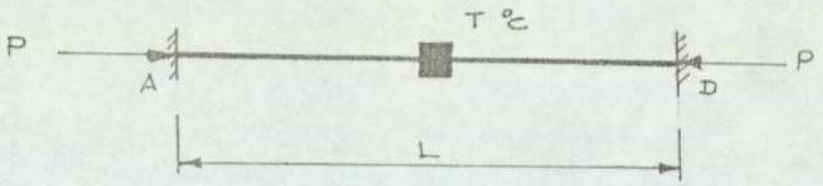

(b)

Fig. 5.0111 The effect of constant temperature distribution in continuous beams

If a continuous beam, such as shown in fig. 5.0111(a) is subjected to a constant temperature change $T^{o}C$ and is supported by "ideally frictionless" bearings, then theoretically it will be free from stresses but will extend or shorten on fall or rise of temperature by:

$$\Delta L = \alpha TL$$

If, on the other extreme, the beam is fully restrained at the far ends A and D, fig. 5.0111(b), then the horizontal force exerted on the abutments could be of the value:

$$P = (\alpha T)\, EA$$

in which αT is the total strain

α being the coefficient of thermal expansion

T the temperature change

E is the modulus of elasticity of the material, and

A is the cross-sectional area of beam.

In practice, the structural members are usually monolithic and continuous and therefore thermal stresses can occur even with uniform temperature.

5.01.2 Linear temperature distribution in a beam

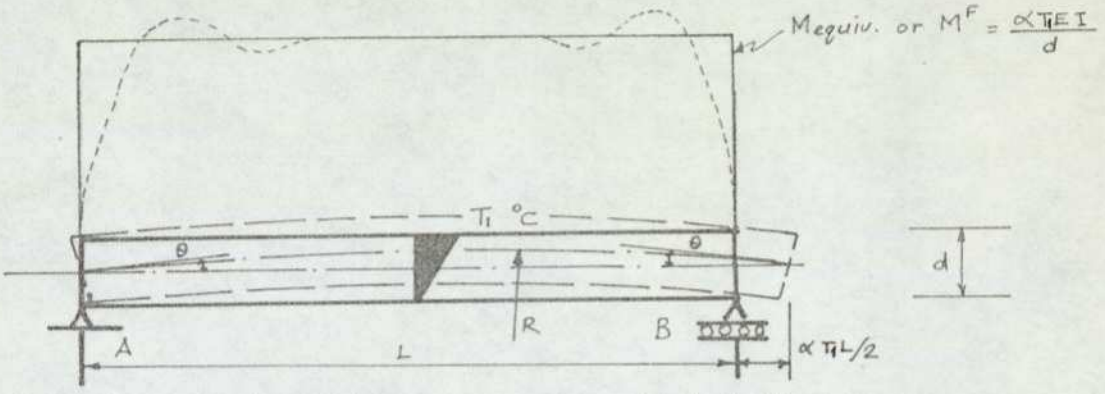

Fig.5.012 The effect of linear temperature distribution in a simply supported beam

Since the curvature of the beam is:

$$\frac{1}{R} = \frac{d\theta}{dx} = \frac{M}{EI} = \frac{\alpha T_1}{d} \qquad - - - \text{(i)}$$

from which

$$R = \frac{d}{\alpha T_1} \; ; \; \theta = \int_0^{L/2} d\theta = \frac{\alpha T_1 L}{2d} \qquad - - - \text{(ii)}$$

and $$\text{Mequiv. or } M^F = \frac{\alpha T_1 E I}{d} \qquad - - - \text{(iii)}$$

The value of M^F represents a bending moment required to prevent the beam from bending, or an equivalent bending moment required to produce curvature similar to that due to change of temperature.

Similarly, by using the unit load method, it can be shown that the maximum deflection,

$$\max \Delta = \frac{\alpha T_1 L^2}{8d} \qquad - - - \text{(iv)}$$

The above equations show that neither θ nor Δ depend on the actual stiffness of the member. However, the equivalent bending moment depends on the actual stiffness of the beam, but does not depend on the length of the beam.

It is interesting to note, however, that when the temperature change is curvilinear throughout the beam depth, then even a simply supported beam is subjected to the internal stresses which are "self-equilibrating". This is, however, outside the scope of this work and will not be discussed further.

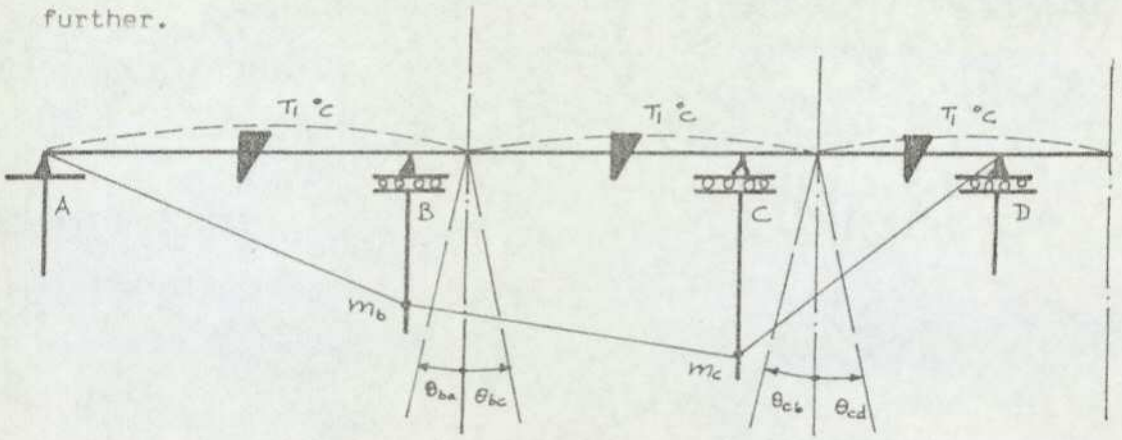

Fig. 5.0122 The effect of linear temperature distribution in a continuous beam

When statically indeterminate structures are subjected to a temperature change, stresses and deformations develop irrespective of whether the heat flow is steady or unsteady, and whether the temperature distribution is linear or curvilinear.

The effect of linear temperature change on continuous structures can be studied using the expression shown in equation (ii), and the compatibility equations can now be written at points B and C. For a three-span beam these are:

at B $\quad Mb\left(\frac{L1}{3EI1} + \frac{L2}{3EI2}\right) + Mc\,\frac{L2}{6EI2} + \theta ba + \theta bc = \frac{\alpha T_1}{2}\left(\frac{L1}{d1} + \frac{L2}{d2}\right)$

at C $\quad Mb\,\frac{L2}{6EI2} + Mc\left(\frac{L2}{3EI2} + \frac{L3}{3EI3}\right) = \theta cb + \theta cd = \frac{\alpha T_1}{2}\left(\frac{L2}{d2} + \frac{L3}{d3}\right)$

from which the bending moments at B and C can be calculated.

It can be seen from the above equations that the statically indeterminate bending moments arising from temperature do not depend on the actual spans but on their ratios L1/L2 and L1/L3 and are directly related to the stiffness of beams EI.

5.02 THERMAL STRESSES IN A CANTILEVER SHEAR WALL OR COLUMN SUBJECTED TO A LINEAR TEMPERATURE DISTRIBUTION

In the analysis of thermal stresses in building frames, it is useful and interesting to find first the deformations of a free standing solid cantilever as shown in fig. 5.021

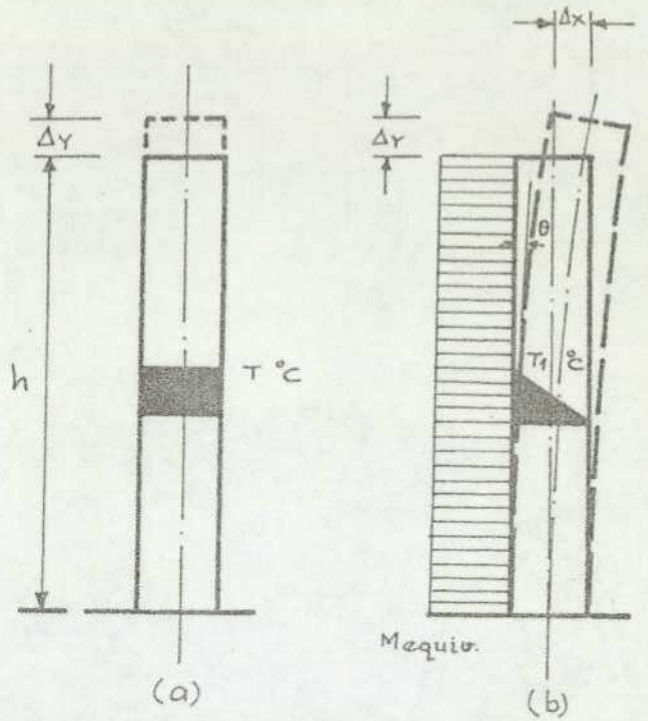

Fig. 5.021 Cantilever shear walls or columns subjected to temperature changes

In the case of constant temperature distribution, as shown in fig. 5.021(a), the cantilever undergoes vertical extension only and no stresses are introduced. The vertical extension would be:

$$\Delta y = \alpha T h$$

When the cantilever is subjected to a linear temperature distribution, as shown in fig. 5.021(b), in addition to the dimensional changes θ, Δx and Δy, bending moments are also introduced. These deformations and bending moments can be calculated by using the force-displacement method as follows:-

$$m \left(\frac{h}{3EI} + \frac{h}{6EI}\right) = \theta = \frac{\alpha T_1 h}{2d}$$

Also $$\theta = \frac{\Delta x}{h}$$

from above $$m = \frac{\alpha T_1 EI}{d}$$

$$\Delta x = \frac{\alpha T_1 h^2}{2d}$$

and $$\Delta y = \frac{\alpha T_1 h}{2}$$

The value of bending moment m represents the bending moment required to restrain the cantilever from bending.

The radius of curvature can be obtained from the equation (ii)

$$R = \frac{d}{\alpha T_1}$$

5.03 ANALYSIS OF A FIXED-END PORTAL FRAME

5.03.1 Introduction

In the analysis of statically indeterminate structures (e.g. portal frames for lateral forces) by the conventional flexibility method, the unknown values are forces (i.e. bending moments or reactions). The term 'force-displacement' or 'mixed flexibility' is used to describe the procedure in which calculations include the unknown forces and displacements of joints simultaneously. This approach is particularly useful in the analysis of tall frames, shear walls and other interconnected structures for primary as well as for secondary effects, such as the effect of temperature, creep and shrinkage. The general assumptions on which the analysis is based are those inherent in all elastic analyses, but can also be extended beyond these limitations.

When statically indeterminate structures are subjected to a temperature change, stresses and deformations develop irrespective of whether the heat flow is steady or unsteady, and whether the temperature is constant, linear or curvilinear. In the following analyses, these stresses and deformations are determined for various framed structures based on the concept of the force-displacement method. As a first example a simple portal frame is analysed.

ANALYSIS OF A FIXED-END PORTAL FRAME

5.03.2 Constant temperature distribution in the beam

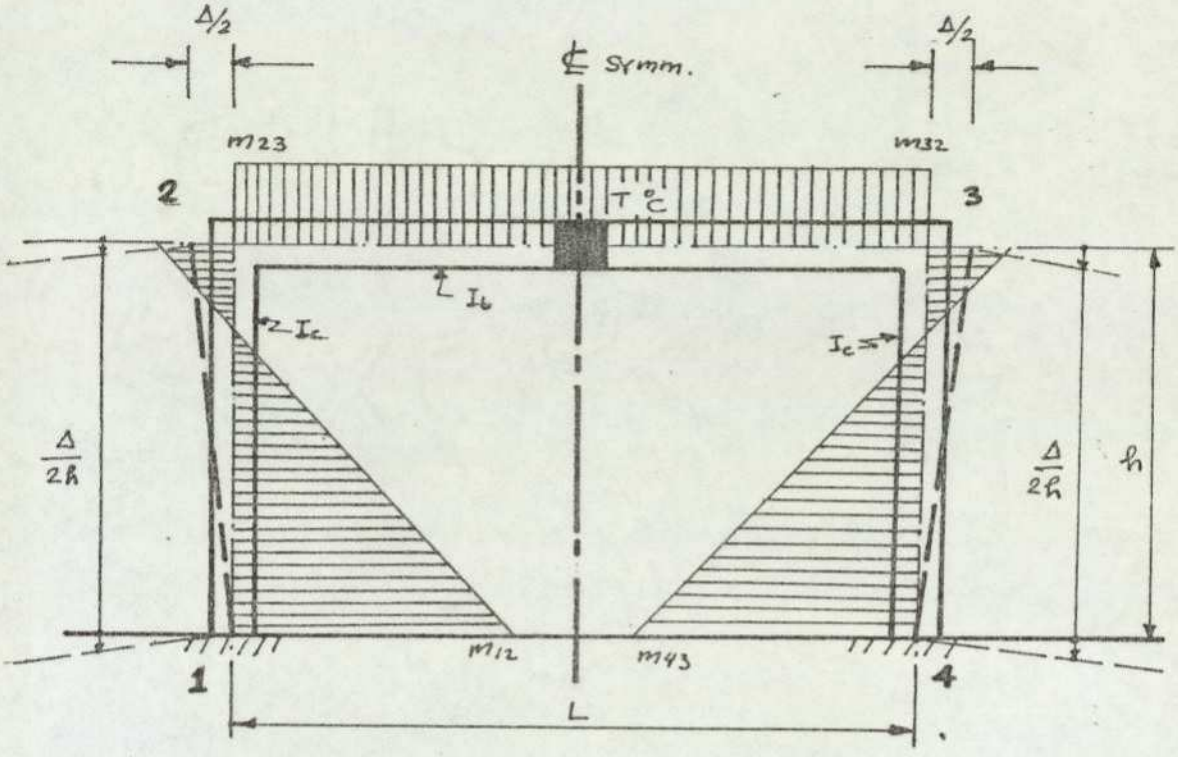

Fig. 5.0321 The effect of constant temperature distribution on a portal frame beam

For a symmetrical frame, the compatibility of deformations at joints (1) and (2) gives

F.1 $$m12\left(\frac{h}{3EIc}\right) - m21\left(\frac{h}{6EIc}\right) = \frac{\Delta}{2h}$$

F.2 $$-m12\left(\frac{h}{6EIc}\right) + m21\left(\frac{h}{3EIc} + \frac{h}{2EIb}\right) = \frac{\Delta}{2h}$$

in which $\Delta = \alpha TL$

from eqns. F.1 and F.2

$$m12 = \frac{3}{2}\,\frac{\Delta E}{h}\left(\frac{Ic}{h} + \frac{Ib}{nh + 2L}\right)$$

and $m21 = \frac{3\Delta}{h} \frac{EIb}{nh + 2l}$

where $n = Ib/Ic$

Numerical Example: Numerical examples are used to assess the magnitude of forces and displacements arising from changes of temperature.

In this numerical example, a frame of the following dimensions and properties is analysed.

$E = 28 \times 10^6$ KN/m^2

$\alpha = 0.00001$ per ^oC

$T = 20\ ^oC$

$Ic = Ib = 0.3 \times 0.6^3/12$
$= 0.0054\ m^4$

$d = 0.6m$

$A = 0.3 \times 0.6 = 0.18m^2$

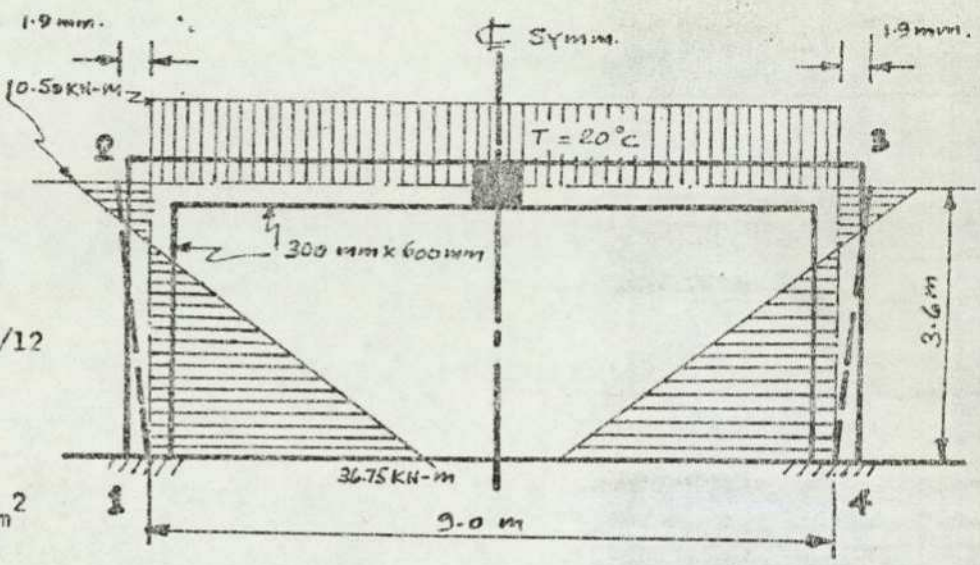

Fig.5.0322 Example frame showing member sizes and bending moments

Substituting the numerical values into eqns. (F.1) and (F.2) gives

$$m12 = \frac{3}{2} \cdot \frac{(0.00001 \times 20 \times 9)\ 28\ 10^6 \times 0.0054}{3.6} \frac{1}{3.6} + \frac{1}{(1 \times 3.6 + 2 \times 9)}$$

$$= 36.75 \text{ KN-m}$$

and $$m21 = \frac{3(0.00001 \times 20 \times 9)}{3.6} \cdot \frac{28 \times 10^6 \times 0.0054}{(1 \times 3.6 + 2 \times 9)}$$

$$= 10.50 \text{ KN-m}$$

and deflection $\Delta = (0.00001 \times 20 \times 9)\ 10^3 = 1.8$ mm

5.03.3 Linear temperature distribution in the beam

The analysis of stresses and deformations for the effects of linear and constant temperature distributions can be carried out simultaneously. However, these are done separately in this work in order to demonstrate clearly the contributions of each type of temperature distribution.

Assuming the same bending moment diagram as in the case of the constant temperature distribution, shown in Fig. 5.0321, the compatibility of deformations at joints (1) and (2) for linear temperature distribution gives:-

F.1 $$m12\left(\frac{h}{3EIc}\right) - m21\left(\frac{h}{6EIc}\right) = \frac{\Delta}{2h}$$

F.2 $$-m12\left(\frac{h}{6EIc}\right) + m21\left(\frac{h}{3EIc} + \frac{L}{2EIb}\right) = \frac{\Delta}{2h} - \theta 21$$

in which $$\Delta = \tfrac{1}{2}\alpha TL$$

and $$\theta 21 = \frac{\alpha TL}{2d}$$

From eqns (F.1) and (F.2)

$$m12 = \frac{3}{2}\frac{\Delta E}{h}\left[\frac{Ic}{h} + \frac{Ib}{(nh + 2L)}\right] - \frac{2\theta 21\, EIb}{(nh + 2L)}$$

and

$$m21 = \left(\frac{3\Delta}{h} - 4\theta 21\right)\frac{EIb}{(nh + 2L)}$$

where $n = Ib/Ic$

Example

In the numerical example, the frame shown in Fig. 5.0321 is now analysed for the effect of linear temperature distribution in the beam.

Substituting the numerical values into eqns. (F.1) and (F.2) gives

$$m12 = \frac{3}{2}\frac{(\frac{1}{2} \times 0.00001 \times 20 \times 9)\ 28 \times 10^6}{3.6}\left[\frac{0.0054}{3.6} + \frac{0.0054}{(1 \times 3.6 + 2 \times 9)}\right] - \frac{2(0.00001 \times 20 \times 9)\ 28 \times 10^6 \times 0.0054}{(1 \times 3.6 + 2 \times 9)}$$

$$= -2.6250 \text{ KN-m}$$

and $$m21 = \left(\frac{3(\frac{1}{2} \times 0.00001 \times 20 \times 9)}{3.6} - \frac{4(0.00001 \times 20 \times 9)}{2 \times 0.6}\right) \frac{28 \times 10^6 \times 0.0054}{(1 \times 3.6 + 2 \times 9)}$$

$$= -36.7500 \text{ KN-m}$$

and $$\Delta = \frac{(0.00001 \times 20 \times 9)}{2} 10^3 = 0.9 \text{ mm}$$

The negative sign indicates that the actual bending moments are of opposite sign to those assumed. Fig. 5.0331 below shows the resulting bending moment diagram for the effect of linear temperature distribution in the beam.

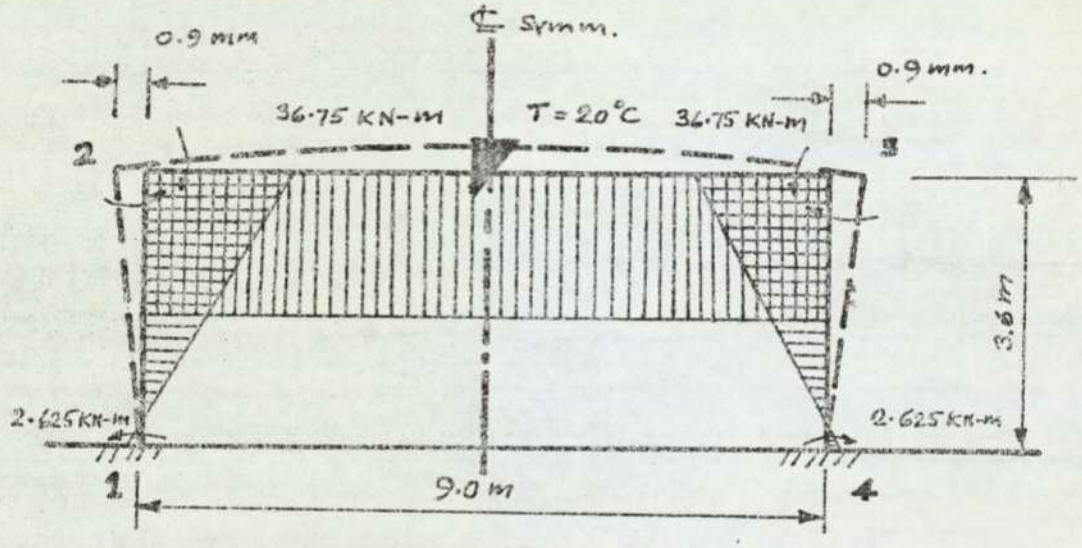

Fig.5.0331 Bending moment diagram for the effect of linear temperature distribution in the beam

5.03.4 Constant temperature distribution in a column

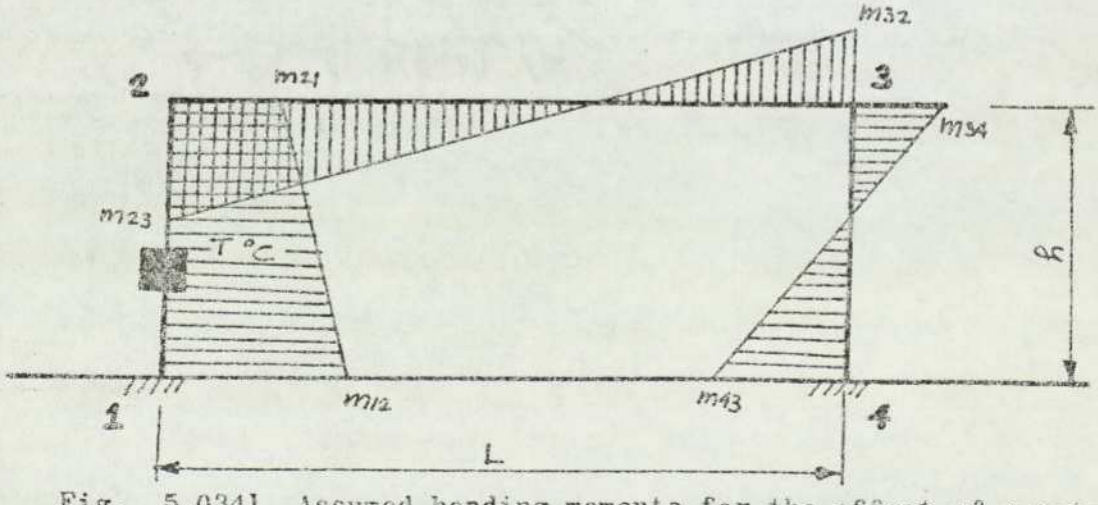

Fig. 5.0341 Assumed bending moments for the effect of constant temperature distribution in the column

For the effect of a constant temperature distribution in one column of a portal frame, the statically indeterminate bending moments and deflections can be obtained by setting out the equations of compatibility and equilibrium as follows:-

F.1 $$m12\left(\frac{h}{3EIc}\right) + m21\left(\frac{h}{6EIc}\right) = -\frac{\Delta}{h}$$

F.2 $$m12\left(\frac{h}{6EIc}\right) + m21\left(\frac{h}{3EIc} + \frac{L}{3EIb}\right) - m34\left(\frac{L}{6EIb}\right) = \frac{\Delta}{h} - \frac{\delta v2}{L}$$

F.3 $$-m21\left(\frac{L}{6EIb}\right) + m34\left(\frac{L}{3EIb} + \frac{h}{3EIc}\right) - m43\left(\frac{h}{6EIc}\right) = \frac{\Delta}{h} - \frac{\delta v2}{L}$$

F.4 $$m43\left(\frac{h}{3EIc}\right) - m34\left(\frac{h}{6EIc}\right) = \frac{\Delta}{h}$$

E.1-4 $$\frac{m12 - m21}{h} - \frac{m43 + m34}{h} = o$$

In the above equations, $\Delta = \alpha Th$, and $\delta v2/L = \frac{\alpha Th}{L}$.

Putting the above equations into matrix form gives:

	1	2	3	4	5			
1	$\frac{h}{3EIc}$	$\frac{h}{6EIc}$	0	0	$+\frac{1}{h}$		m12	0
2	$\frac{h}{6EIc}$	$\left(\frac{h}{3EIc} + \frac{L}{3EIb}\right)$	$-\frac{L}{6EIb}$	0	$-\frac{1}{h}$		m21	$-\frac{\delta v2}{L}$
3	0	$-\frac{L}{6EIb}$	$\left(\frac{L}{3EIb} + \frac{h}{3EIc}\right)$	$-\frac{h}{6EIc}$	$-\frac{1}{h}$		m34	$-\frac{\delta v2}{L}$
4	0	0	$-\frac{h}{6EIc}$	$+\frac{h}{3EIc}$	$-\frac{1}{h}$		m43	0
5	1	-1	-1	-1	0		Δ	0

Table: 500.01

The solution of the above matrix gives the bending moments and deflections in the frame due to the effect of constant temperature distribution in a column.

Example

In the numerical example, the frame shown in Fig. 5.0321 is analysed for the constant temperature distribution in the column. The resulting bending moments and deflections are as follows:-

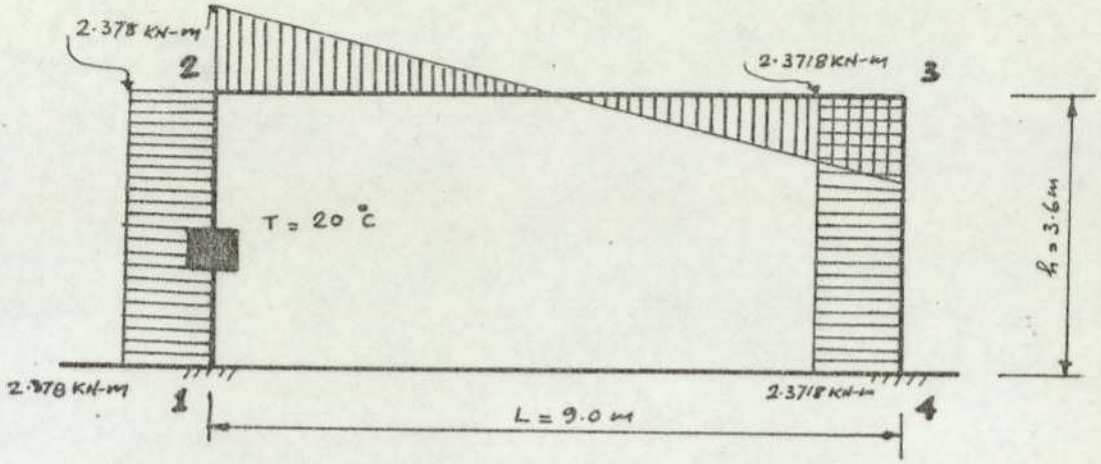

Fig. 5.0342 Actual bending moment diagram for the effect of constant temperature distribution in the column.

5.03.5 Linear temperature distribution in a column

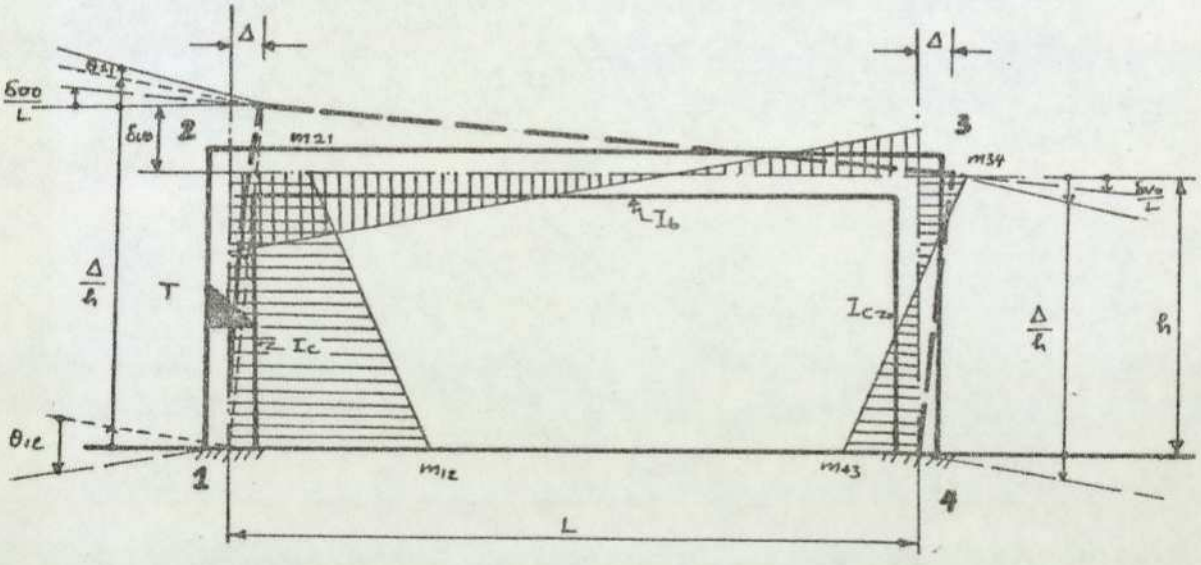

Fig. 5.0351 Stresses due to linear temperature distribution in a portal frame column

The effect of linear temperature distribution affecting one column in a portal frame can be determined from the following equations of compatibility and equilibrium.

F.1 $$m12\left(\frac{h}{3EIc}\right) + m21\left(\frac{h}{6EIc}\right) = -\frac{\Delta}{h} + \theta 12$$

F.2 $$m12\left(\frac{h}{6EIc}\right) + m21\left(\frac{h}{3EIc} + \frac{L}{3EIb}\right) - m34\left(\frac{L}{6EIb}\right) = \frac{\Delta}{h} + \theta 21 - \frac{\delta v2}{L}$$

F.3 $$-m21\left(\frac{L}{6EIb}\right) + m34\left(\frac{L}{3EIb} + \frac{h}{3EIc}\right) - m43\left(\frac{h}{6EIc}\right) = \frac{\Delta}{h} - \frac{\delta v2}{L}$$

F.4 $$m43\left(\frac{h}{3EIc}\right) - m34\left(\frac{h}{6EIc}\right) = \frac{\Delta}{h}$$

E.14 $$\frac{m12 - m21}{h} - \frac{m43 + m34}{h} = 0$$

In the above equations $$\frac{\delta v2}{L} = \frac{\alpha Th}{2L}$$

and $$\theta 12 = \theta 21 = \frac{\alpha Th}{2d}$$

Example

As a numerical example, the frame shown in Fig. 5.0321 is analysed for the linear temperature distribution in the column. The resulting bending moments and deflections are as follows:-

m12 = 52.3024 KN-m

m21 = 20.8024 KN-m

m34 = 12.4024 KN-m

m43 = 19.0976 KN-m

Δ = 0.3685 mm

5.03.6 Linear temperature distribution in a column taking into consideration the secondary effect of axial deformations

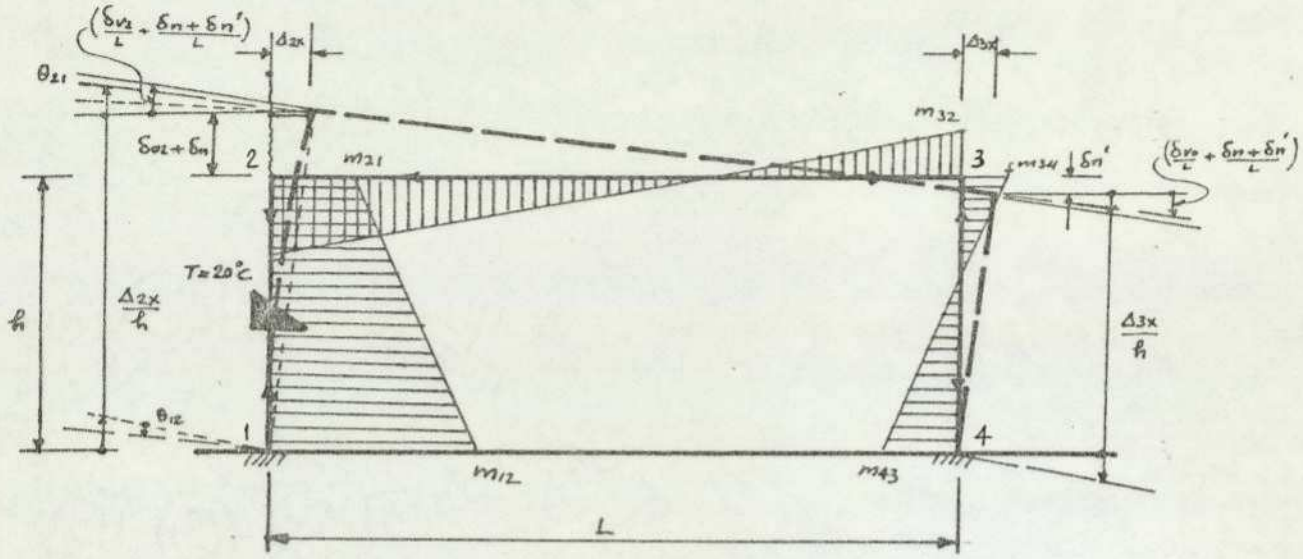

Fig. 5.0361 Assumed stresses due to linear temperature distribution in a portal frame column including the effect of axial deformations

The effect of axial deformations in the analysis of thermal stresses is not usually very high. However, if the problem warrants it, these can be taken into account as follows:-

Denoting $$\delta v2 = \frac{\alpha T h}{2}$$

$$\theta 12 = \theta 21 = \frac{\alpha T h}{2d}$$

$$\delta n = \delta n' = \frac{m23 + m32}{L} \frac{h}{EA} = \frac{N12}{EA} h$$

The equations of compatibility of deformations and equilibrium of forces for this case become:

F.1 $$m12\left(\frac{h}{3EIc}\right) + m21\left(\frac{h}{6EIc}\right) = -\frac{\Delta 2x}{h} + \theta 12$$

or $$2r1\ m12 + r1\ m21 + R\ \Delta 2x \frac{L}{h} = \frac{3C}{d}$$

F.2 $$m12\left(\frac{h}{6EIc}\right) + m21\left(\frac{h}{3EIc} + \frac{L}{3EIb}\right) - m34\left(\frac{L}{6FIb}\right) = \frac{\Delta 2x}{h} + B21 - \frac{\delta v2}{L} - \frac{\delta n + \delta' n}{L}$$

or $$r1m12 + 2(r1 + 1 + P)\, m21 - (1 - 2P)\, m34 - R\,\Delta 2x\,\frac{L}{h} = 3C\left(\frac{1}{d} - \frac{1}{L}\right)$$

F.3 $$-m21\left(\frac{L}{6EIb}\right) + m32\left(\frac{L}{3EIb} + \frac{h}{3EIc}\right) - m43\left(\frac{h}{6EIc}\right) = \frac{\Delta 3x}{h} - \frac{\delta v2}{L} - \frac{\delta n + \delta n'}{L}$$

or $$-(1-2P)\, m21 + 2(r1 + 1 + P)\, m34 - r1m43 - R\,\Delta 3x\,\frac{L}{h} = -\frac{3C}{L}$$

F.4 $$m43\left(\frac{h}{3EIc}\right) - m34\left(\frac{h}{6EIc}\right) = \frac{\Delta 3x}{h}$$

or $$2r1\, m43 - r1\, m34 - R\,\Delta 3x\,\frac{L}{h} = o$$

C.12 $$\frac{\alpha Th}{2} - (\delta v2 + \delta n) = \frac{N12\ L12}{A12\ E12}$$

C.34 $$\delta n' = \frac{N34\ L34}{A34\ E34}$$

or $$r\delta n' - N34\ S34 = o$$

C.23 $$\Delta 2x - \Delta 3x = \frac{N23\ L23}{A23\ E23}$$

or $$r\,\Delta 2x - r\,\Delta 3x - N23\ S23 = o$$

E.2x $$\frac{m12 - m21}{h} = N23$$

or $$m12 - m21 - h\ N23 = o$$

E.2y $$\frac{m21 + m34}{L} = N12$$

or $$m21 + m34 - L\ N12 = o$$

E.3x $$\frac{m34 + m43}{h} = N23$$

or $$m34 + m43 - h\ N23 = o$$

E.3y $$\frac{m34 + m21}{L} = N34$$

or $$m34 + m21 - L\ N34 = o$$

$$S12 = \frac{L12}{A12\ E12} \cdot \frac{An\ En}{Ln} \quad ; \quad S34 = \frac{L34}{A34\ E34} \cdot \frac{An\ En}{Ln} \quad ; \quad S23 = \frac{L23}{A23\ E23} \cdot \frac{An\ En}{Ln}$$

in which $r1 = \frac{h}{L}\frac{Ib}{Ic}$

$r = \frac{An\ En}{Ln}$ where An, En and Ln are properties of any member

$R = \frac{6EIb}{L^2}$

$C = \frac{\alpha\ ThEIb}{L}$

$P = \frac{6hIb}{AL^2}$

Based on the above equations, a general overall matrix can now be set out as shown in Table 500.02.

EQN No.	REF. Jr.	1		2				3			4		LOAD VECTOR
	REF. EQN.	m12	N12	m21	N23	Δ2x	Δ2y = (δv2+δn)	m34	Δ3x	Δ3y= δn'	m43	N34	
1	F.1	2r1	o	r1	o	$R\frac{L}{h}$	o						3 c/d
2	C.12	o	S12	o	o	o	r						$r \propto Th/2$
3	F.2	r1	o	2(r1+1+P)	o	$-R\frac{L}{h}$	o	-(1-2P)					$3c(\frac{1}{d} - \frac{1}{L})$
4	C.23	o	o	o	-S23	r	o		-r				o
5	E.2x	1	o	-1	-h	o	o						o
6	E.2y	o	-L	1	o	o	o	1	o	o	o	o	o
7	F.3			-(1-2P)				2(r1+1+P)	$-R\frac{L}{h}$	o	-r1	o	-3 c/d
8	E.3x				-h			1	o	o	1	o	o
9	E.3y			1				1	o	o	o	-L	o
10	F.4							-r1	$-R\frac{L}{h}$	o	2r1	o	o
11	C.34							o	o	r	o	-S34	o

Table 500.02 General matrix for a single storey portal frame for the effect of linear temperature distribution in a column taking into consideration the secondary effect of axial deformations.

EQN No.	REF JT. / REF EQN.	1		2				3			4		LOAD VECTOR
		m_{12}	N_{12}	m_{21}	N_{23}	Δ_{2X}	Δ_{2Y}	m_{34}	Δ_{3X}	Δ_{3Y}	m_{43}	N_{34}	
1	F.1	0.8	0	0.4	0	28,000	0						60.48
2	C.12	0	0.4	0	0	0	560,000						201.60
3	F.2	0.4	0	2.801778	0	-28,000	0	-0.99822					56.448
4	C.23	0	0	0	-1	560,000	0		-560,000				0
5	E.2x	1	0	-1	-3.6	0	0						0
6	E.2y		-9	1				1	0	0	0	0	0
7	F.3			-0.99822				2.801778	-28,000	0	-0.4	0	-4.032
8	E.3x				-3.6			1	0	0	1	0	0
9	E.3y			1				1	0	0	0	-9	0
10	F.4							-0.4	-28,000	0	0.8	0	0
11	C.34							0	0	560,000	0	-0.4	0

Table 500.03 Numerical matrix for a single storey portal frame for the effect of linear temperature distribution in a column taking into consideration the secondary effect of axial deformations.

Example

In the numerical example, the frame shown in fig. 5.0321 is analysed for the effect of linear temperature distribution in a column taking into consideration the secondary effect of axial deformations.

Before a numerical matrix can be set out, it is necessary to work out the following parameters:-

$$r1 = \frac{h}{L} \cdot \frac{Ib}{Ic} = \frac{3.6}{9} \cdot \frac{0.0054}{0.0054} = 0.4$$

$$r = \frac{Ab\,Eb}{Lb} = \frac{0.18 \times 28 \times 10^6}{9} = 56 \times 10^4 \text{ KN/m}$$

$$R = \frac{6E\,Ib}{L^2} = \frac{6 \times 28 \times 10^6 \times 0.0054}{9^2} = 11200 \text{ KN}$$

$$R\frac{L}{h} = 11200 \times \frac{9}{3.6} = 28000 \text{ KN}$$

$$C = \frac{\alpha\, Th E Ib}{L} = \frac{0.00001 \times 20 \times 3.6 \times 28 \times 10^6 \times 0.0054}{9} = 12.096 \text{ KN-m}^2$$

$$\frac{3C}{d} = \frac{3 \times 12.096}{0.6} = 60.48 \text{ KN-m}$$

$$3C\left(\frac{1}{d} - \frac{1}{L}\right) = 3 \times 12.096 \left(\frac{1}{0.6} - \frac{1}{9}\right) = 56.448 \text{ KN-m}$$

$$\frac{3C}{L} = -3 \times \frac{12.096}{9} = -4.032 \text{ KN-m}$$

$$\frac{rT\alpha h}{2} = 56 \times 10^4 \times 20 \times 0.00001 \times \frac{3.6}{2} = 201.60 \text{ KN}$$

$$P = \frac{6hIb}{AL^2} = \frac{6 \times 3.6 \times 0.0054}{0.18 \times 9^2} = 0.00088889\text{m}$$

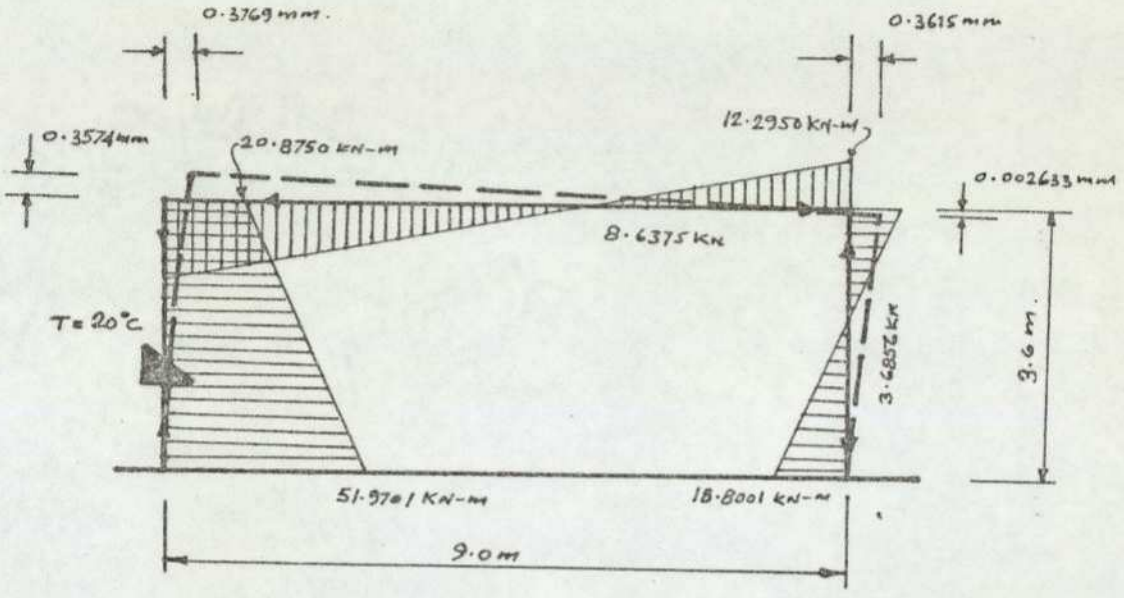

Fig. 5.0362 Diagram showing stresses due to the effect of linear temperature distribution in a column including the effect of axial deformations

5.03.7 DISCUSSION OF RESULTS OF CONSTANT TEMPERATURE AND LINEAR TEMPERATURE DISTRIBUTIONS IN THE ROOF BEAM AND COLUMN OF A PORTAL FRAME

An inspection of the results of sections 5.03.2 and 5.03.3 show that the bending moments in all the members of section 5.03.3 are of opposite sign to those of section 5.03.2 i.e. they have been reversed. In section 5.03.2 tension occurs at the top or outside fibres of the beam. In the columns, the top portion of the column has tension on the outside while the bottom portion has tension on the inside. In section 5.03.3 the reverse take place. It is interesting to note that for the same maximum temperature rise, the maximum bending moment is of the same magnitude in either case, although it does not occur at the same location.

In most practical cases of temperature rises in structural members, the initial rise can be of linear or curvilinear form. As the temperature rises, the distribution will tend towards a combination of constant plus linear or curvilinear. This raises the possibility that a daily reversal of stresses takes place. Further, during this reversal process, two distinct stages could occur in which (1) the bending moment at the joint between the column and the beam may become zero and (2) the bending moment at the base of the column may be zero.

These two stages can be represented diagrammatically as follows:-

Stage (1) When B.M. in beam becomes zero

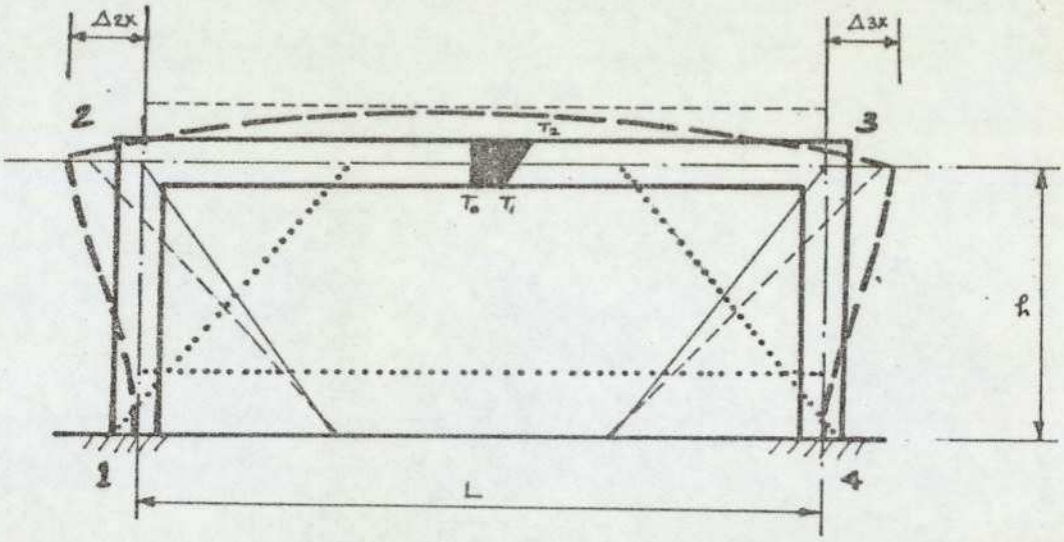

Fig. 5.0371 Special Stage (1)

Assumed bending moment diagrams due to the effects of constant and linear temperature distributions in the beam of a portal frame.

_ _ _ _ _ bending moment diagram for constant temperature distribution

..... bending moment diagram for linear temperature distribution

_____ bending moment diagram for a special Stage (1) of combined constant and linear distributions when bending moment in beam becomes zero.

Now $\Delta 2x = \Delta 3x$ symmetrical frame

and $2\Delta 2x = \alpha T1L + \alpha(T2-T1)\frac{L}{2}$

$$= \frac{\alpha T1L}{2} + \alpha T2\,\frac{L}{2}$$

$$\therefore \quad \Delta 2x = \frac{\alpha T1L}{4} + \alpha T2\,\frac{L}{4}$$

now writing the equations of compatibility of deformations

F.1 $$m12\frac{h}{3EIc} - m21\frac{h}{6EIc} = \frac{\Delta 2x}{h}$$

F.2 $$-m12\frac{h}{6EIc} + m21\left(\frac{h}{3EIc} + \frac{L}{2EIb}\right) = \frac{\Delta 2x}{h} - \theta 23 \quad \text{where } \theta 23 = \alpha(T2-T1)\frac{L}{2d}$$

when $m21 = o$

F.1 becomes $m12\frac{h}{3EIc} = \frac{T1L}{4h} + \frac{\alpha T2L}{4h}$ and

F.2 becomes $-m12\frac{h}{6EIc} = \frac{\alpha T1L}{4h} + \frac{\alpha T2L}{4h} - \left(\frac{\alpha T2L}{2d} - \frac{\alpha T1L}{2d}\right)$

From these equations it can be shown that

$$\frac{T1}{T2} = \frac{4h - 3d}{4h + 3d}$$

For a numerical problem as before i.e. L = 9m ; h = 3.6m ; d = 0.6m

$$T1 = \left(\frac{4 \times 3.6 - 3 \times 0.6}{4 \times 3.6 + 3 \times 0.6}\right) T2$$

i.e.

$$T1 = 0.77777\dot{} \;\; T2$$

and if $T2 = 20^{o}C$

$$T1 = 15.55555\dot{}\;{}^{o}C$$

With the above values of T1 and T2 the bending moment diagrams of constant and linear portions of the temperature distributions and also the combined distributions become as shown below in fig. 5.0372.

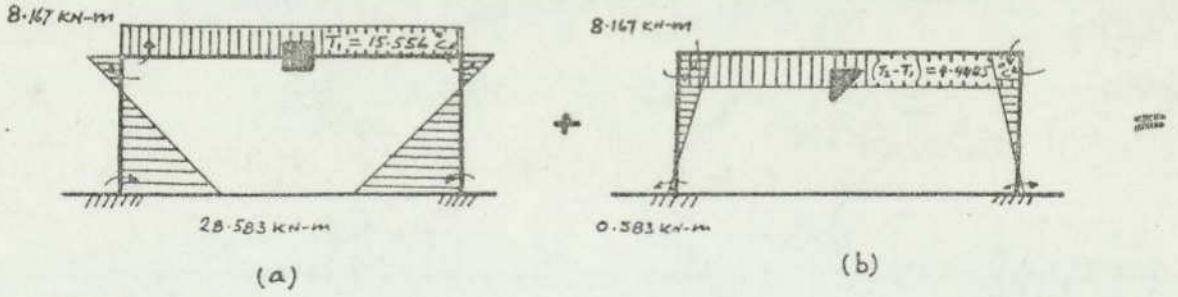

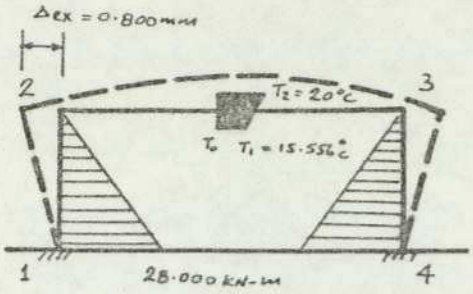

Fig. 5.0372 (c)

Special Stage (1), actual bending moment diagram for a constant and linear temperature distributions when bending moment in the beam becomes zero.

Stage (2) When B.M. at base of columns become zero

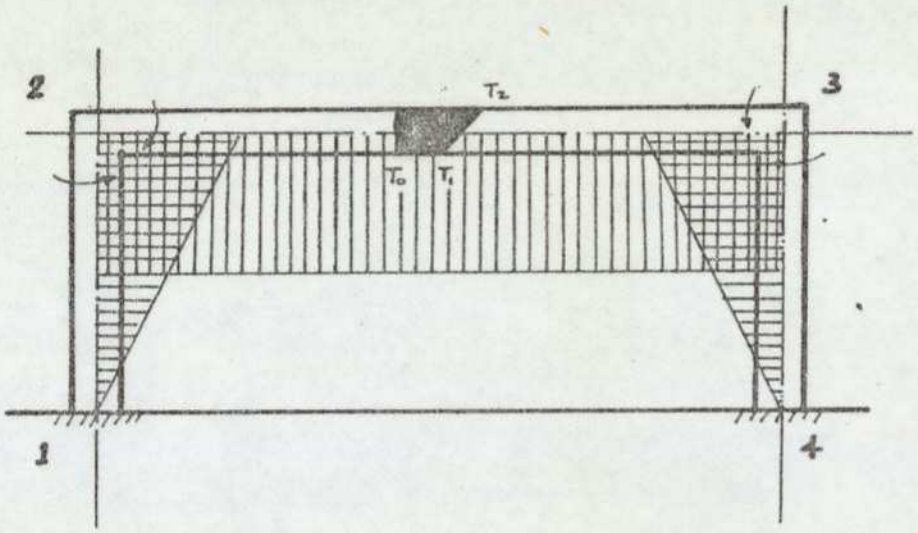

Fig.5.0373 Special Stage (2), assumed bending moment diagram for a constant and linear temperature distributions when bending moments at the base of the columns become zero.

When $m12 = 0$

F.1 becomes $-m21\frac{h}{6EIc} = \frac{\Delta 2x}{h}$ and

F.2 becomes $m21(\frac{h}{3EIc}) + m21(\frac{L}{2EIb}) = \frac{\Delta 2x}{h}$ - 823

It can now be shown that

$$\frac{T1}{T2} = \frac{3Ibhd + 3IcLd - 2Ibh^2}{-3Ibhd - 3IcLd - 2Ibh^2}$$

For the same numerical problem

$$T1 = 0.066666\dot{6}\ T2$$

when $T2 = 20^{o}C$

$$T1 = 0.066666\dot{6} \times 20 = 1.33333\dot{3}\ ^{o}C$$

With the above values of T1 and T2 the bending moment diagrams of constant and linear portions of the temperature distributions and also the combined distributions now become as shown below in fig. 5.0374.

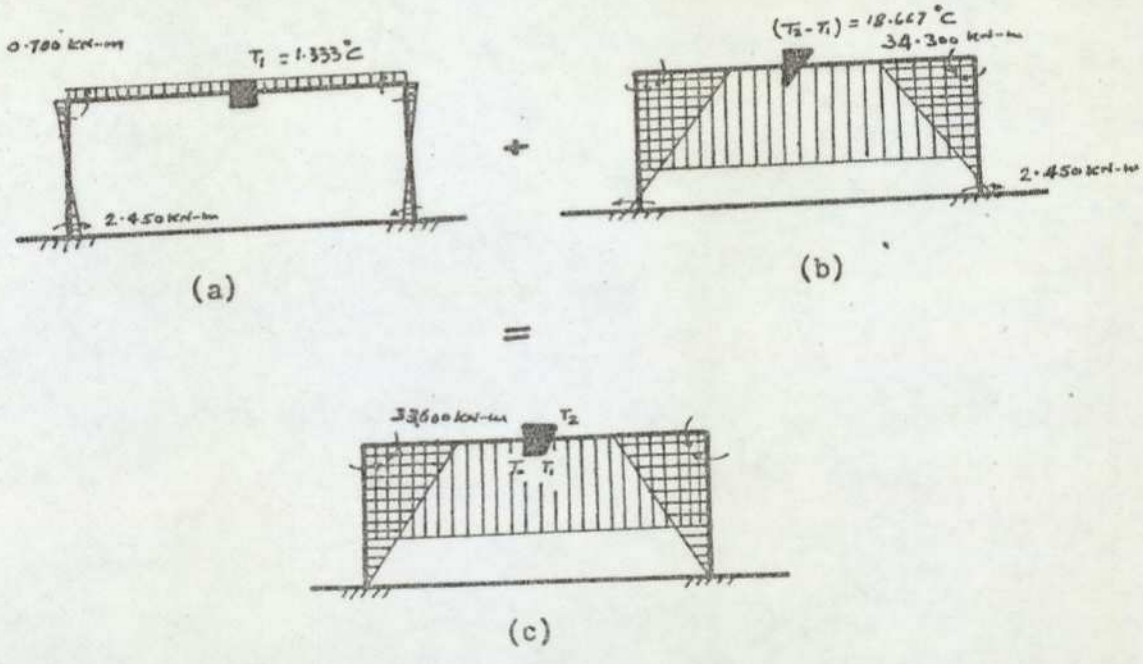

Fig.5.0374

Special stage (2), actual bending moment diagram for a constant and linear temperature distributions when bending moments at base of columns become zero.

The above two stages could occur everyday and sometimes on several occasions during the same day and may explain several phenomena:-

(a) The reasons why cracks occur at certain odd locations in a structure which up to now have had no explanation.

(b) Why some cracks are known to have been observed at some instant and then disappear a short period later even though the temperature does not appear to have altered.

From the bending moment diagrams, tension first occurs on the inside of the structure (mainly due to linear distribution), and if severe, resulting in cracks. The cracks on the columns may not be visible, due to the large gravity forces opposing and cancelling the tensile forces. However, the cracks on the underside of the beams should most likely be visible as the gravity forces will increase tensile stresses at the centre of the span. In many cases these cracks are also not noticeable as they are overhead and very often screened from sight by ceilings.

As more and more heat is absorbed by the structure, the tension reverses to the top surface of the beam. These are the cracks usually noticed, and also cause the greatest damage due to the penetration of rainwater causing corrosion of the reinforcement and spalling of concrete.

The bending diagrams of sections 5.03.4 and 5.03.5 exhibit similar behaviour as sections 5.03.2 and 5.03.3, i.e. as temperature in the column changes from one form to the other, the bending moments reverse signs at all points. During the transition period from one form of temperature to the other, it will pass through 4 distinct stages e.g. (i) bending moment at base of column one becomes zero, (ii) bending moment at base of column two becomes zero, (iii) bending moment at top of column one becomes zero, and (iv) bending moment at top of column two becomes zero.

It is also interesting to note that if the source of heat is at 45^{o} to the structure e.g. sun shining at 45^{o}, thermal effects can occur simultaneously in the roof and the column. The above analysis shows that a very large number of unusual stages can occur when one form of temperature changes to another form.

5.04.1 Introduction

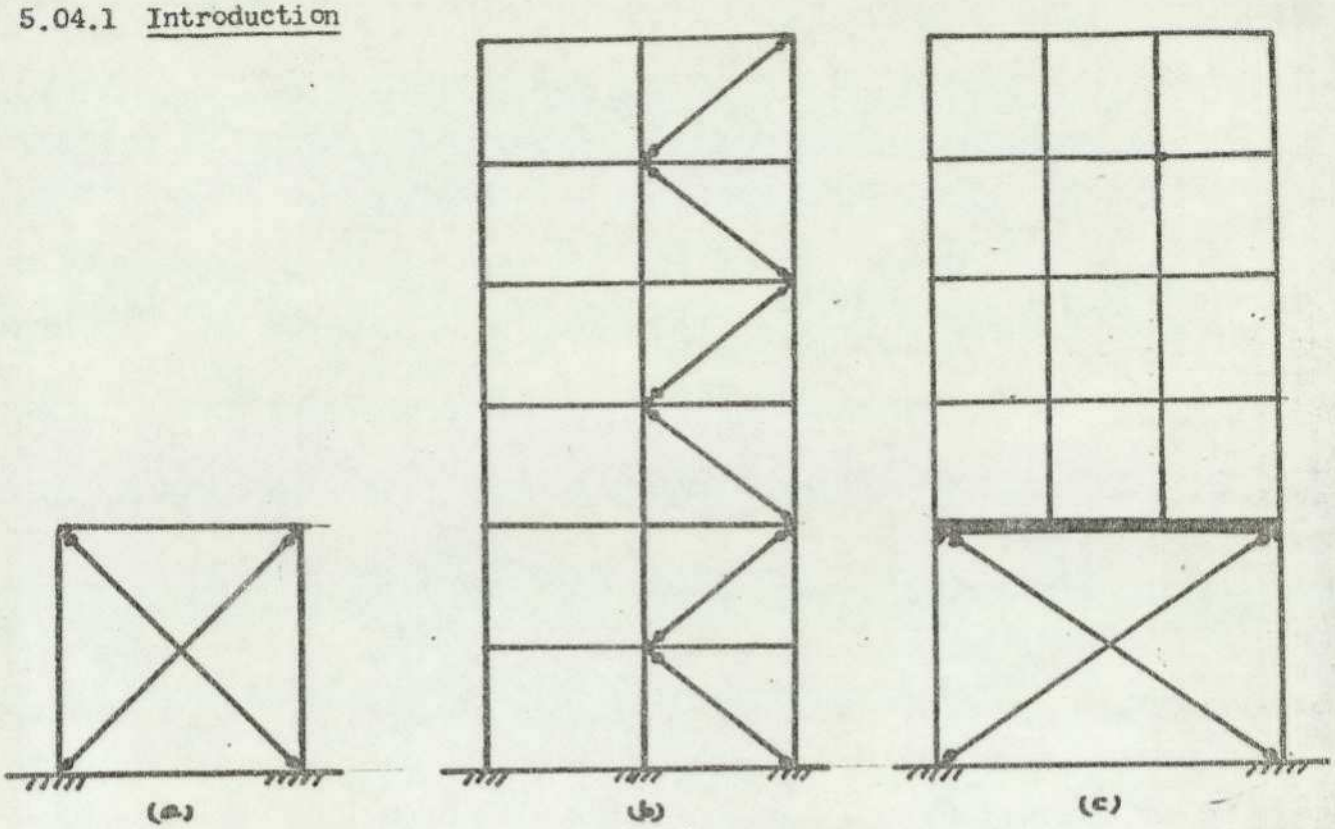

Fig.5.0411 Some examples of braced frames

Braced frames are often used in structural steel buildings and can take various forms, some of which are shown in fig.5.0411. The main functions of bracings are (i) to increase the lateral stiffness of a structure and reduce the deflections and (ii) to reduce the bending moments in the columns. Such bracings in framed structures may be original feature or may be introduced at a late stage if it is found that the structure possesses inadequate stiffness. A structure of this type is specially selected for analysis for the following reasons:-

(i) Having analysed simple portal frames in section 5.03 for the effects of various types of temperature distributions in columns or the beam, it is considered interesting to analyse a simple braced frame structure, such as shown in fig.5.0411(a) for the same thermal effects and to compare the resulting stresses and contributions of the braces.

(ii) By selecting a structure composed of members of different materials, it is intended to demonstrate that these structures are no more difficult to analyse in relation to structures wholly of same material, and to encourage engineers to the use of composite structures if there are distinct advantages and the situation warrants it, and

(iii) To demonstrate how the force-displacement method can be applied to these types of structures.

ANALYSIS

5.04.2 Constant temperature distribution in the beam of a single-storey braced frame

(a) Analysis using the force-displacement method

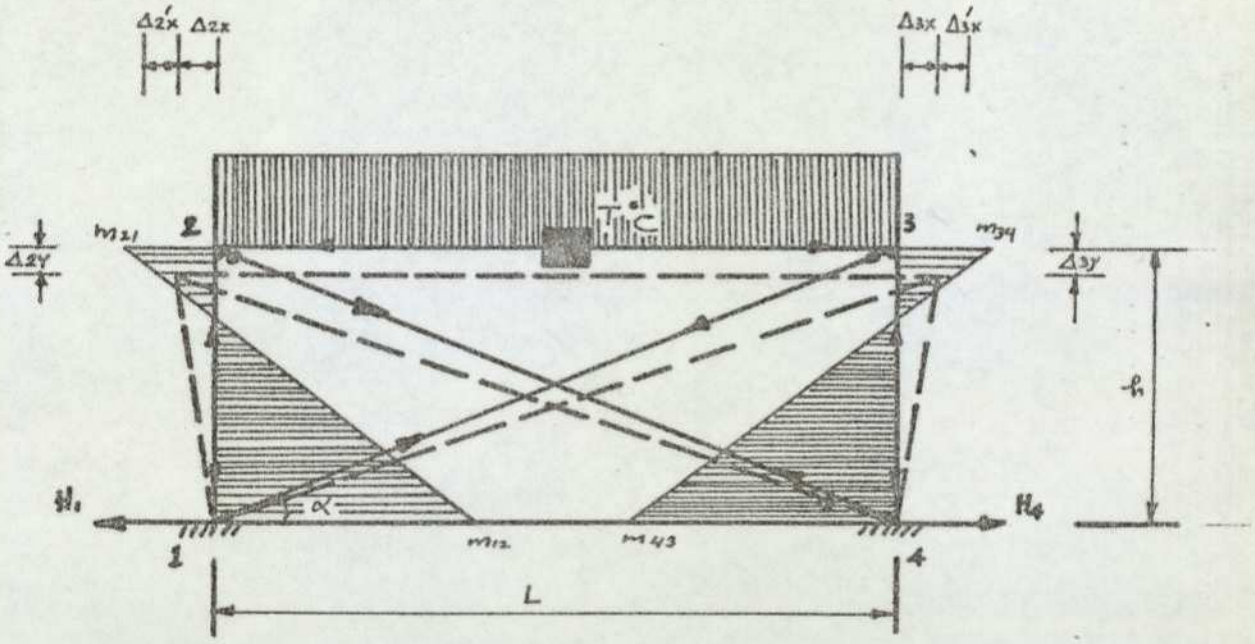

Fig. 5.0421 Assumed bending moments and forces in members

_____ Undeformed structure

_ _ _ _ Deformed structure

$\Delta 2x$, $\Delta 3x$ _ _ horizontal deflections at joints 2 & 3

$\Delta 2'x$, $\Delta 3'x$ _ suppressed horizontal deflections due to action of other members

$\Delta 2y$, $\Delta 3y$ _ _ _ vertical deflections at joints 2 & 3

because of symmetry, $\Delta 2x = \Delta 3x$

$\Delta 2'x = \Delta 3'x$

$\Delta 2x + \Delta 2'x = \Delta 3x + \Delta 3'x = \frac{\alpha TL}{2}$

The conditions of compatibility of deformations and equilibrium of forces can now be written as follows:-

F.1 $m12(\frac{h}{3EIc}) - m21(\frac{h}{6EIc}) = \frac{\Delta 2x}{h}$

or $2r1(\frac{m12}{L}) - r1(\frac{m21}{L}) - r\,\Delta 2x\,K\frac{L}{h} = o$

F.2 $-m12(\frac{h}{6EIc}) + m21(\frac{h}{3EIc} + \frac{L}{3EIb}) + m34(\frac{L}{6EIb}) = \frac{\Delta 2x}{h}$

or $-r1(\frac{m12}{L}) + (2r1 + 3)(\frac{m21}{L}) - r\,\Delta 2x\,K\frac{L}{h} = o$ since $m21 = m34$

C.12 $\Delta 2y = \frac{N12\ L12}{A12\ E12}$

or $r\,\Delta 2y - N12\ S12 = o$

C.13 $r\,\Delta 3x\ \cos\alpha - r\,\Delta 3y\ \sin\alpha = \frac{N13\ L13}{A13\ E13}$

or $r\,\Delta 2x\ \cos\alpha - r\,\Delta 2y\ \sin\alpha - N13\ S13 = o$ since $\Delta 2y = \Delta 3y$

C.23 $\Delta 2'x + \Delta 3'x = \frac{N23\ L23}{A23\ E23}$

or $2r\,\Delta 2x + N23\ S23 = r\alpha TL$ since $\Delta 2'x = \Delta 3'x$ and $\Delta 2x + \Delta 2'x = \Delta 3x + \Delta 3'x = \frac{\alpha TL}{2}$

E.1x $\frac{m12 + m21}{h} + H1 - N13\cos\alpha = o$

$(\frac{m12}{L})\frac{L}{h} + (\frac{m21}{L})\frac{L}{h} + H1 - N13\cos\alpha = o$

E.1y $N13\sin\alpha - N12 = o$ by inspection $V1 = o$

E.2x $\frac{m21 + m12}{h} - N23 + N24\cos\alpha = o$

or $(\frac{m21}{L})\frac{L}{h} + (\frac{m12}{L})\frac{L}{h} - N23 + N13\cos\alpha = o$ since $N13 = N24$

In the above equations, $r1 = \frac{h}{L}\frac{Ib}{Ic}$; $r = \frac{Ab\ Eb}{Lb}$; $K = \frac{6Ib}{AbL^2}$

$$S12 = \frac{L12}{A12E12} \cdot \frac{Ab\ Eb}{Lb} \ ; \quad S13 = \frac{L13}{A13E13} \cdot \frac{AbEb}{Lb} \ ;$$

$$S23 = \frac{L23}{A23E23} \cdot \frac{AbEb}{Lb}$$

Example As a numerical example, the braced frame shown in fig. 5.0422 is analysed for the effect of constant temperature distribution in the beam.

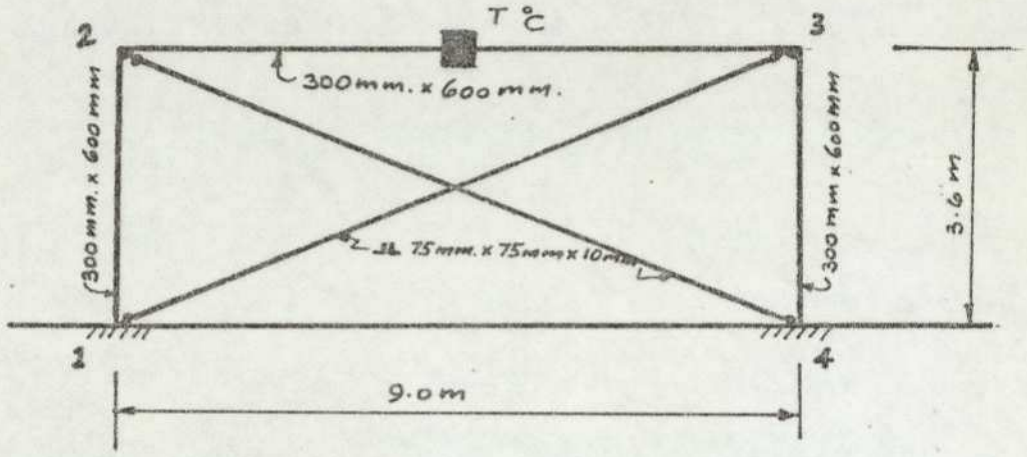

Fig. 5.0422 Braced frame example

Main frame : concrete

bracings : steel

E conc = 28×10^6 KN/m^2

A conc = $0.3 \times 0.6 = 0.18$m^2

I conc = $0.3 \times \frac{0.6^3}{12} = 0.0054$ m^4

Es = 200×10^6 KN/m^2

As = 1.839×10^{-3} m^2

T = 20^oC

α = 0.00001 per ^oC

A numerical matrix is set out as shown in Table 500.04 and based on the equations of compatibility and equilibrium derived earlier. However, before the matrix can be set out, it is necessary to calculate the following parameters:-

$$r1 = \frac{h}{L}\,\frac{Ib}{Ic} = 0.4 \quad ; \quad r = \frac{AbEb}{Lb} = 560 \times 10^3 \text{ KN/m}$$

$$K = \frac{6\,Ib}{AbL^2} = 0.002222 \quad ; \quad K\frac{L}{h} = 0.005555$$

$$S12 = \frac{L12}{A12E12}\,\frac{AbEb}{Lb} = 0.4 \; ; \quad S13 = 14.7582 \; ; \quad S23 = 1$$

$$r\alpha TL = 1{,}008 \text{ KN}$$

The solution of the matrix shown in Table: 500.04 gives direct values of forces, while bending moments are in terms of $(\frac{m}{L})$ and the deflections in terms of $r\Delta$. A diagram of these values is shown in fig. 5.0423.

(b) Analysis using the stiffness method

The above framework is also analysed by the stiffness method. The application of the stiffness method is explained in detail in text later.' Fig.5.0423 shows results of both the force-displacement and the stiffness methods. The small differences in the results can only be accounted for by the degree of errors resulting in the numerical analysis, and not by the differences in theoretical formulations.

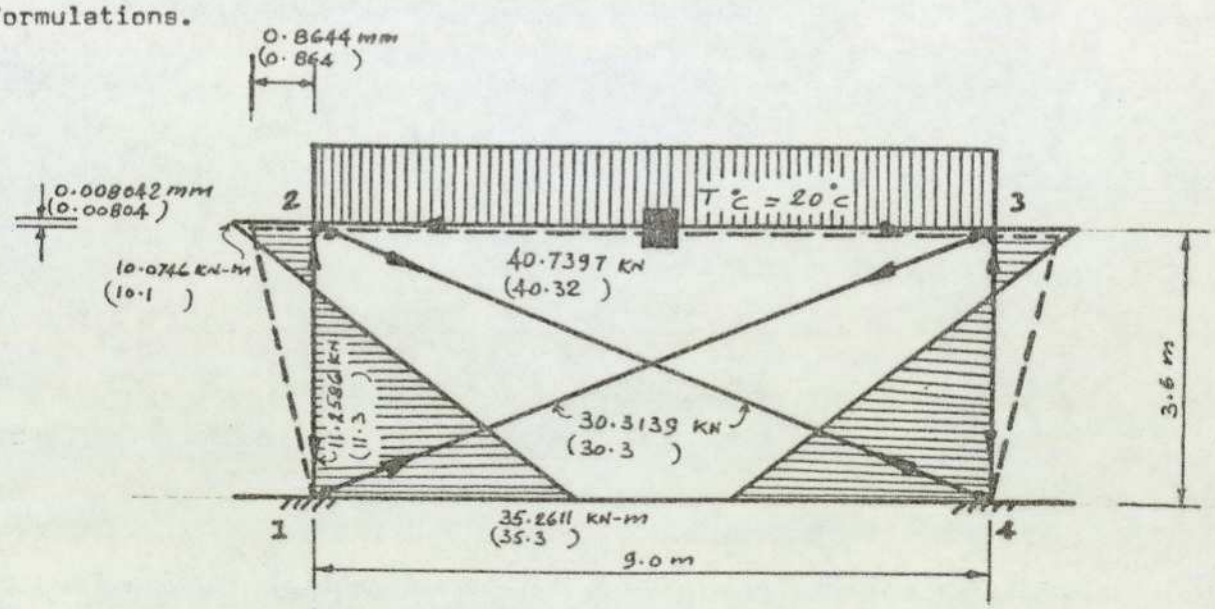

Fig.5.0423 Actual stresses due to the effect of constant temperature distribution in the beam

EQN. NO.	NO.	1	2	3	4	5	6	7	8	LOAD VECTOR
	REF. JTS.	1						2		
	REF.EQNS.	m12/L	N12	N13	H1	m21/L	N23	r Δ2x	r Δ2y	
1	F.1	0.8	0	0	0	-0.4		-0.005556		0
2	C.12	0	-0.4	0	0	0			1	0
3	C.13	0	0	-14.7582	0	0		0.9285	-0.3714	0
4	E.1x	2.5	0	-0.9285	1	2.5				0
5	E.1y	0	-1	0.3714	0	0				0
6	F.2	-0.4				3.8	0	-0.005556	0	0
7	C.23						1	2	0	1,008
8	E.2x	2.5		0.9285		2.5	-1	0	0	0

TABLE: 500.04 Numerical matrix for the effect of constant temperature distribution in the beam of a braced frame.

5.04.3 Linear temperature distribution in the beam

Assuming the same bending diagram as in the case of the constant temperature distribution, shown in Fig. 5.0421, the equations of compatibility of deformations and equilibrium of forces can be formulated as follows:-

F.1 $$m12\left(\frac{h}{3EIc}\right) - m21\left(\frac{h}{6EIc}\right) = \frac{\Delta 2x}{h}$$

or $$2r\left(\frac{m12}{L}\right) - r1\left(\frac{m21}{L}\right) - r\,\Delta 2x\,K\frac{L}{h} = o$$

F.2 $$-m12\left(\frac{h}{6EIc}\right) + m21\left(\frac{h}{3EIc} + \frac{L}{3EIb}\right) + m21\frac{L}{6EIb} = \frac{\Delta 2x}{h} - \theta 23$$

or $$-r1\left(\frac{m12}{L}\right) + 2(r1 + 1.5)\left(\frac{m21}{L}\right) - r\,\Delta 2x\,K\frac{L}{h} = -\frac{3\alpha TEIb}{dL} \qquad m21 = m32 \text{ symmetry}$$

C.13 $$\Delta 3x \cos\alpha - \Delta 3y \sin\alpha = \frac{N13\ L13}{A13\ E13}$$

or $$r\,\Delta 2x \cos\alpha - r\,\Delta 2y \sin\alpha - N13\ S13 = o \qquad \begin{matrix}\Delta 2x = \Delta 3x \\ \Delta 2y = \Delta 3y\end{matrix}\ \text{symmetry}$$

C.12 $$\Delta 2y = \frac{N12\ L12}{A12\ E12}$$

or $$r\,\Delta 2y - N12\ S12 = o$$

C.23 $$\Delta 2'x + \Delta 3'x = \frac{N23\ L23}{A23\ E23} \qquad \Delta 2'x = \Delta 3'x \text{ symmetry}$$

or $$2r\,\Delta 2x + N23\ S23 = \frac{r\alpha TL}{2} \qquad \Delta 2x = \Delta 3x \text{ symmetry}$$

E.1x $$\frac{m12 + m21}{h} = H1 + N13 \cos\alpha$$

or $$\left(\frac{m12}{L}\right)\frac{L}{h} + \left(\frac{m21}{L}\right)\frac{L}{h} - H1 - N13 \cos\alpha = o$$

E.1y $$N13 \sin\alpha - N12 - V1 = o$$

but $$V1 = o \quad \text{by inspection}$$

Therefore $$N13 \sin\alpha - N12 = o$$

E.2x $\quad \frac{m12 + m21}{h} = N13 \cos \alpha - N23 \qquad N13 = N24$ symmetry

or $\quad (\frac{m12}{L})\frac{L}{h} + (\frac{m21}{L})\frac{L}{h} - N13 \cos \alpha + N23 = 0$

In the above equations $\quad \Delta 2x + \Delta 2'x = \frac{\alpha TL}{4}$; $r1 = \frac{h}{L} \frac{Ib}{Ic}$; $r = \frac{Ab\ Eb}{Lb}$; $823 = \frac{\alpha TL}{2d}$

$$K = \frac{6Ib}{Abl^2} \quad ; \quad S13 = \frac{L13}{A13\ E13} \cdot \frac{Ab\ Eb}{Lb} \quad ; \quad S12 = \frac{L12}{A12\ E12} \cdot \frac{Ab\ Eb}{Lb} \quad ;$$

$$S23 = \frac{L23}{A23\ E23} \cdot \frac{A_b\ E_b}{L_b}$$

Example

In the numerical example, the frame shown in Fig. 5.0422 is analysed for the effect of linear temperature distribution in the beam. The following parameters required in the matrix are first calculated:-

$r1 = 0.4$; $r = 560 \times 10^3$ KN/m ; $K\frac{L}{h} = 0.0055555$;

$-3 \frac{\alpha TEIb}{dL2} = -16.8$ KN/m ; $S13 = 14.7582$; $S12 = 0.4$ and $S23 = 1$;

$\frac{r \alpha TL}{2} = 504$ KN

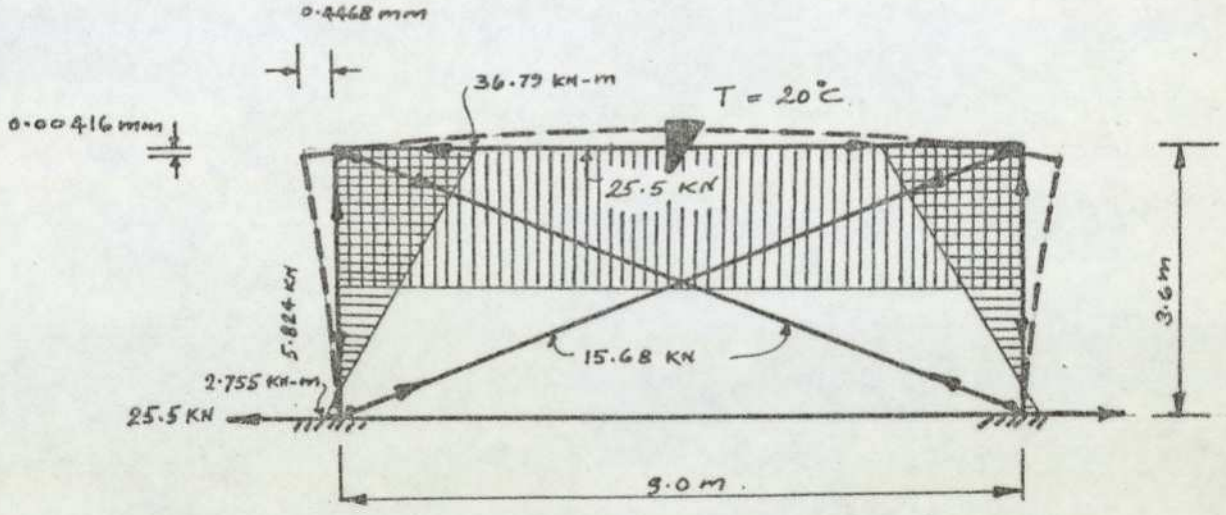

Fig. 5.0431 Actual stresses due to the effect of linear temperature distribution in the beam

EQN. NO.	NO.	1	2	3	4	5	6	7	8	LOAD VECTOR
	REF. JTS.	1				2				
	REF.EQNS.	m12/L	N12	N13	H1	m21/L	N23	rΔ2x	rΔ2y	
1	F.1	0.8	0	0	0	-0.4		-0.005556		0
2	C.12	0	-0.4	0	0				1	0
3	E.1x	2.5	0	-0.9285	-1	2.5				0
4	E.1y	0	-1	0.3714	0					0
5	F.2	-0.4				3.8	0	-0.005556	0	-16.80
6	C.23					0	1	2	0	504.0
7	E.2x	2.5		-0.9285		2.5	1	0	0	0
8	C.13			-14.7582		0	0	0.9285	-0.3714	0

TABLE:500.05 Numerical matrix for the effect of Linear Temperature distribution in the beam of a braced frame

5.04.4 Constant temperature distribution in a column

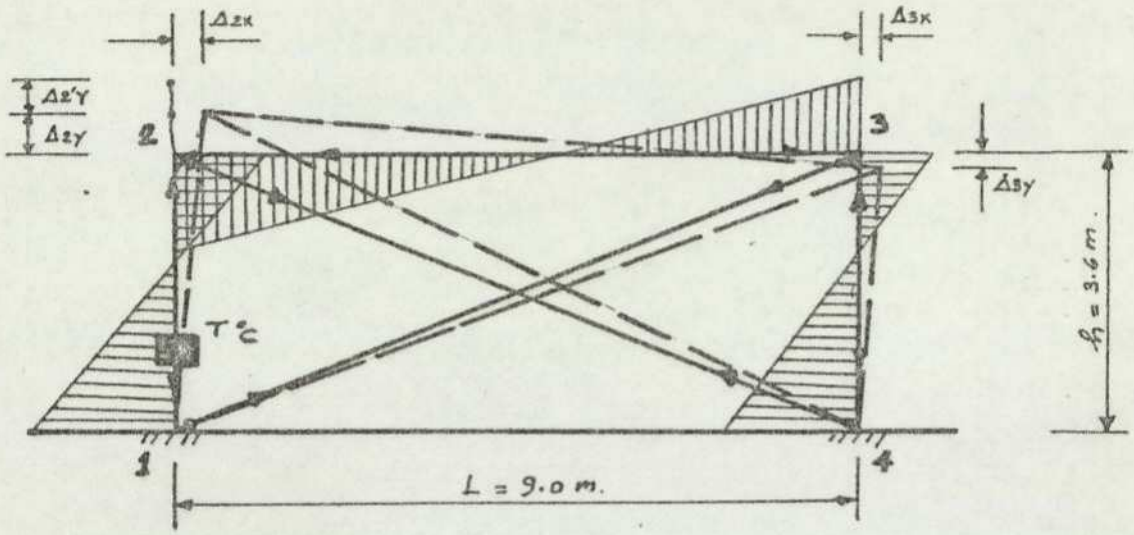

Fig. 5.0441 Assumed bending moments and forces in members due to the effect of constant temperature distribution in a column.

The effect of constant temperature distribution in a column of a braced portal frame can be determined from the following equations of compatibility of deformations and equilibrium of forces:-

F.1 $$m12\left(\frac{h}{3EIc}\right) - m21\left(\frac{h}{6EIc}\right) = \frac{\Delta 2x}{h}$$

or $$2r1\left(\frac{m12}{L}\right) - r1\left(\frac{m21}{L}\right) - r\,\Delta 2x\,K\frac{L}{h} = o$$

F.2 $$-m12\left(\frac{h}{6EIc}\right) + m21\left(\frac{h}{3EIc} + \frac{L}{3EIb}\right) - m34\left(\frac{L}{6EIb}\right) = \frac{\Delta 2x}{h} - \frac{\delta V2}{L}$$

or $$-r1\left(\frac{m12}{L}\right) + 2(r1 + 1)\left(\frac{m21}{L}\right) - \left(\frac{m34}{L}\right) - r\,\Delta 2x\,K\frac{L}{h} + r\,\Delta 2y\,K + r\,\Delta 3y\,K = o$$

F.3 $$-m21\left(\frac{L}{6EIb}\right) + m34\left(\frac{L}{3EIb} + \frac{h}{3EIc}\right) - m43\left(\frac{h}{6EIc}\right) = \frac{\Delta 3x}{h} - \frac{\delta V3}{L}$$

or $$-m21 + 2(r1 + 1)\,m34 - r1\,m43 - r\,\Delta 3x\,K\frac{L}{h} + r\,\Delta 2y\,K + r\,\Delta 3y\,K = o$$

F.4 $$m43\left(\frac{h}{3EIc}\right) - m34\left(\frac{h}{6EIc}\right) = \frac{\Delta 3x}{h}$$

or $$2r1\left(\frac{m43}{L}\right) - r1\left(\frac{m34}{L}\right) - r\,\Delta 3x\,K\frac{L}{h} = o$$

C12 $$\Delta 2'y = \frac{N12\ L12}{A12\ E12}$$

or $$r\,\Delta 2y + N12\ S12 = r\,\alpha Th$$

C.34 $$\Delta 3y = \frac{N34\ L34}{A34\ E34}$$

or $$r\,\Delta 3y - N34\ S34 = o$$

C.13 $$\Delta 3x \cos\alpha - \Delta 3y \sin\alpha = \frac{N13\ L13}{A13\ E13}$$

or $$r\,\Delta 3x \cos\alpha - r\,\Delta 3y \sin\alpha - N13\ S13 = o$$

C.24 $$-\Delta 2x \cos\alpha + \Delta 2y \sin\alpha = \frac{N24\ L24}{A24\ E24}$$

or $$-r\,\Delta 2x \cos\alpha + r\,\Delta 2y \sin\alpha - N24\ S24 = o$$

C.23 $$\Delta 2x - \Delta 3x = \frac{N23\ L23}{A23\ S23}$$

or $$r\,\Delta 2x - r\,\Delta 3x - N23\ S23 = o$$

E.1x $$\frac{m12 + m21}{h} = H1 - N13 \cos\alpha$$

or $$(\frac{m12}{L})\frac{L}{h} + (\frac{m21}{L})\frac{L}{h} - H1 + N13 \cos\alpha = o$$

E.2x $$\frac{m21 + m12}{h} + N23 - N24 \cos\alpha = o$$

or $$(\frac{m21}{L})\frac{L}{h} + (\frac{m12}{L})\frac{L}{h} + N23 - N24 \cos\alpha = o$$

E.2y $$\frac{m21 + m34}{L} + N12 - N24 \sin\alpha = o$$

or $$(\frac{m21}{L})\frac{L}{h} + (\frac{m34}{L})\frac{L}{h} + N12 - N24 \sin\alpha = o$$

E.3x $$\frac{m34 + m43}{h} - N23 + N13 \cos\alpha = o$$

or $$(\frac{m34}{L})\frac{L}{h} + (\frac{m43}{L})\frac{L}{h} - N23 + N13 \cos\alpha = o$$

E.3y $$\frac{m34 + m21}{L} - N34 + N13 \sin\alpha = o$$

or $$(\frac{m34}{L})\frac{L}{h} + (\frac{m21}{L})\frac{L}{h} - N34 + N13 \sin\alpha = o$$

E.4x $$\frac{m43 + m34}{h} + H4 - N24 \cos\alpha = o$$

or $$(\frac{m43}{L})\frac{L}{h} + (\frac{m34}{L})\frac{L}{h} + H4 - N24 \cos\alpha = o$$

In the above equations

$$\Delta 2y + \Delta 2'y = \alpha TL$$

$$r1 = \frac{h}{L}\,\frac{Ib}{Ic} \quad ; \quad r = \frac{Ab\ Eb}{Lb}$$

$$K = \frac{6\ Ib}{Abl^2} \quad ; \quad \delta v2 = \delta v3 = \Delta 2y + \Delta 3y$$

$$S12 = \frac{L12}{A12\ E12}\,\frac{Ab\ Eb}{Lb} \quad ; \quad S34 = \frac{L3y}{A34\ E34} \cdot \frac{Ab\ Eb}{Lb}$$

$$S13 = \frac{L13}{A13\ E13} \cdot \frac{Ab\ Eb}{Lb} \quad ; \quad S24 = \frac{L24}{A24\ E24} \cdot \frac{Ab\ Eb}{Lb}$$

$$S23 = \frac{L23}{A23\ E23} \cdot \frac{Ab\ Eb}{Lb}$$

Example

In the numerical example, the frame shown in Fig. 5.0422 is analysed for the effect of constant temperature distribution in a column. The numerical parameters required for setting up the matrix are:-

$r1 = 0.4$; $r = 560 \times 10^3$ KN/m ; $K\frac{L}{h} = 0.0055555\dot{}$

$r\alpha Th = 403.20$ KN ; $K = 0.002222\dot{}$

$S12 = 0.4$; $S34 = 0.4$; $S13 = 14.7582$

$S24 = 14.7582$; $S23 = 1$

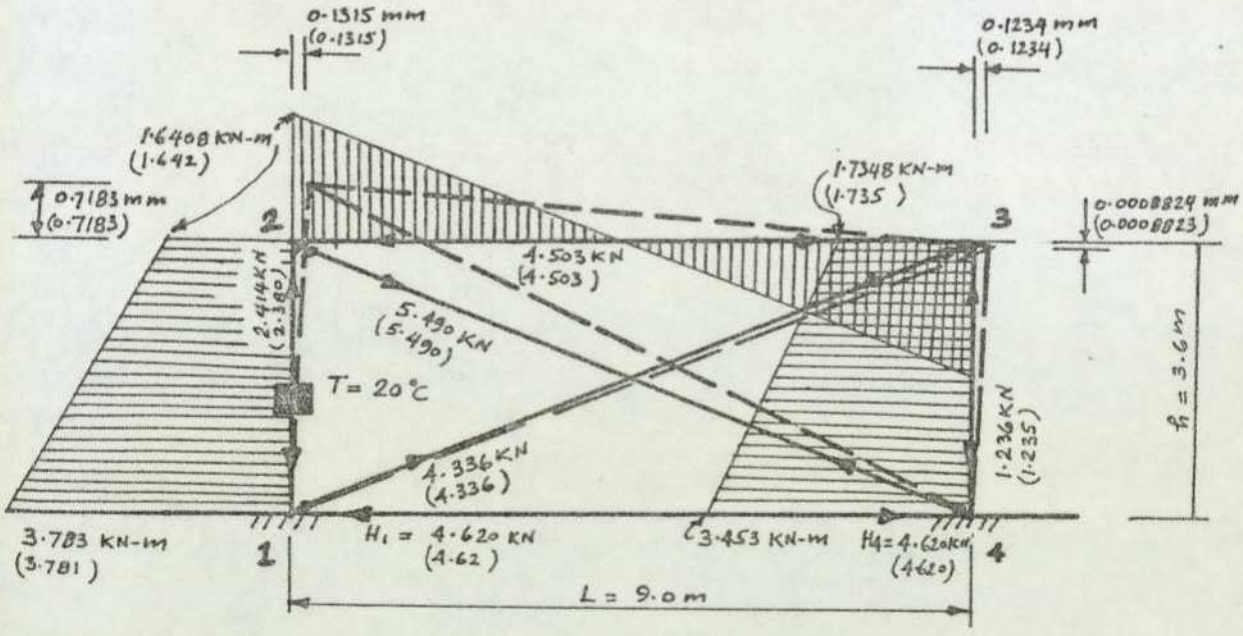

Fig. 5.0442 Actual stresses due to the effect of constant temperature distribution in a column

EQN. NO.		1	2	3	4	5	6	7	8	9	10	11	12	13	14	15	LOAD
NO.	REF. JTS.	1				2					3				4		VECTO
	REF.EQNS.	m12/L	N12	N13	H1	m21/L	N23	N24	r Δ 2x	r Δ 2y	m34/L	N34	r Δ 3x	r Δ 3y	m43/L	H4	
1	F.1	0.8	0	0	0	-0.4			-0.005556								0
2	C.12	0	0.4	0	0					1							403.2
3	C.13	0	0	-14.7582	0								0.9285	-0.3714			0
4	E.1x	2.5	0	0.9285	-1	2.5											0
5	F.2	-0.4				2.8	0	0	-0.005556	0.002222	-1			0.002222			0
6	C.24					0	0	-14.7582	-0.9285	0.3714							0
7	C.23					0	-1	0	1	0			-1				0
8	E.2x	2.5				2.5	1	- 0.9285	0	0							0
9	E.2y		1			1	0	- 0.3714	0	0	1						0
10	F.3					-1				0.002222	2.8	0	-0.005556	0.002222	-0.4		0
11	C.34										0	-0.4	0	1			0
12	E.3x			0.9285			-1				2.5	0	0	0	2.5		0
13	E.3y			0.3714		1					1	-1	0	0			0
14	F.4										-0.4		-0.005556		0.8	0	0
15	E.4x							- 0.9285			2.5				2.5	1	0

TABLE:500.06 Numerical matrix for the effect of Constant Temperature distribution in the column of a braced frame

5.04.5 Linear temperature distribution in a column

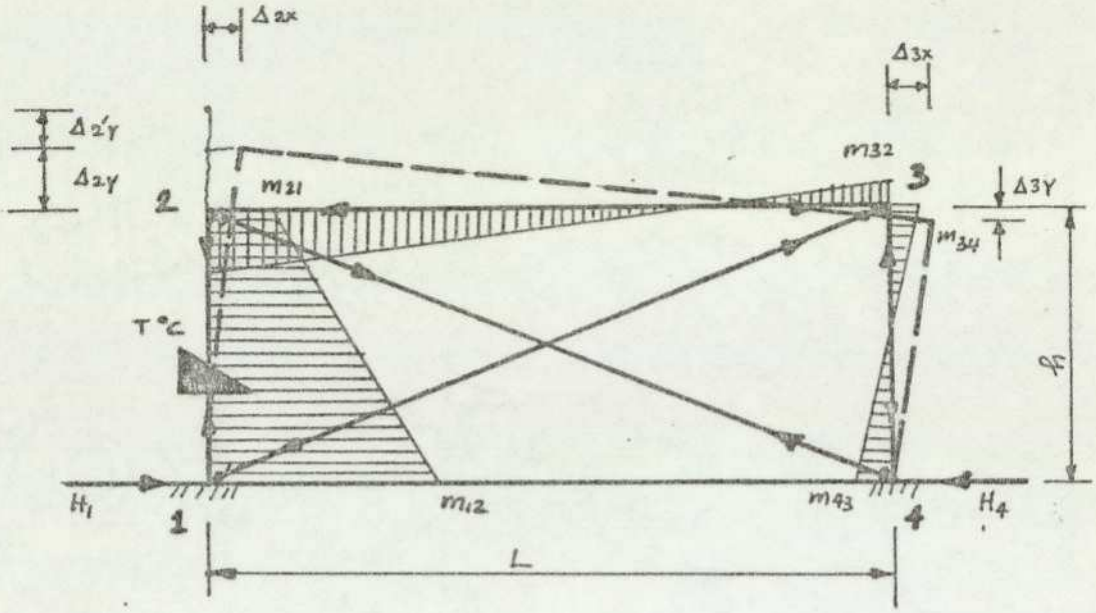

Fig. 5.0451 Assumed bending moments due to the effect of linear temperature distribution in a column

The effect of linear temperature distribution in a colymn of a braced frame can be determined from the following equations of compatibility of deformations and equilibrium of forces:-

F.1 $$m12\left(\frac{h}{3EIc}\right) + m21\left(\frac{h}{6EIc}\right) = -\frac{\Delta 2x}{h} + \theta 12$$

or $$2r1\left(\frac{m12}{L}\right) + r1\left(\frac{m21}{L}\right) + r\,\Delta 2x\,K\frac{L}{h} = \frac{3C}{dL}$$

F.2 $$m12\left(\frac{h}{6EIc}\right) + m21\left(\frac{h}{3EIc} + \frac{L}{3EIb}\right) - m34\left(\frac{L}{6EIb}\right) = \frac{\Delta 2x}{h} + \theta_{21} - \frac{\delta v2}{L}$$

or $$r1\left(\frac{m12}{L}\right) + 2(r1 + 1)\left(\frac{m21}{L}\right) - \left(\frac{m34}{L}\right) - r\,\Delta 2x\,K\frac{L}{h} + r\,\Delta 2y\,K + r\Delta 3y\,K = \frac{3C}{dL}$$

F.3 $$-m21\left(\frac{L}{6EIb}\right) + m34\left(\frac{L}{3EIb} + \frac{h}{3EIc}\right) - m43\left(\frac{h}{6EIc}\right) = \frac{\Delta 3x}{h} - \frac{\delta v3}{L}$$

or $$-\left(\frac{m21}{L}\right) + 2(r1 + 1)\left(\frac{m34}{L}\right) - r1\left(\frac{m43}{L}\right) - r\,\Delta 3x\,K\frac{L}{h} + r\,\Delta 2y\,K + r\,\Delta 3y\,K = o$$

F.4 $$m43\left(\frac{h}{3EIc}\right) - m34\left(\frac{h}{6EIc}\right) = \frac{\Delta 3x}{h}$$

or $$2r1\left(\frac{m43}{L}\right) - r1\left(\frac{m34}{L}\right) - r\,\Delta 3x\,K\frac{L}{h} = o$$

C.12 $$\Delta 2'y = \frac{N12\ L12}{A12\ E12}$$

or $$r\,\Delta 2y + N12\ S12 = \frac{r \alpha Th}{2}$$

C.13 $$-\Delta 3x\ \cos\alpha + \Delta 3y\ \sin\alpha = \frac{N13\ L13}{A13\ E13}$$

or $$-r\,\Delta 3x\ \cos\alpha + r\,\Delta 3y\ \sin\alpha - N13\ S13 = o$$

C.23 $$\Delta 2x - \Delta 3x = \frac{N23\ L23}{A23\ E23}$$

or $$r\,\Delta 2x - r\,\Delta 3x - N23\ S23 = o$$

C.24 $$-\Delta 2x\ \cos\alpha + \Delta 2y\ \sin\alpha = \frac{N24\ L24}{A24\ E24}$$

or $$-r\,\Delta 2x\ \cos\alpha + r\,\Delta 2y\ \sin\alpha - N24\ S24 = o$$

C.34 $$\Delta 3y = \frac{N34\ L34}{A34\ E34}$$

or $$r\,\Delta 3y - N34\ S34 = o$$

E.1x $$\frac{m12 - m21}{h} - H1 + N13\ \cos\alpha = o$$

or $$\left(\frac{m12}{L}\right)\frac{L}{h} - \left(\frac{m21}{L}\right)\frac{L}{h} - H1 + N13\ \cos\alpha = o$$

E.2x $$\frac{m21 - m12}{h} - N24\ \cos\alpha + N23 = o$$

or $$\left(\frac{m21}{L}\right)\frac{L}{h} - \left(\frac{m12}{L}\right)\frac{L}{h} - N24\ \cos\alpha + N23 = o$$

E.2y $$\frac{m21 + m34}{L} - N12 - N24\ \sin\alpha = o$$

or $$\left(\frac{m21}{L}\right)\frac{L}{h} + \left(\frac{m34}{L}\right)\frac{L}{h} - N12 - N24\ \sin\alpha = o$$

E.3x $$\frac{m34 + m43}{L} - N23 - N13\ \cos\alpha = o$$

or $$\left(\frac{m34}{L}\right)\frac{L}{h} + \left(\frac{m43}{L}\right)\frac{L}{h} - N23 - N13\ \cos\alpha = o$$

E.3y $$\frac{m34 + m21}{L} - N34 - N13\ \sin\alpha = o$$

or $$\left(\frac{m34}{L}\right)\frac{L}{h} + \left(\frac{m21}{L}\right)\frac{L}{h} - N34 - N13\ \sin\alpha = o$$

E.4x $$\frac{m43 + m34}{h} - N24\ \cos\alpha - H4 = o$$

or $$\left(\frac{m43}{L}\right)\frac{L}{h} + \left(\frac{m34}{L}\right)\frac{L}{h} - N24\ \cos\alpha - H4 = o$$

In the above equations

$$\Delta 2y + \Delta 2'y = \tfrac{1}{2}\alpha Th$$

$$r1 = \frac{h}{L}\,\frac{Ib}{Ic} \quad ; \quad r = \frac{Ab\,Eb}{Lb}$$

$$K = \frac{6\,Ib}{Ab\ell^2} \quad ; \quad \delta v2 = \delta v3 = \Delta 2y + \Delta 3y$$

$$S12 = \frac{L12}{A12\ E12} \cdot \frac{Ab\ Eb}{Lb} \quad ; \quad S13 = \frac{L13}{A13\ E13} \cdot \frac{Ab\ Eb}{Lb}$$

$$S23 = \frac{L23}{A23\ E23} \cdot \frac{Ab\ Eb}{Lb} \quad ; \quad S24 = \frac{L24}{A23\ E23} \cdot \frac{Ab\ Eb}{Lb}$$

$$S34 = \frac{L34}{A34\ E34} \cdot \frac{Ab\ Eb}{Lb}$$

$$C = \frac{\alpha TEIbh}{L}$$

Example

In the numerical example, the frame shown in Fig. 5.0422 is analysed for the effect of linear temperature distribution in a column. The numerical values required for setting up the matrix are:-

$$r1 = 0.4 \ ; \ r = 560 \times 10^3 \text{ KN/m} \ ; \ K\frac{L}{h} = 0.0055555\dot{}$$

$$\frac{r\alpha Th}{2} = 201.6\text{KN} \ ; \ K = 0.0022222\dot{} \ ; \ \frac{3C}{dL} = 6.72 \text{ KN}$$

$$S12 = 0.4 \ ; \ S13 = 14.7582 \ ; \ S23 = 1.0$$

$$S24 = 14.7582 \ ; \ S34 = 0.4$$

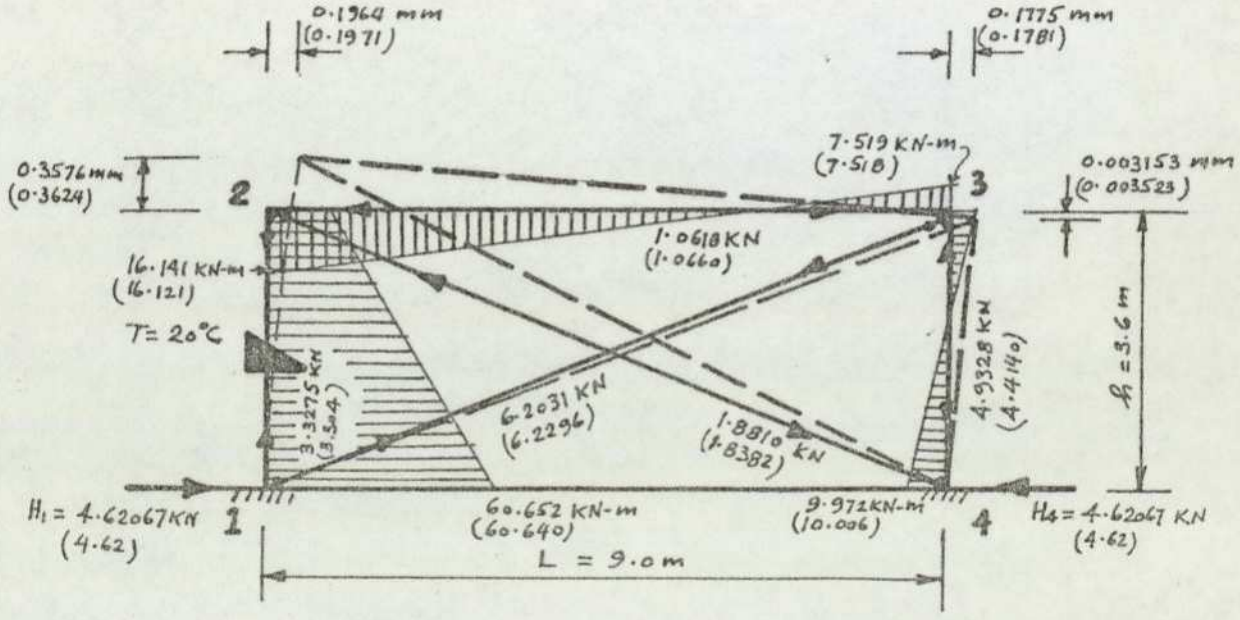

Fig. 5.0452 Actual stresses due to the effect of linear temperature distribution in a column

EQN. NO.	NO.	1	2	3	4	5	6	7	8	9	10	11	12	13	14	15	LOAD VECTOR
	REF.JTS.	1				2					3				4		
	REF.EQNS.	m12/L	N12	N13	H1	m21/L	N23	N24	r Δ2x	r Δ2y	m34/L	N34	r Δ3x	r Δ3y	m43/L	H4	
1	F.1	0.8	0	0	0	0.4			0.005556								6.72
2	C.12	0	0.4	0	0					1							201.6
3	C.13	0	0	-14.7582	0								-0.9285	0.3714			0
4	E.1x	2.5	0	0.9285	-1	-1.5											0
5	F.2	0.4				2.8	0	0	-0.005556	0.002222	-1			0.002222			6.72
6	C.2y					0	0	-14.7582	-0.9285	0.3714							0
7	C.23					0	-1	0	1	0			-1				0
8	E.2x	-2.5				2.5	1	- 0.9285	0	0							0
9	E.2y		-1			2.5	0	- 0.3714	0	0	2.5						0
10	F.3					7				0.002222	2.8	0	-0.005556	0.002222	-0.4		0
11	C.34										0	-0.4	0	1			0
12	E.3x			- 0.9285			-1				2.5	0	0	0	2.5		0
13	E.3y			- 0.3714		2.5					2.5	-1	0	0			0
14	F.4										-0.4		-0.005556		0.8	0	0
15	E.4x							- 0.9285			2.5				2.5	-1	0

TABLE: 500.07 Numerical matrix for the effect of Linear Temperature distribution in the column of a braced frame

5.04.6 Discussion of results of analysis of braced frames

The results of constant temperature distribution in a beam of the braced frame show a small reduction in the bending moments, when compared to the bending moments in the unbraced portal frame. However, the displacements of the braced frame are generally about half of those of the unbraced frame.

The results of linear temperature distribution in a beam of the braced frame show very similar behaviour to that, due to the constant temperature distribution in the beam.

The results of constant and linear temperature distribution in a column of a braced frame also exhibit clearly that displacements can be drastically reduced in relation to those in the unbraced frames. In this respect there is also a significant change in the form of bending moments, i.e. the bending moments at the top of the column are reduced, while those at the bottom increased slightly.

As the frames are identical in both cases, with the exception of the braces, and undergo identical thermal effects, it can be concluded that the braces reduce the deflections (i.e. the stiffness of the structure is increased) significantly. This property of the braces is extremely useful in the design of multi-storey frames. Although the contribution of braces to the resulting stresses is not conclusive, in the case of multi-storey frames braces are often used to reduce bending moments in columns due to lateral forces, such as the effect of wind and earthquakes.

The analysis also demonstrates that braces of different material from that of the frame can be used without any problems, in fact, it is usually advantageous due to the nature of stresses in these members. For example, steel braces are often used in

conjunction with either concrete or timber frames.

These examples further demonstrate the use of the force-displacement method. Whether members are of the same material or otherwise, the method is equally simple to apply.

5.05 ANALYSIS OF MULTI-STOREY SHEAR WALL FRAMES

5.05.1 The effect of constant temperature distribution in a roof beam

(a) Analysis using the force-displacement method

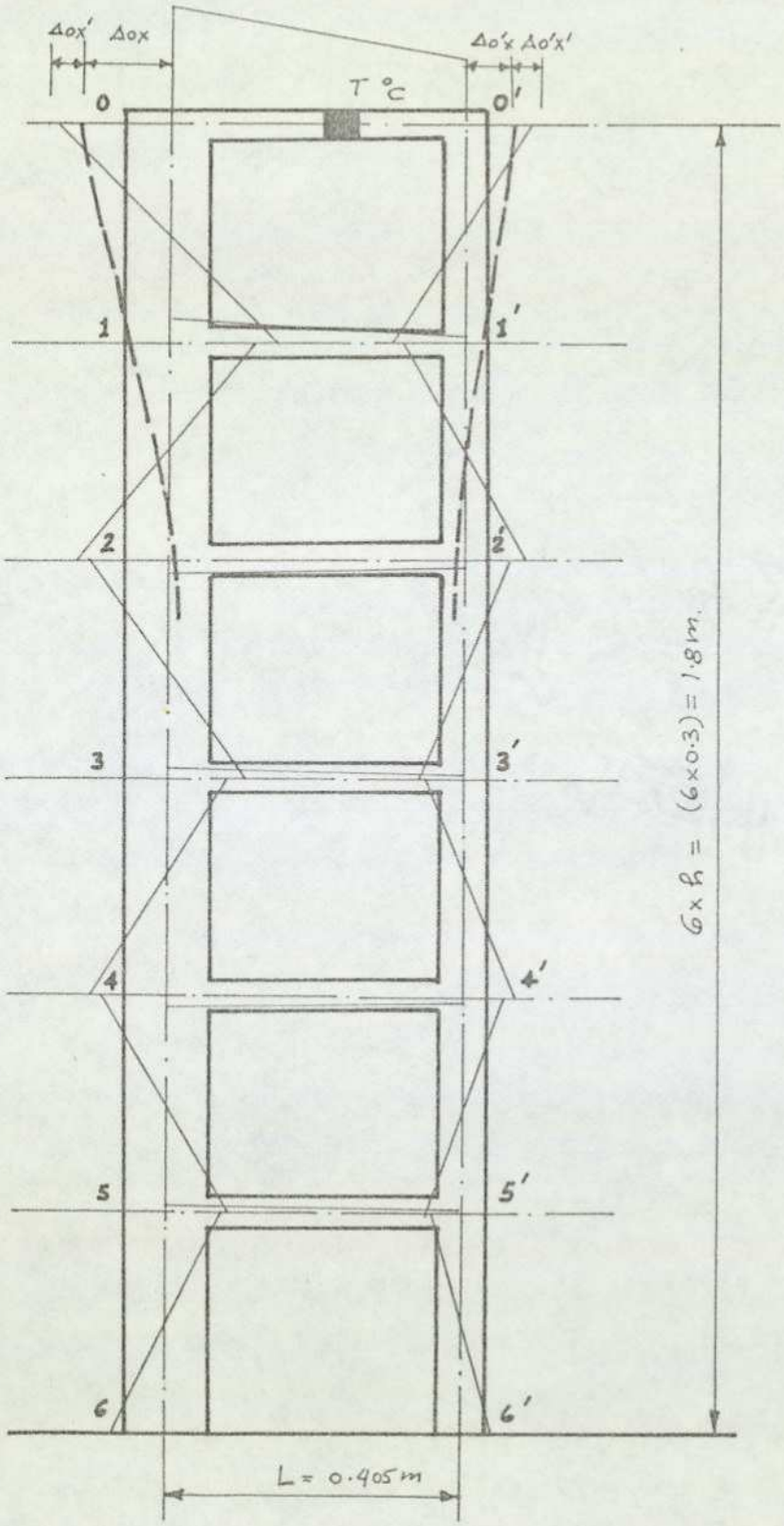

Fig. 5.0511 The effect of constant temperature distribution in roof beam showing reference bending moments assumed in the setting up of a matrix.

Note: This analysis includes the effect of axial deformations of all beams, but excludes the axial deformations of columns, as these are negligible for this case.

Denoting $\Delta ox, \Delta 1x, \text{---}, \Delta o'x, \Delta 1'x, \text{---}$ etc. horizontal displacements at levels oo', 11', --- etc.

$\Delta ox', \Delta 1x', \text{---}, \Delta o'x', \Delta 1'x', \text{---}$ etc. suppressed horizontal displacements at levels oo', 11', etc.

$$\Delta ox + \Delta ox' + \Delta o'x + \Delta o'x' = \alpha TL$$

Referring to Fig.5.0511 the conditions of compatibility of deformations and equilibrium of forces can be written as follows:-

(i) Conditions of Compatibility: 24 conditions of compatibility relating bending moments and displacements at the 12 joints of the frame can be written as follows:-

F.100' $$mo1\left(\frac{L}{3EIb} + \frac{h}{3EIc1}\right) - m10\,\frac{h}{6EIc1} + mo'1'\,\frac{L}{6EIb} = \frac{\Delta ox - \Delta 1x}{h}$$

or $$2(r1+1)\left(\frac{mo1}{L}\right) - r1\left(\frac{m1o}{L}\right) + \left(\frac{mo'1'}{L}\right) - r\Delta ox\,\frac{pL}{h} + r\,\Delta 1x\,\frac{pL}{h} = o$$

F.012 $$-mo1\left(\frac{h}{6EIc1}\right) + m1o\left(\frac{h}{3EIc1}\right) + m12\left(\frac{h}{3EIc1}\right) - m21\left(\frac{h}{6EIc1}\right) = \frac{\Delta ox-\Delta 1x}{h} - \frac{\Delta 1x-(-\Delta 2x)}{h}$$

or $$-r1\left(\frac{mo1}{L}\right) + 2r1\left(\frac{m1o}{L}\right) + 2r1\left(\frac{m12}{L}\right) - r1\left(\frac{m21}{L}\right) - r\Delta ox\,\frac{pL}{h} + 2r\Delta 1x\,\frac{pL}{h} + r\Delta 2x\,\frac{pL}{h} = o$$

F.211' $$-m21\left(\frac{h}{6EIc1}\right) + m12\left(\frac{h}{3EIc1}\right) - (m1o - m12)\left(\frac{L}{3EIb}\right) - (m1'o' - m1'2')\left(\frac{L}{6EIb}\right) = -\left(\frac{\Delta 1x - (-\Delta 2x)}{h}\right)$$

or $$r1\left(\frac{m21}{L}\right) - 2(r1 + 1)\left(\frac{m12}{L}\right) + 2\left(\frac{m1o}{L}\right) + \left(\frac{m1'o'}{L}\right) - \left(\frac{m1'2'}{L}\right) - r\Delta 1x\,\frac{pL}{h} - r\Delta 2x\,\frac{pL}{h} = o$$

F.1'o'o $$-m1'o'\left(\frac{h}{6EIc2}\right) + mo'1'\left(\frac{h}{3EIc2} + \frac{L}{3EIb}\right) + m10\left(\frac{L}{6EIb}\right) = \frac{\Delta o'x-\Delta 1'x}{h}$$

or $$-r2\left(\frac{m1'o'}{L}\right) + 2(r2+1)\left(\frac{mo'1'}{L}\right) + \left(\frac{mo1}{L}\right) - r\Delta o'x\,\frac{pL}{h} + r\Delta 1'x\,\frac{pL}{h} = o$$

F.o'1'2' $-mo'1'(\frac{h}{6EIc2}) + m1'o'(\frac{h}{3EIc2}) + m1'2'(\frac{h}{3EIc2}) = \frac{\Delta o'x-\Delta 1'x}{h} - \frac{\Delta 1'x-(-\Delta 2'x)}{h}$

$-m2'1'(h/6EIc2)$

or $-r2(\frac{mo'1'}{L}) + 2r2(\frac{m1'o'}{L}) + 2r2(\frac{m1'2'}{L}) - r2(\frac{m2'1'}{L}) - r\Delta o'x\frac{pL}{h}$

$+ 2r\Delta 1'x\frac{pL}{h} + r\Delta 2'x\frac{pL}{h} = o$

F.2'1'1 $-m2'1'(\frac{h}{6EIc2}) + m1'2'(\frac{h}{3EIc2}) - (m1'o' - m1'2')(\frac{L}{3EIb}) - (m1o - m12)\frac{L}{6EIb}$

$= -(\frac{\Delta 1'x - (-\Delta 2'x)}{h})$

or $r2(\frac{m2'1'}{L}) - 2(r2 + 1)(\frac{m1'2'}{L}) + 2(\frac{m1'o'}{L}) + (\frac{m1o}{L}) - (\frac{m12}{L}) - r\Delta 1'x\frac{pL}{h}$

$- r\Delta 2'x\frac{pL}{h} = o$

Similarly

F.123 $r1(\frac{m12}{L}) - 2r1(\frac{m21}{L}) - 2r1(\frac{m23}{L}) + r1(\frac{m32}{L}) - r\Delta 1x\frac{pL}{h} - r\Delta 2x\frac{pL}{h} - r\Delta 3x\frac{pL}{h} = o$

F.322' $-r1(\frac{m32}{L}) + 2(r1+1)(\frac{m23}{L}) - 2(\frac{m21}{L}) - (\frac{m2'1'}{L}) + (\frac{m2'3'}{L}) + r\Delta 2x\frac{pL}{h}$

$+ r\Delta 3x\frac{pL}{h} = o$

F.234 $-r1(\frac{m23}{L}) + 2r1(\frac{m32}{L}) + 2r1(\frac{m34}{L}) - r1(\frac{m43}{L}) + r\Delta 2x\frac{pL}{h} + 2r\Delta 3x\frac{pL}{h}$

$+ r\Delta 4x\frac{pL}{h} = o$

F.433' $r1(\frac{m43}{L}) - 2(r1+1)(\frac{m34}{L}) + 2(\frac{m32}{L}) + (\frac{m3'2'}{L}) - (\frac{m3'4'}{L}) - r\Delta 3x\frac{pL}{h}$

$- r\Delta 4x\frac{pL}{h} = o$

F.345 $r1(\frac{m34}{L}) - 2r1(\frac{m43}{L}) - 2r1(\frac{m45}{L}) + r1(\frac{m54}{L}) - r\Delta 3x\frac{pL}{h} - 2r\Delta 4x\frac{pL}{h}$

$- r\Delta 5x\frac{pL}{h} = o$

F.544' $-r1(\frac{m54}{L}) + 2(r1+1)(\frac{m45}{L}) - 2(\frac{m43}{L}) - (\frac{m4'3'}{L}) + (\frac{m4'5'}{L}) + r\Delta 4x\frac{pL}{h}$

$+ r\Delta 5x\frac{pL}{h} = o$

F.456 $-r1(\frac{m45}{L}) + 2r1(\frac{m54}{L}) + 2r1(\frac{m56}{L}) - r1(\frac{m65}{L}) + r\Delta 4x\frac{pL}{h} + 2\Delta 5x\frac{pL}{h} = o$

F.655' $r1\left(\frac{m65}{L}\right) - 2(r1+1)\left(\frac{m56}{L}\right) + 2\left(\frac{m54}{L}\right) + \left(\frac{m5'4'}{L}\right) - \left(\frac{m5'6'}{L}\right) - r\Delta 5 \times \frac{pL}{h} = o$

F.65 $r1\left(\frac{m56}{L}\right) - 2r1\left(\frac{m65}{L}\right) - \Delta 5 \times \frac{pL}{h} = o$

F.1'2'3' $r2\left(\frac{m1'2'}{L}\right) - 2r2\left(\frac{m2'1'}{L}\right) - 2r2\left(\frac{m2'3'}{L}\right) + r2\left(\frac{m3'2'}{L}\right) - r\Delta 1' \times \frac{pL}{h} - 2r\Delta 2' \frac{pL}{h} - r\Delta 3' \times \frac{pL}{h} = o$

F.3'2'2 $-r2\left(\frac{m3'2'}{L}\right) + 2(r2+1)\left(\frac{m2'3'}{L}\right) - 2\left(\frac{m2'1'}{L}\right) - \left(\frac{m21}{L}\right) + \left(\frac{m23}{L}\right) + r\Delta 2' \times \frac{pL}{h} + r\Delta 3' \times \frac{pL}{h} = o$

F.2'3'4' $-r2\left(\frac{m2'3'}{L}\right) + 2r2\left(\frac{m3'2'}{L}\right) + 2r2\left(\frac{m3'4'}{L}\right) - r2\left(\frac{m4'3'}{L}\right) + r\Delta 2' \times \frac{pL}{h} + 2r\Delta 3' \times \frac{pL}{h} + r\Delta 4' \times \frac{pL}{h} = o$

F.4'3'3 $r2\left(\frac{m4'3'}{L}\right) - 2(r2+1)\left(\frac{m3'4'}{L}\right) + 2\left(\frac{m3'2'}{L}\right) + \left(\frac{m32}{L}\right) - \left(\frac{m34}{L}\right) - r\Delta 3' \times \frac{pL}{h} - r\Delta 4' \times \frac{pL}{h} = o$

F.3'4'5' $r2\left(\frac{m3'4'}{L}\right) - 2r2\left(\frac{m4'3'}{L}\right) - 2r2\left(\frac{m4'5'}{L}\right) + r2\left(\frac{m5'4'}{L}\right) - r\Delta 3' \times \frac{pL}{h} - 2r\Delta 4' \times \frac{pL}{h} - r\Delta 5' \times \frac{pL}{h} = o$

F.5'4'4 $-r2\left(\frac{m5'4'}{L}\right) + 2(r2+1)\left(\frac{m4'5'}{L}\right) - 2\left(\frac{m4'3'}{L}\right) - \left(\frac{m43}{L}\right) + \left(\frac{m45}{L}\right) + r\Delta 4' \times \frac{pL}{h} + r\Delta 5' \times \frac{pL}{h} = o$

F.4'5'6' $-r2\left(\frac{m4'5'}{L}\right) + 2r2\left(\frac{m5'4'}{L}\right) + 2r2\left(\frac{m5'6'}{L}\right) - r2\left(\frac{m6'5'}{L}\right) + r\Delta 4 \times \frac{pL}{h} + 2\Delta 5' \times \frac{pL}{h} = o$

F.6'5'5 $r2\left(\frac{m6'5'}{L}\right) - 2(r2+1)\left(\frac{m5'6'}{L}\right) + 2\left(\frac{m5'4'}{L}\right) + \left(\frac{m54}{L}\right) - \left(\frac{m56}{L}\right) - r\Delta 5' \times \frac{pL}{h} = o$

F.5'6' $r2\left(\frac{m5'6'}{L}\right) - 2r2\left(\frac{m6'5'}{L}\right) - r\Delta 5' \times \frac{pL}{h} = o$

For the determination of axial forces in the beams, further 6 conditions of compatibility of deformations relating to axial forces in the beams are required and these are as follows:-

Coo' $\quad \Delta ox' + \Delta o'x' = \frac{Noo'\ Loo'}{Aoo'\ Eoo'}$

or $\quad r\Delta ox + r\Delta o'x + Noo'\ Soo' = r\alpha TL$ $\quad$ since $\Delta ox' + \Delta o'x' = \alpha TL - \Delta ox - \Delta o'x$

Similarly

C11' $\quad r\Delta 1x + r\Delta 1'x - N11\ S11' = o$

C22' $\quad r\Delta 2x + r\Delta 2'x - N22\ S22' = o$

C33' $\quad r\Delta 3x + r\Delta 3'x - N33'\ S33' = o$

C44' $\quad r\Delta 4x + r\Delta 4'x - N44'\ S44' = o$

C55' $\quad r\Delta 5x + r\Delta 5'x - N55'\ S55' = o$

(ii) Conditions of Equilibrium: The 12 required conditions of equilibrium can either all be written at the joints or some at joints and some at levels through the frame. In order to demonstrate the procedure, the latter approach is followed here. The 6 conditions of equilibrium at joints on left hand side of frame are as follows:-

E.ox $\quad \frac{mo1 + m1o}{h} = Noo'$

or $\quad mo1 + m1o + \frac{E\ Ab\ h}{L}\ \Delta ox + \frac{E\ Ab\ h}{L}\ \Delta o'x = TE\alpha Ab\ h$

where $\quad Noo' = (\alpha TL - \Delta ox - \Delta o'x)\ \frac{E\ Ab}{L}$

E.1x $\quad (\frac{m21 + m12}{h}) + (\frac{m1o + mo1}{h}) = N11'$

or $\quad m21 + m12 + m1o = Mo1 - h\ N11' = o$

Similarly

E.2x $\quad m32 + m23 + m21 + m12 - h\ N22' = o$

E.3x $\quad m43 + m34 + m32 + m23 - h\ N33' = o$

E.4x $\quad m54 + m45 + m43 + m34 - h\ N44' = o$

E.5x $\quad m65 + m56 + m54 + m45 - h\ N55' = o$

Further 6 conditions of equilibrium at levels through the frame are as follows:-

$$E.oo' \qquad \left(\frac{mo1 + m1o}{h}\right) - \left(\frac{mo'1' + m1'o'}{h}\right) = o$$

$$E.11' \qquad \left(\left(\frac{m21 + m12}{h}\right) + \left(\frac{m1o + mo1}{h}\right)\right) - \left(\left(\frac{m2'1' + m1'2'}{h}\right) + \left(\frac{m1'o' + mo'1'}{h}\right)\right) = o$$

$$E.22' \qquad \left(\left(\frac{m32 + m23}{h}\right) + \left(\frac{m21 + m12}{h}\right)\right) - \left(\left(\frac{m3'2' + m2'3'}{h}\right) + \left(\frac{m2'1' + m1'2'}{h}\right)\right) = o$$

$$E.33' \qquad \left(\left(\frac{m43 + m34}{h}\right) + \left(\frac{m32 + m23}{h}\right)\right) - \left(\left(\frac{m4'3' + m3'4'}{h}\right) + \left(\frac{m3'2' + m2'3'}{h}\right)\right) = o$$

$$E.44' \qquad \left(\left(\frac{m54 + m45}{h}\right) + \left(\frac{m43 + m34}{h}\right)\right) - \left(\left(\frac{m5'4' + m4'5'}{h}\right) + \left(\frac{m4'3' + m3'4'}{h}\right)\right) = o$$

$$E.55' \qquad \left(\left(\frac{m65 + m56}{h}\right) + \left(\frac{m54 + m45}{h}\right)\right) - \left(\left(\frac{m6'5' + m5'6'}{h}\right) + \left(\frac{m5'4' + m4'5'}{h}\right)\right) = o$$

In the above equations, $r1 = \frac{h}{L}\frac{Ib}{Ic1}$; $r2 = \frac{h}{L}\frac{Ib}{Ic2}$

$$r = \frac{Ab\ E}{L} \quad ; \quad P = \frac{6\ Ib}{Ab\ L^2}$$

$$S11' = \frac{L11'}{A11'\ E11'} \cdot \frac{Ab\ Eb}{Lb} \quad ; \quad S22' = \frac{L22'}{A22'\ E22'} \cdot \frac{Ab\ Eb}{Lb}$$

$$S33' = \frac{L33'}{A33'\ E33'} \cdot \frac{Ab\ Eb}{Lb} \quad ; \quad S44' = \frac{L44'}{A44'\ E44'} \cdot \frac{Ab\ Eb}{Lb}$$

$$S55' = \frac{L55'}{A55'\ E55'} \cdot \frac{Ab\ Eb}{Lb}$$

Example

In the numerical example, a frame of the following dimensions and properties as shown in fig. 5.0511 is analysed:-

L = Lb = 0.405m; h = 0.30m

Large column 50mm x 120mm; Small column 50mm x 60mm

All beams 50mm x 40mm;

$Ac1 = 0.05 \times 0.12 = 0.006m^2$; $Ac2 = 0.05 \times 0.06 = 0.003m^2$

$Ab = 0.05 \times 0.04 = 0.002m^2$

$Ic1 = 0.05 \times 0.12^3/12 = 7.2 \times 10^{-6} m^4$; $Ic2 = 0.05 \times 0.06^3/12 = 9 \times 10^{-7} m^4$

$Ib = 0.05 \times 0.04^3/12 = 2.66667 \times 10^{-7} m^4$

$T = 20^oC$; $\alpha = 0.00001$ per ^oC

$E = 21 \times 10^6$ KN/m^2

The following parameters required in the matrix are first calculated:-

$$r1 = \frac{h}{L} \cdot \frac{Ib}{Ic1} = \frac{0.3}{0.405} \times \frac{2.66667 \times 10^{-7}}{7.2 \times 10^{-6}} = 0.02743484$$

$$r2 = \frac{h}{L} \frac{Ib}{Ic2} = \frac{0.3}{0.405} \times \frac{2.66667 \times 10^{-7}}{9 \times 10^{-7}} = 0.21947874$$

$$r = \frac{Ab\ E}{L} = \frac{0.002 \times 21 \times 10^6}{0.405} = 103703.7037 \text{ KN/m}$$

$$p = \frac{6\ Ib}{Ab\ L^2} = \frac{6 \times 2.66667 \times 10^{-7}}{0.002 \times 0.405^2} = 0.00487731$$

$$r\frac{pL}{h} = \frac{103703.7037 \times 0.00487731 \times 0.405}{0.3} = 682.822716$$

$$r \alpha TL = 103703.7037 \times 0.00001 \times 20 \times 0.405 = 8.40$$

$$\alpha TEAbh = 0.00001 \times 20 \times 21 \times 10^6 \times 0.002 \times 0.3 = 2.520$$

$$\frac{Ab\ Eh}{L} = \frac{0.002 \times 21 \times 10^6 \times 0.3}{0.405} = 31111{\cdot}1111$$

The conditions of compatibility of deformations and equilibrium of forces derived above can now be formulated into matrix form as shown in Table: 500.08, and introducing the above numerical parameters into the general matrix, the numerical matrix shown in Table:500.09 is obtained. The solution of this

matrix gives the bending moments in all members, deflections at all joints and axial forces in the beams. Shearing forces can be obtained from the conditions of static equilibrium. The results are shown in fig. 5.0514.

(b) Analysis using the stiffness method

A two-dimensional stiffness programme written in the Basic Language was developed for use on a Hewlett-Packard Model 9830 Computer. The programme was written for the action of conventional forces on a structure and the effect of temperature was superimposed as explained in text below (it is not considered necessary to show the formulations of the stiffness programme, as the method is now well developed and many text books are now available showing full formulations).

The effect of temperature in any member is to make it expand by the amount αTL, where α is the coefficient of thermal expansion, T is the temperature rise and L is the initial length of the member. However, in indeterminate structures, free and unobstructed expansion is not possible. This results in forces being exerted on connecting members by the expanding member. This force then is the basic cause of stresses in all other members. The force is exerted equally in both directions along the axis of the member being heated and can be calculated as follows:-

Assume that a heated member is fully restrained from expanding

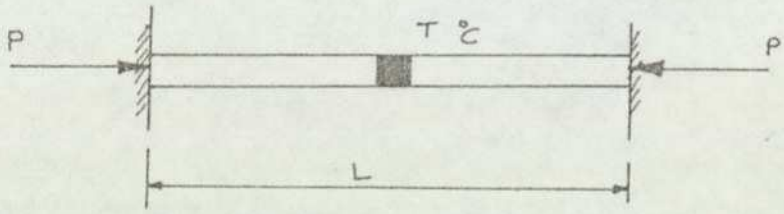

Fig. 5.0512

The force required to stop the member from expanding can be found from the stress/strain relationship as follows:-

Young's Modulus, $E = \frac{\text{Stress}}{\text{Strain}}$

i.e. $$E = \frac{L/A}{e/L} \text{ ------- (1)}$$

where P = force exerted

A = area of cross-section of member

e = extension of member, and

L = initial length of member

but

$$e = \alpha TL \text{ ------- (2)}$$

substituting into equ. (1) and re-arranging gives

$$P = \frac{EA}{L} \alpha TL = EA\alpha T \quad \text{(note that P is independent of L)}$$

In order to determine the effect of constant temperature distribution in the roof beam of the 6-storey frame, equal and opposite forces of magnitude P are applied along the axis of the roof beam in the direction of the possible expansion and the frame analysed similar to any conventional applied load by the stiffness method. The resulting stresses and deformations are correct for all members except the axial force in the heated roof beam. In order to obtain the correct value of the axial force, the force obtained by the stiffness analysis has to be superimposed by a reversed force equal in magnitude to the originally applied force, P.

Analysing the same numerical example as was done with the force-displacement method, the force to be applied is

$$P = AE\alpha T$$
$$= 0.002 \times 21 \times 10^6 \times 0.00001 \times 20$$
$$= 8.40 \text{ KN}$$

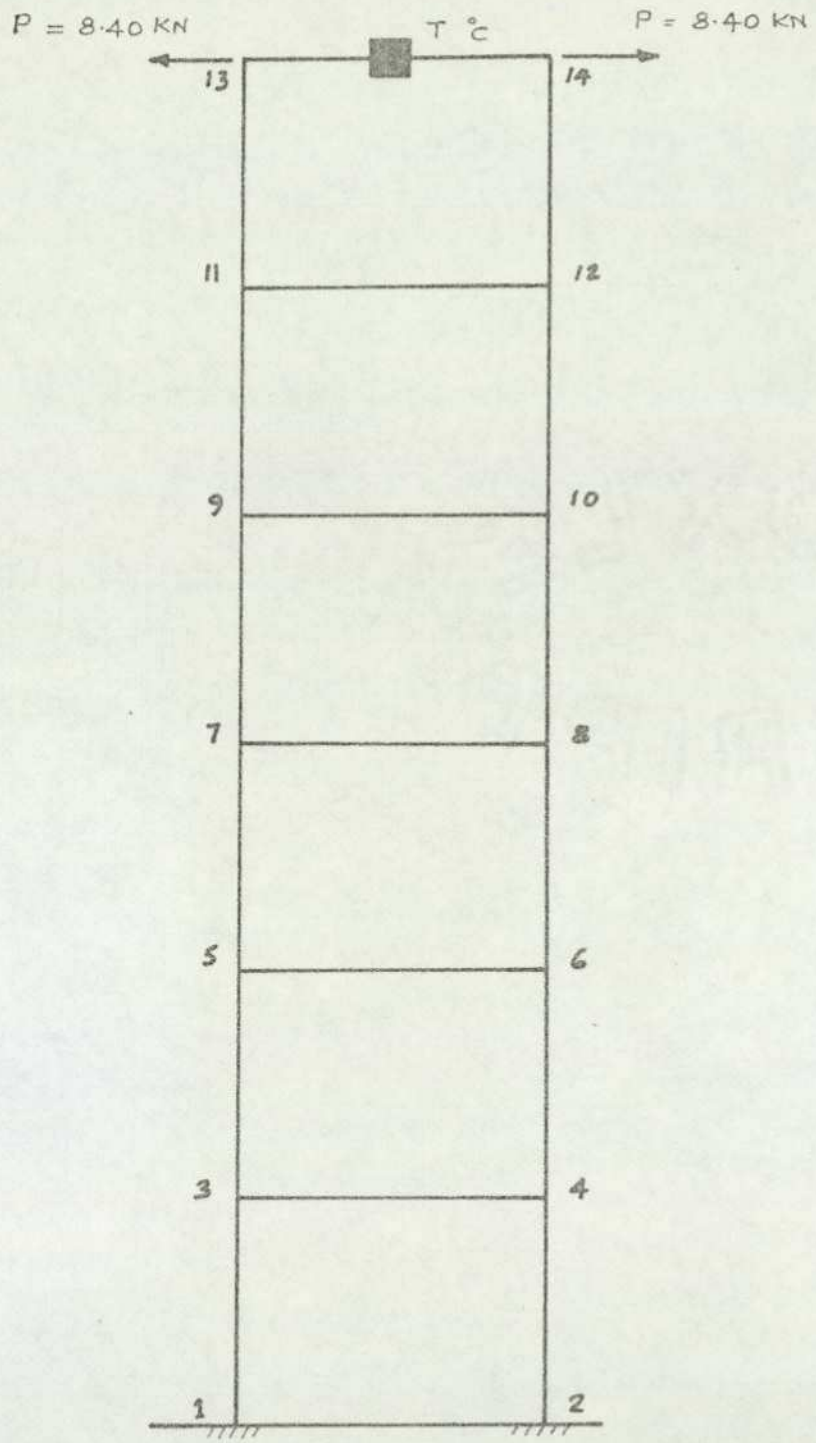

Fig. 5.0513 The effect of constant temperature distribution in the roof beam analysed by the stiffness method

The results of the effect of constant temperature distribution in the roof beam and analysed by the stiffness method are shown in fig. 5.0514.

EQN. NO.		1	2	3	4	5	6	7	8	9	10	11	12	13	14	15	16	17	18	19	20	21	22	23	24	25	26	27	28	29	30	31	32	33	34	35	36	37	38	39	40	41	42	LOAD
	REF. ST.	0					1							2							3								4							5							6		VECTOR
No.	REF. EQN.	m01	m01'	N00'	Δ0x	Δ0x'	m10	m12	m10'	m12'	N11'	Δ1x	Δ1x'	m21	m23	m21'	m23'	N22'	Δ2x	Δ2x'	m32	m34	m32'	m34'	N33'	Δ3x	Δ3x'	m43	m45	m43'	m45'	N44'	Δ4x	Δ4x'	m54	m56	m54'	m56'	N55'	Δ5x	Δ5x'	m65	m65'	
1	F100'	-5.01375	2.46314	0	-182.82274	0	-0.04774	0	0	0	0	182.82274	0																															0
2	F100	2.46314	-6.02212	0	0	-182.82274	0	0	-0.54192	0	0	0	182.82274																															0
3	C00'	0	0	+1	103703.7	103703.7	0	0	0	0	0	0	0																															8.40
4	E00'	+1	-1	0	0	0	+1	0	-1	0	0	0	0																															0
5	E0X	+1	0	0	3111.11	3111.11	+1	0	0	0	0	0	0																															2.520
6	F012	-0.04774	0	0	-182.82274	0	-0.13548	0.13548	0	0	0	1345.68094	0	-0.04774	0	0	0	0	182.82274	0																									0
7	F0'1'2'	0	-0.54192	0	0	-182.82274	0	0	1.08384	1.08384	0	0	1345.68094	0	0	-0.54192	0	0	0	182.82274																									0
8	C11'	0	0	0	0	0	0	0	0	0	-1	103703.7	103703.7	0	0	0	0	0	0	0																									0
9	E11'	+1	-1	0	0	0	+1	+1	-1	-1	0	0	0	+1	0	-1	0	0	0	0																									0
10	E1X	+1	0	0	0	0	+1	+1	0	0	-0.3	0	0	+1	0	0	0	0	0	0																									0
11	F211'						4.93827	5.01375	2.46314	2.46314	0	182.82274	0	-0.04774	0	0	0	0	182.82274	0	0	0	0	0	0	0	0	0																	0
12	F2'11						2.46314	2.46314	4.93827	2.46314	0	0	182.82274	0	0	0.54192	0	0	0	182.82274	0	0	0	0	0	0	0	0																	0
13	F123						0	0.04774	0	0	0	182.82274	0	-0.13548	0.13548	0	0	0	1345.68094	0	0.04774	0	0	0	0	182.82274	0																	0
14	F1'2'3						0	0	0	0.54192	0	0	182.82274	0	0	1.08385	1.08385	0	0	1345.68094	0	0	0.54192	0	0	0	182.82274																	0
15	C22'						0	0	0	0	0	0	0	0	0	0	0	-1	103703.7	103703.7	0	0	0	0	0	0	0																	0
16	E22'						0	+1	0	-1	0	0	0	+1	+1	-1	-1	0	0	0	+1	0	-1	0	0	0	0	0																	0
17	E2X						0	+1	0	0	0	0	0	+1	+1	0	0	-0.3	0	0	+1	0	0	0	0	0	0	0																	0
18	F322'													4.93827	5.01375	2.46314	2.46314	0	182.82274	0	0.04774	0	0	0	182.82274	0	0	0	0	0	0	0	0										0
19	F3'22													2.46314	2.46314	4.93827	6.02212	0	0	182.82274	0	0	0.54192	0	0	0	182.82274	0	0	0	0	0	0	0										0
20	F234													0	-0.04774	0	0	0	182.82274	0	0.13548	0.13548	0	0	1345.68094	0	-0.04774	0	0	0	0	182.82274	0										0
21	F2'3'4													0	0	0	0.54192	0	182.82274	0	0	0	1.08385	0	0	1345.68094	0	0	0	0.54192	0	0	182.82274										0
22	C33'													0	0	0	0	0	0	0	0	0	0	0	-1	103703.7	103703.7	0	0	0	0	0	0										0
23	E33'													0	+1	0	-1	0	0	0	+1	+1	-1	-1	0	0	0	+1	0	-1	0	0	0										0
24	E3X													0	+1	0	0	0	0	0	+1	+1	0	0	-0.3	0	0	+1	0	0	0	0	0										0
25	F433'													4.93827	5.01375	2.46314	2.46314	0	182.82274	0	0.04774	0	0	0	182.82274	0	0	0	0	0	0	0	0										0
26	F4'33													2.46314	2.46314	4.93827	6.02212	0	0	182.82274	0	0	0.54192	0	0	0	182.82274	0	0	0	0	0	0	0										0
27	F345													0	-0.04774	0	0	0	182.82274	0	0.13548	0.13548	0	0	1345.68094	0	-0.04774	0	0	0	0	182.82274	0										0
28	F3'4'5													0	0	0	0.54192	0	182.82274	0	0	0	1.08385	0	0	1345.68094	0	0	0	0.54192	0	0	182.82274										0
29	C44'													0	0	0	0	0	0	0	0	0	0	0	-1	103703.7	103703.7	0	0	0	0	0	0										0
30	E44'													0	+1	0	-1	0	0	0	+1	+1	-1	-1	0	0	0	+1	0	-1	0	0	0										0
31	E4X													0	+1	0	0	0	0	0	+1	+1	0	0	-0.3	0	0	+1	0	0	0	0	0										0
32	F544'																				4.93827	5.01375	2.46314	2.46314	0	182.82274	0	-0.04774	0	0	0	0	182.82274	0	0								0
33	F5'44																				2.46314	2.46314	4.93827	6.02212	0	182.82274	0	0	0	0	0	0	182.82274	0	0								0
34	F456																				0	-0.04774	0	0	0	182.82274	0	0.13548	0.13548	0	0	0	1345.68094	0	-0.04774	0							0
35	F4'5'6'																				0	0	0	0.54192	0	182.82274	0	0	0	0	0	0	1345.68094	0	0.54192	0							0
36	C55'																				0	0	0	0	0	0	0	0	0	1.08385	1.08385	0	0	1345.68094	0	0							0
37	E55'																				0	0	0	0	0	0	0	0	0	0	0	-1	103703.7	103703.7	0	0							0
38	E5X																				0	+1	0	-1	0	0	0	+1	+1	-1	-1	0	0	0	+1	-1							0
39	F655'																				0	+1	0	0	0	0	0	+1	+1	0	0	-0.3	0	0	+1	0							0
40	F6'55																											4.93827	5.01375	2.46314	2.46314	0	182.82274	0	0.04774	0							0
41	F56																											2.46314	2.46314	4.93827	6.02212	0	0	182.82274	0	0.54192							0
42	F5'6'																											0	0.04774	0	0	0	182.82274	0	0.13548	0							0

Table: 500.09 Numerical matrix for the effect of constant temperature distribution in the roof beam of a frame shear wall.

		1	2	3	4	5	6	7	8	9	10	11	12	13	14	15	16	17	18	19	20	21	22	23	24	25	26	27	28	29	30	31	32	33	34	35	36	37	38	39	40	41	42	LOAD
		0-0′					1-1′							2-2′							3-3′							4-4′								5-5′							6-6′		VECTOR
		m01	m01′	N00′	Δ0x	Δ0′x	m10	m12	m10′	m12′	N11′	Δ1x	Δ1′x	m21	m23	m21′	m23′	N22′	Δ2x	Δ2′x	m32	m34	m32′	m34′	N33′	Δ3x	Δ3′x	m43	m45	m43′	m45′	N44′	Δ4x	Δ4′x	m54	m56	m54′	m56′	N55′	Δ5x	Δ5′x	m65	m65′	
1	F.100′	$\frac{(2+2r_1)}{L}$	$\frac{1}{L}$	0	$-rPL/E$	0	$-r_1/L$	0	0	0	0	rPL/E	0																															0
2	F.1′0′0	$\frac{1}{L}$	$\frac{(2+2r_2)}{L}$	0	0	$-rPL/E$	0	0	$-r_2/L$	0	0	0	rPL/E																															0
3	C.00′	0	0	S00′	r	r	0	0	0	0	0	0	0																															rXTL
4	E.00′	1	-1	0	0	0	1	0	-1	0	0	0	0																															0
5	E.0X	1	0	0	EAR/L	EAR/L	1	0	0	0	0	0	0																															αTE-PA
6	F.012	$-r_1/L$	0	0	$-rPL/E$	0	$2r_1/L$	$2r_1/L$	0	0	0	$2rPL/E$	0	$-r_1/L$	0	0	0	0	rPL/E	0																							0
7	F.0′1′2′	0	$-r_2/L$	0	0	$-rPL/E$	0	0	$2r_2/L$	$2r_2/L$	0	0	$2rPL/E$	0	0	$-r_2/L$	0	0	0	rPL/E																							0
8	C.11′	0	0	0	0	0	0	0	0	0	-S11′	r	r	0	0	0	0	0	0	0																							0
9	E.11′	1	-1	0	0	0	1	1	-1	-1	0	0	0	1	0	-1	0	0	0	0																							0
10	E.1X	1	0	0	0	0	1	1	0	0	$-h$	0	0	1	0	0	0	0	0	0																							0
11	F.211′						$2/L$	$\frac{-(2+2r_1)}{L}$	$1/L$	$-1/L$	0	$-rPL/E$	0	r_1/L	0	0	0	0	$-rPL/E$	0	0	0	0	0	0	0	0																	0
12	F.2′1′1						$1/L$	$-1/L$	$2/L$	$\frac{-(2+2r_2)}{L}$	0	0	rPL/E	0	0	r_2/L	0	0	0	$-rPL/E$	0	0	0	0	0	0	0																	0
13	F.123						0	r_1/L	0	0	0	$-rPL/E$	0	$-2r_1/L$	$-2r_1/L$	0	0	0	$-2rPL/E$	0	r_1/L	0	0	0	0	$-rPL/E$	0																	0
14	F.1′2′3						0	0	0	r_2/L	0	0	$-rPL/E$	0	0	$-2r_2/L$	$-2r_2/L$	0	0	$-2rPL/E$	0	0	r_2/L	0	0	0	$-rPL/E$																	0
15	C.22′						0	0	0	0	0	0	0	0	0	0	0	-S22′	r	r	0	0	0	0	0	0	0																	0
16	E.22′						0	1	0	-1	0	0	0	1	1	-1	-1	0	0	0	1	0	-1	0	0	0	0																	0
17	E.2X						0	1	0	0	0	0	0	1	1	0	0	$-h$	0	0	1	0	0	0	0	0	0																	0
18	F.322′													$-2/L$	$\frac{(2+2r_1)}{L}$	$-1/L$	$1/L$	0	rPL/E	0	$-r_1/L$	0	0	0	0	rPL/E	0	0	0	0	0	0	0	0									0
19	F.3′22													$-1/L$	$1/L$	$-2/L$	$\frac{(2+2r_2)}{L}$	0	0	rPL/E	0	0	$-r_2/L$	0	0	0	rPL/E	0	0	0	0	0	0	0									0
20	F.234													0	$-r_1/L$	0	0	0	rPL/E	0	$2r_1/L$	$2r_1/L$	0	0	0	$2rPL/E$	0	$-r_1/L$	0	0	0	0	rPL/E	0									0
21	F.2′3′4′													0	0	0	$-r_2/L$	0	0	rPL/E	0	0	$2r_2/L$	$2r_2/L$	0	0	$2rPL/E$	0	0	$-r_2/L$	0	0	0	rPL/E									0
22	C.33′													0	0	0	0	0	0	0	0	0	0	0	-S33′	r	r	0	0	0	0	0	0	0									0
23	E.33′													0	1	0	-1	0	0	0	1	1	-1	-1	0	0	0	1	0	-1	0	0	0	0									0
24	E.3X													0	1	0	0	0	0	0	1	1	0	0	$-h$	0	0	1	0	0	0	0	0	0									0
25	F.433′																				$2/L$	$\frac{-(2+2r_1)}{L}$	$1/L$	$-1/L$	0	$-rPL/E$	0	r_1/L	0	0	0	0	$-rPL/E$	0	0	0	0	•	0	•	0			0
26	F.4′33																				$1/L$	$-1/L$	$2/L$	$\frac{-(2+2r_2)}{L}$	0	0	$-rPL/E$	0	0	r_2/L	0	0	0	$-rPL/E$	0	0	0	0	0	0	0			0
27	F.345																				0	r_1/L	0	0	0	$-rPL/E$	0	$-2r_1/L$	$-2r_1/L$	0	0	0	$-2rPL/E$	0	r_1/L	0	0	0	0	$-rPL/E$	0			0
28	F.3′4′5′																				0	0	0	r_2/L	0	0	$-rPL/E$	0	0	$-2r_2/L$	$-2r_2/L$	0	0	$-2rPL/E$	0	0	r_2/L	0	0	0	$-rPL/E$			0
29	C.44′																				0	0	0	0	0	0	0	0	0	0	0	-S44′	r	r	0	0	0	0	0	0			0
30	E.44′																				0	1	0	-1	0	0	0	-1	0	0	0	1	1	-1	-1	0	0	0	0			0
31	E.4X																				0	1	0	0	0	0	0	0	0	0	0	1	1	0	0	$-h$	0	0	0			0
32	F.544′																											$-2/L$	$\frac{(2+2r_1)}{L}$	$-1/L$	$1/L$	0	rPL/E	0	$-r_1/L$	0	0	0	0	rPL/E	0	0	0	0	0	0
33	F.5′4′4																											$-1/L$	$1/L$	$-2/L$	$\frac{(2+2r_2)}{L}$	0	0	rPL/E	0	0	$-r_2/L$	0	0	0	rPL/E	0	0	0
34	F.456																											0	$-r_1/L$	0	0	0	rPL/E	0	$2r_1/L$	$2r_1/L$	0	0	0	$2rPL/E$	0	$-r_1/L$	0	0
35	F.4′5′6																											0	0	0	$-r_2/L$	0.	0	rPL/E	0	0	$2r_2/L$	$2r_2/L$	0	0	$2rPL/E$	0	$-r_2/L$	0
36	C.55′																											0	0	0	0	0	0	0	0	0	0	-S55′	r	r	0	0		0
37	E.55′																											0	1	0	-1	0	0	0	1	1	-1	-1	0	0	0	1	-1	0
38	E.5X																											0	1	0	0	0	0	0	1	1	0	0	$-h$	0	0	1	0	0
39	F.655′																																		$2/L$	$\frac{-(2+2r_2)}{L}$	$1/L$	$-1/L$	0	$-rPL/E$	0	r_1/L	0	0
40	F.6′5′5																																		$1/L$	$-1/L$	$2/L$	$\frac{-(2+2r_2)}{L}$	0	0	$-rPL/E$	0	r_2/L	0
41	F.56																																		0	r_1/L	0	0	0	$-rPL/E$	0	$-2r_1/L$	0	0
42	F.5′6′																																		0	0	0	r_2/L	0	0	$-rPL/E$	0	$-2r_2/L$	0

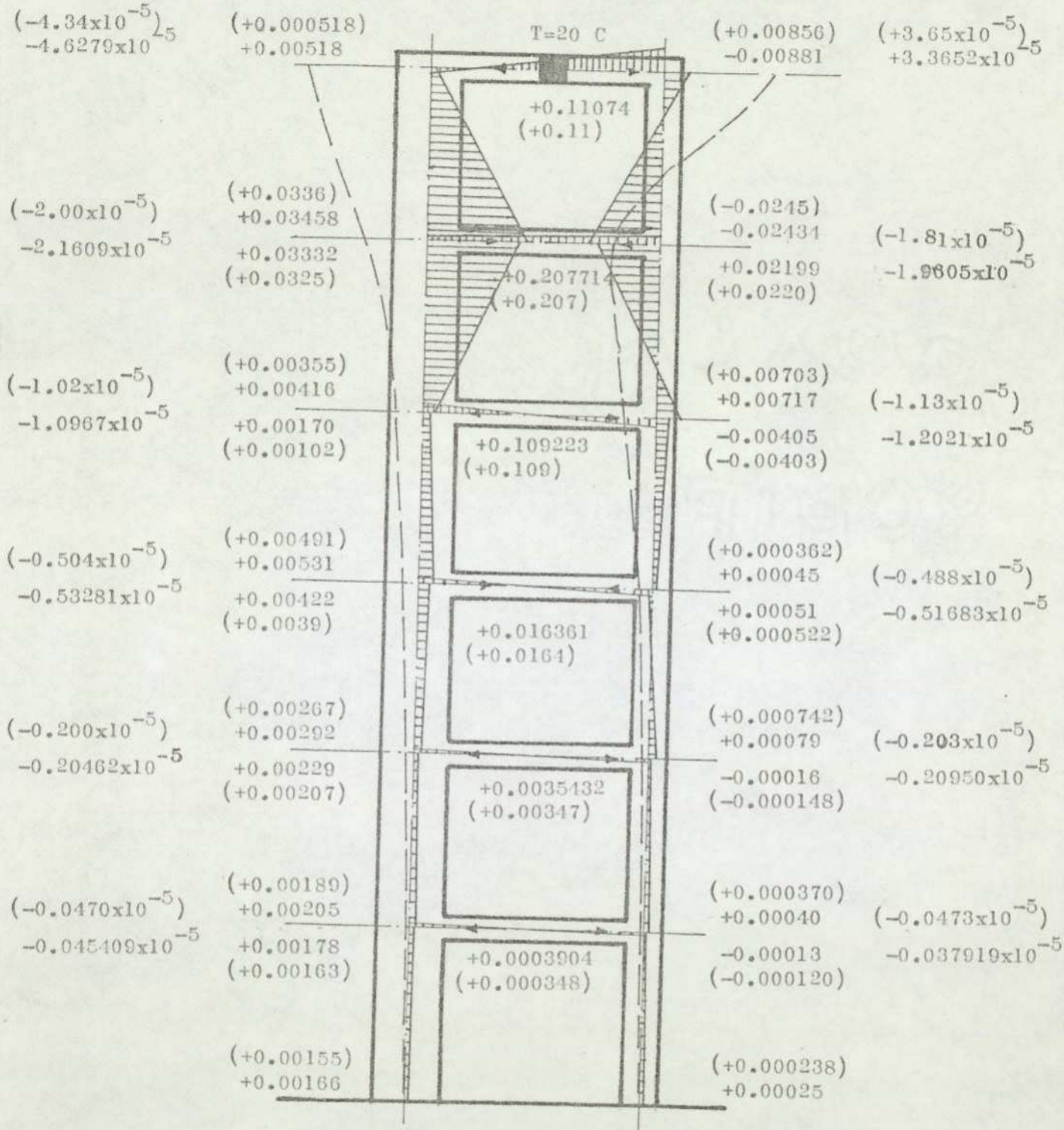

Fig. 5.0514 Shows the results of the effect of Constant Temperature distribution in the roof beam

Unbracketed Figures - - - show results by the Force-Displacement Method

Bracketed Figures - - - show results by the Stiffness Method

(a) Analysis using the force-displacement method

While the analysis for linear and constant temperature distributions can be done simultaneously, here, these are carried out separately so as to show

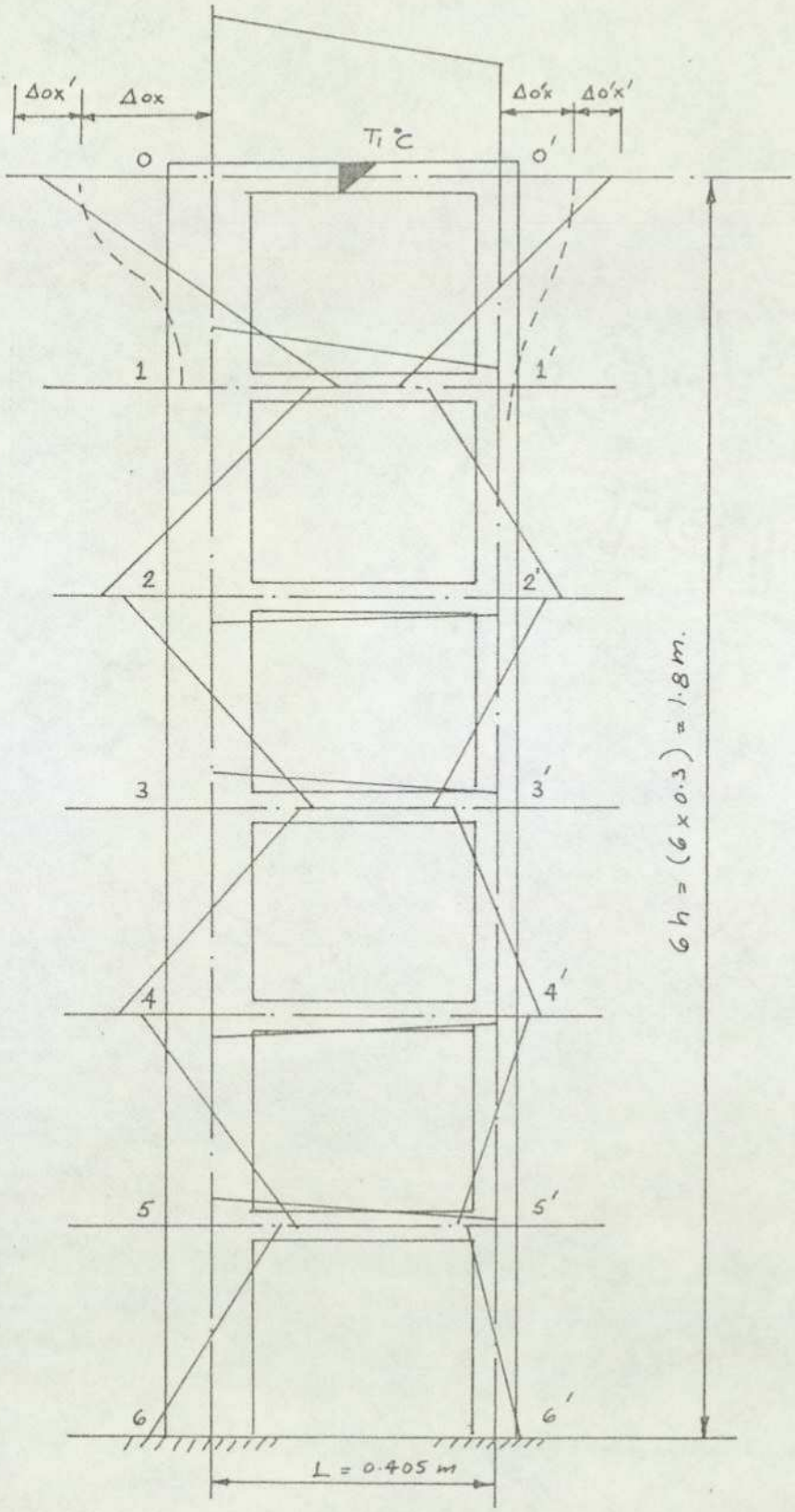

Fig. 5.0521 The effect of linear temperature distribution in roof beam showing assumed bending moments for the setting up of the matrix.

the difference between the effects of the two types of temperature distributions. The following analysis includes the effect of axial deformations of all beams, but excludes the axial deformations of columns as these are expected to be negligible for this case.

Denoting

$$\Delta ox + \Delta ox' + \Delta o'x + \Delta o'x' = \frac{\alpha T1L}{2}$$

Where Δox, $\Delta ox'$, ... etc. are as defined in section 5.05.1.

The conditions of compatibility of deformations and equilibrium of forces remain identical to those derived for the constant temperature distribution, except conditions, F.1oo', F.1'o'o, C.oo', and E.ox, which are modified as follows:-

F.1oo' $$mo1\left(\frac{L}{3EIb} + \frac{h}{3EIc1}\right) - m1o\,\frac{h}{6EIc1} + mo'1'\,\frac{L}{6EIb} = \frac{\Delta ox - \Delta 1x}{h} - \theta oo'$$

or $$2(r1+1)\left(\frac{mo1}{L}\right) - r1\left(\frac{m1o}{L}\right) + \left(\frac{mo'1'}{L}\right) - r\Delta ox\,\frac{pL}{h} + r\Delta 1x\,\frac{pL}{h} = -\frac{3\alpha T1EIb}{Ld}$$

Similarly

F.1'o'o $$-m1'o'\,\frac{h}{6EIc2} + mo'1'\left(\frac{h}{3EIc2} + \frac{L}{3EIb}\right) + mo1\,\frac{L}{6EIb} = \frac{\Delta o'x - \Delta 1'x}{h} - \theta oo'$$

or $$-r2\left(\frac{m1'o'}{L}\right) + 2(r2+1)\left(\frac{mo'1'}{L}\right) + \frac{mo1}{L} - r\Delta o'x\,\frac{pL}{h} + r\Delta 1'x\,\frac{pL}{h} - \frac{3\alpha T1EIb}{Ld}$$

C.oo' $$\Delta ox' + \Delta o'x' = \frac{Noo'\,Loo'}{Aoo'\,Eoo'}$$

or $$r\Delta ox + r\Delta o'x + Noo'\,Soo' = \frac{r\alpha T1L}{2}$$

E.ox $$\frac{mo1 + m1o}{h} = Noo'$$

or $$mo1 + m1o + \frac{EAbh}{L}\Delta ox + \frac{EAbh}{L}\Delta o'x = \frac{\alpha T1EAbh}{2}$$

In the above equations

$$r1 = \frac{h}{L}\frac{Ib}{Ic1} \quad ; \quad r2 = \frac{h}{L}\frac{Ib}{Ic2} \quad ; \quad r = \frac{AbE}{L}$$

$$p = \frac{6Ib}{AbL2} \quad ; \quad \theta oo' = \frac{\alpha T1L}{2d} \quad ; \quad Soo' = \frac{Loo'}{Aoo'Eoo'}\,\frac{AbE}{Lb}$$

and $$Noo' = \left(\frac{\alpha T1L}{2} - \Delta ox - \Delta o'x\right)\frac{EAb}{L}$$

By inspection of the above equations, it can be seen that only the right hand side i.e. the load vector has changed in comparison with the constant temperature distribution case.

The left hand side remains identical. However, the complete matrix is shown in Table 500.10 for the linear temperature distribution in the roof beam.

Example

As a numerical example the frame of section 5.05.1 is analysed for a linear distribution in the roof beam when $T1 = 20^{o}C$. The numerical matrix for this example is shown in Table 500.11. The results of this problem are shown in fig. 5.0524.

(b) Analysis using the stiffness method

When a simply supported homogeneous member is subjected to a linear temperature distribution, axial deformations as well as bending deformations take place. These can be calculated as shown in section 5.01.

It was shown that axial deformation of a beam,

$$\Delta L = \alpha T_{av}.L \quad \ldots\ldots \text{(i)}$$

where $T_{av.} = \frac{T1}{2}$

and angular change in an element

$$d\theta = \frac{de}{h} = \alpha\left(\frac{T1}{2}\right)\frac{dx}{h}$$

from which $\theta = \int_0^{L/2} d\theta = \alpha\left(\frac{T1}{2d}\right) L \quad \ldots\ldots \text{(ii)}$

and bending moment $M = \alpha E T1 \frac{I}{d} \quad \ldots\ldots \text{(iii)}$

It will be shown later, that this bending moment is zero, and represents either the equivalent moment to produce the specified curvature or a fixed-end bending moment if ends are flexurally restrained.

When this member forms part of a structure, free and unobstructed deformations cannot take place. This results in direct axial and bending forces being exerted on the connecting members. In order to keep this member in the original configuration a force 'P' and a bending moment 'M' will have to be applied as shown in fig. 5.0522.

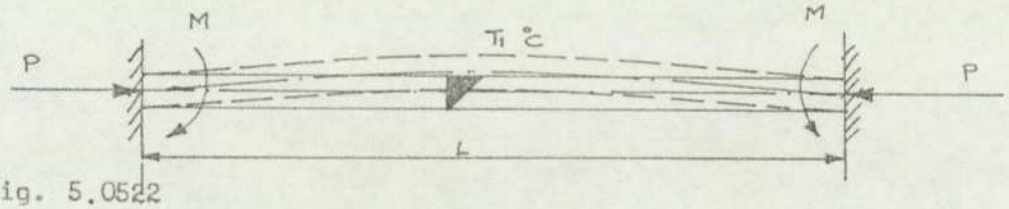

Fig. 5.0522

The magnitudes of the axial force and the bending moment are as follows:-

$$P = EA\alpha\frac{T1}{2} = EA\alpha Tav$$

and $$M = \alpha T1\frac{EI}{d}$$

Therefore, in order to find the effect of linear temperature distribution in the roof beam of the 6-storey frame (i) equal and opposite forces of value, $P = EA\alpha Tav$. are applied along the axis of the roof beam in the direction of the possible expansion and (ii) bending moments of value, $M = \alpha T1\frac{EI}{d}$ are applied at the ends of the member in the direction of the curvature i.e. causing upward hogging as shown in fig. 5.0523.

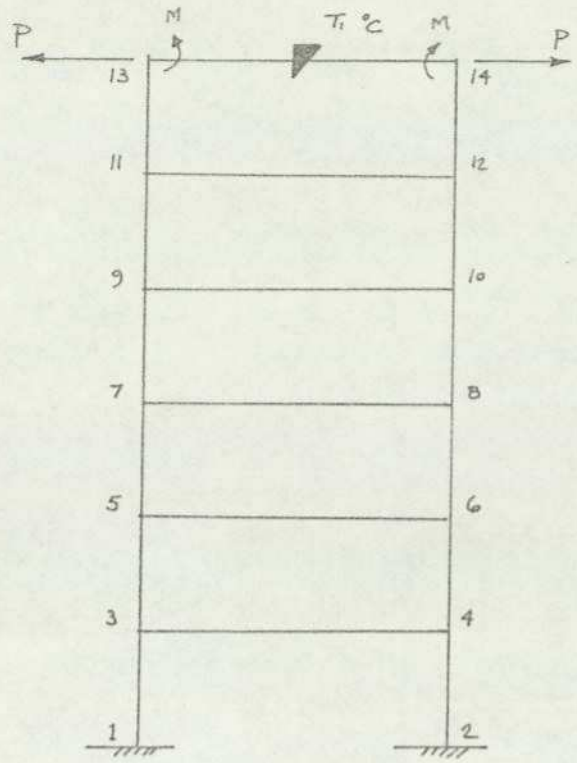

Fig.5.0523 The effect of linear temperature distribution in roof beam analysed by the Stiffness Method.

The frame is now analysed by the usual stiffness method for the two sets of forces shown in fig. 5.0523. The resulting stresses and deformations are correct for all members except the axial force and the bending moments in the heated roof beam itself. In order to obtain the correct values of axial force and bending moments in this member, the axial force and bending moments obtained by the stiffness analysis have to be superimposed by a reversed force and bending moments i.e. of opposite sign, and both equal in magnitude to the originally applied force and bending moments.

Analysing the same numerical example as was done with the force-displacement method in section 5.05.2(a), the axial force and bending moments to be applied are

$$P = AE\alpha T_{av} = 0.002 \times 21 \times 10^{6} \times 0.00001 \times \frac{20}{2} = 4.2 \text{ KN}$$

$$M = \alpha T1 \frac{EI}{d} = 0.00001 \times 20 \times 21 \times 10^{6} \times 2.6667 \times \frac{10^{-7}}{0.04}$$

$$= 0.02800035 \text{ KN-m}$$

The results of the effect of linear temperature distribution in the roof beam and analysed by the stiffness method are shown in fig. 5.0524.

EQN. NO	1	2	3	4	5	6	7	8	9	10	11	12	13	14	15	16	17	18	19	20	21	22	23	24	25	26	27	28	29	30	31	32	33	34	35	36	37	38	39	40	41	42	LOAD
REF. JT.	0					1							2							3							4							5								6		VECTOR
No REF. EQN.	m01	m01'	N00'	Δ0x	Δ0x'	m10	m12	m10'	m12'	N11'	Δ1x	Δ1x'	m21	m23	m21'	m23'	N22'	Δ2x	Δ2x'	m32	m34	m32'	m34'	N33'	Δ3x	Δ3x'	m43	m45	m43'	m45'	N44'	Δ4x	Δ4x'	m54	m56	m54'	m56'	N55'	Δ5x	Δ5x'	m65	m65'		
1 F100'	5.07375	2.46914	0	-1.82270	0	-0.04774	0	0	0	0	1.82270	0																															-0.20741
2 F10'0	2.46914	6.02212	0	0	-1.82270	0	0	-0.59192	0	0	0	1.82270																															-0.20741
3 C00'	0	0	+1	1.03703	1.03703	0	0	0	0	0	0	0																															4.20
4 E00'	+1	-1	0	0	0	+1	0	-1	0	0	0	0																															0
5 E0X	+1	0	0	3.1111	3.1111	+1	0	0	0	0	0	0																															1.260
6 F012	-0.04774	0	0	-1.82270	0	0.13598	0.13598	0	0	0	1.55494	0	-0.04774	0	0	0	0	1.82270	0																									0
7 F01'2'	0	-0.59192	0	0	-1.82270	0	0	1.08385	1.08385	0	0	1.55494	0	0	-0.59192	0	0	0	1.82270																									0
8 C11'	0	0	0	0	0	0	0	0	0	-1	1.03703	1.03703	0	0	0	0	0	0	0																									0
9 E11'	+1	-1	0	0	0	+1	+1	-1	-1	0	0	0	+1	0	-1	0	0	0	0																									0
10 E1X	+1	0	0	0	0	+1	+1	0	0	-0.3	0	0	+1	0	0	0	0	0	0																									0
11 F211'						4.73827	5.07375	2.46914	2.46914	0	1.82270	0	0.04774	0	0	0	0	1.82270	0	0	0	0	0	0	0	0																		0
12 F2'11						2.46914	2.46914	4.73827	6.02212	0	0	1.82270	0	0	0.59192	0	0	0	1.82270	0	0	0	0	0	0	0																		0
13 F123						0	0.04774	0	0	0	1.82270	0	-0.13598	-0.13598	0	0	0	1.55494	0	0.04774	0	0	0	0	0	1.82270																		0
14 F1'23'						0	0	0	0.59192	0	0	1.82270	0	0	-1.08385	-1.08385	0	0	1.55494	0	0	0.59192	0	0	0	1.82270																		0
15 C22'						0	0	0	0	0	0	0	0	0	0	0	-1	1.03703	1.03703	0	0	0	0	0	0	0																		0
16 E22'						0	+1	0	-1	0	0	0	+1	+1	-1	-1	0	0	0	+1	0	-1	0	0	0	0																		0
17 E2X						0	+1	0	0	0	0	0	+1	+1	0	0	-0.3	0	0	+1	0	0	0	0	0	0																		0
18 F322'													4.73827	5.07375	2.46914	2.46914	0	1.82270	0	0.04774	0	0	0	0	1.82270	0	0	0	0	0	0	0										0
19 F'322													2.46914	2.46914	4.73827	6.02212	0	0	1.82270	0	0	0.59192	0	0	0	1.82270	0	0	0	0	0	0										0
20 F234													0	0.04774	0	0	0	1.82270	0	0.13598	0.13598	0	0	0	1.55494	0	0.04774	0	0	0	1.82270	0										0
21 F'234'													0	0	0	0.59192	0	0	1.82270	0	0	1.08385	1.08385	0	0	1.55494	0	0	0.59192	0	0	0	1.82270										0
22 C33'													0	0	0	0	0	0	0	0	0	0	0	-1	1.03703	1.03703	0	0	0	0	0	0										0
23 E33'													0	+1	0	-1	0	0	0	+1	+1	-1	-1	0	0	0	+1	0	-1	0	0	0	0										0
24 E3X													0	+1	0	0	0	0	0	+1	+1	0	0	-0.3	0	0	+1	0	0	0	0	0	0										0
25 F433'																				4.73827	5.07375	2.46914	2.46914	0	1.82270	0	0.04774	0	0	0	0	0	0	0	0	0	0	0					0
26 F'433																				2.46914	2.46914	4.73827	6.02212	0	0	1.82270	0	0	0.59192	0	0	0	1.82270	0	0	0	0	0	0					0
27 F345																				0	0.04774	0	0	0	0	1.82270	0	0	0	0	0	0	1.82270	0	0	0	0	0	0					0
28 F'34'5																				0	0	0	0.59192	0	0	1.82270	0	0	0	0	0	0	1.82270	0	0	0	0	0	0					0
29 C44'																				0	0	0	0	0	0	0	0	0	0	0	0	0	0	0	0	0	0	0	0					0
30 E44'																				0	+1	0	-1	0	0	0	+1	0	-1	0	0	0	0											0
31 E4X																				0	+1	0	0	0	0	0	+1	0	0	0	0	0	0											0
32 F544'																							4.73827	5.07375	2.46914	2.46914	0	0	0	0	0	1.82270	0	0	0	0	0	0	0	0	0			0
33 F'544'																							2.46914	2.46914	4.73827	6.02212	0	0	0.59192	0	0	0	1.82270	0	0	0	0	0	0	0	0			0
34 F456																							0	0.04774	0	0	0.13598	0.13598	0	0	0	1.55494	0	0.04774	0								0
35 F'45'6'																							0	0	0	0.59192	0	0	1.08385	1.08385	0	0	1.55494	0	0.59192								0
36 C55'																							0	0	0	0	0	0	0	0	-1	1.03703	1.03703	0	0								0
37 E55'																							0	+1	0	-1	0	0	+1	+1	0	0	0	+1	-1								0
38 E5X																							0	+1	0	0	0	0	+1	+1	-0.3	0	0	+1	0								0
39 F655'																																4.73827	5.07375	2.46914	2.46914	0	1.82270	0	0.04774	0		0
40 F'65'5																																2.46914	2.46914	4.73827	6.02212	0	0	1.82270	0	0.59192		0
41 F56																																0	0.04774	0	0	0	1.82270	0.13598	0			0
42 F5'6'																																0	0	0	0.59192	0	0	1.82270	0	1.08385		0

Table: 500.11 Numerical matrix for the effect of linear temperature distribution in the roof beam of a 6-storey frame

		1	2	3	4	5	6	7	8	9	10	11	12	13	14	15	16	17	18	19	20	21	22	23	24	25	26	27	28	29	30	31	32	33	34	35	36	37	38	39	40	41	42	LOAD
		0.0′					1-1′							2-2′							3-3′			4-4′											5-5′								6-6′		VECTOR
		m01	m01′	N00′	Δ0x	Δ0′x	m10	m12	m10′	m12′	N11′	Δ1x	Δ1′x	m21	m23	m21′	m23′	N22′	Δ2x	Δ2′x	m32	m34	m32′	m34′	N33′	Δ3x	Δ3′x	m43	m45	m43′	m45′	N44′	Δ4x	Δ4′x	m54	m56	m54′	m56′	N55′	Δ5x	Δ5′x	m65	m65′	
1	F.100′	$\frac{(2+2r_1)}{L}$	$\frac{1}{L}$	0	$-rPL/_2$	0	$-r_1/_L$	0	0	0	0	$rPL/_2$	0																															$-3\alpha TE I_b/_{Ld}$
2	F.1′0′0	$\frac{1}{L}$	$\frac{(2+2r_2)}{L}$	0	0	$-rPL/_2$	0	0	$-r_2/_L$	0	0	0	$rPL/_2$																															$-3\alpha TE I_b/_{Ld}$
3	C.00′	0	0	S00′	r	r	0	0	0	0	0	0	0																															$r\alpha TL/2$
4	E.00′	1	-1	0	0	0	1	0	-1	0	0	0	0																															0
5	E.0X	1	0	0	$EAE_R/_L$	$EAE_R/_L$	1	0	0	0	0	0	0																															$\alpha TE_R A/_2$
6	F.012	$-r_1/_L$	0	0	$-rPL/_2$	0	$2r_1/_L$	$2r_1/_L$	0	0	0	$2rPL/_2$	0	$-r_1/_L$	0	0	0	0	$rPL/_2$	0																								0
7	F.0′1′2′	0	$-r_2/_L$	0	0	$-rPL/_2$	0	0	$2r_2/_L$	$2r_2/_L$	0	0	$2rPL/_2$	0	0	$-r_2/_L$	0	0	0	$rPL/_2$																								0
8	C.11′	0	0	0	0	0	0	0	0	0	$-S_{11}'$	r	r	0	0	0	0	0	0	0																								0
9	E.11′	1	-1	0	0	0	1	1	-1	-1	0	0	0	1	0	-1	0	0	0	0																								0
10	E.1X	1	0	0	0	0	1	1	0	0	$-h$	0	0	1	0	0	0	0	0	0																								0
11	F.211′						$2/_L$	$\frac{-(2+2r_1)}{L}$	$1/_L$	$-1/_L$	0	$-rPL/_2$	0	$r_1/_L$	0	0	0	0	$-rPL/_2$	0	0	0	0	0	0	0	0																		0
12	F.2′1′1						$1/_L$	$-1/_L$	$2/_L$	$\frac{-(2+2r_2)}{L}$	0	0	$+rPL/_2$	0	0	$r_2/_L$	0	0	0	$-rPL/_2$	0	0	0	0	0	0	0																		0
13	F.123						0	$r_1/_L$	0	0	0	$-rPL/_2$	0	$-2r_1/_L$	$-2r_1/_L$	0	0	0	$-2rPL/_2$	0	$r_1/_L$	0	0	0	0	$-rPL/_2$	0																		0
14	F.1′2′3′						0	0	0	$r_2/_L$	0	0	$-rPL/_2$	0	0	$-2r_2/_L$	$-2r_2/_L$	0	0	$-2rPL/_2$	0	0	$r_2/_L$	0	0	0	$-rPL/_2$																		0
15	C.22′						0	0	0	0	0	0	0	0	0	0	0	$-S_{22}'$	r	r	0	0	0	0	0	0	0																		0
16	E.22′						0	1	0	-1	0	0	0	1	1	-1	-1	0	0	0	1	0	-1	0	0	0	0																		0
17	E.2X						0	1	0	0	0	0	0	1	1	0	0	$-h$	0	0	1	0	0	0	0	0	0																		0
18	F.322′													$-2/_L$	$\frac{(2+2r_1)}{L}$	$-1/_L$	$1/_L$	0	$rPL/_2$	0	$-r_1/_L$	0	0	0	0	$rPL/_2$	0	0	0	0	0	0	0	0										0
19	F.3′2′2													$-1/_L$	$1/_L$	$-2/_L$	$\frac{(2+2r_1)}{L}$	0	0	$rPL/_2$	0	0	$-r_2/_L$	0	0	0	$rPL/_2$	0	0	0	0	0	0	0										0
20	F.234													0	$-r_1/_L$	0	0	0	$rPL/_2$	0	$2r_1/_L$	$2r_1/_L$	0	0	0	$2rPL/_2$	0	$-r_1/_L$	0	0	0	0	$rPL/_2$	0										0
21	F.2′3′4′													0	0	0	$-r_2/_L$	0	0	$rPL/_2$	0	0	$2r_2/_L$	$2r_2/_L$	0	0	$2rPL/_2$	0	0	$-r_2/_L$	0	0	0	$rPL/_2$										0
22	C.33′													0	0	0	0	0	0	0	0	0	0	0	$-S_{33}'$	r	r	0	0	0	0	0	0	0										0
23	E.33′													0	1	0	-1	0	0	0	1	1	-1	-1	0	0	0	1	0	-1	0	0	0	0										0
24	E.3X													0	1	0	0	0	0	0	1	1	0	0	$-h$	0	0	1	0	0	0	0	0	0										0
25	F.433′																				$2/_L$	$\frac{-(2+2r_1)}{L}$	$1/_L$	$-1/_L$	0	$-rPL/_2$	0	$r_1/_L$	0	0	0	0	$-rPL/_2$	0	0	0	0	•	0	0	0				0
26	F.4′3′3																				$1/_L$	$-1/_L$	$2/_L$	$\frac{-(2+2r_2)}{L}$	0	0	$-rPL/_2$	0	0	$r_2/_L$	0	0	0	$-rPL/_2$	0	0	0	0	0	0				0
27	F.345																				0	$r_1/_L$	0	0	0	$-rPL/_2$	0	$-2r_1/_L$	$-2r_1/_L$	0	0	0	$-2rPL/_2$	0	$r_1/_L$	0	0	0	0	$-rPL/_2$	0			0
28	F.3′4′5′																				0	0	0	$r_2/_L$	0	0	$-rPL/_2$	0	0	$-2r_2/_L$	$-2r_2/_L$	0	0	$-2rPL/_2$	0	0	$r_2/_L$	0	0	0	$-rPL/_2$			0
29	C.44′																				0	0	0	0	0	0	0	0	0	0	0	$-S_{44}'$	r	r	0	0	0	0	0	0			0
30	E.44′																				0	1	0	-1	0	0	0	1	1	-1	-1	0	0	0	1	0	-1	0	0	0			0
31	E.4X																				0	1	0	0	0	0	0	1	1	0	0	$-h$	0	0	1	0	0	0	0	0			0
32	F.544′																											$-2/_L$	$\frac{(2+2r_1)}{L}$	$-1/_L$	$1/_L$	0	$rPL/_2$	0	$-r_1/_L$	0	0	0	0	$rPL/_2$	0	0	0	0
33	F.5′4′4																											$-1/_L$	$1/_L$	$-2/_L$	$\frac{(2+2r_2)}{L}$	0	0	$rPL/_2$	0	0	$-r_2/_L$	0	0	0	$rPL/_2$	0	0	0
34	F.456																											0	$-r_1/_L$	0	0	0	$rPL/_2$	0	$2r_1/_L$	$2r_1/_L$	0	0	0	$2rPL/_2$	0	$-r_1/_L$	0	0
35	F.4′5′6																											0	0	0	$-r_2/_L$	0	0	$rPL/_2$	0	0	$2r_2/_L$	$2r_2/_L$	0	0	$2rPL/_2$	0	$-r_2/_L$	0
36	C.55′																											0	0	0	0	0	0	0	0	0	0	0	$-S_{55}'$	r	r	0	0	0
37	E.55′																											0	1	0	-1	0	0	0	1	1	-1	-1	0	0	0	1	-1	0
38	E.5X																											0	1	0	0	0	0	0	1	1	0	0	$-h$	0	0	1	0	0
39	F.655′																																		$2/_L$	$\frac{-(2+2r_2)}{L}$	$1/_L$	$-1/_L$	0	$-rPL/_2$	0	$r_1/_L$	0	0
40	F.6′5′5																																		$1/_L$	$-1/_L$	$2/_L$	$\frac{-(2+2r_2)}{L}$	0	0	$-rPL/_2$	0	$r_2/_L$	0
41	F.56																																		0	$r_1/_L$	0	0	0	$-rPL/_2$	0	$-2r_1/_L$	0	0
42	F.5′6′																																		0	0	0	$r_2/_L$	0	0	$-rPL/_2$	0	$-2r_2/_L$	0

Table: 500.10 General matrix for the effect of linear temperature distribution in the roof beam of a 6-storey frame

Deflections (M)	Bend. Mts. (KN-M)		Bend. Mts. (KN - M)	Deflections (M)
(-3.07×10^{-5})	(+0.029120)	$T_1 = 20^\circ C$	(+0.0192004)	$(+1.03\times10^{-5})$
-3.22866×10^{-5}	+0.029558		+0.019068	$+0.864713\times10^{-5}$
		T_0		
	(+0.0155)		(+0.00558)	
(-1.46×10^{-5})	+0.015995		+0.005506	(-1.47×10^{-5})
-1.55434×10^{-5}	+0.014075		+0.006405	-1.56703×10^{-5}
	(+0.0137)		(+0.00640)	
	(+0.00311)		(+C.00311)	
(-0.764×10^{-5})	+0.004489		+0.003183	(-0.797×10^{-5})
-0.814084×10^{-5}	+0.002880		+0.001379	-0.847432×10^{-5}
	(+0.00262)		(+0.00136)	
	(+0.00345)		(+0.000558)	
(-0.372×10^{-5})	+0.0036575		+0.0006008	(-0.367×10^{-5})
-0.396119×10^{-5}	+0.0028413		+0.0001546	-0.391377×10^{-5}
	(+0.00266)		(+0.000165)	
	(+0.00201)		(+0.000514)	
(-0.148×10^{-5})	+0.0021451		+0.0005407	(-0.149×10^{-5})
-0.156925×10^{-5}	+0.0016875		+0.0000916	-0.158501×10^{-5}
	(+0.00157)		(+0.0000825)	
	(+0.00140)		(+0.000279)	
(-0.0347×10^{-5})	+0.0014846		+0.0002939	(-0.035×10^{-5})
-0.0366376×10^{-5}	+0.0012858		+0.0001011	-0.0370245×10^{-5}
	(+0.00120)		(+0.0000926)	
	(+0.00114)		(+0.000174)	
	+0.0012036		+0.0001827	

Fig. 5.0524 Shows the results of the effect of Linear Temperature distribution in the roof beam

Unbracketed Figures - - - show results by the Force-Displacement Method

Bracketed Figures - - - show results by the Stiffness Method

5.05.3 The effect of constant temperature distribution in one column

(a) Analysis using force-displacement method

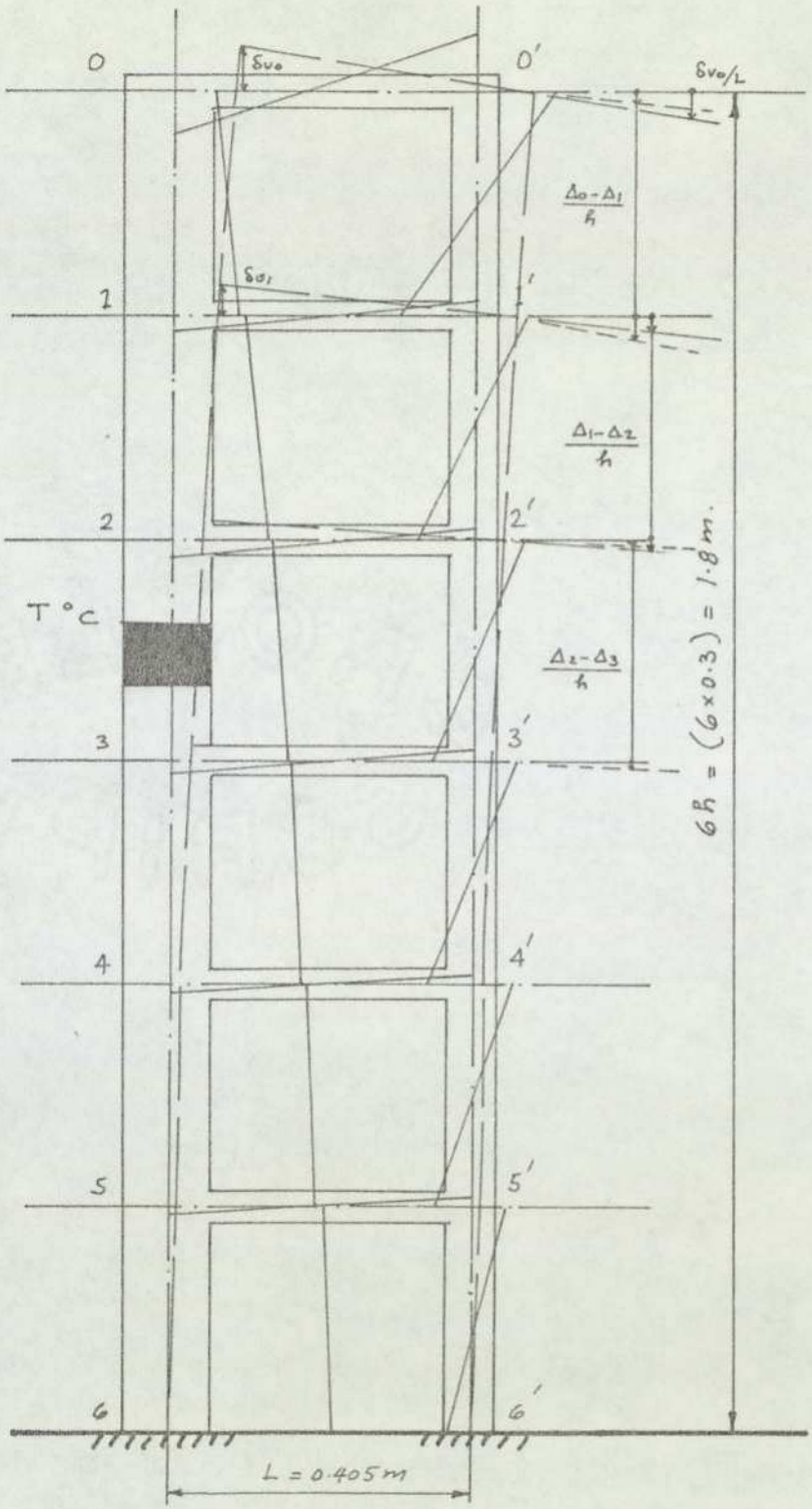

Fig. 5.0531 The effect of constant temperature distribution in the column of a 6-storey Frame showing assumed bending moments for the setting up of the matrix.

Referring to fig. 5.0531 the conditions of compatibility of deformations and equilibrium of forces can be written as follows:-

(a) Conditions of Compatibility

F.1oo' $$m1o\,\frac{h}{6EIc1} + mo1\left(\frac{h}{3EIc1} + \frac{L}{3EIb}\right) - mo'1'\,\frac{L}{6EIb} = \frac{\Delta ox - \Delta 1x}{h} - \frac{\delta oo'}{L}$$

or $$r1\ m1o + 2(r1+1)\ mo1 - mo'1' + R\,\Delta 1x\,\frac{L}{h} - R\,\Delta ox\,\frac{L}{h} = -\frac{6cn}{L}$$

F.o12 $$-mo1\,\frac{h}{6EIc1} - m1o\,\frac{h}{3EIc1} - m12\,\frac{h}{3EIc1} - m21\,\frac{h}{6EIc1} = \left(\frac{\Delta ox - \Delta 1x}{h}\right) - \left(\frac{\Delta 1x - \Delta 2x}{h}\right)$$

or $$r1\ mo1 + 2r1\ m1o + 2r1\ m12 + r1\ m21 - 2R\,\Delta 1x\,\frac{L}{h} + R\,\Delta ox\,\frac{L}{h} + R\,\Delta 2x\,\frac{L}{h} = o$$

F.211' $$m21\,\frac{h}{6EIc1} + m12\,\frac{h}{3EIc1} + (m12 - m1o)\,\frac{L}{3EIb} - (m1'o' + m1'2')\,\frac{L}{6EIb} = \left(\frac{\Delta 1x - \Delta 2x}{h}\right) - \frac{\delta 11'}{L}$$

or $$r1\ m21 + 2(r1+1)\ m12 - 2m1o - m1'o' - m1'2' + R\Delta 2x\,\frac{L}{h} - R\Delta 1x\,\frac{L}{h} = \frac{6c(1-n)}{L}$$

F.1'oo $$-m1'o'\,\frac{h}{6EIc2} + mo'1'\left(\frac{h}{3EIc2} + \frac{L}{3EIb}\right) - mo1\,\frac{L}{6EIb} = \frac{\Delta ox - \Delta 1x}{h} - \frac{\delta oo'}{L}$$

or $$-r2\ m1'o' + 2(r2+1)\ mo'1' - mo1 + R\Delta 1x\,\frac{L}{h} - R\,\Delta ox\,\frac{L}{h} = \frac{-6cn}{L}$$

F.o'1'2' $$-mo'1'\,\frac{h}{6EIc2} + m1'o'\,\frac{h}{3EIc2} - m1'2'\,\frac{h}{3EIc2} + m2'1'\,\frac{h}{6EIc2} = \left(\frac{\Delta ox - \Delta 1x}{h}\right) - \left(\frac{\Delta 1x - \Delta 2x}{h}\right)$$

or $$-r2\ mo'1' + 2r2\ m1'o' - 2r2\ m1'2' + r2\ m2'1' + 2R\Delta 1x\,\frac{L}{h} - R\Delta ox\,\frac{L}{h} - R\Delta 2x\,\frac{L}{h} = o$$

F.2'1'1 $$-m2'1'\,\frac{h}{6EIc2} + m1'2'\,\frac{h}{3EIc2} + (m1'2' + m1'o')\,\frac{L}{3EIb} - (m12 - m1o)\,\frac{L}{6EIb} = \left(\frac{\Delta 1x - \Delta 2x}{h}\right) - \frac{\delta 11'}{L}$$

or $$-r2\ m2'1' + 2(r2+1)\ m1'2' + 2m1'o' - m12 + m1O + R\Delta 2x\,\frac{L}{h} - R\Delta 1x\,\frac{L}{h} = \frac{6c(1-n)}{L}$$

Similarly

F.123 $$r1\ m12 + 2r1\ m21 + 2r1\ m23 + r1\ m32 + R\Delta 1x\,\frac{L}{h} + R\Delta 3x\,\frac{L}{h} - 2R\Delta 2x\,\frac{L}{h} = o$$

F.322' $$r1\ m32 + 2(r1+1)\ m23 - 2\ m21 - m2'1' - m2'3' + R\,\Delta 3x\,\frac{L}{h} - R\Delta 2x\,\frac{L}{h} = \frac{6c(2-n)}{L}$$

F.234 $r1\ m23 + 2r1\ m32 + 2r1\ m34 + r1\ m43 + R\Delta 2x\frac{L}{h} + R\Delta 4x\frac{L}{h} - 2R\Delta 3x\frac{L}{h} = o$

F.433' $r1\ m43 + 2(r1+1)\ m34 - 2\ m32 - m3'2' - m3'4' + R\Delta 4x\frac{L}{h} - R\Delta 3x\frac{L}{h} = \frac{6c(3-n)}{L}$

F.345 $r1\ m34 + 2r1\ m43 + 2r1\ m45 + m54 + R\Delta 3x\frac{L}{h} + R\Delta 5x\frac{L}{h} - 2R\Delta 4x\frac{L}{h} = o$

F.544' $r1\ m54 + 2(r1+1)\ m45 - 2\ m43 - m4'3' - m4'5' + R\Delta 5x\frac{L}{h} - R\Delta 4x\frac{L}{h} = \frac{6c(4-n)}{L}$

F.456 $r1\ m45 + 2r1\ m54 + 2r1\ m56 + r1\ m65 + R\Delta 4x\frac{L}{h} - 2R\Delta 5x\frac{L}{h} = o$

F.655' $r1\ m65 + 2(r1+1)\ m56 - 2\ m54 - m5'4' - m5'6' - R\Delta 5x\frac{L}{h} = \frac{6c(5-n)}{L}$

F.56 $r1\ m56 + 2r1\ m65 + R\Delta 5x\frac{L}{h} = o$

F.1'2'3' $-r2\ m1'2' + 2r2\ m2'1' - 2r2\ m2'3' + r2\ m3'2' + 2R\Delta 2x\frac{L}{h} - R\Delta 1x\frac{L}{h} - R\Delta 3x\frac{L}{h} = o$

F.3'2'2 $-r2\ m3'2' + 2(r2+1)\ m2'3' + 2\ m2'1' - m23 + m21 + R\Delta 3x\frac{L}{h} - R\Delta 2x\frac{L}{h} = \frac{6c(2-n)}{L}$

F.2'3'4' $-r2\ m2'3' + 2r2\ m3'2' - 2r2\ m3'4' + r2\ m4'3' + 2R\Delta 3x\frac{L}{h} - R\Delta 2x\frac{L}{h} - R\Delta 4x\frac{L}{h} = o$

F.4'3'3 $-r2\ m4'3' + 2(r2+1)\ m3'4' + 2\ m3'2' - m34 + m32 + R\Delta 4x\frac{L}{h} - R\Delta 3x\frac{L}{h} = \frac{6c(3-n)}{L}$

F.3'4'5' $-r2\ m3'4' + 2r2\ m4'3' - 2r2\ m4'5' + r2\ m5'4' + 2R\Delta 4x\frac{L}{h} - R\Delta 3x\frac{L}{h} - R\Delta 5x\frac{L}{h} = o$

F.5'4'4 $-r2\ m5'4' + 2(r2+1)\ m4'5' + 2\ m4'3' - m45 + m43 + R\Delta 5x\frac{L}{h} - R\Delta 4x\frac{L}{h} = \frac{6c(4-n)}{L}$

F.4'5'6' $-r2\ m4'5' + 2r2\ m5'4' - 2r2\ m5'6' + r2\ m6'5' + 2R\Delta 5x\frac{L}{h} - R\Delta 4x\frac{L}{h} = o$

F.6'5'5 $-r2\ m6'5' + 2(r2+1)\ m5'6' + 2\ m5'4' - m56 + m54 - R\Delta 5x\frac{L}{h} = \frac{6c(5-n)}{L}$

F.5'6' $-r2\ m5'6' + 2r2\ m6'5' - R\Delta 5x\frac{L}{h} = o$

(b) Conditions of Equilibrium

E.oo' $\left(\frac{mo1-m1o}{h}\right) + \left(\frac{mo'1'+m1'o'}{h}\right) = o$

E.11' $\left(\left(\frac{m21-m12}{h}\right) - \left(\frac{m1o-mo1}{h}\right)\right) - \left(\left(\frac{m2'1'+m1'2'}{h}\right) - \left(\frac{m1'o'+mo'1'}{h}\right)\right) = o$

E.22' $\left(\left(\frac{m32-m23}{h}\right) - \left(\frac{m21-m12}{h}\right)\right) - \left(\left(\frac{m3'2'+m2'3'}{h}\right) \left(\frac{m2'1'+m1'2'}{h}\right)\right) = o$

E.33' $\left(\left(\frac{m43-m34}{h}\right) - \left(\frac{m32-m23}{h}\right)\right) - \left(\left(\frac{m4'3'+m3'4'}{h}\right) - \left(\frac{m3'2'+m2'3'}{h}\right)\right) = o$

E.44' $\left(\left(\frac{m54-m45}{h}\right) - \left(\frac{m43-m34}{h}\right)\right) - \left(\left(\frac{m5'4'+m4'5'}{h}\right) - \left(\frac{m4'3'+m3'4'}{h}\right)\right) = o$

E.55' $\left(\left(\frac{m65-m56}{h}\right) - \left(\frac{m54-m45}{h}\right)\right) - \left(\left(\frac{m6'5'+m5'6'}{h}\right) - \left(\frac{m5'4'+m4'5'}{h}\right)\right) = o$

Example

In the numerical example, the frame shown in fig. 5.0531 is analysed for the constant temperature effect on a column. This is based on the following numerical data:-

L = 0.405m ; h = 0.30m ; d = 0.12m

Large Column Size 50mm x 120mm ; small column size 50mm x 60mm

Size of all beams 50mm x 40mm

$AC1 = 0.05 \times 0.120 = 0.002 m^2$; $AC2 = 0.05 \times 0.06 = 0.003 m^2$

$Ab = 0.05 \times 0.04 = 0.002 m^2$

$IC1 = 0.5 \times 0.12^3/12 = 7.2 \times 10^{-6} m^4$; $IC2 = 0.05 \times 0.06^3/12 = 9 \times 10^{-7} m^4$

$Ib = 0.05 \times 0.04^3/_{12} = 2.6667 \times 10^{-7} m^4$

$T = 20^oC$; $\alpha = 0.00001$ per ^oC ; $E = 21 \times 10^6 KN/m^2$

r1 = 0.02743484 ; r2 = 0.21947874

$C = \frac{\alpha T h E Ib}{L} = 8.2964 \times 10^{-4} KN\text{-}m^2$

$$R = \frac{6EIb}{L^2} = \frac{6 \times 21 \times 10^6 \times 2.6667 \times 10^{-7}}{0.405^2} = 204.849383$$

$$R\frac{L}{h} = 204.849383 \times 0.405/0.30 = 276.546667$$

(i) $$\frac{-6cn}{L} = -6 \times 8.2964 \times 10^{-4} \times \frac{6}{0.405} = -0.07374578$$

(ii) $$\frac{6c(1-n)}{L} = 6 \times 8.2964 \times 10^{-4} \frac{(1-6)}{0.405} = -0.6145481$$

(iii) $$\frac{6c(2-n)}{L} = 6 \times 8.2964 \times 10^{-4} \frac{(2-6)}{0.405} = -0.04916385$$

(iv) $$\frac{6c(3-n)}{L} = 6 \times 8.2964 \times 10^{-4} \frac{(3-6)}{0.405} = -0.03687289$$

(v) $$\frac{6c(4-n)}{L} = 6 \times 8.2964 \times 10^{-4} \frac{(4-6)}{0.405} = -0.02458193$$

(vi) $$\frac{6c(5-n)}{L} = 6 \times 8.2964 \times 10^{-4} \frac{(5-6)}{0.405} = -0.01229096$$

The equations are now presented in matrix form as shown in Table 500.13 and solved. The bending moments and deflections obtained from the solution of the abovementioned matrix are shown in fig. 5.0533.

(b) Analysis using the stiffness method

As in the case of constant temperature distribution in the roof beam, it is only necessary to calculate, the equivalent force that will be exerted by the heated column if it is not allowed to expand. This force will be as follows:-

$$P = EA\alpha T$$

$$= 21 \times 10^6 \times (0.05 \times 0.12)\ 0.00001 \times 20$$

$$= 25.2\ KN$$

Therefore, in order to find the effect of constant temperature distribution in the column of a 6-storey frame, a force of value P is applied along the axis of the column in the direction of the possible expansion, and the frame analysed, similar to any conventional load, by the stiffness method. The resulting stresses and deformations are correct for all members except tha axial force in the heated column. In order to obtain the correct value of the axial force, the force obtained by the stiffness analysis has to be superimposed by a reversed force equal in magnitude to the originally applied force, P.

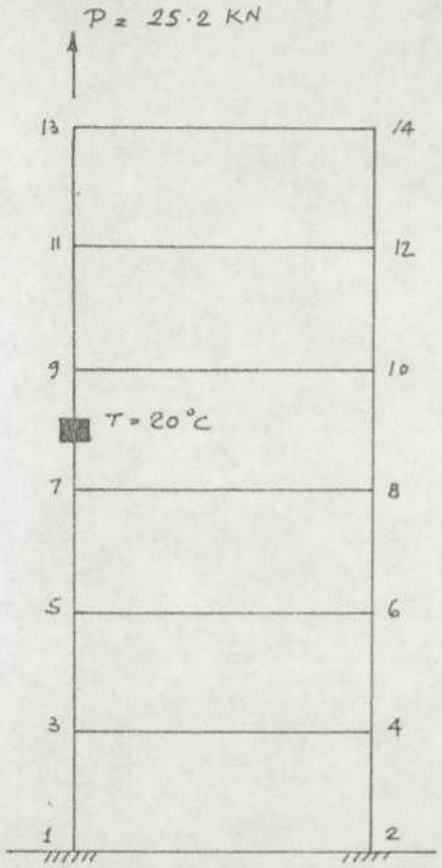

Using the same numerical example as analysed by the force-displacement method, the force, P = 25.2 KN is applied as shown in fig.5.0532. The results of the effect of constant temperature distribution in the column as analysed by the stiffness method are shown in fig.5.0533.

Fig. 5.0532 The effect of constant temperature distribution in a column analysed by the stiffness method.

EQN. NO.		1	2	3	4	5	6	7	8	9	10	11	12	13	14	15	16	17	18	19	20	21	22	23	24	25	26	27	28	29	30	LOAD VECTOR
	REF. JT.	0		0'	1			1'		2			2'		3			3'		4			4'		5			5'		6	6'	
No.	REF. EQN.	m_{01}	Δ_{0x}	$m_{0'1}$	m_{10}	m_{12}	Δ_{1x}	$m_{1'0}$	$m_{1'2'}$	m_{21}	m_{23}	Δ_{2x}	$m_{2'1'}$	$m_{2'3'}$	m_{32}	m_{34}	Δ_{3x}	$m_{3'2'}$	$m_{3'4'}$	m_{43}	m_{45}	Δ_{4x}	$m_{4'3'}$	$m_{4'5'}$	m_{54}	m_{56}	Δ_{5x}	$m_{5'4'}$	$m_{5'6'}$	m_{65}	$m_{6'5'}$	
1	F. 100′	$2(r_1+1)$	$-R_4/L$	-1	r_1	0	R_4/L	0																								$-6cn/L$
2	F. 1′0′0	-1	$-R_4/L$	$2(r_2+1)$	0	0	R_4/L	$-r_1$																								$-6cn/L$
3	E. 00′	1	0	1	-1	0	0	1																								0
4	F. 211′	0	0	0	-2	$2(r_1+1)$	$-R_4/L$	-1	-1	r_1	0	R_4/L	0																			$6c(1-n)/L$
5	F. 2′1′1	0	0	0	1	-1	$-R_4/L$	2	$2(r_2+1)$	0	0	R_4/L	$-r_2$																			$6c(1-n)/L$
6	F. 012	r_1	R_4/L	0	$2r_1$	$2r_1$	$-2R_4/L$	0	0	r_1	0	R_4/L	0																			0
7	F. 0′1′2′	0	$-R_4/L$	$-r_2$	0	0	$2R_4/L$	$2r_2$	$-2r_2$	0	0	$-R_4/L$	r_2																			0
8	E. 11′	1	0	1	-1	-1	0	1	-1	1	0	0	-1																			0
9	F. 322′					0	0	0	0	-2	$2(r_1+1)$	$-R_4/L$	-1	-1	r_1	0	R_4/L	0															$6c(2-n)/L$
10	F. 3′2′2					0	0	0	0	1	-1	$-R_4/L$	2	$2(r_2+1)$	0	0	R_4/L	$-r_2$															$6c(2-n)/L$
11	F. 123					r_1	R_4/L	0	0	$2r_1$	$2r_1$	$-2R_4/L$	0	0	r_1	0	R_4/L	0															0
12	F. 1′2′3′					0	$-R_4/L$	0	$-r_2$	0	0	$2R_4/L$	$2r_2$	$-2r_2$	0	0	$-R_4/L$	r_2															0
13	E. 22′					1	0	0	1	-1	-1	0	1	-1	1	0	0	-1															0
14	F. 433′										0	0	0	0	-2	$2(r_1+1)$	$-R_4/L$	-1	-1	r_1	0	R_4/L	0										$6c(3-n)/L$
15	F. 4′3′3										0	0	0	0	1	-1	$-R_4/L$	2	$2(r_2+1)$	0	0	R_4/L	$-r_2$										$6c(3-n)/L$
16	F. 234										r_1	R_4/L	0	0	$2r_1$	$2r_1$	$-R_4/L$	0	0	r_1	0	R_4/L	0										0
17	F. 2′3′4′										0	$-R_4/L$	0	$-r_2$	0	0	$2R_4/L$	$2r_2$	$-2r_2$	0	0	$-R_4/L$	r_2										0
18	E. 33′										1	0	0	1	-1	-1	0	1	-1	1	0	0	-1										0
19	F. 544′															0	0	0	0	-2	$2(r_1+1)$	$-R_4/L$	-1	-1	r_1	0	R_4/L	0				$6c(4-n)/L$
20	F. 5′4′4															0	0	0	0	1	-1	$-R_4/L$	2	$2(r_2+1)$	0	0	R_4/L	$-r_2$				$6c(4-n)/L$
21	F. 345															r_1	R_4/L	0	0	$2r_1$	$2r_1$	$-2R_4/L$	0	0	r_1	0	R_4/L	0				0
22	F. 3′4′5′															0	$-R_4/L$	0	$-r_2$	0	0	$2R_4/L$	$2r_2$	$-2r_2$	0	0	$-R_4/L$	r_2				0
23	E. 44′															1	0	0	1	-1	-1	0	1	-1	1	0	0	-1				0
24	F. 655′																				0	0	0	0	-2	$2(r_1+1)$	$-R_4/L$	-1	-1	r_1	0	$6c(5-n)/L$
25	F. 6′5′5																				0	0	0	0	1	-1	$-R_4/L$	2	$2(r_2+1)$	0	$-r_2$	$6c(5-n)/L$
26	F. 456																				r_1	R_4/L	0	0	$2r_1$	$2r_1$	$-2R_4/L$	0	0	r_1	0	0
27	F. 4′5′6′																				0	$-R_4/L$	0	$-r_2$	0	0	$2R_4/L$	$2r_2$	$-2r_2$	0	r_2	0
28	E. 55′																				1	0	0	1	-1	-1	0	1	-1	1	-1	0
29	F. 65																									r_1	R_4/L	0	0	$2r_1$	0	0
30	F. 6′5′																									0	$-R_4/L$	0	$-r_2$	0	$2r_2$	0

Table: 500.12 General matrix for the effect of constant temperature distribution in one column of a shear wall frame.

EQN. No.		1	2	3	4	5	6	7	8	9	10	11	12	13	14	15	16	17	18	19	20	21	22	23	24	25	26	27	28	29	30	LOAD
	REF. ST.	0		0'	1			1'		2			2'		3			3'		4			4'		5			5'		6	6'	VECTOR
No.	REF. EQN.	m_{01}	Δ_{0x}	$m_{01'}$	m_{10}	m_{12}	Δ_{1x}	$m_{1'0'}$	$m_{1'2'}$	m_{21}	m_{23}	Δ_{2x}	$m_{2'1'}$	$m_{2'3'}$	m_{32}	m_{34}	Δ_{3x}	$m_{3'2'}$	$m_{3'4'}$	m_{43}	m_{45}	Δ_{4x}	$m_{4'3'}$	$m_{4'5'}$	m_{54}	m_{52}	Δ_{5x}	$m_{5'4'}$	$m_{5'6'}$	m_{65}	$m_{6'5'}$	
1	F.100'	2.05487	276.54467	−1	0.027435	0	276.54467	0																								-0.073746
2	F.1'0'0	−1	276.54467	2.43896	0	0	276.54467	−0.21948																								-0.073746
3	E.00'	+1	0	+1	−1	0	0	+1																								0
4	F.211'	0	0	0	−2	2.05487	276.54467	−1	−1	0.027435	0	276.54467	0																			-0.061455
5	F.2'1'1	0	0	0	+1	−1	276.54467	+2	2.43896	0	0	276.54467	−0.21948																			-0.061455
6	F.012	0.027435	276.54467	0	0.05487	0.05487	553.07334	0	0	0.027435	0	276.54467	0																			0
7	F.0'1'2'	0	276.54467	−0.21948	0	0	553.07334	0.43896	−0.43896	0	0	276.54467	−0.21948																			0
8	E.11'	+1	0	+1	−1	−1	0	+1	−1	+1	0	0	−1																			0
9	F.322'					0	0	0	0	−2	2.05487	276.54467	−1	−1	0.027435	0	276.54467	0															-0.049164
10	F.3'2'2					0	0	0	0	+1	−1	276.54467	+2	2.43896	0	0	276.54467	−0.21948															-0.049164
11	F.123					0.027435	276.54467	0	0	−0.05487	0.05487	553.07334	0	0	0.027435	0	276.54467	0															0
12	F.1'2'3'					0	276.54467	0	−0.21948	0	0	553.07334	0.43896	−0.43896	0	0	276.54467	−0.21948															0
13	E.22'					+1	0	0	+1	−1	−1	0	+1	−1	+1	0	0	−1															0
14	F.433'										0	0	0	0	−2	2.05487	276.54467	−1	−1	0.027435	0	276.54467	0									-0.036873
15	F.4'3'3										0	0	0	0	+1	−1	276.54467	+2	2.43896	0	0	276.54467	−0.21948									-0.036873
16	F.234										0.027435	276.54467	0	0	0.05487	0.05487	553.07334	0	0	0.027435	0	276.54467	0									0
17	F.2'3'4'										0	276.54467	0	−0.21948	0	0	553.07334	0.43896	−0.43896	0	0	276.54467	−0.21948									0
18	E.33'										+1	0	0	+1	−1	−1	0	+1	−1	+1	0	0	−1									0
19	F.544'															0	0	0	0	−2	2.05487	276.54467	−1	−1	0.027435	0	276.54467	0				-0.024582
20	F.5'4'4															0	0	0	0	+1	−1	276.54467	+2	2.43896	0	0	276.54467	−0.21948				-0.024582
21	F.345															0.027435	276.54467	0	0	0.05487	0.05487	553.07334	0	0	0.027435	0	276.54467	0				0
22	F.3'4'5'															0	276.54467	0	−0.21948	0	0	553.07334	0.43896	−0.43896	0	0	276.54467	0.21948				0
23	E.44'															+1	0	0	+1	−1	−1	0	+1	−1	+1	0	0	−1				0
24	F.655'																				0	0	0	0	−2	2.05487	276.54467	−1	−1	0.027435	0	-0.012291
25	F.6'5'5																				0	0	0	0	+1	−1	276.54467	+2	2.43896	0	−0.21948	-0.012291
26	F.456																				0.027435	276.54467	0	0	0.05487	0.05487	553.07334	0	0	0.027435	0	0
27	F.4'5'6'																				0	276.54467	0	−0.21948	0	0	553.07334	0.43896	−0.43896	0	0.21948	0
28	E.55'																				+1	0	0	+1	−1	−1	0	+1	−1	+1	−1	0
29	F.65																															0
30	F.6'5'																															0

Table: 500.13 Numerical matrix for the effect of constant temperature distribution in one column of a shear wall frame.

Deflections (M) | Bend. Mts. (KN - M) | Bend. Mts. (M) | Deflections (KN - M)

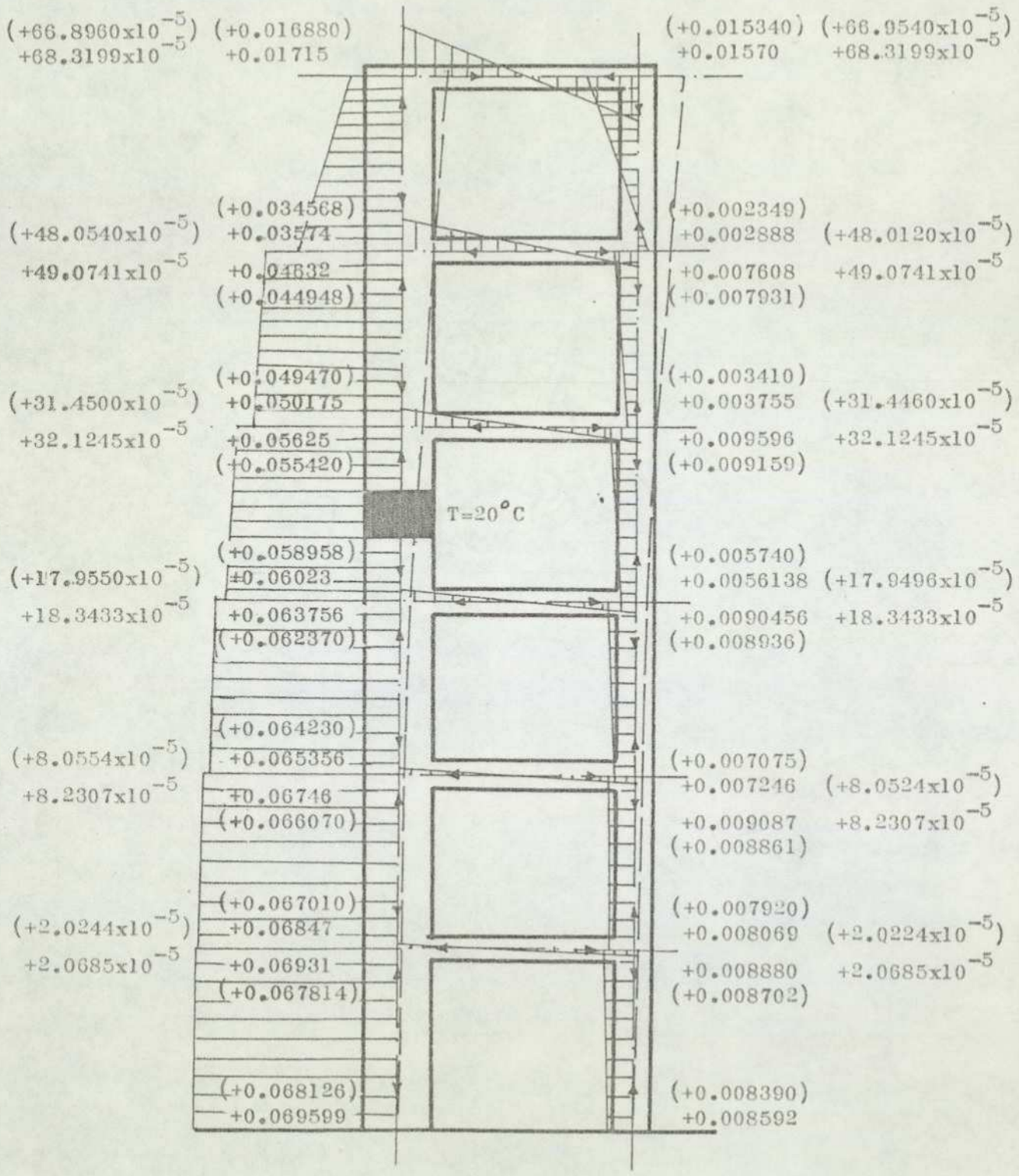

Fig. 5.0533 Shows the results of the effect of Constant Temperature Distribution in a column

Unbracketed Figures - - - show results by the Force-Displacement Method

Bracketed Figures - - - show results by the Stiffness Method

5.05.4 The effect of linear temperature distribution in one column

(a) Analysis using the force-displacement method

The analysis for the effects of linear and constant temperature

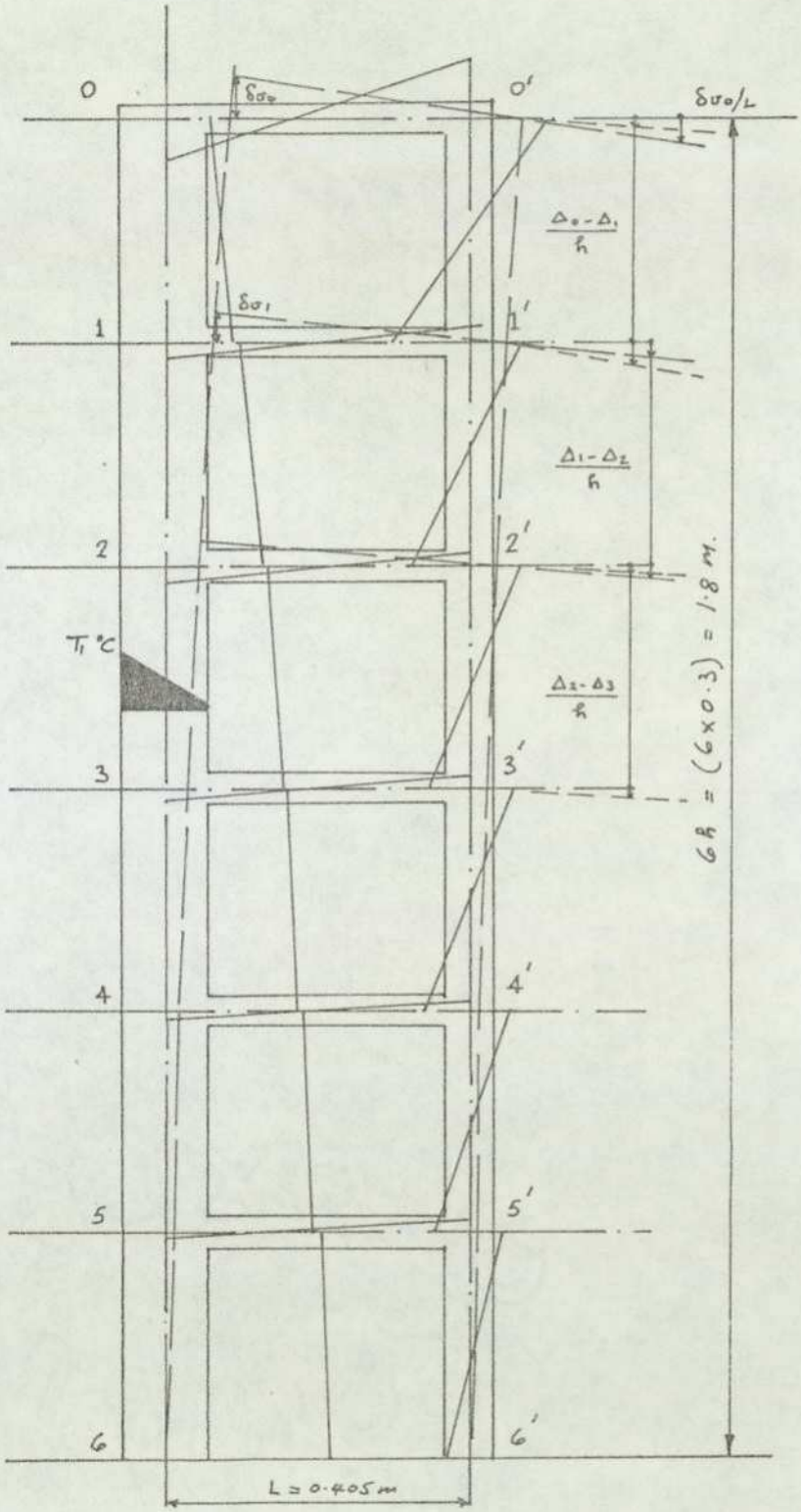

Fig. 5.0541 The effect of linear temperature distribution in the column of a 6-storey frame showing assumed bending moments for the setting up of the matrix

distributions in the column of a 6-storey frame can be done simultaneously. However, these are carried out separately so as to show the difference between the effects of the two types of temperature distributions.

Using the force-displacement method, the equations of compatibility of deformations and equilibrium of forces remain identical to those derived for constant temperature distribution, except the load vector which is modified. However, for clarity all the equations are shown below:-

F.100' $$m1o\frac{h}{6EIc1} + mo1\left(\frac{h}{3EIc1} + \frac{L}{3EIb}\right) - mo'1'\frac{L}{6EIb} = \frac{\Delta ox - \Delta 1x}{h} + \theta o1 - \frac{\delta oo'}{L}$$

where $\theta o1 \frac{\alpha T1h}{2d}$ and $\frac{\delta oo'}{L} = \frac{\alpha T1nh}{2L}$

multiplying the equation by $\frac{6EIb}{L}$ and introducing $r1 = \frac{h}{L}\frac{Ib}{Ic}$,

$r2 = \frac{h}{L}\frac{Ib}{Ic2}$ and $R = \frac{6EIb}{L^2}$, equation is re-written as follows:-

$$r1(m1o) + 2(r1+1)(mo1) - (mo'1') + R\,\Delta 1x\frac{L}{h} - R\,\Delta ox\frac{L}{h} = 3c\left(\frac{1}{d} - \frac{n}{L}\right)$$

where $c = \frac{\alpha T1hEIb}{L}$

F.012 $$-mo1\frac{h}{6EIc1} - m1o\frac{h}{3EIc1} - m12\frac{h}{3EIc1} - m21\frac{h}{6EIc1} = \left(\frac{\Delta ox - \Delta 1x}{h} - \theta 1o\right) - \left(\frac{\Delta 1x - \Delta 2x}{h} + \theta 12\right)$$

By using a similar process as for equation F.100', the above equation can be re-written as follows:-

$$r1(mo1) + 2r1(m1o) + 2r1(m12) + r1(m21) - 2R\,\Delta 1x\frac{L}{h} + R\Delta ox\frac{L}{h} + R\Delta 2x\frac{L}{h} = \frac{6c}{d}$$

Similarly

F.211' $$r1(m21) + 2(r1+1)(m12) - 2(m10) - (m1'o') - (m1'2') + R\,\Delta 2x\frac{L}{h} - R\,\Delta 1x\frac{L}{h} = \frac{3c}{d} + \frac{3c}{L}(1-n)$$

F.123 $$r1(m12) + 2r1(m21) + 2r1(m23) + r1(m32) + R\,\Delta 1x\frac{L}{h} + R\,\Delta 3x\frac{L}{h} - 2R\,\Delta 2x\frac{L}{h} = \frac{6c}{d}$$

F.322' $r1(m32) + 2(r1+1)(m23) - 2(m21) - (m2'1') - (m2'3') + R\,\Delta 3x\,\frac{L}{h} - R\,\Delta 2x\,\frac{L}{h} = \frac{3c}{d} + \frac{3c}{L}(2-n)$

F.234 $r1(m23) + 2r1(m32) + 2r1(m34) + r1(m43) + R\,\Delta 2x\,\frac{L}{h} + R\,\Delta 4x\,\frac{L}{h} - 2R\,\Delta 3x\,\frac{L}{h} = \frac{6c}{d}$

F.433' $r1(m43) + 2(r1+1)(m34) - 2(m32) - (m3'2') - (m3'4') + R\,\Delta 4x\,\frac{L}{h} - R\,\Delta 3x\,\frac{L}{h} = \frac{3c}{d} + \frac{3c}{L}(3-n)$

F.345 $r1(m34) + 2r1(m43) + 2r1(m45) + r1(m54) + R\,\Delta 3x\,\frac{L}{h} + R\,\Delta 5x\,\frac{L}{h} - 2R\,\Delta 4x\,\frac{L}{h} = \frac{6c}{d}$

F.544' $r1(m54) + 2(r1+1)(k45) - 2(m43) - (m4'3') - (m4'5') + R\,\Delta 5x\,\frac{L}{h} - R\,\Delta 4x\,\frac{L}{h} = \frac{3c}{d} + \frac{3c}{L}(4-n)$

F.456 $r1(m45) + 2r1(m54) + 2r1(m56) + r1(m65) + R\,\Delta 4x\,\frac{L}{h} - 2R\,\Delta 5x\,\frac{L}{h} = \frac{6c}{d}$

F.655' $r1(m65) + 2(r1+1)(m56) - 2(m54) - (m5'4') - (m5'6') - R\,\Delta 5x\,\frac{L}{h} = \frac{3c}{d} + \frac{3c}{L}(5-n)$

F.56 $r1(m56) + 2r1(m65) + R\,\Delta 5x\,\frac{L}{h} = \frac{3c}{d}$

F.1'0'0 $-r2\ m1'o8 + 2(r2+1)\ mo'1' - mo1 + R\,\Delta 1'x\,\frac{L}{h} - R\,\Delta o'x\,\frac{L}{h} = -\frac{3cn}{L}$

F.0'1'2' $-r2\ mo'1' + 2r2\ m1'o' - 2r2\ m1'2' + r2\ m2'1' + 2R\,\Delta 1'x\frac{L}{h} - R\,\Delta o'x\,\frac{L}{h} - R\,\Delta 2'x\,\frac{L}{h} = o$

F.2'1'1 $-r2\ m2'1' + 2(r2+1)\ m1'2' + 2\ m1'o' - m12 + m1o + R\,\Delta 2'x\,\frac{L}{h} - R\,\Delta 1'x\,\frac{L}{h} = \frac{3c}{L}(1-n)$

F.1'2'3' $-r2\ m1'2' + 2r2\ m2'1' - 2r2\ m2'3' + r2\ m3'2' + 2R\ \Delta 2' \times \frac{L}{h} - R\ \Delta 1' \times \frac{L}{h} - R\ \Delta 3' \times \frac{L}{h} = o$

F.3'2'2 $-r2\ m3'2' + 2(r2+1)\ m2'3' + 2\ m2'1' - m23 + m21 + R\ \Delta 3' \times \frac{L}{h} - R\ \Delta 2' \times \frac{L}{h} = \frac{3c}{L}(2-n)$

F2'3'4' $-r2\ m2'3' + 2r2\ m3'2' - 2r2\ m3'4' + r2\ m4'3' + 2R\ \Delta 3' \times \frac{L}{h} - R\ \Delta 2' \times \frac{L}{h} - R\Delta 4' \times \frac{L}{h} = o$

F.4'3'3 $-r2\ m4'3' + 2(r2+1)\ m3'4' + 2\ m3'2' - m34 + m32 + R\ \Delta 4' \times \frac{L}{h} - R\ \Delta 3' \times \frac{L}{h} = \frac{3c}{L}(3-n)$

F.3'4'5' $-r2\ m3'4' + 2r2\ m4'3' - 2r2\ m4'5' + r2\ m5'4' + 2R\ \Delta 4' \times \frac{L}{h} - R\ \Delta 3' \times \frac{L}{h} - R\Delta 5' \times \frac{L}{h} = o$

F.5'4'4 $-r2\ m5'4' + 2(r2+1)\ m4'5' + 2\ m4'3' - m45 + m43 + R\ \Delta 5' \times \frac{L}{h} - R\ \Delta 4' \times \frac{L}{h} = \frac{3c}{L}(4-n)$

F.4'5'6' $-r2\ m4'5' + 2r2\ m5'4' - 2r2\ m5'6' + r2\ m6'5' + 2R\ \Delta 5' \times \frac{L}{h} - R\ \Delta 4' \frac{L}{h} = o$

F.6'5'5 $-r2\ m\ 6'5' + 2(r2+1)\ m5'6' + 2\ m5'4' - m56 + m54 - R\ \Delta 5' \times \frac{L}{h} = \frac{3c}{L}(5-n)$

F.5'6' $-r2\ m5'6' + 2r2\ m6'5' - R\Delta 5' \times \frac{L}{h} = o$

Example

In the numerical example, the frame of section 5.05.3 is analysed for the linear temperature distribution in the column. However, before the complete matrix can be set out, it is necessary to calculate the following parameters.

(1) $\frac{3c}{d} - \frac{3cn}{L} = 3 \times 8.2964 \times 10^{-4} \left(\frac{1}{0.12} - \frac{6}{0.405}\right) = -0.01613189$

(2) $\frac{6c}{d} = 6 \times 8.2964 \times \frac{10^{-4}}{0.12} = 0.041482$

(3) $\frac{3c}{d} - \frac{3c(1-n)}{L} = -0.00998641$

(4) $\frac{3c}{d} - \frac{3c}{L}(2-n) = -0.00384093$

(5) $\frac{3c}{d} - \frac{3c}{L}(3-n) = +0.00230456$

(6) $\frac{3c}{d} - \frac{3c}{L}(4-n) = +0.00845004$

(7) $\frac{3c}{d} - \frac{3c}{L}(5-n) = +0.01459552$

(1') $\frac{-3cn}{L} = -0.03687289$

(2') $\frac{3c}{L}(1-n) = -0.03072741$

(3') $\frac{3c}{L}(2-n) = -0.02458193$

(4') $\frac{3c}{L}(3-n) = -0.01843644$

(5') $\frac{3c}{L}(4-n) = -0.01229096$

(6') $\frac{3c}{L}(5-n) = -0.00614548$

The matrix for this case is shown in Table 500.15. The distribution of bending moments and deflections obtained by the solution of the abovementioned matrix is shown in fig. 5.0543.

(b) Analysis using the stiffness method

As in the case of linear temperature distribution in the roof beam, it is necessary to calculate (i) the equivalent direct force which will be exerted by the heated column if it is not allowed to expand and (ii) bending moments which would be necessary to prevent the column from deforming into a curved profile due to the linear temperature distribution. However, in the case of the bending moments, there is a slight difference from the case of the roof beam. As beams are connected to the column at floor levels, it would be necessary to apply equal and opposite bending moments at all joints and in the same direction into which the temperature is tending to curve the column i.e. as shown in fig. 5.0542.

The axial force and bending moments to be applied are

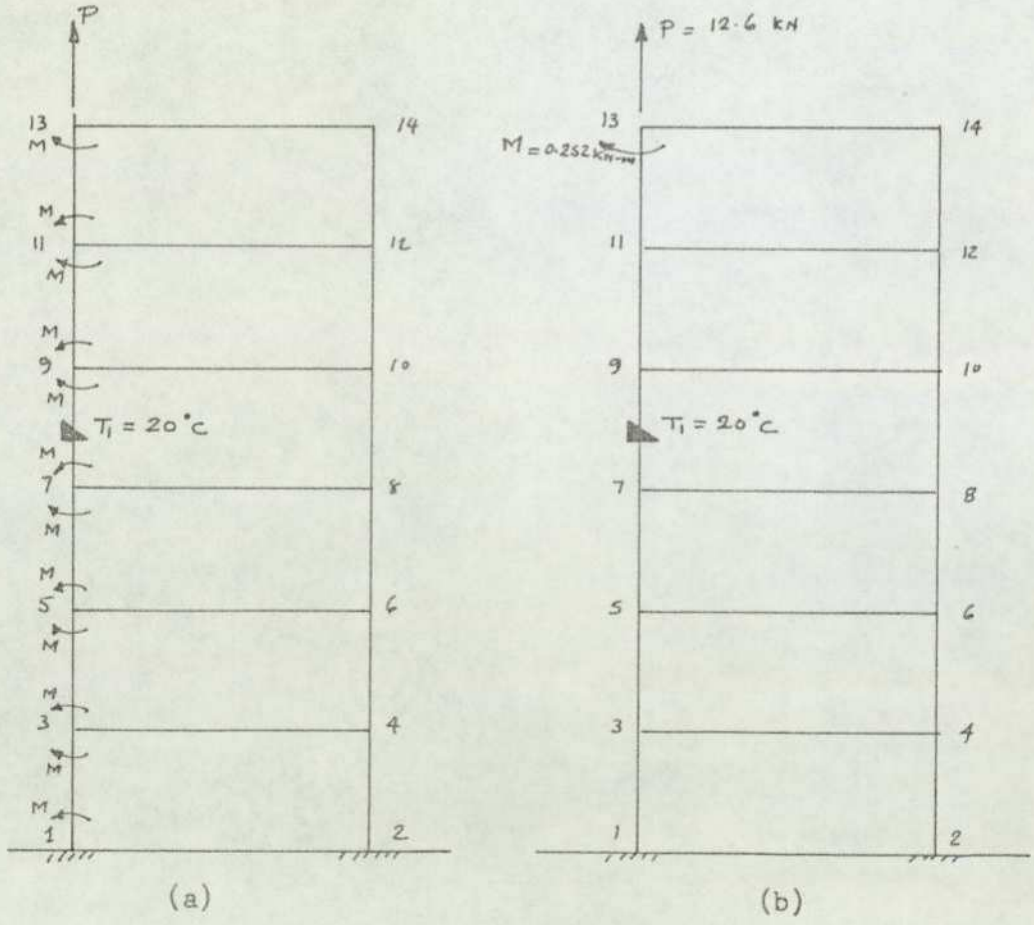

Fig. 5.0542 The effect of linear temperature distribution in a column analysed by the stiffness method

$$P = AE\alpha Tav = AE\alpha\frac{T1}{2} = (0.05 \times 0.12)\ 21 \times 10^6 \times 0.00001 \times {}^{20}/_{2}$$

$$= 12.6 \text{ KN}$$

$$M = \frac{\alpha T1 EIc1}{d} = 0.00001 \times 20 \times 21 \times 10^6 \times 7.2 \times 10^{-6}$$

$$= 0.252 \text{ KN-m}$$

It is interesting to note that equal and opposite bending moments applied at joints 3, 5, 7, 9 and 11 as shown in fig. 5.0542(a) will not really participate in the analysis as these will simply cancel each other out. The bending moment applied at joint 1 also will not participate in the stiffness analysis as this is a fixed joint. Therefore, the actual forces and bending moments which need to be applied are at joint 13 only as shown in fig. 5.0542(b).

However, even though the bending moments at joints 3, 5, 7, 9 and 11 do not participate in the initial stiffness analysis, these moments must be assumed to be acting as shown since it would be necessary to reverse these to get correct bending moments at these joints as will be shown later.

Analysing the same numerical example as used in the force-displacement method, the force, P (= 12.6 KN), and a bending moment, M (= 0.052 KN-m), are applied at joint 13 as shown in fig.5.0542(b) and the frame analysed by the stiffness method. The resulting stresses and deformations are correct for all members, except (i) the axial force in the heated column, (ii) the bending moments at joints 1, 3, 5, 7, 9, 11 and 13, and (iii) the axial forces in all beams as a consequence of the change in bending moments as stated in (ii) above. In order to obtain the correct value of the axial force in the column, the force obtained by the stiffness analysis has to be superimposed by a reversed force equal in magnitude to the originally applied force, P. Similarly, in order to get the correct values of bending moments, reversed bending moments of equal magnitude to the applied bending moment, M, have to be superimposed on those obtained from the stiffness analysis. The correct axial forces in the beams can now be obtained in the usual way from the corrected bending moments in the columns.

The results of the effect of linear temperature distribution in the column, by the stiffness method are shown in fig. 5.0543.

EQN. No.		1	2	3	4	5	6	7	8	9	10	11	12	13	14	15	16	17	18	19	20	21	22	23	24	25	26	27	28	29	30	LOAD
	REF. JT.	0		0'	1			1'		2			2'		3			3'		4			4'		5			5'		6	6'	VECTOR
No.	REF. EQN.	m_{01}	Δ_{0X}	$m_{0'1'}$	m_{10}	m_{12}	Δ_{1X}	$m_{1'0'}$	$m_{1'2'}$	m_{21}	m_{23}	Δ_{2X}	$m_{2'1'}$	$m_{2'3'}$	m_{32}	m_{34}	Δ_{3X}	$m_{3'2'}$	$m_{3'4'}$	m_{43}	m_{45}	Δ_{4X}	$m_{4'3'}$	$m_{4'5'}$	m_{54}	m_{52}	Δ_{5X}	$m_{5'4'}$	$m_{5'2'}$	m_{65}	$m_{6'5'}$	
1	F.100′	$2(r_1+1)$	$-R_L/_L$	-1	r_1	0	$R_L/_L$	0																								$3c(\frac{1}{d}-\frac{n}{L})$
2	F.10′0	-1	$-R_L/_L$	$2(r_2+1)$	0	0	$R_L/_L$	$-r_2$																								$-3cn/_L$
3	E.00′	1	0	1	-1	0	0	1																								0
4	F.211′	0	0	0	-2	$2(r_1+1)$	$-R_L/_L$	-1	-1	r_1	0	$R_L/_L$	0																			$\frac{3c}{d}+\frac{3c}{L}(1-n)$
5	F.2′1′1	0	0	0	1	-1	$-R_L/_L$	2	$2(r_2+1)$	0	0	$R_L/_L$	$-r_2$																			$3c(1-n)/_L$
6	F.012	r_1	$R_L/_L$	0	$2r_1$	$2r_1$	$-2R_L/_L$	0	0	r_1	0	$R_L/_L$	0																			$+6c/_d$
7	F.0′1′2′	0	$-R_L/_L$	$-r_2$	0	0	$2R_L/_L$	$2r_2$	$-2r_2$	0	0	$-R_L/_L$	r_2																			0
8	E.11′	1	0	1	-1	-1	0	1	-1	1	0	0	-1																			0
9	F.322′					0	0	0	0	-2	$2(r_1+1)$	$-R_L/_L$	-1	-1	r_1	0	$R_L/_L$	0															$\frac{3c}{d}+\frac{3c}{L}(2-n)$
10	F.3′2′2					0	0	0	0	1	-1	$-R_L/_L$	2	$2(r_2+1)$	0	0	$R_L/_L$	$-r_2$															$3c(2-n)/_L$
11	F.123					r_1	$R_L/_L$	0	0	$2r_1$	$2r_1$	$-2R_L/_L$	0	0	r_1	0	$R_L/_L$	0															$6c/_d$
12	F.1′2′3′					0	$-R_L/_L$	0	$-r_2$	0	0	$2R_L/_L$	$2r_2$	$-2r_2$	0	0	$-R_L/_L$	r_2															0
13	E.22′					1	0	0	1	-1	-1	0	1	-1	1	0	0	-1															0
14	F.433′										0	0	0	0	-2	$2(r_1+1)$	$-R_L/_L$	-1	-1	r_1	0	$R_L/_L$	0									$\frac{3c}{d}+\frac{3c}{L}(3-n)$
15	F.4′3′3										0	0	0	0	1	-1	$-R_L/_L$	2	$2(r_2+1)$	0	0	$R_L/_L$	$-r_2$									$3c(3-n)/_L$
16	F.234										r_1	$R_L/_L$	0	0	$2r_1$	$2r_1$	$-2R_L/_L$	0	0	r_1	0	$R_L/_L$	0									$6c/_d$
17	F.2′34′										0	$-R_L/_L$	0	$-r_2$	0	0	$2R_L/_L$	$2r_2$	$-2r_2$	0	0	$-R_L/_L$	r_2									0
18	E.33′										1	0	0	1	-1	-1	0	1	-1	1	0	0	-1									0
19	F.544′															0	0	0	0	-2	$2(r_1+1)$	$-R_L/_L$	-1	-1	r_1	0	$R_L/_L$	0				$\frac{3c}{d}+\frac{3c}{L}(4-n)$
20	F.5′4′4															0	0	0	0	1	-1	$-R_L/_L$	2	$2(r_2+1)$	0	0	$R_L/_L$	$-r_2$				$3c(4-n)/_L$
21	F.345															r_1	$R_L/_L$	0	0	$2r_1$	$2r_1$	$-2R_L/_L$	0	0	r_1	0	$R_L/_L$	0				$6c/_d$
22	F.3′4′5′															0	$-R_L/_L$	0	$-r_2$	0	0	$2R_L/_L$	$2r_2$	$-2r_2$	0	0	$-R_L/_L$	r_2				0
23	E.44′															1	0	0	1	-1	-1	0	1	-1	1	0	0	-1				0
24	F.655′																				0	0	0	0	-2	$2(r_1+1)$	$-R_L/_L$	-1	-1	r_1	0	$\frac{3c}{d}+\frac{3c}{L}(5-n)$
25	F.6′5′5																				0	0	0	0	1	-1	$-R_L/_L$	2	$2(r_2+1)$	0	$-r_2$	$3c(5-n)/_L$
26	F.456																				r_1	$R_L/_L$	0	0	$2r_1$	$2r_1$	$-2R_L/_L$	0	0	r_1	0	$6c/_d$
27	F.4′5′6′																				0	$-R_L/_L$	0	$-r_2$	0	0	$2R_L/_L$	$2r_2$	$-2r_2$	0	r_2	0
28	E.55′																				1	0	0	1	-1	-1	0	-1	1	-1	-1	0
29	F.65																									r_1	$R_L/_L$	0	0	$2r_1$	0	$3c/_d$
30	F.6′5′																									0	$-R_L/_L$	0	$-r_2$	0	$2r_2$	0

Table: 500.14 General matrix for the effect of linear temperature distribution in one column of a shear wall frame.

EQN. No.		1	2	3	4	5	6	7	8	9	10	11	12	13	14	15	16	17	18	19	20	21	22	23	24	25	26	27	28	29	30	LOAD
	REF. ST.	0		0'		1		1'		2			2'		3			3'		4			4'		5			5'		6	6'	VECTOR
No.	REP. EQN.	m_{01}	Δ_{0x}	$m_{0'1'}$	m_{10}	m_{12}	Δ_{1x}	$m_{1'6'}$	$m_{1'2'}$	m_{21}	m_{23}	Δ_{2x}	$m_{2'1'}$	$m_{2'3'}$	m_{32}	m_{34}	Δ_{3x}	$m_{3'2'}$	$m_{3'4'}$	m_{43}	m_{45}	Δ_{4x}	$m_{4'3'}$	$m_{4'5'}$	m_{54}	m_{5E}	Δ_{5x}	$m_{5'4'}$	$m_{5'6'}$	m_{65}	$m_{6'5'}$	
1	F.100′	2.054871	276.54467	−1	0.027435	0	276.54467	0																								-0.016131889
2	F.1′0′0	−1	276.54467	2.43896	0	0	276.54467	−0.219481																								-0.03687289
3	E.00′	+1	0	+1	−1	0	0	+1																								0
4	F.211′	0	0	0	−2	2.05487	276.54467	−1	−1	0.027435	0	276.54467	0																			-0.006998491
5	F.2′1′1	0	0	0	+1	−1	276.54467	+2	2.43896	0	0	276.54467	−0.219481																			-0.03072741
6	F.012	0.027435	276.54467	0	0.05487	0.05487	553.07334	0	0	0.027435	0	276.54467	0																			0.041482
7	F.0′1′2′	0	276.54467	−0.219481	0	0	553.07334	−0.43896	−0.43896	0	0	276.54467	0.219481																			0
8	E.11′	+1	0	+1	−1	−1	0	+1	−1	+1	0	0	−1																			0
9	F.322′					0	0	0	0	−2	2.05487	276.54467	−1	−1	0.027435	0	276.54467	0															-0.00184093
10	F.3′2′2					0	0	0	0	+1	−1	276.54467	+2	2.43896	0	0	276.54467	−0.219481															-0.024581935
11	F.123					0.027435	276.54467	0	0	0.05487	0.05487	553.07334	0	0	0.027435	0	276.54467	0															0.041482
12	F.1′2′3′					0	276.54467	0	−0.219481	0	0	553.07334	−0.43896	−0.43896	0	0	276.54467	−0.219481															0
13	E.22′					+1	0	0	+1	−1	−1	0	+1	−1	+1	0	0	−1															0
14	F.433′										0	0	0	0	−2	2.05487	276.54467	−1	−1	0.027435	0	276.54467	0									0.002350956
15	F.4′3′3										0	0	0	0	+1	−1	276.54467	+2	2.43896	0	0	276.54467	−0.21948									-0.018434349
16	F.234										0.027435	276.54467	0	0	0.05487	0.05487	553.07334	0	0	0.027435	0	276.54467	0									0.041482
17	F.2′3′4′										0	276.54467	0	−0.219481	0	0	553.07334	0.43896	−0.43896	0	0	276.54467	0.219481									0
18	E.33′										+1	0	0	+1	−1	−1	0	+1	−1	+1	0	0	−1									0
19	F.544′															0	0	0	0	−2	2.05487	276.54467	−1	−1	0.027435	0	276.54467	0				0.00845004
20	F.5′4′4															0	0	0	0	+1	−1	276.54467	+2	2.43896	0	0	276.54467	−0.219481				-0.012290936
21	F.345															0.027435	276.54467	0	0	0.05487	0.05487	553.07334	0	0	0.027435	0	276.54467	0				0.041482
22	F.3′4′5′															0	276.54467	0	−0.219481	0	0	553.07334	0.43896	0.43896	0	0	276.54467	−0.219481				0
23	E.44′															+1	0	0	+1	−1	−1	0	+1	−1	+1	0	0	−1				0
24	F.655′																				0	0	0	0	−2	2.05487	276.54467	−1	−1	0.027435	0	0.001459552
25	F.6′5′5																				0	0	0	0	+1	−1	276.54467	+2	2.43896	0	−0.219481	-0.006146548
26	F.456																				0.027435	276.54467	0	0	0.05487	0.05487	553.07334	0	0	0.027435	0	0.041482
27	F.4′5′6′																				0	276.54467	0	−0.219481	0	0	553.07334	0.43896	0.43896	0	0.219481	0
28	E.55′																				+1	0	0	+1	−1	−1	0	+1	−1	+1	−1	0
29	F.65																									0.027435	276.54467	0	0	0.05487	0	0.020741
30	F.6′5′																									0	276.54467	0	−0.219481	0	0.43896	0

Table: 500.15 Numerical matrix for the effect of linear temperature distribution in one column of a shear wall frame.

Deflections (M)	Bend. Mts. (KN - M)		Bend. Mts. (KN - M)	Deflections (M)
$(+73.8\times10^{-5})$	(+0.041)		(+0.0338)	$(+73.8\times10^{-5})$
$+70.9985\times10^{-5}$	+0.042182		+0.035151	$+70.9985\times10^{-5}$
	(+0.116)		(+0.0405)	
$(+47.1\times10^{-5})$	+0.120407		+0.043075	$(+47.1\times10^{-5})$
$+45.3387\times10^{-5}$	+0.148264		+0.014633	$+45.3387\times10^{-5}$
	(+0.143)		(+0.0127)	
	(+0.150)		(+0.0197)	
$(+28.4\times10^{-5})$	+0.150976		+0.017348	$(+28.4\times10^{-5})$
$+27.4295\times10^{-5}$	+0.166724		+0.002417	$+27.4295\times10^{-5}$
	(+0.1648)		(+0.00438)	
	$T_1=20^{\circ}C$			
	(+0.1745)		(+0.0144)	
$(+15.3\times10^{-5})$	+0.178816		+0.014513	$(+15.30\times10^{-5})$
$+14.9720\times10^{-5}$	+0.188295		+0.005230	$+14.9720\times10^{-5}$
	(+0.1834)		(+0.00569)	
	(+0.1878)		(+0.0105)	
$(+6.62\times10^{-5})$	+0.193291		+0.010228	$(+6.62\times10^{-5})$
$+6.6582\times10^{-5}$	+0.198801		+0.004942	$+6.6582\times10^{-5}$
	(+0.1926)		(+0.00582)	
	(+0.1947)		(+0.00837)	
$(+1.63\times10^{-5})$	+0.200642		+0.006784	$(+1.63\times10^{-5})$
$+1.7067\times10^{-5}$	+0.195232		+0.007749	$+1.7067\times10^{-5}$
	(+0.1969)		(+0.00629)	
	(+0.1973)		(+0.00717)	
	+0.194362		+0.006879	

Fig. 5.0543 Shows the results of the effect of Linear Temperature Distribution in a column

Unbracketed Figures - - - show results by the Force-Displacement Method

Bracketed Figures - - - show results by the Stiffness Method

5.05.5 Discussion of results of analysis of shear wall frame

The model shear wall frame was analysed for the following 4 different thermal effects:-

(1) Constant temperature distribution in a roof beam

(2) Linear temperature distribution in a roof beam

(3) Constant temperature distribution in one column, and

(4) Linear temperature distribution in one column

Each thermal effect was analysed by using (a) the force - displacement method and (b) the stiffness method.

The results of constant temperature distribution in the roof beam show an interesting pattern of bending moments and axial forces. The highest bending moments occur in the columns at the junction of one floor below the roof. However, these stresses rapidly attenuate in the lower floors. It is also interesting to note that alternate beams are subject to axial tension and compression (as well as bending moments), in other words, tension and compression oscillates from floor to floor. This explains why, in practice, some floors are observed to crack while others appear to be immune to cracks.

The stress pattern and the deflected form of the frame appears to be rather unusual. Also, the level of stress appears at first sight to be rather low. This is due to the unusual geometric properties of the model frame. It will be shown later, that for a frame of practical proportions, very high stresses and deformations can develop in the upper floors when the roof is subjected to moderate ambient temperature changes.

As can be expected, the results of stiffness analysis correspond very closely to those given by the force-displacement method.

The results of linear temperature distribution in the roof show

similar stress pattern and deflected form of the frame except that maximum bending moments now occur at roof level instead of the floor immediately below. The magnitudes of the bending moments are approximately similar, but the deflections and the axial forces in the beams are reduced considerably.

The results of constant temperature distribution in the column of the 6 - storey shear wall frame show that the effect of temperature change is felt most strongly in the upper floors and in the column directly exposed to the temperature change. The far side column shows greatly reduced bending moments. Tensile axial forces occur in the roof beam and the far side column. All other beams show compressive forces.

The results of linear temperature distribution in the column show similar behaviour as for the constant temperature distribution in the column except (i) the signs of bending moments are reversed generally with the exception of lower floors of the far side column, (ii) the magnitudes of the bending moments are increased several times and (iii) the axial forces in the beams reverse signs alternately.

It is to be noted that in all four cases analysed and shown here, the magnitude of the temperature differential was assumed the same i.e. 20 $^{\circ}C$, and a common value of $E = 21 \times 10^6$ KN/m^2 was selected.

However, the frames were also analysed for values of $E = 28 \times 10^6$ KN/m^2 and 11×10^6 KN/m^2. The results show that the deflections are independent of the value of E whereas the values of bending moments are proportional to E.

5.06.1 The effect of constant temperature distribution in the roof beam

(a) Analysis using the force-displacement method

In the following, an example of the analysis of a multi-storey frame of practical proportions is made to assess the order of the magnitude of stresses and deformations arising from temperature changes in real conditions. Included in the analysis is the effect of axial deformations of beams. The effect of axial deformations of the columns is neglected as it is expected to be negligible for this case.

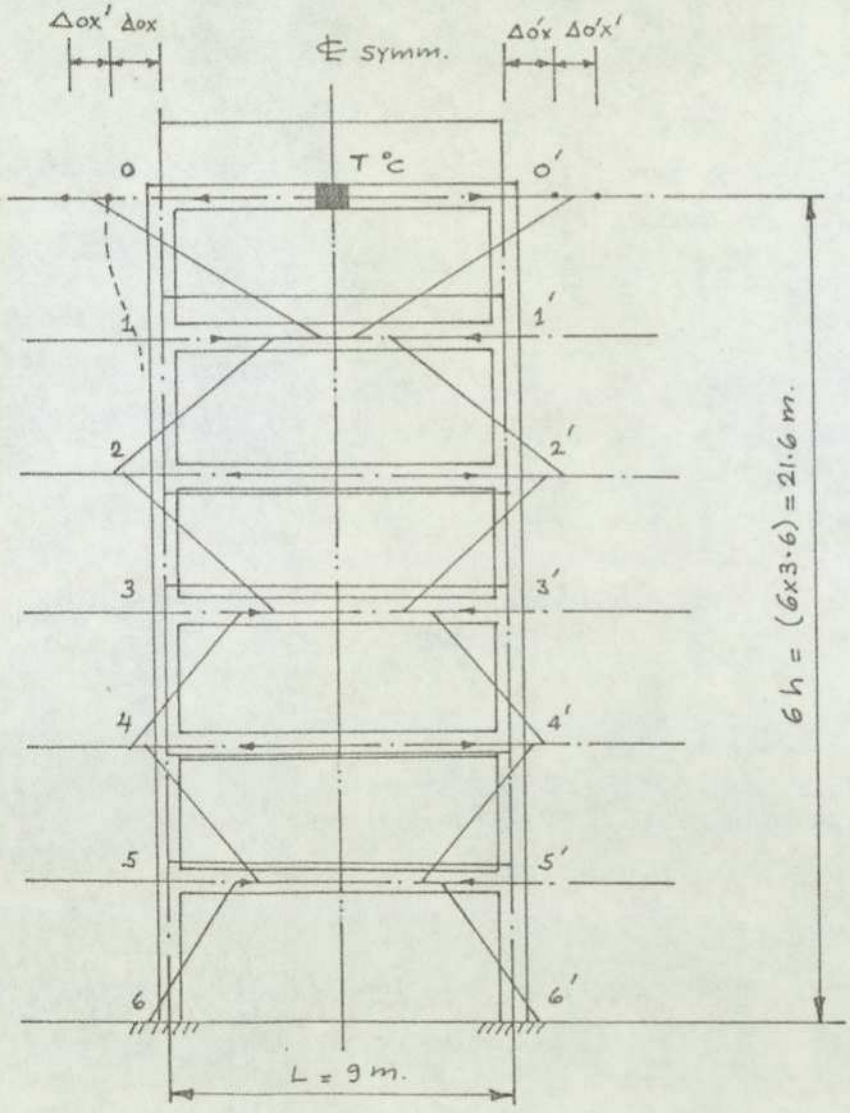

Fig. 5.0611 The effect of constant temperature distribution in roof beam showing assumed bending moments for the setting up of the matrix.

Denoting $\Delta ox + \Delta ox' + \Delta o'x + \Delta o'x' = \alpha TL$ .... (1)

where Δox, $\Delta ox'$, ... etc. are as defined in Section 5.05.1

Also due to symmetry

$$\Delta ox = \Delta o'x \text{ and } \Delta ox' = \Delta o'x' \quad \ldots\ (2)$$

Equation (1) becomes

$$2\,\Delta ox + 2\Delta ox' = \alpha TL \quad \ldots\ (1a)$$

Now, using the force-displacement method, the conditions of compatibility of deformations and equilibrium of forces can be written as follows:-

(NOTE: As the frame is symmetrical, only one half of the frame needs to be analysed).

(a) Conditions of compatibility

F.100' $$mo1\left(\frac{L}{2EIb} + \frac{h}{3EIc}\right) - m1o\left(\frac{h}{6EIc}\right) = \frac{\Delta ox - \Delta 1x}{h}$$

or $$(2r1+3)\left(\frac{mo1}{L}\right) - r1\left(\frac{m1o}{L}\right) - r\,\Delta ox\,\frac{pL}{h} + r\,\Delta 1x\,\frac{pL}{h} = o$$

F.012 $$-mo1 + m1o\left(\frac{h}{3EIc}\right) + m12\left(\frac{h}{3EIc}\right) - m21\left(\frac{h}{6EIc}\right) = \frac{\Delta ox - \Delta 1x}{h} - \frac{\Delta 1x-(-\Delta 2x)}{h}$$

or $$-r1\left(\frac{mo1}{L}\right) + 2r1\left(\frac{m1o}{L}\right) + 2r1\left(\frac{m12}{L}\right) - r1\left(\frac{m21}{L}\right) - r\Delta ox\,\frac{pL}{h} + 2r\Delta 1x\,\frac{pL}{h} + r\Delta 2x\,\frac{pL}{h} = o$$

F.211' $$-m21\left(\frac{h}{6EIc}\right) + m12\left(\frac{h}{3EIc}\right) - (m1o - m12)\left(\frac{L}{2EIb}\right) = -\left(\frac{\Delta 1x-(-\Delta 2x)}{h}\right)$$

or $$-r1\left(\frac{m21}{L}\right) + (2r1+3)\left(\frac{m12}{L}\right) - 3\left(\frac{m1o}{L}\right) + r\Delta 1x\,\frac{pL}{h} + r\Delta 2x\,\frac{pL}{h} = o$$

Similarly

F.123 $$-r1\left(\frac{m12}{L}\right) + 2r1\left(\frac{m21}{L}\right) + 2r1\left(\frac{m23}{L}\right) - r1\left(\frac{m32}{L}\right) + r\Delta 1x\,\frac{pL}{h} + 2r\Delta 2x\,\frac{pL}{h} + r\Delta 3x\,\frac{pL}{h} = o$$

F.322' $$-r1\left(\frac{m32}{L}\right) + (2r1+3)\left(\frac{m23}{L}\right) - 3\left(\frac{m21}{L}\right) + r\Delta 2x\,\frac{pL}{h} + r\Delta 3x\,\frac{pL}{h} = o$$

F.234 $$-r1\left(\frac{m23}{L}\right) + 2r1\left(\frac{m32}{L}\right) + 2r1\left(\frac{m34}{L}\right) - r1\left(\frac{m43}{L}\right) + r\Delta 2x\,\frac{pL}{h} + 2r\Delta 3x\,\frac{pL}{h} + r\Delta 4x\,\frac{pL}{h} = o$$

F.433' $-r1\left(\frac{m43}{L}\right) + (2r1+3)\left(\frac{m34}{L}\right) - 3\left(\frac{m32}{L}\right) + r\Delta 3x\,\frac{pL}{h} + r\Delta 4x\,\frac{pL}{h} = o$

F.345 $-r1\left(\frac{m34}{L}\right) + 2r1\left(\frac{m43}{L}\right) + 2r1\left(\frac{m45}{L}\right) - r1\left(\frac{m54}{L}\right) + r\Delta 3x\,\frac{pL}{h} + 2r\Delta 4x\,\frac{pL}{h} + r\Delta 5x\,\frac{pL}{h} = o$

F.544' $-r1\left(\frac{m54}{L}\right) + (2r1+3)\left(\frac{m45}{L}\right) - 3\left(\frac{m43}{L}\right) + r\Delta 4x\,\frac{pL}{h} + r\Delta 5x\,\frac{pL}{h} = o$

F.456 $-r1\left(\frac{m45}{L}\right) + 2r1\left(\frac{m54}{L}\right) + 2r1\left(\frac{m56}{L}\right) - r1\left(\frac{m65}{L}\right) + r\Delta 4x\,\frac{pL}{h} + 2r\Delta 5x\,\frac{pL}{h} = o$

F.655' $-r1\left(\frac{m65}{L}\right) + (2r1+3)\left(\frac{m56}{L}\right) - 3\left(\frac{m54}{L}\right) + r\Delta 5x\,\frac{pL}{h} = o$

F.56 $-r1\left(\frac{m56}{L}\right) + 2r1\left(\frac{m65}{L}\right) + \frac{r\Delta 5x}{h} = o$

For the determination of axial forces in the beams, further 6 conditions of compatibility of deformations relating to axial forces in the beams are required and these are as follows:-

C.oo' $\Delta ox' + \Delta o'x' = \frac{Noo'\ Loo'}{Aoo'\ Eoo'}$

or $2r\Delta ox + Noo'\ Soo' = r\alpha TL$ since $\Delta ox' = \Delta o'x'$ and $\Delta ox + \Delta ox' = \frac{\alpha TL}{2}$

Similarly

C.11' $2r\ \Delta 1x - N11\ S11' = o$

C.22' $2r\ \Delta 2x - N22'\ S22' = o$

C.33' $2r\Delta 3x - N33'\ S33' = o$

C.44' $2r\Delta 4x - N44'\ S44' = o$

C.55' $2r\Delta 5x - N55'\ S55' = o$

(b) Conditions of Equilibrium

E.ox $\left(\frac{mo1 + m1o}{h}\right) = Noo'$

or $mo1 + m1o + \left(\frac{2EAbh}{L}\right)\Delta ox = \alpha TEAbh$

E.1x $\left(\frac{m21 + m12}{h}\right) + \left(\frac{m1o + mo1}{h}\right) - N11' \doteq o$

or $m21 + m12 + m1o + mo1 - h\,N11' = o$

Similarly

E.2x $m32 + m23 + m21 + m12 - h\,N22' = o$

E.3x $m43 + m34 + m32 + m23 - h\,N33' = o$

E.4x $m54 + m45 + m43 + m34 - h\,N44' = o$

E.5x $m65 + m56 + m54 + m45 - h\,N55' = o$

In the above equations, $r1 = \frac{h}{L}\frac{Ib}{Ic}$; $r = \frac{AbE}{L}$

$p = \frac{6Ib}{AbL^2}$:

$Soo' = \frac{Loo'}{Aoo'}\,Eoo' \cdot \frac{AbEb}{Lb}$; $S11' = \frac{L11'}{A11'}\,E11' \cdot \frac{AbEb}{Lb}$

$S22' = \frac{L22'}{A22'}\,E22' \cdot \frac{AbEb}{Lb}$; $S33' = \frac{L33'}{A33'}\,E33' \cdot \frac{AbEb}{Lb}$

$S44' = \frac{L44'}{A44'}\,E44' \cdot \frac{AbEb}{Lb}$; $S55' = \frac{L55'}{A55'}\,E55' \cdot \frac{AbEb}{Lb}$

Example

In the numerical example, a frame of the following dimensions and properties, as shown in fig. 5.0611, is analysed:-

$L = Lb = 9.0m$; $h = 3.6m$

Columns 300mm x 600mm : All beams 300mm x 600mm

$Ac = Ab = 0.3 \times 0.6 = 0.18m^2$; $Ic = Ib = 0.3 \times 0.6^3/12 = 0.0054m^4$.

$T = 20^oC$; $\alpha = 0.00001$ per ^oC

$E = 28 \times 10^6\ KN/m^2$

The following parameters required in the matrix are first calculated:-

$$r1 = \frac{h}{L} \cdot \frac{Ib}{Ic} = \frac{3.6}{9} = 0.4$$

$$r = \frac{AbE}{L} = \frac{0.18 \times 28 \times 10^6}{9} = 56 \times 10^4 \text{ KN/m}$$

$$p = \frac{6Ib}{AbL^2} = \frac{6 \times 0.0054}{0.18 \times 9^2} = 0.002222$$

$$r\frac{pL}{h} = 56 \times 10^4 \times 0.002222 \times 9/3.6 = 3111.1080 \text{ KN/m}$$

$$\frac{2EAbh}{L} = 2 \times 28 \times 10^6 \times \frac{0.18 \times 3.6}{9} = 4.032 \times 10^6 \text{ KN}$$

$$\alpha TEAbh = 0.00001 \times 20 \times 28 \times 10^6 \times 0.18 \times 3.6 = 3628.8 \text{ KN/m}$$

The conditions of compatibility of deformations and equilibrium of forces derived above can now be formulated into a matrix as shown in Table: 500.16, and introducing the above numerical parameters into the general matrix, the numerical matrix shown in Table: 500.17 is obtained. The solution of this matrix gives the bending moments in all members, deflections at all joints and axial forces in the beams. Shearing forces can be obtained from the conditions of static equilibrium. The results are shown in fig. 5.0613

(b) Analysis using the stiffness method

In analysing the symmetrical frame of fig.5.0611 by the stiffness method, exactly the same procedure was followed as in Section 5.05.1(b). Therefore the force to be applied in this case is as follows:-

$P = EA\alpha T$ where $Ab = 0.3 \times 0.6 = 0.18m^2$

$= 1,008$ KN $E = 28 \times 10^6$ KN/m^2

$\alpha = 0.00001$

$T = 20^{\circ}C$

(Note: The value of $E = 28 \times 10^6$ KN/m^2 selected for this problem is approximately the E value of Grade 30 reinforced concrete. As mentioned above the values of parameters selected for the problems associated with the frame of fig.5.0611 are such that they are likely to be met in reality).

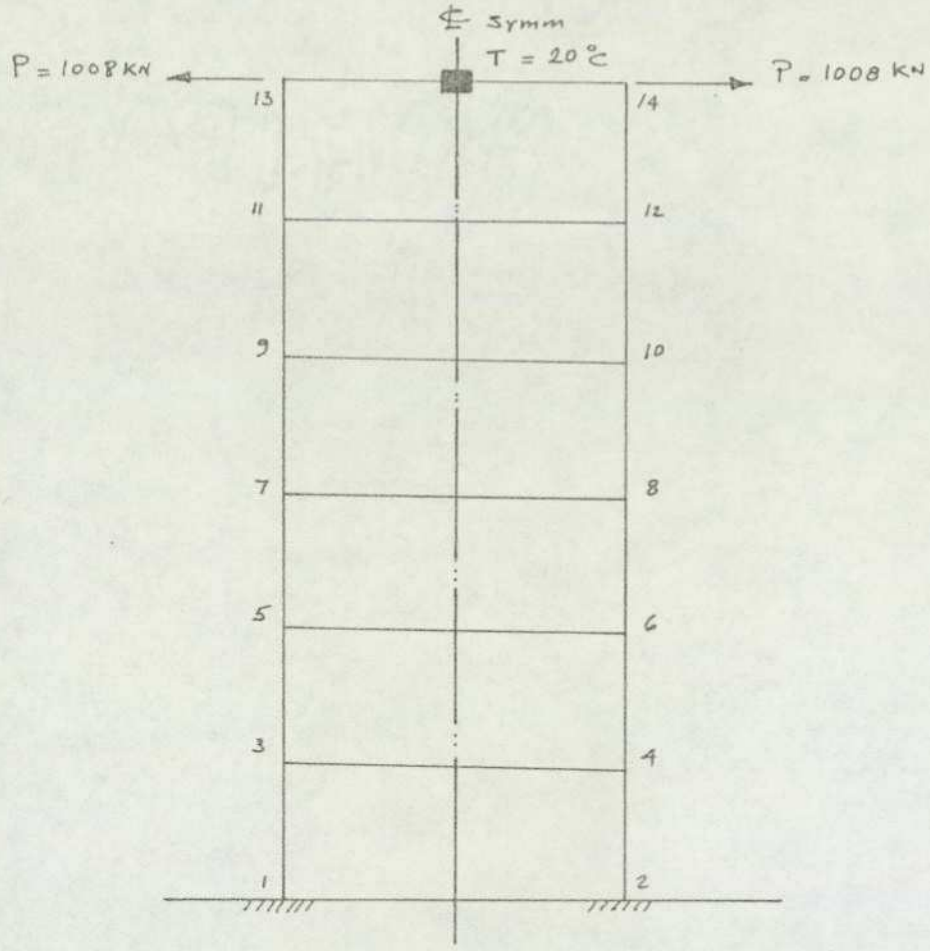

Fig.5.0612 The effect of constant temperature distribution in roof beam of a symmetrical frame analysed by the stiffness method.

The results of the effect of constant temperature distribution in the roof beam of a symmetrical frame and analysed by the stiffness method are shown in fig. 5.0613.

EQN. No.		1	2	3	4	5	6	7	8	9	10	11	12	13	14	15	16	17	18	19	20	21	22	23	24	LOAD VECTOR
No.	REF. JT.	0			1				2				3				4				5				6	
	REF. EQN.	m_{01}	N_{00}'	Δ_{0x}	m_{10}	m_{12}	N_{11}'	Δ_{1x}	m_{21}	m_{23}	N_{22}'	Δ_{2x}	m_{32}	m_{34}	N_{33}'	Δ_{3x}	m_{43}	m_{45}	N_{44}'	Δ_{4x}	m_{54}	m_{56}	N_{55}'	Δ_{5x}	m_{65}	
1	F.100′	-0.42222	0	-3111·108	-0.04444	0	0	3111·108																		0
2	C.00′	0	+1	1120000	0	0	0	0																		1,008
3	E.0x	+1	0	4032000	+1	0	0	0																		3,628·8
4	F.012	-0.04444	0	-3111·108	0.08889	0.08889	0	-6222·216	-0.04444	0	0	3111·108														0
5	C.11′	0	0	0	0	0	-1	1120000	0	0	0	0														0
6	E.1x	+1	0	0	+1	+1	-3·6	0	+1	0	0	0														0
7	F.211′				-0.33333	0.42222	0	-3111·108	-0.04444	0	0	3111·108	0	0	0	0										0
8	F.123				0	-0.04444	0	-3111·108	0.08889	0.08889	0	-6222·216	-0.04444	0	0	3111·108										0
9	C.22′				0	0	0	0	0	0	-1	1120000	0	0	0	0										0
10	E.2x				0	+1	0	0	+1	+1	-3·6	0	+1	0	0	0										0
11	F.322′								-0.33333	0.42222	0	3111·108	-0.04444	0	0	3111·108	0	0	0	0						0
12	F.234								0	-0.04444	0	3111·108	0.08889	0.08889	0	-6222·216	-0.04444	0	0	3111·108						0
13	C.33′								0	0	0	0	0	0	-1	1120000	0	0	0	0						0
14	E.3x								0	+1	0	0	+1	+1	-3·6	0	+1	0	0	0						0
15	F.433′												-0.33333	0.42222	0	3111·108	-0.04444	0	0	3111·108	0	0	0	0		0
16	F.345												0	-0.04444	0	3111·108	0.08889	0.08889	0	-6222·216	-0.04444	0	0	3111·108		0
17	C.44′												0	0	0	0	0	0	-1	1120000	0	0	0	0		0
18	E.4x												0	+1	0	0	+1	+1	-3·6	0	+1	0	0	0		0
19	F.544′																-0.33333	0.42222	0	3111·108	-0.04444	0	0	3111·108	0	0
20	F.456																0	-0.04444	0	3111·108	0.08889	0.08889	0	-6222·216	-0.04444	0
21	C.55′																0	0	0	0	0	0	-1	1120000	0	0
22	E.5x																0	+1	0	0	+1	+1	-3·6	0	+1	0
23	F.655′																				-0.33333	0.42222	0	3111·108	-0.04444	0
24	F.56																				0	-0.04444	0	3111·108	0.08889	0

Table: 500.17 Numerical matrix for the effect of constant temperature distribution in the roof beam of a symmetrical 6-storey frame.

EQN. No.		1	2	3	4	5	6	7	8	9	10	11	12	13	14	15	16	17	18	19	20	21	22	23	24	LOAD
	REF. JT.	0			1				2				3				4				5				6	VECTOR
No.	REF. EQN.	M_{01}	N_{00}'	Δ_{0X}	M_{10}	M_{12}	N_{11}'	Δ_{1X}	M_{21}	M_{23}	N_{22}'	Δ_{2X}	M_{32}	M_{34}	N_{33}'	Δ_{3X}	M_{43}	M_{45}	N_{44}'	Δ_{4X}	M_{54}	M_{52}	N_{55}'	Δ_{5X}	M_{65}	
1	F.100′	$(3+2n)\frac{1}{L}$	0	$-r\frac{PL}{K}$	$-\frac{n}{L}$	0	0	$r\frac{PL}{K}$																		0
2	C.00′	0	S_{00}'	$2r$	0	0	0	0																		$Y_{\alpha TL}$
3	E.0X	+1	0	$\frac{2EAR}{L}$	+1	0	0	0																		α_{TEAR}
4	F.012	$-n/L$	0	$-rPL/K$	$2n/L$	$2n/L$	0	$2rPL/K$	$-n/L$	0	0	rPL/K														0
5	C.11′	0	0	0	0	0	$-S_{11}'$	$2r$	0	0	0	0														0
6	E.1X	+1	0	0	+1	+1	$-h$	0	+1	0	0	0														0
7	F.211′				$-3/L$	$(2n+3)\frac{1}{L}$	0	rPL/K	$-n/L$	0	0	rPL/K	0	0	0	0										0
8	F.123				0	$-n/L$	0	rPL/K	$2n/L$	$2n/L$	0	$2rPL/K$	$-n/L$	0	0	rPL/K										0
9	C.22′				0	0	0	0	0	0	$-S_{22}'$	$2r$	0	0	0	0										0
10	E.2X				0	+1	0	0	+1	+1	$-h$	0	+1	0	0	0										0
11	F.322′								$-3/L$	$(2n+3)\frac{1}{L}$	0	rPL/K	$-n/L$	0	0	rPL/K	0	0	0	0						0
12	F.234								0	$-n/L$	0	rPL/K	$2n/L$	$2n/L$	0	$2rPL/K$	$-n/L$	0	0	rPL/K						0
13	C.33′								0	0	0	0	0	0	$-S_{33}'$	$2r$	0	0	0	0						0
14	E.3X								0	+1	0	0	+1	+1	$-h$	0	+1	0	0	0						0
15	F.433′												$-3/L$	$(2n+3)\frac{1}{L}$	0	rPL/K	$-n/L$	0	0	rPL/K	0	0	0	0		0
16	F.345												0	$-n/L$	0	rPL/K	$2n/L$	$2n/L$	0	$2rPL/K$	$-n/L$	0	0	rPL/K		0
17	C.44′												0	0	0	0	0	0	$-S_{44}'$	$2r$	0	0	0	0		0
18	E.4X												0	+1	0	0	+1	+1	$-h$	0	+1	0	0	0		0
19	F.544′																$-3/L$	$(2n+3)\frac{1}{L}$	0	rPL/K	$-n/L$	0	0	rPL/K	0	0
20	F.456																0	$-n/L$	0	rPL/K	$2n/L$	$2n/L$	0	$2rPL/K$	$-n/L$	0
21	C.55′																0	0	0	0	0	0	$-S_{55}'$	$2r$	0	0
22	E.5X																0	+1	0	0	+1	+1	$-h$	0	+1	0
23	F.655′																				$-3/L$	$(2n+3)\frac{1}{L}$	0	rPL/K	$-n/L$	0
24	F.56																				0	$-n/L$	0	rPL/K	$2n/L$	0

Table: 500.16 General matrix for the effect of constant temperature distribution in the roof beam of a symmetrical 6-storey frame.

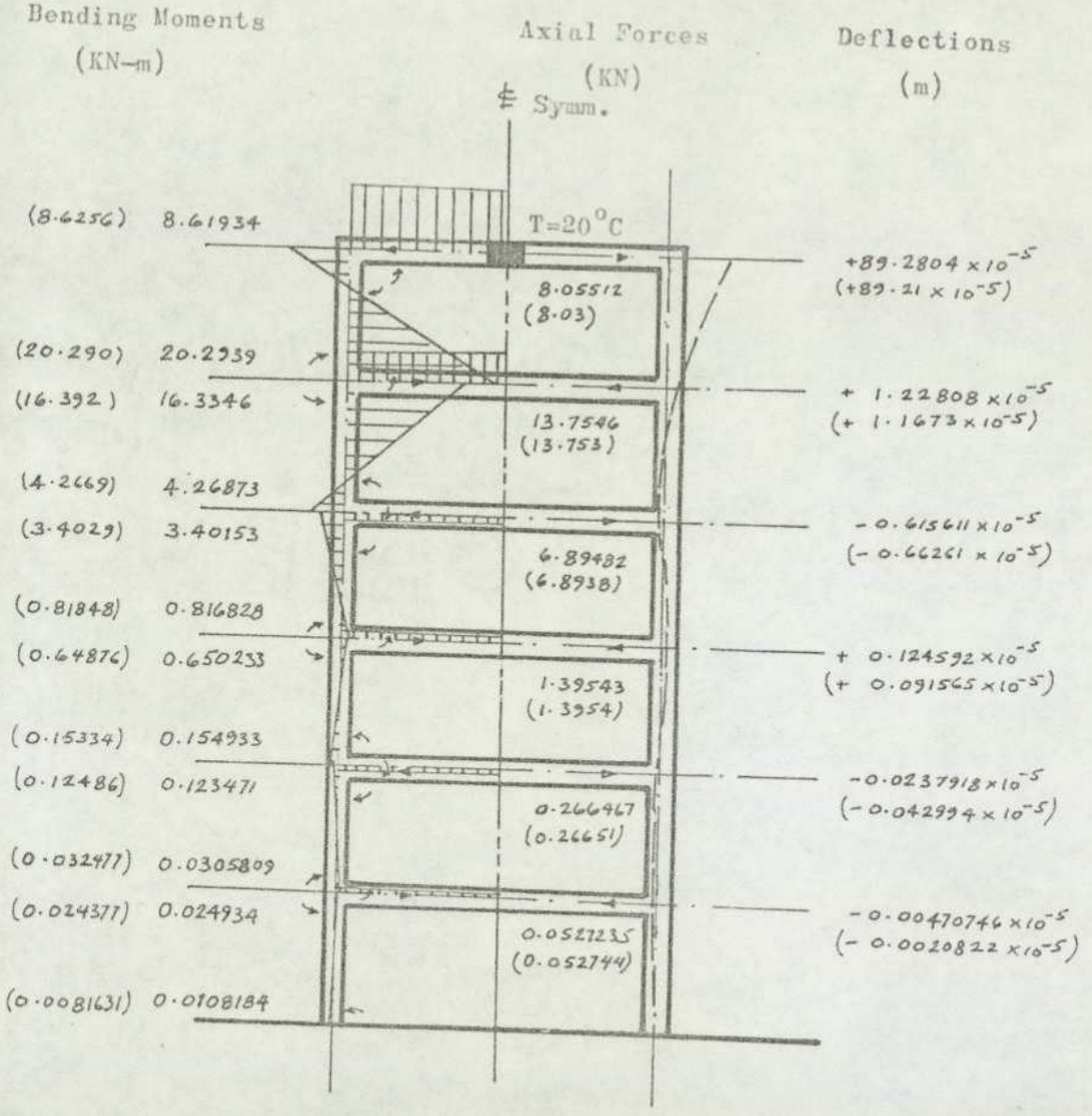

Fig. 5.0613 Shows the results of the effect of constant temperature distribution in the roof beam

Unbracketed figures - - - show results by the force-displacement method

Bracketed figures - - - show results by the stiffness method

5.06.2 The effect of linear temperature distribution in the roof beam

(a) Analysis using the force-displacement method

Note: This analysis includes the effect of axial deformations of all beams but excludes the axial deformations of columns as these are considered negligible for this case.

Denoting ... $\Delta ox' + \Delta ox + \Delta o'x + \Delta o'x' = \frac{\alpha T_1 L}{2}$ ---- (1)

Also because of symmetry

$\Delta ox = \Delta o'x$ and $\Delta ox' = \Delta o'x'$ ---- (2)

$\therefore 2(\Delta ox + \Delta ox') = \frac{\alpha T_1 L b}{2}$ ---- (1a)

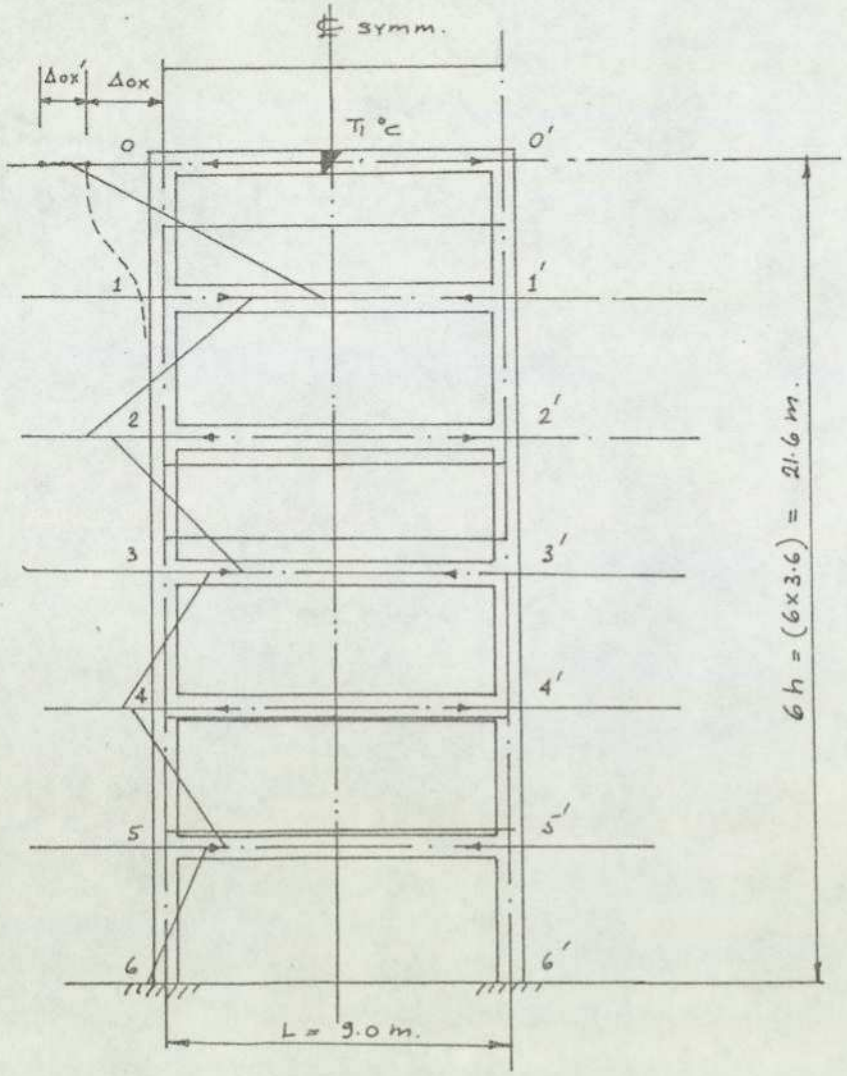

Fig.5.0621 The effect of linear temperature distribution in roof beam showing assumed bending moments for the setting up of the matrix.

Using the force-displacement method, the conditions of compatibility of deformations and equilibrium of forces remain identical to those derived for constant temperature distribution, except equations F1oo', Coo' and Eox, which are modified as follows:-

F.1oo' $\quad mo1\frac{h}{3EIc} - m1o\frac{h}{6EIc} + mo1\frac{L}{3EIb} + mo'1'\frac{L}{6EIb} = \frac{\Delta ox + \Delta 1x}{h} - \theta oo'$

or $\quad (2r1+3)(\frac{mo1}{L}) - r1(\frac{m1o}{L}) - r\Delta ox\,\frac{pL}{h} + r\Delta 1x\,\frac{pL}{h} = \frac{-3\alpha T1EIb}{dL}$

Coo' $\quad \Delta ox' + \Delta o'x' = \frac{Noo'\ Loo'}{Aoo'\ Eoo'}$

or $\quad 2r\Delta ox + Noo'\ Soo' = \frac{r\alpha T1Lb}{2}$

E.ox $\quad (\frac{mo1 + m1o}{h}) = Noo'$

or $\quad mo1 + m1o + \frac{2EAbh}{Lb}\Delta ox = \frac{\alpha T1EAbh}{2}$

In the above equations,

$$\theta oo' = \frac{\alpha T1L}{2d} \quad ; \quad mo1 = mo'1'$$

$$r1 = \frac{h}{L} \cdot \frac{Ib}{Ic} \quad ; \quad r = \frac{AbEb}{Lb}$$

$$P = \frac{6Ib}{AbL^2} \quad ; \quad \Delta ox' = \Delta o'x'$$

$$Soo' = \frac{Loo'}{Aoo'\ Eoo'} \cdot \frac{AbEb}{Lb} = 1$$

$$Noo' = (\frac{\alpha T1Lb}{4} - \Delta ox)\,\frac{2Eb\ Ab}{Lb}$$

As could be expected in the above equations, only the right hand side i.e. the load vector has changed in comparison with the constant temperature distribution case. The left hand side remains identical.

The results of this problem are shown in fig. 5.0422.

(b) Analysis using the Stiffness Method

As before the magnitudes of the axial force and bending moments to be applied are as follows:-

$$P = EAb\alpha\frac{T1}{2} = EAb\alpha Tav = 28 \times 10^6 \times 0.18 \times 0.00001 \times \frac{20}{2} = 504 \text{ KN}$$

and $$M = \alpha T1\frac{E1b}{d} = 0.00001 \times 20 \times 28 \times 10^6 \times \frac{0.0054}{0.6} = 50.4 \text{ KN/m}$$

The results of linear temperature distribution in the roof beam of a symmetrical frame and analysed by the stiffness method are shown in fig.5.0622.

EQN. No.		1	2	3	4	5	6	7	8	9	10	11	12	13	14	15	16	17	18	19	20	21	22	23	24	LOAD VECTOR
	REF. JT.	0			1				2				3				4				5				6	
No.	REF. EQN.	m_{01}	N_{00}'	Δ_{0x}	m_{10}	m_{12}	N_{11}'	Δ_{1x}	m_{21}	m_{23}	N_{22}'	Δ_{2x}	m_{32}	m_{34}	N_{33}'	Δ_{3x}	m_{43}	m_{45}	N_{44}'	Δ_{4x}	m_{54}	m_{56}	N_{55}'	Δ_{5x}	m_{65}	
1	F. 100'	0.42222	0	-3111.108	-0.04444	0	0	3111.108																		-16.8
2	C. 00'	0	+1	1120000	0	0	0	0																		504.0
3	E. 0x	+1	0	4032000	+1	0	0	0																		1814.2
4	F. 012	-0.04444	0	-3111.108	0.08887	0.08887	0	6222.216	-0.04444	0	0	3111.108														0
5	C. 11'	0	0	0	0	0	-1	1120000	0	0	0	0														0
6	E. 1x	+1	0	0	+1	+1	-3.6	0	+1	0	0	0														0
7	F. 211'				-0.33333	0.42222	0	3111.108	-0.04444	0	0	3111.108	0	0	0	0										0
8	F. 123				0	-0.04444	0	3111.108	0.08887	0.08887	0	6222.216	-0.04444	0	0	3111.108										0
9	C. 22'				0	0	0	0	0	0	-1	1120000	0	0	0	0										0
10	E. 2x				0	+1	0	0	+1	+1	-3.6	0	+1	0	0	0										0
11	F. 322'								-0.33333	0.42222	0	3111.108	-0.04444	0	0	3111.108	0	0	0	0						0
12	F. 234								0	-0.04444	0	3111.108	0.08887	0.08887	0	6222.216	-0.04444	0	0	3111.108						0
13	C. 33'								0	0	0	0	0	0	-1	1120000	0	0	0	0						0
14	E. 3x								0	+1	0	0	+1	+1	-3.6	0	+1	0	0	0						0
15	F. 433'												-0.33333	0.42222	0	3111.108	-0.04444	0	0	3111.108	0	0	0	0		0
16	F. 345												0	-0.04444	0	3111.108	0.08887	0.08887	0	6222.216	-0.04444	0	0	3111.108		0
17	C. 44'												0	0	0	0	0	0	-1	1120000	0	0	0	0		0
18	E. 4x												0	+1	0	0	+1	+1	-3.6	0	+1	0	0	0		0
19	F. 544'																-0.33333	0.42222	0	3111.108	-0.04444	0	0	3111.108	0	0
20	F. 456																0	-0.04444	0	3111.108	0.08887	0.08887	0	6222.216	-0.04444	0
21	C. 55'																0	0	0	0	0	0	-1	1120000	0	0
22	E. 5x																0	+1	0	0	+1	+1	-3.6	0	+1	0
23	F. 655'																				-0.33333	0.42222	0	3111.108	-0.04444	0
24	F. 56																				0	-0.04444	0	3111.108	0.08887	0

Table: 500.19 Numerical matrix for the effect of linear temperature distribution in the roof beam of a symmetrical 6-storey frame.

EQN. No.		1	2	3	4	5	6	7	8	9	10	11	12	13	14	15	16	17	18	19	20	21	22	23	24	LOAD VECTOR
	REF. JT.	0			1				2				3				4				5				6	
No.	REF. EQN.	M_{01}	N_{00}'	Δ_{0x}	M_{10}	M_{12}	N_{11}'	Δ_{1x}	M_{21}	M_{23}	N_{22}'	Δ_{2x}	M_{32}	M_{34}	N_{33}'	Δ_{3x}	M_{43}	M_{45}	N_{44}'	Δ_{4x}	M_{54}	M_{52}	N_{55}'	Δ_{5x}	M_{65}	
1	F.100′	$(3+2n)\frac{1}{L}$	0	$-r\frac{PL}{8}$	$-\frac{n}{L}$	0	0	$r\frac{PL}{8}$																		$-3\alpha T E_h/dL$
2	C.00′	0	300′	2r	0	0	0	0																		$r\alpha T L/2$
3	E.0x	+1	0	$\frac{2EAR}{L}$	+1	0	0	0																		$\alpha T E A_h/2$
4	F.01ℓ	$-n/L$	0	$-rPL/8$	$2n/L$	$2n/L$	0	$2rPL/8$	$-n/L$	0	0	$rPL/8$														0
5	C.11′	0	0	0	0	0	$-S_{11}'$	2r	0	0	0	0														0
6	E.1x	+1	0	0	+1	+1	$-h$	0	+1	0	0	0														0
7	F.211′				$-3/L$	$(2n+3)\frac{1}{L}$	0	$rPL/8$	$-n/L$	0	0	$rPL/8$	0	0	0	0										0
8	F.123				0	$-n/L$	0	$rPL/8$	$2n/L$	$2n/L$	0	$2rPL/8$	$-n/L$	0	0	$rPL/8$										0
9	C.22′				0	0	0	0	0	0	$-S_{22}'$	2r	0	0	0	0										0
10	E.2x				0	+1	0	0	+1	+1	$-h$	0	+1	0	0	0										0
11	F.322′								$-3/L$	$(2n+3)\frac{1}{L}$	0	$rPL/8$	$-n/L$	0	0	$rPL/8$	0	0	0	0						0
12	F.234								0	$-n/L$	0	$rPL/8$	$2n/L$	$2n/L$	0	$2rPL/8$	$-n/L$	0	0	$rPL/8$						0
13	C.33′								0	0	0	0	0	0	$-S_{33}'$	2r	0	0	0	0						0
14	E.3x								0	+1	0	0	+1	+1	$-h$	0	+1	0	0	0						0
15	F.433′												$-3/L$	$(2n+3)\frac{1}{L}$	0	$rPL/8$	$-n/L$	0	0	$rPL/8$	0	0	0	0		0
16	F.345												0	$-n/L$	0	$rPL/8$	$2n/L$	$2n/L$	0	$2rPL/8$	$-n/L$	0	0	$rPL/8$		0
17	C.44′												0	0	0	0	0	0	$-S_{44}'$	2r	0	0	0	0		0
18	E.4x												0	+1	0	0	+1	+1	$-h$	0	+1	0	0	0		0
19	F.544′																$-3/L$	$(2n+3)\frac{1}{L}$	0	$rPL/8$	$-n/L$	0	0	$rPL/8$	0	0
20	F.456																0	$-n/L$	0	$rPL/8$	$2n/L$	$2n/L$	0	$2rPL/8$	$-n/L$	0
21	C.55′																0	0	0	0	0	0	$-S_{55}'$	2r	0	0
22	E.5x																0	+1	0	0	+1	+1	$-h$	0	+1	0
23	F.655′																				$-3/L$	$(2n+3)\frac{1}{L}$	0	$rPL/8$	$-n/L$	0
24	F.56																				0	$-n/L$	0	$rPL/8$	$2n/L$	0

Table: 500.18 General matrix for the effect of linear temperature distribution in the roof beam of a symmetrical 6-storey frame.

Bending Moments (KN–m)

Axial Forces in beams (KN)

Horizontal Deflections (mm)

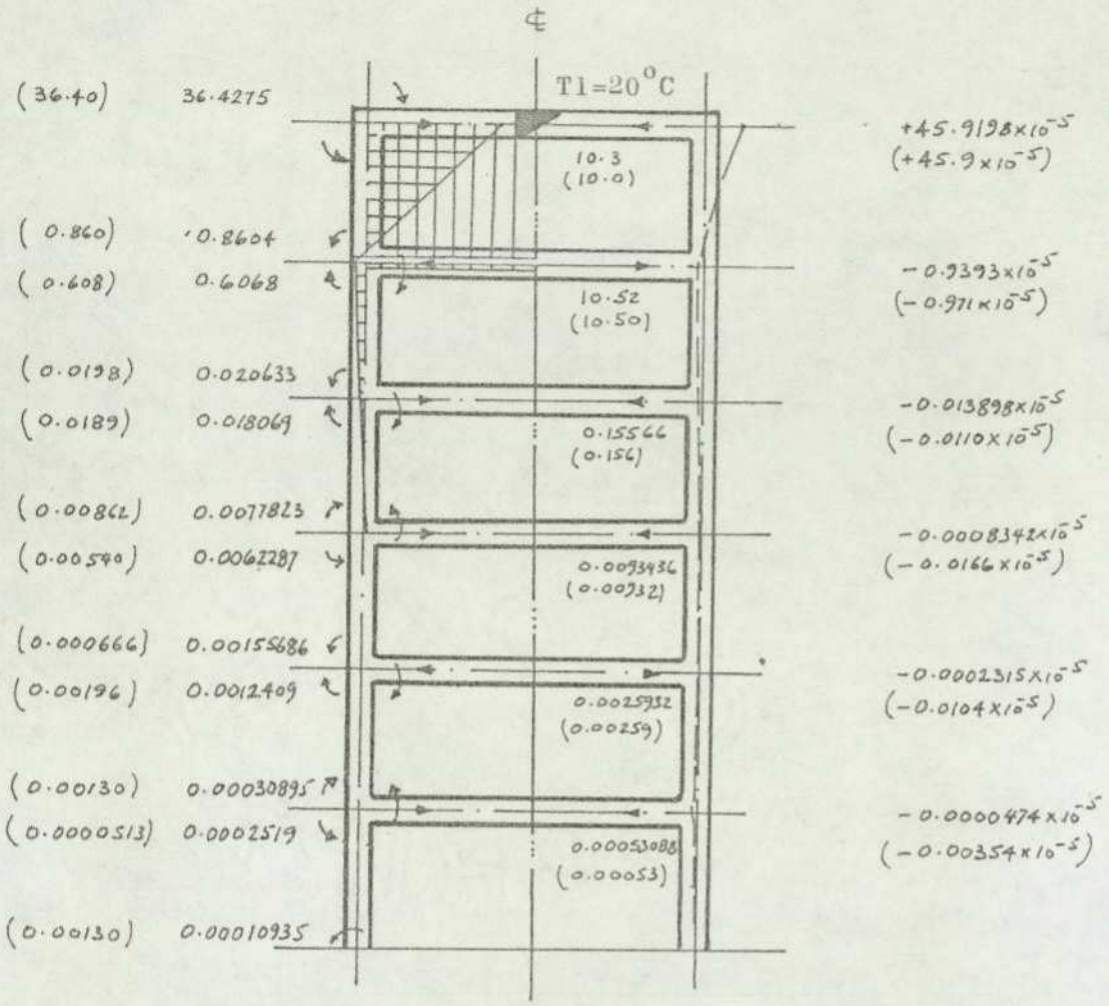

Fig. 5.0622 Shows the results of the effect of linear temperature distribution in the roof beam

Unbracketed figures . . . show results by the force–displacement method

Bracketed figures . . . show results by the stiffness method

5.06.3 The effect of constant temperature distribution in a column

(a) Analysis using force-displacement method

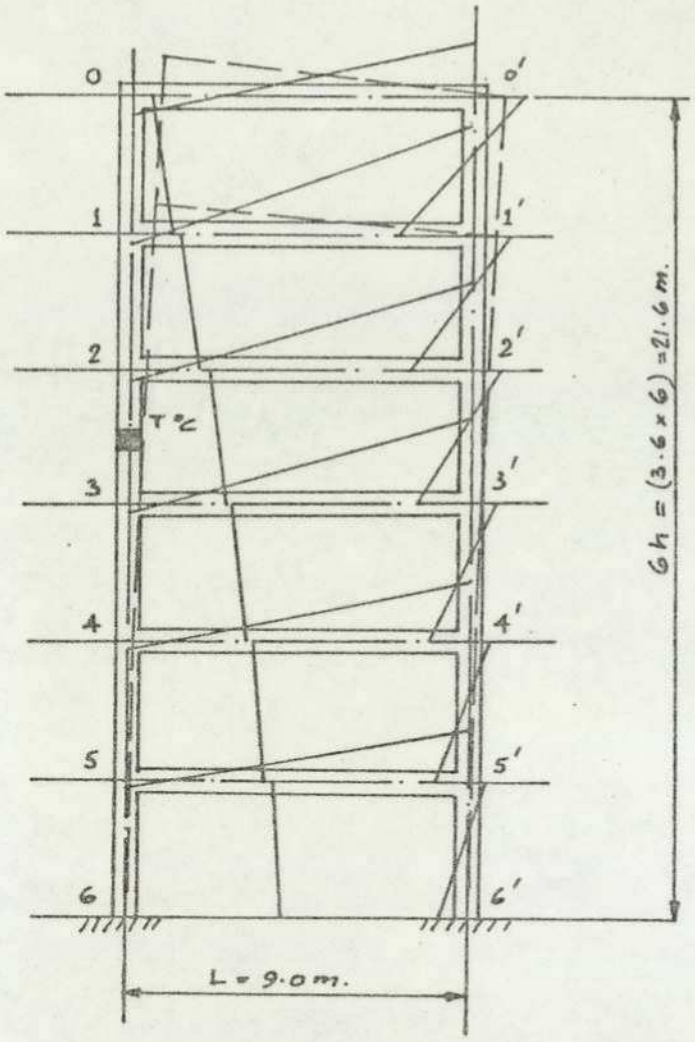

Fig. 5.0631 The effect of constant temperature distribution in the column of a symmetrical 6-storey frame showing assumed bending moments for the setting up of the matrix.

Although the frame itself is symmetrical, but in this case the applied force, i.e. the action of heat on one column, is not symmetrical, therefore it is necessary to analyse the whole frame.

As the assumed bending moment diagram is similar to the one used for the analysis of the shear wall model frame, the conditions of compatibility of deformations and the equilibrium of forces will also be of similar form. Therefore the overall matrix remains the same as in the previous case. However, the numerical values of the elements of the matrix will be different as the properties of the frame are different and for this reason, the complete numerical matrix is shown in Table: 500.21. The results of the solution of the abovementioned matrix are shown in fig. 5.0633.

(b) Analysis Using Stiffness Method

A similar procedure as in the case of the 6-storey shear wall model frame was followed. The force to be applied in this case is as follows:-

$$P = EAc\alpha T$$
$$= 28 \times 10^{6} \times 0.18 \times 0.00001 \times 20$$
$$= 1008 \text{ KN}$$

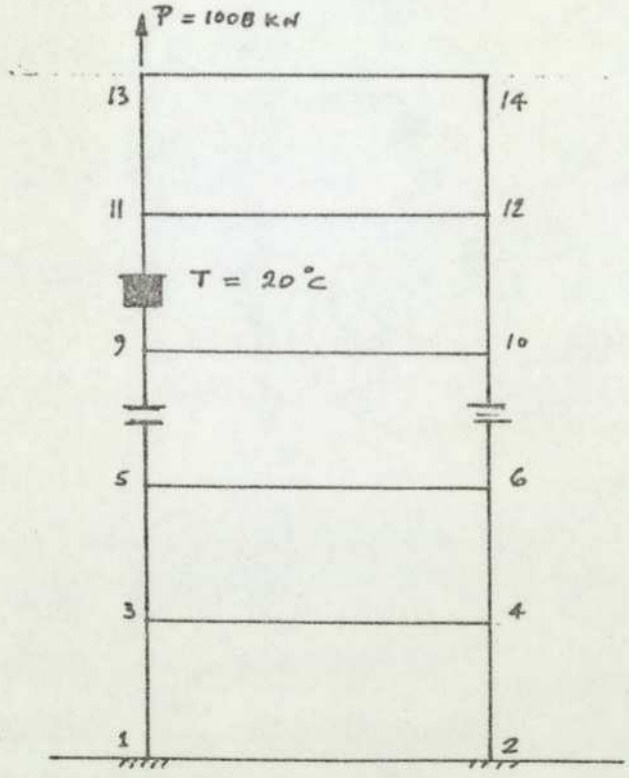

Fig.5.0632 The effect of constant temperature distribution in the column of a symmetrical 6-storey frame analysed by the Stiffness Method.

The results of the effect of constant temperature distribution in the column of a symmetrical 6-storey frame and analysed by the stiffness method are shown in fig. 5.0633.

EQN. No.		1	2	3	4	5	6	7	8	9	10	11	12	13	14	15	16	17	18	19	20	21	22	23	24	25	26	27	28	29	30	LOAD VECTOR
No.	REF. ST.	0		0'	1			1'		2			2'		3			3'		4			4'		5			5'		6	6'	
	REF. EQN.	M01	Δ0x	M0'1'	M10	M12	Δ1x	M1'0'	M1'2'	M21	M23	Δ2x	M2'4'	M2'3'	M32	M34	Δ3x	M3'2'	M3'4'	M43	M45	Δ4x	M4'3'	M4'5'	M54	M52	Δ5x	M5'4'	M5'6'	M65	M6'5'	
1	F.100'	-2·8	28,000	+1	-0·4	0	28,000	0																								-48·384
2	F.1'0'0	+1	28,000	-2·8	0	0	28,000	0·4																								-48·384
3	E.00'	-1	0	-1	+1	0	0	-1																								0
4	F.21'	0	0	0	+2	-2·8	28,000	+1	+1	-0·4	0	28,000	0																			-40·320
5	F.2'1'1	0	0	0	-1	+1	28,000	-2	-2·8	0	0	28,000	-0·4																			-40·320
6	F.012	+0·4	28,000	0	+0·8	+0·8	56,000	0	0	+0·4	0	28,000	0																			0
7	F.0'1'2'	0	28,000	+0·4	0	0	56,000	-0·8	+0·8	0	0	28,000	+0·4																			0
8	E.11'	+1	0	+1	-1	-1	0	+1	-1	+1	0	0	+1																			0
9	F.322'					0	0	0	0	+2	-2·8	28,000	-1	+1	-0·4	0	28,000	0															-32·256
10	F.3'2'2					0	0	0	0	-1	+1	28,000	+2	-2·8	0	0	28,000	-0·4															-32·256
11	F.123					+0·4	28,000	0	0	+0·8	+0·8	56,000	0	0	+0·4	0	28,000	0															0
12	F.1'2'3'					0	28,000	0	+0·4	0	0	56,000	+0·8	+0·8	0	0	28,000	+0·4															0
13	E.22'					+1	0	0	+1	-1	-1	0	-1	-1	+1	0	0	+1															0
14	F.433'										0	0	0	0	+2	-2·8	28,000	-1	+1	-0·4	0	28,000	0									-24·192
15	F.4'3'3										0	0	0	0	-1	+1	28,000	+2	-2·8	0	0	28,000	-0·4									-24·192
16	F.234										+0·4	28,000	0	0	+0·8	+0·8	56,000	0	0	+0·4	0	28,000	0									0
17	F.2'3'4'										0	28,000	0	+0·4	0	0	56,000	+0·8	+0·8	0	0	28,000	+0·4									0
18	E.33'										+1	0	0	+1	-1	-1	0	-1	-1	+1	0	0	+1									0
19	F.544'															0	0	0	0	+2	-2·8	28,000	-1	+1	-0·4	0	28,000	0				-16·128
20	F.54'4															0	0	0	0	-1	+1	28,000	+2	-2·8	0	0	28,000	-0·4				-16·128
21	F.345															+0·4	28,000	0	0	+0·8	+0·8	56,000	0	0	+0·4	0	28,000	0				0
22	F.3'4'5'															0	28,000	0	+0·4	0	0	56,000	+0·8	+0·8	0	0	28,000	+0·4				0
23	E.44'															+1	0	0	+1	-1	-1	0	-1	-1	+1	0	0	+1				0
24	F.655'																				0	0	0	0	+2	-2·8	28,000	-1	+1	-0·4	0	-8·064
25	F.6'5'5																				0	0	0	0	-1	+1	28,000	+2	-2·8	0	-0·4	-8·064
26	F.456																			+0·4	28,000	0	0	+0·8	+0·8	56,000	0	0	+0·4	0	0	0
27	F.4'5'6'																			0	28,000	0	+0·4	0	0	56,000	+0·8	+0·8	0	+0·4	0	0
28	E.55'																			+1	0	0	+1	-1	-1	0	-1	-1	+1	+1	0	0
29	F.65																								+0·4	28,000	0	0	+0·8	0	0	0
30	F.6'5'																								0	28,000	0	+0·4	0	+0·8	0	0

Table 500.21 Numerical matrix for the effect of constant temperature distribution in a column of a symmetrical 6-storey frame.

EQN. No.	1	2	3	4	5	6	7	8	9	10	11	12	13	14	15	16	17	18	19	20	21	22	23	24	25	26	27	28	29	30	LOAD
REF. JT.	0		0'	1			1'		2			2'		3			3'		4			4'		5			5'		6	6'	VECTOR
No. REF. EQN.	m_{01}	Δ_{0x}	$m_{01'}$	m_{10}	m_{12}	Δ_{1x}	$m_{1'0'}$	$m_{1'2'}$	m_{21}	m_{23}	Δ_{2x}	$m_{2'1'}$	$m_{2'3'}$	m_{32}	m_{34}	Δ_{3x}	$m_{3'2'}$	$m_{3'4'}$	m_{43}	m_{45}	Δ_{4x}	$m_{4'3'}$	$m_{4'5'}$	m_{54}	m_{52}	Δ_{5x}	$m_{5'4'}$	$m_{5'6'}$	m_{65}	$m_{6'5'}$	
1 F.100′	$-2(r_1+1)$	$-R_L/_L$	$+1$	$-r_1$	0	$R_L/_L$	0																								$-6Cn/_L$
2 F.1′0′0	$+1$	$-R_L/_L$	$-2(r_1+1)$	2	0	$R_L/_L$	r_1																								0
3 E.00′	-1	0	-1	$+1$	0	0	-1																								$6C(1-n)/_L$
4 F.211′	0	0	0	$+2$	$-2(r_1+1)$	$-R_L/_L$	$+1$	$+1$	$-r_1$	0	$R_L/_L$	0																			$6C(1-n)/_L$
5 F.2′1′1	0	0	0	-1	$+1$	$-R_L/_L$	-2	$-2(r_1+1)$	0	0	$R_L/_L$	$-r_1$																			0
6 F.012	r_1	$-R_L/_L$	0	$2r_1$	$2r_1$	$2R_L/_L$	0	0	$+r_1$	0	$-R_L/_L$	0																			0
7 F.0′1′2′	0	$-R_L/_L$	$+r_1$	0	0	$2R_L/_L$	$-2r_1$	$+2r_1$	0	0	$-R_L/_L$	$+r_1$																			0
8 E.11′	$+1$	0	$+1$	-1	-1	0	$+1$	-1	$+1$	0	0	$+1$																			$6C(2-n)/_L$
9 F.322′					0	0	0	0	$+2$	$-2(r_1+1)$	$-R_L/_L$	-1	$+1$	$-r_1$	0	$R_L/_L$	0															$6C(2-n)/_L$
10 F.3′2′2					0	0	0	0	-1	$+1$	$-R_L/_L$	$+2$	$-2(r_1+1)$	0	0	$R_L/_L$	$-r_1$															$6C(2-n)/_L$
11 F.123					$+r_1$	$-R_L/_L$	0	0	$+2r_1$	$+2r_1$	$+2R_L/_L$	0	0	$+r_1$	0	$-R_L/_L$	0															0
12 F.1′2′3′					0	$-R_L/_L$	0	$+r_1$	0	0	$+2R_L/_L$	$+2r_1$	$+2r_1$	0	0	$-R_L/_L$	$+r_1$															0
13 E.22′					$+1$	0	0	$+1$	-1	-1	0	-1	-1	$+1$	0	0	$+1$															$6C(3-n)/_L$
14 F.433′										0	0	0	0	$+2$	$-2(r_1+1)$	$-R_L/_L$	-1	$+1$	$-r_1$	0	$R_L/_L$	0									$6C(3-n)/_L$
15 F.4′3′3										0	0	0	0	-1	$+1$	$-R_L/_L$	$+2$	$-2(r_1+1)$	0	0	$R_L/_L$	$-r_1$									$6C(3-n)/_L$
16 F.234										$+r_1$	$-R_L/_L$	0	0	$+2r_1$	$+2r_1$	$+2R_L/_L$	0	0	$+r_1$	0	$-R_L/_L$	0									0
17 F.2′3′4′										0	$-R_L/_L$	0	$+r_1$	0	0	$+2R_L/_L$	$+2r_1$	$+2r_1$	0	0	$-R_L/_L$	$+r_1$									0
18 E.33′										$+1$	0	0	$+1$	-1	-1	0	-1	-1	$+1$	0	0	$+1$									0
19 F.544′															0	0	0	0	$+2$	$-2(r_1+1)$	$-R_L/_L$	-1	$+1$	$-r_1$	0	$R_L/_L$	0				$6C(4-n)/_L$
20 F.5′4′4															0	0	0	0	-1	$+1$	$-R_L/_L$	$+2$	$-2(r_1+1)$	0	0	$R_L/_L$	$-r_1$				$6C(5-n)/_L$
21 F.345															$+r_1$	$-R_L/_L$	0	0	$+2r_1$	$+2r_1$	$+2R_L/_L$	0	0	$+r_1$	0	$-R_L/_L$	0	-			0
22 F.3′4′5′															0	$-R_L/_L$	0	$+r_1$	0	0	$+2R_L/_L$	$+2r_1$	$+2r_1$	0	0	$-R_L/_L$	$+r_1$				0
23 E.44′															$+1$	0	0	$+1$	-1	-1	0	-1	-1	$+1$	0	0	$+1$				0
24 F.655′																				0	0	0	0	$+2$	$-2(r_1+1)$	$-R_L/_L$	-1	$+1$	$-r_1$	0	$6C(5-n)/_L$
25 F.6′5′5																				0	0	0	0	-1	$+1$	$-R_L/_L$	$+2$	$-2(r_1+1)$		$-r_1$	$6C(5-n)/_L$
26 F.456																				$+r_1$	$-R_L/_L$	0	0	$+2r_1$	$+2r_1$	$+2R_L/_L$	0	0	$+r_1$	0	0
27 F.4′5′6′																				0	$-R_L/_L$	0	$+r_1$	0	0	$+2R_L/_L$	$+2r_1$	$+2r_1$	0	$+r_1$	0
28 E.55′																				$+1$	0	0	$+1$	-1	-1	0	-1	-1	$+1$	$+1$	0
29 F.65																									$+r_1$	$-R_L/_L$	0	0	$+2r_1$	0	0
30 F.6′5′																									0	$-R_L/_L$	0	$+r_1$	0	$+2r_1$	0

Table: 500.20 General matrix for the effect of constant temperature distribution in a column of a symmetrical 6-storey frame.

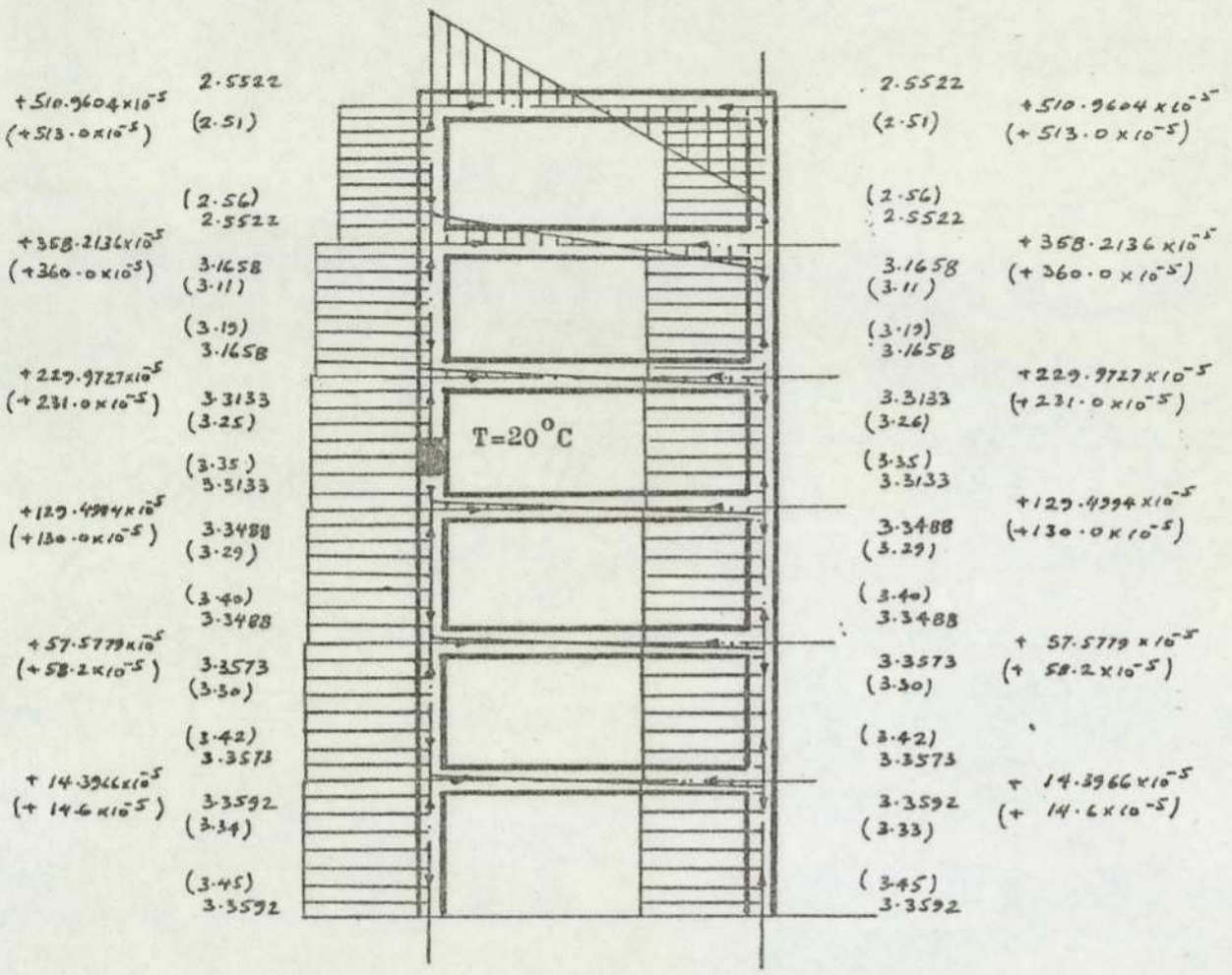

Fig. 5.0633 Shows the results of the effect of constant temperature distribution in a column

Unbracketed figures.....show results by the force–displacement method

Bracketed figures.....show results by the stiffness method

5.06.2 The effect of linear temperature distribution in a column

(a) Analysis using force-displacement method

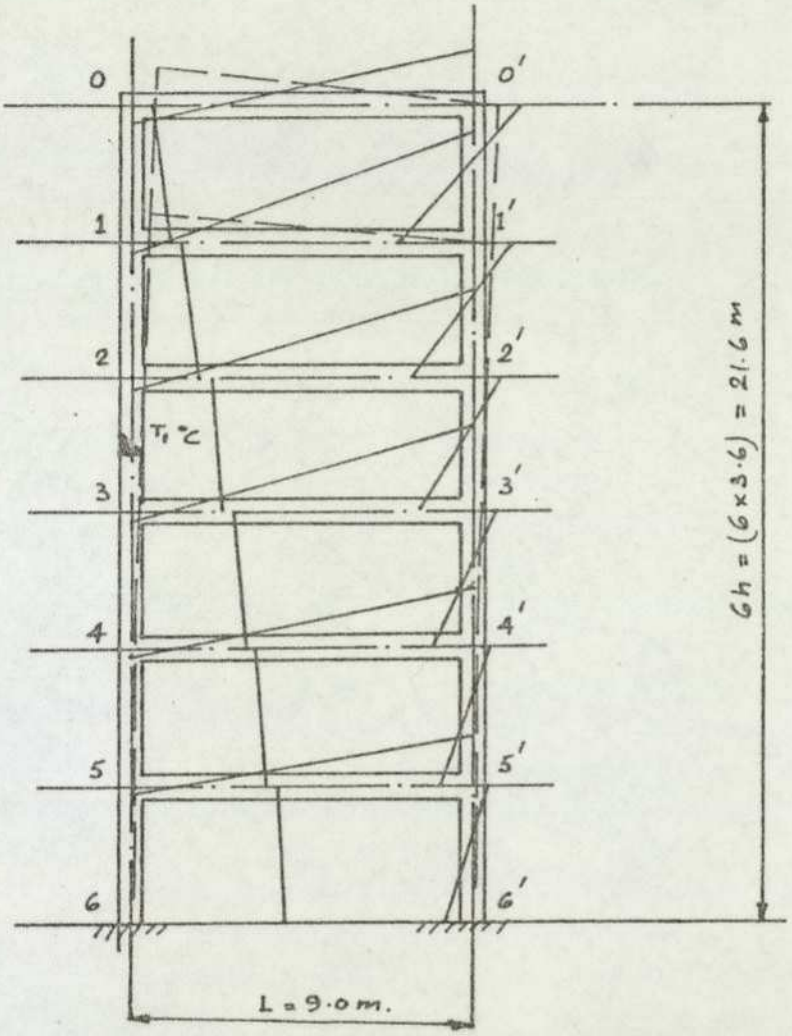

Fig. 5.0641 The effect of linear temperature distribution in the column of a 6-storey symmetrical frame showing assumed bending moments for the setting up of the matrix.

Although the frame is symmetrical, the applied force i.e. the action of heat on one column, is not symmetrical. It is therefore necessary to analyse the whole frame.

Further, since the assumed bending moment diagram is similar to the one used for the shear wall model frame, the equations of compatibility of deformations and the equilibrium of forces will also be of similar form. Therefore, it is not considered necessary to show the derivations of the equations again. However, the numerical values of the elements of the matrix will be different as the properties of the frame are different and for this reason, the complete numerical matrix is shown in Table: 500.23. The results of the abovementioned matrix are shown in fig. 5.0643.

(b) Analysis using the stiffness method

The force and bending moment to be applied in this case are as follows:-

$$P = EAc\alpha\frac{T1}{2} = EAc\alpha Tav = 28 \times 10^6 \times 0.18 \times 0.00001 \times 20/2$$

$$= 504 \text{ KN}$$

$$M = \alpha T1E\frac{Ic}{d} = 0.00001 \times 20 \times 28 \times 10^6 \times \frac{0.18}{0.6}$$

$$= 50.4 \text{ KN/m}$$

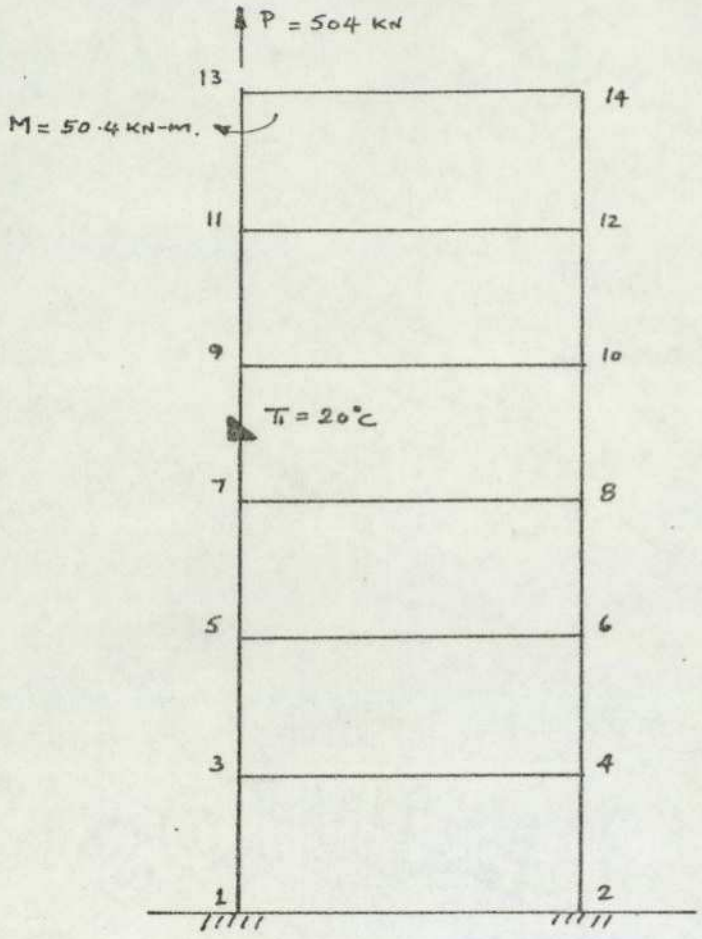

Fig.5.0642 The effect of linear temperature distribution in a column of a 6-storey symmetrical frame and analysed by the stiffness method.

The results of the effect of linear temperature distribution in the column of a symmetrical frame and analysed by the stiffness method are shown in fig. 5.0643.

EQ. No.		1	2	3	4	5	6	7	8	9	10	11	12	13	14	15	16	17	18	19	20	21	22	23	24	25	26	27	28	29	30	LOAD VECTOR
	REF. JT.	0		0'	1			1'			2		2'		3			3'		4			4'		5			5'		6	6'	
No.	REF. EQN	m_{01}	Δ_{0x}	$m_{01'}$	m_{10}	m_{12}	Δ_{1x}	$m_{1'0'}$	$m_{1'2'}$	m_{21}	m_{23}	Δ_{2x}	$m_{2'1'}$	$m_{2'3'}$	m_{32}	m_{34}	Δ_{3x}	$m_{3'2'}$	$m_{3'4'}$	m_{43}	m_{45}	Δ_{4x}	$m_{4'3'}$	$m_{4'5'}$	m_{54}	m_{52}	Δ_{5x}	$m_{5'4'}$	$m_{5'6'}$	m_{65}	$m_{6'5'}$	
1	F.100'	$2(r_1+1)$	$-R_4/\ell$	-1	r_1	0	R_4/ℓ	0																								$3c(\frac{1}{2}-\frac{n}{L})$
2	F.1'0'0	-1	$-R_4/\ell$	$2(r_1+1)$	0	0	R_4/ℓ	$-r_1$																								$-3cn/L$
3	E.00'	1	0	1	-1	0	0	1																								0
4	F.211'	0	0	0	-2	$2(r_1+1)$	$-R_4/\ell$	-1	-1	r_1	0	R_4/ℓ	0																			$\frac{3c}{2}+\frac{3c}{L}(1-n)$
5	F.2'1'1	0	0	0	1	-1	$-R_4/\ell$	2	$2(r_1+1)$	0	0	R_4/ℓ	$-r_1$																			$3c(1-n)/L$
6	F.012	r_1	R_4/ℓ	0	$2r_1$	$2r_1$	$-2R_4/\ell$	0	0	r_1	0	R_4/ℓ	0																			$6c/d$
7	F.0'1'2'	0	$-R_4/\ell$	$-r_1$	0	0	$2R_4/\ell$	$2r_2$	$-2r_1$	0	0	$-R_4/\ell$	r_1																			0
8	E.11'	1	0	1	-1	-1	0	1	-1	1	0	0	-1																			0
9	F.322'					0	0	0	0	-2	$2(r_1+1)$	$-R_4/\ell$	-1	-1	r_1	0	R_4/ℓ	0															$\frac{3c}{2}+\frac{3c}{L}(2-n)$
10	F.3'2'2					0	0	0	0	1	-1	$-R_4/\ell$	2	$2(r_1+1)$	0	0	R_4/ℓ	$-r_1$															$3c(2-n)/L$
11	F.123					r_1	R_4/ℓ	0	0	$2r_1$	$2r_1$	$-2R_4/\ell$	0	0	r_1	0	R_4/ℓ	0															$6c/d$
12	F.1'2'3'					0	$-R_4/\ell$	0	$-r_1$	0	0	$2R_4/\ell$	$2r_1$	$-2r_1$	0	0	$-R_4/\ell$	r_1															0
13	E.22'					1	0	0	1	-1	-1	0	1	-1	1	0	0	-1															0
14	F.433'										0	0	0	0	-2	$2(r_1+1)$	$-R_4/\ell$	-1	-1	r_1	0	R_4/ℓ	0									$\frac{3c}{2}+\frac{3c}{L}(3-n)$
15	F.4'3'3										0	0	0	0	1	-1	$-R_4/\ell$	2	$2(r_1+1)$	0	0	R_4/ℓ	$-r_1$									$3c(3-n)/L$
16	F.234										r_1	R_4/ℓ	0	0	$2r_1$	$2r_1$	$-2R_4/\ell$	0	0	r_1	0	R_4/ℓ	0									$6c/d$
17	F.2'3'4'										0	$-R_4/\ell$	0	$-r_1$	0	0	$2R_4/\ell$	$2r_1$	$-2r_1$	0	0	$-R_4/\ell$	r_1									0
18	E.33'										1	0	0	1	-1	-1	0	1	-1	1	0	0	-1									0
19	F.544'															0	0	0	0	-2	$2(r_1+1)$	$-R_4/\ell$	-1	-1	r_1	0	R_4/ℓ	0				$\frac{3c}{2}+\frac{3c}{L}(4-n)$
20	F.5'4'4															0	0	0	0	1	-1	$-R_4/\ell$	2	$2(r_1+1)$	0	0	R_4/ℓ	$-r_1$				$3c(4-n)/L$
21	F.345															r_1	R_4/ℓ	0	0	$2r_1$	$2r_1$	$-2R_4/\ell$	0	0	r_1	0	R_4/ℓ	0				$6c/d$
22	F.3'4'5'															0	$-R_4/\ell$	0	$-r_1$	0	0	$2R_4/\ell$	$2r_1$	$-2r_1$	0	0	$-R_4/\ell$	r_1				0
23	E.44'															1	0	0	1	-1	-1	0	1	-1	1	0	0	-1				0
24	F.655																			0	0	0	0	-2	$2(r_1+1)$	$-R_4/\ell$	-1	-1	r_1	0	$\frac{3c}{2}+\frac{3c}{L}(5-n)$
25	F.5'5'5																			0	0	0	0	1	-1	$-R_4/\ell$	2	$2(r_1+1)$	0	$-r_1$	$3c(5-n)/L$
26	F.456																			r_1	R_4/ℓ	0	0	$2r_1$	$2r_1$	$-2R_4/\ell$	0	0	r_1	0	$6c/d$
27	F.4'5'6'																			0	$-R_4/\ell$	0	$-r_1$	0	0	$2R_4/\ell$	$2r_1$	$-2r_1$	0	r_1	0
28	E.55'																			1	0	0	1	-1	-1	0	-1	1	-1	0	
29	F.65																								r_1	R_4/ℓ	0	0	$2r_1$	0	$3c/d$
30	F.6'5'																								0	$-R_4/\ell$	0	$-r_1$	0	$2r_1$	0	

Table: 500.22 General matrix for the effect of linear temperature distribution in a column of a symmetrical 6-storey frame.

EQ. No.		1	2	3	4	5	6	7	8	9	10	11	12	13	14	15	16	17	18	19	20	21	22	23	24	25	26	27	28	29	30	LOAD VECTOR
	REF. JT.	0		0'	1			1'			2		2'		3			3'		4			4'		5			5'		6	6'	
No.	REF. EQN	M01	Δ0x	M0'1'	M10	M12	Δ1x	M1'0'	M1'2'	M21	M23	Δ2x	M2'1'	M2'3'	M32	M34	Δ3x	M3'2'	M3'4'	M43	M45	Δ4x	M4'3'	M4'5'	M54	M52	Δ5x	M54'	M5'4'	M65	M6'5'	
1	F.100'	2·8	-28,000	-1	0·4	0	28000	0																								36·288
2	F.1'0'8	-1	28000	2·8	0	0	28000	-0·4																								-24·192
3	E.00'	1	0	1	-1	0	0	1																								0
4	F.211'	0	0	0	-2	2·8	-28000	-1	1	0·4	0	28000	0																			40·320
5	F.2'1'1	0	0	0	1	-1	28000	2	-2·8	0	0	-28000	-0·4																			-20·160
6	F.012	0·4	-28000	0	0·8	0·8	-56000	0	0	0·4	0	28000	0																			120·960
7	F.0'1'2'	0	28000	-0·4	0	0	56000	0·8	0·8	0	0	-28000	0·4																			0
8	E.11'	1	0	1	-1	-1	0	1	1	1	0	0	-1																			0
9	F.322'					0	0	0	0	-2	2·8	-28000	-1	1	0·4	0	28000	0														44·352
10	F.3'2'2					0	0	0	0	1	-1	-28000	2	-2·8	0	0	28000	-0·4														-14·128
11	F.123					0·4	28000	0	0	0·8	0·8	-56000	0	0	0·4	0	56000	0														123·960
12	F.1'2'3'					0	-28000	0	0·4	0	0	56000	0·8	0·8	0	0	-28000	0·4														0
13	E.22'					1	0	0	-1	-1	-1	0	1	1	1	0	0	-1														0
14	F.433'										0	0	0	0	-2	2·8	-28000	-1	1	0·4	0	28000	0									48·384
15	F.4'3'3										0	0	0	0	1	-1	28000	2	-2·8	0	0	28000	-0·4									-12·096
16	F.234										0·4	28000	0	0	0·8	0·8	56000	0	0	0·4	0	28000	0									120·960
17	F.2'3'4'										0	-28000	0	0·4	0	0	56000	0·8	0·8	0	0	28000	0·4									0
18	E.33'										1	0	0	-1	-1	-1	0	1	1	1	0	0	-1									0
19	F.544'															0	0	0	0	-2	2·8	-28000	-1	1	0·4	0	28000	0				52·416
20	F.5'4'4															0	0	0	0	1	-1	28000	2	-2·8	0	0	28000	-0·4				-8·064
21	F.345															0·4	28000	0	0	0·8	0·8	-56000	0	0	0·4	0	28000	0				120·960
22	F.3'4'5'															0	-28000	0	0·4	0	0	56000	0·8	0·8	0	0	-28000	0·4				0
23	E.44'															1	0	0	-1	-1	-1	0	1	1	1	0	0	-1				0
24	F.655'																				0	0	0	0	-2	2·8	-28000	-1	1	0·4	0	56·448
25	F.6'5'5																				0	0	0	0	1	-1	28000	2	-2·8	0	-0·4	-4·032
26	F.456																				0·4	28000	0	0	0·8	0·8	56000	0	0	0·4	0	120·960
27	F.4'5'6'																				0	-28000	0	0·4	0	0	56000	0·8	0·8	0	0·4	0
28	E.55'																				-1	0	0	1	1	1	0	-1	-1	-1	1	0
29	F.65																									0·4	28000	0	0	0·8	0	60·480
30	F.6'5'																									0	-28000	0	0·4	0	0·8	0

Table: 500.23 Numerical matrix for the effect of linear temperature distribution in a column of a symmetrical 6-storey frame.

Horiz. Deflect. (mm)	Bend. Momts. (KN–m)	Bend. Momts. (KN–m)	Horiz. Deflect. (mm)

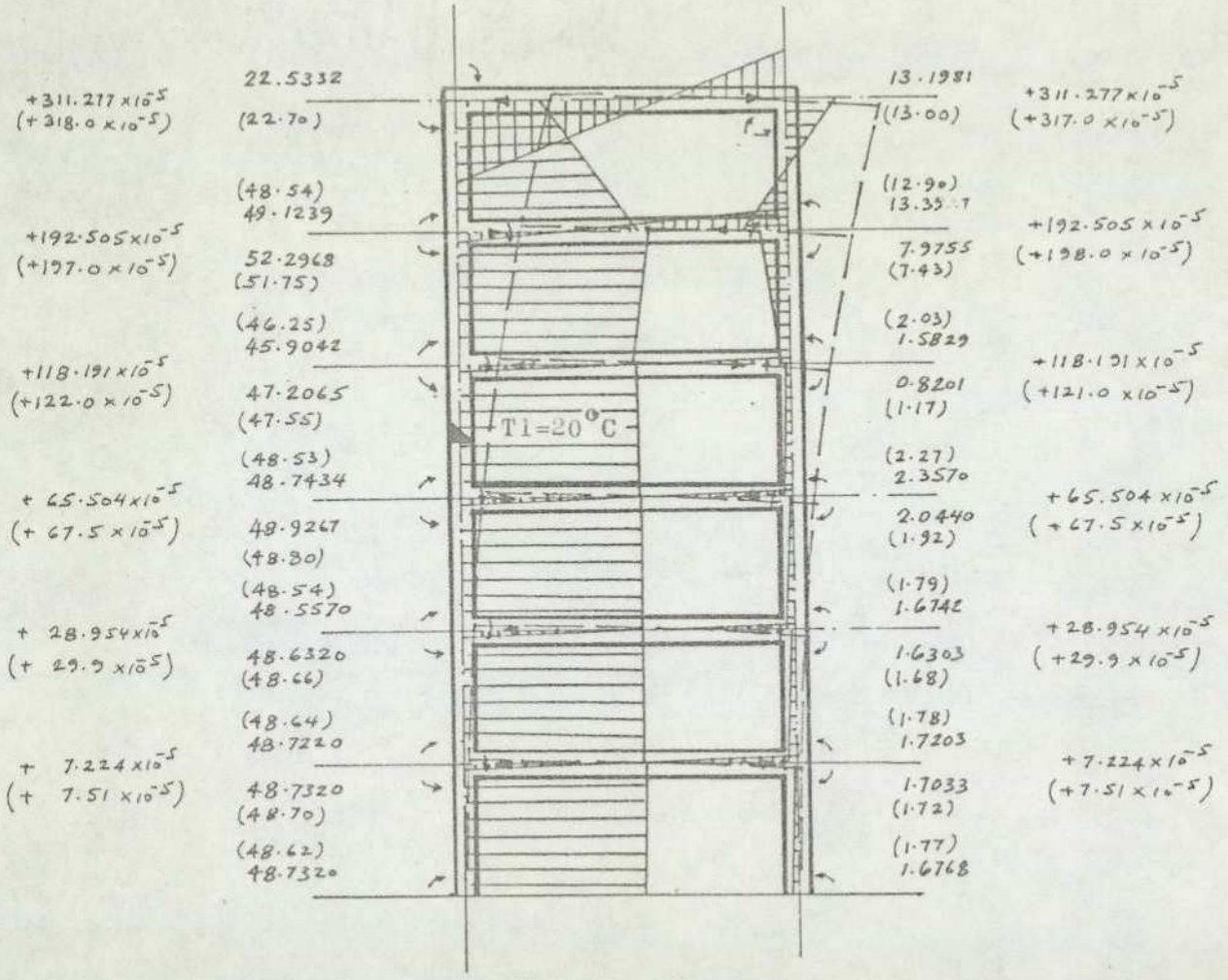

Fig. 5.0643 Shows the results of the effect of linear temperature distribution in a column

Unbracketed figures.....show results by the force-displacement method

Bracketed figures.....show results by the stiffness method

5.06.5 Discussion of results of analysis of a symmetrical 6-storey frame

The multi-storey frame of practical proportions was analysed in order to assess the magnitude and distribution of stresses that can arise in real structures. As for the shear wall frame, constant and linear temperature distributions in the roof beam and constant and linear temperature distributions in one column were analysed. In each case, the magnitude of temperature differential was assumed to be 20 °C.

The effect of constant temperature distribution in the roof beam shows a maximum column bending moment of 20.3 KN - m at the level of floor below the roof, and a maximum beam bending moment of 8.6 KN - m in the roof. The maximum horizontal deflection of 0.89 mm. also occurs at roof level. The distribution of stresses are similar to the shear wall frame.

The effect of linear temperature distribution in the roof beam shows a maximum bending moment of 36.4 KN - m in the column and beam, both occuring at the roof level, which is an increase of about 75% over the constant temperature case. However, the maximum horizontal deflection now is 0.46 mm., i.e. a decrease of about 48%.

The effect of constant temperature distribution in a column of the frame shows the bending moments to be skew symmetrical. On one column the tension occurs entirely on the outside while on the other tension occurs entirely on the inside. The beams show tension on top on one half while the other half shows tension at the bottom. Maximum column bending moments of 3.36 KN - m occur at the lowest storey level and the maximum beam bending moments of 3.55 KN - m occur at the roof. The maximum horizontal deflection at roof level is 5.11 mm.

The results of linear temperature distribution in a column show very large bending moments (maximum 52.30 KN - m) in the column directly exposed to the temperature change. The far side column shows bending moments greatly reduced except at the uppermost level. It is interesting to note that the bending moments in the exposed column are of reversed sign i.e. causing tension on the inside when compared to the case of constant temperature. In the beams, the maximum bending moments occur in the roof. The maximum horizontal deflection in this case is 3.11 mm.

Furthermore, bending moments are considerably greater in each case of linear temperature change, and the horizontal deflections are greater in the case of constant temperature changes.

5.07 ANALYSIS TO DETERMINE THE SECONDARY EFFECT OF AXIAL DEFORMATIONS

5.07.1 Linear temperature distribution in a column of a shear wall frame

(a) Analysis using the force-displacement method

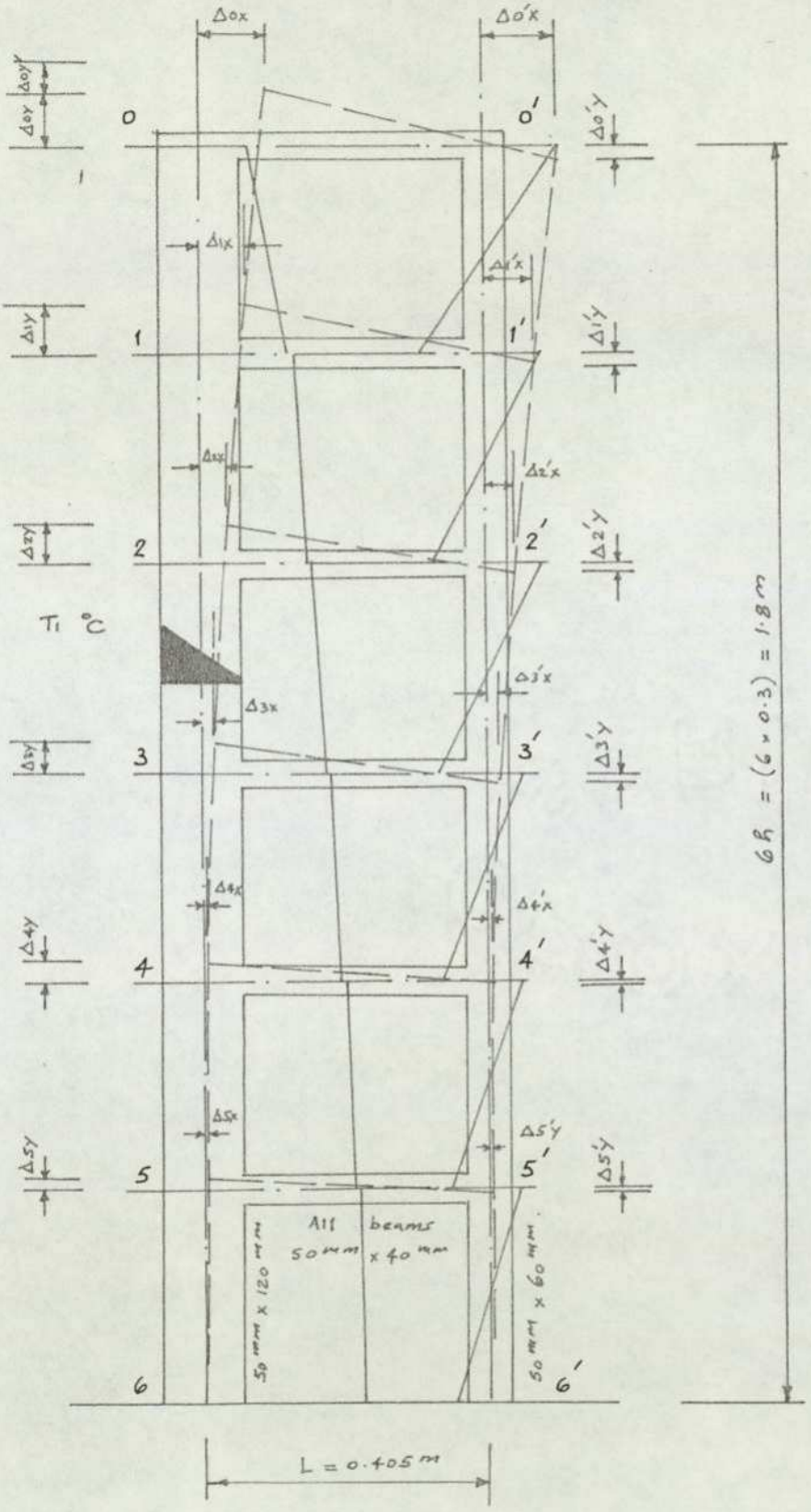

Fig.5.0711 The effect of linear temperature distribution in a column of a shear wall frame showing assumed bending moments and deformations for the setting up of the matrix.

In the following study, the effects of axial deformations in the analysis of thermal stresses for a shear wall shown in fig.5.0711 are investigated. This structure contains 24 unknown bending moments, 24 displacements and 18 axial forces. Therefore, 66 independent conditions of compatibility of deformations and equilibrium of forces are required in the matrix.

The following symbols are used to denote displacements:-

Δoy, $\Delta 1y$, ..., $\Delta o'y$, $\Delta 1'y$, --- etc. Vertical displacements at levels o, 1, o' ... etc.

$\Delta oy'$, $\Delta 1y'$, ..., $\Delta o'y'$, $\Delta 1'y'$ --- etc. Suppressed vertical displacements at levels o, 1, o', etc.

Δox, $\Delta 1x$, ..., $\Delta o'x$, $\Delta 1'x$, --- etc. Horizontal displacements at levels o, 1, o', etc.

Denoting $\Delta oy + \Delta oy' = \frac{1}{2} \alpha T_1 nh$ where n = no. of storeys

$\Delta 1y + \Delta 1y' = \frac{1}{2} \alpha T_1 (n-1)h$

`etc.

Referring to Fig. 5.0711 the conditions of compatibility of deformations and equilibrium of forces can be written as follows:-

1. F.100' $$m1o\frac{h}{6EIc1} + mo1\left(\frac{h}{3EIc1} + \frac{L}{3EIb}\right) - mo'1'\frac{L}{6EIb} = \left(\frac{\Delta ox - \Delta 1x}{h} + \theta o1 - \frac{\delta oo'}{L}\right) - \frac{\delta no1 + \delta no'1'}{L}$$

or $$r1\, m1o + (2r1 + 2 + B+Q)\, mo1 - (1-B-Q)\, mo'1' - R\Delta ox\frac{L}{h} + R\Delta 1x\frac{L}{h} = 3c\left(\frac{1}{d} - \frac{n}{L}\right)$$

NOTE: All symbols used are specified at the end of this section.

2. F.012 $$-mo1 - m1o\frac{h}{3EIc1} - m12\frac{h}{3EIc1} - m21\frac{h}{6EIc1} = \left(\frac{\Delta o - \Delta 1}{h} - \theta 1o\right) - \left(\frac{\Delta 1x - \Delta 2x}{h} + \theta 12\right)$$

or $$-r1mo1 - 2r1m1o - 2r1m12 - r1m21 - R\,\Delta ox\frac{L}{h} + 2R\,\Delta 1x\frac{L}{h} - R\Delta 2x\frac{L}{h} = -\frac{6c}{d}$$

3. F.211' $$m21\,\frac{h}{6EIc1} + m12\,\frac{h}{3EIc1} + (m12 - m1o)\,\frac{L}{3EIb} - (m1'o' + m1'2')\,\frac{L}{6EIb} = \left(\frac{\Delta 1x - \Delta 2x}{h} + \theta 12 - \frac{\delta 11'}{L}\right) - \frac{\delta no1 + \delta no'1'}{L} - \frac{\delta n12 + \delta n1'2'}{L}$$

or $$r1m21 + (2r1 + 2 + B + Q)\,m12 - (2 + B + Q)\,m1o - (1 - B - Q)\,m1'o' - (1-B-Q)\,m1'2' + (B+Q)\,mo1 + (B+Q)\,mo'1' - R\Delta 1x\,\frac{L}{h} + R\Delta 2x\,\frac{L}{h} = \frac{3c}{d} + \frac{3c}{L}(1-n)$$

Similarly

4. F.123 $$r1m12 + 2r1m21 + 2r1m23 + r1m32 + R\Delta 1x\,\frac{L}{h} + R\Delta 3x\,\frac{L}{h} - 2R\Delta 2\,\frac{L}{h} = \frac{6c}{d}$$

5. F.322' $$(B+Q)\,mo1 + (B+Q)\,mo'1' - (B+Q)\,m1o + (B+Q)\,m1'o' + (B+Q)\,m12 + (B+Q)\,m1'2' - (2+B+Q)\,m21 - (1-B-Q)\,m2'1' + (2r1 + 2 + B+Q)\,m23 - (1-B-Q)\,m2'3' + r1m32 + R\Delta 3x\,\frac{L}{h} - R\Delta 2x\,\frac{L}{h} = \frac{3c}{d} + \frac{3c}{L}(2-n)$$

6. F.234 $$r1m23 + 2r1m32 + 2r1m34 + r1m43 + R\Delta 2x\,\frac{L}{h} + R\Delta 4x\,\frac{L}{h} - 2R\Delta 3x\,\frac{L}{h} = \frac{6c}{d}$$

7. F.433' $$(B+Q)\,mo1 + (B+Q)\,mo'1' - (B+Q)\,m1o + (B+Q)\,m1'o' + (B+Q)\,m12 + (B+Q)\,m1'2' - (B+Q)\,m21 + (B+Q)\,m2'1' + (B+Q)\,m23 + (B+Q)\,m2'3' - (2+B+Q)\,m32 - (1-B-Q)\,m3'2' + (2r1+2+B+Q)\,m34 - (1-B-Q)\,m3'4' + r1m43 + R\Delta 4x\,\frac{L}{h} - R\Delta 3x\,\frac{L}{h} = \frac{3c}{d} + \frac{3c}{L}(3-n)$$

8. F.345 $$r1m34 + 2r1m43 + 2r1m45 + r1m54 + R\Delta 3x\,\frac{L}{h} + R\Delta 5x\,\frac{L}{h} - 2R\Delta 3x\,\frac{L}{h} = \frac{6c}{d}$$

9. F.544' $$(B+Q)\,mo1 + (B+Q)\,mo'1' - (B+Q)\,m1o + (B+Q)\,m1'o' + (B+Q)\,m12 + (B+Q)\,m1'2' - (B+Q)\,m21 + (B+Q)\,m2'1' + (B+Q)\,m23 + (B+Q)\,m2'3' - (B+Q)\,m32 + (B+Q)\,m3'2' + (B+Q)\,m34 + (B+Q)\,m3'4' - (2+B+Q)\,m43 - (1-B-Q)\,m4'3' + (2r1 +2+B+Q)\,m45 - (1-B-Q)\,m4'5' + r1m54 + R\Delta 5x\,\frac{L}{h} - R\Delta 4x\,\frac{L}{h} = \frac{3c}{d} + \frac{3c}{L}(4-n)$$

10. F.456 $$r1m45 + 2r1m54 + 2r1m56 + r1m65 + R\Delta 4x\,\frac{L}{h} - 2R\Delta 5x\,\frac{L}{h} = \frac{6c}{d}$$

11. F.655' $(B+Q)\ mo1 + (B+Q)\ mo'1' - (B+Q)\ m1o + (B+Q)\ m1'o' + (B+Q)\ m12 + (B+Q)\ m1'2' - (B+Q)\ m21 + (B+Q)\ m2'1' + (B+Q)\ m23 + (B+Q)\ m2'3' - (B+Q)\ m32 + (B+Q)\ m3'2' + (B+Q)\ m34 + (B+Q)\ m3'4' - (B+Q)\ m43 + (B+Q)\ m4'3' + (B+Q)\ m45 + (B+Q)\ m4'5' - (2+B+Q)\ m54 - (1-B-Q)\ m5'4' + (2r1+2+B+Q)\ m56 - (1-B-Q)\ m5'6' + rm65 - R\Delta5 \times \frac{L}{h} = \frac{3c}{d} + \frac{3c}{L}(5-n)$

12. F.56 $r1m56 + 2r1\ m65 + R\Delta5 \times \frac{L}{h} = \frac{3c}{d}$

13. F.1'o'o $-r2\ m1'o' + (2r2+2+B+Q)\ mo'1' - (1-B-Q)\ mo1 + R\Delta1' \times \frac{L}{h} - R\Delta o' \times \frac{L}{h} = \frac{-3c}{L}$

14. F.o'1'2' $-r2\ mo'1' + 2r2\ m1'o' - 2r2\ m1'2' + r2\ m2'1' + 2R\Delta1' \times \frac{L}{h} - R\Delta o' \times \frac{L}{h} = o$

15. F.2'1'1 $(B+Q)\ mo'1' + (B+Q)\ mo1 + (2+B+Q)\ m1'o' + (1-B-Q)\ m1o + (2r2+2+B+Q)\ m1'2' - (1-B-Q)\ m12 - r2\ m2'1' + R\Delta2' \times \frac{L}{h} - R\Delta1' \times \frac{L}{h} = \frac{3c}{L}(1-n)$

16. F.1'2'3' $-r2\ m1'2' + 2r2\ m2'1' - 2r2\ m2'3' + r2\ m3'2' + 2R\Delta2' \times \frac{L}{h} - R\Delta1' \times \frac{L}{h} - R\Delta3' \times \frac{L}{h} = o$

17. F.3'2'2 $(B+Q)\ mo'1' + (B+Q)\ mo1 + (B+Q)\ m1'o' - (B+Q)\ m1o + (B+Q)\ m1'2' + (B+Q)\ m12 + (2+B+Q)\ m2'1' + (1-B-Q)\ m21 + (2r2+2+B+Q)\ m2'3' - (1-B-Q)\ m23 - r2\ m3'2' + R\Delta3' \times \frac{L}{h} - R\Delta2' \times \frac{L}{h} = \frac{3c}{L}(2-n)$

18. F.2'3'4' $-r2\ m2'3' + 2r2\ m3'2' - 2r2\ m3'4' + r2\ m4'3' + 2R\Delta3' \times \frac{L}{h} - R\Delta2' \times \frac{L}{h} - R\Delta4' \times \frac{L}{h} = o$

19. F.4'3'3 $(B+Q)\ mo'1' + (B+Q)\ mo1 + (B+Q)\ m1'o' - (B+Q)\ m1o + (B+Q)\ m1'2' + (B+Q)\ m12 + (B+Q)\ m2'1' - (B+Q)\ m21 + (B+Q)\ m2'3' + (B+Q)\ m23 + (2+B+Q)\ m3'2' + (1-B-Q)\ m34 + (2r2+2+B+Q)\ m3'4' - (1-B-Q)\ m34 - r2\ m4'3' + R\Delta 4' \times \frac{L}{h} - R\Delta 3' \times \frac{L}{h} = \frac{3c}{L}(3-n)$

20. F.3'4'5' $-r2\ m3'4' + 2r2\ m4'3' - 2r2\ m4'5' + r2\ m5'4' + 2R\Delta 4' \times \frac{L}{h} - R\Delta 3' \times \frac{L}{h} - R\Delta 5' \times \frac{L}{h} = o$

21. F.5'4'4 $(B+Q)\ mo'1' + (B+Q)\ mo1 + (B+Q)\ m1'o' - (B+Q)\ m1o + (B+Q)\ m1'2' + (B+Q)\ m12 + (B+Q)\ m2'1' - (B+Q)\ m21 + (B+Q)\ m2'3' + (B+Q)\ m23 + (B+Q)\ m3'2' - (B+Q)\ m32 + (B+Q)\ m3'4' + (B+Q)\ m34 + (2+B+Q)\ m4'3' + (1-B-Q)\ m43 + (2r2+2+B+Q)\ m4'5' - (1-B-Q)\ m45 - r2\ m5'4' + R\Delta 5' \times \frac{L}{h} - R\Delta 4' \times \frac{L}{h} = \frac{3c}{L}(4-n)$

22. F.4'5'6' $-r2\ m4'5' + 2r2\ m5'4' - 2r2\ m5'6' + r2\ m6'5' + 2R\Delta 5' \times \frac{L}{h} - R\Delta 4' \times \frac{L}{h} = o$

23. F.65'5 $(B+Q)\ mo'1' + (B+Q)\ mo1 + (B+Q)\ m1'o' - (B+Q)\ m1o + (B+Q)\ m1'2' + (B+Q)\ m12 + (B+Q)\ m2'1' - (B+Q)\ m21 + (B+Q\ m2'3' + (B+Q)\ m23 + (B+Q)\ m3'2' - (B+Q)\ m32 + (B+Q)\ m3'4' + (B+Q)\ m34 + (B+Q)\ m4'3' - (B+Q)\ m43 + (B+Q)\ m4'5' + (B+Q)\ m45 + (2+B+Q)\ m5'4' + (1-B-Q)\ m54 + (2r2+2+B+Q)\ m5'6' - (1-B-Q)\ m56 - r2\ m6'5' - R\Delta 5' \times \frac{L}{h} = \frac{3c}{L}(5-n)$

24. F.5'6' $-r2\ m5'6' + 2r2\ m6'5' - R\Delta 5' \times \frac{L}{h} = o$

25. C.oo' $\Delta ox - \Delta o'x = \frac{Noo'\ Loo'}{Aoo'\ Eoo'}$

or $r\Delta ox - r\Delta o'x - Noo'\ Soo' = o$ since $\Delta oy' = \frac{\alpha T_i hn}{2} - \Delta oy$

and $\Delta 1y' = \frac{\alpha T_i h}{2}(n-1) - \Delta 1y$

Similarly

26. C.11' $r\Delta 1x - r\Delta 1'x - N11'\ S11' = o$

27. C.22' $r\Delta 2x - r\Delta 2'x - N22'\ S22' = o$

28. C.33' $r\Delta 3x - r\Delta 3'x - N33'\ S33' = o$

29. C.44' $r\Delta 4x - r\Delta 4'x - N44'\ S44' = o$

30. C.55' $r\Delta 5x - r\Delta 5'x - N55'\ S55' = o$

31. C.1o $r\Delta oy' - r\Delta 1y' - N1o\ S1o = o$

or $r\Delta oy - r\Delta 1y + N1o\ S1o = \frac{r \propto T_h}{2}$ since $\Delta oy + \Delta oy' = \frac{1}{2} \propto T_{nh}$ ---- etc.

32. C.21 $r\Delta 1y' - r\Delta 2y' - N21\ S21 = o$

or $r\Delta 1y - r\Delta 2y + N21\ S21 = \frac{r \propto T_h}{2}$

33. C.32 $r\Delta 2y' - r\Delta 3y' - N32\ S32 = o$

or $r\Delta 2y - r\Delta 3y + N32\ S32 = \frac{r \propto T_h}{2}$

34. C.43 $r\Delta 3y' - r\Delta 4y' - N43\ S43 = o$

or $r\Delta 3y - r\Delta 4y + N43\ S43 = \frac{r \propto T_h}{2}$

35. C.54 $r\Delta 4y' - r\Delta 5y' - N54\ S54 = o$

or $r\Delta 4y - r\Delta 5y + N54\ S54 = \frac{r \propto T_h}{2}$

36. C.65 $r\Delta 5y' - N65\ S65 = o$

or $r\Delta sy + N65\ S65 = \frac{r \propto T_h}{2}\ (n-5)$

37. C.1'o' $r\Delta o'y - r\Delta 1'y - N1'o'\ S1'o' = o$

38. C.2'1' $r\Delta 1'y - r\Delta 2'y = N2'1'\ S2'1' = o$

39. C.3'2' $r\Delta 2'y - r\Delta 3'y - N3'2'\ S\ 3'2' = o$

40. C.4'3' $r\Delta 3'y - r\Delta 4'y - N\ 4'3'\ S4'3' = o$

41. C.5'4' $r\Delta 4'y - r\Delta 5'y - N5'4'\ S5'4' = o$

42. C.6'5' $r\Delta 5'y - N6'5'\ S6'5' = o$

43. E.ox $\frac{m1o - mo1}{h} = Noo'$

or $m1o - mo1 - h\ Noo' = o$

Similarly

44. E.1x $m21 - m12 - m1o + mo1 - h\ N11' = o$

45. E.2x $m32 - m23 - m21 + m12 - h\ N22' = o$

46. E.3x $m43 - m34 - m32 + m23 - h\ N33' = o$

47. E.4x $m54 - m45 - m43 + m34 - h\ N44' = o$

48. E.5x $m65 - m56 - m54 - m45 - h\ N55' = o$

49. E.oy $\frac{N1o\ h}{EC1\ AC1} = \frac{h}{EC1\ AC1}\ (\frac{mo1 + mo'1'}{L})$

or $mo1 + mo'1' - LN1o = o$

50. E.1y $\frac{N21h}{EC1\ AC1} = \frac{h}{EC1\ AC1}\ (\frac{mo1 + mo'1'}{L} + ((\frac{m12 - m1o}{L}) + (\frac{m1'o' + m1'2'}{L}))\ )$

or $mo1 + mo'1' - m1o + m1'o' + m12 + m1'2' - LN21 = o$

Similarly

51. E.2y $mo1 + mo'1' - m1o + m1'o' + m12 + m1'2' + m23 - m21 + m2'1' + m2'3' - LN32 = o$

52. E.3y $mo1 + mo'1' - m1o + m1'o' + m12 + m1'2' + m23 - m21 + m2'1' + m2'3' + m34 - m32 + m3'2' + m3'4' - LN43 = o$

53. E.4y $mo1 + mo'1' - m1o + m1'o' + m12 + m1'2' + m23 - m21 + m2'1' + m2'3' + m34 - m32 + m3'2' + m3'4' + m45 - m43 + m4'3' + m4'5' - LN54 = o$

54. E.5y $mo1 + mo'1' - m1o + m1'o' + m12 + m1'2' + m23 - m21 + m2'1' + m2'3' + m34 - m32 + m3'2' + m3'4' + m45 - m43 + m4'3' + m4'5' + m56 - m54 + m5'4' + m5'6' - LN65 = o$

55. E.o'y $mo'1' + mo1 - LN1'o' = o.$

56. E.1'y $mo'1' + mo1 + m1'o' + m1'2' + m12 - m1o - LN2'1' = o$

57. E.2'y $mo'1' + mo1 + m1'o' + m1'2' + m12 - m1o + m2'1' + m2'3' + m23 - m21 - LN3'2' = o$

58. E.3'y $mo'1' + mo1 + m1'o' + m1'2' + m12 - m1o + m2'1' + m2'3' + m23 - m21 + m3'2 + m3'4' + m34 - m32 - LN4'3' = o$

59. E.4'y $mo'1' + mo1 + m1'o' + m1'2' + m12 - m1o + m2'1' + m2'3' + m23 - m21 + m3'2' + m3'4' + m34 - m32 + m4'3' + m4'5' + m45 - m43 - LN5'4' = o$

60. E.5'y $mo'1' + mo1 + m1'o' + m1'2' + m12 - m1o + m2'1' + m2'3' + m23 - m21 + m3'2' + m3'4' + m34 - m32 + m4'3' + m4'5' + m45 - m43 + m5'4' + m5'6' + m56 - m54 - LN6'5' = o$

61. Eo-o' $(\frac{mo1 - m1o}{h}) + (\frac{mo'1' + m1'o'}{h}) = o$

or $mo1 - m1o + mo'1' + m1'o' = o$

Similarly

62. E.1-1' $m21 - m12 - m1o + mo1 - m2'1' - m1'2' + m1'o' + mo'1' = o$

63. E.2-2' $m32 - m23 - m21 + m12 - m3'2' - m2'3' + m2'1' + m1'2' = o$

64. E.3-3' $m43 - m34 - m32 + m23 - m4'3' - m3'4' + m3'2' + m2'3' = o$

65. E.4-4' $m54 - m45 - m43 + m34 - m5'4' - m4'5' + m4'3' + m3'4' = o$

66. E.5-5' $m65 - m56 - m54 + m45 - m6'5' - m5'6' + m5'4' + m4'5' = o$

In the above equations, the following parameters are used:-

$r1 = \frac{h}{L} \cdot \frac{Ib}{Ic1}$; $r2 = \frac{h}{L} \cdot \frac{Ib}{IC2}$

$R = \frac{6EbIb}{L2}$; $C = \frac{\propto T_i h\ EbIb}{L}$

$B = \frac{6Ibh}{L^3\ AC1}$; $Q = \frac{6Ibh}{L^3\ AC2}$

$\theta o1 = \theta 1o = \theta 12$ ---- etc. $= \frac{\propto T_i h}{2d}$

$\delta oo' = \frac{\propto T_i hn}{2}$; $\delta 11' = \frac{\propto T_i h(n-1)}{2}$

$$\delta_{22'} \text{ ----- etc.} = \frac{\alpha T_{ih}}{2} (n-1) \text{ ---- etc.}$$

$$r = \frac{AbEb}{Lb}$$

$$S_{oo'} = \frac{L_{oo'}}{A_{oo'} E_{oo'}} \cdot \frac{AbEb}{Lb} \; ; \quad S_{11'} = \frac{L_{11'}}{A_{11'} E_{11'}} \cdot \frac{AbEb}{Lb}$$

$$S_{22'} \text{ ----- etc.} = \frac{L_{22'}}{A_{22'} E_{22'}} \cdot \frac{AbEb}{Lb} \text{ ---- etc.}$$

$$\left(\frac{\delta_{no1} + \delta_{no1'}}{L}\right) \frac{6EbIb}{L} = \left(\frac{m_{o1} + m_{o'1'}}{L^2}\right) \frac{h}{EC1\ AC1} \cdot \frac{6EbIb}{L} + \left(\frac{m_{o'1'} + m_{o1}}{L^2}\right)$$

$$\frac{h}{EC2\ AC2} \cdot \frac{6EbIb}{L} = (B+Q)\ m_{o1} + (B+Q)\ m_{o'1'}$$

$$\left(\frac{\delta_{no1} + \delta_{no'1'}}{L}\right) \frac{6EbIb}{L} + \left(\frac{\delta_{n12} + \delta_{n'1'2'}}{L}\right) \frac{6EbIb}{L} = (B+Q)\ m_{o1} + (B+Q)\ m_{o'1'} + (B+Q)\ m_{12} + (B+Q)\ m_{1'2'}$$

Similarly for

$$\left(\frac{\delta_{no1} + \delta_{no'1'}}{L}\right) \frac{6EbIb}{L} + \text{----------} + \left(\frac{\delta_{n23} + \delta_{2'3'}}{L}\right) \frac{6EbIb}{L} =$$

$$(B+Q)\ m_{o1} + \ldots + \ldots + \ldots + (B+Q)\ m_{23} + \ldots. \text{ etc.}$$

Based on the above equations, a matrix can now be set out for the shear wall shown in fig. 5.0711.

Example

The following numerical example is used to illustrate the procedure. Referring to fig. 5.0711 the following numerical values required in the matrix are first evaluated:-

$AC1 = 0.05 \times 0.12 = 0.0006 m^2$; $AC2 = 0.05 \times 0.06 = 0.003 m^2$

$Ab = 0.05 \times 0.04 = 0.002 m^2$; $EC1 = EC2 = Eb = 21 \times 10^6\ KN/m^2$

$IC1 = 0.05 \times 0.12^3/12 = 7.2 \times 10^{-6} m^4$; $IC2 = 0.05 \times 0.06^3/12 = 9 \times 10^{-7} m^4$

$Ib = 0.05 \times 0.04^3/12 = 2.666\dot{6} \times 10^{-7} m^4$; $\alpha = 0.00001$ per ^oC

$T_i = 20^oC$; $r1 = \frac{0.3}{0.405} \cdot \frac{2.6667 \times 10^{-7}}{7.2 \times 10^{-6}} = 0.027435$

$r2 = \frac{0.3}{0.405} \cdot \frac{2.6667 \times 10^{-7}}{9 \times 10^{-7}} = 0.219481$

$$R = \frac{6EIb}{L2} = \frac{6\times21\times10^{6}\times2.6667\times10^{-7}}{0.405^{2}} = 204.849383$$

$$R\frac{L}{h} = 204.849383 \times \frac{0.405}{0.3} = 276.546667$$

$$C = \frac{\alpha T_{h} EIb}{L} = (0.00001 \times 20 \times 0.3 \times 21 \times 10^{6} \times 2.6667 \times 10^{-7})/0.405 = 8.2964 \times 10^{-4} KN\text{-}m^{2}$$

$$B = \frac{6Ibh}{L^{3}AC1} = \frac{6\times2.6667\times10^{-7}\times0.3}{0.405^{3}\times0.006} = 0.00120429$$

$$Q = \frac{6Ibh}{L^{3}AC2} = \frac{6\times2.6667\times10^{-7}\times0.3}{0.405^{3}\times0.003} = 0.00240858$$

$$S_{oo'} = S_{11'} = S_{22'} = S_{33'} = S_{44'} = S_{55'} = \frac{L_{oo'}}{A_{oo'}\,E_{oo'}} \cdot \frac{AbEb}{Lb} = \frac{0.405}{0.002\times21\times10^{6}} \cdot \frac{0.002\times21\times10^{6}}{0.405} = 1$$

$$S_{1o} = S_{21} = S_{32} = S_{43} = S_{54} = S_{65} = \frac{L_{10}}{A_{1o}\,E_{1o}} \cdot \frac{AbEb}{Lb} = \frac{0.3}{0.006\times21\times10^{6}} \cdot \frac{0.002\times21\times10^{6}}{0.405} = 0.24691358$$

$$S_{1'o'} = S_{2'1'} = S_{3'2'} = S_{4'3'} = S_{5'4'} = S_{6'5'} = \frac{L_{1'o'}}{A_{1'o'}\,E_{1'o'}} \cdot \frac{AbEb}{Lb} = \frac{0.3}{0.003\times21\times10^{6}} \cdot \frac{0.002\times21\times10^{6}}{0.405} = 0.49382716$$

$$r = \frac{AbEb}{Lb} = \frac{0.002\times21\times10^{6}}{0.405} = 103703.7037$$

$$\frac{r\alpha T_{h}}{2} = (103703.7037 \times 0.00001 \times 20 \times 0.3)/2 = 3.11111\dot{}$$

(1) $\frac{3c}{d} - \frac{3cn}{L} = -0.01613189$

(2) $\frac{6c}{d} = 0.04148200$

(3) $\frac{3c}{d} + \frac{3c}{L}(1-n) = -0.00998641$

(4) $\frac{3c}{d} + \frac{3c}{L}(2-n) = -0.00384093$

(5) $\frac{3c}{d} + \frac{3c}{L}(3-n) = 0.00230456$

(6) $\frac{3c}{d} + \frac{3c}{L}(4-n) = 0.00845004$

(7) $\frac{3c}{d} + \frac{3c}{L}(5-n) = 0.01459552$

(1') $\frac{-3cn}{L} = -0.03687289$

(2') $\frac{3c(1-n)}{L} = -0.03072741$

(3') $\frac{3c(2-n)}{L}$ = -0.02458193

(4') $\frac{3c(3-n)}{L}$ = -0.01843644

(5') $\frac{3c(4-n)}{L}$ = -0.01229096

(6') $\frac{3c(5-n)}{L}$ = -0.00614548

The complete numerical matrix is shown in Table: 500.24.

The results of the analysis of this problem are shown in fig. 5.0712.

(b) Analysis using the stiffness method

The above problem was also analysed using the stiffness method. The results obtained by this method are also shown in fig. 5.0712.

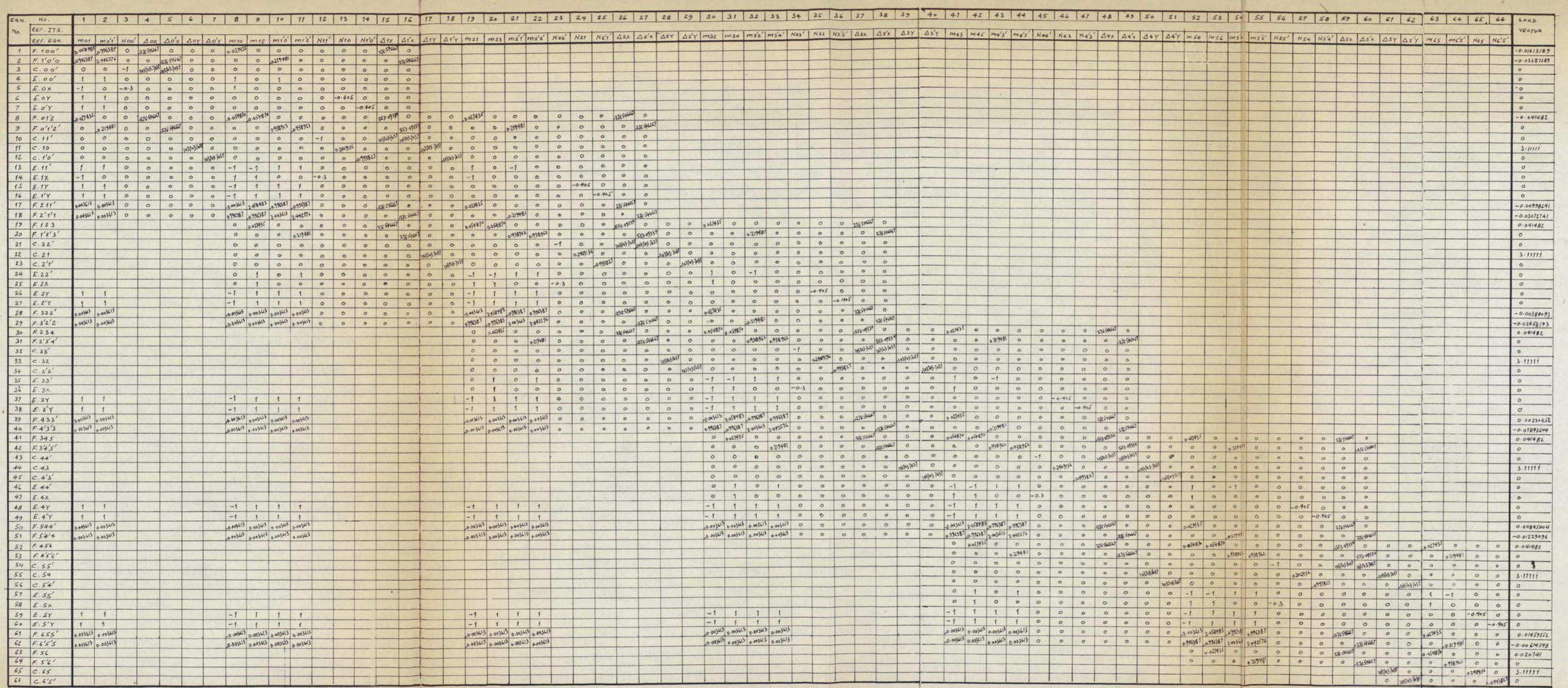

Table: 500.24 Numerical matrix for the effect of linear temperature distribution in a column of a shear wall frame taking into consideration the secondary effect of axial deformations.

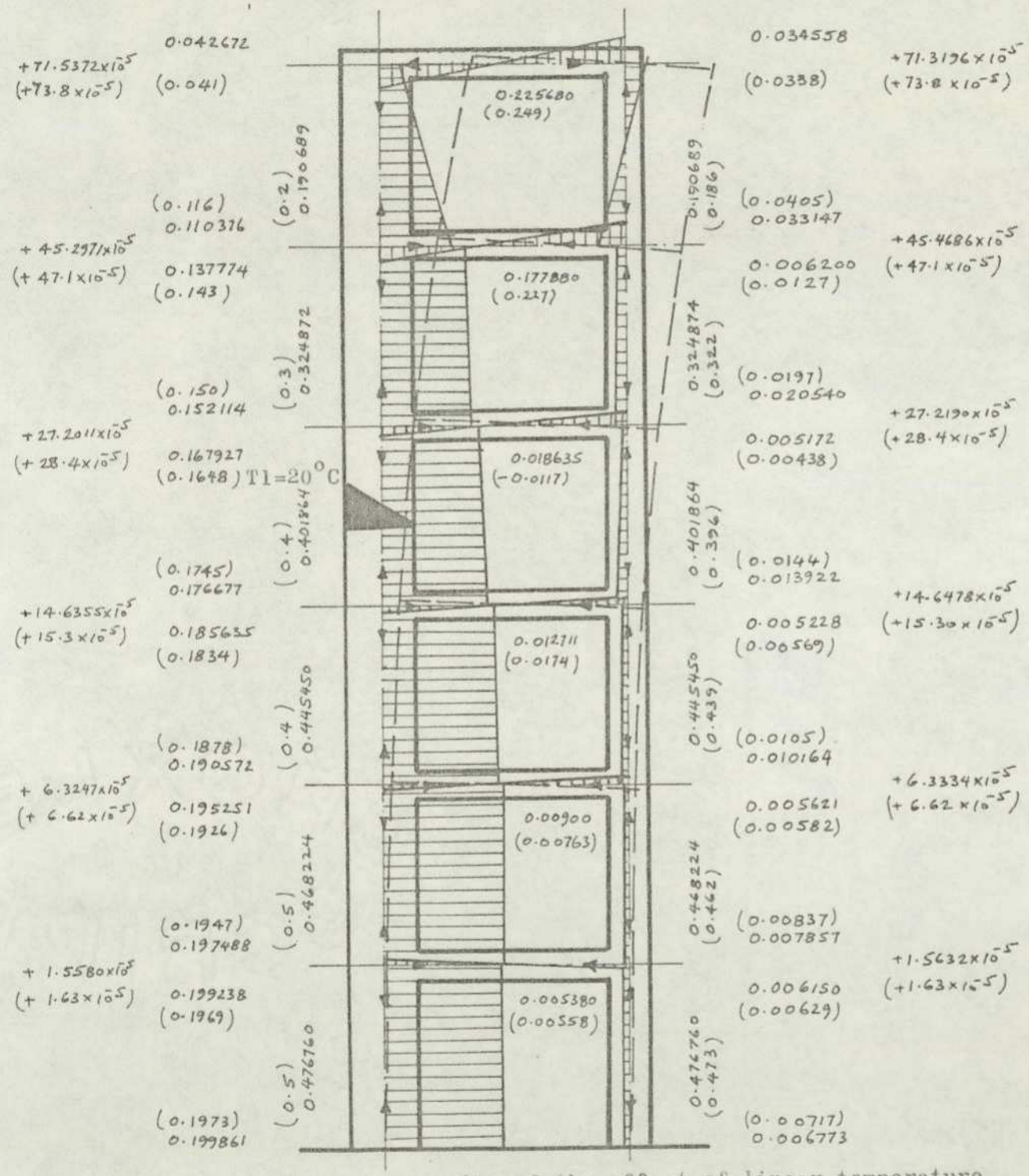

Fig. 5.0712 Shows the results of the effect of linear temperature distribution in a shear wall taking into consideration the secondary effect of axial deformations.

Unbracketed figures.....show results by the force-displacement method

Bracketed figures.....show results by the stiffness method

5.07.2 Linear temperature distribution in a column of a 6-storey frame

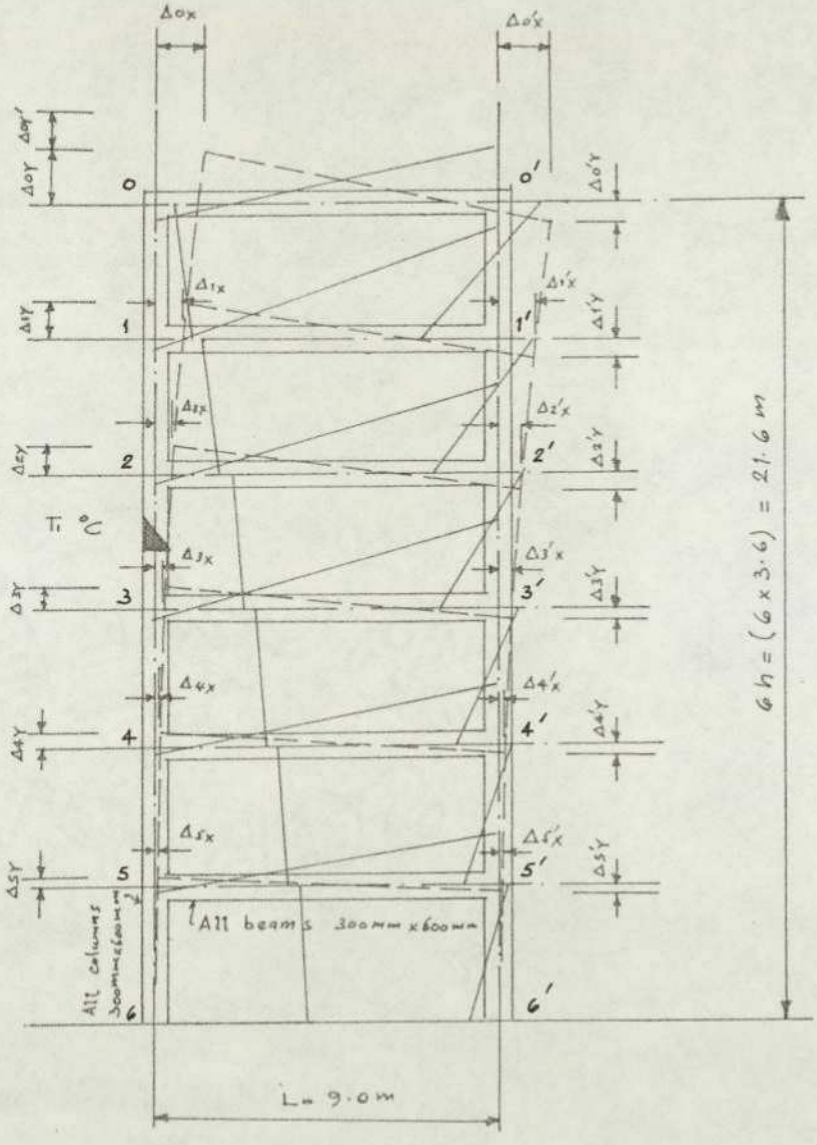

Fig. 5.0721 The effect of linear temperature distribution in one column of a 6-storey symmetrical frame showing assumed bending moments and deformations for the setting up of the matrix.

In the following study, the effects of axial deformations in the analysis of thermal stresses due to a linear temperature distribution in one column of a symmetrical frame are investigated. Although the frame is symmetrical, the applied force i.e. the action of heat on one column, is not symmetrical. It is, therefore, necessary to analyse the whole frame. As in the case of the analysis of a shear wall, the structure contains 24 unknown bending moments, 24 displacements and 18 axial forces. Therefore, 66 independent conditions of compatibility of deformations and equilibrium of forces are required in the matrix.

Assuming a similar bending moment diagram as in the case of the shear wall, the conditions of compatibility and equilibrium would also be of similar form. Therefore, it is not considered necessary to show the derivations of the equations again. However, the numerical values of the elements of the matrix will be different as the properties of the frame are different and for this reason, the complete numerical matrix is shown in Table 500.25

The results of the analysis using the Stiffness Method are shown in the same figure.

EQN. NO.	1	2	3	4	5	6	7	8	9	10	11	12	13	14	15	16	LOAD VECTOR
REF. JTS.																	
REF. EQN.	m_{04}	m_{04}'	N_{00}'	Δ_{0X}	Δ_{0X}'	Δ_{0Y}	Δ_{0Y}'	m_{10}	m_{12}	m_{16}'	m_{12}'	N_{11}'	N_{10}	N_{16}'	Δ_{1X}	Δ_{1X}'	
1 F. 100′	2.801778	2.798222	0	28000.0	0	0	0	0.4	0	0	0	0	0	0	28000.0	0	36.288
2 F. 1′0′0	.798222	2.801778	0	0	28000.0	0	0	0	0	-0.4	0	0	0	0	0	28000.0	-24.192
3 C. 00′	0	0	-1	560000.0	560000.0	0	0	0	0	0	0	0	0	0	0	0	0
4 E. 00′	1	1	0	0	0	0	0	-1	0	0	0	0	0	0	0	0	0
5 E. 0X	-1	0	-3.6	0	0	0	0	1	0	0	0	0	0	0	0	0	0
6 E. 0Y	1	1	0	0	0	0	0	0	0	0	0	0	-9.0	0	0	0	0
7 E. 0′Y	1	1	0	0	0	0	0	0	0	0	0	0	0	-9.0	0	0	0
8 F. 012	-0.51	0	0	28000.0	0	0	0	-0.8	-0.8	0	0	0	0	0	560000.0	560000.0	-120.960
9 F. 0′1′2′	0	-0.4	0	0	28000.0	0	0	0	0	0.8	-0.8	0	0	0	0	560000.0	0
10 C. 11′	0	0	0	0	0	0	0	0	0	0	0	-1	0	0	560000.0	560000.0	0
11 C. 10	0	0	0	0	0	560000.0	0	0	0	0	0	0	0.4	0	0	0	201.600
12 C. 1′0′	0	0	0	0	0	0	560000.0	0	0	0	0	0	0	-0.4	0	0	0
13 E. 11′	1	1	0	0	0	0	0	-1	-1	1	-1	0	0	0	0	0	0
14 E. 1X	-1	0	0	0	0	0	0	1	1	0	0	-3.6	0	0	0	0	0
15 E. 1Y	1	1	0	0	0	0	0	-1	1	1	1	0	0	0	0	0	0
16 E. 1′Y	1	1	0	0	0	0	0	-1	1	1	1	0	0	0	0	0	0
17 F. 211′	0.001778	0.001778	0	0	0	0	0	2.801778	2.801778	.798222	.798222	0	0	0	28000.0	0	40.320
18 F. 2′1′1	0.001778	0.001778	0	0	0	0	0	.798222	.798222	2.801778	2.801778	0	0	0	0	28000.0	-20.160
19 F. 123								0	0.4	0	0	0	0	0	28000.0	0	120.960
20 F. 1′2′3′								0	0	0	-0.4	0	0	0	0	28000.0	0
21 C. 22′								0	0	0	0	0	0	0	0	0	0
22 C. 21								0	0	0	0	0	0	0	0	0	201.600
23 C. 2′1′								0	0	0	0	0	0	0	0	0	0
24 E. 22′								0	1	0	1	0	0	0	0	0	0
25 E. 2X								0	-1	0	0	0	0	0	0	0	0
26 E. 2Y	1	1						-1	1	1	1	0	0	0	0	0	0
27 E. 2′Y	1	1						-1	1	1	1	0	0	0	0	0	0
28 F. 322′	0.001778	0.001778						2.801778	2.801778	.798222	.798222	0	0	0	28000.0	0	44.352
29 F. 3′2′2	0.001778	0.001778						.798222	.798222	2.801778	2.801778	0	0	0	0	28000.0	-16.128
30 F. 234								0	0.4	0	0	0	0	0	28000.0	0	120.960
31 F. 2′3′4′								0	0	0	-0.4	0	0	0	0	28000.0	0
32 C. 33′								0	0	0	0	0	0	0	0	0	0
33 C. 32								0	0	0	0	0	0	0	0	0	201.600
34 C. 3′2′								0	0	0	0	0	0	0	0	0	0
35 E. 33′								0	1	0	1	0	0	0	0	0	0
36 E. 3X								0	-1	0	0	0	0	0	0	0	0
37 E. 3Y	1	1						-1	1	1	1	0	0	0	0	0	0
38 E. 3′Y	1	1						-1	1	1	1	0	0	0	0	0	0
39 F. 433′	0.001778	0.001778						0.001778	0.001778	0.001778	0.001778	0	0	0	28000.0	0	48.384
40 F. 4′3′3	0.001778	0.001778						0.001778	0.001778	0.001778	0.001778	0	0	0	0	28000.0	-12.096
41 F. 345																	120.960
42 F. 3′4′5′																	0
43 C. 44′																	0
44 C. 43																	201.600
45 C. 4′3′																	0
46 E. 44′																	0
47 E. 4X																	0
48 E. 4Y	1	1						-1	1	1	1						0
49 E. 4′Y	1	1						-1	1	1	1						0
50 F. 544′	0.001778	0.001778						0.001778	0.001778	0.001778	0.001778						52.416
51 F. 5′4′4	0.001778	0.001778						0.001778	0.001778	0.001778	0.001778						-8.064
52 F. 456																	120.960
53 F. 4′5′6′																	0
54 C. 55′																	0
55 C. 54																	201.600
56 C. 5′4′																	0
57 E. 55′																	0
58 E. 5X																	0
59 E. 5Y	1	1						-1	1	1	1						0
60 E. 5′Y	1	1						-1	1	1	1						0
61 F. 655′	0.001778	0.001778						0.001778	0.001778	0.001778	0.001778						52.416
62 F. 6′5′5	0.001778	0.001778						0.001778	0.001778	0.001778	0.001778						-8.064
63 F. 56																	60.480
64 F. 5′6′																	0
65 C. 65																	201.600
66 C. 6′5′																	0

EQN. NO.	17	18	19	20	21	22	23	24	25	26	27	28	29	30	31	32	33	34	35	36	37	38	39	LOAD VECTOR
REF. JTS.																								
REF. EQN.	Δ_{1Y}	Δ_{1Y}'	m_{23}	m_{23}'	m_{21}'	m_{32}'	N_{22}'	N_{21}	N_{21}'	Δ_{2X}	Δ_{2X}'	Δ_{2Y}	Δ_{2Y}'	m_{32}	m_{34}	m_{34}'	m_{36}'	N_{33}'	N_{32}	N_{32}'	Δ_{3X}	Δ_{3X}'	Δ_{3Y}	
1 F. 100′																								36.288
2 F. 1′0′0																								-24.192
3 C. 00′																								0
4 E. 00′																								0
5 E. 0X																								0
6 E. 0Y																								0
7 E. 0′Y																								0
8 F. 012	0	0	-0.4	0	0	0	0	0	0	28000.0	0													-120.960
9 F. 0′1′2′	0	0	0	0	0.4	0	0	0	0	0	28000.0													0
10 C. 11′	560000.0	0	0	0	0	0	0	0	0	0	0													0
11 C. 10	560000.0	0	0	0	0	0	0	0	0	0	0													201.600
12 C. 1′0′	0	-560000.0	0	0	0	0	0	0	0	0	0													0
13 E. 11′	0	0	1	0	-1	0	0	0	0	0	0													0
14 E. 1X	0	0	-1	0	0	0	0	0	0	0	0													0
15 E. 1Y	0	0	0	0	0	0	0	0	-3.0	0	0													0
16 E. 1′Y	0	0	0	0	0	0	0	0	0	-9.0	0													0
17 F. 211′	0	0	0.4	0	0	0	0	0	0	0	28000.0													40.320
18 F. 2′1′1	0	0	0	0	-0.4	0	0	0	0	0	0													-20.160
19 F. 123	0	0	0.8	0.8	0	0	0	0	0	560000.0	0	0	0	0.4	0	0	0	0	0	0	28000.0	0		120.960
20 F. 1′2′3′	0	0	0	0	0.8	-0.8	0	0	0	560000.0	560000.0	0	0	0	0.4	0	0	0	0	0	0	28000.0		0
21 C. 22′	0	0	0	0	0	0	-1	0	0	560000.0	560000.0	0	0	0	0	0	0	0	0	0	0	0		0
22 C. 21	560000.0	0	0	0	0	0	0	0.4	0	0	0	560000.0	0	0	0	0	0	0	0	0	0	0		201.600
23 C. 2′1′	0	560000.0	0	0	0	0	0	0	-0.4	0	0	0	560000.0	0	0	0	0	0	0	0	0	0		0
24 E. 22′	0	0	-1	-1	1	-1	0	0	0	0	0	0	0	1	0	-1	0	0	0	0	0	0		0
25 E. 2X	0	0	1	1	0	0	-3.6	0	0	0	0	0	0	-1	0	0	0	0	0	0	0	0		0
26 E. 2Y	0	0	-1	1	1	1	0	0	0	0	0	0	0	0	0	0	0	0	-3.0	0	0	0		0
27 E. 2′Y	0	0	-1	1	1	1	0	0	0	28000.0	0	0	0	0	0	0	0	0	0	-9.0	0	0		0
28 F. 322′	0	0	2.801778	.798222	.798222	2.801778	0	0	0	0	28000.0	0	0	0.4	0	0	0	0	0	0	28000.0	0		44.352
29 F. 3′2′2	0	0	.798222	2.801778	.798222	2.801778	0	0	0	0	0	28000.0	0	0	0	0	0	0	0	0	0	28000.0		-16.128
30 F. 234			0	0.4	0	0	0	0	0	28000.0	0	0	0	0.8	0.8	0	0	0	0	0	560000.0	0	0	120.960
31 F. 2′3′4′			0	0	-0.4	0	0	0	0	0	28000.0	0	0	0	0	0.8	-0.8	0	0	0	0	560000.0	0	0
32 C. 33′			0	0	0	0	0	0	0	0	0	0	0	0	0	0	0	-1	0	0	560000.0	560000.0	0	0
33 C. 32			0	0	0	0	0	0	0	0	0	560000.0	0	0	0	0	0	0	0	0.4	0	0	560000.0	0
34 C. 3′2′			0	0	0	0	0	0	0	0	0	0	560000.0	0	0	0	0	0	0	-0.4	0	0	0	0
35 E. 33′			0	1	0	1	0	0	0	0	0	0	0	-1	-1	1	-1	0	0	0	0	0	0	0
36 E. 3X			0	-1	0	0	0	0	0	0	0	0	0	1	0	0	0	-3.6	0	0	0	0	0	0
37 E. 3Y			-1	1	1	1	0	0	0	0	0	0	0	-1	1	1	1	0	0	0	0	0	0	0
38 E. 3′Y			-1	1	1	1	0	0	0	0	0	0	0	-1	1	1	1	0	0	0	0	0	0	0
39 F. 433′			2.001778	0.001778	0.001778	0.001778	0	0	0	0	0	0	0	2.001778	0.798222	0.798222	0.798222	0	0	0	28000.0	0	0	48.384
40 F. 4′3′3			0.001778	0.001778	0.001778	0.001778	0	0	0	0	0	0	0	0.798222	2.801778	0.798222	0.798222	0	0	0	0	28000.0	0	-12.096
41 F. 345														0	0.4	0	0	0	0	0	28000.0	0		120.960
42 F. 3′4′5′														0	0	0	-0.4	0	0	0	0	28000.0		0
43 C. 44′														0	0	0	0	0	0	0	0	0		0
44 C. 43														0	0	0	0	0	0	0	0	0		201.600
45 C. 4′3′														0	0	0	0	0	0	0	0	0		0
46 E. 44′														0	-1	0	0	0	0	0	0	0		0
47 E. 4X														0	1	0	0	0	0	0	0	0		0
48 E. 4Y			-1	1	1	1								-1	1	1	1	0	0	0	0	0		0
49 E. 4′Y			-1	1	1	1								-1	1	1	1	0	0	0	0	0		0
50 F. 544′			0.001778	0.001778	0.001778	0.001778								2.001778	0.798222	0.798222	0.798222	0	0	0	28000.0	0		52.416
51 F. 5′4′4			0.001778	0.001778	0.001778	0.001778								0.798222	2.801778	0.798222	0.798222	0	0	0	0	28000.0		-8.064
52 F. 456																					0	0	0	120.960
53 F. 4′5′6′																					0	0	0	0
54 C. 55′																					0	0	0	0
55 C. 54																					0	0	0	201.600
56 C. 5′4′																					0	0	0	0
57 E. 55′																					0	0	0	0
58 E. 5X																					0	0	0	0
59 E. 5Y			-1	1	1	1								-1	1	1	1	0	0	0	0	0		0
60 E. 5′Y			-1	1	1	1								-1	1	1	1	0	0	0	0	0		0
61 F. 655′			0.001778	0.001778	0.001778	0.001778								2.001778	0.798222	0.798222	0.798222	0	0	0	28000.0	0		52.416
62 F. 6′5′5			0.001778	0.001778	0.001778	0.001778								0.798222	2.801778	0.798222	0.798222	0	0	0	0	28000.0		-8.064
63 F. 56														0	0.4	0	0	0	0	0	28000.0	0		60.480
64 F. 5′6′														0	0	0	-0.4	0	0	0	0	28000.0		0
65 C. 65																					560000.0	0		201.600
66 C. 6′5′																					0	560000.0		0

EQN. NO.	40	41	42	43	44	45	46	47	48	49	50	51	52	53	54	55	56	57	58	59	60	61	62	63	64	65	66	LOAD VECTOR
REF. JTS.																												
REF. EQN.	Δ_{3Y}	m_{43}	m_{45}	m_{45}'	m_{41}'	N_{44}'	N_{43}	N_{45}'	Δ_{4X}	Δ_{4X}'	Δ_{4Y}	Δ_{4Y}'	m_{54}	m_{52}	m_{56}'	m_{52}'	N_{55}'	N_{54}	N_{54}'	Δ_{5X}	Δ_{5X}'	Δ_{5Y}	Δ_{5Y}'	m_{65}	m_{65}'	N_{65}	N_{65}'	
1 F. 100′																												36.288
2 F. 1′0′0																												-24.192
3 C. 00′																												0
4 E. 00′																												0
5 E. 0X																												0
6 E. 0Y																												0
7 E. 0′Y																												0
8 F. 012																												-120.960
9 F. 0′1′2′																												0
10 C. 11′																												0
11 C. 10																												201.600
12 C. 1′0′																												0
13 E. 11′																												0
14 E. 1X																												0
15 E. 1Y																												0
16 E. 1′Y																												0
17 F. 211′																												40.320
18 F. 2′1′1																												-20.160
19 F. 123																												120.960
20 F. 1′2′3′																												0
21 C. 22′																												0
22 C. 21																												201.600
23 C. 2′1′																												0
24 E. 22′																												0
25 E. 2X																												0
26 E. 2Y																												0
27 E. 2′Y																												0
28 F. 322′																												44.352
29 F. 3′2′2																												-16.128
30 F. 234																												120.960
31 F. 2′3′4′																												0
32 C. 33′																												0
33 C. 32																												201.600
34 C. 3′2′																												0
35 E. 33′																												0
36 E. 3X																												0
37 E. 3Y																												0
38 E. 3′Y																												0
39 F. 433′																												48.384
40 F. 4′3′3																												-12.096
41 F. 345																												120.960
42 F. 3′4′5′																												0
43 C. 44′																												0
44 C. 43																												201.600
45 C. 4′3′																												0
46 E. 44′																												0
47 E. 4X																												0
48 E. 4Y																												0
49 E. 4′Y																												0
50 F. 544′																												52.416
51 F. 5′4′4																												-8.064
52 F. 456																												120.960
53 F. 4′5′6′																												0
54 C. 55′																												0
55 C. 54																												201.600
56 C. 5′4′																												0
57 E. 55′																												0
58 E. 5X																												0
59 E. 5Y																												0
60 E. 5′Y																												0
61 F. 655′																												52.416
62 F. 6′5′5																												-4.032
63 F. 56																												60.480
64 F. 5′6′																												0
65 C. 65																												201.600
66 C. 6′5′																												0

Table: 500.25 Numerical matrix for the effect of linear temperature distribution in a column of a 6-storey symmetrical frame taking into consideration the secondary effect of axial deformations.

Horiz. Deflect. (mm)	Bend. Momts. (KN–m)	Axial Forces (KN)	Axial Forces (KN)	Axial Forces (KN)	Bend. Momts. (KN–m)	Horiz. Deflect. (mm)

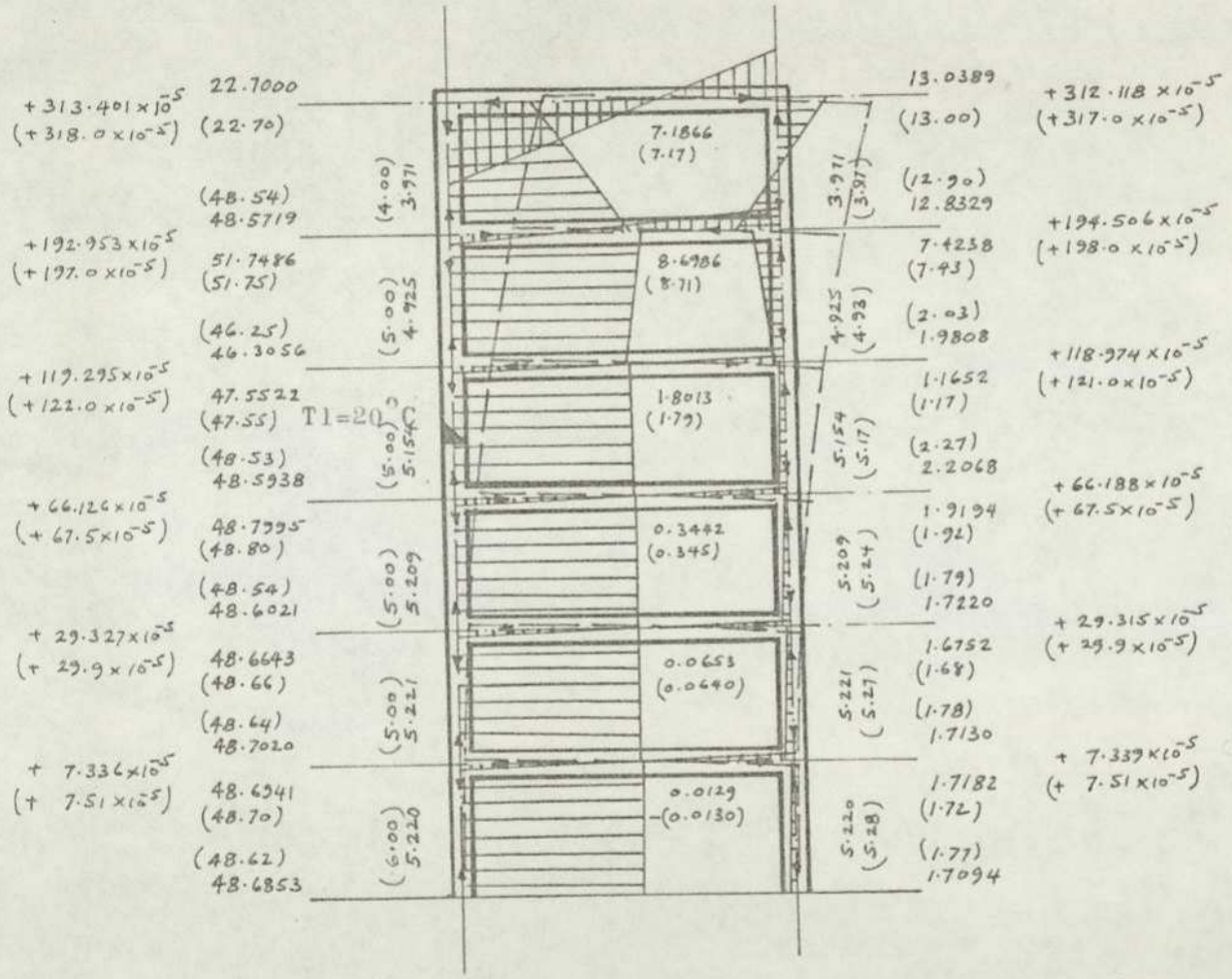

Fig. 5.0722 Shows the results of the effect of linear temperature distribution in a column taking into consideration the secondary effect of axial deformations.

Unbracketed figures.....show results by the force-displacement method

Bracketed figures.....show results by the stiffness method

5.07.3 Discussion of results of the effect of linear temperature distribution in a shear wall and a symmetrical 6-storey frame, taking into consideration the secondary effect of axial deformations

The results show that the effect of axial deformations in the analysis of thermal stresses is not very high. However, if required, the effect of axial deformations can be taken into account by the force-displacement method. Although the formulation of the equations (i.e. the matrix) is fairly easy and straightforward, the size of the matrix grows so fast that not only does it become very cumbersome and easy to make mistakes, but large computer storage capacity would be required for its solution. Under normal circumstances, the difference between the accuracies of results, with or without consideration of axial deformations, is so small that the extra effort and expense required does not justify the inclusion of the effect of axial deformations.

6.00 THERMAL STRESSES IN TRUSSES

6.01 Introduction

Thermal stresses and deformations can occur in all structures. So far this work has mainly dealt with framed structures, which are primarily subjected to bending stresses. Trusses, in contrast to frames, are subjected mainly to axial forces and deformations. However, bending stresses are nearly always present in trusses due to various factors, but these are seldom evaluated in practice and are usually considered secondary and small. The evaluation of these secondary stresses involves a large amount of work and time in relation to their importance. For this same reason, some simple forms of trusses are analysed for axial forces and deformations in this work, using the force-displacement method. The analysis is based on the usual assumptions, e.g.

(i) that the response of members is linearly elastic

(ii) that the deformations are sufficiently small for equilibrium to be satisfied in the original configuration of the structure

(iii) that the principle of superposition is valid

(However, it should be pointed out, that these limitations can be by-passed and high order effects arising from this can be taken into account.)

6.02 Application of the force displacement method

The application of the force displacement method to the analysis of forces and displacements in trusses is, in principle, similar to the analysis of frames. In this method matrices are set out by expressing the conditions of compatibility of deformation and equilibrium of forces at joints. The load-deflection characteristics of members are used in the form of linear flexibility coefficients resulting from a unit axial force. These provide the relationship between the applied load and deformations of an element. However, before the compatibility conditions can be written, it is necessary to develop a relationship between the displacements of one joint in a triangulated truss with respect to another joint.

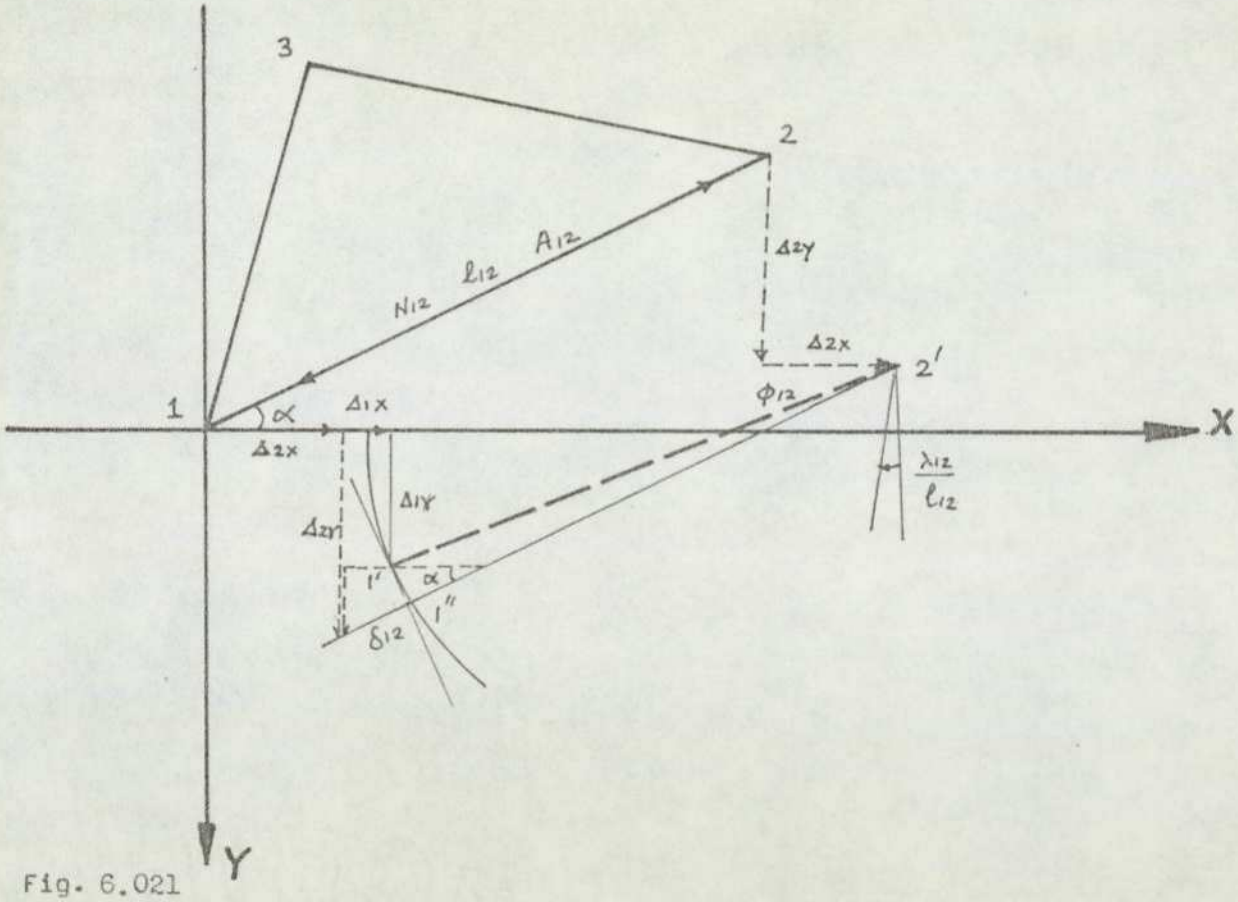

Fig. 6.021

Referring to fig.6.021 and assuming that a member 1-2 in a truss is subjected to an axial force N12, displacements Δ_{1x} and Δ_{1y} at joint 1, Δ_{2x} and Δ_{2y} at joint 2, and also a rotation ϕ_{12}, it can be

seen that for deformations to be compatible the following relationship must be satisfied:

C.12. $$\delta_{12} = (\Delta_{1x} - \Delta_{2x})\cos\alpha + (\Delta_{2y} - \Delta_{1y})\sin\alpha$$

or $$(\Delta_{1x} - \Delta_{2x})\cos\alpha + (\Delta_{2y} - \Delta_{1y})\sin\alpha - \delta_{12} = 0 \quad \text{--- (a)}$$

the angle of rotation ϕ is of no relevance when the joints are hinged, but for trusses with rigid joints this angle is the source of secondary bending moments. For most trusses these moments are known to be small, but in some cases they can be very high e.g. in masts or in cable-stayed bridges.

Compatibility condition C.12 can now be re-arranged by multiplying throughout by $\frac{E_n A_n}{\ell_n}$ and substituting $\delta_{12} = \frac{N_{12}\,\ell_{12}}{E_{12}\,A_{12}}$ (or a similar linear or non-linear relationship) and becomes

C12 $$\frac{E_n A_n}{\ell_n}(\Delta_{1x} - \Delta_{2x})\cos\alpha + \frac{E_n A_n}{\ell_n}(\Delta_{2y} - \Delta_{1y})\sin\alpha - \frac{N_{12}\,\ell_{12}}{E_{12}\,A_{12}} \cdot \frac{E_n A_n}{\ell_n} = 0$$

or $$r(\Delta_{1x} - \Delta_{2x})\cos\alpha + r(\Delta_{2y} - \Delta_{1y})\sin\alpha - N_{12}\,S_{12} = 0 \quad \text{--- (b)}$$

where $$r = \frac{E_n A_n}{\ell_n} \quad \text{and} \quad S_{12} = \frac{\ell_{12}}{E_{12}\,A_{12}} \cdot \frac{E_n A_n}{\ell_n} \quad \text{--- (c)}$$

in the above relationship, En, An and ℓ_n are the reference properties of any member which can be arbitrarily selected.

In the last term of equation, the lack of fit 'ρ' of a member can also be included as follows:-

C.12 $$r(\Delta_{1x} - \Delta_{2x})\cos\alpha + r(\Delta_{2y} - \Delta_{1y})\sin\alpha - N_{12}\,S_{12} \pm \rho = 0 \quad \text{---(d)}$$

When a member is either horizontal or vertical the compatibility equation reduces to very simple expressions which are extremely useful in the analysis of trusses with horizontal and vertical members.

For a horizontal member, angle $\alpha = 0^{\circ}$ and the compatibility equation C.12 reduces to

$$r(\Delta_{1x} - \Delta_{2x}) - N_{12}\, S_{12} = 0 \quad \text{---- (e)}$$

and, for the vertical member, angle $\alpha = 90^{\circ}$ and the compatibility equation C.12 reduces to

$$r(\Delta_{2y} - \Delta_{1y}) - N_{12}\, S_{12} = 0 \quad \text{---- (f)}$$

The above relationship have been derived on the assumptions that point 1' in Fig. 6.021 moves along the tangent instead of along a circular path. More accurate relationships can be obtained, based on the actual circular rotation of the member 12 with respect to point 1', as follows:-

From Fig. 6.021 and assuming circular rotation, it can be written that

$$\left[x - (\ell_{12}\cos\alpha + \Delta_{1x})\right]^2 + \left[y - (\ell_{12}\sin\alpha - \Delta_{1y})\right]^2 = \left[\ell_{12} + \delta_{12}\right]^2 \text{--- (g)}$$

Introducing the boundary conditions for the displacements of the point 1" i.e. for $x = \Delta_{1x}$, $y = \Delta_{1y}$

expression (g) becomes

$$\left[\Delta_{1x} - \ell_{12}\cos\alpha_{12} - \Delta_{2x}\right]^2 + \left[\Delta_{1y} - \ell_{12}\sin\alpha_{12} - \Delta_{2y}\right]^2 = \left[\ell_{12} + \delta_{12}\right]^2 \text{--- (h)}$$

The expression (h) is more accurate than (b), but it leads to more complicated non-linear analysis.

6.03 Analysis of statically determinate trusses for thermal stresses

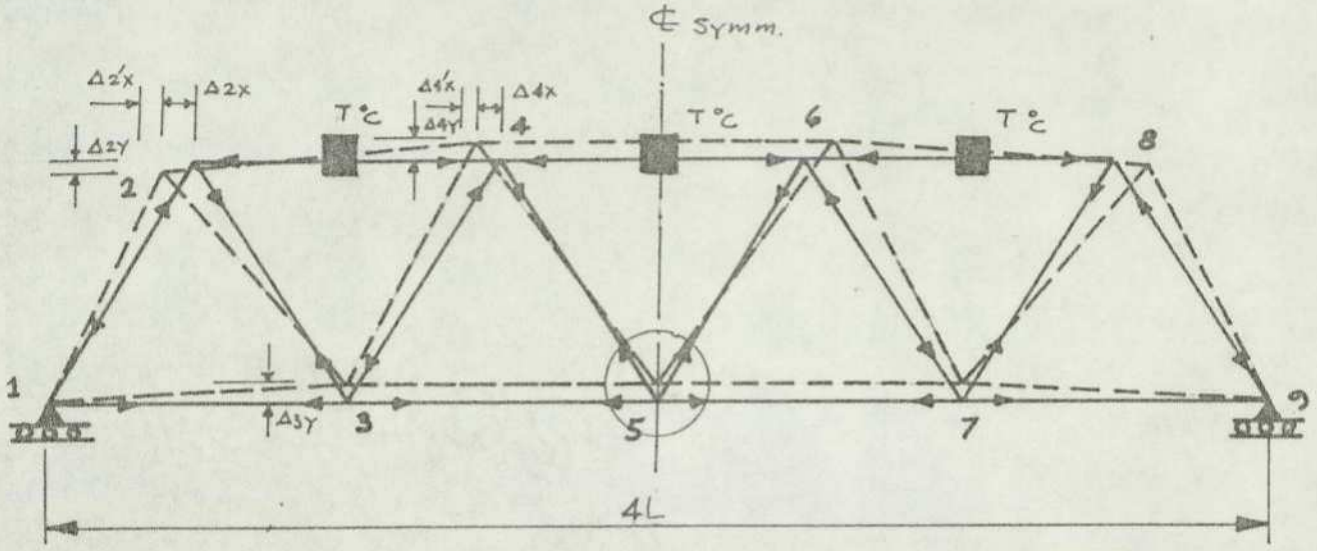

Fig. 6.031 The effect of constant temperature distribution in the top chord of a statically determinate truss

$\Delta 2x$, $\Delta 4x$	actual horizontal displacements at joints 2 and 4
$\Delta 2'x$, $\Delta 4'x$	suppressed " " " " " " "
$\Delta 2y$, $\Delta 4y$	actual vertical displacements at joints 2 and 4

Denoting

$$\Delta_{2x} + \Delta_{2'x} = \frac{3}{2} \alpha T L \quad \text{--- (1)}$$

$$\Delta_{4x} + \Delta_{4'x} = \frac{1}{2} \alpha T L \quad \text{--- (2)}$$

By inspection of the truss, it can be seen that whichever type of force is assumed in the member, the equilibrium of all joints cannot be satisfied unless the forces in all members are zero, e.g. for the assumed forces shown by arrows, joint 5 is not in equilibrium. This happens in all statically determinate trusses indicating that in statically determinate trusses, temperature changes result only in displacements of joints without any stresses in members.

The displacement of members can be determined from the conditions of compatibility of deformations as shown below:

Referring to fig. 6.031

$\Delta 2'x = \Delta 4'x = o$ Since force in member 2-4 is zero.

therefore from eqns. (1) and (2)

$\Delta 2x = \frac{3}{2} \alpha TL$ and $\Delta 4x = \frac{1}{2} \alpha TL$

The conditions of compatibility of deformations can now be written as follows:-

C.12 $\Delta 1x \cos \alpha + \Delta 2x \cos \alpha + \Delta 2y \sin \alpha = o$

C.13 $-\Delta 1x + \Delta 3x = o$

C.23 $\Delta 2x \cos \alpha + \Delta 3x \cos \alpha - \Delta 2y \sin \alpha - \Delta 3y \sin \alpha = o$

C.34 $\Delta 3x \cos \alpha - \Delta 4x \cos \alpha + \Delta 3y \sin \alpha - \Delta 4y \sin \alpha = o$

C.35 $-\Delta 3x \pm \overset{o}{\cancel{\Delta 5x}} = o$ (due to symmetry $\Delta 5x = o$)

C.45 $\Delta 4x \cos \alpha \pm \Delta 5x \overset{o}{\cancel{\cos \alpha}} + \Delta 4y \sin \alpha - \Delta 5y \sin \alpha = o$

From eqn. C.35 $\Delta 3x = o$

substituting into eqn. C.13 gives

$\Delta 1x = o$ (This is only true if the change in angle α is very small. A non-linear analysis would yield a more accurate solution).

from eqn. C.12 $\Delta 2y = \Delta 2x \frac{\cos \alpha}{\sin \alpha}$

$= -\frac{3}{2} \alpha TL \frac{\cos \alpha}{\sin \alpha}$ (by subst. for $\Delta 2x$)

substituting into eqn. C.23 gives

$$\frac{3}{2} \alpha TL \cos \alpha - \left(-\frac{3}{2} \alpha TL \frac{\cos \alpha}{\sin \alpha} \cdot \sin \alpha\right) - \Delta 3y \sin \alpha = o$$

i.e. $3\alpha TL \cos\alpha - \Delta 3y \sin\alpha = 0$

or $\Delta 3y = 3\alpha TL \frac{\cos\alpha}{\sin\alpha}$

Substituting into eqn. C.34 gives

$$-\frac{\alpha TL}{2}\cos\alpha + 3\alpha TL \frac{\cos\alpha}{\sin\alpha} \cdot \sin\alpha - \Delta 4y \sin\alpha = 0$$

i.e. $\frac{5}{2}\alpha TL \cos\alpha - \Delta 4y \sin\alpha = 0$

or $\Delta 4y = \frac{5}{2}\alpha TL \frac{\cos\alpha}{\sin\alpha}$

substituting into eqn. C.45 gives

$$\frac{\alpha TL}{2}\cos\alpha + \frac{5}{2}\alpha TL \frac{\cos\alpha}{\sin\alpha} \cdot \sin\alpha - \Delta 5y \sin\alpha = 0$$

i.e. $3\alpha TL \cos\alpha - \Delta 5y \sin\alpha = 0$

or $\Delta 5y = 3\alpha TL \frac{\cos\alpha}{\sin\alpha}$

6.04 Analysis of statically indeterminate trusses for thermal stresses

6.04.1 Example (1) Effect of temperature in the top chord of a simple statically indeterminate truss

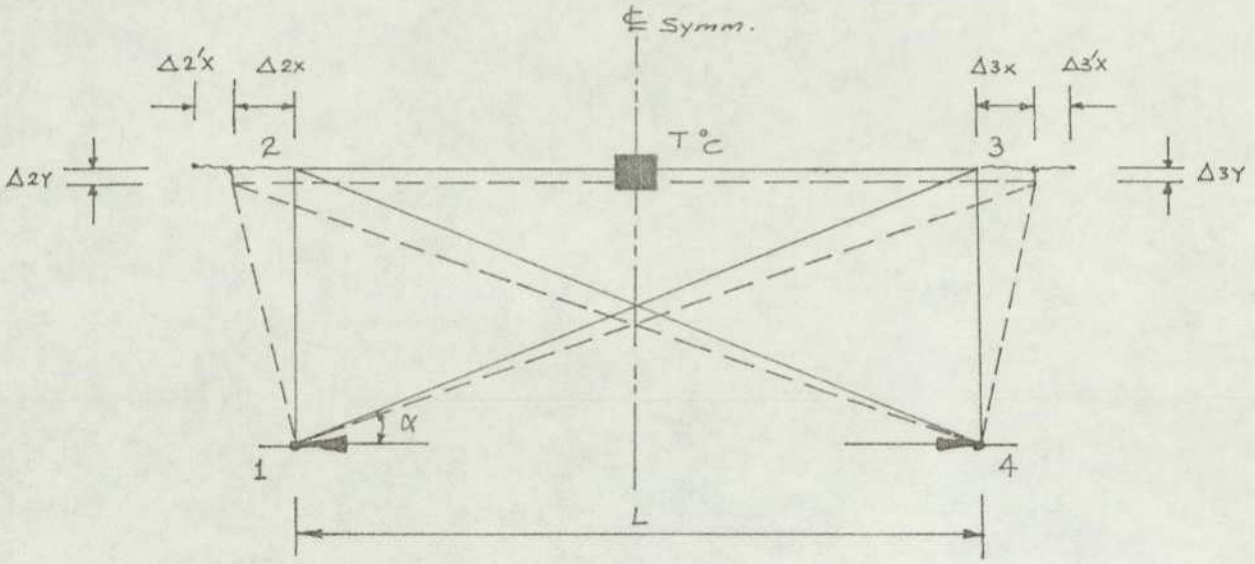

Fig. 6.0411 Effect of temperature in the top chord of a simple statically indeterminate truss

Denoting

$\Delta 2x, \Delta 3x$ __ __ __ horizontal displacements at joints 2 & 3

$\Delta 2y, \Delta 3y$ __ __ __ vertical displacements at joints 2 & 3

$\Delta 2'y, \Delta 3'x$ __ __ __ suppressed horizontal displacements at joints 2 & 3

By making use of the symmetry, only half the truss needs to be analysed.

The necessary conditions of compatibility of deformations and equilibrium of forces are as follows:-

Denoting $\Delta 2x + \Delta 2'x = \frac{1}{2} \alpha T L$

C.12 $\Delta 2y = \frac{N12\ L12}{A12\ E12}$

or $r\Delta 2y - N12\ S12 = o$ where $S12 = \frac{L12}{A12\ L12} \cdot \frac{An\ En}{Ln}$

and $r = \frac{An\ En}{Ln}$

C.13 $\Delta 3x \cos\alpha - \Delta 3y \sin\alpha = \frac{N13\ L13}{A13\ E13}$

or $r\,\Delta 3x \cos\alpha - r\Delta 3y \sin\alpha - N13\ S13 = o$ where $S13 = \frac{L13}{A13\ L13} \cdot \frac{An\ En}{Ln}$

C.23 $\Delta 2'x = \frac{N23\ L23/2}{A23\ E23}$

or $r\Delta 2x + N23\ \frac{S23}{2} = \frac{1}{2} r\alpha TL$ where $S23 = \frac{L23}{A23\ L23} \cdot \frac{An\ En}{Ln}$

E.1x $H1 - N13 \cos\alpha = o$

E.2x $N23 - N24 \cos\alpha = o$

or $N23 - N13 \cos\alpha = o$ since $N24 = N13$

E.2y $N12 - N2y \sin\alpha = o$

or $N12 - N13 \sin\alpha = o$

The general matrix for the analysis of the effect of temperature change in the truss shown in fig. 6.0411 can now be formulated as follows:-

EQN. No.	No.	1	2	3	4	5	6	LOAD VECTOR
	REF.JOINT	1			2			
	REF.EQN.	12	13	H1	23	r Δ2x	r Δ2y	
1	C.12	-S12	0	0			1	0
2	C.13	0	-S13	0		cos α	-Sin α	0
3	E.1x	0	-cos α	1				0
4	C.23				S23/2	1	0	½ r α TL
5	E.2x		-cos α		1	0	0	0
6	E.2y	1	-Sin α					0

Table 600.01 General matrix for the analysis of thermal stresses in the truss shown in fig. 6.0411

Taking $\alpha = 30^{\circ}$, L = Ln and assuming that the cross-sectional area A is constant throughout, the forces and displacements derived are shown in fig. 6.0412. The forces are in terms of r α TL and the displacements in terms of α TL.

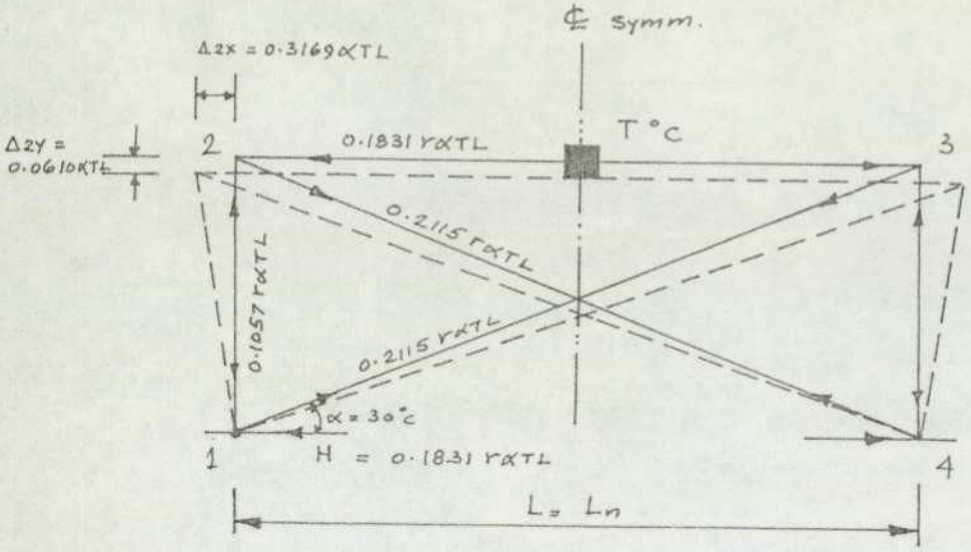

Fig. 6.0412 Showing stresses and deformations due to the temperature distribution in the top chord.

6.04.2 Example (2) Analysis of thermal stresses in a column of a simple statically indeterminate truss shown in fig. 6.0421

The conditions of compatability of deformations and equilibrium of forces are formulated in a similar way as shown above, but in this case symmetry cannot be used and a matrix for the whole truss has to be set out as shown in Table 600.02.

Taking $\alpha = 30^{\circ}$, L = Ln and cross-sectional area A, constant throughout, the forces and displacements derived are shown in fig. 6.0421. The forces are again in terms of r α TL and the displacements in terms of α TL.

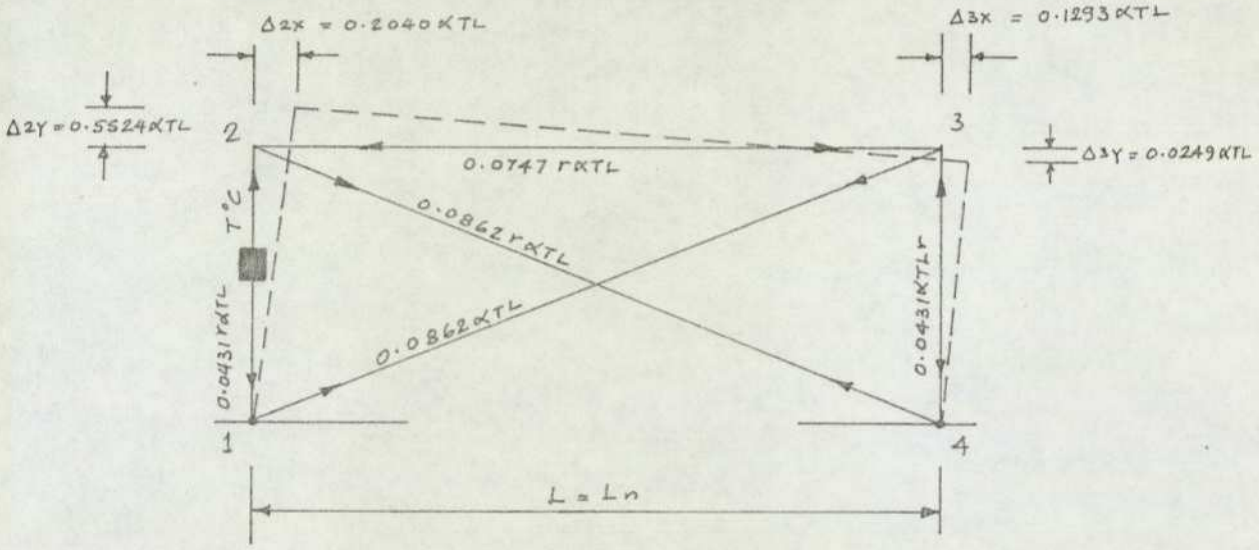

Fig. 6.0421 Showing stresses and deformations due to the temperature distribution in one column.

EQN. NO.	NO.	1	2	3	4	5	6	7	8	9	10	11	LOAD VECTOR
	REF.JOINT	1			2				3			4	
	REF. EQN.	12	13	H1	24	23	r Δ2x	r Δ2y	34	r Δ3x	r Δ3y	H4	
1	C.12	S13	0	0				1					r∝ Th
2	C.13	0	-S14	0						cos ∝	-Sin ∝		0
3	E.1x	0	cos ∝	-1									0
4	C.24				-S24	0	-cos ∝	Sin ∝					0
5	C.23				0	-S23	1	0		-1			0
6	E.2x				cos ∝	-1	0	0					0
7	E.2y	-1			Sin ∝	0	0	0					0
8	C.34								-S34	0	1		0
9	E.3x		cos ∝			-1			0	0	0		0
10	E.3y		sin ∝						-1	0	0		0
11	E.4x				cos ∝							-1	0

Table 600.02 General matrix for the analysis of the effect of temperature changes in the column of a truss shown in fig. 6.0421

6.04.3 Example (3) Analysis of thermal stresses in a cross-braced truss due to the effect of temperature variation in the top chord shown in fig. 6.0431

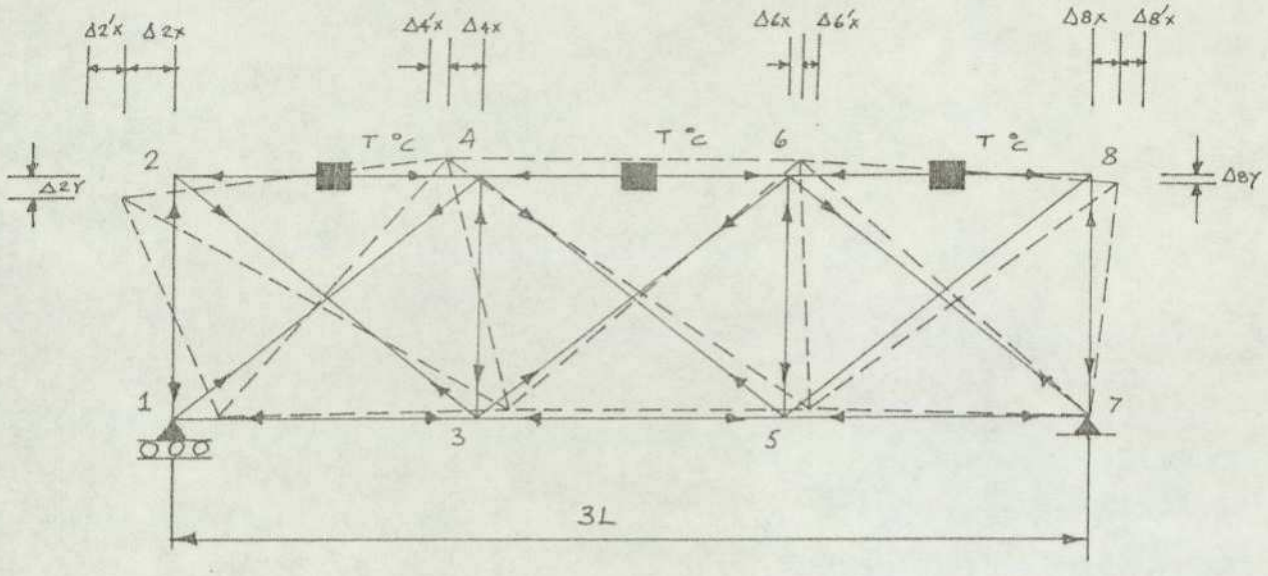

Fig. 6.0431

Denoting $\Delta 4x + \Delta 4x' + \Delta 6x + \Delta 6x' = \alpha TL$ ----- (i)

$\Delta 2x + \Delta 2x' + \Delta 8x + \Delta 8X' = 3\alpha TL$ ----- (ii)

$\Delta 2x + \Delta 2x' + \Delta 6x + \Delta 6x' = 2\alpha TL$ ----- (iii)

$\Delta 4x + \Delta 4x' + \Delta 8x + \Delta 8x' = 2\alpha TL$ ----- (iv)

In view of the support conditions, symmetry cannot be assumed and the equations of compatibility of deformations and equilibrium of forces have to be formulated for the whole structure as follows:-

C.24 $\Delta 2x' - \Delta 4'x = \frac{N24\ L24}{A24\ E24}$

or $r\Delta 4x - r\Delta 2x - N24\ S24 = -r\alpha TL$ using the above relationships

C.46 $\Delta 4x' + \Delta 5x' = \frac{N46\ L46}{A46\ E46}$

or $r\Delta 4x + r\Delta 6x + N46\ S46 = r\alpha TL$

C.68 $\Delta 8x - \Delta 6x' = \frac{N68\ L68}{A68\ E68}$

or $r\Delta 6x - r\Delta 8x - N68\ S68 = -r\alpha TL$

C.12 $\Delta 2y = \frac{N12\ L12}{A12\ E12}$

or $r\Delta 2y - N12\ S12 = o$

Similarly

C.12 $r\Delta 1x - r\Delta 3x - N13\ S13 = o$

C.14 $-r\Delta 1x \cos\alpha - r\Delta 4x \cos\alpha + r\Delta 4y \sin\alpha - N14\ S14 = o$

C.23 $r\Delta 2x \cos\alpha + r\Delta 3x \cos\alpha - r\Delta 3y \sin\alpha - r\Delta 2y \sin\alpha - N23\ S23 = o$

C.34 $r\Delta 3y - r\Delta 4y - N34\ S34 = o$

C.35 $r\Delta 3x - r\Delta 5x - N35\ S35 = o$

C.36 $-r\Delta 3x \cos\alpha - r\Delta 3y \sin\alpha + r\Delta 6x \cos\alpha + r\Delta 6y \sin\alpha - N36\ S36 = o$

C.45 $r\Delta 4x \cos\alpha + r\Delta 4y \sin\alpha + r\Delta 5x \cos\alpha - r\Delta 5y \sin\alpha - N45\ S45 = o$

C.56 $r\Delta 5y - r\Delta 6y - N56\ S56 = o$

C.57 $r\Delta 5x - N57\ S57 = o$

C.58 $-r\Delta 5x \cos\alpha - r\Delta 5y \sin\alpha + r\Delta 8x \cos\alpha - r\Delta 8y \sin\alpha - N58\ S58 = o$

C.67 $-r\Delta 6x \cos\alpha + r\Delta 6y \sin\alpha - N67\ S67 = o$

C.78 $r\Delta 8y - N78\ S78 = o$

E.1x $N13 - N14 \cos\alpha = o$

E.1y $N12 - N14 \sin\alpha - R1 = o$

E.2x $N24 - N23 \cos\alpha = o$

E.2y $N12 - N23 \sin\alpha = o$

E.3x $N13 - N35 - N23 \cos\alpha + N36 \cos\alpha = o$

E.3y $N34 - N23 \sin\alpha - N36 \sin\alpha = o$

E.4x $N24 - N46 + N45 \cos\alpha - N14 \cos\alpha = o$

E.4y $N34 - N14 \sin\alpha - N45 \sin\alpha = o$

E.5x $N35 - N57 - N45 \cos\alpha + N58 \cos\alpha = o$

E.5y $N56 - N45 \sin\alpha - N58 \sin\alpha = o$

E.6x $N46 - N68 - N36 \cos\alpha + N67 \cos\alpha = o$

E.6y $N56 - N36 \sin\alpha - N67 \sin\alpha = o$

E.7x N57 - N67 cos α - H7 = o

E.7y N78 - N67 Sin α - R7 = o

E.8x N68 - N58 cos α = o

E.8y N78 - N58 Sin α = o

The overall general matrix is shown in Table 600.03.

Assuming that $\alpha = 30^{o}$, L = Ln = 2000mm, A = 2.409 x $10^{3}mm^{2}$ throughout, E = 200 KN/mm^{2}, the forces and displacements obtained are shown in fig. 6.0432 T = $10^{o}C$

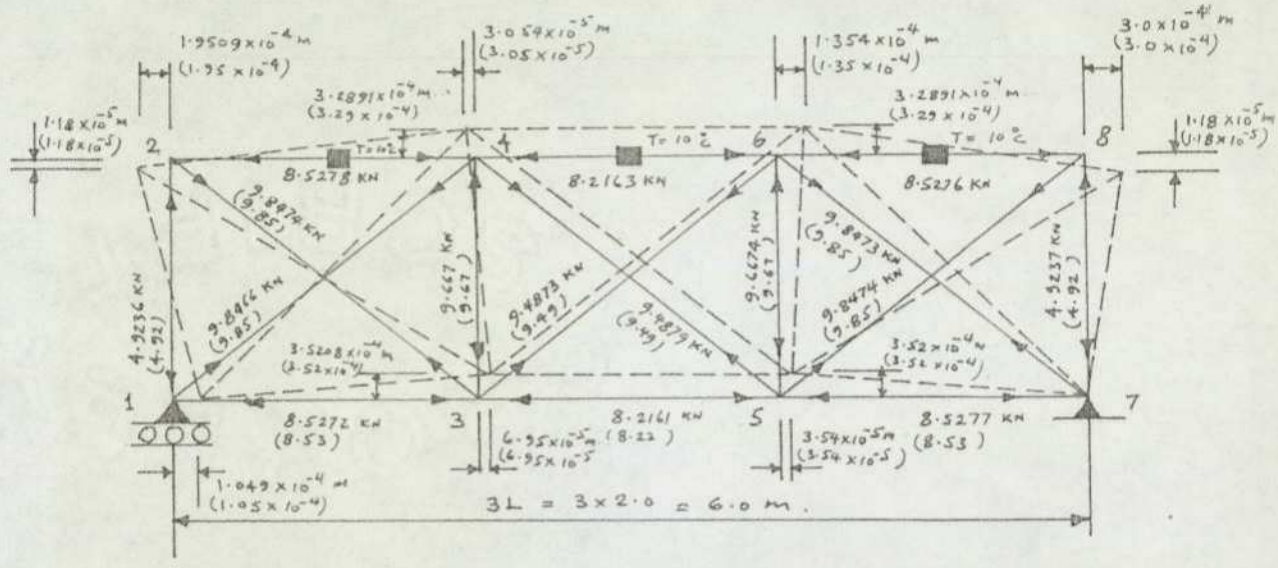

Fig. 6.0432 Showing stresses and deformations in a cross-braced truss due to the temperature distribution in the entire top chord as shown.

REF. No		1	2	3	4	5	6	7	8	9	10	11	12	13	14	15	16	17	18	19	20	21	22	23	24	25	26	27	28	29	30	31	32	LOAD VECTOR
	REF. JT.	1					2				3					4				5					6				7			8		
	REF. EQN.	12	13	14	R_1	$r\Delta_{1x}$	23	24	$r\Delta_{2x}$	$r\Delta_{2y}$	34	35	36	$r\Delta_{3x}$	$r\Delta_{3y}$	45	46	$r\Delta_{4x}$	$r\Delta_{4y}$	56	57	58	$r\Delta_{5x}$	$r\Delta_{5y}$	67	68	$r\Delta_{6x}$	$r\Delta_{6y}$	78	R_7	H_7	$r\Delta_{8x}$	$r\Delta_{8y}$	
1	C 12	$-S_{12}$	0	0	0	0				1																								0
2	C 13	0	$-S_{13}$	0	0	1								-1		4																		0
3	C 14	0	0	$-S_{14}$	0	$-\cos\alpha$								-				$-\cos\alpha$	$\sin\alpha$															0
4	E 1X	0	1	$-\cos\alpha$	0	0																												0
5	E 1Y	1	0	$-\sin\alpha$	-1	0																												0
6	C 23						$-S_{23}$	0	$\cos\alpha$	$-\sin\alpha$				$\cos\alpha$	$-\sin\alpha$																			0
7	C 24						0	$-S_{24}$	-1	0								1																	$-r\alpha T1$
8	E 2X						$-\cos\alpha$	1	0	0																									0
9	E 2Y	1					$-\sin\alpha$	0	0	0																										0
10	C 34										$-S_{34}$	0	0	0	1				-1																0
11	C 35										0	$-S_{35}$	0	1	0								-1												0
12	C 36										0	0	$-S_{36}$	$-\cos\alpha$	$-\sin\alpha$												$\cos\alpha$	$\sin\gamma$						0
13	E 3X		1				$-\cos\alpha$				0	-1	$\cos\alpha$	0	0																				0
14	E 3Y						$-\sin\alpha$				1	0	$-\sin\alpha$	0	0																				0
15	C 45															$-S_{45}$	0	$\cos\alpha$	$\sin\alpha$				$\cos\alpha$	$-\sin\alpha$										0
16	C 46															0	S_{46}	1	0								1								$r\alpha T1$
17	E 4X			$-\cos\alpha$				1								$\cos\alpha$	-1	0	0																0
18	E 4Y			$-\sin\alpha$							1					$-\sin\alpha$	0	0	0																0
19	C 56																			$-S_{56}$	0	0	0	1				-1						0
20	C 57																			0	$-S_{57}$	0	1	0										0
21	C 58																			0	0	$-S_{58}$	$-\cos\alpha$	$-\sin\alpha$								$\cos\alpha$	$-\sin\alpha$	0
22	E 5X											1				$-\cos\alpha$				0	-1	$\cos\alpha$	0	0										0
23	E 5Y															$-\sin\alpha$				1	0	$-\sin\alpha$	0	0										0
24	C 67																								$-S_{67}$	0	$-\cos\alpha$	$\sin\alpha$						0
25	C 68																								0	$-S_{68}$	1	0				-1		$-r\alpha T1$
26	E 6X												$-\cos\alpha$				1								$\cos\alpha$	-1	0	0						0
27	E 6Y												$-\sin\alpha$							1					$-\sin\alpha$	0	0	0						0
28	C 78																												$-S_{78}$	0	0	0	1	0
29	E 7X																				1				$-\cos\alpha$				0	0	-1	0	0	0
30	E 7Y																								$-\sin\alpha$				1	-1	0	0	0	0
31	E 8X																					$-\cos\alpha$				1								0
32	E 8Y																					$-\sin\alpha$							1					0

Table: 600.03 General matrix for the analysis of the effect of temperature change in the entire top chord of the cross-braced truss shown in fig. 6.0431

6.05 Analysis of thermal stresses due to temperature distribution in individual members of statically indeterminate trusses

6.05.1 Example (4) Stresses due to temperature distribution in end segment of top chord

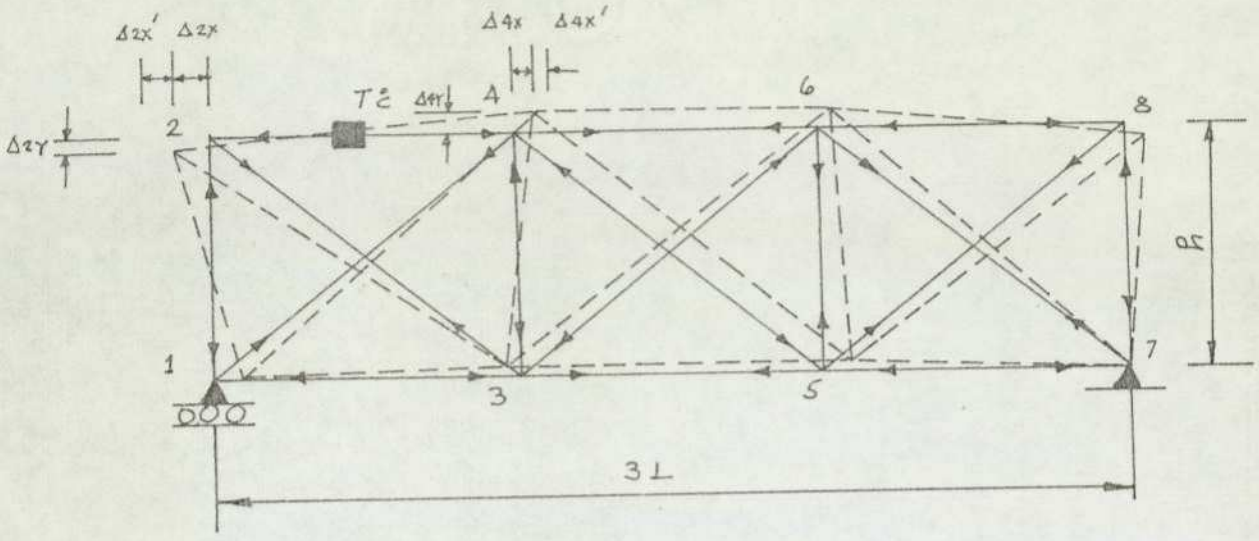

Fig.6.0511 Analysis of thermal stresses due to temperature distribution in one member as shown.

Denoting $\Delta 2x$, $\Delta 4x$ - actual Horizontal displacements at joints 2 & 4

$\Delta 2x'$, $\Delta 4x'$ - suppressed horizontal displacements at joints 2 & 4

$$\Delta 2x + \Delta 2x' + \Delta 4x + \Delta 4x' = \alpha TL$$

The conditions of compatibility of deformations and equilibrium of forces can now be set out as before. Assuming that $\alpha = 30^0$ and L13 = Ln = 2000mm, A = 2.409×10^3mm throughout, E = 200 KN/mm^2, $\alpha = 0.00001$ per ^{0}C and T = 10^0C, the numerical matrix is shown in Table 600.04.

The results of the solution of the matrix in Table 600.04 are shown in fig. 6.0512.

REF. No		1	2	3	4	5	6	7	8	9	10	11	12	13	14	15	16	17	18	19	20	21	22	23	24	25	26	27	28	29	30	31	32	LOAD VECTOR
	REF. JT.	1					2				3					4				5							6		7			8		
	REF. EQN.	12	13	14	R_1	$r\Delta_{1X}$	23	24	$r\Delta_{2X}$	$r\Delta_{2Y}$	34	35	36	$r\Delta_{3X}$	$r\Delta_{3Y}$	45	46	$r\Delta_{4X}$	$r\Delta_{4Y}$	56	57	58	$r\Delta_{5X}$	$r\Delta_{5Y}$	67	68	$r\Delta_{6X}$	$r\Delta_{6Y}$	78	R_7	M_7	$r\Delta_{8X}$	$r\Delta_{8Y}$	
1	C 12	-.5774	0	0	0	0				+1																								0
2	C 13	0	-1	0	0	+1								+1																				0
3	C 14	0	0	+1.1547	0	-.8660												+.8660	+0.5															0
4	E 1X	0	+1	-.8660	0	0																												0
5	E 1Y	+1	0	-0.5	-1	0																												0
6	C 23						-1.1547	0	+.8660	+0.5				-.8660	-0.5																			0
7	C 24						0	+1	+1	0								+1																$\Gamma_{RTL} = +48.18 \times 10^3$
8	E 2X						-.8660	+1	0	0																								
9	E 2Y	+1					-0.5	0	0	0																								0
10	C 34										-.5774	0	0	0	+1				-1															0
11	C 35										0	-1	0	+1	0								+1											0
12	C 36										0	0	-1.1547	-.8660	+0.5												-.8660	-0.5						0
13	E 3X		+1				-.8660				0	+1	-.8660	0	0																			0
14	E 3Y						-0.5				+1	0	+0.5	0	0																			0
15	C 45															+1.1547	0	+.8660	-0.5				-.8660	+0.5										0
16	C 46															0	-1	-1	0								+1							0
17	E 4X			-.8660				+1								-.8660	+1	0	0															0
18	E 4Y			-0.5							+1					+0.5	0	0	0															0
19	C 56																			-.5774	0	0	0	-1				+1						0
20	C 57																			0	-1	0	+1	0										0
21	C 68																			0	0	-1.1547	-.8660	-0.5										0
22	E 5X											+1				-.8660				0	+1	-.8660	0	0								+.8660	-0.5	0
23	E 5Y															-0.5				+1	0	+0.5	0	0										0
24	C 67																								-1.1547	0	-.8660	+0.5						0
25	C 68																								0	-1	+1	0				-1		0
26	E 6X												-.8660				+1								-.8660	+1	0	0						0
27	E 6Y												-0.5							+1					+0.5	0	0	0						0
28	C 7B																												-.5774	0	0	0	+1	0
29	E 7X																				+1				-.8660				0	0	-1	0	0	0
30	E 7Y																								-0.5				+1	-1	0	0	0	0
31	E 8X																					-.8660	0	0	0	+1	0	0	0					0
32	E 8Y																					-0.5	0	0	0	0	0	0	+1					0

Table: 600.04 Numerical matrix for the analysis of the effect of temperature change in end segment of top chord of a cross-braced truss as shown in fig. 6.0511

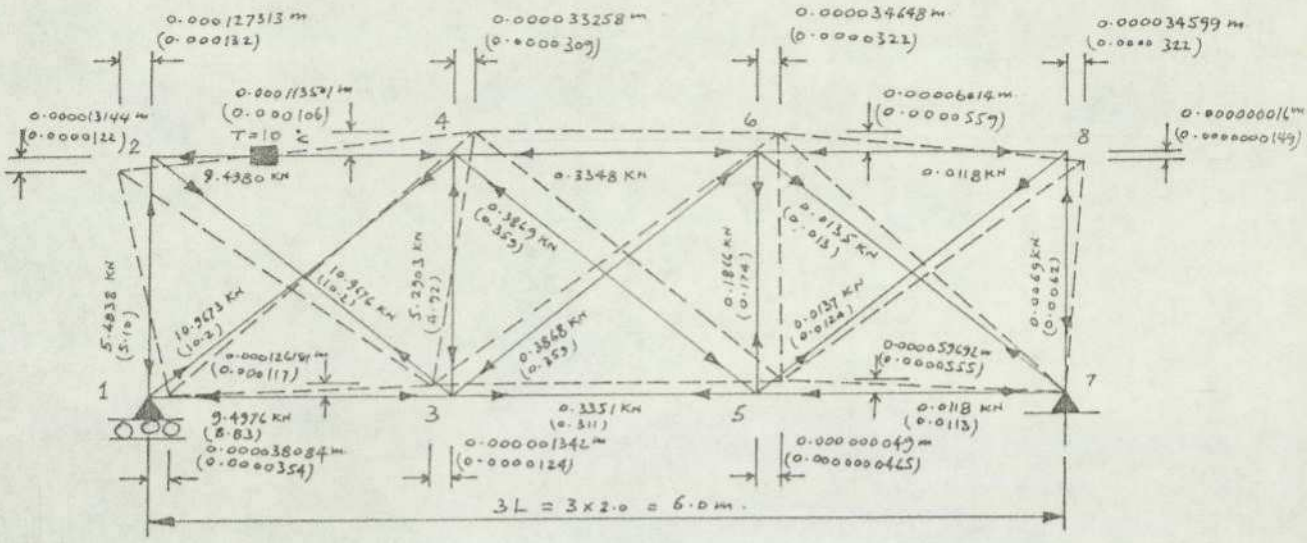

Fig. 6.0512 Showing stresses and deformations in a cross-braced truss due to the temperature distribution in one member as shown.

6.05.2 Example (5) Stresses due to temperature distribution in the middle segment of top chord

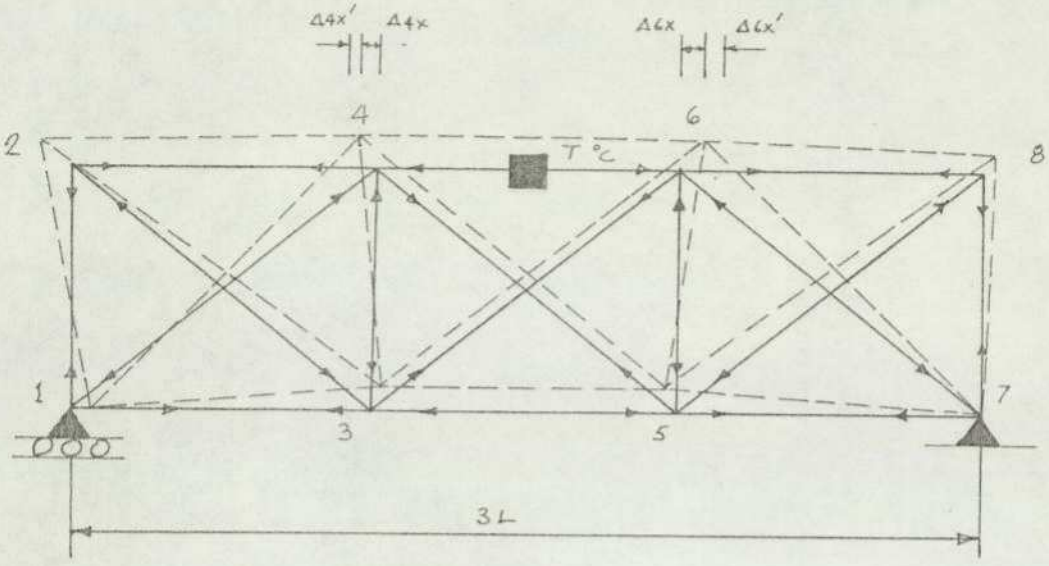

Fig.6.0521 Analysis of thermal stresses due to temperature change in one member only

Denoting $\Delta 4x$, $\Delta 6x$ - horizontal displacements at joints 4 & 6

$\Delta 4x'$, $\Delta 6x'$ - suppressed horizontal displacements at joints 4 & 6

$$\Delta 4x + \Delta 4x' + \Delta 6x + \Delta 6x' = \alpha TL$$

For a truss of similar properties as in example (3) the numerical matrix is shown in Table 600.05 and the resulting forces and displacements are indicated in fig. 6.0522.

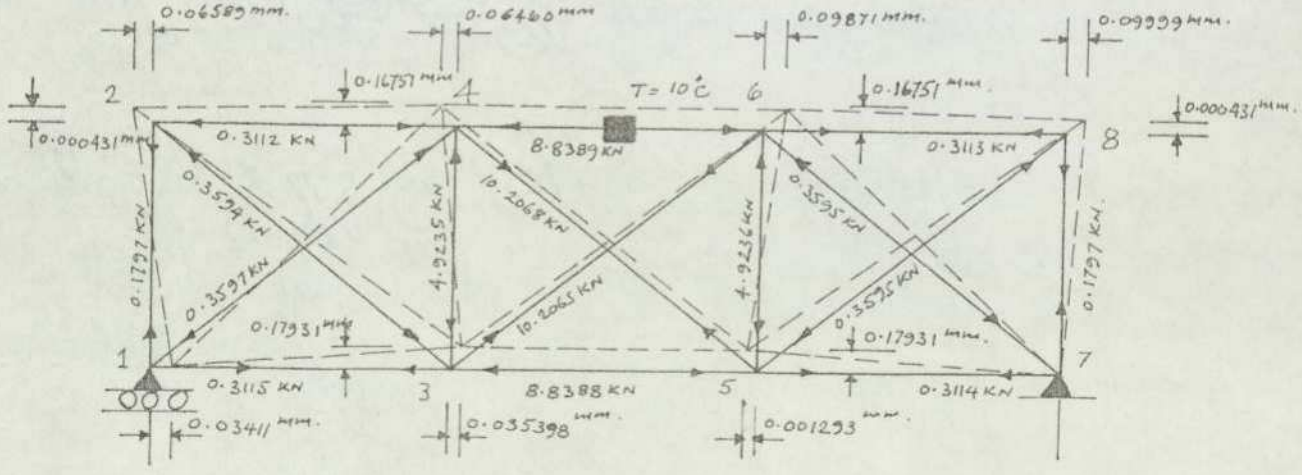

Fig. 6.0522 Showing stresses and deformations due to temperature distribution in one member as shown.

REF. No		1	2	3	4	5	6	7	8	9	10	11	12	13	14	15	16	17	18	19	20	21	22	23	24	25	26	27	28	29	30	31	32	LOAD VECTOR
No	REF. JT.	1					2				3					4				5					6				7			8		
	REF. EQN.	12	13	14	R_1	$r\Delta_{1x}$	23	24	$r\Delta_{2x}$	$r\Delta_{2y}$	34	35	36	$r\Delta_{3x}$	$r\Delta_{3y}$	45	46	$r\Delta_{4x}$	$r\Delta_{4y}$	56	57	58	$r\Delta_{5x}$	$r\Delta_{5y}$	67	68	$r\Delta_{6x}$	$r\Delta_{6y}$	78	R7	H7	$r\Delta_{8x}$	$r\Delta_{8y}$	
1	C 12	-0.5774	0	0	0	0				+1																								0
2	C 13	0	-1	0	0	-1								+1																				0
3	C 14	0	0	-1.1547	0	+0.866												+0.866	-0.5															0
4	E 1X	0	+1	-0.866	0	0																												0
5	E 1Y	+1	0	-0.5	+1	0																												0
6	C 23						-1.1547	0	-0.866	-0.5				-0.866	+0.5																			0
7	C 24						0	-1	+1	0								-1																0
8	E 2X						+0.866	+1	0	0																								0
9	E 2Y	+1					-0.5	0	0	0																								0
10	C 34										-0.5774	0	0	0	+1				-1															0
11	C 35										0	-1	0	+1	0								+1											0
12	C 36										0	0	+1.1547	-0.866	-0.5												+0.866	+0.5						0
13	E 3X		+1				-0.866				0	+1	-0.866	0	0																			0
14	E 3Y						+0.5				+1	0	-0.5	0	0																			0
15	C 45															-1.1547	0	+0.866	+0.5				+0.866	-0.5										0
16	C 46															0	+1	+1	0								+1							$T \times TL = 48.18 \times 10^3$
17	E 4X			-0.866				+1								-0.866	+1	0	0															0
18	E 4Y			+0.5							+1					-0.5	0	0	0															0
19	C 56																			-0.5774	0	0	0	+1				-1						0
20	C 57																			0	-1	0	+1	0										0
21	C 58																			0	0	-1.1547	-0.866	+0.5								-0.866	-0.5	0
22	E 5X											+1				-0.866				0	+1	-0.866	0	0										0
23	E 5Y															-0.5				+1	0	+0.5	0	0										0
24	C 67																								-1.1547	0	+0.866	-0.5						0
25	C 68																								0	-1	-1	0				+1		0
26	E 6X												-0.866				+1								-0.866	+1	0	0						0
27	E 6Y												-0.5							+1					+0.5	0	0	0						0
28	C 78																												-0.5774	0	0	0	+1	0
29	E 7X																				+1				-0.866				0	0	-1	0	0	0
30	E 7Y																								-0.5				+1	+1	0	0	0	0
31	E 8X																					-0.866				+1								0
32	E 8Y																					-0.5							+1					0

Table: 600.05 Numerical matrix for the analysis of the effect of temperature change in one member of the cross-braced truss as shown in fig. 6.0521

6.06 Discussion of results of thermal stress analysis of trusses

The results of this section show that stresses and deformations caused by thermal changes in members of trusses can also be analysed with equal ease by the method of force-displacement. In this method, the load-deflection characteristics of members are used in the form of the linear flexibility coefficients and these provide an analytical link between the geometry of structure, system of loading, compatibility of deformations and equilibrium of forces. In contrast to the traditional methods, the force-displacement method shows one distinct superiority, that is, the ease with which deflections, whether due to thermal stresses or gravity loads, can be calculated.

The analysis of a statically determinate truss for thermal stresses shows a very interesting phenomenon: That in statically determinate trusses, temperature changes result only in displacements of joints without any stresses in the members. This result can be concluded by a mere inspection of the structure without having to do any calculations.

The analysis of displacements of joints show that the displacements are proportional to the length of members, the coefficient of extension and the temperature change. The cross-sectional areas of members, or the modulus of elasticity of the material, has no bearing on the magnitude of the displacements.

The analysis of statically indeterminate trusses for thermal stresses show that in addition to displacements of joints, members are also subject to axial forces and deformations. It has been shown, that even for a small temperature change of $10^{\circ}C$ large stresses and deformations can take place. An inspection of the results of examples (3), (4) and (5) confirm the validity of the principle of superposition, which is adequate for practical purposes.

As in the case of statically determinate trusses, the displacements are proportional to the length of members, the coefficient of extension and the temperature change. However, the stresses in the members are not only proportional to the above parameters, but also to the modulus of elasticity of the material. This aspect is of great importance in practical application in the design.

7.00 THERMAL STRESSES IN BRIDGES

7.01 Introduction

Observations show, that temperature variations in bridge decks can cause high stresses and even cracks. For this reason, it is a requirement of the code of practice, that all bridges should be designed for the effects of differential temperature. The draft code gives the minimum and maximum temperatures and the range of temperatures to be considered as affecting the structure. These are based on Transport & Road Research Laboratory Report LR 765, "Temperature differentials in bridges". The effective minimum and maximum temperatures are dependent on the depth of surfacing and the type of construction. The chart on the following sheet gives the recommended "Temperature Differences for Different Types of Construction".

In the following sections, an attempt is made to develop an approximate method of analysing the stresses in different forms of bridge decks due to the effects of differential temperatures.

PERATURE DIFFERENCES FOR DIFFERENT TYPES OF CONSTRUCTION

ROUP	TYPE OF CONSTRUCTION	TEMPERATURE DIFFERENCE °C

Steel deck on steel box girders

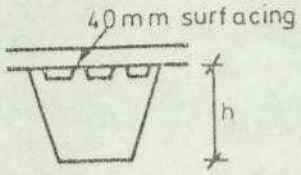

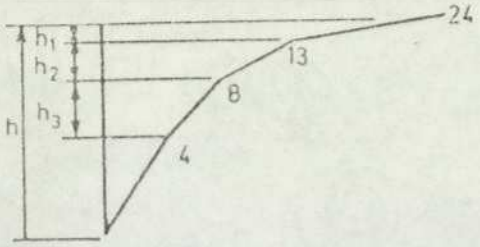

h_1 = 0·1 metres
h_2 = 0·2 metres
h_3 = 0·3 metres

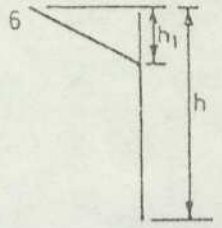

h_1 = 0·5 metres

Steel deck on steel truss or plate girders

Use differences as for Group 1

Concrete deck on steel box, truss or plate girders.

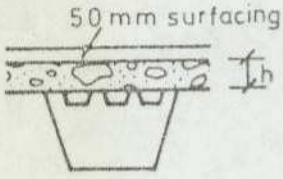

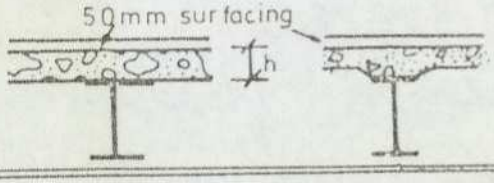

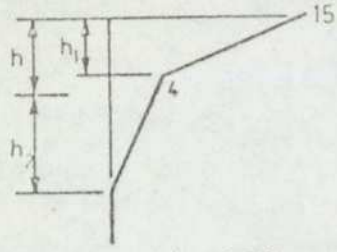

h_1 = 0·75h
h_2 = 0·4 metres

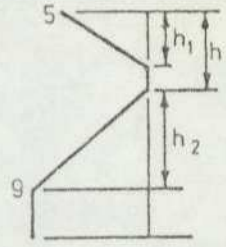

---

4 Concrete slab or concrete deck on concrete beams or box girders

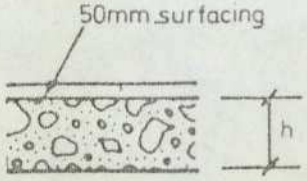

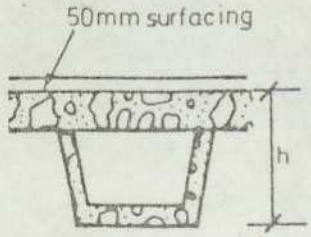

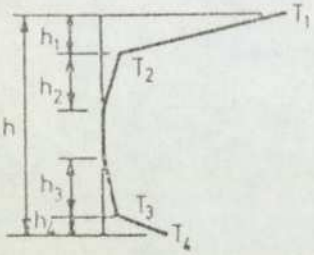

h_1 = 0·6h ± 0·2m
h_2 = 0·4(h-h_1) ± 0·3m
h_4 = 0·4(h-h_1) ± 0·1m
h_3 = h-(h_1+h_2+h_4) ± 0·2m

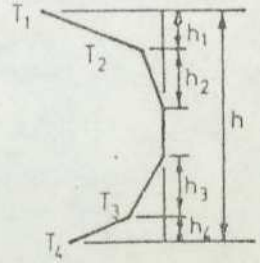

h_1 = 0·4h ± 0·2m
h_2 = 0·3h ± 0·3m
h_4 = 0·4(h-h_1) ± 0·1m
h_3 = h-(h_1+h_2+h_4) ± 0·2m

h metres	T_1	T_2	T_3	T_4
	°centigrade			
0·2	9·5	0·5	0·2	0·5
0·4	13·5	0·75	0·5	2·5
0·6	15·0	1·0	1·0	4·0
0·8	16·0	1·75	1·5	5·0
≥ 0·9	16·0	2·0	1·5	5·0

h metres	T_1	T_2	T_3	T_4
	°centigrade			
0·2	3·5	0·5	0·25	1·5
0·4	6·5	0·75	0·5	3·5
0·6	8·5	1·0	1·5	5·0
0·8	10·0	1·5	2·5	6·5
≥ 0·9	10·5	2·0	3·5	7·0

7.02 General formulations for the effects of differential temperature on any structural member

So far, the effect of temperature changes on prismatic members with rectangular cross-sections have been considered, and in each case the problem has been treated as a specific individual case and not as a general solution. However, in practice one very often encounters problems of members of any cross-section subjected to complex temperature differentials, e.g. various forms of bridge structures, some of which will be dealt with later in the text.

In the following section, general formulations are developed for the effects of differential temperature on any structural element.

The element to be considered, as shown in fig. 7.021(a), is divided into horizontal segments such that the temperature distribution across any segment is linear. If the member is fully restrained from expanding, the force required would be $P = AE\alpha T$

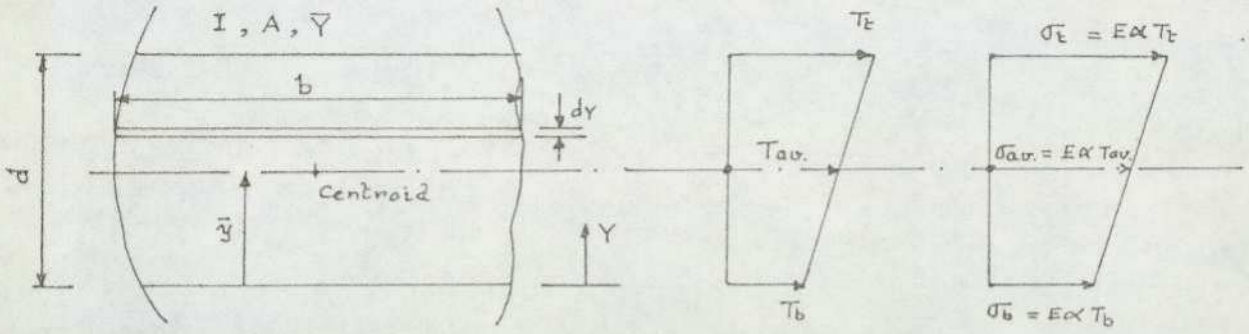

(a) (b) strain diagram (c) stress diagram

Fig. 7.021

and the magnitude of stress, Total $= E\alpha T$

and the stress at any level, $= E\alpha Tb\ (1-\frac{Y}{d}) + E\alpha Tt\ (\frac{Y}{d})$

For the section under consideration, the stress diagram is as shown in Fig. 7.021(c).

If now the restraint is removed, a condition of plane strain is set up with the resultant localised stresses whose net moment and axial force on the section are zero. In order to define this plane strain condition, it is necessary to equate the released moment and the axial force, with the moment and axial force due to the original stress in the restrained condition.

7.021 Effect of linear temperature distribution on a fully restrained section

Consider the effect of temperature on a small element, dy of a segment of thickness d

(i) Axial force on segment,

$$P = \int_o^d b.\sigma.\,dy$$

$$= \int_o^d b.E.\alpha\left(Tb\left(1 - \frac{y}{d}\right) + Tt\,\frac{y}{d}\right) dy$$

$$= E\alpha\left\{Tb\left(\int_o^d b.dy - \frac{1}{d}\int_o^d b.y.\,dy\right) + \frac{Tt}{d}\int_o^d b.y.\,dy\right\}$$

$$= E\alpha\int_o^d b.dy\left\{Tb\left(1 - \frac{1}{d}\cdot\frac{\int_o^d b.y.\,dy}{\int_o^d b.dy}\right) + \frac{Tt}{d}\cdot\frac{\int_o^d b.y.dy}{\int_o^d b.dy}\right\}$$

$$= E.\alpha.A\left\{Tb\left(1 - \frac{\bar{y}}{d}\right) + Tt\,.\,\frac{\bar{y}}{d}\right\}$$

$$= E.\alpha.A.Tav.$$

$\therefore$ Total axial force on section for n segments $= \sum_{i=1}^{n} (E.\alpha.Ai.Tav.i)$

(ii) Moment on segment about its own centroid

$$m = \int_o^d b.\sigma.(y-\bar{y})\,dy$$

$$= \int_o^d b.E.\alpha\left\{Tb\left(1 - \frac{y}{d}\right) + Tt.\,\frac{y}{d}\right\}(y - \bar{y})\,dy$$

$$= E.\alpha.\left\{Tb\left(\int_o^d b\,\cancel{(y-\bar{y})}^{\,0}\,dy - \frac{1}{d}\int_o^d b.y\,(y-\bar{y})\,dy\right) + \frac{Tt}{d}\int_o^d b.y\,\cancel{(y-\bar{y})}^{\,0}\,dy\right\}$$

but $\int_o^d b(y-\bar{y})\,dy = 0$ i.e. the moment of area about its own centroid is zero

$$\therefore M = E.\alpha\left(-\frac{Tb}{d}\int_o^d b.y\ (y-\bar{y})\ dy + \frac{Tt}{d}\int_o^d b.y\ (y-\bar{y})\ dy\right)$$

$$= E.\alpha\left(\frac{Tt-Tb}{d}\right)\left\{\int_o^d b\ (y-\bar{y})^2 dy + \bar{y}\int_o^d b\ (y-\bar{y})\, dy\right\}$$

$$= E.\alpha\left(\frac{Tt-Tb}{d}\right) I$$

$$= E\alpha I\ \frac{\Delta T}{d} \qquad \text{where } \Delta T = Tt-Tb$$

Now, if the height of the centroid of segment above the bottom of section is given by y', then the moment about the base is given by:-

M = moment of forces on segment about its own centroid

+ Axial force on segment x y'

$$= E.\alpha.I.\ \frac{\Delta T}{d} + E\alpha A\ Tav.y'$$

$\therefore$. The total moment of a fully restrained section about the bottom of the section, $M = \sum_{i=1}^{n} \left(E.\alpha.Ii\ \frac{\Delta Ti}{di} + E.\alpha.\ Ai\ Tav.i\ y'i\right)$

7.02.2 For plane strain release

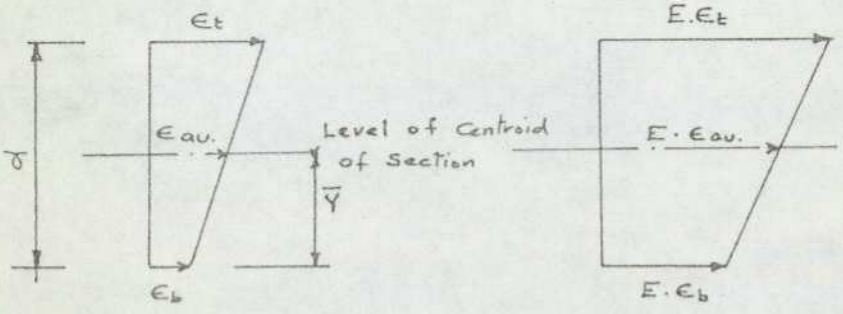

(a) Plane Strain (b) Stress released by Plane Strain

Fig. 7.0221

By similar argument as for the effect of temperature above,

Total axial force on section

$$Pps = E.A.\epsilon av.$$

and total moment at bottom of section

$$M = E\ I\ \frac{\Delta\epsilon}{d} + E.A.\epsilon av.\ \bar{y}$$

where $\Delta\epsilon = (\epsilon t - \epsilon b)$

Now equating the axial forces and moments for the two conditions considered above gives

Axial Force $\sum_{i=1}^{n} (E.\alpha.Ai.\ Tav.i) = E.A.\epsilon av.$

i.e. $\sum_{i=1}^{n} \alpha(Ai.Tav.i) = A.\epsilon av.$ ..... (1)

Moment $\sum_{i=1}^{n} (E.\alpha.Ii\frac{\Delta Ti}{di} + E.\alpha.Ai.Tav.i\ y'i) = EI\ \frac{\Delta\epsilon}{d} + E.A.\epsilon av.\bar{y}$

i.e. $\sum_{i=1}^{n} \alpha(Ii\ \frac{\Delta Ti}{di} + Ai.Tav.i.y'i) = I\ \frac{\Delta\epsilon}{d} + A.\epsilon av.\bar{y}$ --- (2)

The equations (1) and (2) can now be used as simultaneous equations in ϵ_b and ϵ_t (the strains at the bottom and top of the section).

EXAMPLES

7.03 Plate Bridges

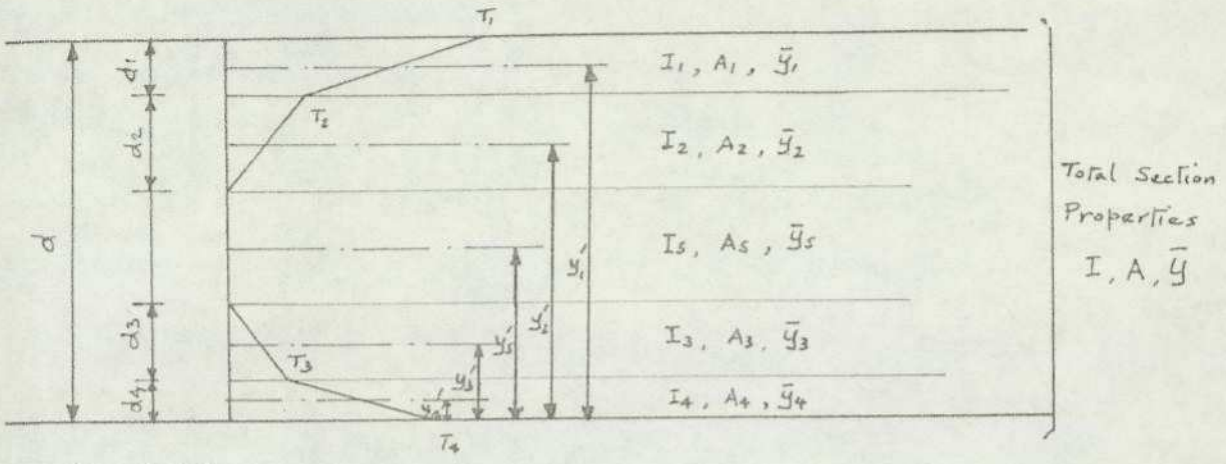

Fig. 7.031

Equating the axial forces in the fully restrained section to the axial force released by allowing plane strain gives

$$\alpha\left[A1\left\{T1\left(\frac{\bar{y}1}{d1}\right) + T2\left(1-\frac{\bar{y}1}{d1}\right)\right\} + A2.T2.\left(\frac{\bar{y}2}{d2}\right) + A3.T3\left(1-\frac{\bar{y}3}{d3}\right) + A4\left\{T3\left(\frac{\bar{y}4}{d4}\right) + T4\left(1-\frac{\bar{y}4}{d4}\right)\right\}\right] = A\left\{\epsilon b\left(1-\frac{\bar{y}}{d}\right) + \epsilon t\left(\frac{\bar{y}}{d}\right)\right\} \quad \text{--------- (1)}$$

By equating the bending moment about the bottom of the slab in the fully restrained section to the moment released by allowing plane strain we obtain

$$\alpha\left[\left(\frac{T1-T2}{d1}\right) \cdot I1 + A1\left\{T1\left(\frac{\bar{y}1}{d1}\right) + T2\left(1-\frac{\bar{y}1}{d1}\right)\right\} y1' + \frac{T2}{d2} \cdot I2 + A2.T2\left(\frac{\bar{y}2}{d2}\right)y2' + \left(\frac{-T3}{d3}\right) I3 + A3.T3\left(1-\frac{\bar{y}3}{d3}\right)y3' + \frac{(T3-T4)}{d4} I4 + A4\left\{T3\left(\frac{\bar{y}4}{d4}\right) + T4\left(1-\frac{\bar{y}4}{d4}\right)\right\} y4'\right] = \frac{(\epsilon t-\epsilon b)}{d} \cdot I + A\left\{\epsilon b\left(1-\frac{\bar{y}}{d}\right) + \epsilon t\left(\frac{\bar{y}}{d}\right)\right\}\bar{y} \quad \text{- - - - - (2)}$$

If $d1 = 200mm$

$d2 = 300mm$

$d3 = 200mm$

$d4 = 100mm$

$d = 1000mm$

For a section 10m wide

$A1 = 10 \times 0.2 = 2m^2$: $I1 = 10 \times \frac{0.2^3}{12} = 0.0067m^4$; $\bar{y}1 = 0.1m$

$A2 = 10 \times 0.3 = 3m^2$; $I2 = 10 \times \frac{0.3^3}{12} = 0.0225m^4$; $\bar{y}2 = 0.15m$

$A3 = 10 \times 0.2 = 2m^2$: $I3 = 10 \times \frac{0.2^3}{12} = 0.00667m^4$; $\bar{y}3 = 0.1m$

$A4 = 10 \times 0.1 = 1m^2$: $I4 = 10 \times \frac{0.1^3}{12} = 0.00083m^4$; $\bar{y}4 = 0.05m$

$A = 10 \times 1 = 10m^2$: $I = 10 \times \frac{1^3}{12} = 0.83333m^4$; $\bar{y} = 0.50m$

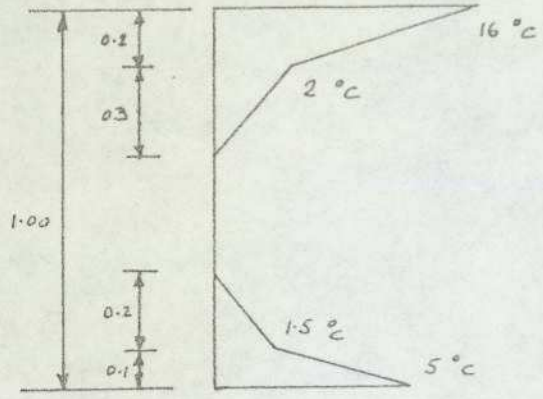

Fig. 7.032

Member	Area of heated zone of Slab (m^2)	Lever arm, La, from centre of heated zone to base of Slab in (m)	Temp. Tav. ^{o}C at centroid of heated zone	Axial Force in section due to Temp., F= AlEα Tav.	Temp. gradient across heated zone in $^{o}C/m$.	Bending Moment at base of section = F.La + IlE $\Delta T \alpha/d$
A	2	0.900	9	18 Eα	70.00	16.6690 Eα
B	3	0.650	1	3 Eα	6.6667	2.1000 Eα
C	2	0.400	0	0	0	0
D	2	0.200	0.75	1.5 Eα	-7.50	0.2500 Eα
E	1	0.050	3.25	3.25 Eα	-35.00	0.1335 Eα

Table: 700.01

Σ 25.75 Eα

Σ 19.1525 Eα

Plane Strain

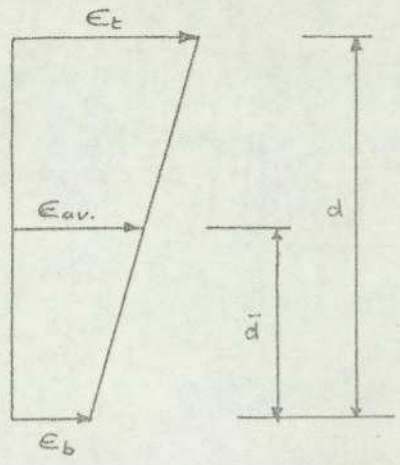

Fig. 7.033

Strain at any point is given by the expression

$$\epsilon = \epsilon_b\left(1-\frac{\bar{d}}{d}\right) + \epsilon_t\left(\frac{\bar{d}}{d}\right)$$

Axial Force released, $F = A.E.\epsilon = 10E\left\{\epsilon_b\left(1-\frac{\frac{1}{2}d}{d}\right) + \epsilon_t\left(\frac{\frac{1}{2}d}{d}\right)\right\}$

$$= 10E\ \{0.5\,\epsilon_b + 0.5\,\epsilon_t\}$$

Bending moment " , $M = A.E.\epsilon.\bar{d} + I.E\ \frac{\Delta\epsilon}{d}$

$$= 10E\left\{0.5\epsilon_b + 0.5\epsilon_t\right\}0.5 + 0.83333E\left\{\frac{\epsilon_t-\epsilon_b}{1.0}\right\}$$

$$= \left\{1.66667\epsilon_b + 3.33333\epsilon_t\right\}E$$

$\therefore$ Equating Forces gives

$$10E\{0.5\,\epsilon_b + 0.5\epsilon_t\} = 25.75\,E\alpha \qquad \text{------ (1)}$$

$$E\{1.66667\epsilon_b + 3.33333\epsilon_t\} = 19.1525\,E\alpha \qquad \text{------ (2)}$$

From (1) $\epsilon_b = \{25.75\,\alpha - 5\epsilon_t\}\frac{1}{5}$ ------ (1a)

Substituting into (2) gives

$$1.66667\ (25.75\,\alpha - 5\epsilon_t)\frac{1}{5} + 3.33333\epsilon_t = 19.1525\alpha$$

$$1.66666\epsilon_t = 19.1525\,\alpha - 8.58335\,\alpha$$

$$\therefore\ \epsilon_t = \frac{10.56915}{1.66666}\,\alpha = 6.34152\,\alpha$$

Substituting into (1a)

$$\epsilon_b = -1.19152\,\alpha$$

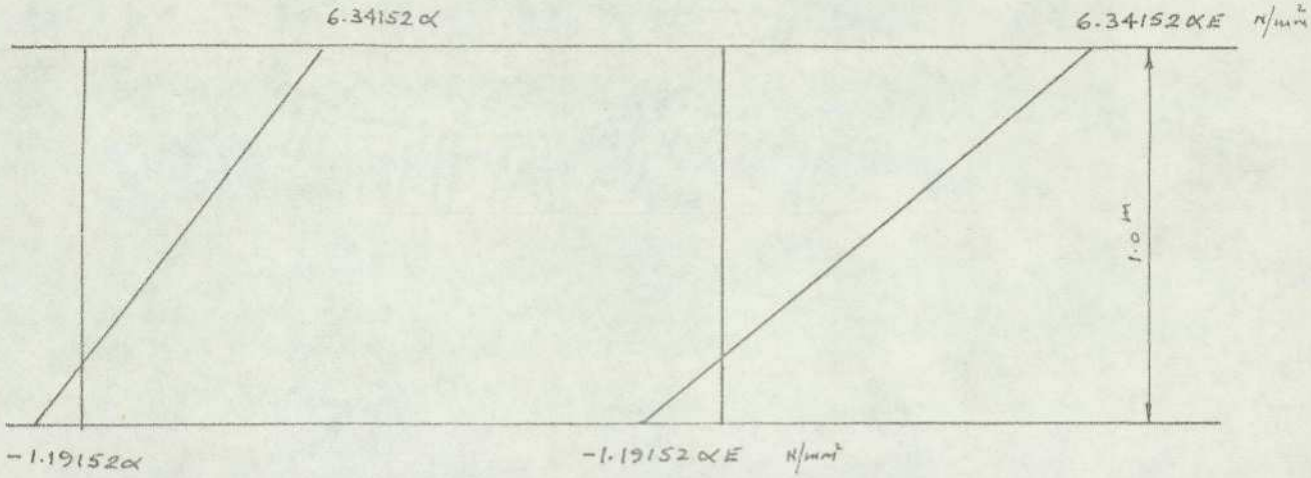

(a) Strain Diagram

(b) Stress Diagram

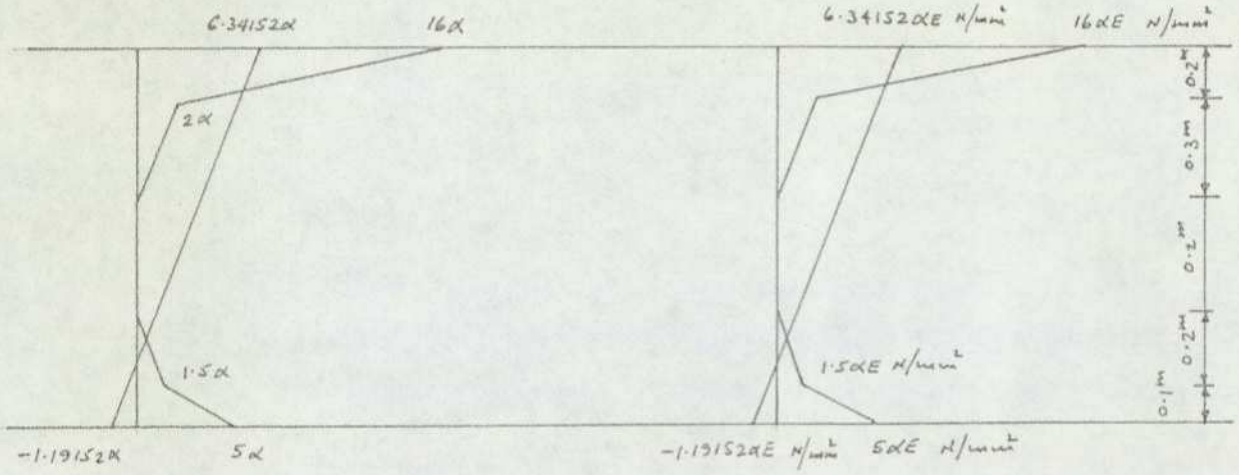

(c) Primary strain due to temperature distribution

(d) Primary stress due to temperature distribution

Fig. 7.034 Final primary stresses and strains due to the effect of temperature distribution.

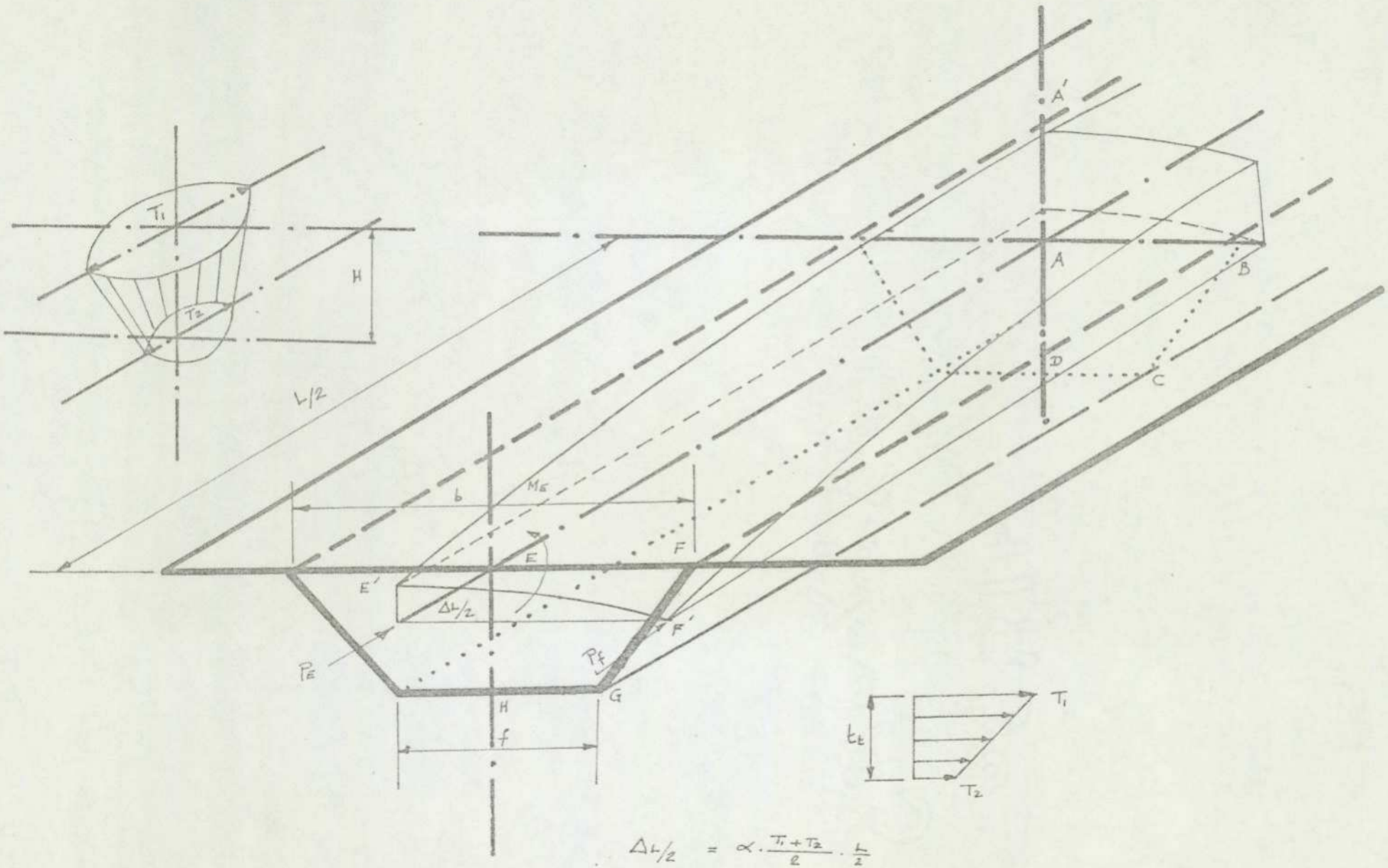

$$\Delta L/2 = \alpha \cdot \frac{T_1 + T_2}{2} \cdot \frac{L}{2}$$

$$\Delta b/2 = \alpha \cdot \frac{T_1 + T_2}{2} \cdot \frac{b}{2}$$

Fig. 7.041

7.04.1 Cantilevered box bridges type (a)

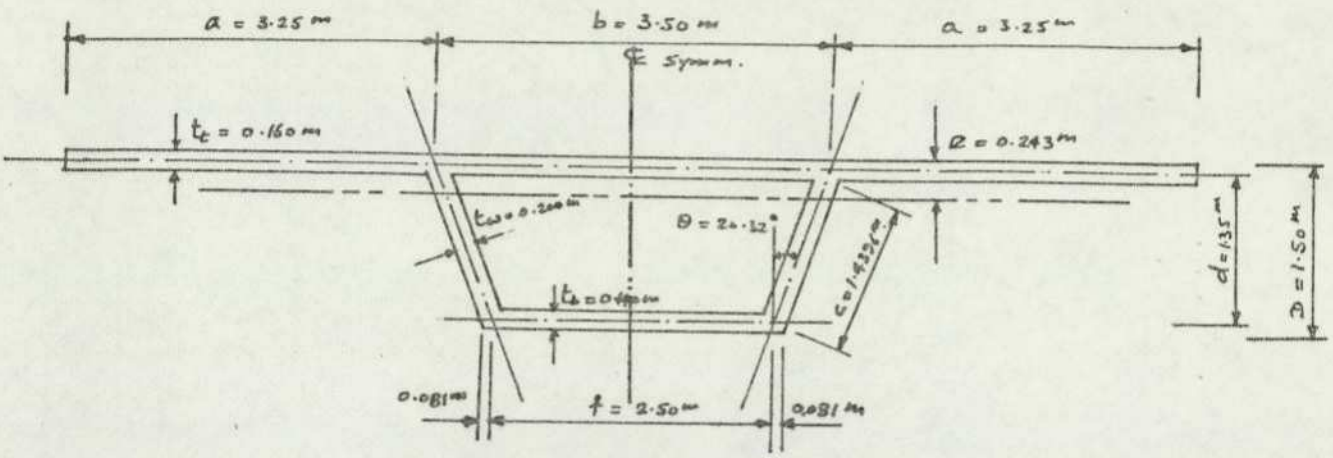

Fig. 7.0411

1 Properties of top deck slab

area of slab (top) A_1 = 10 x 0.16 = 1.6 m^2

$\bar{y}_1$ = 0.08 m

$\bar{I}_1$ = 10 x $0.16^3/_{12}$ = 0.0034133 m^4.

2 Properties of total bridge section

area slab (top) = 10 x 0.16 = 1.6 m^2

area webs + bottom slab = $\frac{1}{2}$ ((2.50 + 0.81 x 2) + (2.662 + 0.496 x 2)) 1.34
− (2.338 + (2.662 + 0.496 x 2 − 213.15 x 2)) $\frac{1}{2}$ x
(1.50 − 0.16 − 0.14)

= 4.01464 − 3.33942 = 2.27522 m^2

∴ Total area, ΣA = 1.6 + 0.67522 = 2.27522 m^2

Taking moments about base of bottom slab gives :

$A\bar{y}$ = 1.6 (1.5 − 0.08) + (2.5 + 0.81 x 2 + 0.496 x 2)
x $\frac{1.34^2}{2}$ − (2.338 x 1.2 (0.6 + 0.14) + 0.44485 x
1.2 x $\frac{1}{2}$ x 2($\frac{2}{3}$ x 1.2 + 0.14) + 0.496 (1.5 − 0.16)
$\frac{1}{2}$ x 2 x 1/3 (1.5 − 0.16))

$$= 2.272 + 3.281 - 2.076 - 0.502 - 0.297 = 2.678$$

$$\therefore \bar{y} = \frac{2.678}{2.27522} = 1.177\text{m}$$

$$\begin{aligned}
\text{I of Total Section} &= 10 \times 0.16^3/12 + 1.6(1.5 - 1.177 - 0.08)^2 + \\
&\quad 3.654 \times 1.34^3/12 + (3.654 \times 1.34)\,(1.34/2 - 1.177)^2 \\
&\quad - \{2.338 \times 1.2^3/12 + (2.338 \times 1.2)(0.6 + 0.14 - 1.177)^2\} \\
&\quad -2\{0.44485 \times 1.2^3/36 + 0.44485 \times 1.2/2\,(2/3 \times 1.2 + 0.14 - 1.77)^2\} \\
&\quad -2\{0.496 \times 1.34^3/36 + 0.496 \times 1.34/2\,(1/3 \times 1.34 - 1.177)^2\} \\
&= (0.00341333 + 0.0944784) + (0.73265867 + 1.25860444) \\
&\quad -(0.336672 + 0.53578263 - 2(0.02135280 + 0.01499207) \\
&\quad -2(0.03315077 + 0.17725509) \\
&= 0.72319876\text{m}^4
\end{aligned}$$

Now eccentricity of heated section from centre of area of total section,

$e = 1.5 - 1.177 - 0.08 = 0.243\text{m}.$

$T1 = Tt = 15^{\circ}C$

$T2 = Tb = 5^{\circ}C$

$\alpha = 0.000012$ per $1^{\circ}C$

$E = 28\ \text{KN/mm}^2$

Member	Area of heated Zone of Slab m^2	Lever arm from centre of heated Zone to base of Section La (m)	Temp. Tav.^oC at centroid of Heated Zone ^oC	Axial Force in Section due to Temp. effect F = A.E.α.Tav in KN	Temp. Gradient across heated Zone $^oC/m$	Bending Moment at base of section $M = F.La + IE\frac{\Delta T\alpha}{d}$
Top Slab	1.6	1.42	10	5376	62.50	7705.60

Table: 700.02

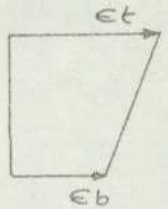

Assumed Strain Diagram

Fig. 7.0412

$$\epsilon = \epsilon b\left(1 - \frac{\bar{d}}{d}\right) + \epsilon t\,\frac{\bar{d}}{d} = \epsilon b\left(1 - \frac{1.177}{1.5}\right) + \epsilon t\,\frac{1.177}{1.5}$$

$$= 0.21533\,\epsilon b + 0.78467\,\epsilon t$$

$$F = AE\epsilon = 2.27522 \times 28 \times 10^6\,(0.21533\,\epsilon b + 0.78467\,\epsilon t)$$

$$M = AE\epsilon La + IE\,\frac{\Delta\epsilon}{d} = 2.27522 \times 28 \times 10^6 \times 1.177\,(0.21533\,\epsilon b + 0.78467\,\epsilon t) + 0.72319876 \times 28 \times 10^6\,\left(\frac{\epsilon t - \epsilon b}{1.5}\right)$$

$$= 16{,}145{,}906.43\,\epsilon b + 58836243.89\,\epsilon t + 13499710.19\,\epsilon t - 13{,}499{,}710.19\,\epsilon b$$

$$= 2{,}646{,}196.24\,\epsilon b + 72335954.08\,\epsilon t$$

$$2.27522 \times 28 \times 10^6\,(0.21533\,\epsilon b + 0.78467\,\epsilon t) = 5376 \text{ ---------- (1)}$$

$$2646196.24\,\epsilon b + 72335954.08\,\epsilon t = 7705.60 \text{ ------- (2)}$$

from eqn. (1) $\epsilon b = \left(\frac{5376}{2.27522 \times 28 \times 10^6} - 0.78467\,\epsilon t\right)\,\frac{1}{0.21533}$

i.e. $\epsilon b = 0.00039190 - 3.64403474\,\epsilon t$ ---------- (1a)

Subst. into eqn. (2) gives

$$2646196.24\left\{0.00039190 - 3.64403474\epsilon_t\right\} + 72335954.08\epsilon_t = 7705.60$$

$$1037.044306 - 9642831.027\epsilon_t + 72335954.08\epsilon_t = 7705.60$$

$$62693123.05\epsilon_t = 7705.60 - 1037.044306$$

$$\therefore \epsilon_t = \frac{6668.555694}{62693123.05}$$

$$= 0.00010637$$

$$\therefore \epsilon_b = 0.0003919 - 3.64403474\ (0.00010637)$$

$$= 0.0003919 - 0.00038761$$

$$= -0.00000429$$

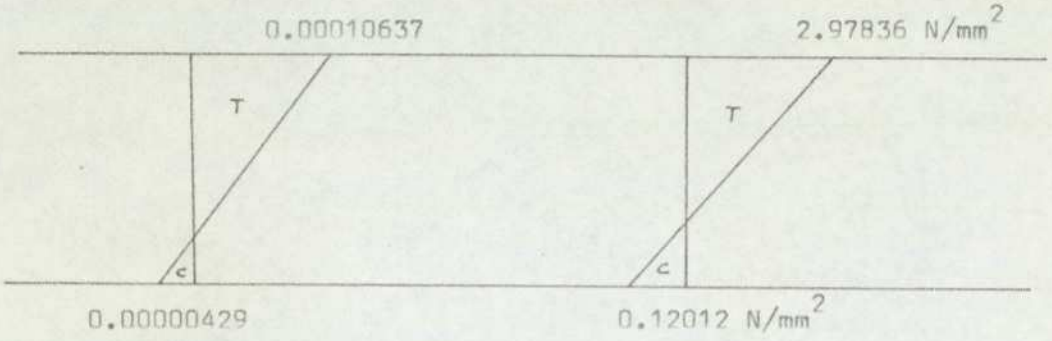

(a) Strain Diagram (b) Stress Diagram

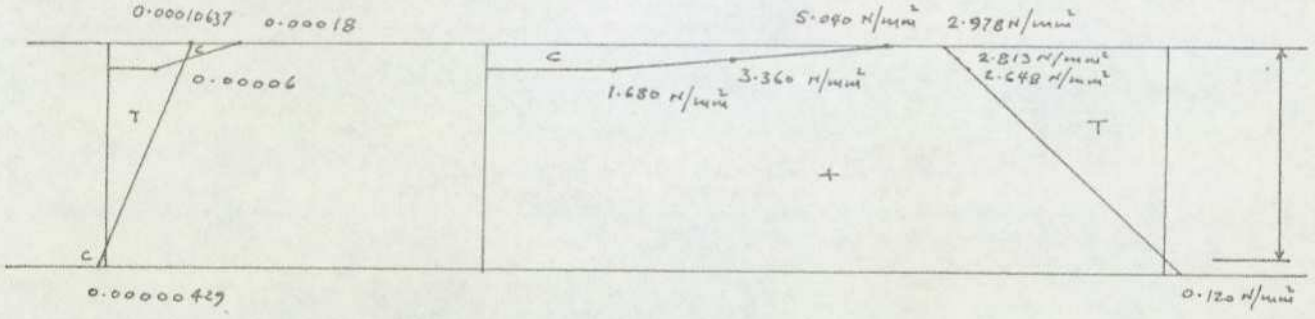

(d) Primary stresses due to temp. distribution

(c) Primary strain due to temp. distribution

=

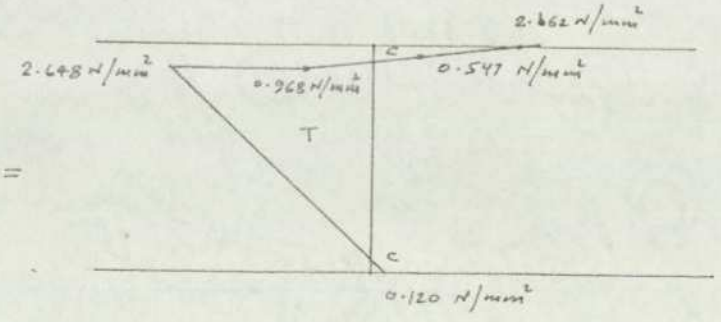

Fig. 7.0413

Flexural stresses in the longitudinal direction due to the effect of temperature distribution

Assuming a bridge of 2 x 30m spans as shown below:

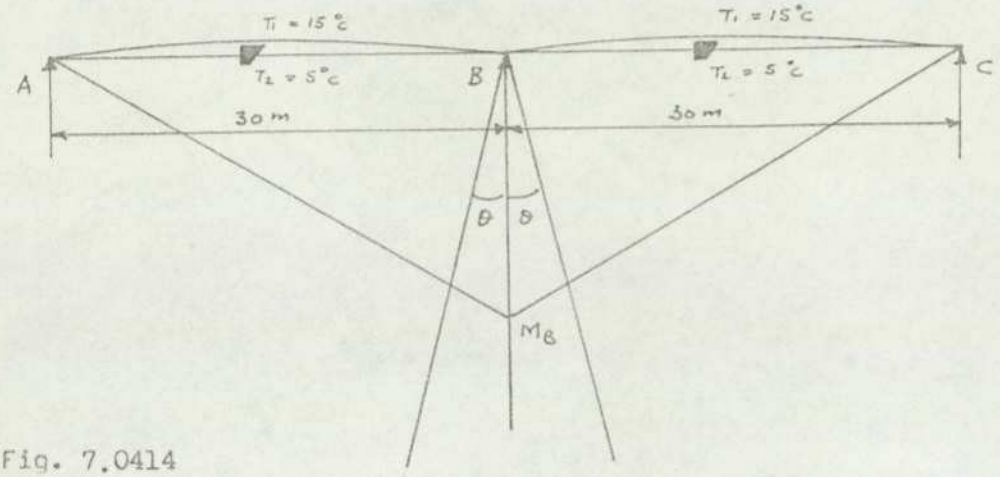

Fig. 7.0414

Bending Moment at Centroid of Section, $M = Fe + I1E \frac{\Delta T}{d} \alpha$

$= 5376 \times 0.243 + 0.0034133 \times 28 \times 10^6 \times 0.000012 \times 62.5$

$= 1306.368 + 71.679$

$= 1378.047$ KN-m

$$\theta = \frac{ML}{2EI} = \frac{1378.047 \times L}{2EI}$$

$$M_B \frac{L}{3EI} = \frac{1378.047 \times L}{2EI}$$

$\therefore M_B = 1378.047 \times 3/2 = 2067.071$ KN-m

I (Total) $= 0.72320\ m^4$

$$\sigma_B \text{ top} = \frac{2067.071}{0.72320/0.323} = 923.208\ KN/m^2\ (0.9232\ N/mm^2)$$

$$\sigma_B \text{ bottom} = \frac{2067.071}{0.72320/1.177} = 3364.135\ KN/m^2\ (3.364\ N/mm^2)$$

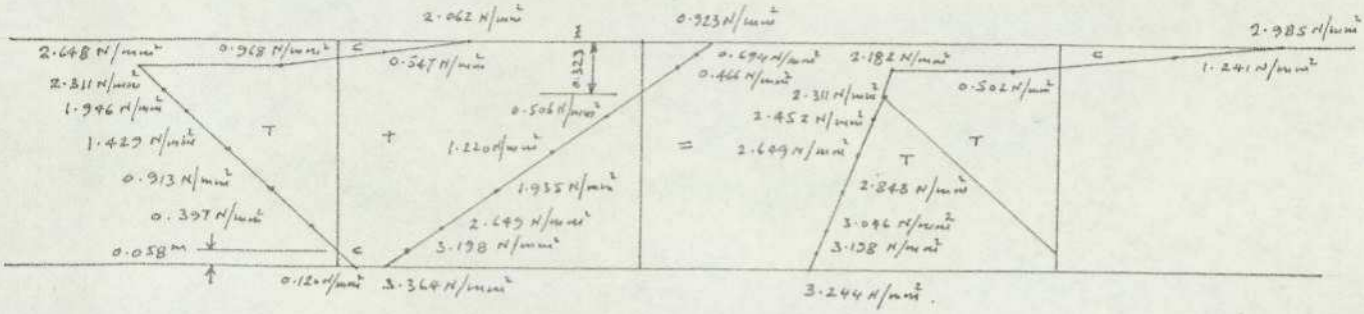

Fig. 7.0415 Final stress diagram in the longitudinal direction due to the effect of temperature distribution

Stresses in transverse direction

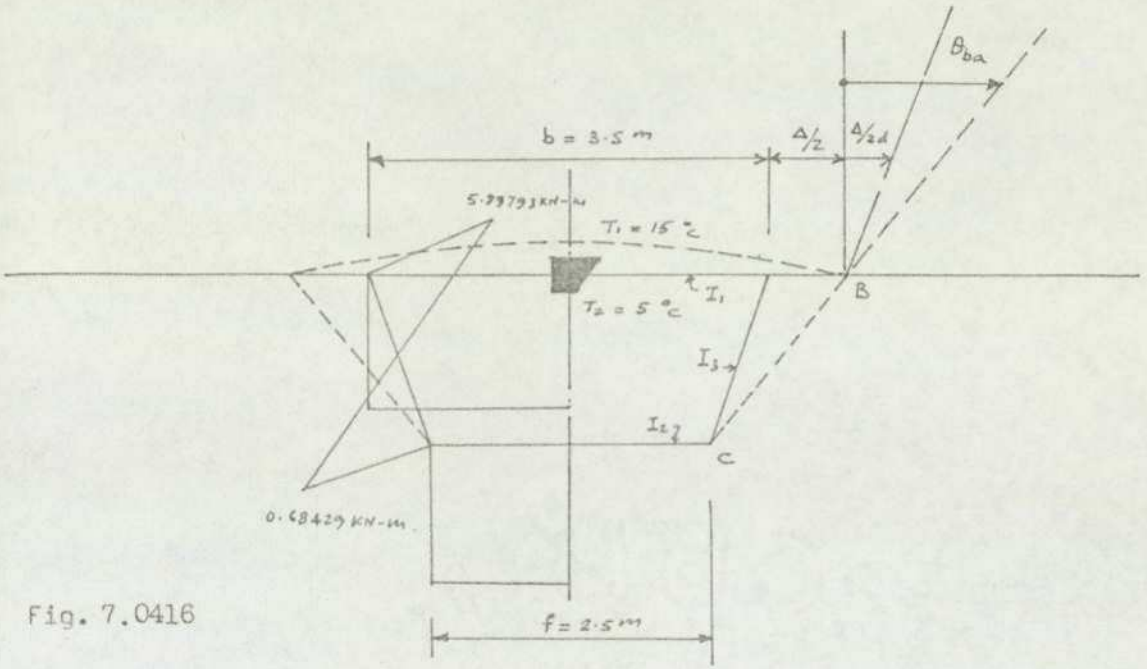

Fig. 7.0416

$d = 1.5 - 0.16/2 - 0.14/2 = 1.35$ m.

$$\theta_{ba} = \frac{\alpha(T1-T2)b}{2t_t} = \frac{0.000012\ (15-5)3.5}{2 \times 0.160} = 0.0013125 \text{ rad.}$$

$$\delta_a{}^o = \frac{\alpha(T1-T2)b^2}{8t_t} = \frac{0.000012\ (15-5)3.5^2}{8 \times 0.16} = 0.0011484$$

$$I_1 = \frac{1}{12} \times 1 \times 0.16^3 = 0.0003413 \text{ m}^4$$

$$I_2 = \frac{1}{12} \times 1 \times 0.2^3 = 0.0006667 \text{ m}^4$$

$$I_3 = \frac{1}{12} \times 1 \times 0.14^3 = 0.0002287 \text{ m}^4$$

$$\Delta = \frac{\alpha(T1+T2)}{2} .b = \frac{0.000012\ (15-5)3.5}{2} = 0.000210$$

Writing the compatibility of deformation equations:-

At B $\quad M_b \left(\frac{b}{2EI1} + \frac{d}{3EI2}\right) - Mc \frac{d}{6EI2} = \theta_{ba} - \frac{\Delta}{2d}$

At C $\quad -M_b \frac{d}{6EI2} + Mc \left(\frac{d}{3EI2} + \frac{f}{2EI3}\right) = \frac{\Delta}{2d}$

$$\frac{Mb}{E}\left(\frac{3.5}{2\times0.0003413} + \frac{1.35}{3\times0.0006667}\right) - \frac{Mc}{E}\frac{1.35}{6\times0.0006667} = 0.0013125 - \frac{0.00021}{2\times1.35}$$

$$-\frac{Mb}{E}\frac{1.35}{6\times0.0006667} + \frac{Mc}{E}\left(\frac{1.35}{3\times0.0006667} + \frac{2.5}{2\times0.0002287}\right) = \frac{0.00021}{2\times1.35}$$

$$5802.42011 \frac{Mb}{E} - 337.48313 \frac{Mc}{E} = 0.0012347$$

$$\therefore M_b = (0.0012347 + 337.48313 \frac{Mc}{E}) \frac{E}{5802.42011}$$

$$-337.48313 \frac{Mb}{E} + 6140.64181 \frac{Mc}{E} = 0.00007778$$

Subst. from above

$$-337.48313 \times \frac{1}{E}(0.0012347 + 337.48313 \frac{Mc}{E})E/5802.42011 + 6140.64181\frac{Mc}{E}$$

$$= 0.00007778$$

$$-0.00007181 - 19.62886\frac{Mc}{E} + 6140.64181 \frac{Mc}{E} = 0.00007778$$

$$6121.01296 \frac{Mc}{E} = 0.00014959$$

$$\therefore Mc = 0.00014959 \times \frac{E}{6121.01296}$$

$$= 2.4438765 \times 10^{-8} E$$

$$= 0.68429 \text{ KN-m}$$

$$Mb = 2.1421194 \times 10^{-7} E$$

$$= 5.99793 \text{ KN-m}$$

Stresses due to continuity at abutments or end diaphragm

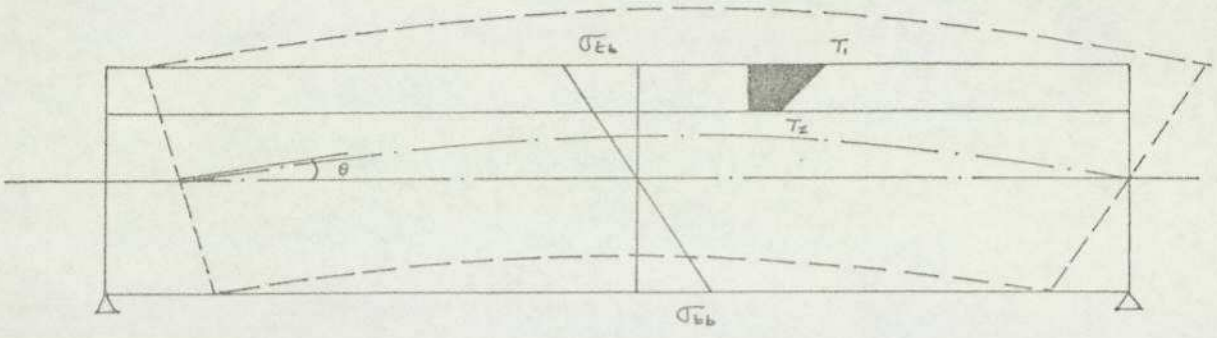

Fig. 7.0417

Angular deformation θ results only because of bending stresses. Since the curvature is constant, we can write:

$$\theta = \frac{ML}{2EI_{total}}$$

where $$M = Fe + IE\frac{\Delta T}{d}\alpha = \tfrac{1}{2}\alpha E(T1+T2)\ (2a+b)\ t_t.e + IE\ (T1-T2)\frac{\alpha}{d}$$

i.e. M = (Force on Segment) .e + Moment about its own centroid.

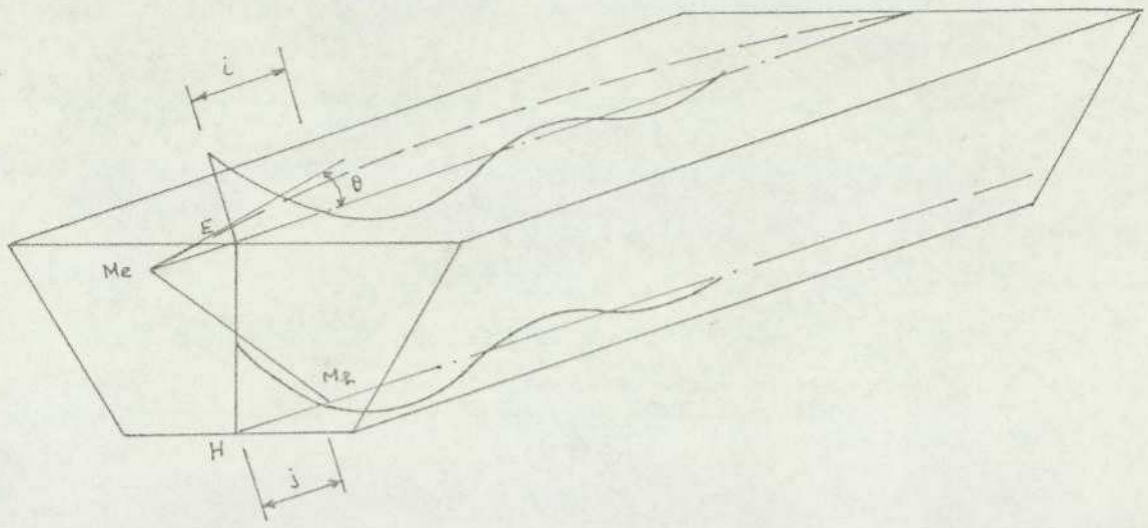

Fig. 7.0418

Writing the equations of compatibility of deformations at E & H gives

At E $\quad Me\left(\frac{i}{3EI1} + \frac{d}{3EI2}\right) - M_h \frac{d}{6EI2} = \theta e$

At H $\quad -Me \frac{d}{6EI2} + M_h \left(\frac{d}{3EI2} + \frac{j}{3EI3}\right) = 0$

If the value of i and j can be found, the magnitude of moments at E and H can be found.

Assuming $i = j = \frac{d}{2} = \frac{1.35}{2} = 0.675m$

$$\frac{Me}{E}\left(\frac{0.675}{3\times0.0003413} + \frac{1.35}{3\times(1.35\times0.2^3/12)}\right) - \frac{Mh}{E}\frac{1.35}{6\times1.35\times0.2^3/12} = \frac{1378.047\times L}{2EI}$$

$$-\frac{Me}{E}\frac{1.35}{6\times1.35\times0.2^3/12} + \frac{Mh}{E}\left(\frac{1.35}{3\times1.35\times0.2^3/12} + \frac{0.675}{3\times0.0002287}\right) = 0$$

$$1159.24\frac{Me}{E} - 250.00\frac{Mh}{E} = \frac{1378.047\times30}{2\times E\times0.7232}$$

$$-250\frac{Me}{E} + 983.82\frac{Mh}{E} = 0$$

$$M_e = \left(\frac{28582.28}{E} + 250.00\ \frac{M_h}{E}\right) \frac{E}{1159.24}$$

$$= 24.6561 + 0.2160\ M_h$$

Substituting into (2) gives

$$-250\ \left\{24.6561 + 0.2160\ M_h\right\} \frac{1}{E} + 983.82\ \frac{M_h}{E} = 0$$

$$-\frac{6164.0250}{E} - 54.0078\ \frac{M_h}{E} + 983.82\ \frac{M_h}{E} = 0$$

$$929.8122\ \frac{M_h}{E} = \frac{6164.0250}{E}$$

$$\therefore M_h = 6.6293 \text{ KN-m}$$

$$\therefore M_e = 24.6561 + 0.2160 \times 6.6293$$

$$= 26.0880 \text{ KN-m.}$$

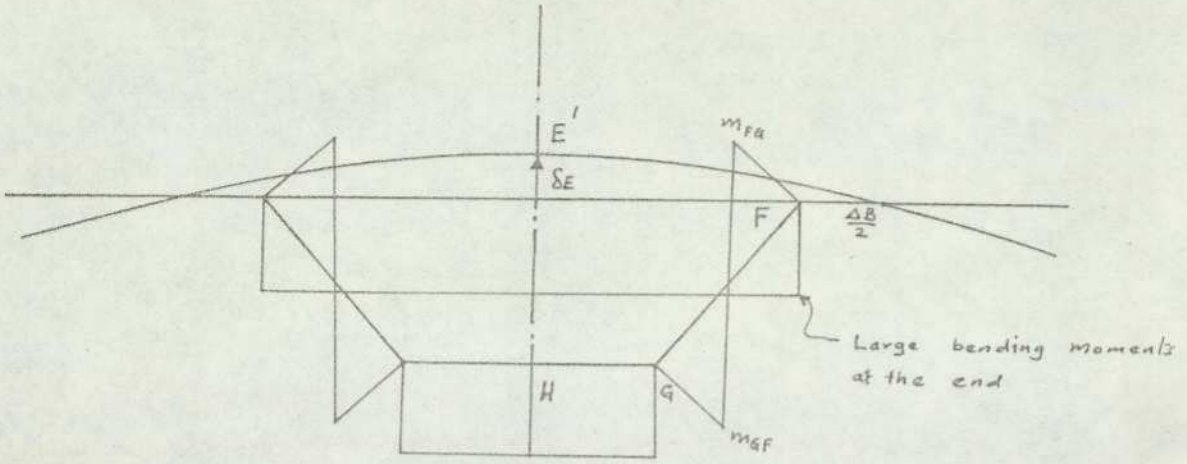

(a) CROSS-SECTION AT THE END

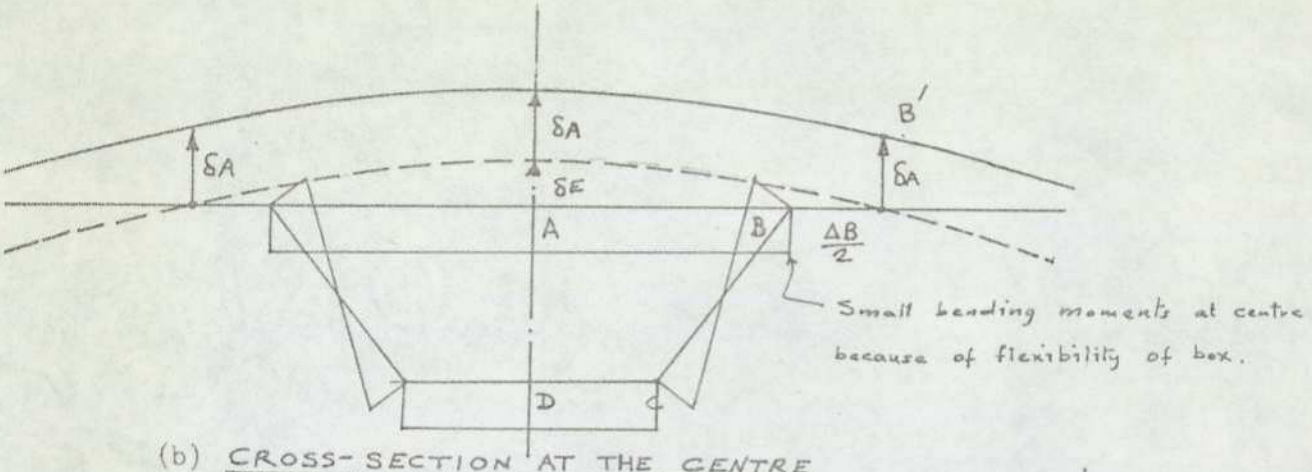

(b) CROSS-SECTION AT THE CENTRE

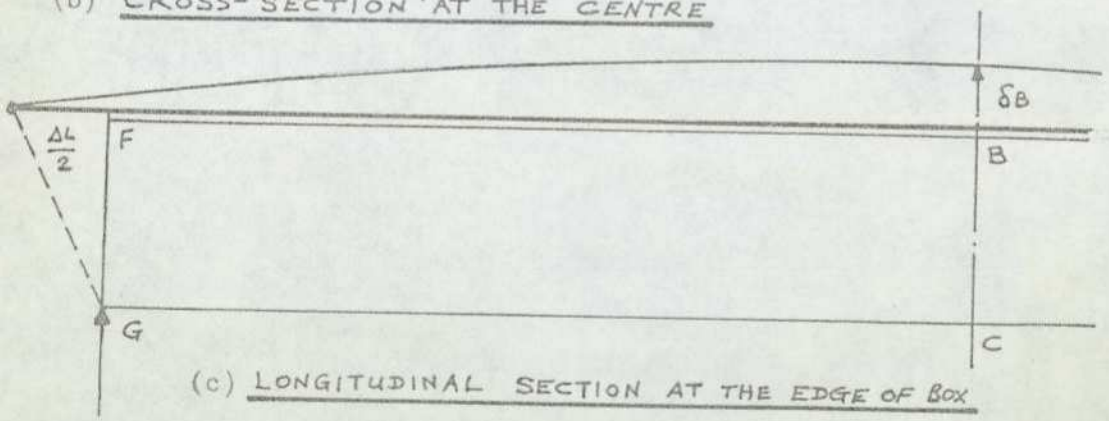

(c) LONGITUDINAL SECTION AT THE EDGE OF BOX

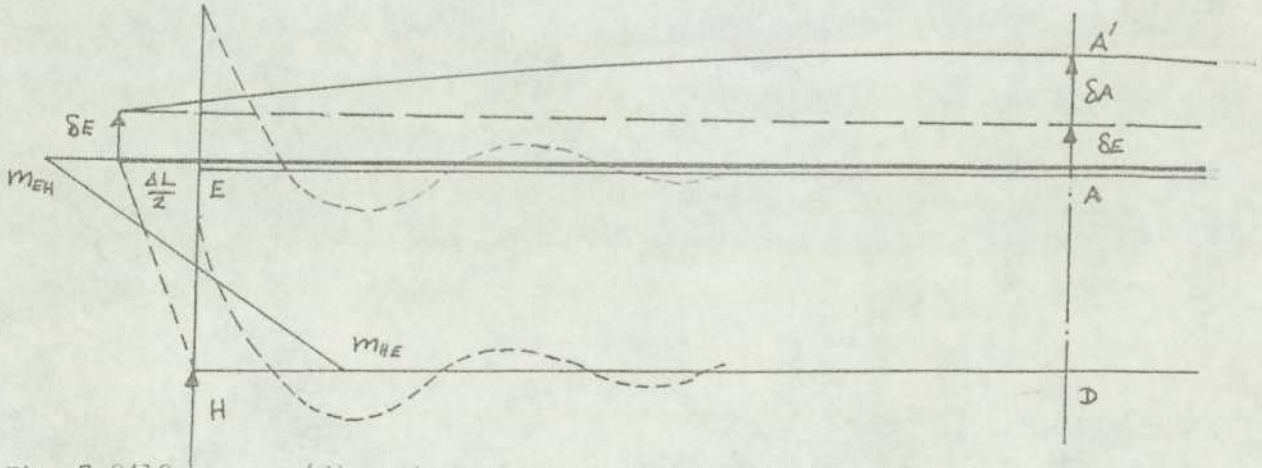

Fig. 7.0419 (d) LONGITUDINAL SECTION AT THE CENTRE

7.04.2 Cantilevered box bridges type (b)

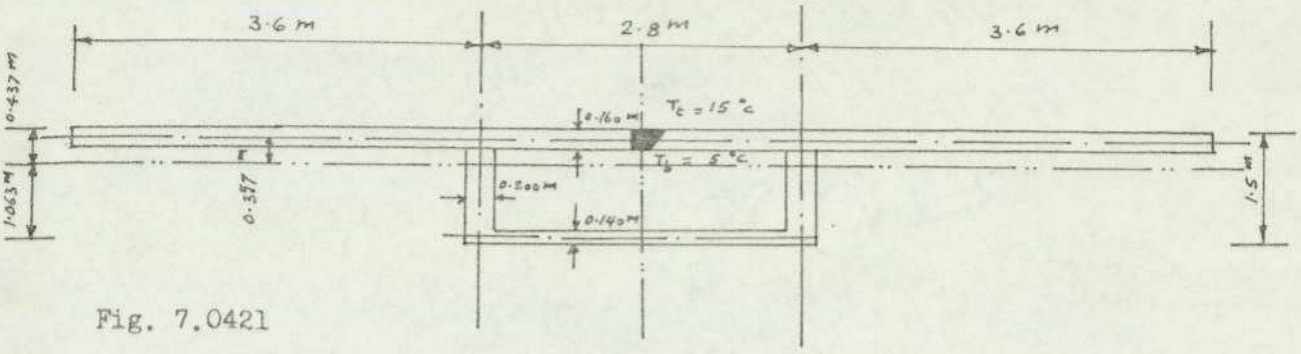

Fig. 7.0421

1. Properties of Top Deck Slab

Area A1 = 0.160 x 10 = 1.6 m^2

$\bar{y}1$ = 0.08 m

I1 = 10 x $0.16^3/12$ = 0.0034133 m^3

2. Properties of Total Section

Calculation of the position of neutral axis:

Area of Slab (top) : 10 m x 0.160 m = 1.6 m^2

Webs : 2 x 1.2 m x 0.20 m = 0.48 m^2

Slab (bott.) : 3 m x 0.140 m = 0.42 m^2

ΣA = 2.50 m^2

Taking moments about the base of bottom Slab gives:

$A\bar{y}$ = 1.6 (1.5 - 0.08) + 0.48 (0.6 + 0.14) + 0.42 (0.07)

= 2.6566

$$\bar{y} = \frac{2.6566}{2.50} = 1.063 \text{ m}$$

$$I \text{ of Total Section} = 10 \times 0.16^3/12 + 1.6(0.0437 - 0.08)^2 + 3.0 \times 0.14^3/12$$

$$+ 0.42(1.063 - 0.07)^2 + 2\left(0.2 \times \frac{1.2^3}{12}\right)$$

$$+ 0.48(1.063 - 0.6 - 0.14)^2$$

$$= 0.0034133 + 0.2039184 + 0.000686 + 0.41414058$$

$$+ 0.0576 + 0.05007792$$

$$= 0.72983623 m^3$$

$T1 = Tt = 15^{\circ}C$

$T2 = Tb = 5^{\circ}C$

$\alpha = 0.000012$ per $1^{\circ}C$

$E = 28\ KN/mm^2$

Member	Area of heated Zone of Slab m^2	Lever arm, La, from Centre of heated Zone to base of Slab in (m)	Temp. Tav. ^oC at Centroid of heated Zone	Axial Force in Section due to Temp., F = A1Eα Tav.	Temp. Gradient across heated Zone in $^oC/m$	Bending Moment at base of Section = F.La + I1E $\frac{\Delta T \alpha}{d}$
	1.6	1.42	10	5376	62.50	7705.60

Table: 700.03

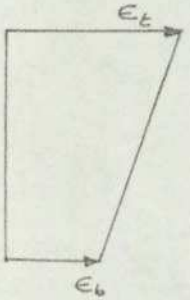

Assumed Strain Diagram

Fig. 7.0422

$$\epsilon = \epsilon_b(1 - \frac{\bar{d}}{d}) + \epsilon_t \frac{\bar{d}}{d} = \epsilon_b(1 - \frac{1.063}{1.500}) + \epsilon_t \frac{1.063}{1.500}$$

$$= 0.29133\,\epsilon_b + 0.70867\,\epsilon_t$$

$$F = AE.\epsilon = 2.5 \times 28 \times 10^6\,(0.29133\,\epsilon_b + 0.70867\,\epsilon_t)$$

$$M = AE\epsilon\,La + IE\,\frac{\Delta\epsilon}{d} = 2.5 \times 28 \times 10^6 \times 1.063\,(0.29133\,\epsilon_b + 0.70867\,\epsilon_t) + 0.72983623$$

$$\times 28 \times 10^6 \times (\frac{\epsilon_t - \epsilon_b}{1.5})$$

$$= 21{,}677{,}865.3\epsilon_b + 52732134.7\epsilon_t + 13623609.63\epsilon_t - 13623609.63\epsilon_b$$

$$= 8{,}054{,}255.67\epsilon_b + 66355744.33\epsilon_t$$

$$2.5 \times 28 \times 10^6(0.29133\epsilon_b + 0.70867\epsilon_t) = 5367 \quad \text{------ (1)}$$

$$8054255.67\epsilon_b + 66355744.33\epsilon_t = 7705.60 \text{ ------ (2)}$$

From eqn (1)

$$0.29133\epsilon_b + 0.70867\epsilon_t = \frac{5376}{25 \times 28 \times 10^6}$$

$$\therefore \epsilon_b = .(0.0000768 - 0.70867\epsilon_t) \frac{1}{0.29133}$$

$$= 0.00026362 - 2.43253355\,\epsilon_t$$

Substituting into eqn (2) gives

$$8054255.67(0.00026362 - 2.43253355\epsilon_t) + 66355744.33\epsilon_t = 7705.60$$

$$2123.26288 - 19592247.14\epsilon_t + 66355744.33\epsilon_t = 7705.60$$

$$46763497.19\epsilon_t = 5582.34$$

$$\epsilon_t = 1.1937382 \times 10^{-4} = 0.00011937382$$

$$\epsilon_b = -0.00002676$$

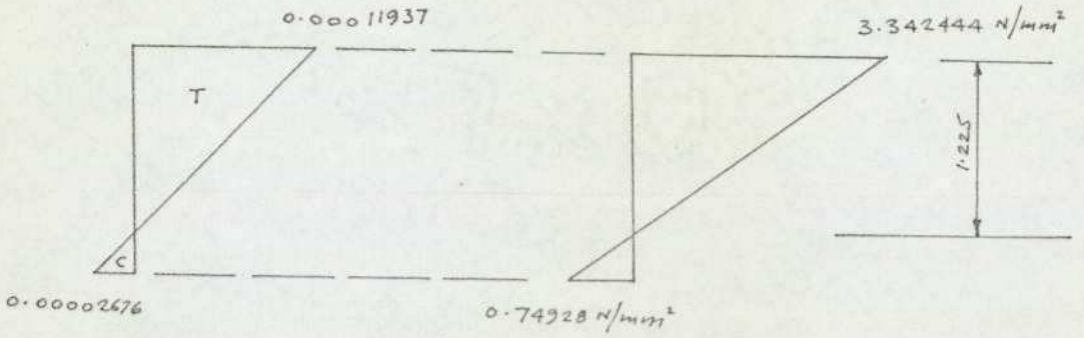

(a) Strain Diagram (b) Stress Diagram

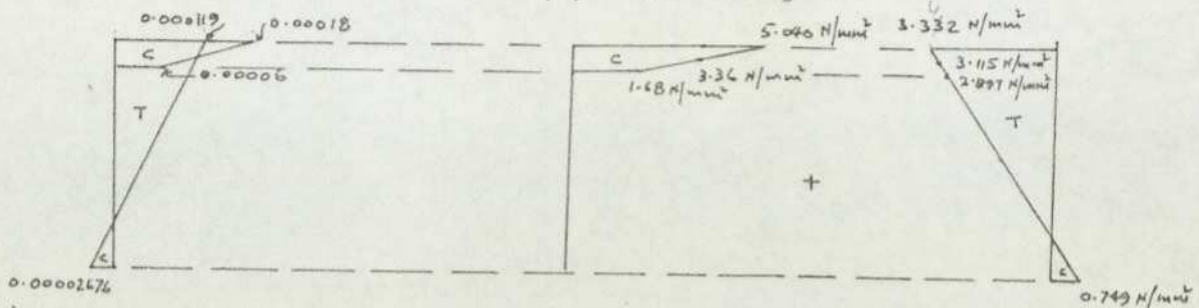

(c) Primary strain due to temp. distribution

(d) Primary stresses due to temp. distribution

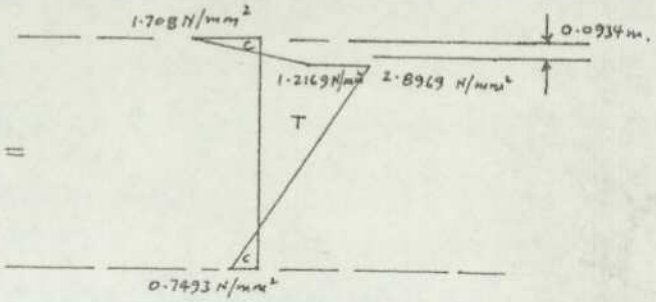

Fig. 7.0423
Final primary stresses and strains due to the effect of temperature distribution.

Flexural stresses in the longitudinal direction due to the effect of temperature distribution

Assuming a bridge of 2 x 30 m spans as shown below:-

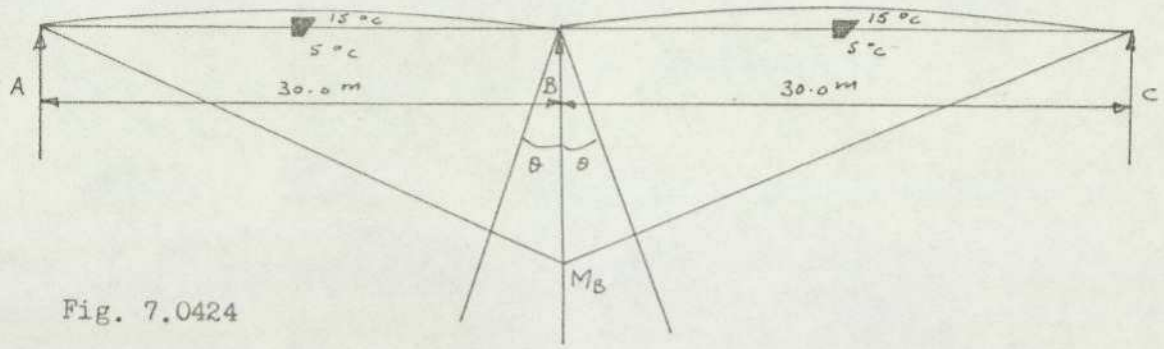

Fig. 7.0424

Bending Moment at Centroid of Section, $M = F.e + IE \frac{\Delta T}{d} \alpha$

$= 5376 \times (0.357) + 0.0034133 \times 28 \times 10^6 \times 0.000012 \times 62.5$

$= 1919.232 + 71.679$

$= 1990.911$ KN-m

$\theta = \frac{ML}{2EI} = \frac{1990.911 \times L}{2EI}$

$M_B \frac{L}{3EI} = \frac{1990.911 \times L}{2EI}$

$\therefore M_B = \frac{1990.911 \times 3}{2} = 2986.367$ KN - m

Now I (total) = 0.72984 m^4

σ_B top $= \frac{2986.367}{0.72984/0.437} = 1788.121$ KN/m^2 (1.788121 N/mm^2)

σ_B bott. $= \frac{2986.367}{0.72984/1.063} = 4349.594$ KN/m^2 (4.3495 N/mm^2)

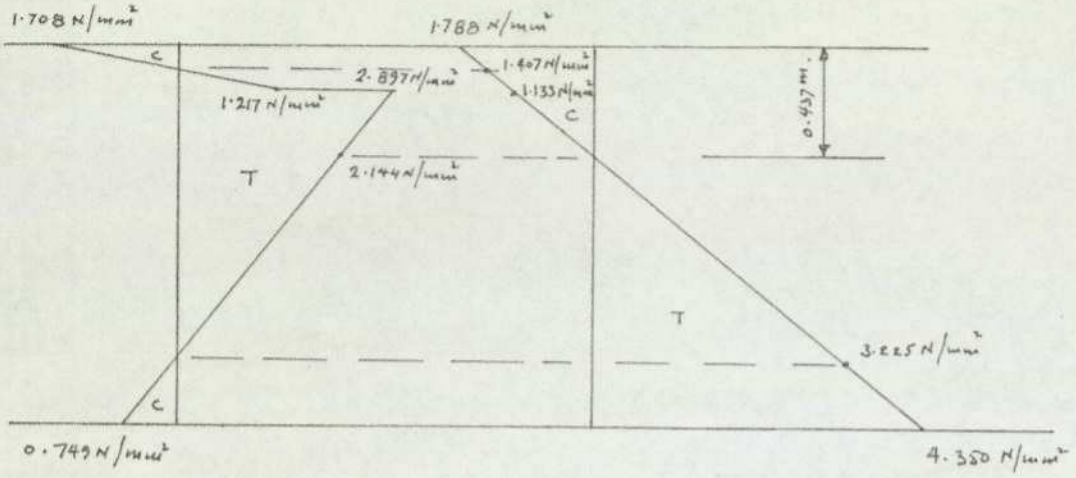

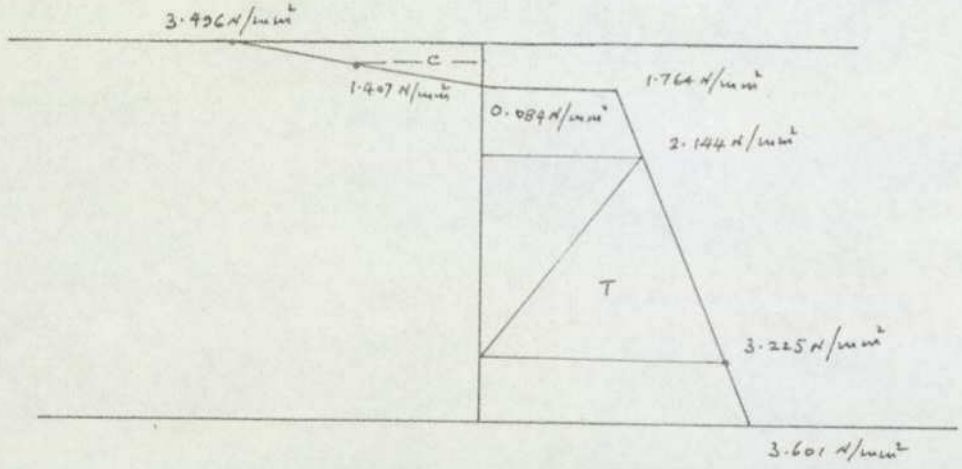

Fig. 7.0425 Final stress diagram in the longitudinal direction due to the effect of temperature distribution

Stresses in transverse direction

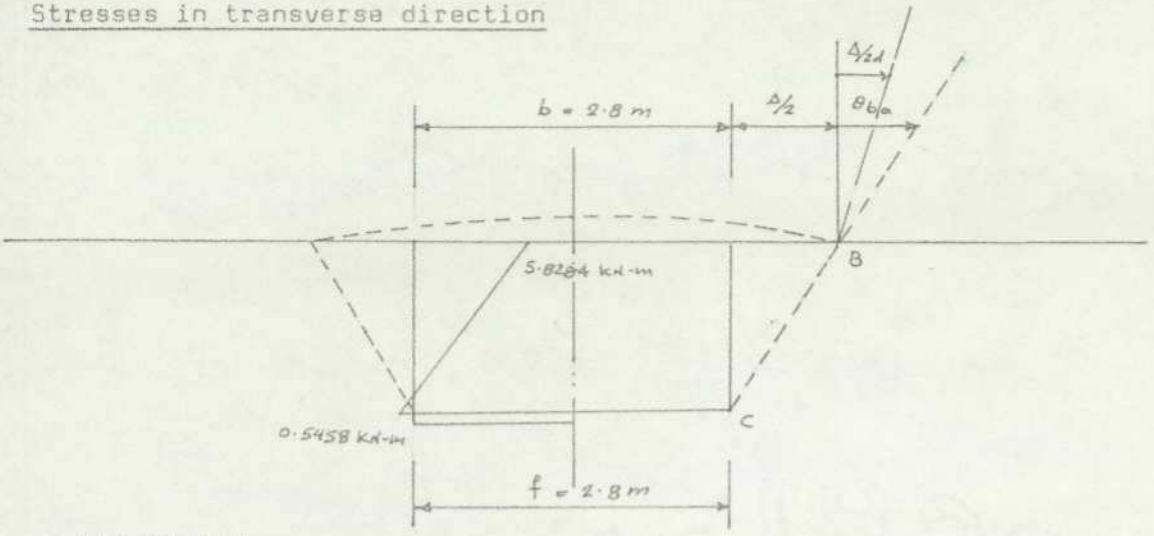

Fig. 7.0426

$$d = 1.5 - \frac{0.16}{2} - \frac{0.14}{2} = 1.35\ m$$

$$\theta_{ba} = \frac{\alpha(T1 - T2)b}{2\ t1} = \frac{0.000012(15 - 5)}{2 \times 0.16} \times 2.8 = 0.00105^{rad.}$$

$$\delta_a{}^o = \frac{\alpha(T1 - T2)b^2}{8\ t1} = \frac{0.000012\ (15 - 5)\ 2.8^2}{8 \times 0.16} = 0.000735\ m$$

$$I1 = \frac{1}{12} \times 1 \times 0.16^3 = 0.003413\ m^4$$

$$I2 = \frac{1}{12} \times 1 \times 0.2^3 = 0.0006667\ m^4$$

$$I3 = \frac{1}{12} \times 1 \times 0.14^3 = 0.0002287\ m^4$$

$$\Delta = \frac{\alpha(T1 + T2)b}{2} = \frac{0.000012 \times (15 - 5) \times 2.8}{2} = 0.000168$$

Writing the equations of compatibility of deformations gives

At B $$M_b\left(\frac{b}{2EI1} + \frac{d}{3EI2}\right) - Mc\ \frac{d}{6EI2} = \theta ba - \frac{\Delta}{2d}$$

At C $$-Mb\ \frac{d}{6EI2} + Mc\ \left(\frac{d}{3EI2} + \frac{f}{2EI3}\right) = \frac{\Delta}{2d}$$

$$\frac{Mb}{E}\left(\frac{2.8}{2\times0.0003413} + \frac{1.35}{3\times0.0006667}\right) - \frac{Mc}{E}\ \frac{1.35}{6\times0.0006667} = 0.00105 - \frac{0.000168}{2\times1.35}$$

$$-\frac{Mb}{E}\ \frac{1.35}{6\times0.0006667} + \frac{Mc}{E}\ \left(\frac{1.35}{3\times0.0006667} + \frac{2.8}{2\times0.0002287}\right) = \frac{0.000168}{2 \times 1.35}$$

$$4776.92933 \frac{Mb}{E} - 337.48313 \frac{Mc}{E} = 0.00098778$$

$$\therefore Mb = (0.00098778 + 337.48313 \frac{Mc}{E}) \frac{E}{4776.92933}$$

Subst. into (2)

$$\frac{-337.48313}{E} (0.00098778 + 337.48313 \frac{Mc}{E}) \frac{E}{4776.92933}$$

$$+ 6796.52288 \frac{Mc}{E} = 0.00006222$$

$$- 0.00006979 - 23.84269 \frac{Mc}{E} + 6796.52288 \frac{Mc}{E} = 0.00006222$$

$$6772.68019 \frac{Mc}{E} = 0.00013201$$

$$\therefore Mc = 0.54576 \text{ KN-m}$$

$$Mb = 5.82844 \text{ KN-m}$$

7.04.3 Voided slab bridges

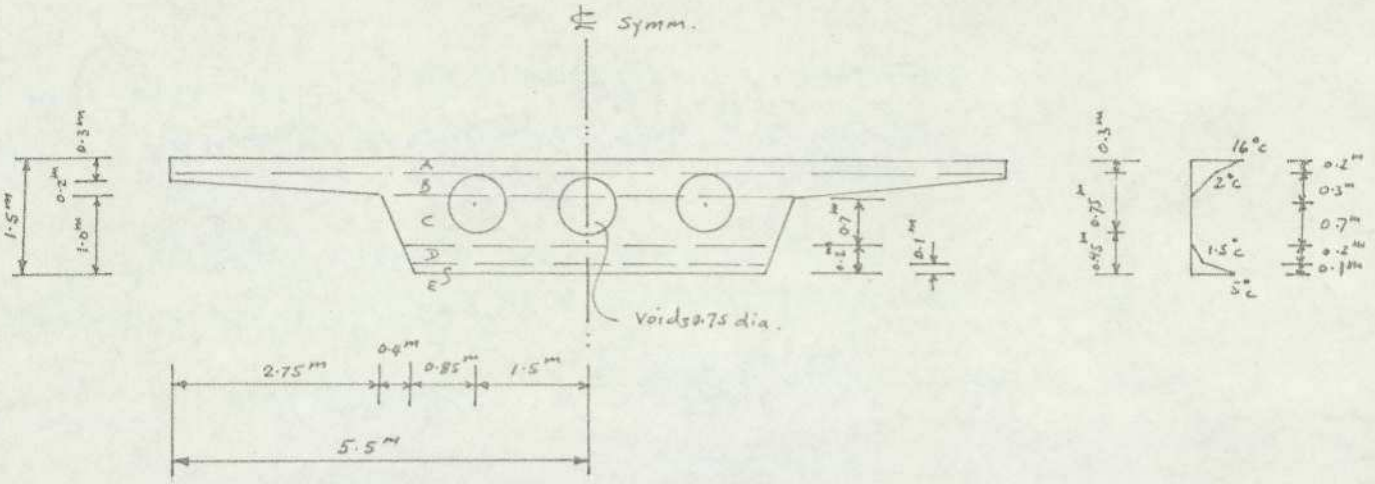

Fig. 7.043l

1. Considering Area 'A'

Section Properties

Area A = $11.000 \times 0.200 = 2.200m^2$

$I_A = 11.000 \times 0.200^3/12 = 0.00733m^4$

Centroid of area from base of section = 1.500 - 0.1 = 1.400m.

2. Considering Area 'B'

Section Properties

Area B = $11.000 \times 0.300 - (2.750 \times \frac{0.200}{2})2 - 0.09454 \times 3$

$= 3.300 - 0.550 - 0.2836 = 2.4664m^2$

$I_B = 0.01644m^4$

Centroid from base of section = (0.300 - 0.123 + 1.000) = 1.177m

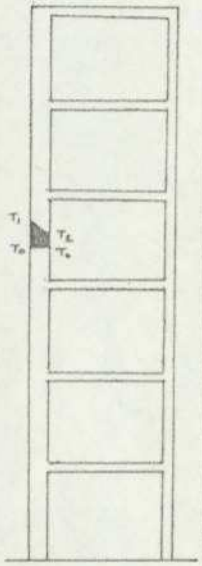

Date	2nd February 1976			2nd February 1976			2nd February 1976			2nd February 1976		
Thermocouple No.	Time	Thermo-Couple Reading	True Temp. °C	Time	Thermo-Couple Reading	True Temp. °C	Time	Thermo-Couple Reading	True Temp. °C	Time	Thermo-Couple Reading	True Temp. °C
	Voltage Applied = 100 Volts			Voltage Applied = 100 Volts			Voltage Applied = 100 Volts			Voltage Applied = 150 Volts		
T1	10.06	15.5	16.5	11.40	26.5	24.0	12.05	32.0	27.50	13.37	58.50	45.50
T2	10.06	15.5	16.5	11.40	23.0	21.50	12.06	27.0	24.25	13.38	50.10	39.75
T3	10.06	15.5	16.5	11.405	18.0	18.25	12.06	21.50	20.50	13.39	39.00	32.25
T4	10.06	15.5	16.5	11.405	17.0	17.50	12.07	16.50	17.25	13.40	17.40	17.80
T5	10.06	15.5	16.5	11.41	17.0	17.50	12.07	16.50	17.25	13.41	17.40	17.80
T6	10.06	15.5	16.5	11.41	17.0	17.50	12.07	16.50	17.25	13.42	17.50	17.75
T7	10.06	15.5	16.5	11.415	17.0	17.50	12.07	16.50	17.25	13.42	17.50	17.75
T8	10.06	15.5	16.5	11.415	26.0	23.50	12.07	31.00	27.00	13.43	59.25	46.00
T9	10.06	15.5	16.5	11.42	21.0	20.25	12.08	25.50	23.25	13.44	48.05	38.25
T10	10.06	15.5	16.5	11.42	18.0	18.25	12.08	21.00	20.25	13.45	39.40	32.50
T11	10.06	15.5	16.5	11.425	16.5	17.25	12.09	16.00	16.75	13.46	16.25	17.25
T12	10.06	15.5	16.5	11.425	16.5	17.25	12.09	16.00	16.75	13.47	16.25	17.00
T13	10.06	15.5	16.5	11.43	16.5	17.25	12.09	16.00	16.75	13.47	16.60	17.30
T14	10.06	15.5	16.5	11.43	16.0	16.75	12.09	16.00	16.75	13.48	17.00	17.50
T15	10.06	15.5	16.5	11.435	26.0	23.50	12.09	31.00	27.00	13.48	56.10	43.75
T16	10.06	15.5	16.5	11.435	20.0	19.75	12.10	24.00	22.25	13.49	44.0	35.75
T17	10.06	15.5	16.5	11.44	17.5	17.75	12.10	20.50	20.00	13.50	36.10	30.25
T18	10.06	15.5	16.5	11.44	15.0	16.50	12.11	15.50	16.50	13.51	15.50	16.50
T19	10.06	15.5	16.5	11.445	15.0	16.50	12.11	15.50	16.50	13.52	15.50	16.50
T20	10.06	15.5	16.5	11.445	15.0	16.50	12.11	15.50	16.50	13.52	15.60	16.50
T21	10.06	15.5	16.5	11.45	15.0	16.50	12.11	15.50	16.50	13.52	16.00	16.75

Table: 800.01(a)

TEMPERATURE EFFECT ON A MULTI-STOREY FRAME COLUMN

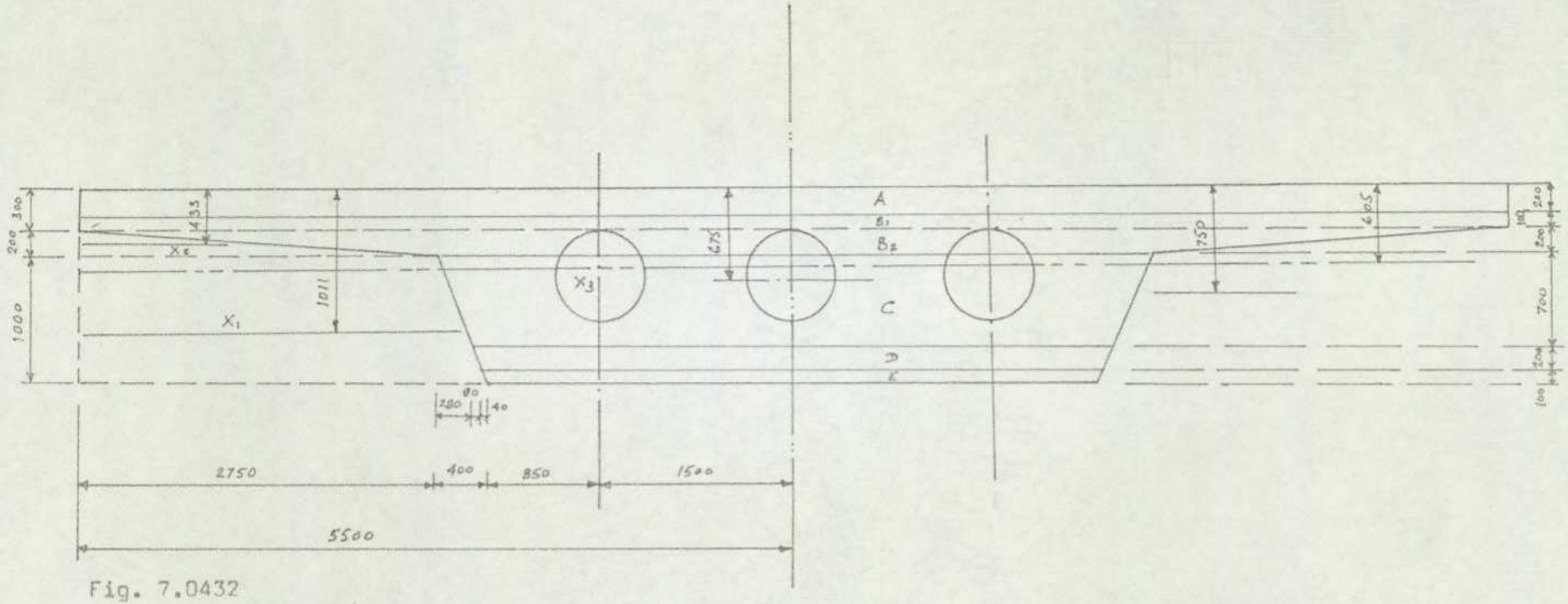

Fig. 7.0432

Segment	Area	$\bar{y}$ (from top)	I
A	22E5 mm^2	100 mm	73333E5 mm^4
B	24.66E5 mm^2	123 mm	164400E5 mm^4
C	26.14E5 mm^2	383 mm	1280000E5 mm^4
D	9.72E5 mm^2	99 mm	32397E5 mm^4
E	4.74E5 mm^2	50 mm	3950E5 mm^4

$\bar{A}$ = 87.26E5 mm^2 $\bar{y}$ = 605 mm $\bar{I}$ = 1.91E12 mm^4

Table: 700.04

Assume Base Line at the Top of Section

Segment	Area	$\bar{y}$	$\bar{y}^o$	$A*\bar{y}^o$
A	200x5500x2=2200E3	100	100	220000E3
C	$\frac{(5500+4940)}{2}$x700=3654E3	$\frac{700(2\times4940+5500)}{3(4940+5500)}$=344	500+344	3083976E3
D	$\frac{(4780+4940)}{2}$x200=972E3	$\frac{200(2\times4780+4940)}{3(4780+4940)}$=99	1200+99	1262628E3
E	$\frac{(4700+4780)}{2}$x100=474E3	$\frac{100(2\times4700+4780)}{3(4700+4780)}$=50	1400+50	687300E3
*F	$\frac{3}{4}\times\pi\times750^2$=1326E3	$\frac{750}{2}$ = 375	300+375	895050E3
B1	100x11000=1100E3	50	200+50	275000E3
B2	$\frac{(5500+11000)\times200}{2}$=1650E3	$\frac{200(2\times5500+11000)}{3(5500+11000)}$=89	89+300	641856E3

ΣA = 8724E3 $\Sigma A\bar{y}o$ = 5275704E3

yc = 5275704/8724 = 605mm

Table: 700.05

Segment	Area	I	y
Whole	$11{,}000 \times 1500 = 165E5$	$\frac{1}{12} \times 11000 \times 1500^3 = 30937500E5$	$\frac{1500}{2} = 750$
X1	$2 \times \frac{(2750+3150)1000}{2} = 59E5$	$2 \times \frac{1000^3 \times (2750^2 + 4 \times 2750 \times 3150 + 3150^2)}{36 \times (2750+3150)} = 4909134E5$	$\frac{1000(2 \times 2750 + 3150)}{3(2750+3150)} = 489$
X2	$2 \times \frac{200 \times 2750}{2} = 515E5$	$2 \times \frac{2750 \times 200^3}{36} = 12222E5$	$\frac{200}{3} = 67$
X3	$3 \times \frac{\times 750^2}{4} = 13.25E5$	$3 \times \frac{\times 750^4}{64} = 465948E5$	Center

Table: 700.06

$$I = 30937500E5 + 165E5 \times (750 - 605)^2$$
$$- 465948E5 - 13.25E5 \times (675 - 605)^2$$
$$- 4909134E5 - 59E5 \times (1011 - 605)^2$$
$$- 12222E5 - 5.5E5 \times (605 - 433)^2$$
$$= 1.907E12mm^4$$
$$= 1.907m^4$$

Member	Area of heated Zone of slab m^2	Lever arm, la, from centre of heated Zone to base of slab in (m)	Temp. Tav ^{o}C at centroid of heated Zone	Axial force in Section due to Temp. $F = A1E\alpha Tav.$	Temp. Gradient across heated Zone in $^{o}C/m$	Bending Moment at base of Section $BM = F.La + \frac{I1E\Delta T\alpha}{d}$
A	2.200	1.400	9	18.180Eα	70.0	18.180Eα x 1.4+0.00733x70.0Eα = 25.9651Eα
B	2.4664	1.177	1.18	1.9104Eα	6.6667	2.9104Eα x1.177+ 0.01644x6.6667Eα = 3.5351Eα
C	2.6129	0.617	0	0	0	0
D	0.9720	0.201	0.7425	0.7217Eα	-7.50	0.7217Eα x 0.201 + 0.0032397 x (-7.50)Eα = 0.1208Eα
E	0.474	0.050	3.250	1.5405Eα	-35.00	1.5405Eα x 0.050 + 0.0003950 x (-35.00) Eα = 0.0632Eα
				Σ 23.3526Eα		Σ 29.6842Eα

Table: 700.07

Plane Strain

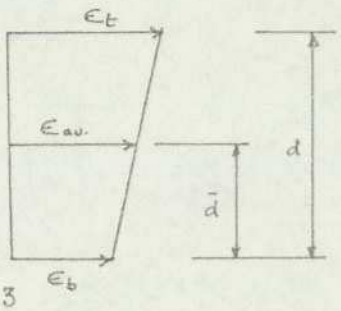

Fig. 7.0433

Strain at any point is given by the expression

$$\epsilon = \epsilon_b \left(1 - \frac{\bar{d}}{d}\right) + \epsilon_t \left(\frac{\bar{d}}{d}\right)$$

Axial force released, $F = AE\epsilon = 8.7253E \left\{\epsilon_b \left(1 - \frac{0.895}{1.50}\right) + \epsilon_t \left(\frac{0.895}{1.50}\right)\right\}$

$$= E\left[3.5192\epsilon_b + 5.2061\epsilon_t\right]$$

Bending Moment, $M = AE\epsilon\bar{d} + IE\frac{\Delta\epsilon}{d}$

$$= E\left[3.5192\,\epsilon_b + 5.2061\,\epsilon_t\right] 0.895 + 1.907E \left(\frac{\epsilon_t - \epsilon_b}{1.5}\right)$$

$$= E\left[3.1497\,\epsilon_b + 4.6595\,\epsilon_t + 1.2713\epsilon_t - 1.2713\epsilon_b\right]$$

$$= E\left[1.8784\,\epsilon_b + 5.9308\,\epsilon_t\right]$$

$\therefore$ Equating Forces gives

$$E\left[3.5192\,\epsilon_b + 5.2061\,\epsilon_t\right] = 23.3526E\alpha \qquad (1)$$

$$E\left[1.8784\,\epsilon_b + 5.9308\,\epsilon_t\right] = 29.6842E\alpha \text{ ------ } (2)$$

from (1) $\epsilon_b = (23.3526\alpha - 5.2061\,\epsilon_t)\frac{1}{3.5192}$ ------ (1a)

Subst. into (2)

$$1.8784\,(23.3526\alpha - 5.2061\,\epsilon_t)\frac{1}{3.5192} + 5.9308\,\epsilon_t = 29.6842\alpha$$

$$12.4646\alpha - 2.7788\,\epsilon_t + 5.9308\,\epsilon_t = 29.6842\alpha$$

$$3.1520\,\epsilon_t = 17.2196\alpha$$

$$\therefore \epsilon_t = \frac{17.2196\alpha}{3.1520} = 5.4631\alpha$$

Subst. into(1a) gives

$$\epsilon_b = (23.3526\alpha - 5.2061 \times 5.4631\alpha)\frac{1}{3.5192}$$

$$= -1.4460\alpha$$

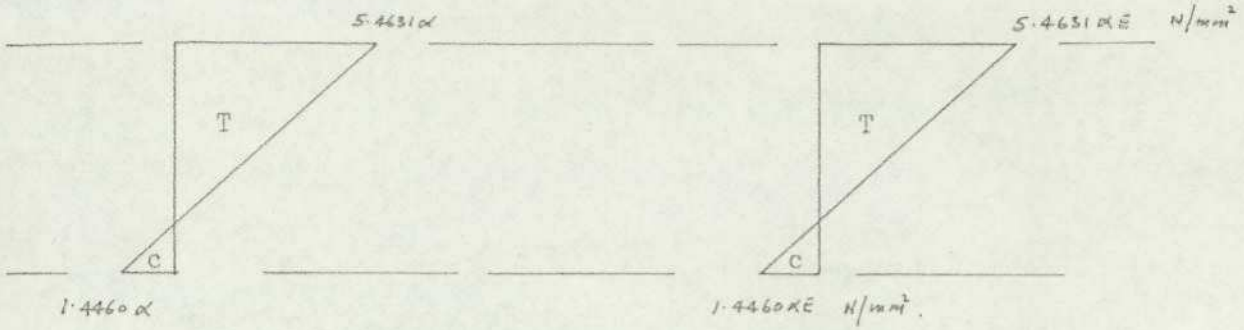

(a) Strain diagram (b) Stress diagram

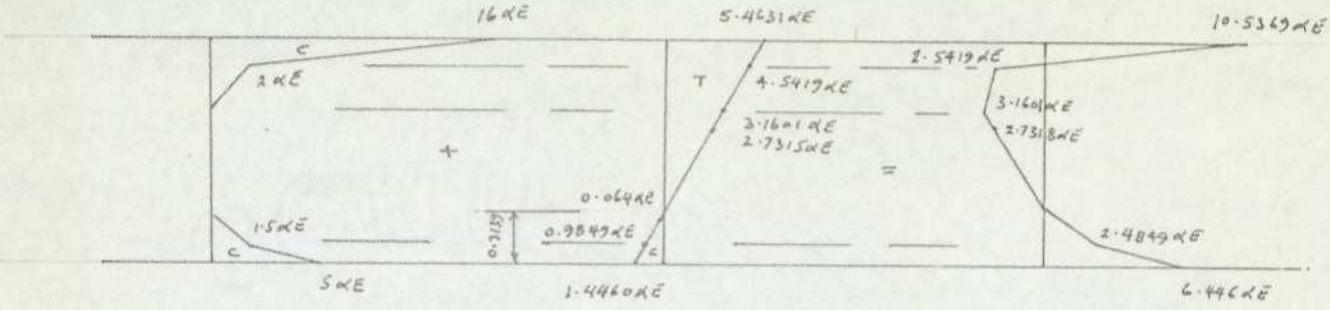

(c) Stress diagram (primary stresses due to temperature distribution)

Fig. 7.0434

Flexural stresses in the longitudinal direction due to the effect of temperature distribution.

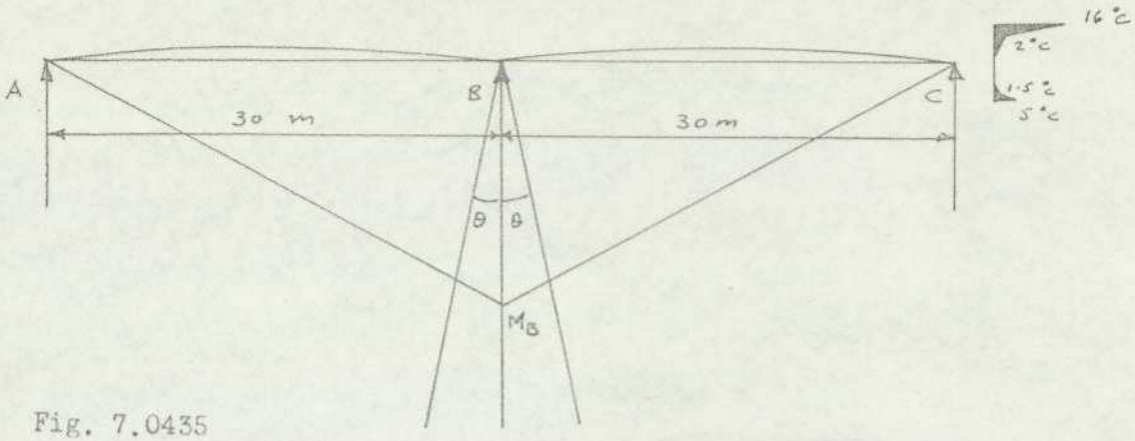

Fig. 7.0435

Bending Moment in section due to temperature distribution, $M = EI \frac{\alpha t_e}{d}$

where $t_e = 5.4631 + 1.4460 = 6.9091$

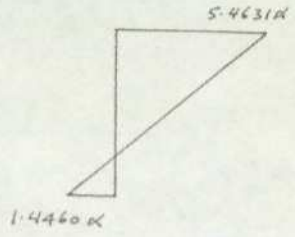

Fig. 7.0436

$$\therefore M = 28 \times 10^6 \times 1.907 \times 0.000012 \times \frac{6.9091}{1.5}$$

$$= 2951.35 \text{ KN-m}$$

$$\theta = \frac{ML}{2EI} = \frac{2951.35L}{2EI} = \frac{1475.675L}{EI}$$

$$MB \frac{L}{3EI} = \frac{1475.675L}{EI}$$

$$\therefore MB = 4427.025 \text{ KN-m}$$

$$\sigma_B \text{ top} = \frac{4427.025}{1.907/.605} = 1404.48 \text{ KN/m}^2 \quad (1.4045 \text{ N/mm}^2)$$

$$\sigma_B \text{ bott.} = \frac{4427.025}{1.907/0.895} = 2077.71 \text{ KN/m}^2 \quad (2.0777 \text{ N/mm}^2)$$

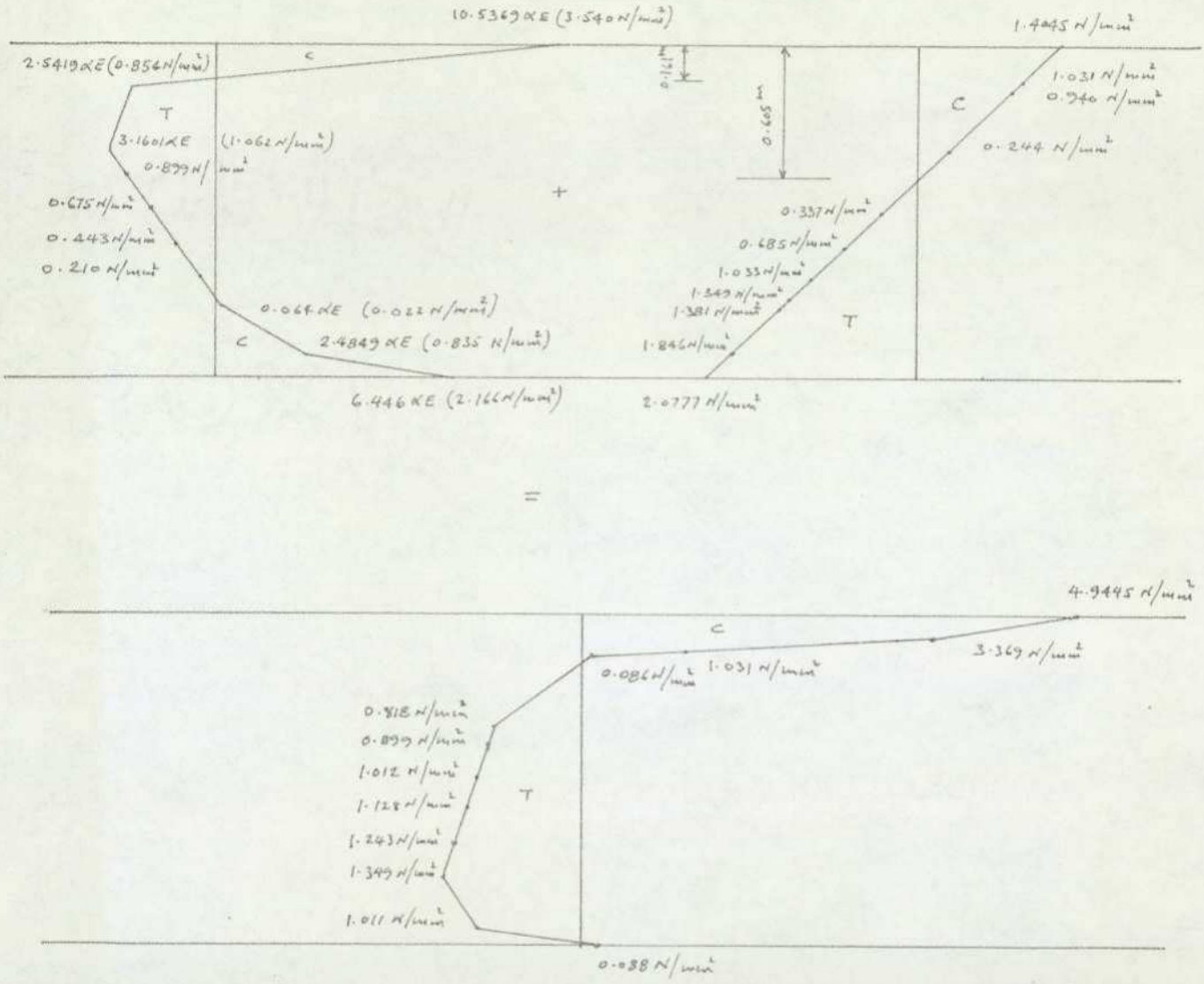

Fig. 7.0437 Final stress diagram in the longitudinal direction due to the effect of temperature distribution.

7.05 Discussion of results of thermal stresses in bridges

The first part of this section on Thermal Stresses in bridges shows that general equations can be formulated for all shapes of bridge cross-sections and for any form of temperature differential. Although the equations look very formidable at first sight, in reality they are very simple and easy to apply. This simplicity of application is demonstrated amply by solving several types of bridge forms for various temperature differentials in the second part of this section. The same general principles can be applied for the solution of thermal stresses in other structures.

The four examples of bridge decks analysed show similar thermal stress distributions. It is interesting to note that the deck surface undergoes high compressive stresses whereas the rest of the structure undergoes tensile stresses. This is quite contrary to what one would expect. However, this explains why bridge structures are known to deteriorate rapidly from underneath. The situation is further aggrevated by the fact that the majority of bridges span over waterways which cause steep temperature differentials by keeping the underside cool. The rising water vapour due to evaporation accelerates the deterioration even more. This situation is not much different even in the case of bridges which do not cross waterways, e.g. flyovers over roadways. The underside usually remains cool due to its own shading and trees and bushes planted alongside.

The results show that the thermal stresses are greater in the case of bridge decks where the structural thicknesses are greater.

From the results it follows that prestressing of beam bridges would be advantageous over conventional r.c. members, not only that greater spans can be designed, but also for providing better resistance against thermal stresses.

CHAPTER EIGHT

8.00 EXPERIMENTAL VERIFICATIONS OF THE ANALYSIS OF THERMAL STRESSES AND DEFORMATIONS

8.01 EXPERIMENTS ON 6-STOREY CONCRETE MODEL SHEAR WALL FRAME

8.01.1 Introduction

Two experiments were conducted on the Micro-concrete frame detailed in Fig. 8.001, 2 & 3. The first experiment was to determine the response of the frame due to the effect of temperature variation on the larger column. The second experiment was carried out to observe the response of the frame due to the effect of temperature variation in the roof beam.

The objectives of these experiments were (a) to check and to correlate theoretical predictions of thermal stresses and deformations with the experimental results, and (b) to check the validity of the assumptions made in the analytical formulation.

8.01.2 Model Frame

A 6-storey Micro-concrete model frame made by a previous researcher was available in good condition. It was therefore decided to use this model rather than make a new one. The dimensions and reinforcement details of the model frame are shown in figs. 8.001 and 8.002 respectively.

8.01.3 Temperature Measurement

For the purpose of measurement of temperature, 21 thermocouples had been cast into the frame at suitable locations (as shown in fig. 8.003) during the manufacture of the model. (As has been mentioned elsewhere, the measurement of temperature was carried out by the use of thermocouples because they offer the most reliable way of measuring internal temperatures).

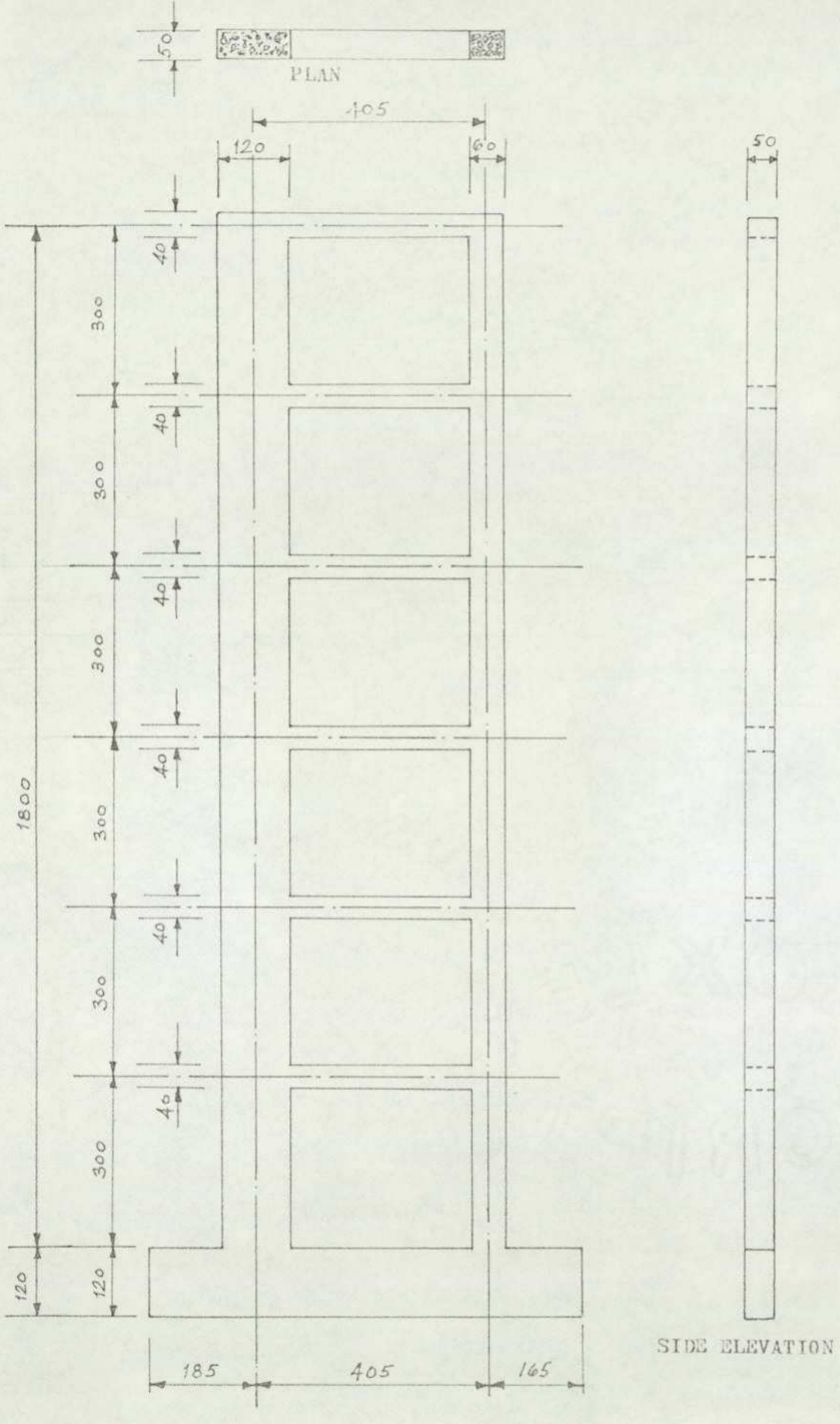

Fig. 8.001 Dimensional Details of Model Frame

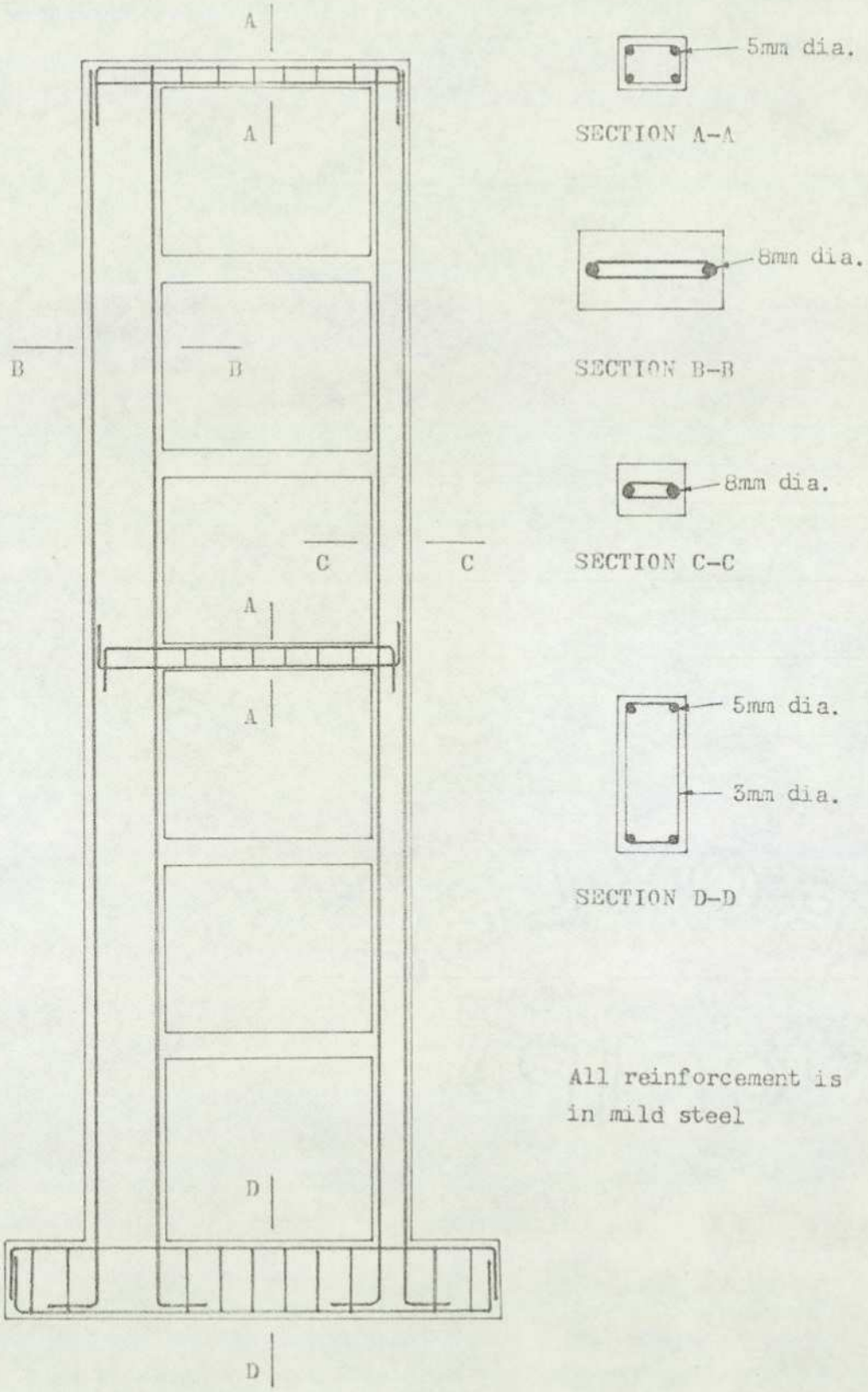

Fig. 8.002 Reinforcement in Model

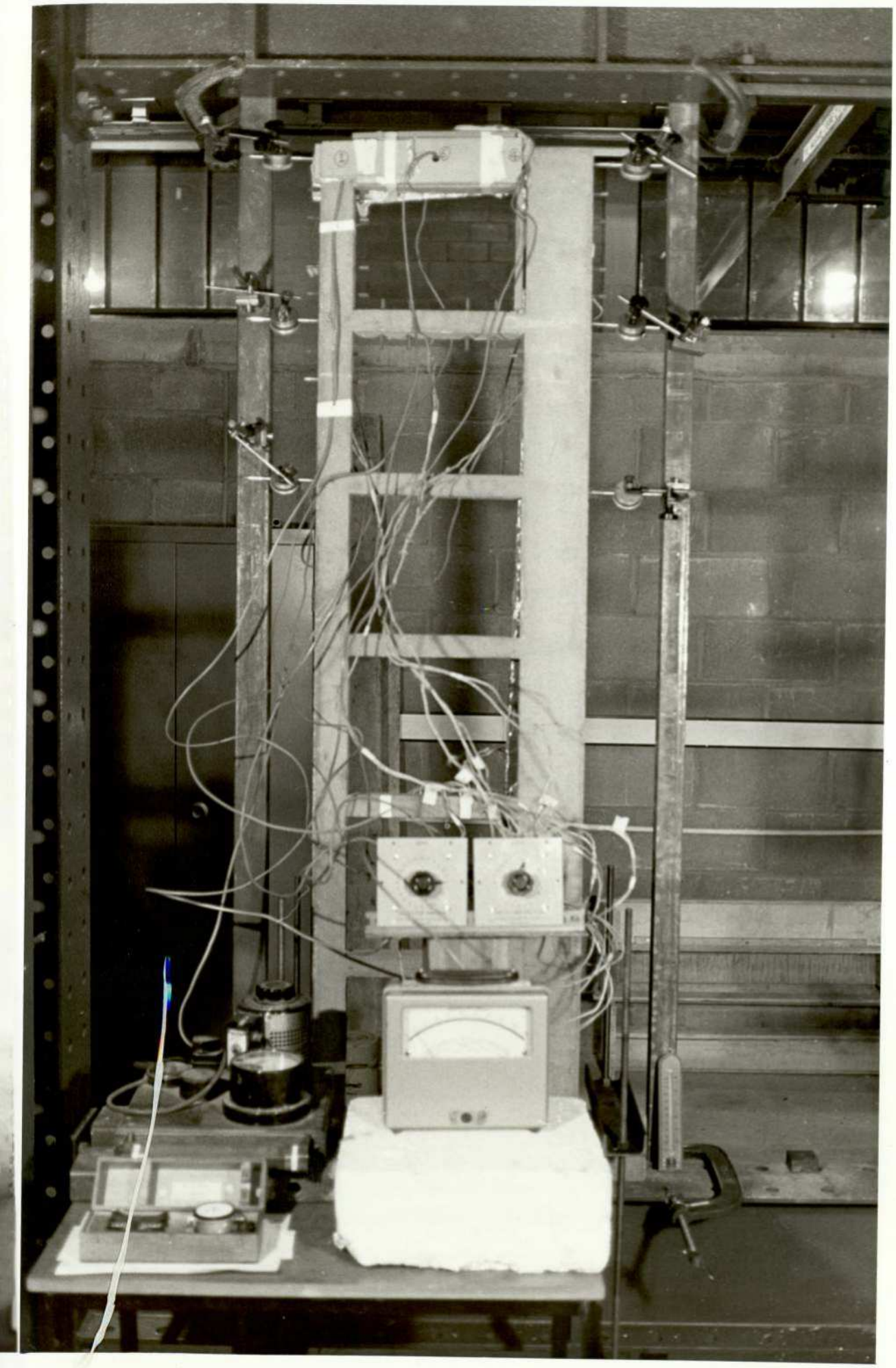

PLPLATE: VI 6-storey micro-concrete shear wall frame under test for the effect of temperature change in the roof beam

8.01.4 Strain Measurement

For the purpose of measurement of strains, demec studs (of the cast-in-socket type) at 36 locations (as shown in fig. 8.003) had been cast into the frame during its manufacture. For the measurement of strains caused by heat, demec gauges are considered superior to strain gauges as the latter has to be compensated for temperature and can give very misleading results if this is not done. In the case of demec gauges, only the studs are in contact with the heated member and the demec gauge itself is therefore not effected by the heat.

8.01.5 Deflection Measurement

For the purpose of direct measurement of deflections, dial gauges were used at various suitable locations as shown in fig. 8.003. The model frame was placed inside a larger steel frame as shown in Plate VI so as to fix the model in a stable position and allow the fixing of dial gauges.

8.01.6 Heat Input

Heating tapes were used for the purpose of heat input. For the first experiment, i.e. effect of temperature distribution in a column, heating tapes were applied on one face of the member to be heated. Insulation softboard, 12mm thick and lined with aluminium foil, was applied on the outside to stop heat loss from the tape to the atmosphere. Similarly insulating softboard lined with aluminium foil was applied to the 2 adjacent faces of the member. The opposite face to the heated face was left open to the atmosphere so that a flow of heat could take place from one face to the opposite face, thus giving a linear (or curvilinear) temperature distribution.

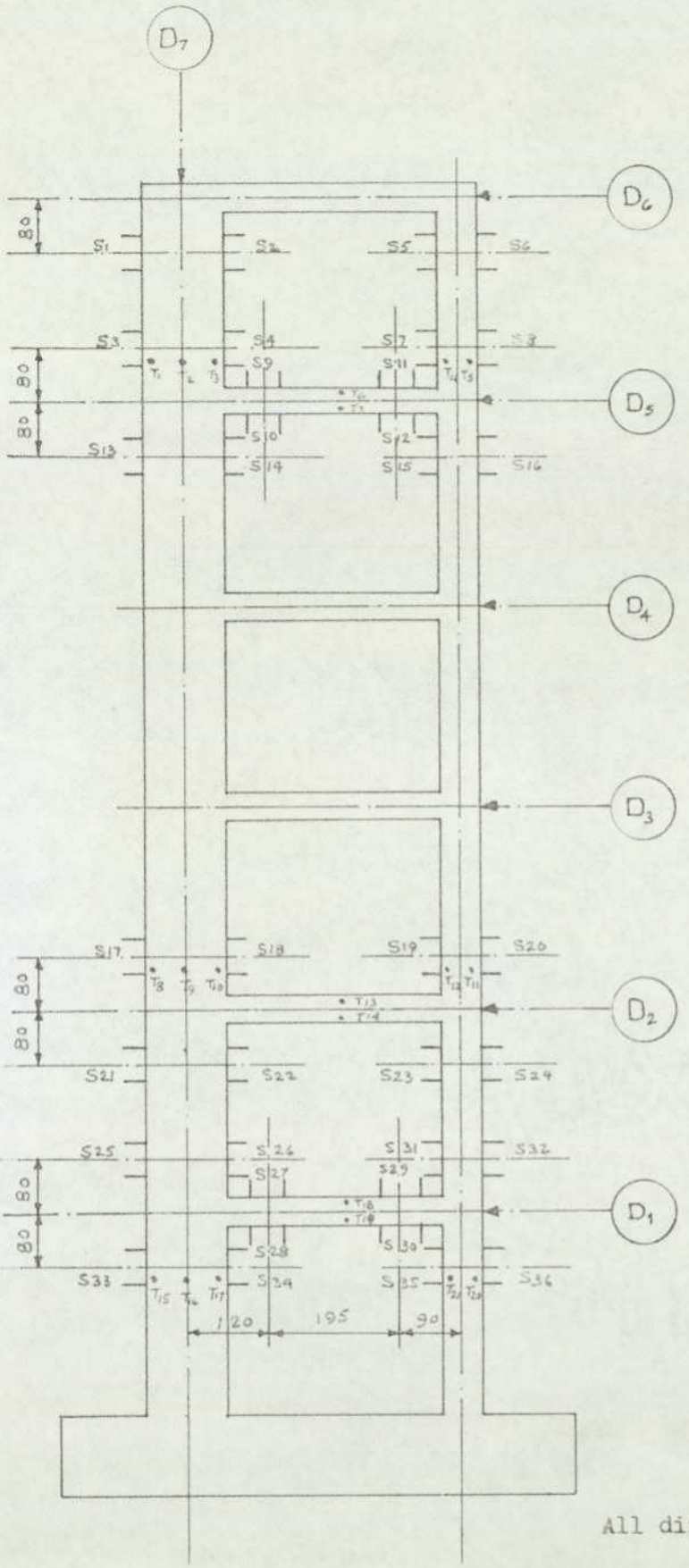

All dimensions are in mm.

Fig. 8.003 Instrumentation: S1—S36 Demec Gauges
T1—T21 Thermocouples

For the second experiment, i.e. effect of temperature distribution in the roof beam, the heating tap was wrapped round the entire beam and insulated on all sides with aluminium foil lined softboard. This was done in order to try and obtain a constant temperature distribution in the member.

8.01.7 Experiment No.1 - The effect of temperature distribution in the larger column of a 6-storey frame

It was decided to test the model frame in a vertical position so as to be as near reality as possible. The thermocouples were connected to a temperature indicator "Resilia" instrument through a 24 station multi-switch. (As the thermocouples were made of iron and the "Resilia" was a direct reading instrument for copper constantan thermocouples, it had to be calibrated before use in the experiment. This was done separately and the calibration results are shown in Appendix: B. The "Resilia" was also fitted with a mercury thermometer. A separate alcohol thermometer was used to compare the room temperature with that shown by the "Resilia" thermometer.

The heating tape was connected to a power supply through a VARIAC DURATRACK Type V6 HMT INPUT 230V OUTPUT 270V 3A (Range 0 to 268 volts) and an ampere Meter (reading up to a max. of 5 amperes).

The dial gauges were positioned at locations as shown in fig. 8.003.

Before switching on the electric power supply, the initial readings of (i) all the thermocouples and the ambient room temperature, (ii) all demec gauges, and (iii) all dial gauges were noted and recorded. The voltage was then set to 100 volts and the current switched on. From

this stage onwards periodic readings, at intervals of 1 to 2 hours, were taken of all the instruments and the time noted. As the temperature rise was small and slow, it was decided to raise the voltage to 150 volts after about 2 hours of heating. The power supply was then continued for the rest of the day. Readings of all instruments were recorded at regular intervals. The power supply was switched off overnight at 5.00 pm.

The power supply was again switched on at 9.00 am. the following day and the experiment continued recordings of all instruments at regular intervals throughout the day. The experiment was finally concluded at 5.00 pm. of the second day.

The results of the experiment are shown in Table 800.01. From these results, at least two actual temperature distributions throughout all the members were determined and are shown in figs. 8.0171 and 8.0172. Other temperature distributions (8 nos.) are available, but it was considered that 2 distributions were adequate to determine the effect of temperature distribution in a column. From the two temperature distributions selected, stresses and deflections were calculated. The stresses calculated from the demec gauges and the deflections shown by the dial gauges were compared with those obtained from the analysis.

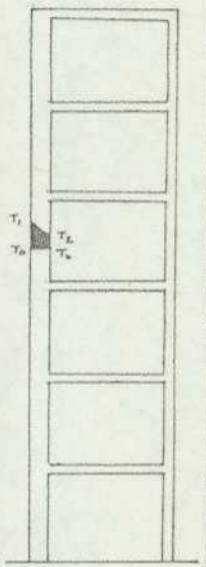

Date	2nd February 1976			2nd February 1976			2nd February 1976			2nd February 1976		
Thermocouple No.	Time	Thermo-Couple Reading	True Temp. ^{o}C	Time	Thermo-Couple Reading	True Temp. ^{o}C	Time	Thermo-Couple Reading	True Temp. ^{o}C	Time	Thermo-Couple Reading	True Temp. ^{o}C
	Voltage Applied = 100 Volts			Voltage Applied = 100 Volts			Voltage Applied = 100 Volts			Voltage Applied = 150 Volts		
T1	10.06	15.5	16.5	11.40	26.5	24.0	12.05	32.0	27.50	13.37	58.50	45.50
T2	10.06	15.5	16.5	11.40	23.0	21.50	12.06	27.0	24.25	13.38	50.10	39.75
T3	10.06	15.5	16.5	11.405	18.0	18.25	12.06	21.50	20.50	13.39	39.00	32.25
T4	10.06	15.5	16.5	11.405	17.0	17.50	12.07	16.50	17.25	13.40	17.40	17.80
T5	10.06	15.5	16.5	11.41	17.0	17.50	12.07	16.50	17.25	13.41	17.40	17.80
T6	10.06	15.5	16.5	11.41	17.0	17.50	12.07	16.50	17.25	13.42	17.50	17.75
T7	10.06	15.5	16.5	11.415	17.0	17.50	12.07	16.50	17.25	13.42	17.50	17.75
T8	10.06	15.5	16.5	11.415	26.0	23.50	12.07	31.00	27.00	13.43	59.25	46.00
T9	10.06	15.5	16.5	11.42	21.0	20.25	12.08	25.50	23.25	13.44	48.05	38.25
T10	10.06	15.5	16.5	11.42	18.0	18.25	12.08	21.00	20.25	13.45	39.40	32.50
T11	10.06	15.5	16.5	11.425	16.5	17.25	12.09	16.00	16.75	13.46	16.25	17.25
T12	10.06	15.5	16.5	11.425	16.5	17.25	12.09	16.00	16.75	13.47	16.25	17.00
T13	10.06	15.5	16.5	11.43	16.5	17.25	12.09	16.00	16.75	13.47	16.60	17.30
T14	10.06	15.5	16.5	11.43	16.0	16.75	12.09	16.00	16.75	13.48	17.00	17.50
T15	10.06	15.5	16.5	11.435	26.0	23.50	12.09	31.00	27.00	13.48	56.10	43.75
T16	10.06	15.5	16.5	11.435	20.0	19.75	12.10	24.00	22.25	13.49	44.0	35.75
T17	10.06	15.5	16.5	11.44	17.5	17.75	12.10	20.50	20.00	13.50	36.10	30.25
T18	10.06	15.5	16.5	11.44	15.0	16.50	12.11	15.50	16.50	13.51	15.50	16.50
T19	10.06	15.5	16.5	11.445	15.0	16.50	12.11	15.50	16.50	13.52	15.50	16.50
T20	10.06	15.5	16.5	11.445	15.0	16.50	12.11	15.50	16.50	13.52	15.60	16.50
T21	10.06	15.5	16.5	11.45	15.0	16.50	12.11	15.50	16.50	13.52	16.00	16.75

Table: 800.01(a)

TEMPERATURE EFFECT ON A MULTI-STOREY FRAME COLUMN

Date	2nd February 1976			2nd February 1976			2nd February 1976			3rd February 1976		
Thermocouple No.	Time	Thermo-couple Reading	True Temp. °C	Time	Thermo-couple Reading	True Temp. °C	Time	Thermo-couple Reading	True Temp. °C	Time	Thermo-couple Reading	True Temp. °C
	Voltage Applied = 150 Volts			Voltage Applied = 150 Volts			Voltage Applied = 150 Volts			Voltage Applied = 150 Volts		
T1	14.34	68.00	52.00	15.44	75.50	57.00	16.51	81.00	60.75	13.43	81.00	60.75
T2	14.35	60.00	46.50	15.44	67.50	51.50	16.51	72.00	54.75	13.44	72.50	55.00
T3	14.36	48.00	38.25	15.45	55.00	43.00	16.51	60.00	46.50	13.45	60.00	46.50
T4	14.36	17.50	17.75	15.45	17.00	17.50	16.52	17.50	17.75	13.46	17.50	17.75
T5	14.37	17.50	17.75	15.46	17.00	17.50	16.52	17.50	17.75	13.47	17.50	17.75
T6	14.37	18.00	18.25	15.46	19.50	19.25	16.53	20.00	19.75	13.47	20.50	20.00
T7	14.37	18.00	18.25	15.46	19.50	19.25	16.53	20.00	19.75	13.47	20.50	20.00
T8	14.37	68.00	52.00	15.47	75.50	57.00	16.53	81.00	60.75	13.48	82.50	61.75
T9	14.38	57.50	44.75	15.48	65.00	50.00	16.54	70.00	53.25	13.48	71.00	54.00
T10	14.38	48.00	38.25	15.48	55.00	43.00	16.54	60.00	46.50	13.48	61.00	47.25
T11	14.39	16.00	16.75	15.49	16.00	16.75	16.55	16.00	16.75	13.49	17.00	17.50
T12	14.39	16.00	16.75	15.49	16.00	16.75	16.55	16.00	16.75	13.49	17.00	17.50
T13	14.40	18.00	18.25	15.49	19.00	19.00	16.55	20.00	19.75	13.49	20.50	20.00
T14	14.40	18.00	18.25	15.49	19.00	19.00	16.55	20.00	19.75	13.50	21.00	20.25
T15	14.40	61.00	47.25	15.50	64.50	49.50	16.56	66.50	51.00	13.50	67.50	52.75
T16	14.41	50.00	39.75	15.50	53.50	42.00	16.57	55.50	43.50	13.51	56.00	43.75
T17	14.41	42.00	34.50	15.51	45.50	36.75	16.57	47.50	38.00	13.51	48.00	38.50
T18	14.41	15.50	16.50	15.51	16.00	16.75	16.58	15.50	16.50	13.52	15.00	16.50
T19	14.42	15.50	16.50	15.51	16.00	16.75	16.58	15.50	16.50	13.52	15.00	16.50
T20	14.42	16.00	16.75	15.52	16.50	17.25	16.58	17.00	17.50	13.52	17.50	17.75
T21	14.42	16.00	16.75	15.52	16.00	16.75	16.58	16.00	16.75	13.52	18.00	18.25

Table: 800.01(b)

TEMPERATURE EFFECT ON A MULTI-STOREY FRAME COLUMN

Date	3rd February 1976			3rd February 1976			3rd February 1976		
Thermocouple No.	Time	Thermo-Couple Reading	True Temp. °C	Time	Thermo-Couple Reading	True Temp. °C	Time	Thermo-Couple Reading	True Temp. °C
	Voltage Applied = 150 Volts			Voltage Applied = 150 Volts			Voltage Applied = 150 Volts		
T1	15.40	86.50	64.50	17.05	90.00	66.75	9.04	16.50	17.25
T2	25.40	78.20	58.75	17.06	80.60	60.25	9.04	16.50	17.25
T3	15.40	64.50	49.50	17.07	67.30	51.75	9.04	16.50	17.25
T4	15.41	17.80	18.00	17.08	18.50	18.75	9.04	16.50	17.25
T5	15.41	17.50	17.75	17.09	18.50	18.75	9.04	16.50	17.25
T6	15.41	21.00	20.25	17.09	22.30	21.25	9.04	16.50	17.25
T7	15.41	21.00	20.25	17.10	22.30	21.25	9.04	16.50	17.25
T8	15.42	87.50	65.00	17.11	88.80	65.75	9.04	16.50	17.25
T9	15.42	75.50	57.00	17.12	77.50	58.25	9.04	16.50	17.25
T10	15.43	65.00	50.00	17.12	67.50	52.75	9.04	16.50	17.25
T11	15.44	16.50	17.25	17.13	17.50	17.75	9.04	16.50	17.25
T12	15.44	16.25	17.00	17.13	17.50	17.75	9.04	16.50	17.25
T13	15.45	21.50	20.50	17.14	22.30	21.25	9.04	16.00	16.75
T14	15.45	22.00	20.75	17.14	23.00	21.50	9.04	16.00	16.75
T15	15.46	68.00	52.00	17.15	68.10	52.00	9.04	16.00	16.75
T16	15.47	57.00	44.50	17.16	57.50	44.75	9.04	16.00	16.75
T17	15.48	48.80	38.75	17.17	49.50	39.50	9.04	16.00	16.75
T18	15.48	15.00	16.50	17.18	15.00	16.50	9.04	16.00	16.75
T19	15.45	15.00	16.50	17.18	15.00	16.50	9.04	16.00	16.75
T20	15.49	17.50	17.75	17.18	18.00	18.25	9.04	16.00	16.75
T21	15.50	15.00	16.50	17.19	17.52	17.75	9.04	16.00	16.75

Table: 800.01(c)

TEMPERATURE EFFECT ON A MULTI-STOREY FRAME COLUMN

TEMPERATURE EFFECT ON A MULTI-STOREY FRAME COLUMN
SHEET 3
DEMEC GAUGE READINGS

Date	3rd February 1976			3rd February 1976			3rd February 1976		
Demec Gauge No.	Time	Demec Gauge Reading	Ch.in Demec Read.	Time	Demec Gauge Reading	Ch.in Demec Read.	Time	Demec Gauge Reading	Change in Demec Reading
1	9.04	571	9	13.53	626	64	15.58	611	49
2		810	0	13.54	815	5	15.56	825	15
3		392	36	13.53	401	45	15.58	395	39
4		1040	- 43	10.54	1035	- 48	15.55	1041	- 42
5		530	- 6	13.55	521	- 15	15.55	528	- 8
6		2189	89	13.56	2180	80	15.54	2193	93
7		730	- 6	13.54	720	- 16	15.55	718	- 18
8		1554	7	13.56	1541	- 6	15.54	1540	- 7
9		1454	1	13.54	1459	6	15.55	1458	5
10		591	36	13.57	543	- 12	15.57	564	9
11		820	19	13.54	795	- 6	15.55	818	17
12		683	15	13.57	679	11	15.57	679	11
13		1610	- 21	13.58	1650	19	15.58	1643	12
14		1090	- 15	13.55	1094	- 11	15.56	1114	9
15		2093	- 7	13.55	2080	- 20	15.54	2084	- 16
16		939	21	13.56	919	1	15.54	954	36
17		1430	17	13.57	1468	55	15.58	1460	47
18		1540	- 6	13.57	1559	13	15.59	1560	14
19		1486	97	13.58	1502	113	15.59	1470	81
20		608	- 3	13.58	604	- 7	15.59	602	- 9
21		-		-	-		-	-	
22		706	0	13.59	715	9	16.00	718	12
23		873	- 2	13.58	865	- 10	16.00	877	2
24		574	- 13	13.58	567	- 20	15.59	577	- 10
25		482	5	13.59	498	21	16.00	505	28
26		1129	377	13.59	910	158	16.00	834	82
27		523	- 19	13.59	528	- 14	16.01	528	- 14
28		-		-	-		-	-	
29		678	9	14.00	664	- 5	16.01	667	- 2
30		1162	0	14.01	1171	9	16.02	1164	2
31		595	14	14.00	598	17	16.01	601	20
32		1477	- 23	14.02	1456	- 46	16.01	1470	- 30
33		2094	- 2	14.01	2115	19	16.02	2118	22
34		672	31	14.01	647	6	16.02	661	20
35		2116	16	14.01	2112	12	16.02	2116	16
36		1955	5	14.00	1870	- 80	16.01	1950	0

Table 800.02(a)

TEMPERATURE EFFECT ON A MULTI-STOREY FRAME COLUMN

SHEET 1

DEMEC GAUGE READINGS

DEMEC No.846
DIAL No.242758
RESEARCH & DEVELOPMENT DIVISION
ONE DIV. REPRESENTS A STRAIN OF 2.47×10^{-5}

Date	2nd February 1976			2nd February 1976			2nd February 1976		
Demec Gauge No.	Time	Demec Gauge Reading	Ch.in Demec Read.	Time	Demec Gauge Reading	Ch.in Demec Read.	Time	Demec Gauge Reading	Change in Demec Reading
1	11.15	562	0	12.21	600	38	13.54	590	28
2	11.15	810	0	12.21	818	8	13.54	814	4
3	11.15	356	0	12.13	368	12	13.54	205	- 51
4	11.15	1083	0	12.21	1039	- 44	13.55	1048	- 35
5	11.15	536	0	12.20	533	- 3	13.55	534	- 2
6	11.16	2100	0	12.23	2128	28	13.58	2158	58
7	11.16	736	0	12.20	708	- 28	13.56	733	- 3
8	11.16	1547	0	12.23	1556	9	13.56	1564	17
9	11.16	1453	0	12.21	1452	- 1	13.55	1453	0
10	11.16	555	0	12.22	511	- 44	13.59	584	29
11	11.17	801	0	12.21	818	17	13.55	813	12
12	11.17	668	0	12.22	674	6	13.59	674	12
13	11.17	1631	0	12.13	1650	19	13.54	1533	- 98
14	11.17	1105	0	12.20	1020	- 85	13.56	1073	- 32
15	11.17	2100	0	12.19	2102	2	13.57	2121	21
16	11.18	918	0	12.24	956	38	13.58	911	- 7
17	11.18	1413	0	12.13	1420	7	13.59	1447	34
18	11.18	1546	0	12.17	1547	1	14.00	1555	9
19	11.18	1389	0	12.17	1474	85	14.01	1472	83
20	11.18	611	0	12.19	612	1	14.02	605	- 6
21	11.19	-		-	-		-	-	
22	11.19	706	0	12.17	707	1	14.00	714	8
23	11.19	875	0	12.17	884	9	14.01	875	0
24	11.19	587	0	12.19	570	- 17	14.02	564	- 21
25	11.19	477	0	12.14	486	9	14.00	502	25
26	11.20	752	0	12.15	865	13	14.01	899	47
27	11.20	542	0	12.16	540	- 2	14.04	538	- 4
28	11.20	-		-	-		-	-	
29	11.20	669	0	12.16	671	2	14.04	661	- 8
30	11.20	1162	0	12.15	1151	- 11	14.03	1161	- 1
31	11.21	581	0	12.16	579	- 2	14.01	579	- 2
32	11.21	1500	0	12.18	1490	- 10	14.02	1460	- 40
33	11.21	1096	0	12.14	2102	6	14.00	2110	14
34	11.21	641	0	12.14	660	19	14.03	668	27
35	11.21	2100	0	12.16	2122	22	14.03	2113	13
36	11.21	1950	0	12.18	1898	- 52	14.02	1932	- 18

Table: 800.02 (b)

TEMPERATURE EFFECT ON A
MULTI-STOREY FRAME COLUMN
SHEET 2
DEMEC GAUGE READINGS

Date	2nd February 1976			2nd February 1976			2nd February 1976		
Demec Gauge No.	Time	Demec Gauge Reading	Ch.in Demec Read.	Time	Demec Gauge Reading	Ch.in Demec Read.	Time	Demec Gauge Reading	Change in Demec Reading
1	14.43	591	29	15.53	627	65	16.59	647	85
2	14.44	816	6	15.54	817	7	17.00	817	17
3	14.44	387	31	15.53	394	38	16.59	402	46
4	14.45	1051	- 32	15.54	1042	- 41	17.00	1049	- 34
5	14.46	539	3	15.55	532	- 4	17.01	541	5
6	14.47	2145	45	15.56	2212	112	17.01	2191	91
7	14.46	732	- 4	15.55	729	- 7	17.01	732	- 4
8	14.47	1553	6	15.56	1551	4	17.02	1552	5
9	14.45	1457	4	15.54	1457	4	17.00	1455	2
10	14.48	520	- 35	15.58	532	- 23	17.03	557	2
11	14.45	804	3	15.55	801	0	17.00	804	3
12	14.49	669	1	15.58	686	18	17.03	664	- 4
13	14.44	1650	19	15.53	1654	23	16.59	1672	41
14	14.58	1081	- 24	15.58	1118	13	17.02	1127	22
15	14.47	2111	11	15.58	2106	6	17.03	2115	15
16	14.48	922	4	15.57	938	20	17.02	925	7
17	14.50	1442	29	15.59	1455	42	17.06	1448	35
18	14.50	1552	6	15.59	1556	10	17.07	1564	18
19	14.49	1457	68	15.59	1514	125	17.11	1512	123
20	14.49	609	- 2	15.59	604	- 7	17.04	605	- 6
21	-	-		-	-		-	-	
22	14.50	712	6	16.00	721	15	17.05	712	6
23	14.51	883	8	16.02	877	2	17.05	866	- 9
24	14.51	569	- 18	16.02	582	- 5	17.04	569	- 18
25	14.55	495	18	16.07	503	26	17.06	500	23
26	14.54	914	162	16.08	867	115	17.06	891	139
27	14.54	536	- 6	16.01	541	- 1	17.05	532	- 10
28	14.57			16.06			17.07		
29	14.54	652	- 17	16.01	668	- 1	17.05	658	- 11
30	14.57	1158	- 4	16.06	1156	- 6	17.08	1149	- 13
31	14.52	588	7	16.02	592	11	17.05	589	8
32	14.51	1465	- 35	16.02	1505	5	17.04	1494	- 6
33	14.55	2113	17	16.05	2111	15	17.06	2114	18
34	14.56	670	29	16.04	684	43	17.07	663	22
35	14.56	2118	18	16.03	2125	25	17.08	2117	17
36	14.56	1896	- 54	16.03	1926	- 24	17.04	1925	- 25

Table: 800.02 (c)

TEMPERATURE EFFECT ON A
MULTI-STOREY FRAME COLUMN
SHEET 4
DEMEC GAUGE READINGS

Date	3rd February 1976		
Demec Gauge No.	Time	Demec Gauge Reading	Ch. in Demec Read.
1	16.48	603	41
2	16.49	816	6
3	16.48	391	35
4	16.49	1043	- 40
5	16.50	537	1
6	16.50	2185	85
7	16.50	712	- 24
8	16.51	1547	0
9	16.49	1453	0
10	16.52	568	13
11	16.50	826	25
12	16.52	677	- 9
13	16.49	1644	13
14	16.52	1085	- 20
15	16.51	1098	- 2
16	16.51	920	2
17	16.52	1464	51
18	16.53	1557	11
19	16.53	1469	80
20	16.53	605	- 6
21	-	-	
22	26.55	714	8
23	16.54	859	- 16
24	16.53	571	- 16
25	16.55	501	24
26	16.55	829	77
27	16.54	529	- 13
28	-	-	
29	16.54	666	- 3
30	16.56	1147	- 15
31	16.54	595	14
32	16.50	1493	- 7
33	16.55	2113	17
34	16.56	648	7
35	16.54	2112	12
36	16.53	1955	5

Table: 800.02 (d)

Date	2nd February, 1976			2nd February, 1976			2nd February, 1976			2nd February, 1976		
Dial Gauge Position & no.	Time	Dial Gauge Reading	Displace-ments in mm.	Time	Dial Gauge Reading	Displace-ments in mm.	Time	Dial Gauge Reading	Displace-ments in mm.	Time	Dial Gauge Reading	Displace-ments in mm.
1st Fl. Level D1	10.06	0.67	0	11.23	0.67	0	11.43	0.67	0	12.05	0.675	0.005
2nd Fl. Level D2	10.06	0.55	0	11.23	0.54	-0.01	11.43	0.55	0	12.05	0.56	0.01
3rd Fl. Level D3	10.06	1.21	0	11.23	1.22	0.01	11.43	1.235	0.025	12.05	1.265	0.055
4th Fl. Level D4	10.06	2.36	0	11.23	2.40	0.04	11.43	1.44	0.08	12.05	1.495	0.135
5th Fl. Level D5	10.06	0.56	0	11.23	0.625	0.065	11.43	0.69	0.13	12,05	0.78	0.220
6th Fl. Level D6	10.06	1.46	0	11.23	1.57	0.11	11.43	1.68	0.22	12.05	1.82	0.360
Roof Level D7	10.06	5.06	0	11.23	5.06	0	11.43	5.065	0.005	12.05	5.11	0.050

Table: 800.03(a) TEMPERATURE EFFECT ON A MULTI-STOREY FRAME COLUMN
DIAL GAUGE READINGS (0.01 mm. per DIVISION)

Date	2nd February 1976			2nd February 1976			2nd February 1976			2nd February 1976		
Dial Gauge Position & No.	Time	Dial Gauge Reading	Displace-ments in mm	Time	Dial Gauge Reading	Displace-ments in mm	Time	Dial Gauge Reading	Displace-ments in mm	Time	Dial Gauge Reading	Displace-ments in mm
1st Fl. Level D1	13.31	0.69	0.02	14.32	0.70	0.03	15.40	0.71	0.04	15.59	0.71	0.04
2nd Fl. Level D2	13.31	0.629	0.079	14.32	0.655	0.105	15.41	0.68	0.13	15.59	0.695	0.145
3rd Fl. Level D3	13.32	1.41	0.20	14.32	1.49	0.28	15.41	1.535	0.325	16.49	1.57	0.36
4th Fl. Level D4	13.33	2.76	0.40	14.33	2.895	0.535	15.41	2.98	0.62	16.49	3.045	0.685
5th Fl. Level D5	13.33	1.22	0.66	14.33	1.46	0.90	15.41	1.60	1.04	16.49	1.695	1.135
6th Fl. Level D6	13.34	2.5025	1.0425	14.33	2.80	1.34	15.43	3.01	1.55	16.49	3.15	1.69
Roof L. D7	13.35	5.344	0.284	14.33	5.41	0.35	15.43	5.52	0.46	16.49	5.56	0.50

Table: 800.03(b)

TEMPERATURE EFFECT ON A MULTI-STOREY FRAME COLUMN
DIAL GAUGE READINGS (0.01mm PER DIVISION)

Date	3rd February 1976			3rd February 1976			3rd February 1976			3rd February 1976		
Dial Gauge Position & No.	Time	Dial Gauge Reading	Displace-ments in mm	Time	Dial Gauge Reading	Displace-ments in mm	Time	Dial Gauge Reading	Displace-ments in mm	Time	Dial Gauge Reading	Displace-ments in mm
1st Fl. Level D1	9.04	0.67	0	13.40	0.715	0.045	15.51	0.714	0.044	17.03	0.712	0.042
2nd Fl. Level D2	9.04	0.54	0	13.40	0.691	0.151	15.51	0.712	0.172	17.03	0.708	0.168
3rd Fl. Level D3	9.04	1.22	0	13.41	1.528	0.308	15.51	1.602	0.382	17.03	1.605	0.385
4th Fl. Level D4	9.04	2.37	0	13.41	3.04	0.67	15.51	3.11	0.74	17.03	3.112	0.742
5th Fl. Level D5	9.04	0.59	0	13.41	1.659	1.069	15.52	1.789	1.199	17.04	1.802	1.212
6th Fl. Level D6	9.04	1.48	0	13.41	3.111	1.631	15.52	3.272	1.792	17.04	3.294	1.814
Roof L. D7	9.04	5.04	0	13.42	5.62	0.58	15.52	5.62	0.58	17.02	5.67	0.63

Table: 800.03(c)

TEMPERATURE EFFECT ON A MULTI-STOREY FRAME COLUMN
DIAL GAUGE READINGS (0.01mm PER DIVISION)

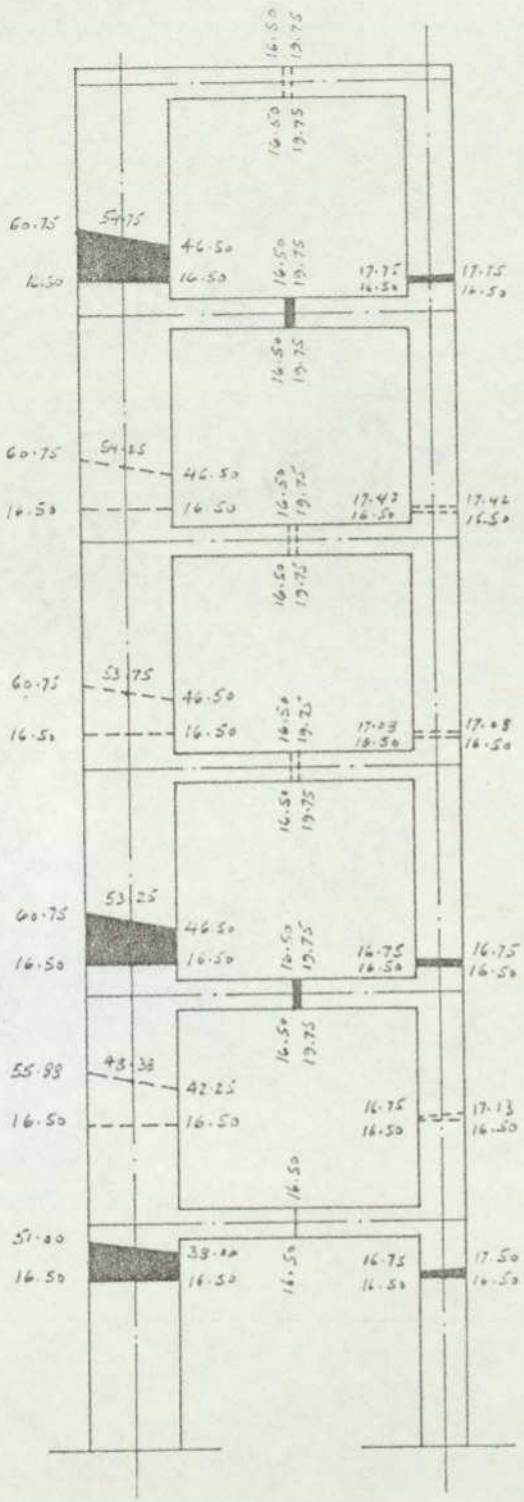

Fig. 8.0171 Temperature distribution in all members of the frame due to heating of the larger column. CASE (1)

(All temperatures shown are in ^{o}C)

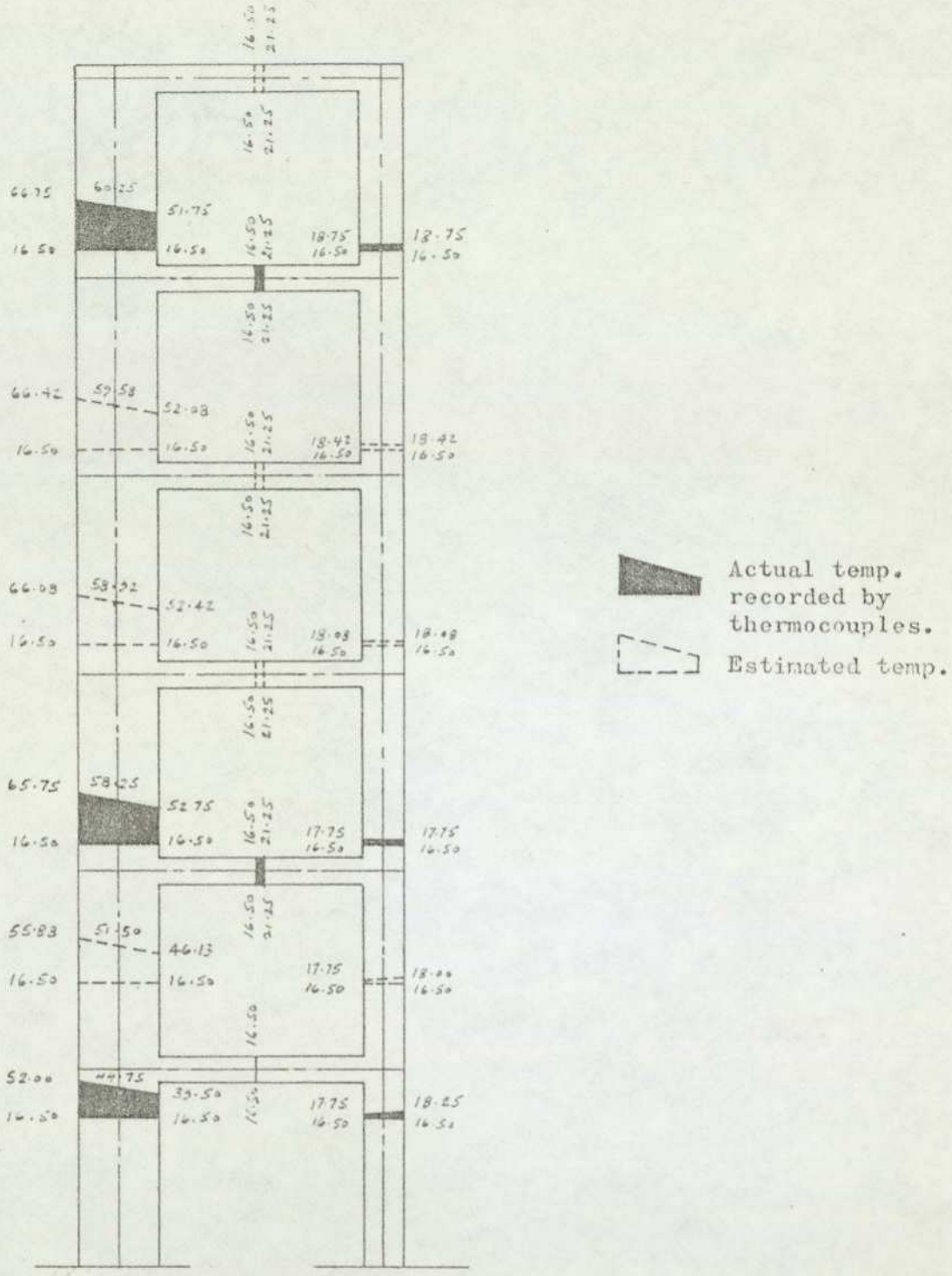

Fig. 8.0172 Temperature distribution in all members of the frame due to heating of the larger column. CASE (2)

(All temperatures shown are in ^{o}C)

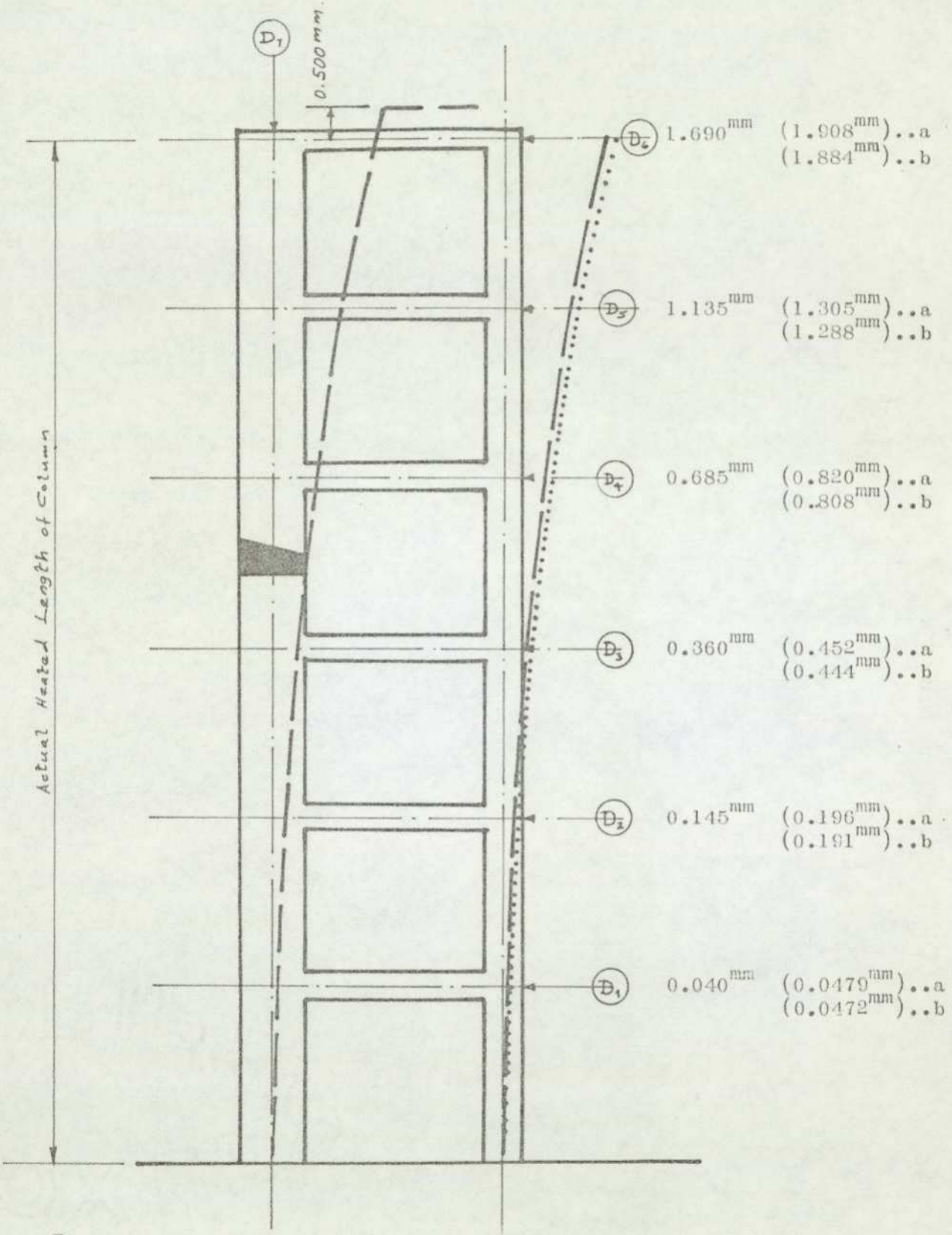

Fig. 8.0173 Shows deflection of a frame subjected to temperature changes affecting one column only (CASE 1)

Unbracketed Figures—— show experimental results

Bracketed Figures——— show (a) theoretical primary results

(b) theoretical results including secondary effects.

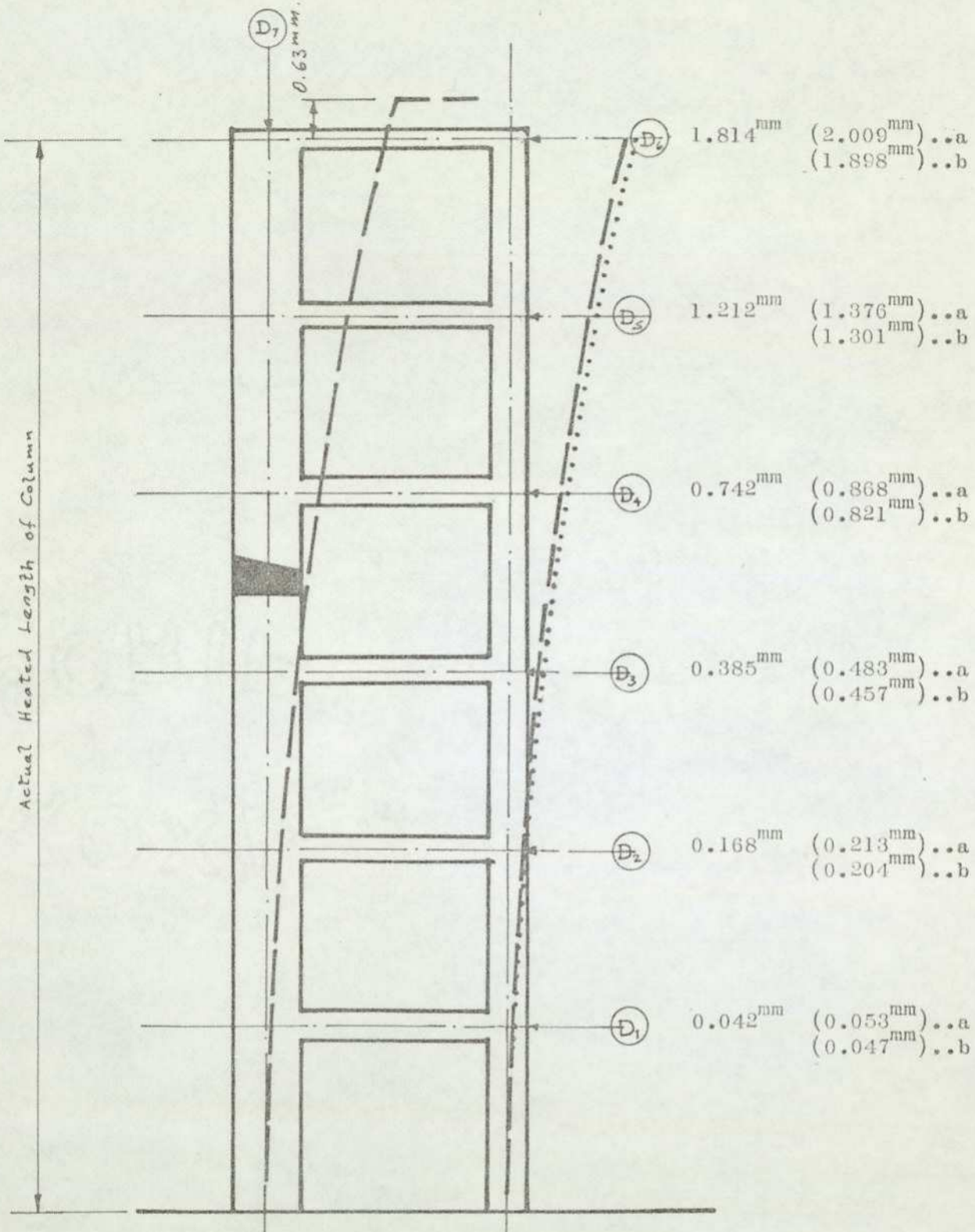

Fig. 8.0174 Shows deflection of a frame subjected to temperature changes affecting one column only (CASE 2)

Unbracketed Figures—— show experimental results

Bracketed Figures——— show (a) theoretical primary results

(b) theoretical results including secondary effects

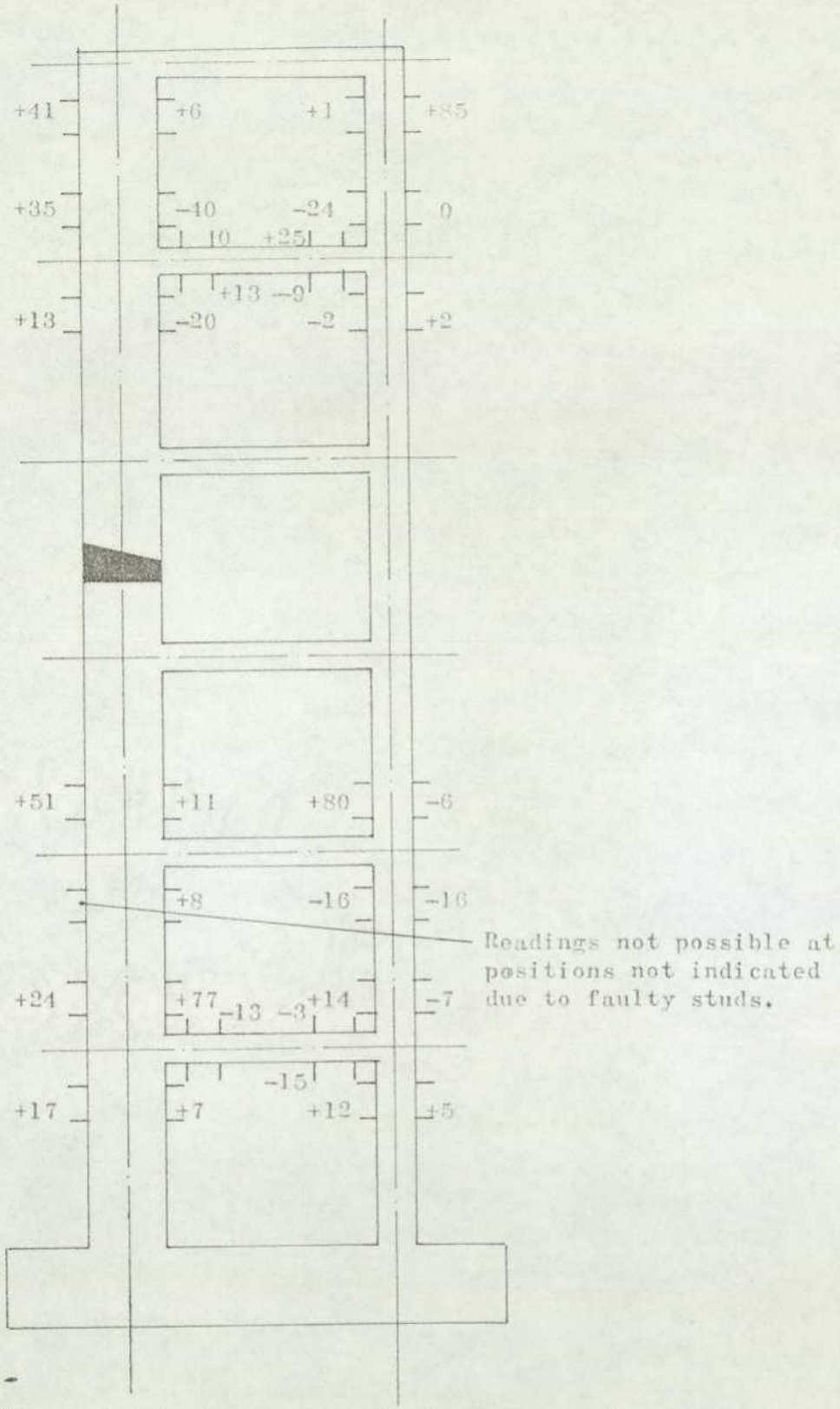

Fig. 8.0175 Summary of net change in readings recorded at demec gauge positions

8.01.8 Experiment No. 2 - The effect of temperature variation in the roof beam of a 6-storey frame.

The second experiment was carried out exactly in the same way as the first experiment. This experiment was conducted continuously over a period of 3 days. For the control and measurement of temperature in the heated beam, a set of 6 additional thermocouples was fixed to the roof beam. For the measurement of direct deflections, 6 dial gauges were repositioned as shown in figs. 8.0183 and 8.0184.

The readings of all the instruments were taken at suitable intervals of time and are shown in Tables 800.4, 5 & 6. From these readings, once again two actual temperature distributions throughout all the members were determined and are shown in figs. 8.0181 and 8.0182. Further temperature distributions are available, but it was considered that 2 distributions were adequate to determine the effect of temperature distribution in the roof beam. From the two temperature distributions selected, stresses and deflections were then calculated, and compared with those obtained by the analysis.

TEMPERATURE EFFECT ON A MULTI-STOREY FRAME ROOF BEAM

Date	9th February 1976			10th February 1976			10th February 1976			10th February 1976		
Thermocouple No.	Time	Thermo-couple Readings	True Temp. °C	Time	Thermo-couple Readings	True Temp. °C	Time	Thermo-couple Readings	True Temp. °C	Time	Thermo-couple Readings	True Temp. °C
T1	10.08	13.90	15.25	14.06	16.50	17.25	15.38	16.50	17.25	17.02	20.20	19.80
T2	10.08	13.90	15.25	14.06	16.50	17.25	15.38	16.50	17.25	17.03	20.10	19.80
T3	10.08	13.90	15.25	14.06	16.50	17.25	15.38	16.50	17.25	17.03	20.20	19.80
T4	10.08	13.90	15.25	14.06	16.50	17.25	15.38	20.00	19.75	17.04	23.80	22.00
T5	10.05	13.90	15.25	14.06	16.50	17.25	15.38	20.00	19.75	17.05	23.80	22.00
T6	10.05	13.90	15.25	14.06	16.50	17.25	15.39	19.00	19.00	17.05	20.00	19.75
T7	10.05	13.90	15.25	14.06	16.50	17.25	15.39	18.00	18.25	17.06	19.80	19.50
T8	10.05	13.90	15.25	14.06	16.50	17.25	15.39	16.50	17.25	17.06	16.50	17.25
T9	10.05	13.90	15.25	14.06	16.50	17.25	15.39	16.20	17.10	17.07	16.30	17.20
T10	10.05	13.90	15.25	14.06	16.50	17.25	16.40	16.10	17.00	17.07	16.30	17.20
T11	10.05	13.90	15.25	14.06	16.50	17.25	16.40	16.10	17.00	17.08	16.30	17.20
T12	10.05	13.90	15.25	14.06	16.50	17.25	16.40	16.10	17.00	17.08	16.30	17.20
T13	10.06	13.90	15.25	14.07	16.50	17.25	16.40	16.10	17.00	17.08	16.30	17.20
T14	10.06	13.90	15.25	14.07	16.50	17.25	16.40	16.10	17.00	17.08	16.30	17.20
T15	10.06	13.90	15.25	14.07	16.50	17.25	16.40	16.00	16.75	17.09	16.10	17.00
T16	10.06	13.90	15.25	14.07	16.00	16.75	16.40	16.00	16.75	17.09	16.05	17.00
T17	10.06	13.90	15.25	14.08	16.00	16.75	16.41	15.90	16.90	17.09	16.00	16.75
T18	10.06	13.90	15.25	14.08	17.50	17.75	16.41	17.00	17.50	17.10	16.30	17.20
T19	10.06	13.90	15.25	14.08	16.00	16.75	16.41	16.00	16.75	17.10	16.20	17.10
T20	10.06	13.90	15.25	14.08	16.00	16.75	16.41	16.00	16.75	17.10	16.20	17.10
T21	10.05	13.90	15.25	14.08	17.00	17.50	16.41	17.00	17.50	17.11	16.50	17.25
C1	10.05	13.90	15.25	14.03	18.00	18.00	15.27	67.00	67.00	16.46	79.00	79.00
C2	10.05	13.90	15.25	14.03	18.00	18.00	15.28	74.00	74.00	16.58	86.00	86.00
C3	10.05	13.90	15.25	14.03	18.00	18.00	15.29	55.80	55.80	16.59	65.20	65.20
C4	10.05	13.90	15.25	14.03	18.00	18.00	15.30	52.50	52.50	17.00	61.50	61.50
C5	10.05	13.90	15.25	14.03	17.80	17.80	15.26	138.50	138.50	16.45	164.00	164.00
C6	10.05	13.90	15.25	14.03	17.80	17.80	15.24	141.80	141.80	16.44	171.00	171.00

Table: 800.04(a)

Date	11th February 1976			11th February 1976			11th February 1976		
Thermocouple No.	Time	Thermo-couple Readings	True Temp. °C	Time	Thermo-couple Readings	True Temp. °C	Time	Thermo-couple Readings	True Temp. °C
T1	9.38	25.50	23.25	13.47	27.00	24.25	16.36	25.00	23.00
T2	9.38	25.00	23.00	13.48	26.50	23.88	16.36	25.00	23.00
T3	9.38	25.50	23.25	13.48	27.00	24.25	16.37	25.50	23.25
T4	9.39	26.00	23.50	13.48	26.50	23.88	16.37	25.50	23.25
T5	9.39	25.90	23.50	13.48	26.00	23.50	16.37	25.50	23.25
T6	9.39	22.00	20.75	13.49	22.00	20.75	16.37	21.00	20.25
T7	9.39	21.00	20.25	13.49	22.00	20.75	16.37	21.00	20.25
T8	9.40	18.00	18.25	13.49	19.50	19.25	16.38	17.00	17.50
T9	9.40	18.00	18.25	13.49	19.50	19.25	16.38	17.00	17.50
T10	9.40	17.90	18.10	13.50	18.00	18.25	16.38	17.00	17.50
T11	9.40	17.90	18.10	13.50	18.00	18.25	16.38	17.00	17.50
T12	9.40	17.50	17.75	13.50	18.00	18.25	16.38	17.00	17.50
T13	9.40	17.50	17.75	13.50	18.00	18.25	16.38	17.00	17.50
T14	9.40	17.50	17.75	13.51	17.50	17.75	16.38	17.00	17.50
T15	9.40	16.50	17.25	13.52	17.50	17.75	16.38	16.50	17.25
T16	9.41	16.00	16.75	13.52	17.50	17.75	16.38	16.00	16.75
T17	9.41	16.00	16.75	13.52	17.50	17.75	16.39	16.00	16.75
T18	9.41	17.00	17.50	13.52	18.00	18.25	16.39	18.00	18.25
T19	9.41	17.00	17.50	13.52	17.50	17.75	16.39	17.00	17.50
T20	9.43	16.50	17.25	13.53	17.00	17.50	16.39	17.00	17.50
T21	9.43	17.50	17.75	13.53	17.50	17.75	16.39	17.00	17.50
C1	9.34	86.30	86.30	13.43	87.80	87.80	16.35	87.50	87.50
C2	9.35	92.30	92.30	13.44	95.00	95.00	16.34	94.00	94.00
C3	9.36	70.30	70.30	13.41	72.50	72.50	16.34	70.50	70.50
C4	9.37	66.50	66.50	13.45	68.00	68.00	16.33	66.00	66.00
C5	9.30	181.50	181.50	13.46	182.00	182.00	16.33	183.50	183.50
C6	9.29	189.00	189.00	13.42	190.00	190.00	16.32	190.50	190.50

Table: 800.04(b)

TEMPORARY EFFECT ON A
MULTI-STOREY FRAME ROOF
Sheet 1
DEM&C GAUGE READINGS

Date	9th February 1976			9th February 1976			10th February 1976		
Demec Gauge No.	Time	Demec Gauge Reading	Change in Demec Reading	Time	Demec Gauge Reading	Change in Demec Reading	Time	Demec Gauge Reading	Change in Demec Reading
1	9.53	555	0	11.31	547	- 8	13.51	551	4
2	-	-		-	-		-	-	
3	9.53	400	0	11.31	358	- 42	13.51	445	45
4	9.54	1038	0	11.30	1036	- 2	13.52	1023	- 15
5	-	-		-	-		-	-	
6	10.05	2157	0	11.23	2135	- 22	13.54	2131	- 26
7	9.56	728	0	11.30	737	9	13.53	724	- 4
8	10.05	1553	0	11.23	1532	- 21	13.55	1560	1
9	9.53	1453	0	11.30	1456	3	13.52	1454	1
10	9.57	554	0	11.39	520	- 34	13.54	482	- 28
11	9.53	823	0	11.30	795	- 28	13.52	823	0
12	9.57	682	0	11.28	675	- 7	13.54	644	- 38
13	9.44	1594	0	11.32	1598	4	13.52	1607	13
14	9.56	982	0	11.29	1011	29	13.53	1034	52
15	9.56	2098	0	11.29	2081	- 17	13.53	2100	2
16	10.05	903	0	11.24	864	- 39	13.55	877	- 26
17	9.58	1447	0	11.26	1455	8	13.55	1463	16
18	9.58	1541	0	11.26	1547	6	13.56	1544	3
19	9.59	1482	0	11.28	1459	- 23	13.56	1511	29
20	9.59	604	0	11.24	613	9	13.56	608	4
21	-	-		-	-		-	-	
22	10.03	703	0	11.26	710	7	13.58	700	- 3
23	9.59	876	0	11.28	870	- 6	13.56	858	- 18
24	-	-		-	-		-	-	
25	10.02	474	0	11.26	474	0	13.59	482	8
26	10.03	881	0	11.27	818	- 63	13.58	990	9
27	10.01	536	0	11.27	536	0	13.57	538	2
28	-	-		-	-		-	-	
29	10.01	670	0	11.27	668	- 2	13.57	666	- 4
30	10.04	763	0	11.25	1148	385	14.00	847	84
31	9.59	597	0	11.27	606	9	13.56	598	1
32	10.00	1493	0	11.24	1555	52	13.56	1450	- 43
33	10.02	2090	0	11.26	2092	2	13.59	2100	10
34	10.02	636	0	11.25	644	8	13.59	665	29
35	10.01	2031	0	11.24	2155	124	13.57	2109	78
36	10.01	375	0	11.24	420	45	13.57	520	145

Table: 800.05(a)

TEMPERATURE EFFECT ON A
MULTI-STOREY FRAME ROOF
SHEET 2
DEMEC GAUGE READINGS

Date	10th. February 1976			10th. February 1976			10th. February 1976		
Demec Gauge No.	Time	Demec Gauge Read.	Change in Dem. Read.	Time	Demec Gauge Read.	Change in Dem. Read.	Time	Demec Gauge Read.	Change in Dem. Read.
1	15.42	550	- 5	16.44	548	- 7	9.45	553	- 2
2	-	-		-	-		-	-	
3	15.43	440	40	16.44	356	- 44	9.49	361	- 39
4	15.43	1035	- 3	16.42	1045	7	9.44	1040	2
5	-	-		-	-		-	-	
6	15.45	2125	- 32	16.43	2125	- 32	9.47	2146	- 11
7	15.44	756	28	16.42	728	0	9.45	773	45
8	15.45	1532	- 21	16.43	1509	- 44	9.48	1515	- 38
9	15.44	1460	7	16.42	1463	10	9.44	1460	7
10	15.46	516	- 38	16.45	519	- 35	9.50	570	16
11	15.44	809	- 14	16.42	829	6	9.44	831	8
12	15.46	680	- 2	16.45	680	- 2	9.50	680	- 2
13	15.43	1605	11	16.45	1599	5	9.49	1598	4
14	15.44	1065	83	16.43	1047	65	9.46	1082	100
15	15.44	2102	4	16.43	2094	- 4	9.46	2114	16
16	15.45	886	- 17	16.44	875	- 28	9.48	858	- 45
17	15.46	1461	14	16.45	1455	8	9.50	1464	17
18	15.47	1546	5	16.46	1542	1	9.50	1546	5
19	15.47	1515	33	16.46	1474	- 8	9.51	1509	27
20	15.47	593	- 11	16.46	612	8	9.51	608	4
21	-	-		-	-		-	-	
22	15.48	706	3	16.49	705	2	9.53	707	4
23	15.47	836	40	16.46	873	- 3	9.51	860	- 16
24	-	-		-	-		-	-	
25	15.48	474	0	16.49	482	8	9.53	473	- 1
26	15.48	885	4	16.48	830	- 51	9.52	834	- 47
27	15.48	538	2	16.47	539	3	9.52	537	1
28	15.48	-		-	-		-	-	
29	15.48	668	- 2	16.50	665	- 5	9.52	654	- 16
30	15.49	852	89	16.48	867	104	9.55	854	91
31	15.47	599	2	16.47	599	2	9.52	600	3
32	15.50	1354	-139	16.50	1360	-133	9.55	1325	-168
33	15.49	2092	2	16.49	2100	10	9.54	2087	- 3
34	15.49	667	31	16.48	660	24	9.54	650	14
35	15.49	2116	85	16.48	2114	83	9.54	2112	141
36	15.50	406	31	16.47	533	158	9.55	555	180

Table: 800.05 (b)

TEMPERATURE EFFECT ON A
MULTI-STOREY FRAME ROOF
SHEET 3
DEMEC GAUGE READINGS

Date	11th. February 1976			11th. February 1976		
Demec Gauge No.	Time	Demec Gauge Reading	Change in Demec Reading	Time	Demec Gauge Reading	Change in Demec Reading
1	14.00	549	- 6	16.46	544	- 11
2	-	-		-	-	
3	14.00	358	- 42	16.46	358	- 42
4	14.00	1041	3	16.44	1038	0
5	-	-		-	-	
6	14.02	2138	- 19	16.42	2135	- 22
7	14.01	758	30	16.43	740	12
8	14.03	1520	- 33	16.42	1513	- 40
9	14.01	1463	10	16.44	1460	7
10	14.03	528	- 26	16.45	532	- 22
11	14.01	833	10	16.43	832	9
12	14.04	670	- 12	16.46	697	- 3
13	14.00	1597	3	16.47	1594	0
14	14.01	1065	83	16.45	1030	48
15	14.02	2117	19	16.44	2104	6
16	14.03	874	- 29	16.43	873	- 30
17	14.04	1458	11	16.47	1460	13
18	14.05	1540	- 1	16.47	1550	9
19	14.07	1476	- 6	16.48	1518	36
20	14.07	608	4	16.48	623	19
21	14.07	-		-	-	
22	14.05	703	0	16.50	709	6
23	14.07	874	- 2	16.48	861	- 15
24	-	-		-	-	
25	14.04	484	10	16.50	484	10
26	14.06	901	20	16.49	740	-141
27	14.06	543	7	16.49	535	- 1
28	-	-		-	-	
29	14.06	673	3	16.49	675	5
30	14.09	849	86	16.51	858	95
31	14.06	598	1	16.49	594	- 3
32	14.10	1331	-162	16.48	1363	-130
33	14.04	2100	10	16.50	2097	7
34	14.09	641	5	16.53	640	4
35	14.07	2109	78	16.52	2130	99
36	14.07	510	135	16.50	602	227

Table: 800.05 (c)

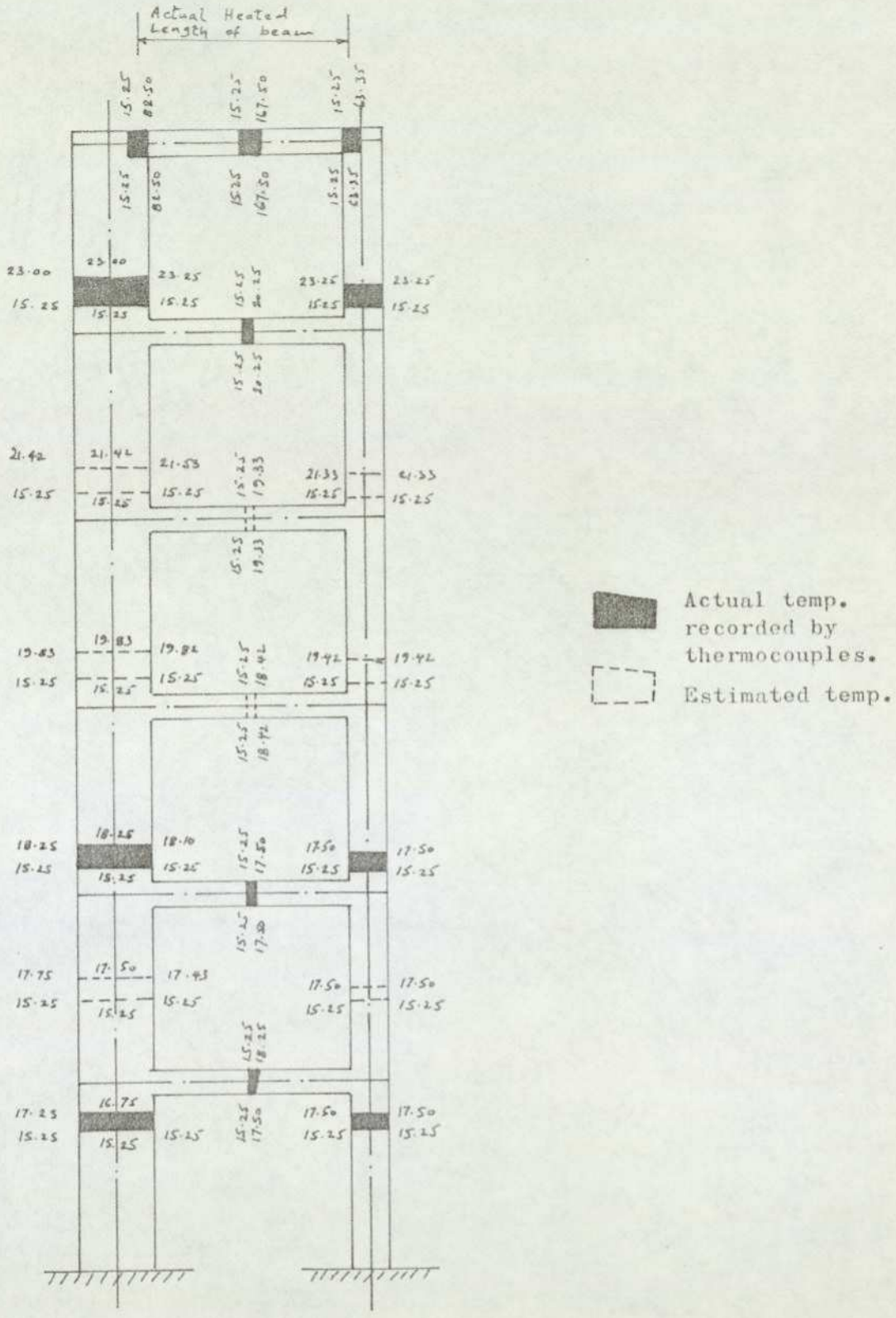

Fig. 8.0181 Temperature distribution in all members of the frame due to heating of the roof beam. CASE (1)

(All temperatures shown are in ^{o}C)

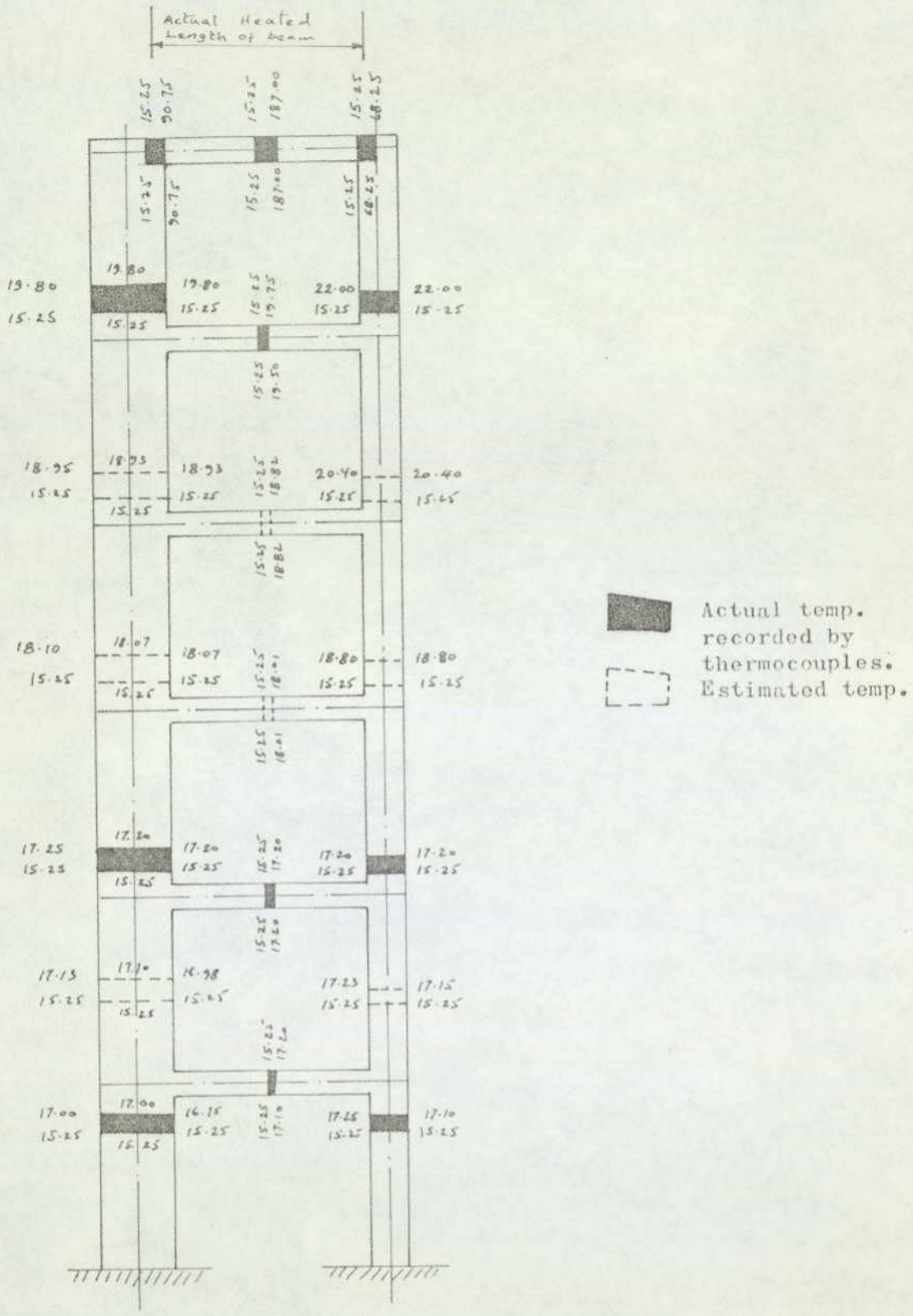

Fig. 8.0182 Temperature distribution in all members of the frame due to heating of the roof beam. CASE (2)

(All temperatures shown are in ^{o}C

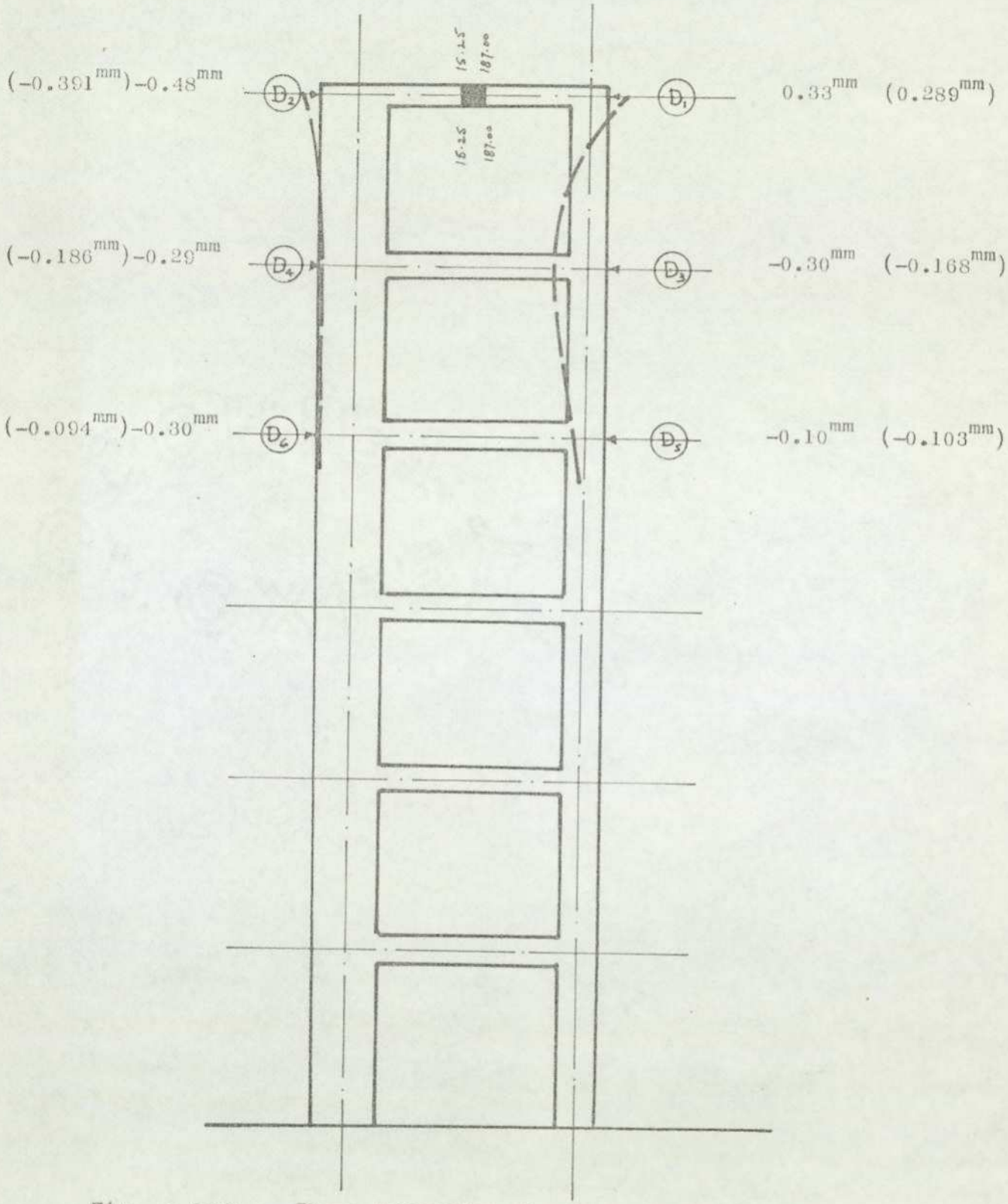

Fig. 8.0183 Shows deflection of a frame subjected to temperature changes affecting roof beam only (CASE 1)

Unbracketed Figures—— show experimental results

Bracketed Figures———— show theoretical primary results

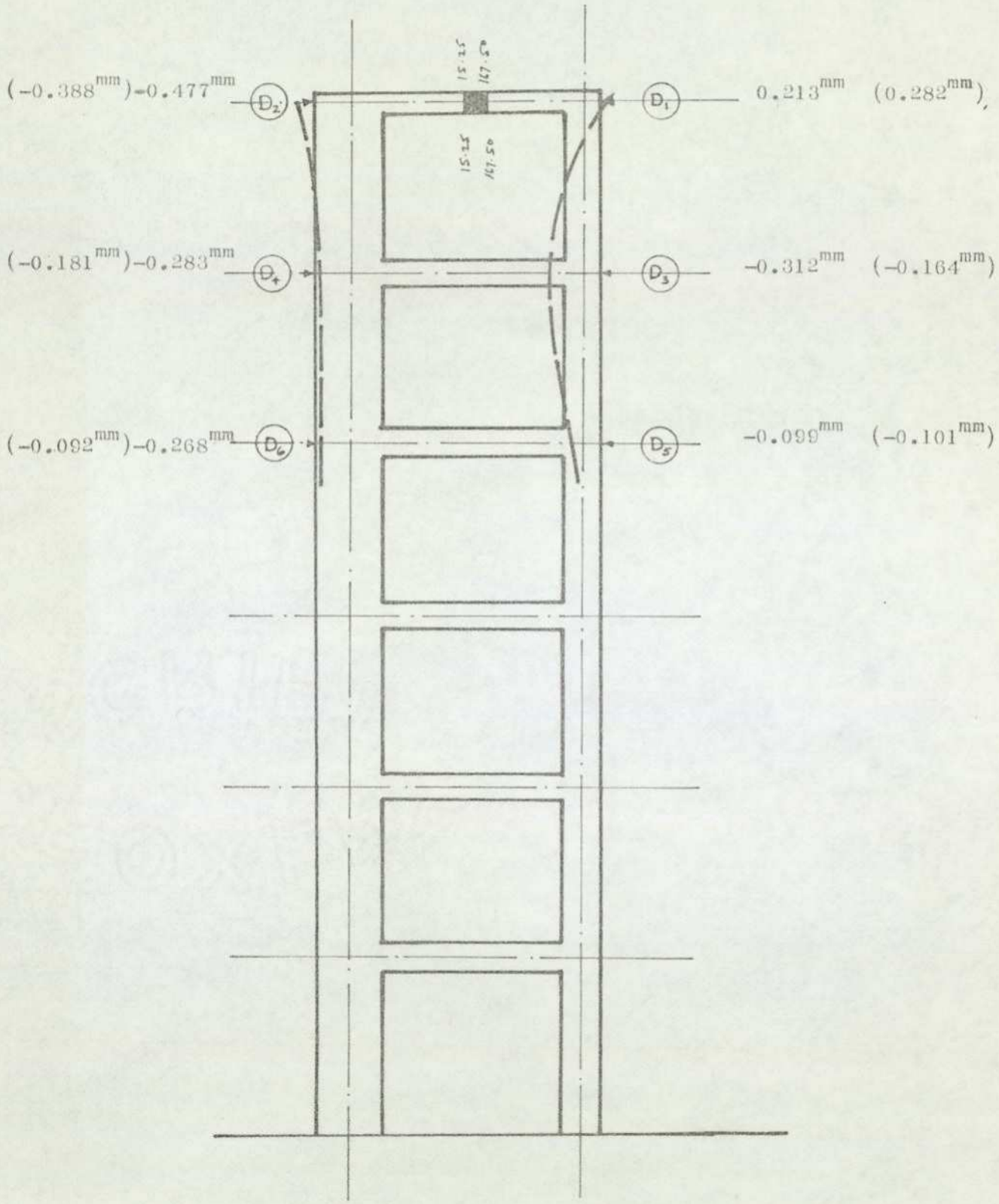

Fig. 8.0184 Shows deflection of a frame subjected to temperature changes affecting roof beam only (CASE 2)

Unbracketed Figures--- show experimental results

Bracketed Figures------ show theoretical primary results

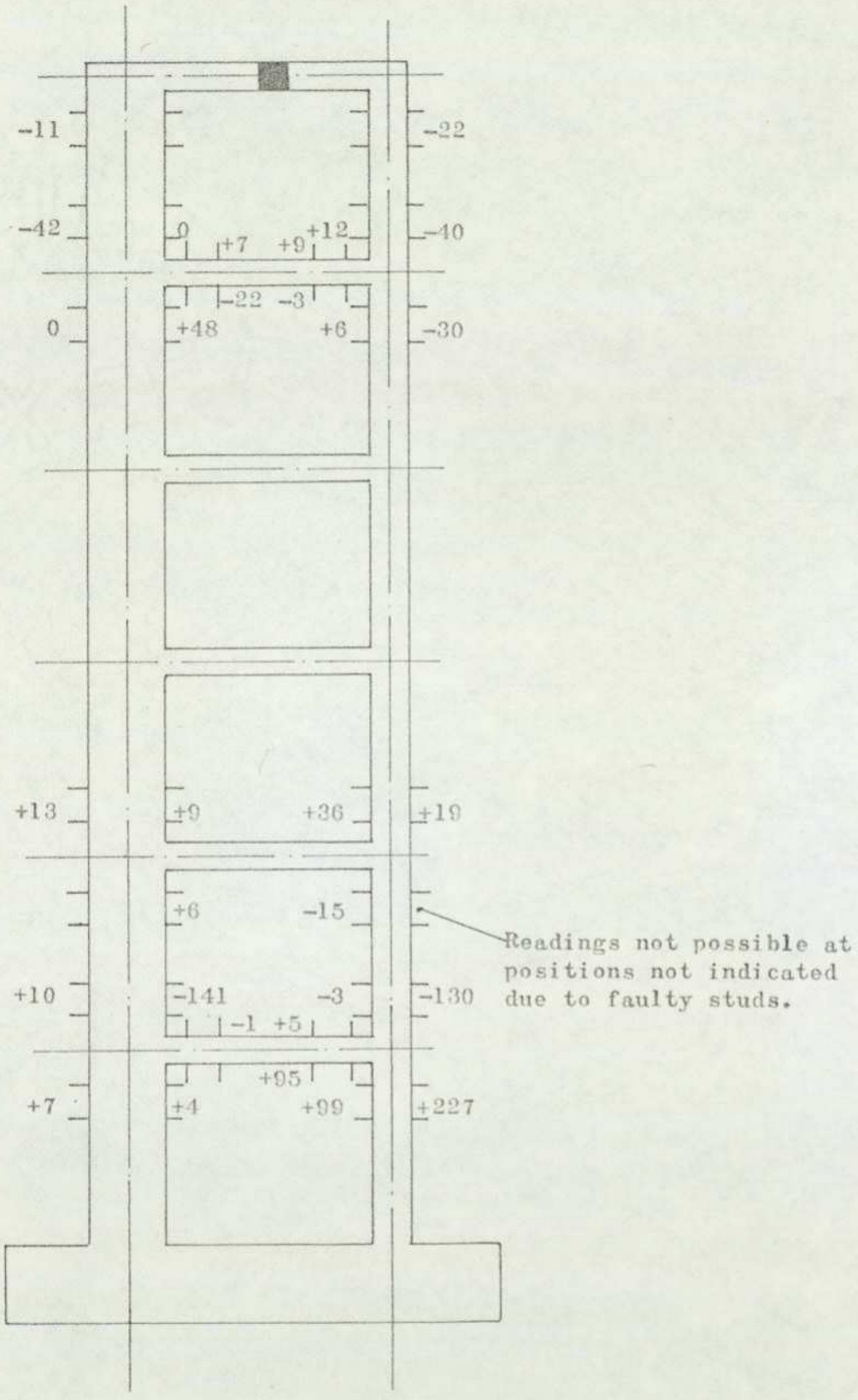

Fig. 8.0185 Summary of net change in readings recorded at demec gauge positions

TEMPERATURE EFFECT ON A MULTI - STOREY ROOF BEAM

DIAL GAUGE READINGS & DISPLACEMENTS

Date	9th. February, 1976			10th. February, 1976			10th. February, 1976			10th. February, 1976		
Dial Gauge Position & No.	Time	Dial Gauge Reading	Displacements in mm.	Time	Dial Gauge Reading	Displacements in mm.	Time	Dial Gauge Reading	Displacements in mm.	Time	Dial Gauge Reading	Displacements in mm.
6th Floor Level D_1	10.42	4.71	0	13.49	4.67	- 0.04	15.36	4.89	0.18	16.41	4.923	0.213
6th Floor Level D_2	10.43	0.37	0	13.49	0.41	0.04	15.36	0.737	0.367	16.41	0.847	0.477
5th Floor Level D_3	10.43	4.20	0	13.49	4.05	- 0.15	15.36	3.914	- 0.286	16.42	3.888	- 0.312
5th Floor Level D_4	10.43	0.87	0	13.49	0.85	- 0.02	15.37	1.050	0.18	16.42	1.153	0.283
4th Floor Level D_5	10.43	2.93	0	13.49	2.93	0	15.37	2.832	- 0.098	16.42	2.831	- 0.099
4th Floor Level D_6	10.44	0.84	0	13.50	0.84	0	15.37	1.09	0.25	16.42	1.118	0.268

Table: 800.06(a)

TEMPERATURE EFFECT ON A MULTI - STOREY ROOF BEAM

DIAL GAUGE READINGS & DISPLACEMENTS

Date	11th. February, 1976			11th. February, 1976			11th. February, 1976		
Dial Gauge Position & No.	Time	Dial Gauge Reading	Displacements in mm.	Time	Dial Gauge Reading	Displacements in mm.	Time	Dial Gauge Reading	Displacements in mm.
6th Floor Level D_1	9.26	5.059	0.349	14.00	5.06	0.35	17.00	5.04	0.33
6th Floor Level D_2	9.26	0.820	0.45	14.00	0.78	0.41	17.00	0.85	0.48
5th Floor Level D_3	9.26	3.916	- 0.284	14.00	3.92	- 0.28	17.00	3.90	- 0.30
5th Floor Level D_4	9.26	1.132	0.262	14.00	1.06	0.19	17.00	1.16	0.29
4th Floor Level D_5	9.27	2.834	- 0.096	14.00	2.85	- 0.08	17.00	2.83	- 0.10
4th Floor Level D_6	9.27	1.111	0.271	14.00	1.02	0.18	17.00	1.14	0.30

Table: 00.06(b)

8.01.9 Discussion of results of Experiment No.1

The effect of temperature variation in the larger column of a 6-storey frame

The results of deflections as given by dial gauges are very satisfactory when compared with the theoretical results of heating of the larger column only, i.e. assuming no change of temperature occurs in any other member. However, as can be seen from figs. 8.0171 and 8.0172 a considerable amount of heat was observed to have dissipated by conduction into other members. The additional deflections due to the effect of this change in temperature in other members are also considered. The final deflections, taking into consideration the effect of change of temperature in all members, compared even more satisfactorily with the theoretical results.

However, the calculations of experimental bending moments from the results of Demec Gauges presented some problems as these were found to be erratic and did not correlate well.
For this reason, simulated temperature experiments were carried out on perspex models, in attempts to achieve even better results as shown in section 8.02.

Thermal experiments are known to be difficult to perform for many reasons, some of which are as follows:-

1. Heating and Thermocouples

Theoretically, it is normally assumed that any one member is heated in relation to the others which are assumed to be unheated. Practically, this is impossible to achieve. Heat travels by conduction into adjoining members. While it is possible to consider some effect of secondary heat, as is done in these experiments, it would be extremely difficult or almost impossible

to consider full effect e.g. at junctions of members, where complex heat changes occur.

A linear distribution of temperature is assumed in the derivation of theoretical values, but this is not the case in experimental work. The distributions so obtained are taken to be approximately linear in the derivation of experimental results. More accurate results might have been obtained based on the curvilinear temperature distribution. However, this was not pursued.

The measure of temperature is also a factor which contributes towards inaccuracy. Past experiences have shown that the measurement of surface temperature with thermocouples is unlikely to give a realistic indication of the surface temperature, due to the unstable conditions which exist at the air-concrete boundary. The thermocouples require to have their hot junctions surrounded by one material. In order to overcome this problem, hot junctions of thermocouples were fixed under the surface by drilling holes in the concrete. However, inaccuracies still occurred due to the rapid dissipation of heat to the atmosphere at surfaces.

2. Demec-Gauges

Although demec gauges were considered superior for measurement of strains caused by heat in relation to strain gauges, as the latter have to be compensated for temperature, the former did not fulfil the expectations. It is to be noted that several other researchers experienced similar difficulties with demec gauges, as well as difficulties with ordinary strain gauges. However, the results given in fig. 8.0175 show (as can be expected) that the large column suffered appreciably more strain than the smaller one.

3. Axial Forces and Extensions

In experimental thermal stress analysis two components of axial effects take place, i.e. the first effect is the "free" extension of a member due to the applied heat, and the second effect is the extension or compression induced by the presence of axial forces, generated because of continuity of members. Difficulties were encountered in separating these two effects by the instrumentation used, particularly that for the temperature changes obtained experimentally. The effect of axial forces is usually small, whereas direct extensions can be very much larger than the latter.

8.01.10 Discussion of results of Experiment No.2

The effect of temperature variation in the roof beam of a 6-storey frame

The results of deflection as measured by the dial gauges are satisfactory, but not quite as good as in the case of Experiment No.1. The evaluation of experimental bending moments from the results of Demec Gauges did not correlate well. However, the deflected shape of the frame as shown in figs. 8.0183 and 8.0184 resembles closely that predicted by theoretical analysis.

The causes of discrepancies are similar to those in Experiment No.1.

8.02 EXPERIMENT ON THE EFFECT OF SIMULATED TEMPERATURE IN THE COLUMN OF A SIX-STOREY PERSPEX SHEAR WALL

8.02.1 Introduction

To overcome the difficulties associated with the heating of Micro-concrete models, it was decided to carry out some experiments on the effect of simulated temperature on perspex models. It was hoped that this simulated effect may produce an overall effect in a structure of similar form as that of temperature change!

8.02.2 Model Frame

A 6-storey perspex model frame, similar in dimensions in every respect except the thickness to the Micro-concrete frame, was made. The dimensions and instrumentation details of the model frame are shown in fig. 8.021. Clear transparent perspex was used for the model.

8.02.3 Strain Measurement

For the purpose of measurement of strains, 36 Nos. strain gauges of F-8 type, each 8mm long, were used. These were fixed at various locations (in areas of expected maximum strain) as shown in fig. 8.021 The strain gauges were then connected via four junction boxes to a voltage measuring instrument (Dynamco 6600) which gave a digital display of strain gauge voltage as well as a printed record. Four 'dummy' gauges attached to separate perspex beams were also connected to the voltage measuring instrument.

8.02.4 Deflection Measurement

For the purpose of direct measurement of deflections, ten dial gauges were positioned at the junctions, as shown in fig. 8.021.

8.02.5 Theoretical Philosophy of Heat Simulation

It has been expected that the effect of temperature in any member can be simulated by the effect of gravity forces acting on the same member. The effect of heat on any member is to make the member expand by an amount αTL, (where α is the coefficient of thermal expansion, T is the temperature rise and L is the initial length of the member). If the member is free to expand, there will be no stresses due to the heat. However, in an indeterminate structure, free and unobstructed expansion cannot take place, resulting in a force being exerted by the expanding member on all connecting members. This force is exerted equally in both directions along the axis of the member being heated and can be related to the applied temperature as follows:-

It is well known and it has been shown earlier in the text that if a heated member is fully restrained from expanding, the force required to stop the member from expanding can be found from the stress/strain relationship, which is

$$P = \frac{EA}{L} \alpha TL = EA\alpha T$$

$$\text{or} \qquad T = \frac{P}{EA\alpha}$$

The above relationship shows therefore that analytically the force P, exerted on an element, can be interchanged with T, the applied temperature. Thus in a simulated experiment, the effect of temperature variation can be replaced by an equivalent force P to give the same effect, i.e. the resulting stresses will be the same.

8.02.6 The Experiment

The purpose of the experiment was to check stresses and deformations in the frame arising from the effect of simulated temperature change in the larger column, and to compare these with the analytical values. At

first, the model was fixed in a vertical position and instead of heat, loads were applied vertically along the axis of the column through a system of pulleys attached to a supporting steel frame. It was soon realised that this method had several flaws. The major flaws were (i) the pulleys generated a certain amount of friction and (ii) the wire rope restricted the deflections of the frame from the vertical position.

It was then decided to hang the model upside down from the top beam of the supporting steel frame. This allowed the loads to be applied directly without passing through any pulleys. The frame was then free to deflect in any direction. For each increment of applied load, readings of dial gauges and strain gauges were taken. The applied loads were increased in suitable increments until deflections of a discernible magnitude (but still within the elastic range) were obtained. Then the applied loads were decreased step by step (the decrements being equal to the increments), each time recording the readings of dial gauges and strain gauges. For the calculations of deflections and bending moments, average of the loading and unloading readings was taken.

The results of the experiment are shown on the following sheets. Fig. 8.0261 shows the deflected form of the frame as measured by dial gauges. For comparison purposes, the theoretical deflections are also shown.

For the calculation of stresses, a calibration perspex beam was tested in flexure (Appendix 'C'). The resulting stresses from loading of the test model were analysed by equating the frame stresses to those resulting from the calibration beam test. Typical calculations are shown in Table 800.09. Fig. 8.0262 shows the bending moments due to the applied load (or equivalent temperature). Also shown for comparison are the theoretical bending moments.

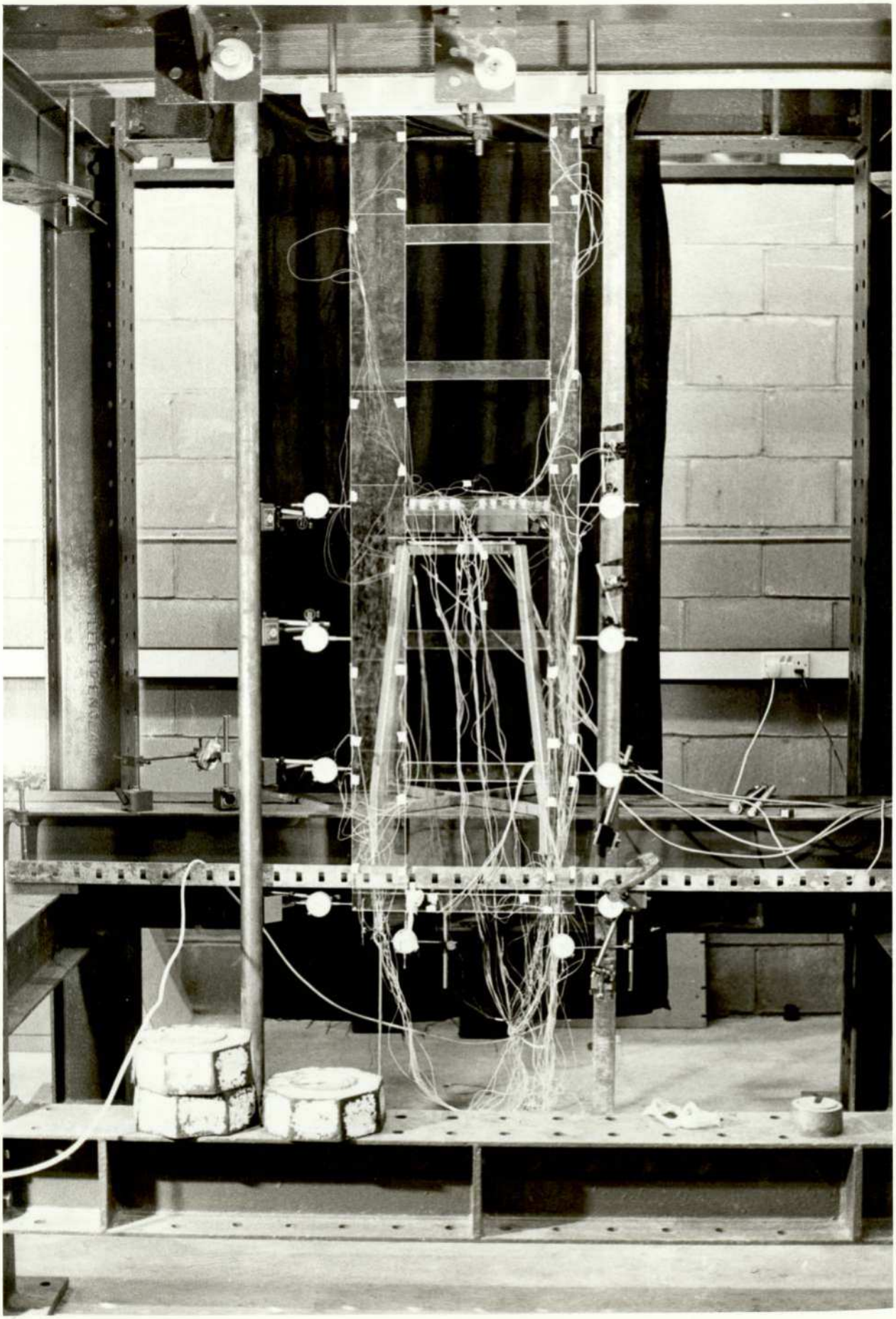

PLATE: V11 6-Storey perspex shear wall frame under test for the effect of simulated temperature change in the larger column.

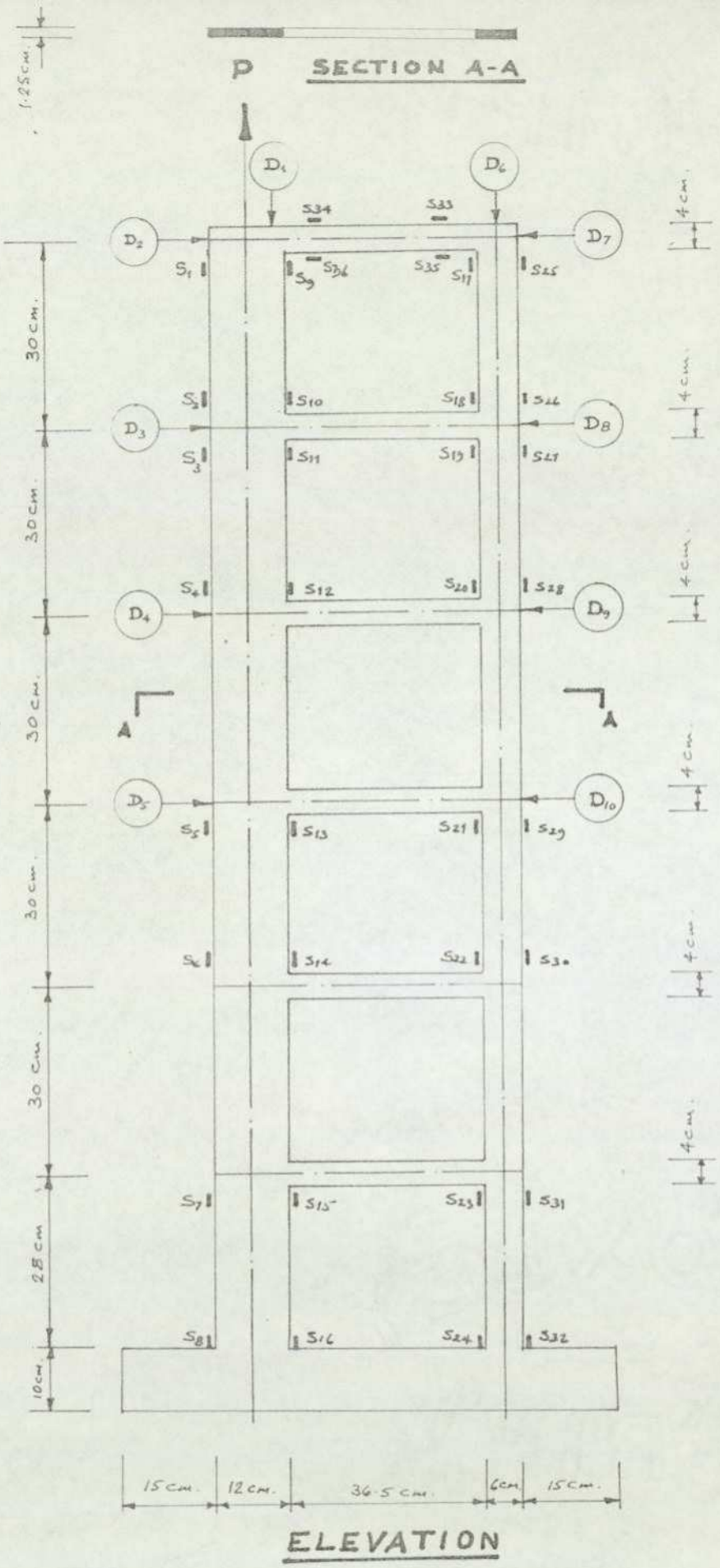

Fig. 8.021 Shows perspex model of a 6-storey frame for the simulated temperature effect on the larger column.

S1 to S36..Strain gauges

D1 to D10..Dial gauges

SIMULATED TEMPERATURE EFFECT ON A MULTI-STOREY FRAME COLUMN

DIAL GAUGE READINGS (0.01 mm. PER DIVISION)

APPLIED LOAD \ DIAL GAUGE NO.	D_1	D_2	D_3	D_4	D_5	D_6	D_7	D_8	D_9	D_{10}
0 N.	10.465	7.482	4.942	3.645	7.245	8.510	12.714	8.182	6.189	8.508
200 N.	10.537	7.356	4.842	3.577	7.228	8.530	12.860	8.273	6.232	8.547
400 N.	10.590	7.221	4.745	3.502	7.206	8.539	13.010	8.380	6.302	8.578
600 N.	10.644	7.066	4.614	3.430	7.178	8.542	13.170	8.500	6.392	8.622
777.92 N.	10.725	6.919	4.518	3.343	7.132	8.568	13.332	8.599	6.438	8.661
955.84 N.	10.797	6.781	4.410	3.289	7.100	8.588	13.485	8.711	6.513	8.704
1133.76 N.	10.865	6.665	4.356	3.227	7.070	8.595	13.605	8.802	6.566	8.730
1311.68 N.	10.931	6.536	4.268	3.167	7.027	8.596	13.743	8.900	6.627	8.762
1133.76 N.	10.878	6.632	4.332	3.210	7.060	8.595	13.643	8.826	6.591	8.735
955.84 N	10.812	6.751	4.389	3.263	7.090	8.589	13.519	8.740	6.533	8.710
777.92 N.	10.757	6.891	4.490	3.338	7.130	8.584	13.378	8.635	6.478	8.673
600 N.	10.705	7.028	4.592	3.412	7.171	8.578	13.222	8.529	6.406	8.630
400 N.	10.652	7.144	4.692	3.462	7.185	8.578	13.100	8.443	6.348	8.609
200 N.	10.582	7.330	4.821	3.558	7.232	8.562	12.917	8.325	6.280	8.560
0 N.	10.542	7.482	4.919	3.632	7.252	8.558	12.774	8.225	6.223	8.525
0* N.	10.527	7.499	4.942	3.650	7.252	8.561	12.735	8.191	6.195	8.512

* Readings taken after half hour interval

Table: 800.07

EXPERIMENT ON THE EFFECT OF SIMULATED TEMPERATURE IN THE LARGER COLUMN OF A SIX-STOREY PERSPEX FRAME

THURSDAY, 26TH MAY, 1977

LOADING			LOADING			LOADING			LOADING
LOAD 00 N									
-0707	+0242	+0349	+0761	-0900	+0242	+0059	+0173	+0517	+0168
-0410	-0198	-0268	-0165	+0021	-0012	-0319	-0488	-0476	-0487
-0207	-0825	-0619	-0063	-0178	-1289	-0996	-0725	-0758	-0157
-0345	-0269	-0654	-0599	-0655	-0494				
-0708	+0242	+0349	+0760	-0899	+0241	+0059	+0172	+0517	+0168
-0408	-0198	-0268	-0164	+0022	-0013	-0319	-0487	-0476	-0487
-0208	-0824	-0619	-0063	-0179	-1290	-0994	-0725	-0757	-0157
-0344	-0269	-0652	-0599	-0654	-0493				
LOAD 200 N									
-0709	+0234	+0342	+0753	-0907	+0237	+0051	+0165	+0514	+0161
-0414	-0203	-0274	-0171	+0017	-0018	-0318	-0487	-0478	-0488
-0208	-0826	-0621	-0063	-0179	-1289	-0993	-0725	-0758	-0157
-0343	-0268	-0652	-0599	-0656	-0492				
-0710	+0233	+0340	+0753	-0908	+0236	+0051	+0164	+0513	+0161
-0414	-0204	-0274	-0170	+0017	-0017	-0318	-0488	-0477	-0488
-0210	-0827	-0621	-0064	-0180	-1290	-0994	-0725	-0757	-0159
-0342	-0268	-0652	-0600	-0655	-0492				
LOAD 400 N									
-0714	+0227	+0335	+0746	-0914	+0230	+0044	+0156	+0511	+0154
-0421	-0210	-0281	-0178	+0011	-0023	-0320	-0489	-0479	-0489
-0211	-0827	-0621	-0064	-0180	-1290	-0994	-0725	-0757	-0158
-0341	-0267	-0651	-0601	-0657	-0494				
-0714	+0226	+0333	+0744	-0916	+0230	+0043	+0155	+0511	+0153
-0421	-0211	-0281	-0177	+0012	-0023	-0320	-0489	-0479	-0489
-0211	-0828	-0623	-0065	-0181	-1289	-0993	-0725	-0756	-0158
-0343	-0268	-0651	-0602	-0657	-0493				
LOAD 600 N									
-0713	+0224	+0332	+0743	-0919	+0228	+0040	+0153	+0514	+0152
-0427	-0217	-0286	-0184	+0007	-0028	-0321	-0489	-0480	-0488
-0213	-0829	-0624	-0066	-0181	-1289	-0992	-0724	-0754	-0157
-0341	-0269	-0651	-0604	-0657	-0493				
-0712	+0223	+0331	+0742	-0920	+0228	+0040	+0152	+0513	+0152
-0427	-0215	-0284	-0183	+0008	-0027	-0319	-0487	-0479	-0488
-0214	-0829	-0623	-0065	-0182	-1288	-0993	-0723	-0753	-0158
-0342	-0270	-0651	-0603	-0658	-0494				

Table: 800.08 (a)

LOAD 600 N + 40 Lb

-0716	+0216	+0324	+0735	-0926	+0223	+0032	+0146	+0511	+0146
-0432	-0221	-0291	-0191	+0003	-0032	-0321	-0489	-0480	-0488
-0214	-0830	-0624	-0066	-0183	-1289	-0992	-0724	-0754	-0158
-0341	-0269	-0651	-0604	-0659	-0495				
-0716	+0215	+0324	+0734	-0920	+0223	+0033	+0145	+0510	+0146
-0432	-0221	-0289	-0190	+0004	-0031	-0321	-0489	-0480	-0488
-0216	-0831	-0625	-0067	-0184	-1289	-0992	-0724	-0752	-0158
-0342	-0268	-0652	-0607	-0661	-0496				

LOAD 600 N + 80 Lb

-0718	+0209	+0318	+0728	-0934	+0217	+0027	+0138	+0508	+0140
-0438	-0227	-0295	-0196	-0000	-0037	-0321	-0489	-0482	-0488
-0216	-0832	-0626	-0065	-0184	-1288	-0992	-0724	-0751	-0158
-0340	-0270	-0651	-0607	-0660	-0495				
-0718	+0208	+0318	+0728	-0933	+0217	+0025	+0138	+0509	+0139
-0439	-0227	-0296	-0196	-0001	-0036	-0322	-0489	-0482	-0489
-0216	-0833	-0625	-0066	-0183	-1289	-0990	-0723	-0750	-0158
-0341	-0270	-0652	-0606	-0662	-0495				

LOAD 600 N + 120 Lb

-0720	+0204	+0313	+0721	-0940	+0213	+0019	+0132	+0506	+0134
-0442	-0232	-0299	-0202	-0005	-0041	-0321	-0489	-0481	-0489
-0217	-0832	-0627	-0066	-0184	-1289	-0991	-0722	-0751	-0157
-0340	-0271	-0650	-0608	-0663	-0495				
-0720	+0203	+0312	+0721	-0940	+0213	+0019	+0131	+0505	+0133
-0445	-0234	-0301	-0203	-0006	-0043	-0324	-0490	-0482	-0490
-0217	-0832	-0627	-0067	-0184	-1289	-0991	-0723	-0751	-0158
-0340	-0271	-0650	-0607	-0661	-0494				

LOAD 600 N + 160 Lb

-0723	+0197	+0306	+0715	-0947	+0206	+0012	+0125	+0505	+0128
-0449	-0239	-0307	-0209	-0011	-0048	-0325	-0491	-0483	-0491
-0217	-0833	-0628	-0065	-0184	-1289	-0991	-0722	-0750	-0157
-0339	-0271	-0650	-0609	-0661	-0495				
-0724	+0197	+0306	+0716	-0947	+0207	+0012	+0124	+0505	+0128
-0450	-0239	-0306	-0208	-0010	-0047	-0325	-0491	-0483	-0490
-0218	-0833	-0627	-0066	-0185	-1289	-0991	-0722	-0750	-0158
-0338	-0271	-0649	-0609	-0660	-0494				

LOAD		UNLOADING			UNLOADING			UNLOADING	

LOAD 600 N + 120 Lb

-0720	+0204	+0311	+0722	-0942	+0212	+0019	+0130	+0507	+0133
-0445	-0233	-0302	-0203	-0007	-0042	-0324	-0490	-0482	-0490
-0217	-0833	-0627	-0067	-0184	-1289	-0990	-0724	-0750	-0158
-0340	-0271	-0651	-0608	-0662	-0495				
-0721	+0203	+0312	+0720	-0942	+0212	+0019	+0131	+0505	+0132
-0445	-0234	-0304	-0204	-0006	-0043	-0324	-0491	-0483	-0490
-0218	-0832	-0627	-0067	-0185	-1289	-0992	-0722	-0750	-0158
-0341	-0270	-0650	-0609	-0661	-0496				

Table: 800.08 (b)

LOAD 600 N + 80 Lb

-0719	+0209	+0318	+0723	-0936	+0217	+0025	+0137	+0507	+0139
-0440	-0230	-0297	-0197	-0002	-0038	-0322	-0489	-0482	-0489
-0218	-0833	-0626	-0067	-0186	-1289	-0991	-0723	-0750	-0158
-0341	-0270	-0651	-0607	-0662	-0495				
-0718	+0207	+0318	+0726	-0935	+0216	+0025	+0136	+0508	+0137
-0440	-0228	-0299	-0198	-0003	-0038	-0324	-0489	-0483	-0490
-0216	-0833	-0626	-0068	-0185	-1290	-0992	-0723	-0750	-0158
-0342	-0270	-0653	-0607	-0661	-0496				

LOAD 600 N + 40 Lb

-0717	+0215	+0322	+0733	-0929	+0221	+0032	+0142	+0509	+0145
-0434	-0224	-0292	-0190	-0003	-0034	-0321	-0490	-0480	-0488
-0216	-0834	-0625	-0068	-0186	-1287	-0992	-0721	-0751	-0159
-0343	-0270	-0654	-0607	-0661	-0498				
-0717	+0215	+0323	+0732	-0930	+0222	+0032	+0144	+0509	+0143
-0434	-0224	-0293	-0191	+0003	-0032	-0322	-0490	-0482	-0488
-0218	-0833	-0624	-0067	-0186	-1289	-0991	-0721	-0749	-0159
-0341	-0270	-0654	-0608	-0660	-0496				

LOAD 600 N

-0715	+0221	+0329	+0739	-0923	+0226	+0037	+0150	+0512	+0149
-0430	-0219	-0288	-0185	+0006	-0029	-0321	-0488	-481	-0488
-0216	-0832	-0625	-0068	-0186	-1288	-0991	-0722	-0750	-0158
-0343	-0271	-0655	-0607	-0662	-0498				
-0715	+0221	+0331	+0740	-0923	+0227	+0039	+0152	+0512	+0148
-0429	-0218	-0287	-0183	+0008	-0029	-0321	-0489	-0480	-0489
-0217	-0832	-0625	-0068	-0186	-1288	-0993	-0722	-0749	-0158
-0342	-0271	-0655	-0606	-0661	-0496				

LOAD 400 N

-0712	+0226	+0336	+0746	-0916	+0232	+0044	+0158	+0513	+0154
-0423	-0213	-0283	-0177	+0011	-0024	-0322	-0489	-0480	-0489
-0216	-0832	-0624	-0068	-0188	-1287	-0992	-0722	-0749	-0159
-0344	-0269	-0656	-0604	-0661	-0497				
-0714	+0227	+0335	+0746	-0915	+0232	+0046	+0157	+0512	+0155
-0424	-0212	-0282	-0178	+0012	-0025	-0321	-0490	-0481	-0489
-0217	-0831	-0624	-0068	-0188	-1287	-0992	-0722	-0750	-0159
-0342	-0270	-0655	-0604	-0662	-0496				

LOAD 200 N

-0711	+0233	+0342	+0752	-0909	+0238	+0053	+0165	+0513	+0160
-0418	-0207	-0276	-0171	+0016	-0019	-0321	-0489	-0481	-0488
-0214	-0832	-0624	-0069	-0187	-1288	-0993	-0723	-0749	-0159
-0345	-0270	-0656	-0604	-0661	-0496				
-0712	+0233	+0342	+0753	-0908	+0239	+0054	+0165	+0514	+0159
-0417	-0205	-0275	-0169	-0017	-0019	-0321	-0490	-0481	-0488
-0216	-0831	-0623	-0070	-0188	-1288	-0993	-0721	-0750	-0159
-0345	-0270	-0657	-0604	-0663	-0498				

Table: 800.08 (c)

LOAD 00 N

-0710	+0240	+0348	+0759	-0902	+0244	+0060	+0173	+0515	+0167
-0411	-0202	-0270	-0163	+0022	-0014	-0321	-0490	-0478	-0488
-0216	-0830	-0621	-0070	-0189	-1288	-0993	-0722	-0751	-0160
-0344	-0270	-0658	-0603	-0661	-0498				
-0709	+0239	+0348	+0761	-0902	+0245	+0059	+0173	+0517	+0167
-0412	-0202	-0269	-0164	+0020	-0014	-0322	-0489	-0481	-0167
-0216	-0831	-0621	-0072	-0186	-1288	-0994	-0721	-0751	-0159
-0346	-0269	-0658	-0604	-0662	-0498				
-0711	+0240	+0348	+0760	-0902	+0244	+0059	+0173	+0517	+0168
-0408	-0198	-0268	-0162	+0023	-0013	-0319	-0488	-0478	-0487
-0216	-0832	-0621	-0069	-0189	-1285	-0991	-0720	-0748	-0160
-0345	-0269	-0656	-0602	-0659	-0494				

Table: 800.08 (d)

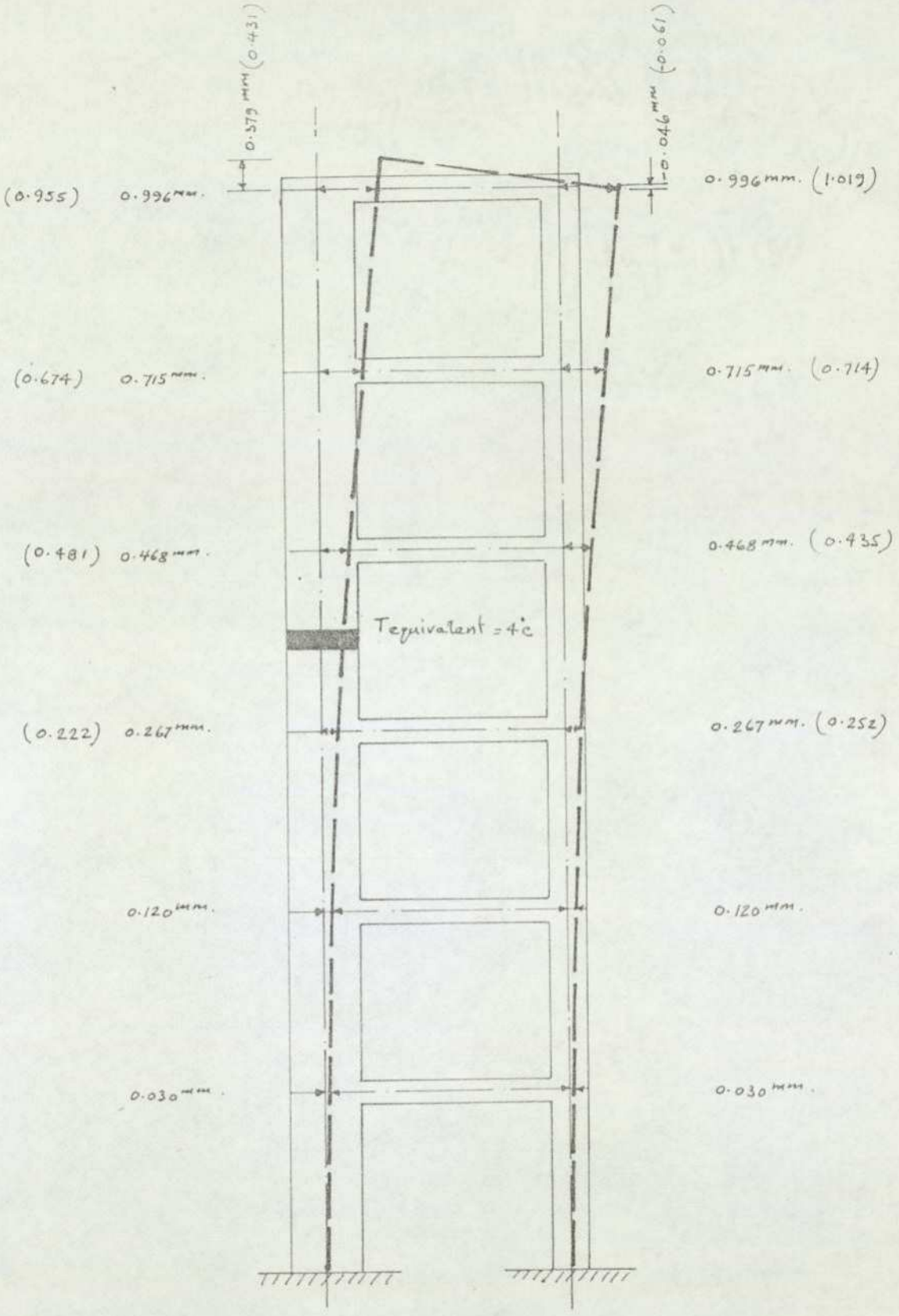

Fig. 8.0261 Shows deflection of frame due to the effect of simulated temperature in the larger column of a 6-storey frame.

Unbracketed figures.....Show theoretical results.

Bracketed figures.....Show experimental results.

1. CALCULATIONS OF FRAME BENDING MOMENTS

Applied Load in N.	Strain Gauge Location	Strain Gauge Av. Zero Reading	Strain Gauge Reading for applied Load	Diff. between Strain Gauge Readings	Experimental Bending Moments	Theoretical Bending Moments
1311.68	1	-708.75	-723.50	14.75	$(14.75 - 11.67)\frac{1}{2} \times 0.02432$	892.88
	9	+516.67	+505.00	11.67	$\times 13 \times \frac{120^2}{6} = 1168.53$ N-mm	N-mm
	2	+240.83	+197.00	43.83	$(43.83 - 39.67)\frac{1}{2} \times 0.02432$	1860.15
	10	+167.67	+128.00	39.67	$\times 13 \times \frac{120^2}{6} = 1578.27$ N-mm	N-mm
	3	+348.50	+306.00	42.50	$(42.50 - 39.83)\frac{1}{2} \times 0.02432$	2411.62
	11	-409.67	-449.50	39.83	$\times 13 \times \frac{120^2}{6} = 1012.98$ N-mm	N-mm
	4	+760.25	+715.50	44.75	$(44.75 - 39.67)\frac{1}{2} \times 0.02432$	2612.12
	12	-199.33	-239.00	39.67	$\times 13 \times \frac{120^2}{6} = 1927.31$ N-mm	N-mm
	5	-900.75	-947.00	46.25	$(46.25 - 38.00)\frac{1}{2} \times 0.02432$	3318.55
	13	-268.50	-306.50	38.00	$\times 13 \times \frac{120^2}{6} = 3129.98$ N-mm	N-mm
	6	+242.92	+206.50	36.42	$(36.42 - 44.75)\frac{1}{2} \times 0.02432$	3412.24
	14	-163.75	-208.50	44.75	$\times 13 \times \frac{120^2}{6} = 3160.34$ N-mm	N-mm
	7	+ 59.17	+ 12.00	47.17	$(47.17 - 32.08)\frac{1}{2} \times 0.02432$	3607.12
	15	+ 21.58	- 10.50	32.08	$\times 13 \times \frac{120^2}{6} = 5725.03$ N-mm	N-mm
	8	+172.75	+124.50	48.25	$(48.25 - 34.42)\frac{1}{2} \times 0.02432$	3622.17
	16	- 13.08	- 47.50	34.42	$\times 13 \times \frac{120^2}{6} = 5246.99$ N-mm	N-mm
	17	-319.83	-325.00	5.17	$(5.17 - 1.25)\frac{1}{2} \times 0.02432$	877.55
	25	-183.25	-184.50	1.25	$\times 13 \times \frac{60^2}{6} = 371.80$ N-mm	N-mm
	18	-488.25	-491.00	2.75	$(2.75 - 0.75)\frac{1}{2} \times 0.02432$	149.87
	26	-1288.25	-1289.00	0.75	$\times 13 \times \frac{60^2}{6} = 189.70$ N-mm	N-mm

Table: 800.09 (a)

CALCULATIONS OF FRAME BENDING MOMENTS						
Applied Load in N.	Strain Gauge Location	Strain Gauge Av. Zero Reading	Strain Gauge Reading for applied Load	Diff. between Strain Gauge Readings	Experimental Bending Moments	Theoretical Bending Moments
1311.68	19	-477.50	-483.00	5.50	$(5.50 - 2.83)\frac{1}{2} \times 0.02432$	396.54
	27	-993.83	-991.00	2.83	$\times 13 \times \frac{60^2}{6} = 253.24$ N-mm	N-mm
	20	-487.67	-490.50	2.83	$(2.83 - 1.00)\frac{1}{2} \times 0.02432$	195.07
	28	-723.00	-722.00	1.00	$\times 13 \times \frac{60^2}{6} = 173.57$ N-mm	N-mm
	21	-211.75	-217.50	5.75	$(5.75 - 3.75)\frac{1}{2} \times 0.02432$	471.64
	29	-753.75	-750.00	3.75	$\times 13 \times \frac{60^2}{6} = 189.70$ N-mm	N-mm
	22	-827.75	-833.00	0.83	$(5.25 - 0.83)\frac{1}{2} \times 0.0243$	377.01
	30	-158.33	-157.50	0.83	$\times 13 \times \frac{60^2}{6} = 419.23$ N-mm	N-mm
	23	-620.00	-627.50	7.50	$(7.50 - 6.25)\frac{1}{2} \times 0.02432$	462.27
	31	-344.75	-338.50	6.25	$\times 13 \times \frac{60^2}{6} = 118.56$ N-mm	N-mm
	24	- 66.67	- 65.50	1.17	$(1.17 - 1.83)\frac{1}{2} \times 0.02432$	447.10
	32	-269.17	-271.00	1.83	$\times 13 \times \frac{60^2}{6} = 62.60$ N-mm	N-mm
	33	-655.17	-649.50	5.67	$(5.67 - 2.92)\frac{1}{2} \times 0.02432$	877.55
	35	-657.58	-649.50	2.92	$\times 13 \times \frac{60^2}{6} = 260.83$ N-mm	N-mm
	34	-601.00	-609.00	8.00	$(8.00 - 0.58)\frac{1}{2} \times 0.02432$	892.88
	36	-495.08	-494.50	0.58	$\times 13 \times \frac{60^2}{6} = 703.77$ N-mm	N-mm

Table: 800.09 (b)

2. CALCULATIONS OF EQUIVALENT TEMPERATURE

Applied Max. Load = 1311.68 N.

Subst. into $T = \frac{P}{EA\alpha}$ where $E = 3{,}000\ N/mm^2$

$A = 13 \times 120$

$\alpha = 7.3 \times 10^{-5}$

$$T = \frac{1311.68}{3{,}000 \times 13 \times 120 \times 7.3 \times 10^{-5}} = 3.84\ ^\circ C \quad \text{say} \approx 4\ ^\circ C$$

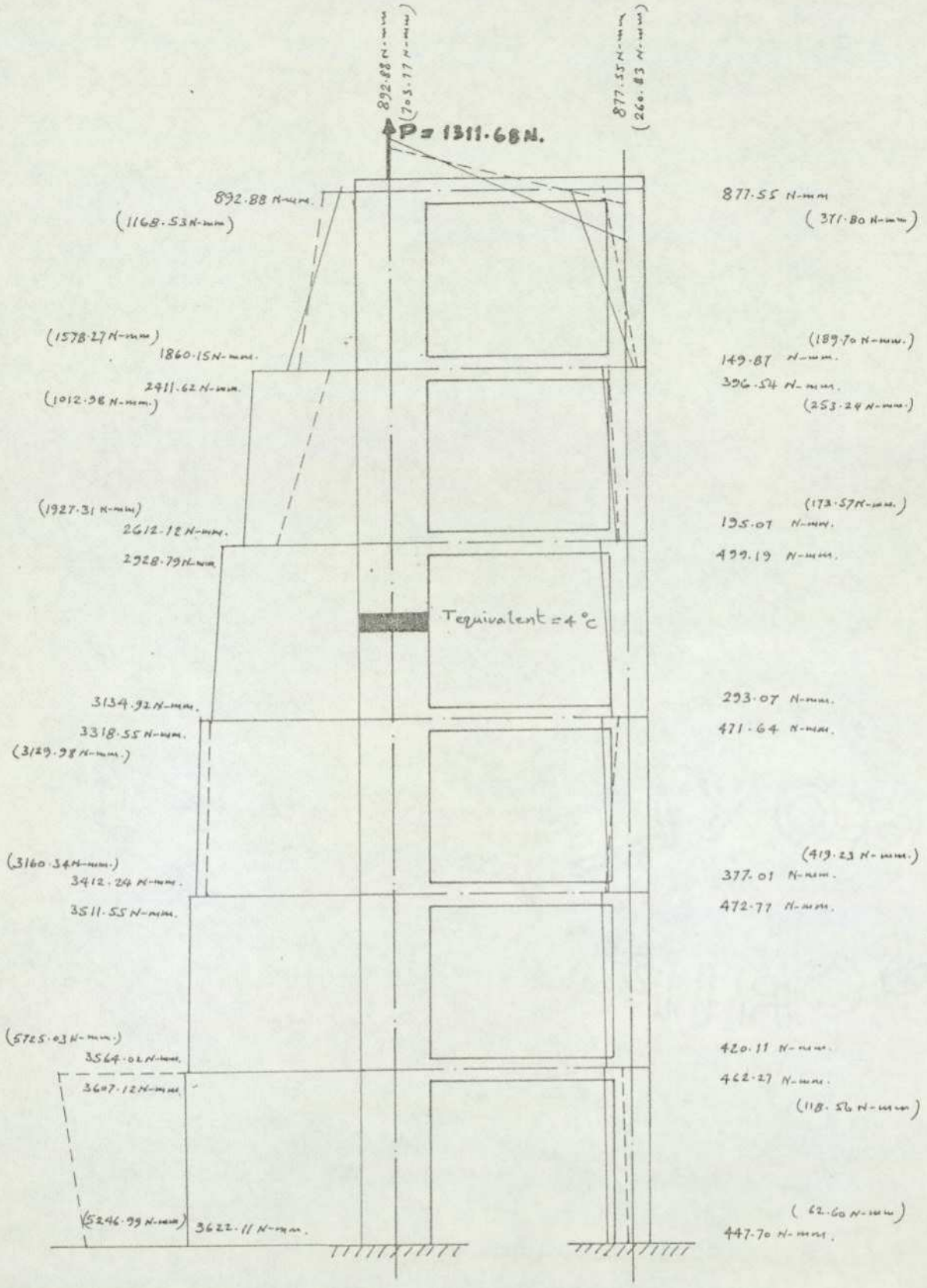

Fig. 8.0262 Shows bending moments due to the applied vertical load (simulated temperature effect on the larger column of a 6-storey frame).

———————— Theoretical bending moments by the force-displacement method. (Unbracketed figures)

– – – – – – Experimental bending moments. (Bracketed figures)

8.02.7 Discussion of results of experiment of simulated temperature in a column of a six-storey perspex shear wall

The displacement results, as given by dial gauges, show very good correlation with the theoretical displacements. Some of the displacements are correct to within ± 2%, while the majority are correct to within ± 5%. Only one location shows a greater discrepancy. This is at the top of the unheated column, showing a reduction in length caused by the compressive stress and induced by the simulated heating (applied tension) of the other column. It has been mentioned elsewhere in the text that members undergoing compressive stresses do not generally show good results. The main reason for this discrepancy is believed to be due to the tendency of the perspex to buckle.

The calculations of bending moments from the readings of strain gauges show reasonable correlation with the theoretical results. Generally, better accuracy is attained at points of maximum displacements. This would indicate that the level of experimental stress was perhaps not high enough.

Based on the above, it is concluded that the calculated stresses and deformations correlate reasonably well with those obtained from simulated experiments. The discrepancy range from ± 2% to ± 5% is accepted as being the result of approximate assumptions made in the analysis as well as inevitable imperfections of laboratory work. This experiment, however, has demonstrated adequately that simulated temperature experiments can yield more accurate results than experiments based on actual heating.

8.03 EXPERIMENTAL ANALYSIS OF A SIMULATED TEMPERATURE EFFECT ON A PERSPEX TRUSS

8.03.1 Introduction

In order to compare the theoretical results of thermal stress analysis of trusses, an experiment was carried out on the effect of simulated temperature on a perspex truss.

The dimensions and instrumentation details of the model truss are shown in fig. 8.031. For practical reasons, such as most readily available and suitable laboratory equipment and facilities, it was decided to hang the truss by one of the short sides and to test for the effect of temperature in one of the longer sides. Although this is not a common position in which one would use a truss of this type, it is adequate to demonstrate the simulated temperature effect on one of the chords.

As in the case of the perspex frame, strain gauges were used to measure the strains in all members, and dial gauges were used to measure deflections at joints.

8.03.2 The Experiment

The purpose of the experiment was to find, in a simulated experiment, the axial forces and deflections of all members of the truss due to the effect of temperature in one chord. It has been shown earlier in the text that if a heated member is fully restrained from expanding, the force required to stop the member from expanding can be found from the stress/strain relationship,

$$P = \frac{EA}{L} \alpha TL = EA\alpha T$$

or

$$T = \frac{P}{EA\alpha}$$

The perspex truss was fixed in a vertical position as shown in fig. 8.031 and instead of heat, loads were applied vertically along the axis of one chord. For each increment of applied load, readings of dial gauges and strain gauges were taken. The applied loads were increased in suitable increments until deflections and strain reading of a discernible magnitude were obtained. Then the applied loads were decreased by similar steps, each time recording the readings of dial gauges and strain gauges. For the calculations of deflections and axial forces, average of the loading and unloading readings was taken.

The results of the experiment are shown on the following sheets. Fig. 8.0321 shows the deflected form of the truss as measured by dial gauges. For comparison purposes, the theoretical deflections are also shown.

For the calculations of axial forces, a calibration perspex piece was tested in tension (Appendix 'D'). The resulting axial forces from the loading of the test model were analysed by equating the truss forces to those resulting from the calibration piece. Typical calculations are shown on Table 800.12. Also shown in fig. 8.0321 is the equivalent temperature for the case of maximum applied load. For comparison, the theoretical axial forces are also shown.

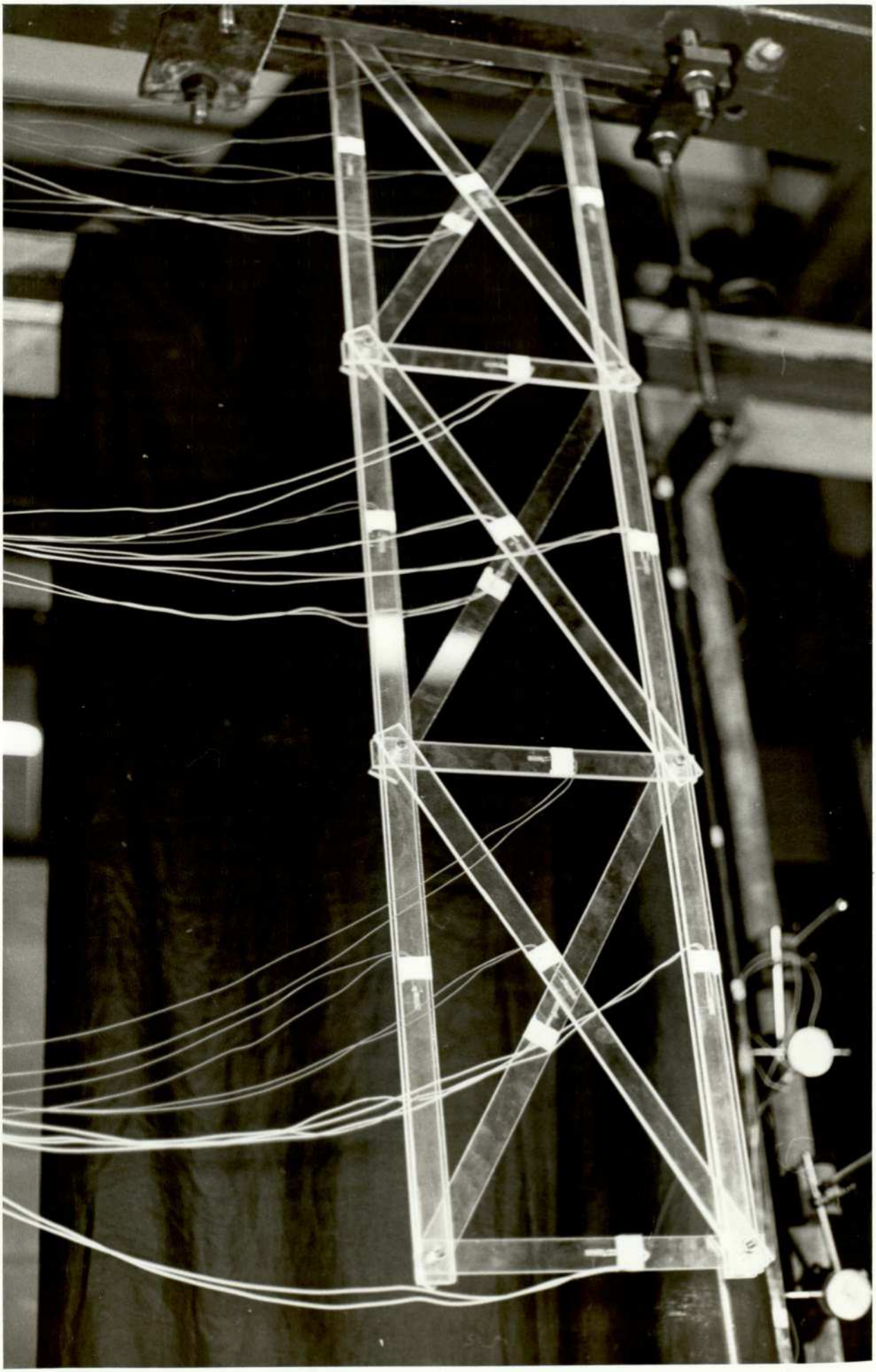

PLATE: V111 A perspex truss under test for the effect of simulated temperature change in one chord.

Fig. 8.051

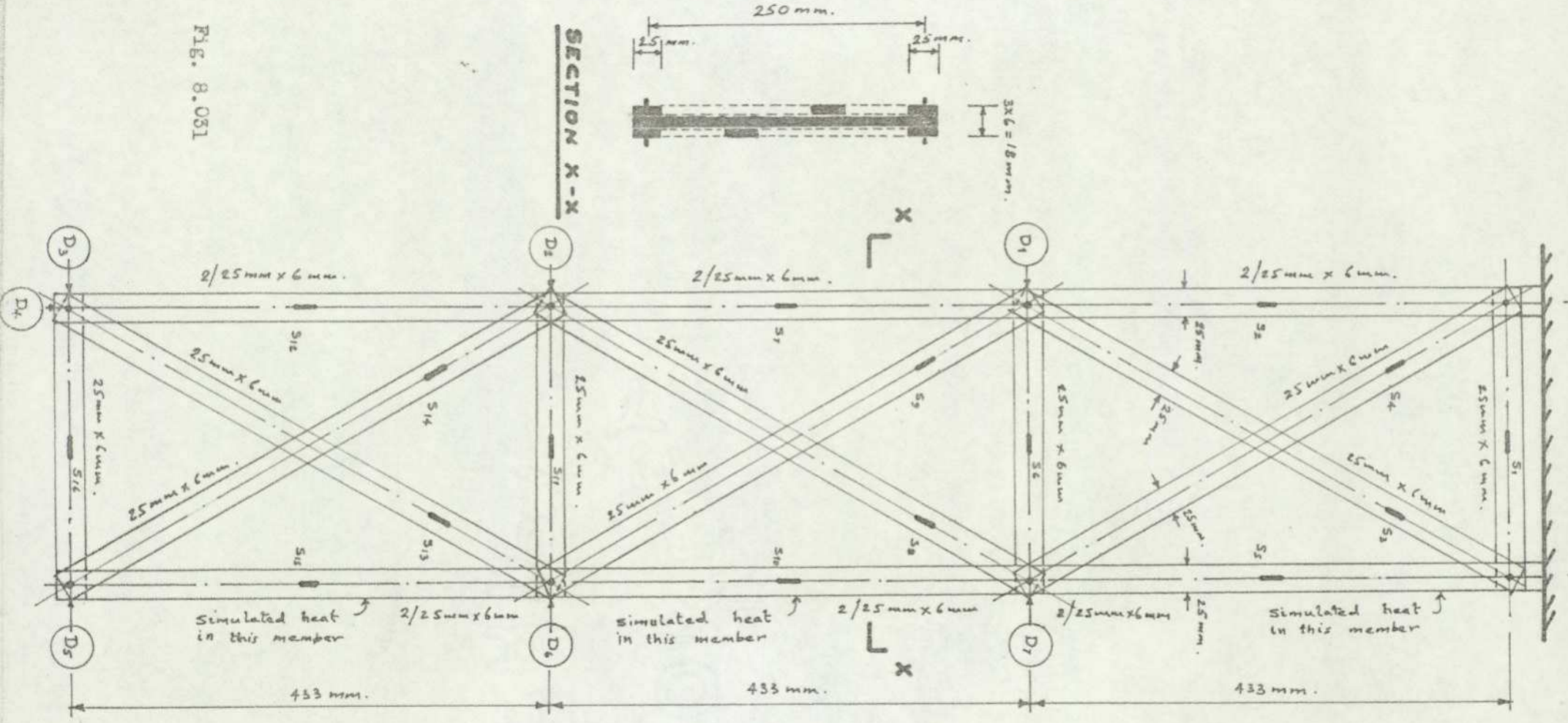
250 mm.
25 mm.
25 mm.
3x6 = 18 mm.
SECTION X-X
X
X
D1
D2
D3
D4
D5
D6
D7
2/25mm x 6mm.
2/25mm x 6mm.
2/25mm x 6mm.
25mm x 6mm
25mm x 6mm
25mm x 6mm
25mm x 6mm
25mm x 6mm
25mm x 6mm
25mm x 6mm
25mm x 6mm
25mm x 6mm
25mm x 6mm
S1
S2
S3
S4
S5
S6
S7
S8
S9
S10
S11
S12
S13
S14
S15
S16
25mm.
25mm.
25mm.
25mm.
Simulated heat in this member
2/25mm x 6mm
simulated heat in this member
2/25mm x 6mm
2/25mm x 6mm
Simulated heat in this member
433 mm.
433 mm.
433 mm.
250 mm.

SIMULATED TEMPERATURE EFFECT ON A CHORD OF A TRUSS

DIAL GAUGE READINGS (0.01 mm. PER DIVISION)

3rd. June, 1977.

APPLIED LOAD P \ DIAL GAUGE No.	D_1	D_2	D_3	D_4	D_5	D_6	D_7
0 N.	10.856	3.494	3.785	10.760	5.774	10.838	10.908
200 N.	11.024	3.887	4.507	10.789	4.811	10.418	10.751
400 N.	11.127	4.249	5.317	10.815	4.061	10.087	10.639
600 N.	11.282	4.716	6.102	10.828	3.182	9.677	10.502
777.92 N.	11.368	4.987	6.713	10.832	2.516	9.401	10.405
955.84 N	11.477	5.325	7.938	10.850	1.819	9.730	10.296
UNLOADING							
777.92 N.	11.420	5.160	6.895	10.829	2.319	9.292	10.367
600 N.	11.311	4.797	6.281	10.819	2.990	9.602	10.470
400 N.	11.199	4.550	5.557	10.817	3.788	9.956	10.592
200 N.	11.077	4.048	4.797	10.817	4.594	10.309	10.706
0 N.	10.930	3.692	3.964	10.813	5.484	10.721	10.850

Table: 800.10

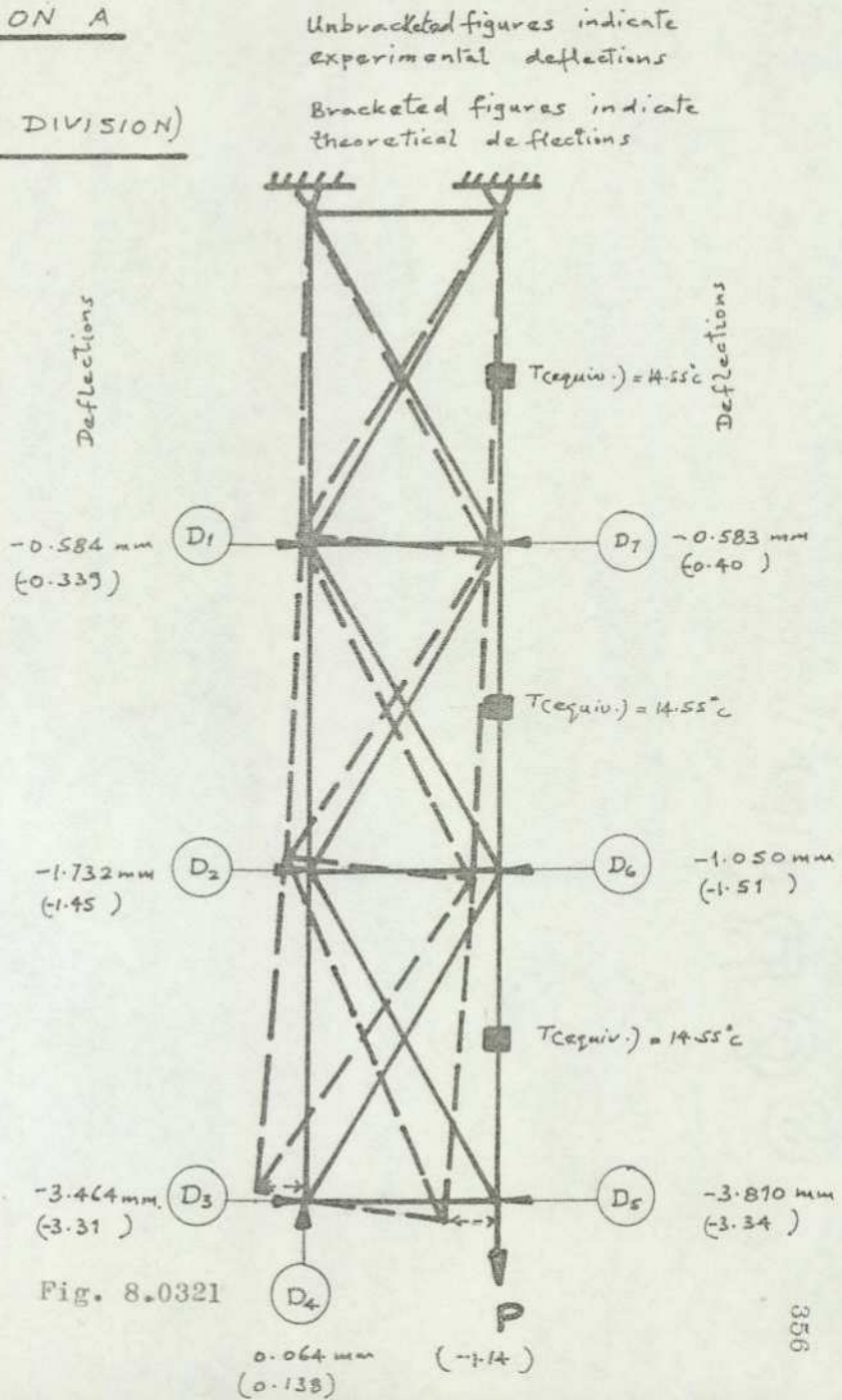

Fig. 8.0321

REPEAT OF EXPERIMENT ON SIMULATED EFFECT OF TEMPERATURE ON A TRUSS

3RD JUNE, 1977

LOADING			LOADING			LOADING			LOADING
LOAD 00 N									
+0295	+0157	+0412	+0306	+0350	+0117	-0001	+0051	+0004	+0062
-0263	-0127	+0016	+0196	+0059	-0023				
+0295	+0159	+0412	+0305	+0350	+0117	-0002	+0050	+0004	+0062
-0265	-0128	+0015	+0195	+0058	-0025				
+0295	+0159	+0411	+0305	+0350	+0117	-0001	+0051	+0004	+0061
-0265	-0128	+0014	+0195	+0058	-0025				
LOAD 200 N									
+0296	+0145	+0404	+0302	+0296	+0122	-0009	+0048	+0006	+0016
-0262	-0132	+0010	+0194	-0000	-0024				
+0296	+0147	+0404	+0301	+0296	+0120	-0008	+0049	+0006	+0017
-0261	-0130	+0010	+0194	+0001	-0023				
+0296	+0149	+0404	+0300	+0300	+0122	-0007	+0048	+0003	+0017
-0262	-0133	+0009	+0193	-0000	-0022				
LOAD 400 N									
+0296	+0139	+0399	+0298	+0255	+0124	-0010	+0049	+0007	-0021
-0258	-0131	+0012	+0195	-0045	-0017				
+0296	+0140	+0399	+0297	+0255	+0125	-0009	+0048	+0007	-0022
-0258	-0133	+0009	+0194	-0047	-0019				
+0296	+0140	+0400	+0298	+0253	+0125	-0009	+0050	+0007	-0022
-0258	-0132	+0009	+0194	-0047	-0019				
LOAD 600 N									
+0297	+0130	+0399	+0298	+0209	+0124	-0011	+0052	+0010	-0061
-0257	-0132	+0013	+0196	-0090	-0015				
+0297	+0132	+0397	+0298	+0208	+0125	-0011	+0052	+0010	-0062
-0255	-0133	+0011	+0197	-0092	-0016				
+0297	+0130	+0396	+0297	+0206	+0125	-0012	+0050	+0010	-0062
-0254	-0132	+0011	+0195	-0092	-0014				
LOAD 600 N + 40 Lb									
+0296	+0127	+0393	+0294	+0173	+0131	-0014	+0051	+0010	-0099
-0249	-0130	+0012	+0197	-0133	-0009				
+0297	+0125	+0394	+0294	+0171	+0131	-0013	+0051	+0011	-0099
-0248	-0132	+0013	+0196	-0134	-0009				
+0297	+0126	+0392	+0295	+0171	+0131	-0013	+0051	+0011	-0099
-0248	-0131	+0012	+0198	-0135	-0007				
LOAD 600 N + 80 Lb									
+0297	+0121	+0389	+0291	+0135	+0135	-0015	+0052	+0010	-0133
-0244	-0131	+0011	+0197	-0174	-0003				
+0296	+0121	+0389	+0291	+0134	+0135	-0015	+0052	+0010	-0135
-0244	-0132	+0010	+0197	-0176	-0003				
+0296	+0121	+0390	+0291	+0134	+0135	-0015	+0052	+0009	-0135
-0244	-0131	+0011	+0198	-0176	-0003				

Table: 800.11 (a)

UNLOADING UNLOADING UNLOADING UNLOADING

LOAD 600 N + 40 Lb

+0297 +0126 +0394 +0294 +0165 +0127 −0014 +0052 +0011 −0103
−0252 −0131 +0012 +0197 −0137 −0010

LOAD 600 N + 0 Lb

+0297 +0131 +0398 +0296 +0199 +0124 −0011 +0051 +0010 −0069
−0255 −0132 +0012 +0197 −0098 −0014
+0297 +0131 +0397 +0297 +0202 +0124 −0012 +0050 +0009 −0069
−0257 −0132 +0011 +0196 −0099 −0015
+0296 +0131 +0397 +0298 +0200 +0123 −0012 +0050 +0008 −0069
−0257 −0133 +0012 +0195 −0099 −0014

LOAD 400 N

+0298 +0136 +0400 +0298 +0242 +0119 −0011 +0048 +0009 −0031
−0260 −0132 +0012 +0195 −0054 −0019
+0298 +0136 +0401 +0298 +0243 +0119 −0011 +0048 +0008 −0031
−0260 −0133 +0012 +0195 −0053 −0018
+0296 +0136 +0400 +0297 +0242 +0118 −0012 +0047 +0006 −0032
−0276 −0123 +0019 +0205 −0027 +0013

LOAD 200 N

+0301 +0146 +0407 +0304 +0286 +0120 −0007 +0051 +0009 +0011
−0241 −0109 +0034 +0216 +0014 −0000
+0301 +0145 +0406 +0303 +0288 +0118 −0008 +0048 +0007 +0010
−0242 −0111 +0033 +0214 +0014 −0000
+0300 +0145 +0404 +0302 +0286 +0117 −0009 +0048 +0006 +0010
−0240 −0110 +0034 +0216 +0017 +0001

LOAD 00 N

+0299 +0151 +0408 +0303 +0334 +0111 −0009 +0044 +0002 +0052
−0245 −0112 +0036 +0217 +0072 −0005

Table: 800.11 (b)

1. CALCULATION OF FORCES IN TRUSS MEMBERS

Applied Load in N.	Strain Gauge Location	Strain Gauge Average Zero Reading	Strain Gauge Reading for App. Load	Diff. between Strain Gauge Readings	Experimental Force in each Member in N.	Theoretical Force in each Member in N.
955.34	1	+297.00	+296.33	0.67	0.67 × 0.015449 (25 × 6) = 1.55	0
	2	+154.67	+121.00	33.67	33.67 × 0.015449 (25×6×2)=156.05	108.0
	3	+409.83	+389.33	20.50	20.50 × 0.015449 (25 × 6) = 47.51	124.0
	4	+304.17	+291.00	13.17	13.17 × 0.015449 (25 × 6) = 30.52	124.0
	5	+342.00	+ 134.33	207.67	207.67×0.015449 (25×6×2)=962.49	849.0
	6	+114.00	+135.00	21.00	21.00 × 0.015449 (25 × 6) = 49.66	119.0
	7	+ 5.17	+ 15.00	9.83	9.83 × 0.05449 (25×6×2)=45.56	98.1
	8	+ 47.33	+ 52.00	4.67	4.67 × 0.015449 (25 × 6) = 10.82	113.0
	9	+ 3.00	+ 9.67	6.67	6.67 × 0.015449 (25 × 6) = 15.46	113.0
	10	+ 56.83	-134.33	191.16	191.16×0.015449 (25×6×2)=885.97	858.0
	11	-254.67	-244.00	10.67	10.67 × 0.015449 (25 × 6) = 24.73	116.0
	12	-119.83	-131.33	11.50	11.50 × 0.015449 (25×6×2)=53.30	103.0
	13	+ 25.50	+ 10.67	14.83	14.83 × 0.015449 (25 × 6) = 34.37	119.0
	14	+206.17	+197.33	8.84	8.84 × 0.015449 (25 × 6) = 20.49	119.0
	15	+ 65.17	-175.33	240.50	240.50×0.015449 (25×6×2)=1114.65	853.0
	16	- 14.67	- 3.00	11.67	11.67 × 0.015449 (25 × 6) = 27.04	59.2

Table: 800.12

2. CALCULATION OF EQUIVALENT TEMPERATURE

Applied Max. Load = 955.84N

Subst. into $T = \frac{P}{EA\alpha}$ gives

$$T = 955.84/3000 \quad (2 \times 25 \times 6) \quad 7.3 \times 10^{-5} = 14.55\,^{\circ}C$$

8.03.3 Discussion of results of experiment of simulated temperature on a perspex truss

The displacement results as given by the dial gauges show reasonable correlation with the theoretical displacements. At nodes showing maximum displacements the discrepancy is only of the order of 5%. Greater discrepancies occur at other joints where the displacements are small. Similarly, the axial forces in the members show good correlation for members with maximum forces, and greater discrepancies for members with small forces.

The reasons for the discrepancies are attributed to the following factors:-

1. The grade of perspex selected for the truss model was too strong. A weaker (or thinner) perspex would have given greater displacements at all points and consequently better results.

2. The bolted connections of the truss members, assumed to be pin-connected, showed considerable friction. It was found that the truss could be given an arbitrary displacement by simply moving it by hand, and it would remain in the displaced position. In view of this, an arbitrary small load (not taken into account) was applied to remove initial kinks etc. at the joints.

3. The members in compression always showed a tendency to buckle, thus indicating that perspex is not a suitable material for model members having large compressive forces.

However, in spite of the above factors, the results show that simulated experiments can be carried out to assess thermal stresses in trusses.

9.00 THE EFFECT OF TEMPERATURE OF HYDRATION OF CEMENT AND EARLY SHRINKAGE OF CONCRETE IN STRUCTURES

9.01 INTRODUCTION

It is well known that the chemical reaction of cement with water appears to continue in concrete over a period of many years. However, this reaction is the most vigorous during the first 7 to 14 days. During this period, while the constituents of concrete i.e. cement, sand, gravel and water are undergoing complex chemical changes, two very important and observable aspects are also taking place. First, the chemical reaction generates a great quantity of heat of hydration. In large concrete pours, this heat of hydration can raise the temperature of setting concrete to such an extent that concrete can become too hot to touch with a bare hand. Second, shrinkage of concrete is taking place and is at its highest rate at this early age of hydration of concrete.

Theoretically, if a mass of concrete could shrink uniformly without any internal or external restraints, then no internal stresses would be induced in the concrete. This however seldom happens in practice, since usually any free movement of concrete is restricted internally by reinforcement and aggregate embedded in the concrete, and often externally by other members.

When concrete in a reinforced beam or slab shrinks, tension stresses develop in concrete and compression in steel. The latter takes place through the bond stress (and mechanical anchorage) along the surface of reinforcement.

In the following, an attempt is made to assess the effect of shrinkage and temperature of hydration on stresses and deformations as well as to predict the approximate spacing of the potential cracks.

Observation shows that concrete members can develop severe cracks even at a very early stage within one to seven days after casting. At this stage concrete is usually fully supported by formwork so that no stresses and deformations take place from own weight. The cracks are attributed therefore to the effect of temperature of hydration, shrinkage of concrete and possibly creep.

Concrete strength and particularly tensile strength is very low within the first few days after casting and if tension develops in concrete, it can result in cracks, often very wide. To minimise this effect, concrete is often "cured" for a period of 7 to 14 days, various moisture-retaining paints are used or concrete is specified with low shrinkage and heat of hydration.

In the following, an effort is made to assess the magnitude of these stresses by analytical method. However, no experimental work is carried out because this warrants a separate study on a large scale.

In the following analysis, it is assumed that:-

(i) the principle of superposition can be applied, so that the effect of shrinkage can be added to the effect of temperature of hydration.

(ii) that shrinkage strains are linearly disposed through the depth of the concrete member.

(iii) shrinkage stresses are proportional to strains and that

(iv) the temperature of hydration can be represented by a mathematical expression to facilitate the solution.

9.02 The effect of shrinkage on Rectangular Concrete Members:

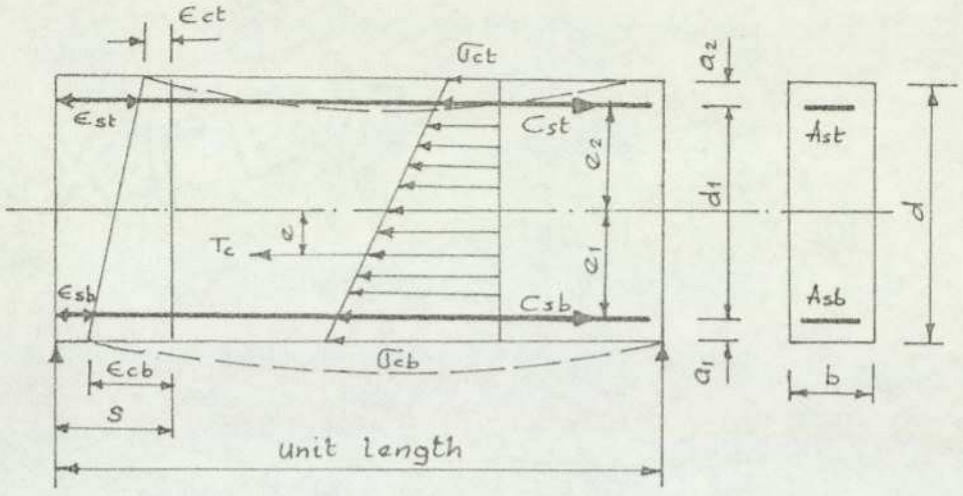

Fig. 9.021

Fig. 9.021 shows a simply-supported beam of unit length which is subjected to a potential shrinkage 's' of a plain concrete. If reinforcement is present (Asb and Ast) then the full amount of this shrinkage cannot take place and external fibres of the beam will be subjected to tensile strains ϵ_{cb} and ϵ_{ct}, these strains will produce tensile stresses σ_{cb} and σ_{ct} with an overall tensile force Tc. For equilibrium, steel will be subjected to compression Csb and Cst respectively.

To calculate these stresses in concrete and in steel the required values are the strains ϵ_{cb} and ϵ_{ct}, these can be calculated using the conditions of equilibrium of forces and moments:

$$Tc = Csb + Cst \qquad \ldots\ldots\ldots 9.02.01$$

and $$Tc.e = Csb.e_1 - Cst.e_2 \qquad \ldots\ldots\ldots 9.02.02$$

By expressing the values of forces in terms of stresses or strains we obtain:

$$T_c = \tfrac{1}{2}(\sigma_{cb} + \sigma_{ct})\, A_c = \tfrac{1}{2} A_c E_c (\epsilon_{cb} + \epsilon_{ct})$$

$$C_{sb} = A_{sb}.E_s.\epsilon_{sb}$$

$$C_{st} = A_{st}.E_s.\epsilon_{st}$$

$$\epsilon_{sb} = S - \left(\frac{e_1}{d} + \frac{1}{2}\right)\epsilon_{cb} + \left(\frac{e_1}{d} - \frac{1}{2}\right)\epsilon_{ct} \qquad \text{..... 9.02.03}$$

$$\epsilon_{st} = S + \left(\frac{e_2}{d} - \frac{1}{2}\right)\epsilon_{cb} - \left(\frac{e_2}{d} + \frac{1}{2}\right)\epsilon_{ct} \qquad \text{..... 9.02.04}$$

Denoting:

$$K = \frac{A_c.E_c}{A_{sb}.E_s}, \quad K_s = \frac{A_{st}}{A_{sb}}$$

$$\mu_1 = \frac{e_1}{d} \quad \text{and} \quad \mu_2 = \frac{e_2}{d}$$

we obtain from 9.02.01 and 9.02.02

$$\left[\frac{K}{2} + \mu_1 + K_s\left(\frac{1}{2} - \mu_2\right) + \frac{1}{2}\right]\epsilon_{cb} +$$

$$\left[\frac{K}{2} - \mu_1 + K_s\left(\frac{1}{2} + \mu_2\right)\right]\epsilon_{cb} = S(K_s + 1) \qquad \text{..... 9.02.05}$$

$$\left[\frac{K}{12} + \mu_1\left(\mu_1 + \frac{1}{2}\right) + K_s.\mu_2\left(\mu_2 - \frac{1}{2}\right)\right]\epsilon_{cb} -$$

$$\left[\frac{K}{12} + \mu_1\left(\mu_1 - \frac{1}{2}\right) + K_s.\mu_2\left(\mu_2 + \frac{1}{2}\right)\right]\epsilon_{ct} = S(\mu_1 - K_s.\mu_2)$$

..... 9.02.06

Equations 9.02.03 and 9.02.04 can be solved in general form if the following abbreviations are used:

$$A = \frac{K}{2} + \mu_1 + K_s\left(\frac{1}{2} - \mu_2\right) + \frac{1}{2}$$

$$B = \frac{K}{2} + \mu_1 + K_s\left(\frac{1}{2} + \mu_2\right) + \frac{1}{2}$$

$$C = 1 + K_s$$

$$D = \frac{K}{12} + \mu_1\left(\mu_1 + \frac{1}{2}\right) + K_s.\mu_2\left(\mu_2 - \frac{1}{2}\right)$$

$$E = \frac{K}{12} + \mu_1\left(\mu_1 - \frac{1}{2}\right) + K_s.\mu_2\left(\mu_2 + \frac{1}{2}\right)$$

$$F = \mu_1 - K_s.\mu_2$$

Equations 9.02.05 and 9.02.06 can now be re-written in the form:

$$A.\epsilon_{cb} + B.\epsilon_{ct} = C.S \qquad \text{..... 9.02.07}$$

$$D.\epsilon_{cb} - E.\epsilon_{ct} = F.S \qquad \text{..... 9.02.08}$$

from which:

$$\epsilon_{cb} = \frac{BF + CE}{AE + BD}.S \qquad \text{..... 9.02.09}$$

$$\epsilon_{ct} = \frac{CD - AF}{AE + BD}.S \qquad \text{..... 9.02.10}$$

the strains in the steel can now be determined from eqns. 9.02.03 and 9.02.04.

For a beam with symmetrical reinforcement at the top and bottom

$$Ast = Asb \text{ and } \quad e_1 = e_2$$

Equations 9.02.09 and 9.02.10 reduce to

$$\epsilon cb = \epsilon ct = \frac{S}{A} \qquad \ldots\ldots\ldots 9.02.11$$

$$\text{and } \epsilon sb = \epsilon st = S\left(1 - \frac{1}{A}\right) \qquad \ldots\ldots\ldots 9.02.12$$

Since in this case Ks = 1, the value of A reduces to

$$A = \frac{K}{2} + 1 \qquad \ldots\ldots\ldots 9.02.13$$

Eqns 9.02.11 and 9.02.12 show that the strains in concrete and in steel in symmetrically reinforced members are independent of the position of the steel, but depend on the magnitude of the reinforcement used.

If the centre of gravity of the steel area is denoted be 'e'

$$\text{then } \epsilon cb = S.\frac{BF + E}{AE + BD} = S.\frac{6\mu + 1}{K + 12\mu^2 + 1} \quad \text{where } \mu = \frac{e}{d} \qquad \ldots\ldots\ldots 9.02.14$$

$$\epsilon ct = S.\frac{D + AF}{AE + BD} = S.\frac{1 - 6\mu}{K + 12\mu^2 + 1} \qquad \ldots\ldots\ldots 9.02.15$$

$$\text{and } \epsilon s = S.\frac{K + 12\mu^2 - 8\mu + 1}{K + 12\mu^2 + 1} \qquad \ldots\ldots\ldots 9.02.16$$

which, for e = o, and ks = 1 reduces to eqn. 9.02.11

9.03 The Effect of Temperature of Hydration of Cement:

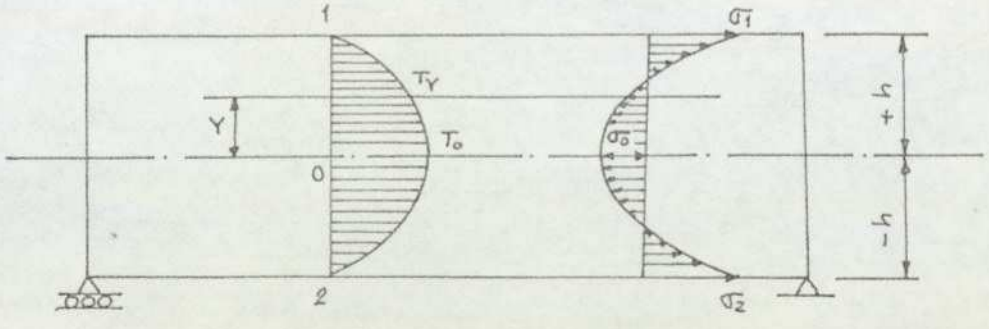

Fig. 9.031

It is well known that when a beam is subjected to a variable temperature change throughout the depth, then the stress at any distance 'y' from the neutral axis can be expressed as:

$$\sigma x = \alpha . E \left[- T_Y + \frac{1}{2h} \int_{-h}^{+h} T_Y . dY + \frac{3Y}{2h^3} \int_{-h}^{+h} T_Y . Y . dY \right] \qquad \ldots\ldots\ldots 9.03.01$$

in which Ty must be an even function of y.

If the temperature of hydration is assumed to be parabolic with the maximum To at the neutral axis, then at any distance y the Temperature Ty can be expressed as:

$$Ty = To\left[1-\left(\frac{Y}{h}\right)^2\right] \qquad \ldots\ldots\ldots 9.03.02$$

Introducing eqns. 9.03.02 and 9.03.01 we obtain:

$$\sigma_x = \alpha E T_o \left[\left(\frac{Y}{h}\right)^2 - \frac{1}{3}\right]$$

from which for $y = o$, $\sigma_o = -\frac{1}{3}\alpha E T_o$

and for $y = \pm h$, $\sigma_{1,2} = +\frac{2}{3}\alpha E T_o$

These stresses are "self- equilibrating" i.e. the sum of all forces and their moments with respect to any point are zero.

9.04 Resultant Stresses:

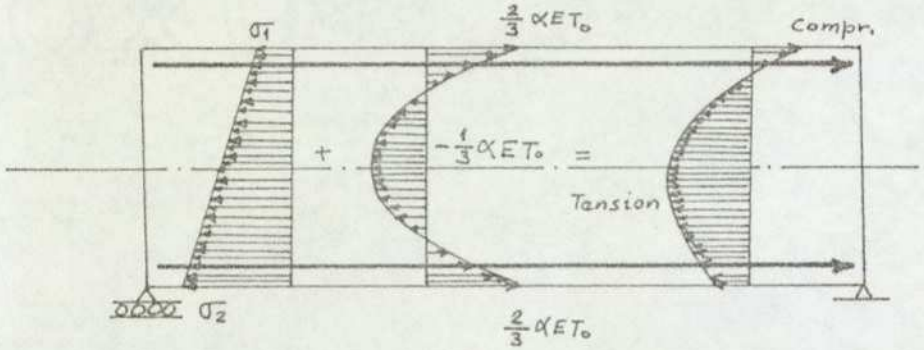

Fig. 9.041

When shrinkage and temperature of hydration are taking place simultaneously then the combined stresses can be of the form as shown in Fig. 9.041. Tensile stresses can be at their maximum at or near the neutral axis and are the sum of the two effects. These stresses can diminish towards the extreme fibres and can change into compressive stresses at the top surface.

If tensile resistance of concrete at this stage of its maturity is less than this stress, then cracks may develop at spacings, as shown in text later.

9.05 EXAMPLES

The following examples are used to illustrate the changing pattern of stresses and their magnitude with the changing pattern of reinforcement for the combined effect of Temperature of hydration and early shrinkage of concrete.

9.05.1 Example 1

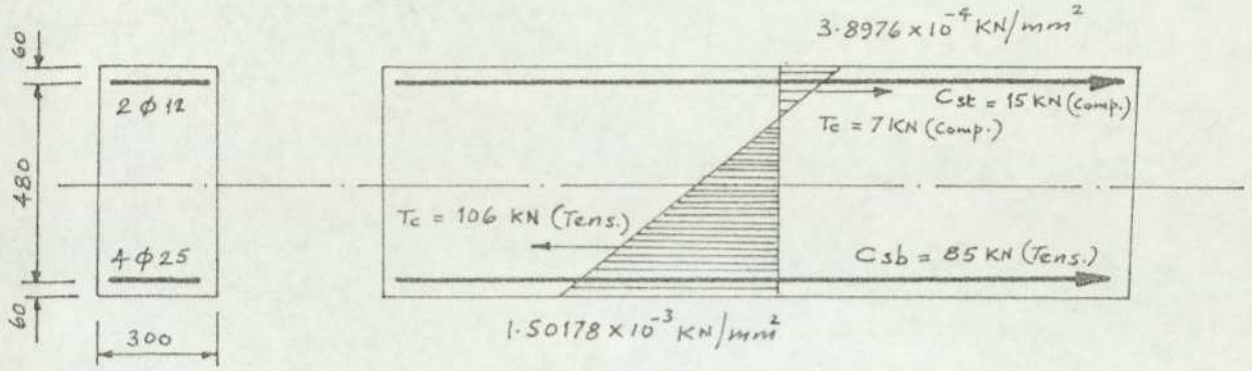

Fig. 9.0511 Reinforced concrete section and stress distribution due to shrinkage

Asb	= 1,962.5 mm²	Ast	= 226.08 mm²
Ac	= 177,811.42 mm²	Ec	= 14 KN/mm²
Es	= 210 KN/mm²	s	= 0.0003

The reinforced concrete section shown in fig. 9.0511 and having the properties shown above is analysed as follows:

First, the following parameters are evaluated:-

$K = 6.0403$ $\qquad$ $Ks = 0.1152$

$\mu_1 = \mu_2 = \frac{240}{600} = 0.4$

$A = \frac{6.0403}{2} + 0.4 + 0.1152\ (\frac{1}{2} - 0.4) + \frac{1}{2} = 3.93162$

$B = \frac{6.0403}{2} - 0.4 + 0.1152\ (\frac{1}{2} + 0.4) + \frac{1}{2} = 3.13162$

$C = 1 + 0.1152 = 1.1152$

$D = \frac{6.0403}{12} + 0.4\ (0.4 + \frac{1}{2}) + 0.1152 \times 0.4\ (0.4 - \frac{1}{2}) = 0.858750$

$E = \frac{6.0403}{12} + 0.4\ (0.4 - \frac{1}{2}) + 0.1152 \times 0.4\ (0.4 + \frac{1}{2}) = 0.504830$

$F = 0.4 - 0.1152 + 0.4 = 0.35392$

and from eqns 9.02.01, 02, 03 and 04.

$$\epsilon_{cb} = S\frac{BF + CE}{AE + BD} = 0.0003 \times \frac{3.13162 \times 0.35392 + 1.1152 \times 0.504830}{3.93162 \times 0.504830 + 3.13162 \times 0.858750}$$

$$= 0.00010727$$

$$\epsilon_{ct} = S\frac{CD - AF}{AE + BD} = -0.00002784$$

$$\epsilon_{sb} = S-(\frac{e_1}{d} + \tfrac{1}{2})\,\epsilon_{cb} + (\frac{e_1}{d} - \tfrac{1}{2})\,\epsilon_{ct}$$

$$= 0.0003 - (\frac{240}{600} + \tfrac{1}{2})\ 0.00010727 + (\frac{240}{600} - \tfrac{1}{2})(-0.00002784)$$

$$= 0.00020624$$

$$\epsilon_{st} = S + (\frac{e_2}{d} - \tfrac{1}{2})\ \epsilon_{cb} - (\frac{e_2}{d} + \tfrac{1}{2})\,\epsilon_{ct}$$

$$= 0.0003 + (\frac{240}{600} - \tfrac{1}{2})\ 0.00010727 - (\frac{240}{600} + \tfrac{1}{2})(-0.00002784)$$

$$= 0.00031433$$

The stresses are now calculated, based on the assumed moduli of elasticity, as follows:-

$$\sigma_{cb} = 1.50178 \times 10^{-3}\ KN/mm^2$$

$$\sigma_{ct} = -3.8976 \times 10^{-4}\ KN/mm^2$$

$$\sigma_{sb} = 0.0433104\ KN/mm^2$$

$$\sigma_{st} = 0.066093\ KN/mm^2$$

The resulting forces in concrete and steel are:-

$$Tc(tension) = \tfrac{1}{2}(0.00150178) \times (476.3674 \times 300 - 1962.50)$$

$$= 105.8362\ KN$$

$$Tc(Comp.) = \tfrac{1}{2}(0.00038976)\ (123.6326 \times 300 - 226.08)$$

$$= 7.1840\ KN$$

$$Csb = Asb.Fs\ \epsilon sb = 1962.50 \times 210 \times 0.00020624 = 84.9967\ KN$$

$$Cst = Ast.Fs\ \epsilon st = 226.08 \times 210 \times 0.00031433 = 14.9234\ KN$$

In this example, it is assumed that the heat of hydration of cement generates a temperature of $T_o = 10^oC$, at the neutral axis and that no temperature changes take place at the external fibres, so that $T_1 = T_2 = 0^oC$. The stress distribution is as shown in fig. 9.0512.

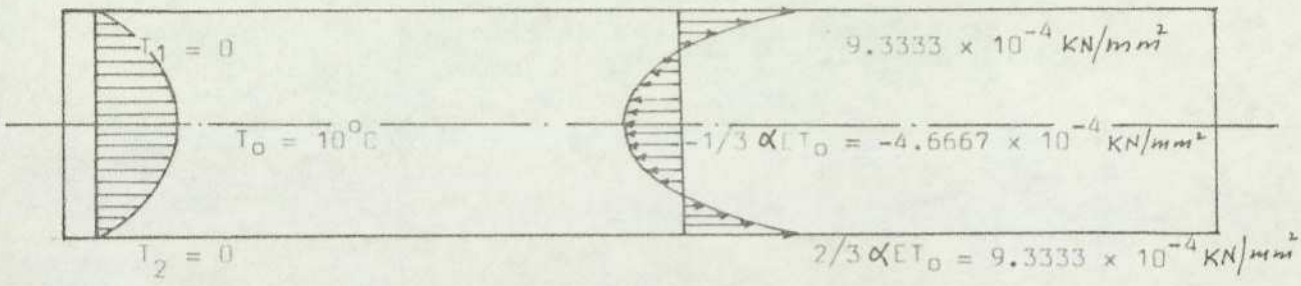

Fig. 9.0512 Stress distribution due to temperature of hydration of Cement

The stress distributions shown in figs. 9.0511 and 9.0512 for shrinkage and temperature of hydration can occur simultaneously during the early stage of casting.

The combined stress distribution is shown in fig. 9.0513.

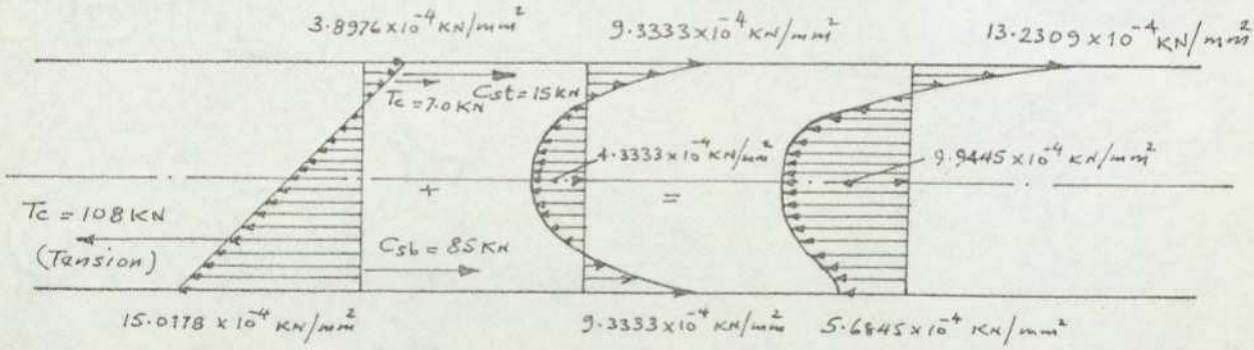

Fig. 9.0513 Stress distribution due to the combined effect of temperature of hydration and early shrinkage of concrete

9.05.2 Example 2

If the same beam is reinforced symmetrically with 2 Ø 12 bars top and bottom (fig. 9.0521) or with 4 Ø 25 bars (fig. 9.0522) the tensile stresses in concrete due to shrinkage and heat of hydration of cement are as follows:

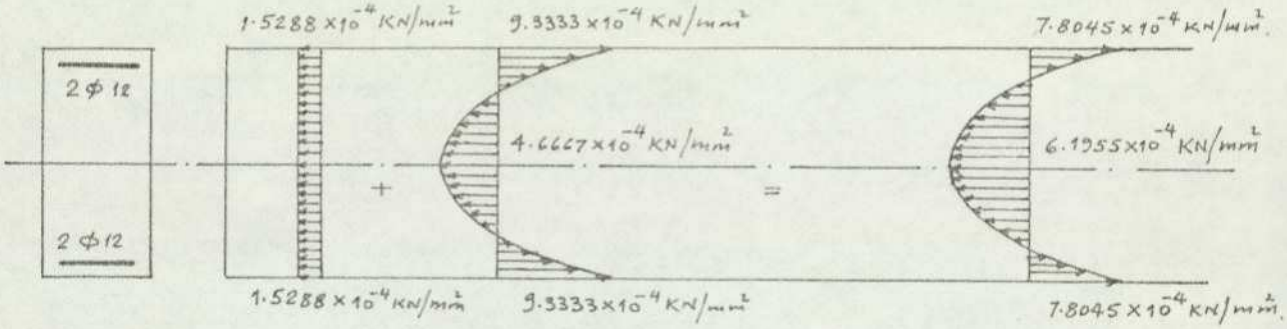

Fig. 9.0521

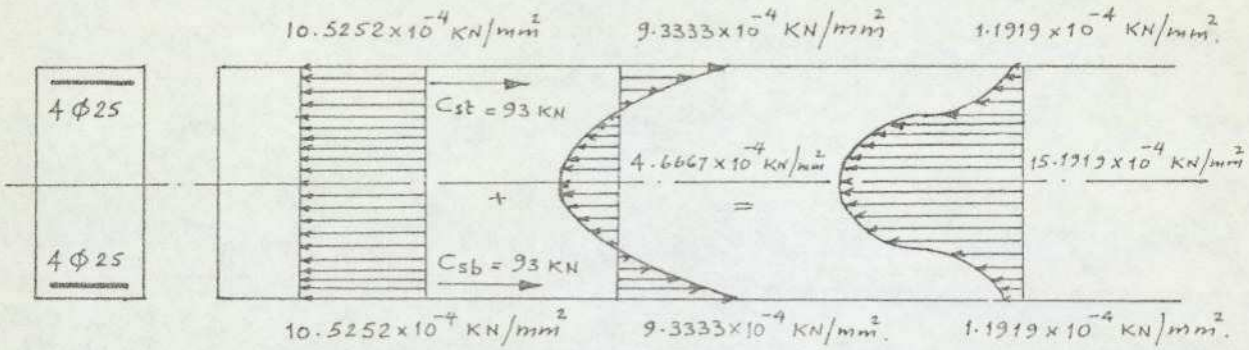

Fig. 9.0522

If only bottom reinforcement is used with 4 Ø 25 bars as in (fig. 9.0523) then the tensile stress in concrete is as follows:

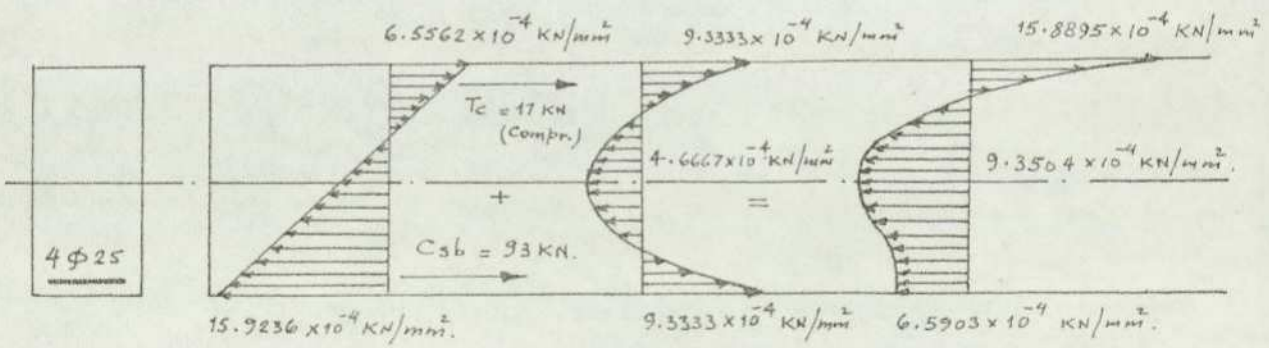

Fig. 9.0523

9.06 APPROXIMATE ANALYSIS OF DISTRIBUTION OF POTENTIAL CRACKS IN REINFORCED CONCRETE

In the following, an attempt is made to assess the effect of shrinkage and temperature of hydration on stresses and deformations as well as to predict the spacing and the size of the potential cracks.

Observations indicate that large tensile stresses can develop in the concrete due to the combined effect of temperature of hydration and shrinkage, and when the magnitude of these tensile stresses exceed the modulus of rupture of concrete, cracks can develop in concrete.

Although temperature and shrinkage cracks in concrete members occur frequently, not all members crack. During the setting period both the magnitude of temperature, shrinkage and the modulus of rupture of concrete vary with time and curing period. If the latter is sufficiently long, concrete strength, its modulus of elasticity and particularly the tensile strength may reach a higher value than the shrinkage stresses, and cracks will not form. This is shown diagrammatically in fig. 9.061.

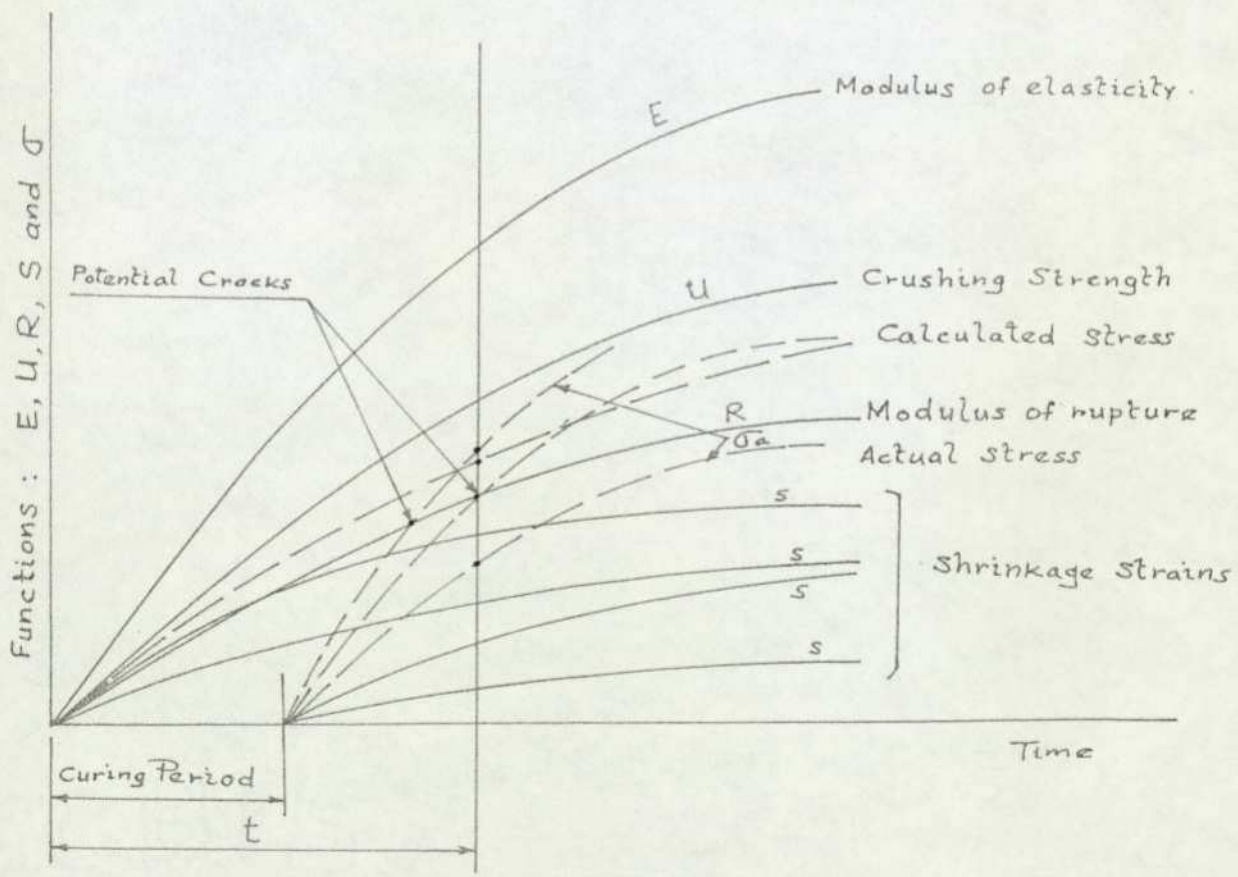

Fig.9.061 Formation of cracks in beams or slabs

If, however, temperature and shrinkage stresses increase at a higher rate than the increase of modulus of rupture, a time may be reached when the latter value is exceeded and cracks may develop.

Based on the analysis shown in section 9.02 the theoretical distribution of potential cracks can be approximately assessed as follows:-

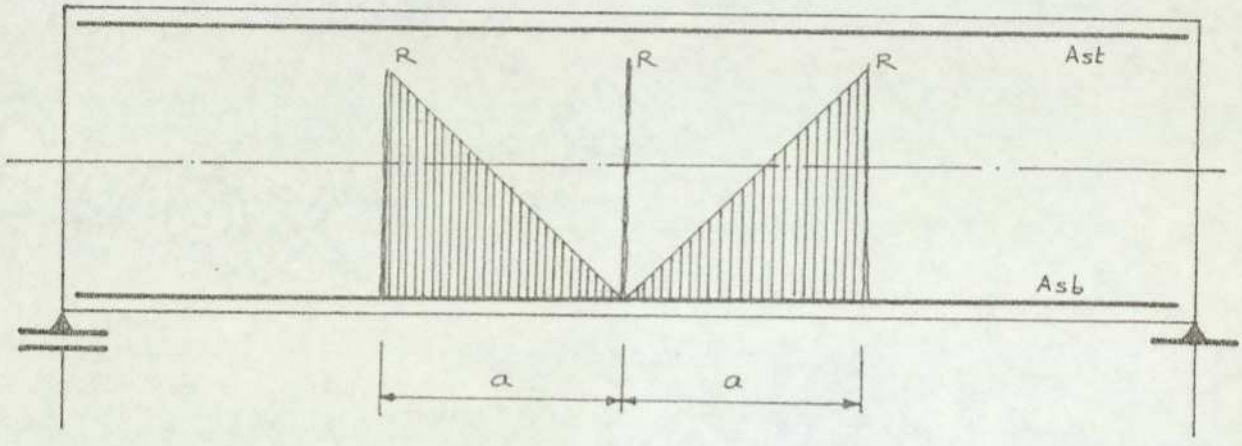

Fig. 9.062

Fig. 9.062 shows a beam assumed to crack at distances 'a' apart under the effect of temperature and shrinkage stresses only. At the crack longitudinal stress σ must vanish, and then build up by bond to a full value of the modulus of rupture of concrete at a particular time. In certain cases, this full value of the modulus of rupture may not be reached at all and cracks will not form. However, assuming that the full value of modulus of rupture is developed by bond, and a stage is reached where cracks are just developing, then, for equilibrium the following equation must hold:-

$$C_s = \frac{aRP}{2}$$

from which

$$a = \frac{2C_s}{RP}$$

or substituting values from Eqns. 9.02.04, 9.02.14, 15 and 16

$$a = \frac{2s}{RP} \quad As\ Es \quad \frac{K + 12\mu^2 + 1 - 8\mu}{K + 12\mu^2 + 1}$$

in which:

C_s - is total compression in steel

R - modulus of rupture of concrete at a time considered

$K = \frac{AcEc}{AsEs}$, $\mu = \frac{e}{d}$

P - Perimeter of steel

From the above equation, it can be seen that the spacing of the potential cracks depends only marginally on the position of steel in the cross-section (μ), but depends to a considerable extent on the ratio of steel to concrete area, on the modular ration Es/Ec and is inversely proportional to the modulus of rupture of concrete and the perimeter of steel used. This confirms the well known fact that the smaller the diameters of bars, for the same overall area of steel, the smaller and more closely spaced are the cracks.

The average values of the modulus of rupture related to 28 days cube strength are given by Prof. Evans as follows:-

Cube Strength		Tensile Strength of concrete	
N/mm^2	($lb/in.^2$)	N/mm^2	($lb/in.^2$)
6.9	1,000	1.4	200
13.8	2,000	2.0	290
20.7	3,000	2.5	360
27.6	4,000	2.8	410
41.4	6,000	3.4	500
68.9	10,000	4.5	650

9.06.1 Example (3)

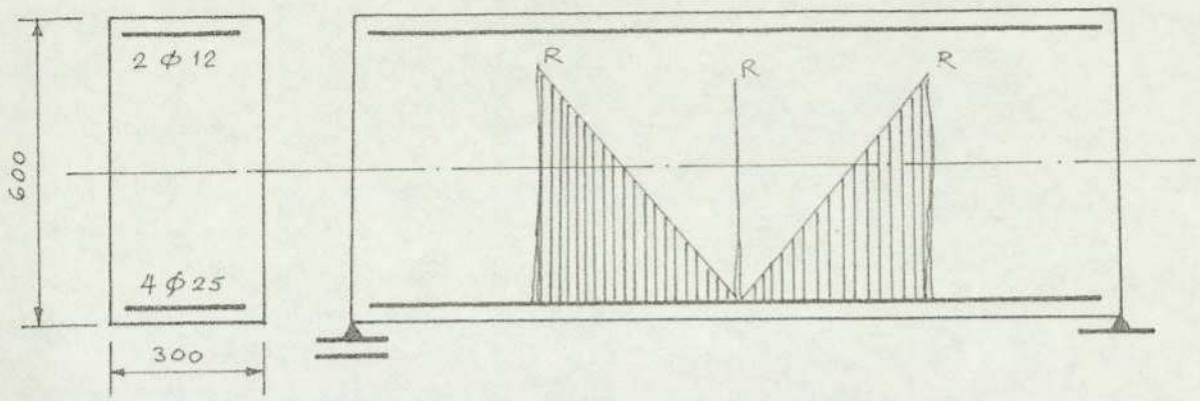

Fig. 9.0611

C_{sb} = 84.9967 KN R = 2.75 N/mm^2

and p = 319.02 mm

$$a = \frac{2 \times 84.9967 \times 10^3}{2.75 \times 319.02} = 193.77 \text{ mm}$$

9.07 DISCUSSION ON THE EFFECT OF TEMPERATURE OF HYDRATION OF CEMENT AND EARLY SHRINKAGE OF CONCRETE IN STRUCTURES

The results of the investigation confirm that very high stresses and deformations can be introduced in structures by the combined effect of the temperature of hydration of cement and the early shrinkage of concrete.

Barry P. Hughes (ref. 12) states that even with the use of low-heat portland cement for a foundation raft structure, a temperature rise of 47°C was recorded during the first 24 hours after placing the concrete. In spite of several other precautions taken, such as addition of extra reinforcement and flooding the surface, cracking of concrete still occurred. This shows that neither reinforcement nor better curing can fully control these stresses, and other means must be found to reduce these stresses and the development of cracks.

It is also shown that in reinforced concrete members shrinkage generally produces tension in concrete and compression in steel, and these are additive to stresses produced by gravity, wind loads, prestressing, creep and temperature. Shrinkage strains and stresses in concrete and in steel in symmetrically reinforced members are independent of the position of the steel, but depend on the magnitude of the reinforcement used. Also, the greater the magnitude of reinforcement, the greater are the stresses and strains in the concrete.

On the assumption of parabolic temperature of hydration of cement, a beam is subjected to compressive stresses near the surface, and tensile stresses at the centre, which is additive to the tensile stresses produced by shrinkage of concrete.

An approximate method of calculating the theoretical spacing of potential cracks in beams is also presented. However, they depend in a complex way on the relative magnitude of the shrinkage of concrete, its modulus of elasticity, modulus of rupture and bond. The parameters change continuously throughout the life of concrete and particularly at early stages after casting.

CHAPTER TEN

10.00 DISCUSSIONS AND CONCLUSIONS

10.01 DISCUSSION AND COMPARISON OF ANALYTICAL SOLUTIONS

The force-displacement method of analysis was mainly used in this work. However, a large number of problems were also analysed by the stiffness method, so that a comparison could be made between the two methods. As both methods are based on "energy principles", it is not surprising that the results correspond very closely in the two cases. There is, therefore, not much to choose between the methods. Each method has its own merits and demerits. While the stiffness method is now very well developed, the force- displacement method, being new, requires further development, before it is possible to say whether one is superior to the other. It may be conjectured, however, that it is a matter of time before it is postulated that certain problems may be more suited to one method than the other. At this stage, it would appear that the force-displacement method may appeal more to the engineer for the following two features:-

(1) The method gives directly the values of statically indeterminate bending moments and deflections, which are usually of prime interest to the designer.

(2) The philosophy of the method is easier to understand as it is based on the clear, physical interpretation of the actual response of the structure.

10.02 COMPARISON OF ANALYTICAL AND EXPERIMENTAL RESULTS

It may be justifiably claimed that a reasonable degree of correlation was obtained between the theoretical and experimental results. Various difficulties associated with heating of models, as indicated in the text, were anticipated from the outset of this work. It was, therefore, not surprising that inspite of very careful and repeated experimentation, based on actual heating, calculations of stresses (i.e. bending moments) were not satisfactory in the case of multi-storey frame, although quite satisfactory in the case of a continuous beam. However, this was more than made up by the accuracy of deflections and the general behaviour of the frame.

In the case of experiments based on the effect of "simulated temperature" on perspex models, the results were even more encouraging. The multi-storey frame shows some deflections correct to within $\pm$ 2%, while the majority are correct to within $\pm$ 5%. In the case of bending moments, reasonable correlation was obtained at points of maximum displacements. The inaccuracies in the bending moments are mainly attributed to low level of applied experimental stress.

Similarly, the results of an experiment on the effect of simulated temperature on a truss show good accuracy ($\pm$ 5%) in deflections and axial forces at points of maximum displacements. These results of simulated temperature effects justify and show encouraging prospects of future experimentation on improved models, and have provided future researchers with a new approach to thermal problems.

Based on the above facts, that calculated stresses and deformations correlate reasonably well with those obtained from experiments, it is concluded that the assumptions made in the theories of thermal stresses are valid.

Furthermore, the experimental work on (i) the concrete block, (ii) cylinder and cubes of various mixes, and (iii) micro-concrete beams, has established the thermal response and properties of concrete.

10.03 SUMMARY AND CONCLUSIONS

The results of this work have fulfilled the objectives in all aspects, from acceptable to excellent degree of accuracies. The results are discussed in detail at the end of each section.

Within the scope of this work, the following conclusions can be drawn.

(1) the response of concrete to the outside temperature changes is subject to two important phenomena:

   (a) a time lag Δt, i.e. concrete does not respond instantaneously to the temperature change and

   (b) attenuation of temperature, i.e. the temperature in concrete does not rapidly reach the value of the temperature applied.

(2) at low or intermediate temperatures, there is no significant change in the modulus of elasticity, Ec, of concrete.

(3) at 100°C the value of 'Ec' begins to drop rather rapidly.

(4) concretes made from other types of aggregates, such as Aglite and Lytag Mixes, also exhibit similar properties.

(5) within the test temperature range (up to 100°C) compressive strength of concrete increases with age and increase in temperature.

(6) although strength and elasticity ($\frac{1}{EI}$) show about the same temperature dependence, elasticity is more severely reduced at temperatures of 100°C.

(7) high stresses, but without any strains, can be induced in a beam, restrained at the ends, when subjected to a constant temperature change.

(8) on the other hand, large deformation strains, but without any stress, can be induced in a beam, simply supported at the ends, when subjected to a linear temperature change.

(9) in statically determinate beams, subjected to a linear temperature change, the slope and deflection are independent of the stiffness EI (where slope $\theta = \alpha T_1 L/2d$ and deflection $\delta = \alpha T_1 L^2/8d$). On the other hand, the equivalent bending moment, $M = \alpha T_1 EI/d$ producing a curvature similar to the effect of temperature, is independent of the span.

(10) in continuous beams, the statically indeterminate bending moments from temperature do not depend on the actual spans but on their ratios L_1/L_2 and L_1/L_3, and are directly related to the stiffness of beams EI. However, the reactions depend on the actual lengths of beams. This is contrary to the case of gravity loads, where bending moments depend on the actual lengths of the beams and only on the ratio of their stiffnesses.

(11) points of contraflexure due to temperature changes need not coincide with the zero bending moments, as in the case of gravity loads.

(12) if a cantilever shear wall or column is subjected to a linear temperature variation, the bending moment, $M = \alpha T_1 EI/d$, required to restrain the cantilever from bending, is independent of the height. The deflections in the x and y directions (where $\delta x = \alpha Th^2/2d$ and $\delta y = \alpha Th/2$) are independent of the cantilever stiffness EI.

(13) in framed structures, due to temperature variations, stress reversals take place daily and sometimes on several occasions on the same day. This would indicate that structures could eventually fail due to fatigue, even at low stresses. Since concrete is not known to suffer from fatigue, it follows that in regions where temperature variations are large or very frequent, steel structures are likely to deteriorate at a much faster rate.

(14) tensile stresses can occur at many odd locations, which explains the reasons for cracks for which, up to now, there was either no explanation or it was erroneously attributed to shrinkage.

(15) bracing of framed structures reduces deflections due to temperature effects, significantly.

(16) in multi-storey buildings, the effect of temperature changes in the roof and/or side of the building is felt most strongly in the upper two to three floors, and in the columns directly exposed to the temperature change.

(17) temperature changes in the roof cause alternate floors to be subjected to axial tension and compression in addition to bending moments, i.e. tension and compression oscillates from floor to floor. This explains why, in practice, some floors are observed to crack while others appear to be immune to cracks.

(18) linear temperature changes cause greater bending moments in relation to constant temperature changes, whereas the latter cause greater deflections, predominantly at the top of the structure.

(19) the secondary effect of axial forces in the analysis of thermal stresses in frames is small.

(20) in statically determinate trusses, temperature changes result only in displacements of joints without any stresses in members.

(21) in statically indeterminate trusses, temperature changes result not only in displacementsof joints, but members are also subjected to axial forces and deformations.

(22) in both determinate and indeterminate trusses, the displacements are independent of cross-sectional areas of members and the modulus of elasticity of the material, depending only on the length of members, the coefficient of extension and the temperature change. However, in indeterminate trusses the forces in the members, in addition to the above properties, are also proportional to the cross-sectional areas of members and the modulus of elasticity of the material.

(23) in reinforced concrete members, shrinkage generally produces tension in concrete and compression in steel, in addition to stresses produced by gravity, wind loads, prestressing, creep and temperature.

(24) shrinkage strains and stresses in concrete and in steel in symmetrically reinforced members are independent of the position of the steel, but depend on the magnitude of the reinforcement used. Also, the greater the magnitude of reinforcement, the greater are the stresses and strains in the concrete.

(25) temperature of hydration of cement causes compressive stresses near the surface and tensile stresses at the centre of a beam which are additive to other stresses.

(26) high stresses and deformations can develop in reinforced concrete beams due to the combined effect of temperature of hydration and shrinkage, and these stresses cannot be fully controlled by either extra reinforcement or better curing.

(27) the theoretical spacing of potential cracks can be approximately evaluated. However, they depend in a complex way on the relative magnitude of the shrinkage of concrete, its modulus of elasticity, modulus of rupture and bond.

In summarising this work it is fair to claim that, for the first time, a comprehensive method of analysis of thermal stresses and deformations in structures is presented. This project has demonstrated that thermal changes, even at ambient temperatures, can create high stresses and deformations in full-size structures (as shown in the analysis of a 6-storey symmetrical frame. During the author's extensive research into past papers and literature, he was surprised to discover that relatively little information was available on the effect of ambient temperature changes in relation to the effect of elevated temperature or fire. This was particularly evident in the case of 'analysis' for thermal effects. Most efforts appear to have been concentrated on the effect of temperature on individual isolated members of a structure or on the changes in the material properties. The result has been that the designer was no wiser in how to deal with a complete structure. This topic is, however, beginning to receive its due attention, especially in view of the rapid development of the Middle East Countries.

Due to the lack of proven information, Engineers in the past had to depend very often on their rational powers of reasoning. This has sometimes resulted in serious problems. One particular aspect of interest is the belief that concretes made from aggregates of low coefficient of expansion (e.g. limestone aggregate) would be most suitable for building in areas where temperature changes are large. This has now been proved wrong (ref. 36) in the Middle East and some Mediterranean Countries where limestone is predominantly used as an aggregate for concrete. It has now been shown that the relative difference in the coefficients of expansion of the constituent materials is more important than the common coefficient of the

finished product. Rapid deterioration of structures made from limestone aggregate concrete has taken place in the Middle East. This is attributed to the relative differences of coefficients of expansion of aggregates, hardened cement paste and reinforcing steel.

This work covers a very wide spectrum of structural problems most frequently encountered in a design office. Other forms not discussed here may also be dealt with in a similar way, based on the principles developed for the basic forms. However, like all other topics, there is plenty of scope for future research. From the designers point of view, perhaps the most urgent need is to formulate simple guidelines on the methods of design for thermal stresses for incorporation into the Code of Practice. One area which is still not fully resolved is 'how and how much of the thermal stresses should be taken care of by reinforcement or by other means, such as insulations'! clearly, to try and provide reinforcement for the full thermal stress could not only make the structure very expensive, but may also not be altogether effective (as mentioned in the section on temperature of hydration of cement and shrinkage). A further study is necessary to investigate the properties and comparative costs of the available insulators before an effective and economic combination can be recommended. This, however, is outside the scope of this work.

10.04 APPENDIX A: DETERMINATION OF ELASTIC MODULUS AND STRAIN CALIBRATION OF MODEL MATERIALS

This appendix gives the details of the experimental determination of Young's Modulus of Elasticity for micro-concrete used in the test models. Also included are the calibration data relating strain to data logger output for the model materials.

Flexural test on concrete cantilever representative of concrete used in experimental work on 6 - storey Frame

For a simple cantilever, the deflection at the free end is given by the well known relationship:

$$\Delta = \frac{PL^3}{3EI}$$

Where P = point load applied to the free end.

L = length of cantilever

Transposing gives $E = \frac{PL^3}{3\Delta I}$

To establish E and also obtain the relationship between gauge reading and stress, a model cantilever of micro-concrete was manufactured and strain gauges applied as shown in Fig. 10.041.

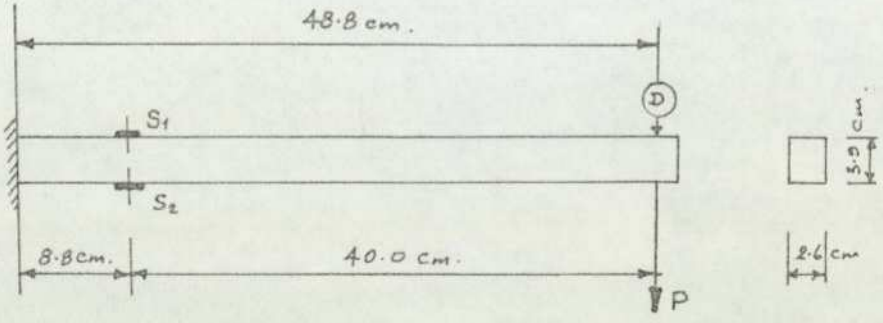

Fig. 10.041 Model Concrete Cantilever used in Test

From $I = \frac{bd^3}{12}$, $I = \frac{1}{12} \times 26 \times 39^3 = 128524.5 \text{ mm}^4$

$$E = \frac{P}{\Delta} \quad \frac{488^3}{3 \quad 128524.5} = \frac{P}{\Delta} \quad 301.4063$$

Where the value of (i) P/Δ from Graph $\quad Exp(1) = \frac{11.50-0.55}{0.348-0.05} = 36.745$

(ii) P/Δ " " $\quad Exp(2) = \frac{11.00-0.35}{0.346-0.04} = 34.800$

Average value of $P/\Delta = (36.745 + 34.800)\ \frac{1}{2} = 35.773$

Therefore $E = 301.4063 \times 35.773 = 10782.21\ N/mm^2$

This is rounded up to $E = 11000\ N/mm^2$

Further, from the data logger print, load increment of $P = 10$ N resulted in a strain gauge reading of 4.5 divisions i.e.

$$4.5 \text{ divisions} = M = 10 \times 400 = 4000 \text{ N-mm}$$

$$\text{i.e. } M = \frac{4000}{4.5} = 888.89 \text{ N-mm per division}$$

Relationship between gauge reading and stress is derived from

$$\sigma = \frac{MY}{I} = \frac{PLY}{I}$$

$$\text{Max. } \sigma_{(P=12N)} = \frac{12 \times 488 \times 39}{128524.5 \times 2} = 0.8885\ N/mm^2$$

Corresponding strain gauge reading for this load, $G_1 = 4.33$, $G_2 = 6.67$ (from Fig. 10.043)

Average for G_1 and $G_2 = (4.33 + 6.67)\ \frac{1}{2} = 5.50$

Therefore Stress per division $= \frac{0.8885}{5.50} = 0.1615\ N/mm^2$

EXPERIMENT 1			
Load in N.	Dial Gauge Readings	Strain Readings from Data Logger	
		Bottom Gauge	Top Gauge
0	10.86	46.67	272.67
2	10.85	45.50	274.00
4	10.75	44.00	274.00
6	10.70	44.00	275.00
8	10.635	43.00	276.00
10	10.57	41.50	276.50
12	10.50	40.00	277.00
10	10.535	41.00	276.00
8	10.58	43.00	276.00
6	10.625	43.50	275.00
4	10.68	44.50	275.00
2	10.735	46.00	273.50
0	10.79	46.33	272.33

Table: 1000.1

EXPERIMENT 2			
Load in N.	Dial Gauge Readings	Strain Readings from Data Logger	
		Bottom Gauge	Top Gauge
0	12.40	66.00	293.50
2	12.34	64.50	294.00
4	12.275	63.50	295.00
6	12.215	62.50	296.00
8	12.16	61.00	296.50
10	12.11	60.00	297.00
12	12.04	59.50	298.00
10	12.06	60.00	297.00
8	12.11	61.00	297.00
6	12.16	62.00	296.00
4	12.225	64.00	295.00
2	12.285	65.00	294.00
0	12.37	66.00	294.00

Table: 1000.2


EXPERIMENT 1
DEFLECTION (FROM DIAL GAUGE READINGS)
0.35
0.30
0.20
0.10
0
2N.
4N.
6N.
8N.
10N.
12N.
APPLIED LOAD

Fig. 10.042

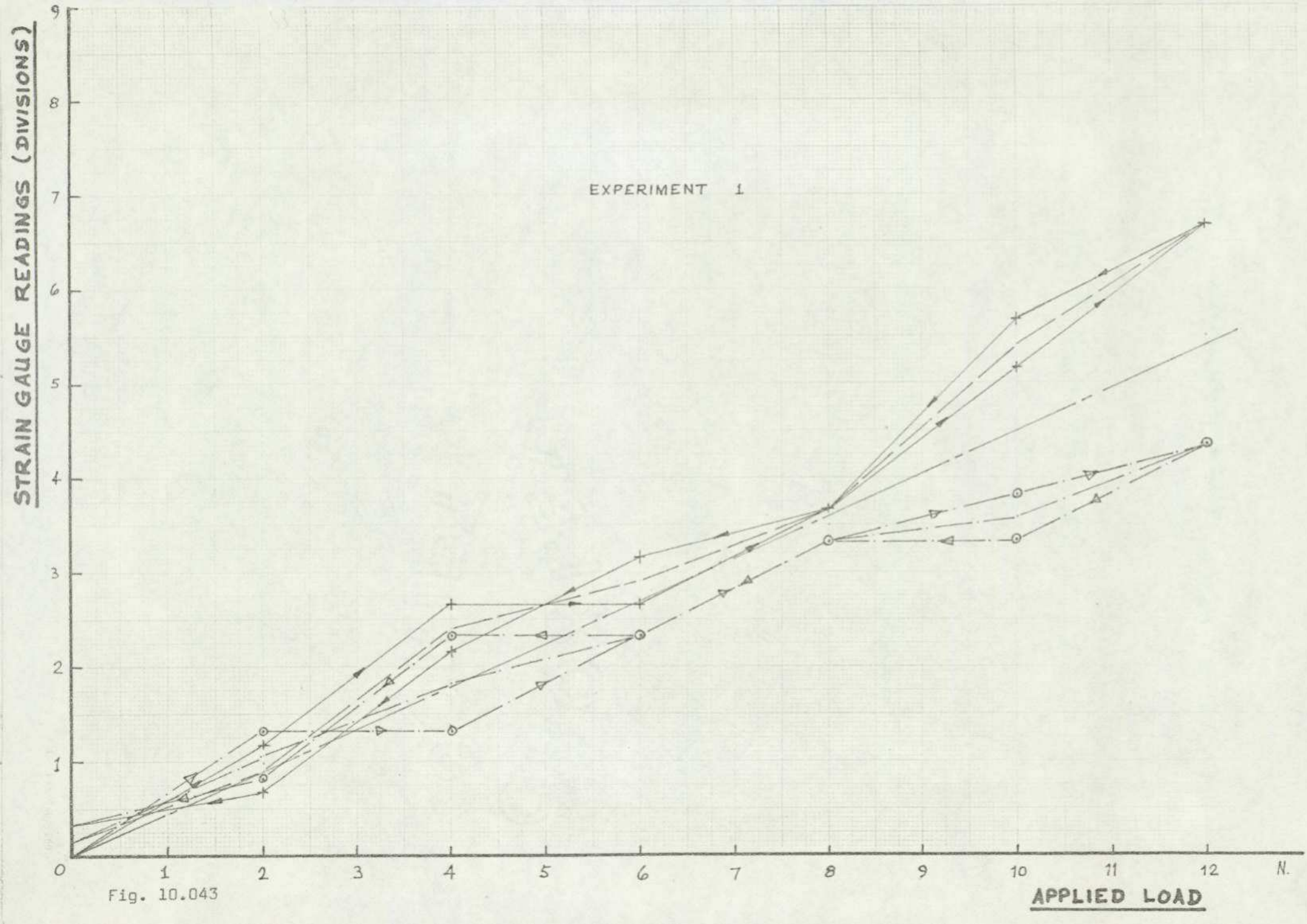
STRAIN GAUGE READINGS (DIVISIONS)
EXPERIMENT 1
0
1
2
3
4
5
6
7
8
9
10
11
12
N.
APPLIED LOAD

Fig. 10.043

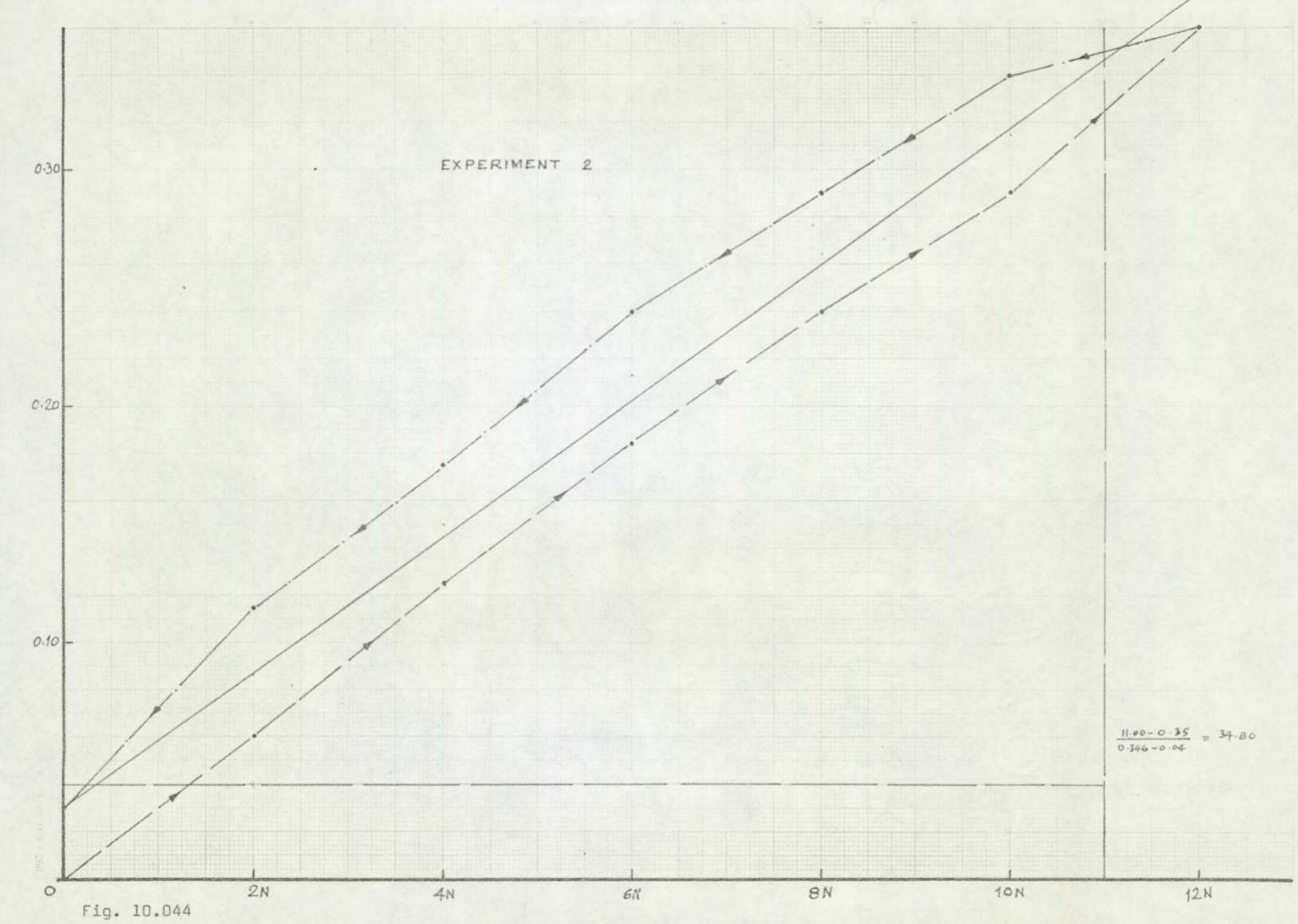
EXPERIMENT 2
0·30
0·20
0·10
0
2N
4N
6N
8N
10N
12N
11.00 - 0.35 / 0.346 - 0.04 = 34.80

Fig. 10.044

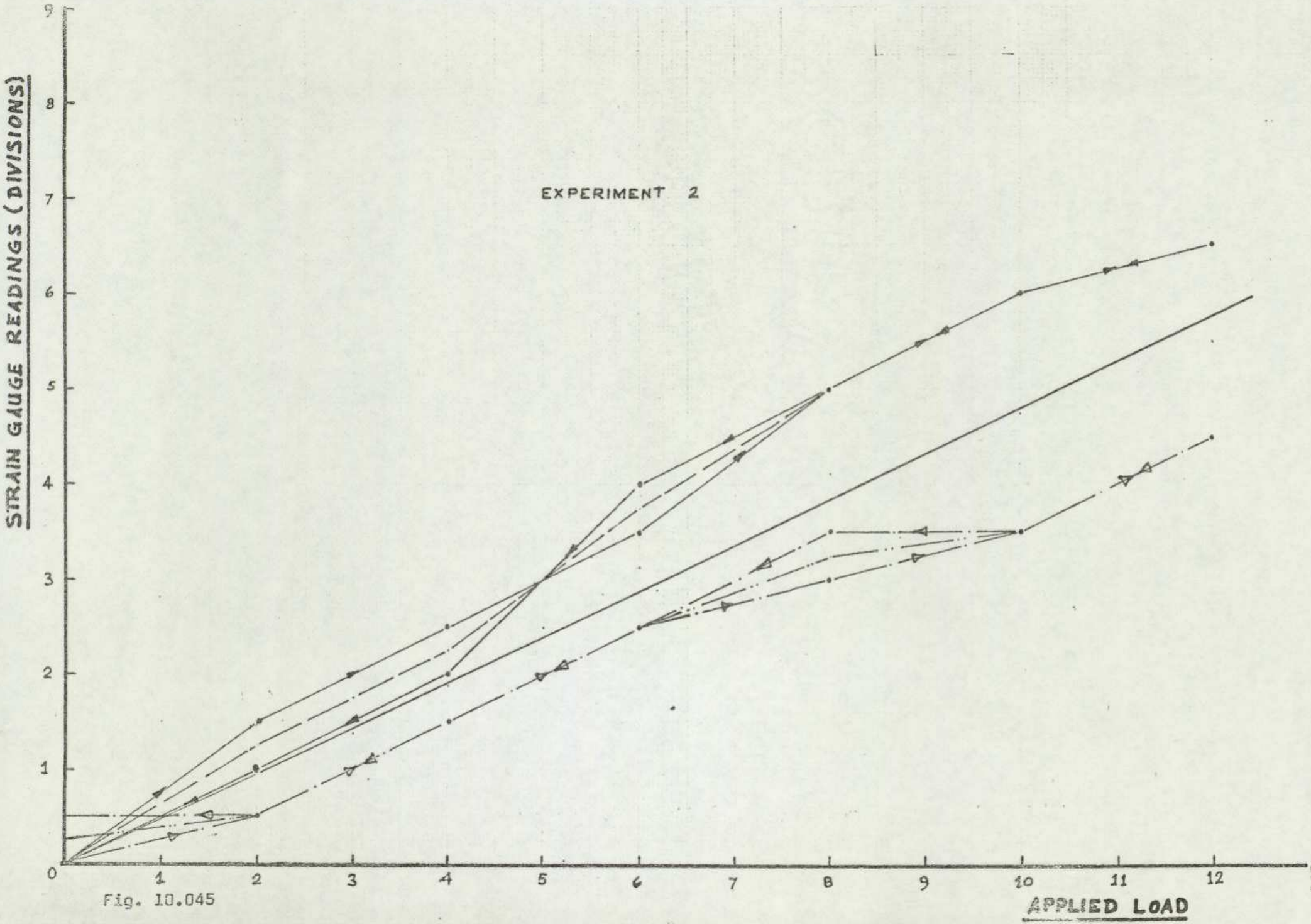
EXPERIMENT 2
STRAIN GAUGE READINGS (DIVISIONS)
0
1
2
3
4
5
6
7
8
9
1
2
3
4
5
6
7
8
9
10
11
12
APPLIED LOAD

Fig. 10.045

10.05 APPENDIX B: CALIBRATION OF FOSTER RESILIA GAUGE FOR IRON THERMOCOUPLES

Thermometer Readings in °C	Gauge Readings (Foster Resilia Serial No. 163537)	Remarks
18	32	Room Temperature
16	18	Water Temperature
20	20.5	
30	36	
40.5	51	
50	65	
61	80	
70	94.5	
80	110.5	
90	125.5	
98.5	139	

Table: 1000.3

CALIBRATION OF FOSTER 'RESILIA' GAUGE

FOR IRON THERMOCOUPLES

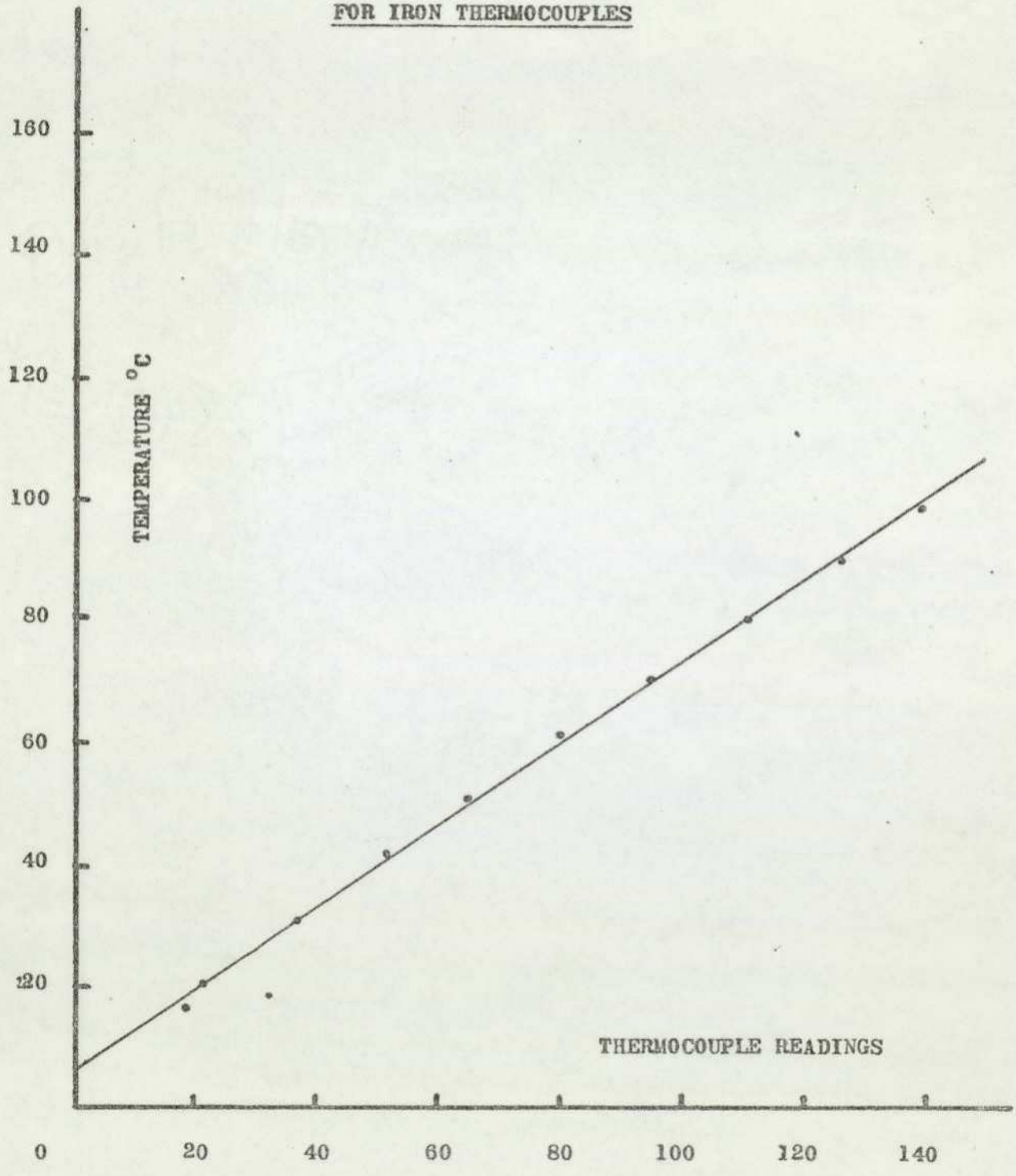

10.06 APPENDIX C: CALIBRATION BEAM TEST FOR PERSPEX MODEL

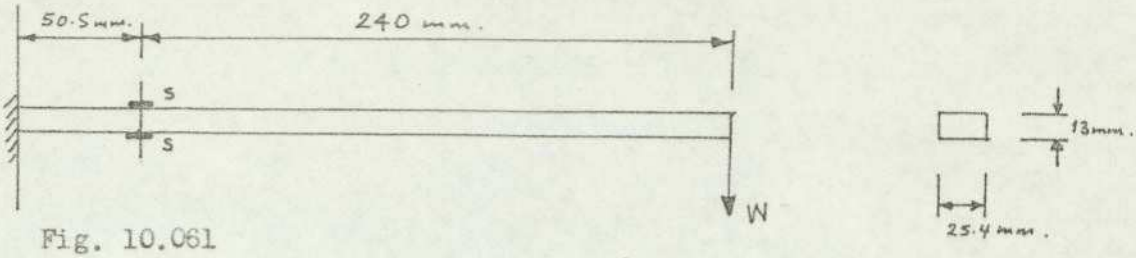

Fig. 10.061

A_B = Cross-sectional area of beam

A_F = Cross-sectional area of frame member

M_B = Beam bending moment

M_F = Frame member bending moment

Z_B = Beam section modulus

Z_F = Frame member section modulus

$(DLR)_1$ = Frame Data Logger readings for bending

$(DLR)_2$ = Frame Data Logger readings for axial loads

From Data Logger, average readings for applied load (W=12N) = 165.5

Beam bending stress, $\sigma B_b = \frac{M_B}{Z_B} = 165.5$

$$\therefore \quad 1(DLR)_1 \text{ div.} = \frac{M_B}{165.5 Z_B} = \frac{240 \times 12 \times 6}{165.5 \times 25.4 \times 13^2}$$

Now Frame bending stress, $\sigma F_b = \frac{M_F}{Z_F} = \frac{M_B (DLR)_1}{165.5\ Z_B} = \frac{2880 \times 6 (DLR)_1}{165.5 \times 25.4 \times 13^2}$

$$M_F = 0.02432346\ (DLR)_1\ Z_F$$

and Frame direct stresses, $\sigma F_d = \frac{M_B\ (DLR)_2}{Z_B\ (165.5)}$

Frame axial forces, $F_F = \frac{M_B\ (DLR)_2\ A_F}{Z_B (165.5)}$

CALIBRATION TEST ON A CANTILEVER BEAM (PERSPEX)

LOADING

Load 00 N

+0269 +0864

Load 2 N

+0242 +0890

Load 4 N

+0216 +0918

Load 6 N

+0188 +0943

Load 8 N

+0158 +0973

Load 10 N

+0131 +1002

Load 12 N

+0100 +1031

UNLOADING

Load 10 N+0127 +1006

Load 8 N

+0154 +0980

Load 6 N

+0181 +0951

Load 4 N+0210 +0924

Load 2 N

+0238 +0897

Load 00 N

+0265 +0870

Table: 1000.4

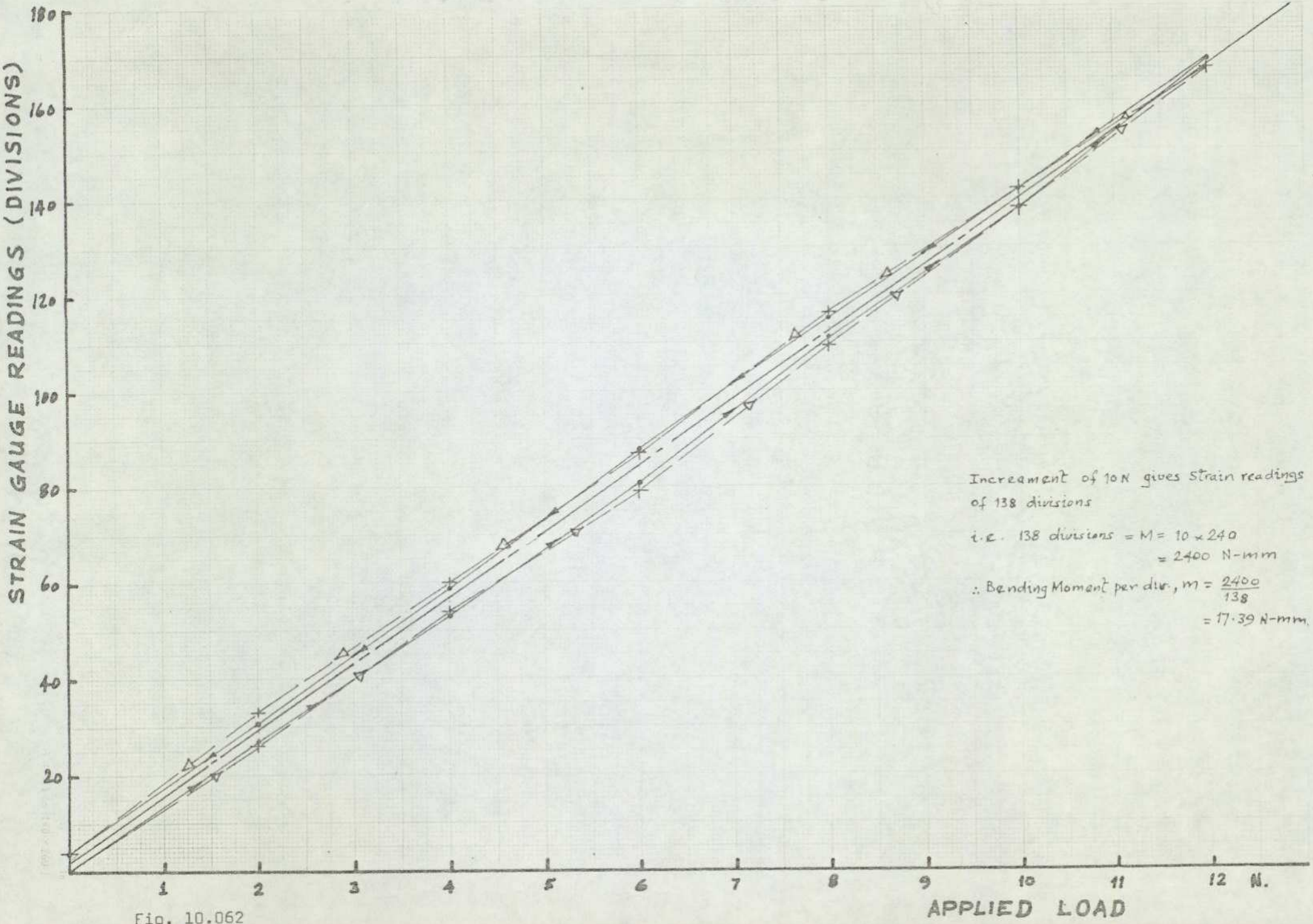
STRAIN GAUGE READINGS (DIVISIONS)
180
160
140
120
100
80
60
40
20
1
2
3
4
5
6
7
8
9
10
11
12 N.
APPLIED LOAD
Increament of 10 N gives Strain readings of 138 divisions
i.e. 138 divisions = M = 10 × 240
= 2400 N-mm
∴ Bending Moment per div., m = 2400/138
= 17·39 N-mm.

Fig. 10.062

10.07 APPENDIX D: CALIBRATION OF A PERSPEX MEMBER FOR AXIAL LOADS

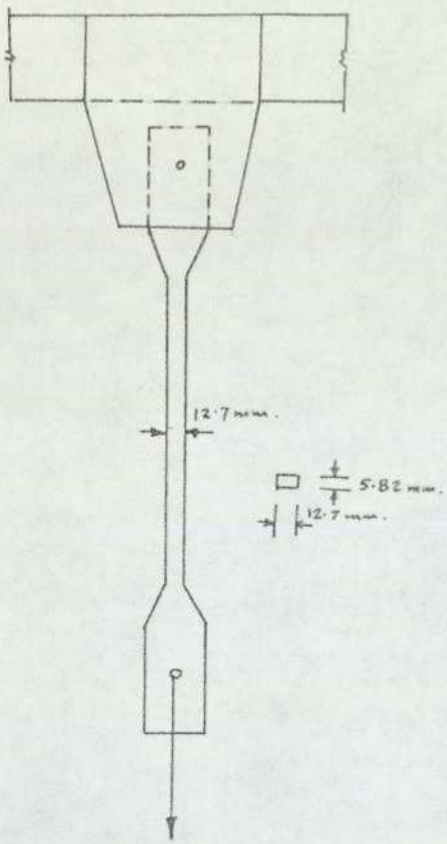

Fig. 10.071

A_{TP} = Cross Sectional Area of Test Piece

A_T = Cross Sectional Area of Truss Member = bxd

F_{TP} = Force in Test Piece

F_T = Force in Truss Member

$$\text{Test Piece direct Stress} = \frac{F_{TP}}{A_{TP}} \quad \frac{(D.L.R.)}{613}$$

$$\text{Truss direct Stress, } \frac{F_T}{A_T} = \frac{F_{TP}}{A_{TP}} \quad \frac{(D.L.R.)}{613}$$

$$\text{Truss direct Force, } F_T = \frac{F_{TP}}{A_{TP}} \quad \frac{(D.L.R.)}{613} \; A_T$$

$$\frac{700}{12.7 \times 5.82} \quad \frac{(D.L.R.)}{613} \; A_T$$

$$= 0.015449 \times A_T$$

CALIBRATION OF STRAIN GAUGE IN TENSION

8TH JUNE, 1977.

LOADING --- LOADING

LOAD 00 N

-0244 -9999
-0246 -9999
-0244 -9999

LOAD 200 N

-0410 -9999
-0411 -9999
-0412 -9999

LOAD 400 N

-0591 -9999
-0592 -9999
-0592 -9999

LOAD 400 N + 20 Lb

-0672 -9999
-0672 -9999
-0672 -9999

LOAD 400 N + 40 Lb

-0745 -9999
-0745 -9999
-0745 -9999

LOAD 400 N + 60 Lb

-0825 -9999
-0827 -9999
0826 -9999

UNLOADING

LOAD 400 N + 40 Lb

-0756 -9999
-0756 -9999
-0757 -9999

LOAD 400 N + 20 Lb

-0682 -9999
-0681 -9999
-0679 -9999

LOAD 400 N

-0603 -9999
-0602 -9999
-0602 -9999

LOAD 200 N

-0425 -9999
-0424 -9999
-0426 -9999

LOAD 00 N

-0256 -9999
-0255 -9999
-0254 -9999

Table: 1000.5

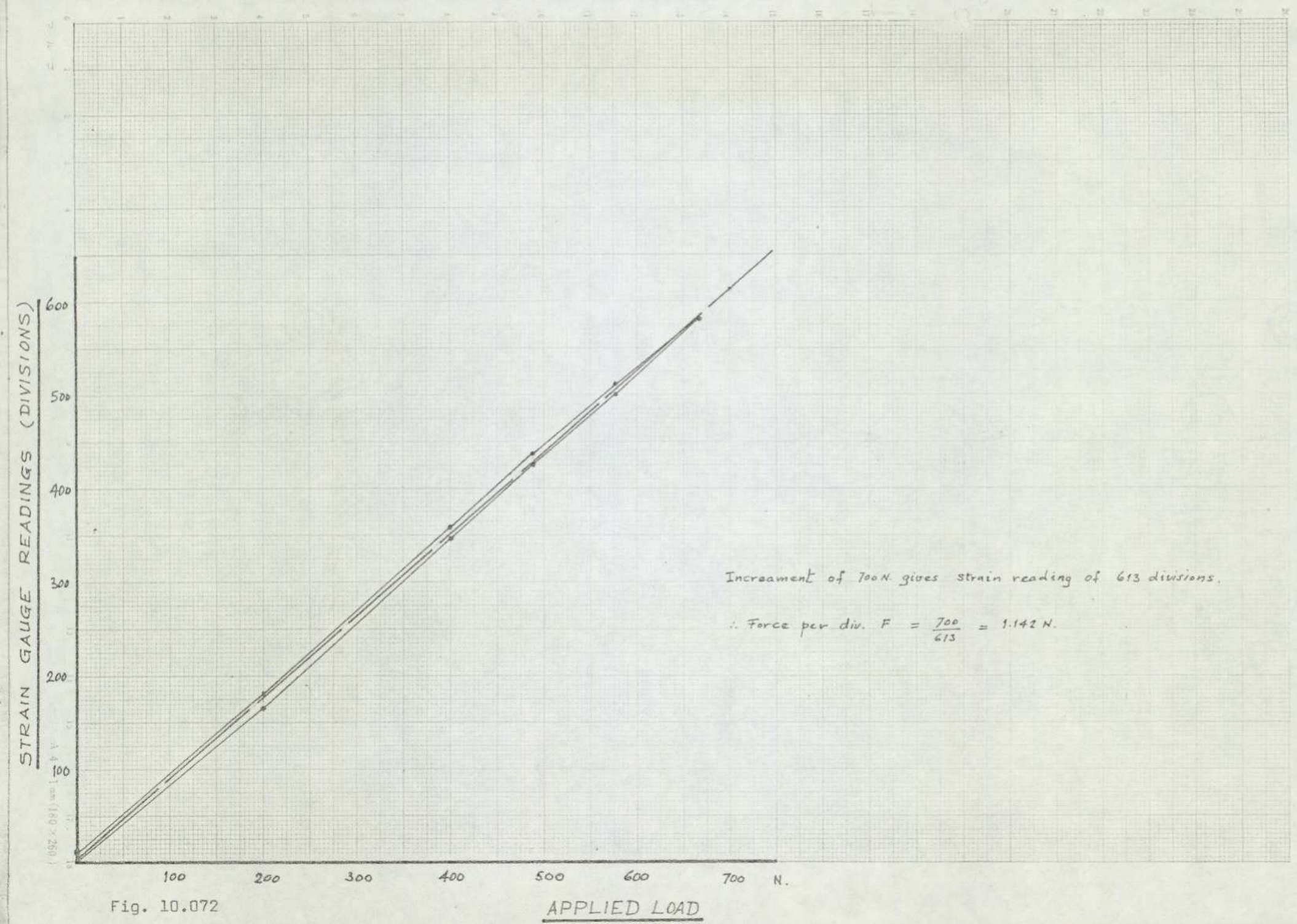
STRAIN GAUGE READINGS (DIVISIONS)
600
500
400
300
200
100
0
100
200
300
400
500
600
700
N.
APPLIED LOAD
Increament of 700 N. gives strain reading of 613 divisions.
∴ Force per div. F = 700/613 = 1.142 N.

Fig. 10.072

REFERENCES

1. B.A. Boley and J.H. Weiner, 'Theory of Thermal Stresses', John Wiley & Sons Limited, New York, 1964.

2. H.S. Carslaw and J.C. Jaeger, 'Conduction of Heat in Solids', Oxford University Press, London, 1959.

3. W.H. McAdams, 'Heat Transmission', McGraw-Hill, London, 1954.

4. S. Timoshenko and J.N. Goodier, 'Theory of Elasticity', McGraw-Hill Book Co. Inc., New York, 1951.

5. S. Timoshenko and S. Woinowsky-Krieger,'Theory of Plates and Shells', McGraw-Hill Book Co. Inc., 1959.

6. M. Smolira, 'Analysis of Tall Buildings by the Force-Displacement Method', McGraw-Hill Book Company (U.K.) Limited, 1975.

7. D.J. Johns, 'Thermal Stress Analysis', Pergamon Press Ltd., London, 1965.

8. Glyn Evans, 'The Effect of Temperature Changes on a Reinforced Concrete Frame', M.Sc. Thesis, The City University, 1973.

9. M.E.T. Taitt, 'Theoretical and Experimental Investigation of Thermal Stresses and Deformations in Structures', M.Sc. Thesis, The City University, 1975.

10. C.B. Wilby, 'Concrete for Structural Engineers - A Text to CP 110', Newnes - Butterworths - London, 1977.

11. C.G. Schilling, K.H. Klippstein, J.M. Basom, S.R. Novak and G.T. Blake, 'Low - Temperature Tests on Simulated Bridge Members', Journal of the Structural Division, ASCE, Jan. 1975.

12. B.P. Hughes, 'Temperature Rises in Low-Heat Cement Concrete', Journal of the Structural Division, ASCE, Dec. 1971.

13. N.G. Zoldners, 'Effect of High Temperatures on Concretes Incorporating Different Aggregates', American Society for

Testing and Materials, Vol. 60, 1960

14. D. Campbell - Allen and C.P. Thorne, 'The Thermal Conductivity of Concrete', Magazine of Concrete Research, Vol. 15, No. 43, Mar. 1963, pp. 39 - 48.

15. H.L. Malhotra, 'The Effect of Temperature on the Compressive Strength of Concrete', Magazine of Concrete Research, Vol. 8, No. 23, Aug. 1956.

16. K.W. Nasser and R.P. Lohtia, 'Mass Concrete Properties at High Temperatures', ACI Journal, March 1971.

17. Tasnim Uddin, 'Effects of Elevated Temperature on Structural Members', Journal of the Structural Division, ASCE, July 1975.

18. R.D. Browne, 'Thermal Movement of Concrete', Current Practice Sheet, Cement and Concrete Association, ref. 55.201, Vol. 6, No. 11

19. ACI, Ad Hoc C-S-T Symposium Committee, 'Designing for Effects of Creep Shrinkage Temperature in Concrete Structures', Am. Conc. Inst. Special Publication SP - 27, 1971, Detroit.

20. Z.F. Baczynski, J. Ignaczak, 'Thermoelastic Stress Analysis of Reactor Secondary Containment', Institute of Fundamental Technological Research, Polish Academy of Sciences, Warsaw, Poland.

21. D.G.R. Bonnell and F.C. Harper, 'The Thermal Expansion of Concrete', National Building Studies, Technical Paper No. 7 Department of Scientific and Industrial Research (Building Research Station).

22. A.K. Kar, 'Thermal Effects in Concrete Members', Ebasco Services, Inc. 21 West Street, New York, N.Y. 10006, U.S.A.

23. George T. Taska, Michael Hogan, Fazlur Khan and Robert H. Scanlan, 'Ambient Response Analysis of some Tall Structures', Journal of the Structural Division, ASCE, Jan. 1975.

24. Building Research Station Digest No. 98, May 1957, 'Light Cladding - Part 1, General Principles of Design'.

25. Building Research Station Digest No. 12, 'The Design of Flat Concrete Roofs in Relation to Thermal Effects'.

26. R.J. Roark, 'Formulas for Stress & Strain', McGraw-Hill Book Company, Inc.

27. G.H. Ryder, 'Strength of Materials', Macmillan and Co. Ltd. 1969.

28. D.A.R. Clark, 'Materials and Structures', Blackie & Son Limited, 1963.

29. R.K. Livesly, 'Matrix Methods of Structural Analysis', Pergamon Press, The Macmillan Company, 1964.

30. S.P.Timashenko & D.H. Young, 'Theory of Structures', Second Edition, Mcgraw-Hill Book Company, 1965.

31. Kazuo Ohno, Mamoru Obata, 'The Movement of Actual Reinforced Concrete Buildings caused by the Atmospheric Temperature', Symposium, Design of Concrete Structures for Creep, Shrinkage and Temperature Changes, Madrid - 1970. Volume - Band 5.

32. Fookes, P.G. and L. Collis, 'Problems in the Middle East', 1975 Concrete, Vol. 9, No. 7.

33. Fookes, P.G. and L. Collis, 'Aggregate and the Middle East', 1975 Concrete, Vol. 9, No. 11.

34. French, W.J. and A.B. Poole, 'Alkali-aggregate Reactions and the Middle East', 1976 Concrete, Vol. 10, No. 1.

35. Fookes, P.G. and L. Collis, 'Cracking and the Middle East', 1976 Concrete, Vol. 10, No. 2.

36. Venecanin, Srdan D., 'Influence of Temperature on Deterioration of Concrete in the Middle East', 1977, Concrete, Vol. 11, No. 8.